Protein engineering and enzyme cascade in the sustainable stereoselective synthesis of β-nitroalcohols

A thesis submitted for the degree of

DOCTOR OF PHILOSOPHY

By

AYON CHATTERJEE

हैदराबाद विश्वविद्यालय
University of Hyderabad

प्रतिष्ठित संस्थान
INSTITUTION OF EMINENCE
राष्ट्रीय अपेक्षाएँ, वैश्विक मानक
National Needs, Global Standards

Department of Biochemistry

School of Life Sciences

University of Hyderabad

Hyderabad – 500046, India

Enrollment No: 17LBPH08 **May, 2024**

University of Hyderabad
Hyderabad – 500046, India

Declaration

I, **Ayon Chatterjee**, hereby declare that this thesis entitled '**Protein engineering and enzyme cascade in the sustainable stereoselective synthesis of β-nitroalcohols'** submitted by me under the guidance and supervision of **Dr. Santosh Kumar Padhi**, is an original and independent research work, I also declare that it has not been submitted previously in part or in full to this university or any other university or institution for the award of any degree or diploma.

Date: 22/05/2024

Ayon Chatterjee.

Signature of the student

Name: Ayon Chatterjee

Regd. No. 17LBPH08

22/05/2024

Signature of the supervisor

Dr. Santosh Kumar Padhi
Associate Professor
Department of Biochemistry
School of Life Science
University of Hyderabad
Hyderabad-500 046. India.

University of Hyderabad
Hyderabad – 500046, India

CERTIFICATE

This is to certify that the thesis entitled '**Protein engineering and enzyme cascade in the sustainable stereoselective synthesis of β-nitroalcohols**' submitted by Ayon Chatterjee to University of Hyderabad, Hyderabad, for the award of the degree of Doctor of Philosophy is bonafide record of research work carried out by him under my supervision. The contents of this thesis, in full or parts, have not been submitted to any other University or Institution for the award of any degree or diploma.

Place: Hyderabad

22/05/2024

Dr. Santosh Kumar Padhi
Supervisor

Dr. Santosh Kumar Padhi
Associate Professor
Department of Biochemistry
School of Life Science
University of Hyderabad
Hyderabad-500 046. India.

S. V. Naidu

Head
Department of Biochemistry

प्रो. नरेश बाबु वी. शेपूरी
Prof. NARESH BABU V. SEPURI
अध्यक्ष / Head
जीवरसायनविभाग / Department of Biochemistry
जीवविज्ञान संकाय / School of Life Sciences
हैदराबाद विश्वविद्यालय / University of Hyderabad
हैदराबाद / Hyderabad-500046. INDIA

Dean
School of Life sciences

संकाय अध्यक्ष / Dean
जीवन विज्ञान संकाय / School of Life Sciences
हैदराबाद विश्वविद्यालय / University of Hyderabad
हैदराबाद / Hyderabad-500 046.

University of Hyderabad
Hyderabad – 500046, India

CERTIFICATE

This is to certify that the thesis entitled '**Protein engineering and enzyme cascade in the sustainable stereoselective synthesis of β-nitroalcohols'** submitted by Ayon Chatterjee bearing registration number 17LBPH08 in partial fulfillment of the requirements for the award of Doctor of Philosophy in the Department of Biochemistry, School of Life Sciences, is a bonafide work carried out by him under my supervision and guidance.

This thesis is free from plagiarism and has not been submitted previously in part or in full to this or any other University or Institution for the award of any degree or diploma.

Parts of this thesis have been:

A. Published in the following publications:

1) **A. Chatterjee**, D.H.S. Rao, and S. K. Padhi, One-Pot Enzyme Cascade Catalyzed Asymmetrization of Primary Alcohols: Synthesis of Enantiocomplementary Chiral β-Nitroalcohols. ***Adv. Synth. Catal.,*** **2021**, 363, 5310-5318.

2) D.H.S. Rao, **A. Chatterjee**, and S. K. Padhi, Biocatalytic approaches for enantio and diastereoselective synthesis of chiral β-nitroalcohols. ***Org. Biomol. Chem.,*** **2021**, 19, 322-337.

B. Published in the following patents:

1) Variants of hydroxynitrile lyase and their use in diastereoselective synthesis of β-nitroalcohols. SANTOSH KUMAR PADHI, **AYON CHATTERJEE**, BADIPATLA VISHNU PRIYA, University of Hyderabad, Date: 2023/05/03. Ref. No./Application No: 202341031596. status: published

2) Baliospermum montanum hydroxynitrile lyase in the stereoselective synthesis of optically active β-nitroalcohols of one or more chiral centers. SANTOSH KUMAR PADHI, **AYON CHATTERJEE**, SUKADEV RANA, University of Hyderabad, Date: 2023/07/15. Ref. No./Application No: 202341047813 status: published

C. Presented in the following conferences:

1) **Poster presentation and flash talk** on 'A dehydrogenase-hydroxynitrile lyase cascade for one-pot transformation of primary alcohols into enantiocomplementary chiral β-nitroalcohols'

in '**BIOCAT-2022' organized by Hamburg University of Technology (TUHH), Hamburg, Germany**, August 2022.

2) **Poster presentation** on 'A new biocatalytic route for the synthesis of Chiral β-nitroalcohols' in '**Bioquest – 2019 Cellular Homeostasis: From Basics to Translational Research'** organized by School of Life Sciences, University of Hyderabad, and **won 3rd prize for the same**, March 2019.

Further, the student has passed the following courses towards fulfillment of coursework requirement for Ph.D.

Course code	Name	Credits	Pass/fail
BC 801	Research methodology/Analytical techniques	4	Pass
BC 802	Research Ethics, Biosafety, Data Analysis and Biostatistics	4	Pass
BC 803	Scientific Writing and Research Proposal	4	Pass

22/05/2024

Research Supervisor
Dr. Santosh Kumar Padhi
Associate Professor
Department of Biochemistry
School of Life Science
University of Hyderabad
Hyderabad-500 046. India.

Head
Department of Biochemistry
प्रो. नरेश बाबु वी. शेपूरी
Prof. NARESH BABU V. SEPURI
अध्यक्ष / Head
जीवरसायनविभाग / Department of Biochemistry
जीवविज्ञान संकाय / School of Life Sciences
हैदराबाद विश्वविद्यालय / University of Hyderabad
हैदराबाद / Hyderabad-500046. INDIA

Dean
School of Life sciences
संकाय अध्यक्ष / Dean
जीव विज्ञान संकाय / School of Life Sciences
हैदराबाद विश्वविद्यालय / University of Hyderabad
हैदराबाद / Hyderabad-500 046.

ACKNOWLEDGEMENTS

It's not possible to acknowledge all the people in only few words who made this Ph.D thesis possible. However, I will try to express my gratitude to everyone who helped me throughout this study.

First and foremost, I express my gratitude to my supervisor, **Dr. Santosh Kumar Padhi**, for his unwavering guidance and support throughout my research program. He not only introduced me to the realm of biocatalysis but also nurtured me into a proficient researcher. One of the invaluable lessons I imbibed from him is the virtue of patience, a quality I developed significantly while working under his mentorship. Even when confronted with less-than-ideal data, I learned to meticulously analyze it with patience, extracting valuable insights before considering repeating the experiment. Throughout my tenure, Dr. Padhi never imposed restrictions on my planning or execution of experiments, granting me full autonomy to think innovatively. His enthusiasm and accessibility at any hour for guidance were particularly noteworthy. Importantly, I owe my qualification for the CSIR-JRF to his initial support and belief in me during the early days of my Ph.D. Though initially hesitant due to my limited knowledge, joining his lab in UOH Biochemistry turned out to be one of the most rewarding decisions of my academic journey.

I would like to thank my doctoral committee members: **Prof. N. Siva Kumar** and **Prof. Mrinal Kanti Bhattacharyya** for their critical comments and invaluable suggestions on my PhD work.

I would like to express my gratitude to **Prof. Naresh BV Sepuri,** Head, Department of Biochemistry and **Prof. Krishnaveni Mishra, and Prof. Mrinal Kanti Bhattacharyya**, former Head, Department of Biochemistry for providing encouragement and necessary facilities for carrying out the research work.

I would like to thank to **Prof. Anand. K. Kondapi,** Dean, School of Life Sciences**, Prof. S. Dayananda**, **Prof. K.V.A. Ramaiah, Prof. MNV Prasad** and **Prof. P. Reddanna former** Deans of School of Life Sciences for allowing me to use all the central facilities of school.

I would like to thank all the **faculty members** of department of biochemistry and school of life sciences for their timely help.

I express my gratitude to **Dr. T. Saravanan** from School of Chemistry, University of Hyderabad for their kind help to record NMR spectra of the synthesized standards used in my Ph.D thesis work.

I would like to thank UOH-Infrastructure and School of Life Sciences facilities provided by **DST-COE**, **DBT-CREB**, **UGC-SAP UPE**, **CSIR** & **ICMR**.

I would like to thank funding bodies **UGC-SAP, DST-SERB, CSIR** & **IOE-UOH** for providing funding to our lab.

I would like to thank **University Grants Commission** (UGC), New Delhi, for providing me the fellowship

I want to acknowledge **S. B. Chary** and all the **non-teaching staff** of Department of Biochemistry and School of Life Sciences for their help.

I would like to thank all my lab-mates **Nisha Jangid, D.H.S. Rao, Nivedita Rai, Vishnu Priya, Ghufrana, Mohit, Sukadev, Vinay** for their help and cooperation during my research work.

I would like to thank to my Friends of SLS - **Prodosh da, Saumashish, my brother Arpan, Supriya and Avishek**

I would like to thank to my family members **Mother, Father & Brother** for their care and support.

TABLE OF CONTENTS

Chapter 1: Introduction

1.1. Chiral β-nitroalcohols and their importance ……1

1.2. Asymmetric synthesis of β-nitroalcohols ……1

1.2.1. Asymmetric synthesis of β-nitroalcohols by chemical catalyst ...…….1

1.2.2. Biocatalytic approaches for synthesis of chiral β-nitroalcohols ……3

1.2.2.1. Lipase catalyzed kinetic resolution (KR) ……..….4

1.2.2.2. Dynamic Kinetic resolution (DKR) ……...6

1.2.2.3. Direct C–C bond formation ……...8

1.2.2.3.1. Hydroxynitrile lyase (HNL) ……...8

1.2.2.3.2. HNLs and other enzyme catalyzed synthesis of optically pure β-nitroalcohols …….9

1.2.2.4. Stereoselective cleavage of racemic β-nitroalcohols (retro-Henry reaction) ……4

1.2.2.5. Biocatalytic asymmetric reduction ……14

1.2.2.6. Stereooselective epoxide ring opening ……16

1.3. Outline of the thesis ……...18

1.4. Objectives ……18

1.5. References ……19

Chapter 2: One-pot enzyme cascade in the synthesis of enantiocomplementary chiral β-nitroalcohols starting from aromatic primary alcohols

2.1. Introduction ……...24

2.2. Objectives ……26

2.3. Materials and methods ……..….26

2.3.1. Chemicals and materials ……26

2.3.2. Heterologous expression, purification, and assay of enzymes ……26

2.3.2.1. Heterologous expression, purification, and assay of HLADH ……26

2.3.2.2. Heterologous expression, purification, and assay of *At*HNL ……..27

2.3.2.3. Heterologous expression, purification, and assay of *Bm*HNL ……27

2.3.3. Kinetics and inhibition studies ……...27

2.3.3.1. Steady-state kinetics of HLADH ……27

2.3.3.2. Inhibition of HLADH by benzaldehyde ……..27

2.3.3.3. Inhibitory effects of benzyl alcohol and benzaldehyde on *At*HNL ……...28

2.3.3.4. Inhibitory effects of benzyl alcohol and benzaldehyde on *Bm*HNL ……28

2.3.4. Optimization of reaction conditions of HLADH-*At*HNL cascade ……..28
2.3.4.1. Optimization of buffer system and its pH ……28
2.3.4.2 Screening for cofactor recycling agent ……29
2.3.4.3. Optimization of *At*HNL content ……..29
2.3.4.4. Optimization of cofactor (NAD^+) concentration ……29
2.3.4.5. Optimization of HLADH content ……29
2.3.4.6. Optimization of concentration of KPB pH 6.0 ……30
2.3.4.7. Optimization of nitromethane concentration ……..30
2.3.4.8. Optimization of the biphasic system ……30
2.3.4.9. Optimization of organic solvent content ……30
2.3.4.10. Intermittent addition of benzyl alcohol and HLADH ……30
2.3.4.11. Optimization of substrate concentration ……31
2.3.4.12. Optimization of protein stabilizer ……..32
2.3.4.13. Optimization of cofactor recycling agent (acetaldehyde) concentration ……..32
2.3.4.14. Optimization of reaction time ……32
2.3.4.15. Optimization of sorbitol concentration ……32
2.3.5. Synthesis of racemic β-nitro alcohols ……33
2.3.6. HLADH-*At*HNL cascade catalyzed enantioselective synthesis of different (*R*)-β-nitroalcohols ……33
2.3.7. Optimization of reaction parameters of *Bm*HNL catalyzed nitroaldol reaction …….33
2.3.7.1. Optimization of *Bm*HNL enzyme content using benzaldehyde as the substrate ……...33
2.3.7.2. Optimization of buffer system and its pH ……34
2.3.7.3. Optimization of organic solvent ……..….34
2.3.7.4. Optimization of protein stabilizer or reaction additive ……34
2.3.7.5. Optimization of substrate ……34
2.3.7.6. Optimization of *Bm*HNL content using 3,5-dimethoxybenzaldehyde as the substrate ….34
2.3.8. Optimization of HLADH content in the HLADH-*Bm*HNL cascade using 3,5-dimethoxybenzyl alcohol as the substrate ……35
2.3.9. HLADH-*Bm*HNL cascade catalyzed enantioselective synthesis of different (*S*)-β-nitroalcohols ……35
2.4. Results ……..…….35
2.4.1. NMR characterization of racemic β-nitroalcohols ……..……35
2.4.2. HPLC conditions for chiral resolution of racemic β-nitroalcohols …….47

2.4.3. SDS-PAGE of purified HLADH, *At*HNL, and *Bm*HNL enzymes and their specific activity determination ……..47
2.4.4. Kinetics and inhibition studies ……...48
2.4.4.1. Steady-state kinetics of HLADH ……48
2.4.4.2. Inhibition of HLADH by benzaldehyde ……..49
2.4.4.3. Inhibitory effects of benzyl alcohol and benzaldehyde on *At*HNL ……...49
2.4.4.4. Inhibitory effects of benzyl alcohol and benzaldehyde on *Bm*HNL ……50
2.4.5. Optimization of reaction conditions of HLADH-*At*HNL cascade ……..50
2.4.5.1 Optimization of buffer system and its pH ……50
2.4.5.2. Screening of cofactor recycling agent ……51
2.4.5.3. Optimization of *At*HNL content ……..51
2.4.5.4. Optimization of cofactor (NAD^+) concentration ……52
2.4.5.5. Optimization of HLADH content ……52
2.4.5.6. Optimization of KPB concentration ……53
2.4.5.7. Optimization of nitromethane concentration ……...53
2.4.5.8. Optimization of the biphasic system ……54
2.4.5.9. Optimization of organic solvent content ……..54
2.4.5.10. Intermittent addition of benzyl alcohol and HLADH ……55
2.4.5.11. Optimization of substrate concentration ……56
2.4.5.12. Optimization of protein stabilizer ……..56
2.4.5.13. Optimization of cofactor recycling agent (acetaldehyde) concentration ……57
2.4.5.14. Optimization of reaction time ……58
2.4.5.15. Optimization of sorbitol concentration ……..58
2.4.6. HLADH-*At*HNL cascade catalyzed enantioselective synthesis of different (*R*)-β-nitroalcohols ……59
2.4.7. Optimization of reaction parameters of *Bm*HNL catalyzed nitroaldol reaction ……..61
2.4.7.1. Optimization of *Bm*HNL enzyme content using benzaldehyde as the substrate ……...61
2.4.7.2. Optimization of buffer system and its pH ……61
2.4.7.3. Optimization of organic solvent ……..62
2.4.7.4. Optimization of protein stabilizer or reaction additive ……62
2.4.7.5. Optimization of substrate ……63
2.4.7.6. Optimization of *Bm*HNL content using 3,5-dimethoxybenzaldehyde as the substrate …..63
2.4.8. Optimization of HLADH content in the HLADH-*Bm*HNL cascade using 3,5-dimethoxybenzyl alcohol as the substrate ……64

2.4.9. HLADH-*Bm*HNL cascade catalyzed enantioselective synthesis of different (*S*)-β-nitroalcohols ……65
2.4.10. HPLC chromatograms of products of HLADH-*At*HNL and HLADH-*Bm*HNL cascade …66
2.5. Discussion ……87
2.5.1. Inhibition study of the enzymes used in the cascade ……87
2.5.2. Overcoming the pH hurdle of the HLADH-*At*HNL cascade 87
2.5.3. Reaction condition optimization of HLADH-*At*HNL cascade 87
2.5.4. Stereoselective syntheses of (*R*)-β-nitroalcohols by HLADH-*At*HNL cascade ……..88
2.5.5. Study of the promiscuous activity of *Bm*HNL in stereoselective nitroaldol reactions ….89
2.5.6. Optimization of *Bm*HNL catalysed nitroaldol reaction ……...89
2.5.7. Stereoselective syntheses of (*S*)-β-nitroalcohols by HLADH-*Bm*HNL cascade …….89
2.6. Conclusions ……...90
2.7. References ……90

Chapter 3: Engineered *At*HNL variants catalyzed diastereoselective synthesis of β-nitroalcohols with broad substrate scope and high enantioselectivity

3.1. Introduction ……...94
3.2. Objectives ……95
3.3. Materials and methods ……..96
3.3.1. Chemicals and materials ……96
3.3.2. Chromatography ……96
3.3.3. Cloning ……...96
3.3.4. Preparation of *At*HNL variant library ……97
3.3.5. Expression and purification of WT *At*HNL and its variants ……97
3.3.6. Screening of *At*HNL library for diastereoselective synthesis of 2-nitro-1-phenylpropanol (2-NPP) ……97
3.3.7. Optimization of biocatalytic parameters for diastereoselective synthesis of 2-NPP …...98
3.3.7.1. Buffer and pH optimization ……98
3.3.7.2. Organic solvent optimization ……..98
3.3.7.3. Nitroethane concentration optimization ……..98
3.3.7.4. Citrate phosphate buffer concentration optimization ……...98
3.3.7.5. Enzyme content optimization ……..99

3.3.8. Y14C catalyzed diastereoselective Henry reaction in the synthesis of diverse β-nitroalcohols using nitroethane as a nucleophile ……..99

3.3.9. Y14C-F179L catalyzed diastereoselective Henry reaction in the synthesis of diverse β-nitroalcohols using nitroethane as a nucleophile ……..99

3.3.10. Screening of *At*HNL library for diastereoselective synthesis of 2-nitro-1-phenyl butan-1-ol (2-NPB) ……99

3.3.11. Optimization of biocatalytic parameters for diastereoselective synthesis of 2-NPB ...100

3.3.11.1. Optimization of reaction time and catalyst amount ……100

3.3.11.2. Optimization of 1-nitropropane concentration ……100

3.3.12. Y14A catalyzed diastereoselective Henry reaction in the synthesis of diverse β-nitroalcohols using 1-nitropropane as the nucleophile ……...100

3.3.13. Determination of kinetics parameters ……100

3.3.14. The pH dependence of Y14C kinetic parameters: Probing proton donation role of Cys14 in diastereoselective nitroaldol synthesis ……...101

3.3.15. Comparison of cyanogenesis and retro-nitroaldolase activity of WT *At*HNL, Y14C, and Y14A ……101

3.3.16. Gram scale synthesis of (*1R,2S*)-2-NPP using Y14C crude enzyme as the catalyst …101

3.3.17. Synthesis of L-norephedrine drug intermediate from (*1R,2S*)-2-NPP ……102

3.3.18. Deciphering the reaction mechanism of diastereoselective Henry reaction by selective deuteration ……102

3.3.18.1. Synthesis of monodeuterated nitroethane by replacing a proton at its α-carbon with deuterium ……...102

3.3.18.2. Synthesis of β-deuterated-2-NPP ……102

3.3.19. Recycling *At*HNL-Y14C for the synthesis of (*1R,2S*)-2-NPP ……103

3.3.20. Chemical synthesis of racemic β-nitroalcohol standards ……103

3.4. Results ……103

3.4.1. Barium hydroxide catalyzed synthesis of different racemic β-nitroalcohols starting from their corresponding aromatic aldehydes and nitroethane ……...103

3.4.2. NMR characterization of nitroethane corresponding racemic β-nitroalcohols ……104

3.4.3. Barium hydroxide catalyzed synthesis of different racemic β-nitroalcohols starting from their corresponding aromatic aldehydes and 1-nitropropane ……..125

3.4.4. NMR characterization of 1-nitropropane corresponding racemic β-nitroalcohols …...125

3.4.5. Screening of *At*HNL mutant libraries towards the promiscuous nitroaldol reaction to synthesize 2-nitro-1-phenyl propanol (2-NPP) ……..142

3.4.6. Optimization of reaction conditions towards the stereoselective synthesis of (*1R,2S*)-2-NPP using *At*HNL-Y14C crude enzyme ……144

3.4.6.1. Buffer and pH optimization ……...144

3.4.6.2. Organic solvent optimization ……145

3.4.6.3. Nitroethane concentration optimization ……145

3.4.6.4. Reaction buffer concentration optimization ……..146

3.4.6.5. Enzyme content optimization ……146

3.4.7. SDS-PAGE of purified *At*HNL mutants selected from screening study ……...147

3.4.8. Substrate scope of *At*HNL-Y14C catalyzed diastereoselective synthesis of *anti* β-nitroalcohols using nitroethane as the co-substrate ……148

3.4.9. Evaluation of *At*HNL double variants in the diastereoselective Henry reaction using aldehydes that were poorly accepted by Y14C ……...150

3.4.10. Screening of *At*HNL mutant libraries towards the stereoselective synthesis of 2-nitro-1-phenyl butanol (2-NPB) via Henry reaction between benzaldehyde and 1-nitropropane …151

3.4.11. Optimization of reaction conditions towards the stereoselective synthesis of (*1R,2S*)-2-NPB using *At*HNL-Y14A ……..153

3.4.11.1. Optimization of reaction time and catalyst amount ……153

3.4.11.2. Optimization of 1-nitropropane concentration ……153

3.4.12. Substrate scope of *At*HNL-Y14A catalyzed diastereoselective synthesis of *anti* β-nitroalcohols using 1-nitropropane as the co-substrate ……...154

3.4.13. Determination of the kinetic parameters of Y14C and Y14A towards the diastereoselective Henry reaction ……..155

3.4.14. pH dependence of Y14C kinetic parameters: probing proton donation role of Cys14 in diastereoselective nitroaldol synthesis ……...156

3.4.15. Comparison of cyanogenesis and retro-nitroaldolase activity of *At*HNL WT, Y14C, and Y14A ……..157

3.4.16. Gram scale synthesis of (*1R,2S*)-2-NPP by using Y14C crude enzyme as the catalyst …158

3.4.17. NMR characterization of (*1R,2S*)-2-NPP synthesized in gram scale using *At*HNL-Y14C crude enzyme ……159

3.4.18. Synthesis of L-norephedrine from (*1R,2S*)-2-NPP ……160

3.4.19. NMR characterization of racemic and (*1R,2S*)-2-amino-1-phenylpropan-1-ol ……..161

3.4.20. Deciphering the reaction mechanism of diastereoselective Henry reaction by selective deuteration at the β-carbon of the nitroaldol product ……..164
3.4.21. Recycling *At*HNL-Y14C for the synthesis of (*1R,2S*)-2-NPP ……167
3.4.22. HPLC conditions and HPLC traces of racemic standard β-nitroalcohols and enantiopure product synthesized by *At*HNL-Y14C mutant enzyme ……..167
3.4.23. HPLC conditions and HPLC traces of racemic standard β-nitroalcohols and enantiopure product synthesized by *At*HNL-Y14A mutant enzyme ……..197
3.4.24. HPLC traces of (*1R,2S*)-2-NPP synthesized in gram scale by using *At*HNL-Y14C crude enzyme ……...218
3.4.25. HPLC traces of racemic and (*1R,2S*)-2-amino 1-phenylpropan-1-ol (2-APP) ……220
3.4.26. HPLC traces of racemic 2-NPP and deuteriated β-nitroalcohol product ……221
3.5. Discussion ……...222
3.5.1. Screening of *At*HNL mutant library towards promiscuous nitroaldol reaction to synthesize 2-NPP ……...222
3.5.2. Optimization of reaction conditions towards *At*HNL-Y14C catalyzed stereoselective synthesis of (*1R,2S*)-2-NPP ……223
3.5.3. *At*HNL-Y14C catalyzed diastereoselective synthesis of *anti* stereoisomers of different β-nitroalcohols using nitroethane as the co-substrate ……223
3.5.4. Gram scale synthesis of (*1R,2S*)-2-NPP by using Y14C crude enzyme as the catalyst …...224
3.5.5. Recycling *At*HNL-Y14C for the synthesis of (*1R,2S*)-2-NPP ……...224
3.6. Conclusions ……224
3.7. References ……...225

Chapter 4: Diastereoselective synthesis of different β-nitroalcohols by using *Bm*HNL as the biocatalyst

4.1. Introduction ……228
4.2. Objectives ……...228
4.3. Materials and methods ……229
4.3.1. Chemicals and materials ……...229
4.3.2. Chromatography ……..229
4.3.3. Cloning ……229
4.3.4. Expression, crude enzyme preparation, and purification of *Bm*HNL and preparation of extracts ……..230

4.3.5. Assessing the effectiveness of purified wild-type *Bm*HNL in the stereoselective synthesis of 2-nitro-1-phenylpropanol (2-NPP), using benzaldehyde as the substrate and nitroethane as the nitroalkane ……...….230
4.3.6. Optimization of biocatalytic parameters for diastereoselective synthesis of 2-NPP ……...230
4.3.6.1 Buffer and pH optimization ……230
4.3.6.2. Organic solvent optimization ……...…….231
4.3.6.3. Nitroethane concentration optimization ……231
4.3.6.4. Citrate phosphate buffer concentration optimization …….……231
4.3.6.5. Enzyme content optimization ……231
4.3.6.6. Determining the tolerable substrate loading ……..232
4.3.7. Biocatalytic diastereoselective Henry reaction in the synthesis of different β-nitroalcohols starting from their corresponding aldehydes using nitroethane as the nucleophile …….…..232
4.3.8. Assessing the effectiveness of purified wild-type *Bm*HNL in the stereoselective synthesis of 2-nitro-1-phenylbutanol (2-NPB), using benzaldehyde and 1-nitropropane ……..232
4.3.9. Optimization of biocatalytic parameters for diastereoselective synthesis of 2-nitro 1-phenyl butanol (2-NPB) …….……232
4.3.9.1. Optimization of reaction time and catalyst amount ……232
4.3.9.2. Optimization of 1-nitropropane concentration ……..232
4.3.10. Biocatalytic diastereoselective Henry reaction in the synthesis of diverse β-nitroalcohols using 1-nitropropane as the nucleophile ……...……233
4.3.11. Determination of kinetics parameters towards the synthesis of (*1S,2R*)-2-NPP ……..233
4.3.12. Evolution of promiscuous nitroaldolase activity over hydrocyanation ……..…….233
4.3.13. Determination of *Bm*HNL's stability in the reaction medium and recycling of the enzyme …….……..233
4.3.14. Gram scale synthesis of (*1S,2R*)-2-NPP by recycling the *Bm*HNL ……..…234
4.3.15. Conversion of *anti* (*1S,2R*)-2-NPP to *syn* (*1S,2S*)-2-NPP by *Bm*HNL ……234
4.3.16. Synthesis of enantiopure *syn* (*1S,2S*)-β-nitroalcohols ……235
4.3.17. Chemical synthesis of racemic β-nitroalcohols ……..235
4.4. Results ……..……235
4.4.1. Barium hydroxide catalyzed synthesis of different racemic β-nitroalcohols starting from their corresponding aromatic aldehydes and nitroethane or 1-nitropropane ……...……235
4.4.2. NMR characterization of nitroethane and 1-nitropropane corresponding racemic β-nitroalcohols ……..……235

4.4.3. *Bm*HNL catalysed promiscuous diastereoselective nitroaldol reaction to synthesize 2-NPP ……...….236
4.4.4. Optimization of reaction conditions of *Bm*HNL catalyzed diastereoselective synthesis of (*1S,2R*)-2-NPP ……...…236
4.4.4.1. Buffer and pH optimization ……...236
4.4.4.2. Organic solvent optimization ……236
4.4.4.3. Nitroethane concentration optimization ……...…….237
4.4.4.4. Citrate phosphate buffer concentration optimization ……237
4.4.4.5. Optimization of *Bm*HNL amount ……..……238
4.4.4.6. Determining the tolerable substrate loading ……..239
4.4.5. SDS-PAGE of purified *Bm*HNL ……...……239
4.4.6. Purified *Bm*HNL catalyzed diastereoselective synthesis of *anti* (*1S,2R*)-stereoisomers of different β-nitroalcohols using nitroethane ……240
4.4.7. Promiscuous nitroaldol reaction to synthesize 2-nitro-1-phenyl butanol (2-NPB) by using 1-nitropropane ……..…….241
4.4.8. Optimization of reaction conditions towards *Bm*HNL catalysed diastereoselective synthesis of (*1S,2R*)-2-NPB ……...242
4.4.8.1. Optimization of reaction time and catalyst amount ……...….242
4.4.8.2. Optimization of 1-nitropropane concentration …….…….242
4.4.9. Purified *Bm*HNL catalyzed diastereoselective synthesis of *anti* (*1S,2R*)-stereoisomers of different β-nitroalcohols using 1-nitropropane ……...……243
4.4.10. Determination of the kinetic parameters of *Bm*HNL in the diastereoselective synthesis of 2-NPP ……244
4.4.11. Comparing *Bm*HNL's hydrocyanation and nitroaldol activity by spectrophotometric cleavage assay ……245
4.4.12. Determination of *Bm*HNL's stability in the reaction medium and recycling of the enzyme ……..…….245
4.4.13. Gram scale synthesis of (*1S,2R*)-2-NPP by recycling the *Bm*HNL enzyme ……....246
4.4.14. *Bm*HNL catalysed conversion of *anti* (*1S,2R*)-2-NPP to *syn* (*1S,2S*)-2-NPP ……..….246
4.4.15. *Bm*HNL catalysed diastereoselective synthesis resulting a mixture of *anti* (*1S,2R*)- and *syn* (*1S,2S*)-β-nitroalcohols …….……...……248
4.4.16. Synthesis of enantiopure *syn* (*1S,2S*)-β-nitroalcohols ……...…….249
4.4.17. HPLC conditions for the chiral resolution of chemically synthesized standard racemic β-nitroalcohols ……...……250

4.4.18. HPLC chromatograms of biocatalytically synthesized (*1S,2R*)-nitrophenyl propanol derivatives starting from different aromatic aldehydes and nitroethane ……251
4.4.19. HPLC chromatograms of (*1S,2R*)-2-NPP synthesized in gram scale by using *Bm*HNL enzyme ……...277
4.4.20. HPLC chromatograms of biocatalytically synthesized 1-nitropropane corresponding β-nitroalcohols starting from different aromatic aldehydes ……...……278
4.4.21. HPLC chromatograms of biocatalytically synthesized *syn* (*1S,2S*)-β-nitroalcohols starting from different aromatic aldehydes and nitroethane via *Bm*HNL catalyzed concomitant Henry and retro-Henry reaction …….297
4.5. Discussion ……...….304
4.5.1. Promiscuous diastereoselective nitroaldol reaction to synthesize (1*S*,2*R*)-2-NPP ……304
4.5.2. Optimization of reaction conditions of *Bm*HNL catalyzed stereoselective synthesis of (*1S,2R*)-2-NPP ……..…….304
4.5.3. *Bm*HNL catalysed stereoselective synthesis of *anti* (*1S,2R*)- stereoisomers of different β-nitroalcohols ……..……305
4.5.4. Gram scale synthesis of (*1S,2R*)-2-NPP by recycling the *Bm*HNL enzyme …..……305
4.6. Conclusions ……...……..306
4.7. References ……...306

LIST OF FIGURES

Chapter 1: Introduction

Figure 1.1: Examples of pharmaceuticals, biologically active molecules, and natural products derived from enantiopure (*S*)- (upper), (*R*)-β-nitroalcohols (middle), and chiral β-nitroalcohol diastereomers (lower dotted box) ……..…….3
Figure 1.2: Different biocatalytic routes for synthesis of chiral β-nitroalcohols …….4

Chapter 2: One-pot enzyme cascade in the synthesis of enantiocomplementary chiral β-nitroalcohols starting from aromatic primary alcohols

Figure 2.1: Representative examples of enantiopure aromatic β-nitroalcohols as chiral intermediates of some pharmaceuticals and biologically active molecules (the reduced forms of β-nitroalcohols are shown in color) ……..26
Figure 2.2.1: ^{1}H NMR and ^{13}C NMR spectra of 2-nitro-1-phenyl ethanol ……....38
Figure 2.2.2.: ^{1}H NMR and ^{13}C NMR spectra of 1-(3-methoxylphenyl)-2-nitroethanol …..…39

Figure 2.2.3: ^{1}H NMR and ^{13}C NMR spectra of 1-(3,5-dimethoxyphenyl)-2-nitroethanol …..40
Figure 2.2.4: ^{1}H and ^{13}C NMR spectra of 1-(2-chlorophenyl)-2-nitroethanol ……..41
Figure 2.2.5: ^{1}H and ^{13}C NMR spectra of 1-(3-chlorophenyl)-2-nitroethanol ……..42
Figure 2.2.6: ^{1}H NMR and ^{13}C NMR spectra of 1-(4-chlorophenyl)-2-nitroethanol ……43
Figure 2.2.7: ^{1}H NMR and ^{13}C NMR spectra of 1-(3,4-dichlorophenyl)-2-nitroethanol ……..44
Figure 2.2.8: ^{1}H NMR and ^{13}C NMR spectra of 1-(3-nitrophenyl)-2-nitroethanol ……...45
Figure 2.2.9: ^{1}H NMR and ^{13}C NMR spectra of 1-(4-nitrophenyl)-2-nitroethanol ……...…46
Figure 2.2.10: ^{1}H NMR and ^{13}C NMR spectra of 1-(4-benzoloxyphenyl)-2-nitroethanol ….....47
Figure 2.3: SDS-PAGE of purified HLADH, *At*HNL, and *Bm*HNL protein. (A) SDS-PAGE analysis of purified HLADH ……49
Figure 2.4: Michaelis–Menten kinetics of HLADH for benzyl alcohol oxidation ……....50
Figure 2.5: Michaelis–Menten kinetics of HLADH using benzyl alcohol oxidation assay shows inhibitory effect by benzaldehyde ……....50
Figure 2.6: Inhibitory effect of benzyl alcohol and benzaldehyde on the specific activity of *At*HNL determined using mandelonitrile cleavage assay ……...……..51
Figure 2.7: Inhibitory effect of benzyl alcohol and benzaldehyde on the specific activity of *Bm*HNL determined using mandelonitrile cleavage assay ……...51
Figure 2.8: Optimization of biocatalytic conditions of the HLADH-*At*HNL cascade: different pH and buffer ……...52
Figure 2.9: Optimization of biocatalytic conditions of the HLADH-*At*HNL cascade: different cofactor recycling agents …….……52
Figure 2.10: Optimization of biocatalytic conditions of the HLADH-*At*HNL cascade: *At*HNL content …….53
Figure 2.11: Optimization of biocatalytic conditions of the HLADH-*At*HNL cascade: NAD^{+} concentration …….……..53
Figure 2.12: Optimization of biocatalytic conditions of the HLADH-*At*HNL cascade: HLADH amount …….54
Figure 2.13: Optimization of biocatalytic conditions of the HLADH-*At*HNL cascade: KPB concentration ……...……54

Figure 2.14: Optimization of biocatalytic conditions of the HLADH-*At*HNL cascade: nitromethane concentration ……..……55

Figure 2.15: Optimization of biocatalytic conditions of the HLADH-*At*HNL cascade: organic solvent content ……...……..56

Figure 2.16: Effect of the % of organic solvent on the HLADH-*At*HNL cascade catalysis …...56

Figure 2.17: Effect of different intermittent addition strategies on the HLADH-*At*HNL cascade catalysis ……..…….57

Figure 2.18: Optimization of biocatalytic conditions of the HLADH-*At*HNL cascade substrate concentration ……...……57

Figure 2.19: Optimization of biocatalytic conditions of the HLADH-*At*HNL cascade substrate concentration …….……..58

Figure 2.20: Effect of addition of extra 800 U of *At*HNL on the biocatalytic cascade after 4 h …...58

Figure 2.21: Effect of different acetaldehyde concentrations on the HLADH-*At*HNL cascade catalysis ……..…….59

Figure 2.22: Reaction progression curve of HLADH-*At*HNL cascade …….59

Figure 2.23: Effect of different sorbitol concentrations on the HLADH-*At*HNL cascade catalysis ……...…60

Figure 2.24: Summary of all the parameters optimized for HLADH-*At*HNL cascade to achieve maximum % conversion and % *ee* of (*R*)-NPE …….……60

Figure 2.25: Optimization of *Bm*HNL content in the synthesis of (*S*)-NPE from benzaldehyde ….62

Figure 2.26: Effect of different buffers and their pH in the *Bm*HNL catalyzed synthesis of (*S*)-NPE …….…….63

Figure 2.27: Effect of different organic solvents in the *Bm*HNL catalyzed synthesis of (*S*)-NPE ...63

Figure 2.28: Effect of different additives in the *Bm*HNL catalyzed synthesis of (*S*)-NPE ……64

Figure 2.29: Study of different aromatic aldehydes in the *Bm*HNL catalyzed synthesis of the corresponding (*S*)-nitroaldol products …….64

Figure 2.30: Optimization of *Bm*HNL content in the synthesis of the corresponding (*S*)-nitroaldol from 3,5-dimethoxy benzaldehyde …….……65

Figure 2.31: Summary of optimization of biocatalytic parameters of *Bm*HNL catalyzed nitroaldol reaction ……65

Figure 2.32: Study of the amount of HLADH in HLADH-*Bm*HNL cascade in the synthesis of (*S*)-NPE ……66
Figure 2.33: HPLC chromatograms of 2-nitro-1-phenylethanol ……..69
Figure 2.34: HPLC chromatograms of 1-(3-methoxyphenyl)-2-nitroethanol ……..……71
Figure 2.35: HPLC chromatograms of 1-(3, 5-dimethoxyphenyl)-2-nitroethanol ……...73
Figure 2.36: HPLC chromatograms of 1-(2-chlorophenyl)-2-nitroethanol ……..75
Figure 2.37: HPLC chromatograms of 1-(3-chlorophenyl)-2-nitroethanol ……77
Figure 2.38: HPLC chromatograms of 1-(4-chlorophenyl)-2-nitroethanol ……79
Figure 2.39: HPLC chromatograms of 1-(3, 4-dichlorophenyl)-2-nitroethanol ……...…81
Figure 2.40: HPLC chromatograms of 1-(3-nitrophenyl)-2-nitroethanol ……83
Figure 2.41: HPLC chromatograms of 1-(4-nitrophenyl)-2-nitroethanol ……85
Figure 2.42: HPLC chromatograms of 1-(4-benzyloxyphenyl)-2-nitroethanol ……87

Chapter 3: Engineered *At*HNL variants catalyzed diastereoselective synthesis of β-nitroalcohols with broad substrate scope and high enantioselectivity

Figure 3.1: Different pharmaceutical molecules with chiral β-amino alcohol moiety that can be derived from corresponding β-nitro alcohols with two chiral centers ……...…95
Figure 3.2: ^{1}H NMR and ^{13}C NMR spectra of 2-nitro-1-phenylpropan-1-ol ……..106
Figure 3.3: ^{1}H NMR and ^{13}C NMR spectra of 1-(3-chlorophenyl)-2-nitropropan-1-ol ……..107
Figure 3.4: ^{1}H NMR and ^{13}C NMR spectra of 1-(3-methoxyphenyl)-2-nitropropan-1-ol …..108
Figure 3.5: ^{1}H NMR and ^{13}C NMR spectra of 1-(3-methylphenyl)-2-nitropropan-1-ol ….....109
Figure 3.6: ^{1}H NMR and ^{13}C NMR spectra of 1-(4-chlorophenyl)-2-nitropropan-1-ol …….110
Figure 3.7: ^{1}H NMR and ^{13}C NMR spectra of 1-(2,5-dimethoxyphenyl)-2-nitropropan-1-ol …...111
Figure 3.8: ^{1}H NMR and ^{13}C NMR spectra of 1-(2-methylphenyl)-2-nitropropan-1-ol ...…..112
Figure 3.9: ^{1}H NMR and ^{13}C NMR spectra of 1-(naphthalen-5-yl)-2-nitropropan-1-ol …….113
Figure 3.10: ^{1}H NMR and ^{13}C NMR spectra of 4-nitro-1-phenylpentan-3-ol ……114
Figure 3.11: ^{1}H NMR and ^{13}C NMR spectra of 1-(4-methylphenyl)-2-nitropropan-1-ol ….....115

Figure 3.12: ^{1}H NMR and ^{13}C NMR spectra of 1-(2-chlorophenyl)-2-nitropropan-1-ol …....116

Figure 3.13: ^{1}H NMR and ^{13}C NMR spectra of 1-(2-methoxyphenyl)-2-nitropropan-1-ol ……..118

Figure 3.14: ^{1}H NMR and ^{13}C NMR spectra of 1-(4-nitrophenyl)-2-nitropropan-1-ol …..…118

Figure 3.15: ^{1}H NMR and ^{13}C NMR spectra of 1-(3-bromophenyl)-2-nitropropan-1-ol …....119

Figure 3.16: ^{1}H NMR and ^{13}C NMR spectra of 1-(2-bromophenyl)-2-nitropropan-1-ol …..120

Figure 3.17: ^{1}H NMR and ^{13}C NMR spectra of 1-(2,3-dichlorophenyl)-2-nitropropan-1-ol …....121

Figure 3.18: ^{1}H NMR and ^{13}C NMR spectra of 1-(2,3-dimethoxyphenyl)-2-nitropropan-1-ol …123

Figure 3.19: ^{1}H NMR and ^{13}C NMR spectra of 1-(2-nitrophenyl)-2-nitropropan-1-ol ……...124

Figure 3.20: ^{1}H NMR and ^{13}C NMR spectra of 1-(3-(benzyloxy)phenyl)-2-nitropropan-1-ol …..125

Figure 3.21: ^{1}H NMR and ^{13}C NMR spectra of 2-nitro-1-phenylbutan-1-ol ……...……127

Figure 3.22: ^{1}H NMR and ^{13}C NMR spectra of 1-(3-bromophenyl)-2-nitrobutan-1-ol ……..128

Figure 3.23: ^{1}H NMR and ^{13}C NMR spectra of 1-(2-bromophenyl)-2-nitrobutan-1-ol ……..130

Figure 3.24: ^{1}H NMR and ^{13}C NMR spectra of 1-(2,3-dichlorophenyl)-2-nitrobutan-1-ol 131

Figure 3.25: ^{1}H NMR and ^{13}C NMR spectra of 1-(2-nitrophenyl)-2-nitrobutan-1-ol ……..…132

Figure 3.26: ^{1}H NMR and ^{13}C NMR spectra of 1-(furan-2-yl)-2-nitrobutan-1-ol ……...…133

Figure 3.27: ^{1}H NMR and ^{13}C NMR spectra of 1-(2-methoxyphenyl)-2-nitrobutan-1-ol …...135

Figure 3.28: ^{1}H NMR and ^{13}C NMR spectra of 1-(3-methylphenyl)-2-nitrobutan-1-ol …….136

Figure 3.29: ^{1}H NMR and ^{13}C NMR spectra of 1-(3-chlorophenyl)-2-nitrobutan-1-ol ……..137

Figure 3.30: ^{1}H NMR and ^{13}C NMR spectra of 1-(3-methoxyphenyl)-2-nitrobutan-1-ol …...138

Figure 3.31: ^{1}H NMR and ^{13}C NMR spectra of 1-(4-methylphenyl)-2-nitrobutan-1-ol …….139

Figure 3.32: ^{1}H NMR and ^{13}C NMR spectra of 1-(4-chlorophenyl)-2-nitrobutan-1-ol ……..140

Figure 3.33: ^{1}H NMR and ^{13}C NMR spectra of 4-nitro-1-phenylhexan-3-ol ……..142

Figure 3.34: ^{1}H NMR and ^{13}C NMR spectra of 1-(4-nitrophenyl)-2-nitrobutan-1-ol ……....143

Figure 3.35: Summary of screening of F179L and *At*HNL-Y14 series towards the diastereoselective synthesis of 2-NPP ……144

Figure 3.36: Effect of different pH and buffer in *At*HNL-Y14C catalyzed diastereoselective synthesis of 2-NPP ……146

Figure 3.37: Effect of different organic solvents in a biphasic medium in *At*HNL-Y14C catalyzed diastereoselective synthesis of 2-NPP ……146

Figure 3.38: Optimization of *At*HNL-Y14C catalyzed diastereoselective synthesis of 2-NPP by varying nitroethane concentration ……..147

Figure 3.39: Optimization of *At*HNL-Y14C catalyzed diastereoselective synthesis of 2-NPP by varying CPB concentration ……147

Figure 3.40: Effect of amount of enzyme on *At*HNL-Y14C catalyzed diastereoselective synthesis of 2-NPP ……148

Figure 3.41: Summary of optimization of biocatalytic parameters of Y14C catalysed diastereoselective nitroaldol reaction using benzaldehyde and nitroethane as the substrate in synthesizing (*1R,2S*)-2-NPP ……..148

Figure 3.42: SDS-PAGE of purified *At*HNL variant proteins ……149

Figure 3.43: Y14C catalyzed stereoselective synthesis of (*1R,2S*) isomers of different β-nitroalcohols from their corresponding aldehydes and nitroethane ……150

Figure 3.44: *At*HNL-Y14C-F179L catalysed stereoselective synthesis of (*1R,2S*) isomers of different β-nitroalcohols from their corresponding aldehydes and nitroethane ……..152

Figure 3.45: Purified *At*HNL mutants screening towards the diastereoselective synthesis of 2-NPB ……...153

Figure 3.46: Optimization of biocatalytic conditions for the *At*HNL-Y14A: enzyme content and reaction time ……154

Figure 3.47: Optimization of biocatalytic conditions for the *At*HNL-Y14A: 1-nitropropane concentration ……155

Figure 3.48: Summary of optimization of biocatalytic parameters of Y14A catalyzed nitroaldol reaction using benzaldehyde and 1-nitropropane as the substrate in synthesizing (*1R,2S*)-2-NPB ……...155

Figure 3.49: Stereoselective synthesis of (*1R,2S*) isomers of different β-nitroalcohols from their corresponding aldehyde substrates and 1-nitropropane by Y14A mutein ……..156

Figure 3.50: Michaelis-Menten plots of *At*HNL A. Y14C, B. WT and C. Y14A towards diastereoselective synthesis of β-nitroalcohol ……157

Figure 3.51: Michaelis-Menten plots of *At*HNL A. Y14C and B. WT at pH 8.2 towards diastereoselective synthesis of β-nitroalcohol ……....158

Figure 3.52: Comparison of cyanogenesis and retro-nitroaldolase activity of WT *At*HNL, Y14C, Y14A by spectrophotometric cleavage assay ……..159

Figure 3.53: Reaction setup for the gram scale synthesis of (*1R,2S*)-2-NPP using Y14C crude enzyme ……...160

Figure 3.54: ^{1}H NMR and ^{13}C NMR spectra of (*1R,2S*)-2-nitro-1-phenylpropan-1-ol synthesized using *At*HNL-Y14C ……161

Figure 3.55: Reaction setup for the gram scale synthesis of (*1R,2S*)-2-amino phenyl propanol (2-APP) ……..…….162

Figure 3.56: ^{1}H NMR and ^{13}C NMR spectra of racemic 2-amino-1-phenylpropan-1-ol ……163

Figure 3.57: ^{1}H NMR and ^{13}C NMR spectra of (*1R,2S*)-2-amino-1-phenylpropan-1-ol ……165

Figure 3.58: Deuterium exchange at the C_1 of nitroethane at different time points ……167

Figure 3.59: Deuterium exchange at the β-carbon of 2-NPP ……...168

Figure 3.60: Reusability of *At*HNL-Y14C to synthesize (*1R,2S*)-2-NPP ……...……168

Figure 3.61: HPLC chromatograms of 2-nitro-1-phenylpropan-1-ol ……170

Figure 3.62: HPLC chromatograms of 1-(3-chlorophenyl)-2-nitropropan-1-ol …….…….....171

Figure 3.63: HPLC chromatograms of 1-(3-methoxyphenyl)-2-nitropropan-1-ol ……173

Figure 3.64: HPLC chromatograms of 1-(3-methylphenyl)-2-nitropropanol ……175

Figure 3.65: HPLC chromatograms of 1-(4-chlorophenyl)-2-nitropropan-1-ol …….……176

Figure 3.66: HPLC chromatograms of 1-(2,5-Dimethoxyphenyl)-2-nitropropan-1-ol ……178

Figure 3.67: HPLC chromatograms of 1-(2-methylphenyl)-2-nitropropan-1-ol ……179

Figure 3.68: HPLC chromatograms of 1-(naphthalen-1-yl)-2-nitropropan-1-ol ……181

Figure 3.69: HPLC chromatograms of 4-nitro-1-phenylpentan-3-ol ……182

Figure 3.70: HPLC chromatograms of 1-(4-methylphenyl)-2-nitropropanol ……184

Figure 3.71: HPLC chromatograms of 1-(2-chlorophenyl)-2-nitropropan-1-ol …….……185

Figure 3.72: HPLC chromatograms of 1-(2-methoxyphenyl)-2-nitropropan-1-ol ……187

Figure 3.73: HPLC chromatograms of 1-(4-nitrophenyl)-2-nitropropan-1-ol ……189

Figure 3.74: HPLC chromatograms of 1-(3-bromophenyl)-2-nitropropan-1-ol …….191

Figure 3.75: HPLC chromatograms of 1-(2-bromophenyl)-2-nitropropan-1-ol ……..…192

Figure 3.76: HPLC chromatograms of 1-(2,3-dichlorophenyl)-2-nitropropan-1-ol ……...194

Figure 3.77: HPLC chromatograms of 1-(2,3-dimethoxyphenyl)-2-nitropropan-1-ol ……...195

Figure 3.78: HPLC chromatograms of 1-(2-nitrophenyl)-2-nitropropanol ……...…….197

Figure 3.79: HPLC chromatograms of 1-(3-(benzyloxy)phenyl)-2-nitropropan-1-ol ……198

Figure 3.80: HPLC chromatograms of 2-nitro 1-phenyl butanol ……..….199

Figure 3.81: HPLC chromatograms of 1-(3-bromophenyl)-2-nitrobutan-1-ol ……...201

Figure 3.82: HPLC chromatograms of 1-(2-bromophenyl)-2-nitro butanol ……...……203

Figure 3.83: HPLC chromatograms of 1-(2,3-dichlorophenyl)-2-nitrobutan-1-ol …….204

Figure 3.84: HPLC chromatograms of 1-(2-nitrophenyl)-2-nitrobutan-1-ol …….….206

Figure 3.85: HPLC chromatograms of 2-nitro 1-fural butanol ……...……207

Figure 3.86: HPLC chromatograms of 1-(2-methoxyphenyl)-2-nitrobutan-1-ol …….…..209

Figure 3.87: HPLC chromatograms of 1-(3-methylphenyl)-2-nitrobutan-1-ol ……..210

Figure 3.88: HPLC chromatograms of 1-(3-chlorophenyl)-2-nitrobutan-1-ol ……...……211

Figure 3.89: HPLC chromatograms of 1-(3-methoxyphenyl)-2-nitrobutan-1-ol ……..….213

Figure 3.90: HPLC chromatograms of 1-(4-methylphenyl)-2-nitrobutan-1-ol ……..214

Figure 3.91: HPLC chromatograms of 1-(4-chlorophenyl)-2-nitrobutan-1-ol ……...216

Figure 3.92: HPLC chromatograms of 1-(4-nitrophenyl)-2-nitrobutanol ……..219

Figure 3.93: HPLC chromatograms of biocatalytically synthesized (*1R,2S*)-2-nitro-1-phenyl propanol ……...……..221

Figure 3.94: HPLC chromatograms of 1-(2-aminophenyl)-2-nitropropanol ……..222

Figure 3.95: HPLC chromatograms of racemic 2-NPP and deuteriated β-nitroalcohol product …223

Chapter 4: Diastereoselective synthesis of different β-nitroalcohols by using *Bm*HNL as the biocatalyst

Figure 4.1: Reaction setup for the gram-scale synthesis of (*1S,2R*)-2-NPP using *Bm*HNL …..…234

Figure 4.2: Effect of different pH and buffer on *Bm*HNL catalysed diastereoselective Henry reaction in the synthesis of 2-NPP ……..236

Figure 4.3: Effect of different organic solvents on *Bm*HNL catalysed diastereoselective Henry reaction in the synthesis of 2-NPP ……..……237

Figure 4.4: Effect of different nitroethane concentration on *Bm*HNL catalysed diastereoselective Henry reaction in the synthesis of 2-NPP ……..……237

Figure 4.5: Effect of CPB concentration on *Bm*HNL catalysed diastereoselective Henry reaction in the synthesis of 2-NPP ……..238

Figure 4.6: Effect of enzyme content on *Bm*HNL catalysed diastereoselective Henry reaction in the synthesis of 2-NPP ……....238

Figure 4.7: Summary of optimization of biocatalytic parameters of *Bm*HNL catalyzed nitroaldol reaction in synthesis of (*1S,2R*)-2-NPP using benzaldehyde and nitroethane ……..…..238

Figure 4.8: Determining the tolerable substrate concentration towards the *Bm*HNL catalyzed diastereoselective synthesis of 2-NPP ……....239

Figure 4.9: SDS-PAGE analysis of purified *Bm*HNL …….……239

Figure 4.10: Stereoselective synthesis of *anti* (*1S,2R*)- stereoisomers of different β-nitroalcohols from their corresponding aldehydes and nitroethane by *Bm*HNL ……...…..241

Figure 4.11: Effect of enzyme content and reaction time on *Bm*HNL catalysed diastereoselective Henry reaction in the synthesis of 2-NPB …….……242

Figure 4.12: Effect of 1-nitropropane concentration on *Bm*HNL catalysed diastereoselective Henry reaction in the synthesis of 2-NPB …….……..242

Figure 4.13: Summary of optimization of biocatalytic parameters of *Bm*HNL catalyzed nitroaldol reaction in the synthesis of (*1R,2S*)-2-NPB using benzaldehyde and 1-nitropropane ……...243

Figure 4.14: Stereoselective synthesis of *anti* (*1S,2R*)- stereoisomers of different β-nitroalcohols from their corresponding aldehydes and 1-nitropropane by *Bm*HNL …..……244

Figure 4.15: Michaelis-Menten plots of *Bm*HNL catalysed diastereoselective synthesis of (*1S,2R*)-2-NPP ……..…….244

Figure 4.16. Comparing *Bm*HNL's hydrocyanation and nitroaldolase activity by spectrophotometric cleavage assay ……..……..245

Figure 4.17: Determining *Bm*HNL's stability and recyclability in the reaction medium. (A): percentage of remaining specific activity of *Bm*HNL at different time points ……...….246

Figure 4.18: Conversion of (*1S,2R*)-2-NPP in to (*1S,2S*)-2-NPP with increase of time …..…247

Figure 4.19: *Bm*HNL catalyzed cleavage of (*1S,2R*) 2-NPP in (A) absence and (B) presence of nitroethane ……...……..248

Figure 4.20: ^{1}H NMR chromatograms showing transformation of (*1S,2R*)-2-NPP to (*1S,2S*)-2-NPP over the time ……...……248

Figure 4.21: Synthesis of different (*1S,2S*)-β-nitroalcohols from corresponding achiral aromatic aldehydes ……250

Figure 4.22: ^{1}H NMR depicting the formation of (*1S,2S*)-2-NPP ……...250

Figure 4.23: HPLC chromatograms of 2-nitro 1-phenylpropan-1-ol ……..……252

Figure 4.24: HPLC chromatograms of 1-(3-chlorophenyl)-2-nitropropan-1-ol ……..…253

Figure 4.25: HPLC chromatograms of 1-(2-chlorophenyl)-2-nitropropan-1-ol …….254

Figure 4.26: HPLC chromatograms of 1-(3-methoxyphenyl)-2-nitropropan-1-ol ……....255

Figure 4.27: HPLC chromatograms of 1-(3-methylphenyl)-2-nitropropan-1-ol ……...….257

Figure 4.28: HPLC chromatograms of 1-(4-methylphenyl)-2-nitropropan-1-ol ……258

Figure 4.29: HPLC chromatograms of 1-(4-nitrophenyl)-2-nitropropan-1-ol ……261

Figure 4.30: HPLC chromatograms of 1-(2,5-dimethoxyphenyl)-2-nitropropan-1-ol ……...262

Figure 4.31: HPLC chromatograms of 1-(4-chlorophenyl)-2-nitropropan-1-ol …….263

Figure 4.32: HPLC chromatograms of 4 nitro-1-phenylpentan-3-ol ……..265

Figure 4.33: HPLC chromatograms of 1-(3-benzyloxyphenyl)-2-nitropropan-1-ol ……..…266

Figure 4.34: HPLC chromatograms of 1-(2-methylphenyl)-2-nitropropan-1-ol ……268

Figure 4.35: HPLC chromatograms of 1-(2-methoxyphenyl)-2-nitropropan-1-ol ……..…269

Figure 4.36: HPLC chromatograms of 1-napthal-2-nitropropan-1-ol ……270

Figure 4.37: HPLC chromatograms of 1-(3-bromophenyl)-2-nitropropan-1-ol …….272

Figure 4.38: HPLC chromatograms of 1-(2-bromophenyl)-2-nitropropan-1-ol ……..……273

Figure 4.39: HPLC chromatograms of 1-(2,3-dichlorophenyl)-2-nitropropan-1-ol ……...275

Figure 4.40: HPLC chromatograms of 1-(2,3-dimethoxyphenyl)-2-nitropropan-1-ol ……..276

Figure 4.41: HPLC chromatograms of 1-(2-nitrophenyl)-2-nitropropan-1-ol ……..277

Figure 4.42: HPLC chromatograms of biocatalyticatally synthesized (*1S,2R*)-2-nitro-1-phenylpropan-1-ol …….278

Figure 4.43: HPLC chromatograms of 2-nitro 1-phenylbutan-1-ol ……..…..280

Figure 4.44: HPLC chromatograms of 1-(2-metoxyphenyl)-2-nitrobutan-1-ol …….....281

Figure 4.45: HPLC chromatograms of 1-(4-chlorophenyl)-2-nitrobutan-1-ol ……...282

Figure 4.46: HPLC chromatograms of 1-(4-methylphenyl)-2-nitrobutan-1-ol ……..283

Figure 4.47: HPLC chromatograms of 1-(3-chlorophenyl)-2-nitrobutan-1-ol ……...285

Figure 4.48: HPLC chromatograms of 1-(3-methoxyphenyl)-2-nitrobutan-1-ol ……...286

Figure 4.49: HPLC chromatograms of 1-(3-methylphenyl)-2-nitrobutan-1-ol ……..……287

Figure 4.50: HPLC chromatograms of 2-nitro 1-furalbutan-1-ol ……..…..289

Figure 4.51: HPLC chromatograms of 1-(3-bromophenyl)-2-nitrobutan-1-ol ……...290

Figure 4.52: HPLC chromatograms of 1-(2-bromophenyl)-2-nitrobutan-1-ol ……...291

Figure 4.53: HPLC chromatograms of 1-(2,3-dichlorophenyl)-2-nitrobutan-1-ol ……..…293

Figure 4.54: HPLC chromatograms of 1-(2-nitrophenyl)-2-nitrobutan-1-ol ……..294

Figure 4.55: HPLC chromatograms of 1-(4-nitrophenyl)-2-nitrobutan-1-ol ……..297

Figure 4.56: HPLC chromatograms of 2-nitro 1-phenyl propan-1-ol …….298

Figure 4.57: HPLC chromatograms of 1-(3-methoxyphenyl)-2-nitropropan-1-ol ……299

Figure 4.58: HPLC chromatograms of 1-(2-methylphenyl)-2-nitropropan-1-ol ……300

Figure 4.59: HPLC chromatograms of 1-(3-methylphenyl)-2-nitropropan-1-ol ……301

Figure 4.60: HPLC chromatograms of 1-(4-methylphenyl)-2-nitropropan-1-ol ……303

Figure 4.61: HPLC chromatograms of 1-(2-methoxyphenyl)-2-nitropropan-1-ol ……304

LIST OF SCHEMES

Chapter 1: Introduction

Scheme 1.1: CALB catalyzed KR of a racemic β-nitro alcohol with ketal functionality to enable chemo-enzymatic synthesis of aminocyclitol ……4

Scheme 1.2: Lipase PS catalyzed KR of aromatic β-nitroalcohols ……....5

Scheme 1.3: *Pseudomonas flourescens* lipase catalyzed KR in the synthesis of β-nitroalcohol diastereomers ……....5

Scheme 1.4: Lipase catalyzed KR of racemic 2-nitrocyclohexanol and 2-nitrocyclohexyl acetate via transesterification and hydrolysis in the synthesis of β-nitroalcohol diastereomers ……....6

Scheme 1.5: Two-step process of DKR using calcium alginate beads catalyzed racemic β-nitroalcohol synthesis followed by lipase PS catalyzed KR ……...7

Scheme 1.6: *Burkholderia cepacia* catalyzed double parallel dynamic resolution in the enantioselective synthesis of β-nitroalcohol esters ……..……7

Scheme 1.7: One-pot DKR based chemo-enzymatic cascade using *Candida antarctica* lipase A in the synthesis of (*S*)-β-nitroalcohol esters ……8

Scheme 1.8: One-pot DKR with repeated interconversion and lipase based KR ……....8

Scheme 1.9: catabolism of cyanogen glycoside to carbonyl compound and HCN ……..…..9

Scheme 1.10: Enantioselective nitroaldol catalyzed by *Gt*HNL and *Ac*HNL muteins ……..10

Scheme 1.11: Enantioselective nitroaldol catalyzed by acyl peptide releasing enzyme from *Sulfolobus tokodaii* (ST0799) ……..…11

Scheme 1.12: *Hb*HNL catalyzed diastereoselective Henry reaction ……12

Scheme 1.13: *Gt*HNL and *Ac*HNL muteins catalyzed diastereoselective Henry reaction ……12

Scheme 1.14: Retro-Henry reaction by *Hb*HNL and *At*HNL produces (*R*)- and (*S*)-NPE respectively, while Henry reaction by them is shown in grey ……...12

Scheme 1.15: *At*HNL catalyzed synthesis of (*S*)-β-nitroalcohols by retro-Henry approach ……...14

Scheme 1.16: Baker's yeast catalyzed asymmetric reduction of an α-nitro ketone ……..….14
Scheme 1.17: Alcohol dehydrogenase catalyzed asymmetric reduction of α-nitro ketones ……15
Scheme 1.18: *Candida parapsilosis* ATCC7330 catalyzed asymmetric reduction of aliphatic α-nitro ketones ……15
Scheme 1.19: Alcohol dehydrogenase catalyzed reduction of prochiral α-nitro ketones …..…16
Scheme 1.20: KREDs catalyzed reduction of α-nitro ketones ……..17
Scheme 1.21: Halohydrin dehalogenase catalyzed regio and enantioselective ring opening of epoxide by nitrite in the synthesis of chiral β-nitroalcohols …….….18
Scheme 1.22: Halohydrin dehalogenase catalyzed ring opening by nitrite in the synthesis of β-nitroalcohol diastereomer ……....18

Chapter 2: One-pot enzyme cascade in the synthesis of enantiocomplementary chiral β-nitroalcohols starting from aromatic primary alcohols

Scheme 2.1: Chemical (top left), biocatalytic (right), and current method (bottom left) of syntheses of enantiopure β-nitroalcohols ……....26
Scheme 2.2. HLADH-*At*HNL cascade catalyzed stereoselective conversion of benzylic alcohols to (*R*)-β-nitroalcohols ……62
Scheme 2.3: HLADH-*Bm*HNL cascade catalyzed stereoselective conversion of benzylic alcohols to (*S*)-β-nitroalcohols ……67

Chapter 3: Engineered *At*HNL variants catalyzed diastereoselective synthesis of β-nitroalcohols with broad substrate scope and high enantioselectivity

Scheme 3.1. Chemical synthesis of racemic β-nitroalcohols using nitroethane as a nucleophile ..105
Scheme 3.2. Chemical synthesis of racemic β-nitroalcohols using 1-nitropropane as a nucleophile …….……127
Scheme 3.3: Chemo-enzymatic synthesis of L-norephedrine starting from benzaldehyde ……..163
Scheme 3.4: *At*HNL-Y14C catalyzed diastereoselective synthesis deuterated 2-NPP …..….168

Chapter 4: Diastereoselective synthesis of different β-nitroalcohols by using *Bm*HNL as the biocatalyst

Scheme 4.1: *Bm*HNL catalyzed synthesis of both diastereomers, (*1S,2R*)- and (*1S,2S*)-β-nitroalcohols ……..250

LIST OF TABLES

Chapter 1: Introduction

Table 1.1: Modern HNLs and their ancestral enzymes in the stereoselective Henry reaction in the synthesis of chiral NPE ……..….11

Table 1.2: HNLs including their ancestral enzymes in the stereoselective cleavage of NPE …13

Chapter 2: One-pot enzyme cascade in the synthesis of enantiocomplementary chiral β-nitroalcohols starting from aromatic primary alcohols

Table 2.1: Details of intermittent addition of HLADH and benzyl alcohol in the cascade ……..32

Table 2.2: Reaction conditions used for this substrate concentration optimization study ……...33

Table 2.3: HPLC conditions for chiral resolution of racemic β-nitroalcohols ……...…48

Table 2.4: HLADH-*At*HNL cascade catalyzed synthesis of enantioenriched (*R*)-β-nitroalcohols from corresponding primary alcohols ……..…62

Table 2.5: HLADH-*Bm*HNL cascade catalyzed synthesis of (*S*)-β-nitroalcohols from corresponding primary alcohols ……...67

Chapter 3: Engineered *At*HNL variants catalyzed diastereoselective synthesis of β-nitroalcohols with broad substrate scope and high enantioselectivity

Table 3.1: List of primers employed in the above work. Italicized nucleotides are the site of mutation ……...98

Table 3.2: List of racemic β-nitroalcohols synthesized using nitroethane as nucleophile …...105

Table 3.3: List of racemic β-nitroalcohols synthesized using 1-nitropropane as nucleophile …...127

Table 3.4: Screening of Y14C and F179L *At*HNL library for the diastereoselective synthesis of 2-NPP ……..……145

Table 3.5: Screening of Y14C and F179L *At*HNL libraries towards the diastereoselective synthesis of 2-NPB ……154

Chapter 4: Diastereoselective synthesis of different β-nitroalcohols by using *Bm*HNL as the biocatalyst

Table 4.1: *Bm*HNL catalyzed synthesis of both diastereomers, *anti* (*1S,2R*)- and *syn* (*1S,2S*)-β-nitroalcohols …….…….250

Chapter 1

Introduction

1.1. Chiral β-nitroalcohols and their importance

Chiral β-nitroalcohols are key building blocks that find application in the synthesis of pharmaceuticals and bioactive molecules.[1] The distinct structural features of optically pure β-nitroalcohols having two versatile, functional groups, a nitro and a hydroxyl, attached to the vicinal carbon centers of which either one or both are asymmetric, makes them attractive synthetic analogs to manufacture a diverse range of functionally rich fine chemicals, by further transformation.[2] Chiral vicinal amino alcohols that are key building blocks of several β-blockers and pharmaceutical intermediates, are synthesized by a simple reduction of the nitro group of corresponding chiral β-nitroalcohols.[3] The nitro group of a β-nitroalcohol can be converted to a carbonyl using Nef reaction to produce α-hydroxy carbonyl.[4] It can also undergo denitration for the synthesis of secondary alcohol intermediate.[5] Similarly, the hydroxyl group can be subjected to elimination, Ritter reaction, oxidation, acetylation, etc. Simple elimination in case of a β-nitroalcohol produces nitro alkene.[6] In Ritter reaction, the hydroxyl group reacts with a nitrile under acidic conditions and converts it into corresponding *N*-(β-nitro)amide.[7] A few examples of different drug molecules and natural products which can be synthesized from (*S*)-β-nitroalcohols are chelonin A[8] (antimicrobial), and (*S*)-tembamide[9] (anti-HIV), (*S*)-toliprolol, (*S*)-moprolol[10], and (*S*)-propranolol[11], (*S*)-norphenylephrine[12] (β-adrenergic receptor blocking agents), (*S*)-sotalol[13] (antiarrhythmic agents), and (*S*)-miconazole[14] (antifungal) (**Figure 1.1**, upper). Similarly (*R*)-β-nitroalcohols can be used as precursors of several bioactive molecules. Some typical examples include important drug intermediates such as (*R*)-tembamide[15] a natural product with hypoglycemic activity, (*R*)-isoproterenol[16] a β_1-adrenergic receptor agonist, (*R*)-salmeterol[17] and (*R*)-nifenalol[18] both are β_2-adrenoreceptor agonist, and (*R*)-denopamine[19] a β_1-adrenoreceptor agonist (**Figure 1.1**, middle). Representative examples of natural products, biologically active molecules, and pharmaceuticals carrying β-nitroalcohol diastereomers as structural components are spisulosine[20], sphingosine[21], (*R*,*S*)-ephedrine, (*R*,*S*)-metaraminol[22], (*R*,*S*)-methoxamine[23], (*R*,*R*)-chloramphenicol[24], and AZD-5423[25] (shown with stereochemistry in **Figure 1.1**).

1.2. Asymmetric synthesis of β-nitroalcohols

The catalysts used in various synthetic approaches available for the synthesis of enantiopure β-nitroalcohols can be broadly classified into the following two types, a) chemical catalysts and b) biocatalysts such as enzymes.

1.2.1. Asymmetric synthesis of β-nitroalcohols by chemical catalysts

Chemists have developed several proven methods for synthesizing chiral β-nitroalcohols using chemical catalysts. Among them the Henry reaction stands out as a major one. The versatility and efficacy of the reaction makes it an attractive choice for chemists seeking to produce different important building blocks. By utilizing inexpensive and readily available inorganic bases such as potassium carbonate[26], imidazole[27] and NaOH in the presence of a cationic surfactant such as cetyltrimethylammonium chloride (CTACl) [28] chemists can achieve

impressive results across a range of substrates with varying backbone structures. Different copper based catalysts such as chiral Cu^{I}–[H_4]salen catalyst[29], copper-aminopyridine catalysts [30], chiral copper complex[31], chiral tetrahydrosalen-Cu(I) complex [32], and chiral diamine–Cu^{I} complex [33] are also found to be useful in this stereoselective transformation. A few representative organocatalysts, such as guanidine-thiourea bifunctional organocatalysts [34], thiazoline tridentate ligands [35], C1-symmetric dinitrogen ligand [36], chiral thioureas, guanidines, cinchona alkaloids derivatives, phase transfer organocatalysts and La-Li-BINOL Complex [37-39] have also proven effective in promoting direct stereoselective nitroaldol reactions with high yields and enantiomeric excess. With these powerful tools at their disposal, chemists continue to explore and unlock the full potential of asymmetric Henry reaction in the production of chiral β-nitroalcohols and their derivatives.

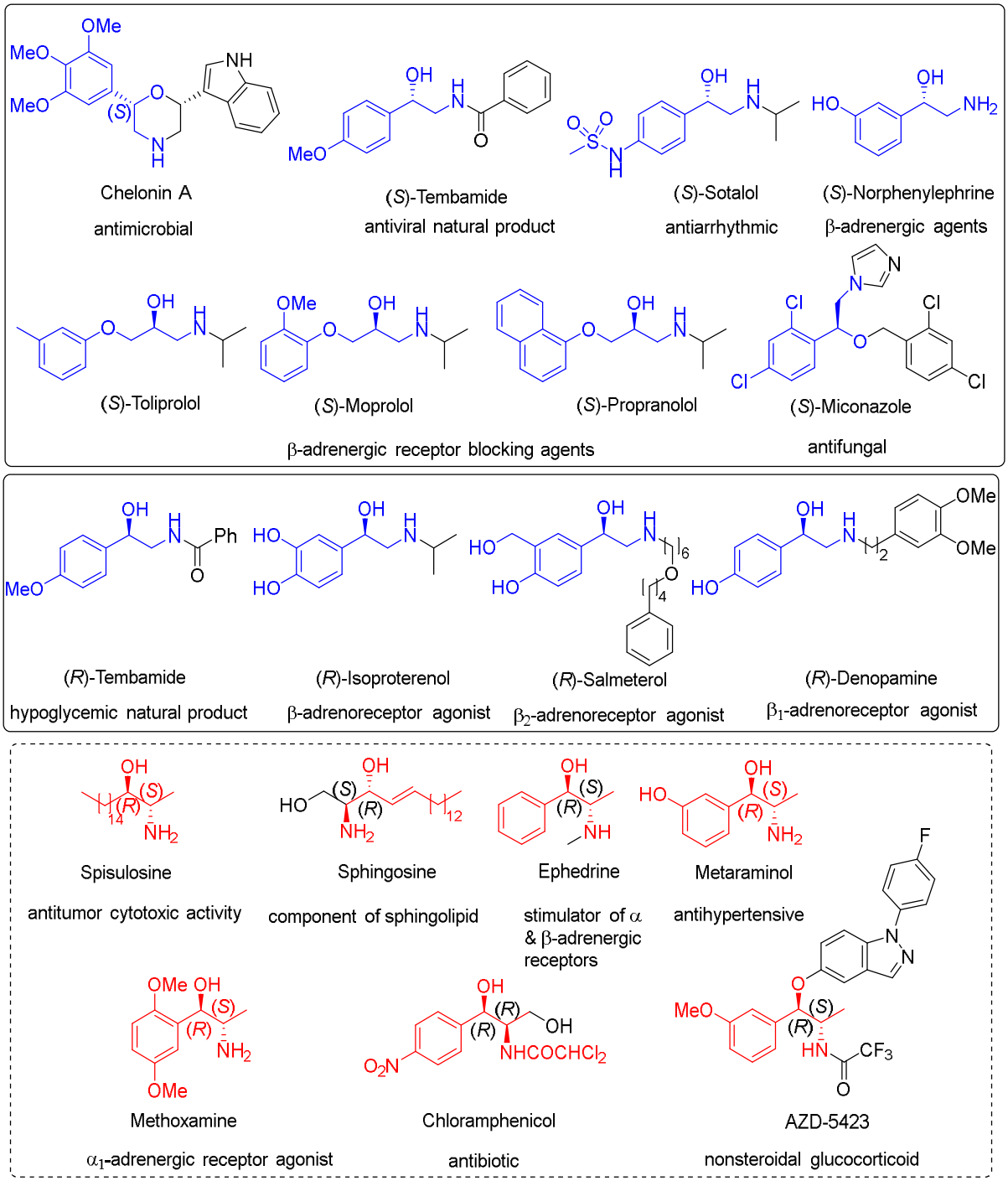


Figure 1.1: Examples of pharmaceuticals, biologically active molecules, and natural products derived from enantiopure (*S*)- (upper), (*R*)-β-nitroalcohols (middle), and chiral β-nitroalcohol diastereomers (lower dotted box).

1.2.2. Biocatalytic approaches for synthesis of chiral β-nitroalcohols

As several chiral β-nitroalcohols are precursors to pharmaceuticals, there is a growing demand to develop clean and green catalysts for their synthesis. Biocatalysts are nature evolved catalysts and their use in organic synthesis brings several advantages, such as, (i) avoids the use of toxic/metal/hazardous catalysts, (ii) high selectivity which often results in high stereoselective products, (iii) work under mild reaction conditions, (iv) does not require

protection of functional groups in the substrate, (v) makes fewer by-products, and (vi) re-usable if immobilized. Hence, use of biocatalysts could provide a sustainable solution to the asymmetric synthesis of β-nitroalcohols. Different biocatalytic approaches to synthesize chiral β-nitroalcohol stereoisomers can be classified into the following six categories. They are (a) kinetic resolution of racemic β-nitroalcohols, mostly catalyzed by lipases, (b) dynamic kinetic resolution that uses multi-enzymes or a chemo-enzymatic system, (c) Henry reaction by direct C-C bond formation between a carbonyl and nitroalkane, mostly catalyzed by a hydroxynitrile lyases (HNL), (d) stereoselective cleavage of racemic β-nitroalcohols (retro-Henry reaction), (e) asymmetric reduction of α-nitroketones catalyzed by alcohol dehydrogenase (ADH) or corresponding whole cells, and (f) halohydrin dehalogenase (HheC) catalyzed enantioselective epoxide ring-opening (**Figure 1.2**).

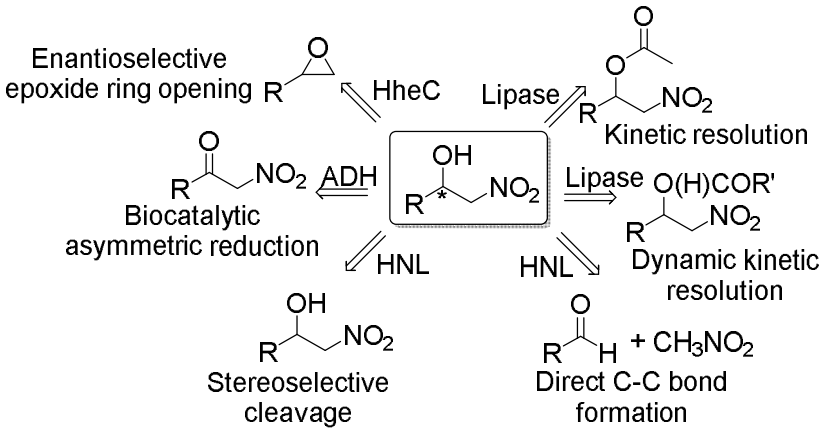
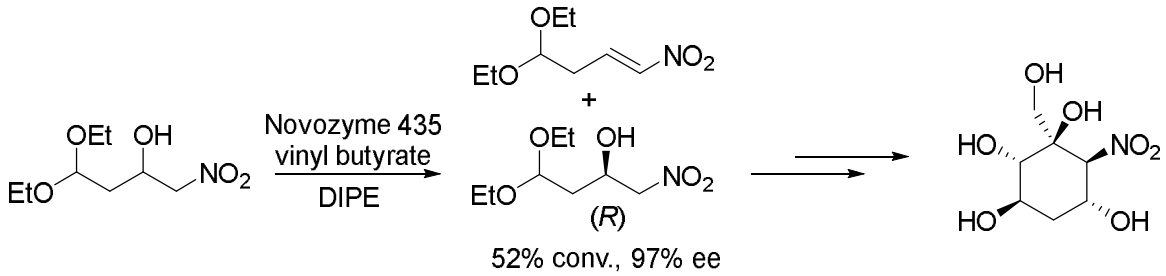


Figure 1.2: Different biocatalytic routes for synthesis of chiral β-nitroalcohols.

1.2.2.1. Lipase catalyzed kinetic resolution (KR)

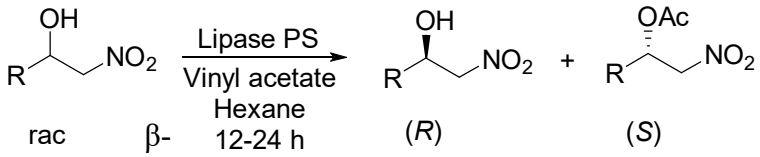
KR is one of the early biocatalytic approaches that majorly used lipases and hydrolases in the enantioselective preparation of β-nitroalcohols. Among the different lipases tested in the KR, *Pseudomonas* sp.,[40-41] *Candida antarctica* lipase B (CALB),[42] *Pseudomonas fluorescens*,[43] and *Burkholderia cepacia* lipase (lipase PS, Amano IM)[44] were found to be effective against a number of aliphatic and aromatic β-nitroalcohols.

Among the three lipases, CAL-B (Novozyme 435), lipase PS and PC (Amano AK and PS) tested in the KR of 4,4-diethoxy-1-nitrobutan-2-ol. Efficient resolution was found in case of CAL-B in DIPE using vinyl butyrate as an acylating agent (**Scheme 1.1**).



Scheme 1.1: CALB catalyzed KR of a racemic β-nitro alcohol with ketal functionality to enable chemo-enzymatic synthesis of aminocyclitol.

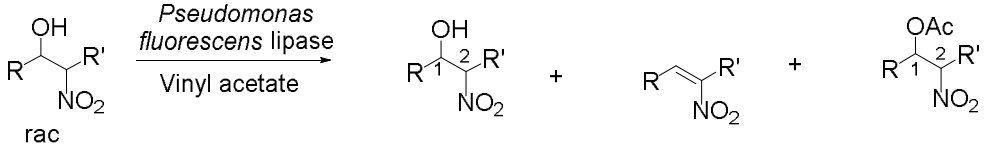
Burkholderia cepacia lipase (lipase PS, Amano IM) catalyzed enantioselective transesterification of eight racemic aromatic β-nitroalcohols has produced enantiopure (*R*)-2-nitroalcohols and the corresponding (*S*)-acetylated products (**Scheme 1.2**).[45] In 12 h, using 5:1 (w/w) of the enzyme to substrate ratio in hexane, the KR has produced 49% conversion, 98% ee of the (*R*)-2-nitro-1-phenylethanol (NPE), while (*S*)-acetylated NPE was obtained in >99% ee and a *E* value was found to be >200. Both *para* and *meta* substituted aromatic β-nitroalcohols could undergo resolution efficiently, however, *ortho* substituted ones (R=*o*-Me, *o*-Cl, **Scheme 1.2**) gave poor performance. KR of 1-nitro-3- phenylpropan-2-ol gave only 72% ee of its (*R*)-alcohol, and 81% of the (*S*)-acetate. This suggests that the presence of a phenyl group adjacent to the chiral center in the substrate is important for the KR in case of lipase PS.



R= Ph, 4-ClPh, 4-MePh	98 to >99% ee	98 to >99% ee	*E*= >200
R= 3-ClPh, 3-MePh	>99% ee	91 to 98% ee	*E*= 61-116

Scheme 1.2: Lipase PS catalyzed KR of aromatic β-nitroalcohols

In addition to the racemic β-nitroalcohols with one chiral center, lipases were also tested towards the KR racemic β-nitroalcohols having two chiral centers to produce β-nitroalcohol diastereomers. *Pseudomonas flourescens* lipase catalyzed KR of three aromatic β-nitroalcohols each having two chiral centers. Two substrate where R= 4-ClPh and 4-COOMePh and R'=Me, have produced the (*R*)-β-nitroalcohols, however, the chirality of the second chiral carbon with $–NO_2$ was not specified in case of both the products (**Scheme 1.3**). [43] KR of the third substrate 2-hydroxy-3-nitro-3-phenyl-1-benzyl-oxypropane has resulted in the synthesis of the (*R*,*S*)-diastereomer in 85% ee, 50% yield, and the (*S*,*R*)-diastereomer of the 2-acetoxy-3-nitro-3-phenyl-1-benzyl-oxypropane in 82% ee, 45% yield.

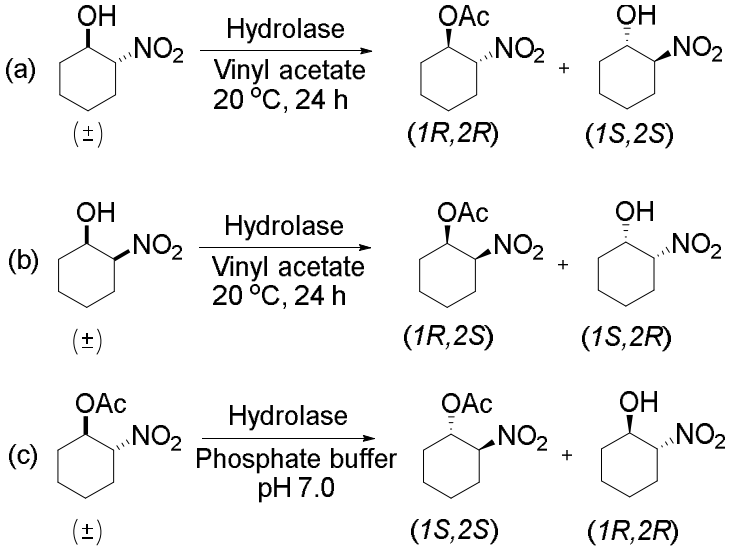


R= 4-Cl-C_6H_4	R'=Me	66% conv., 71% ee (1*R*)	27%	not found
R= 4-COOMe-C_6H_4	R'=Me	68% conv., 82% ee (1*R*)	30%	not found
R= $C_6H_5CH_2$-OCH_2	R'=Ph	50% conv., 85% ee (1*R*,2*S*)	not found	45% conv., 82% ee (1*S*,2*R*)

Scheme 1.3: *Pseudomonas flourescens* lipase catalyzed KR in the synthesis of β-nitroalcohol diastereomers.

In the KR based stereoselective transacetylation of racemic *trans*-2-nitrocyclohexanol using vinyl acetate as an acylating agent, *Pseudomonas flourescens* lipase and CALB have produced 49-50% conversion and >98% ee of each of the stereoisomers (**Scheme 1.4a**) [48]. Preparative scale transacetylation by *Pseudomonas flourescens* lipase has produced (1*R*,2*R*)-*trans*-2-nitrocyclohexyl acetate in 99% ee, 49% yield, and (1*S*,2*S*)-*trans*-2-nitrocyclohexanol in 99%

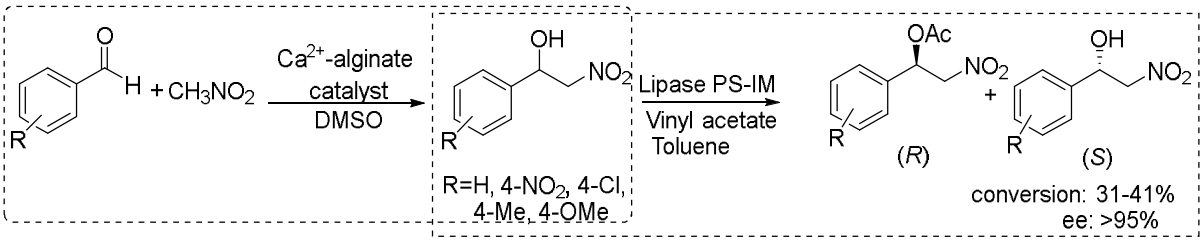
ee, 48% yield. In the transesterification of racemic *cis*-2-nitrocyclohexanol using vinyl acetate, four enzymes, *Candida cylindracea* C1, *Pseudomonas stutzeri*, *Alcaligenes* spp. and *Pseudomonas flourescens* showed *E* >400, with a conversion range of 47-81% and up to >98% ee of the product (**Scheme 1.4b**). The *cis*-2-nitrocyclohexanol on preparative scale transesterification produced (1*R*,2*S*)-*cis*-2-nitrocyclohexyl acetate and (1*S*,2*R*)-*cis*-2-nitrocyclohexanol in 99% ee, however, the *cis*-acetate was decomposed during silica gel based separation. For the hydrolysis of racemic *trans*-2-nitrocyclohexyl acetate, *Candida cylindracea* C1, *Alcaligenes* spp., *Pseudomonas cepacia* P1, *Pseudomonas stutzeri*, and *Pseudomonas cepacia* P2 have shown high enantioselectivity (**Scheme 1.4c**). The hydrolysis based KR by these enzymes has produced (1*S*,2*S*)-*trans*-2-nitrocyclohexyl acetate in 88-99% ee, 47-53% conversion, and (1*R*,2*R*)-*trans*-2-nitrocyclohexanol in 91-99% ee.



Scheme 1.4: Lipase catalyzed KR of racemic 2-nitrocyclohexanol and 2-nitrocyclohexyl acetate via transesterification and hydrolysis in the synthesis of β-nitroalcohol diastereomers.

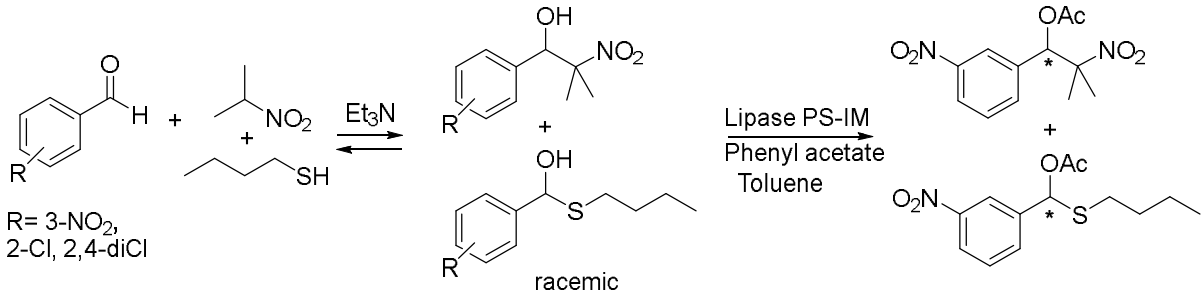
1.2.2.2. Dynamic Kinetic resolution (DKR)

Kühbeck et al. reported a two-step chemoenzymatic reaction in the production of (*S*)-β-nitroalcohols.[49] The first step involved a Ca^{2+}-alginate beads catalyzed racemic β-nitroalcohol synthesis in DMSO and second, immobilized lipase PS-catalyzed kinetic resolution of aromatic racemic β-nitroalcohols in toluene (**Scheme 1.5**). A combination of these two steps in one pot was not possible due to the incompatibility of the solvents used in the two different reactions. The lipase PS catalyzed KR has produced (*S*)-β-nitroalcohols and (*R*)-β-nitroalcohol esters. Five aromatic β-nitroalcohols studied in the KR have provided their corresponding enantiopure (*S*)-β-nitroalcohols in 31-41% yield and >95% ee. The limited (maximum of 50%) yield of chiral β-nitroalcohols by KR has been overcome by DKR.



Scheme 1.5: Two-step process of DKR using calcium alginate beads catalyzed racemic β-nitroalcohol synthesis followed by lipase PS catalyzed KR.

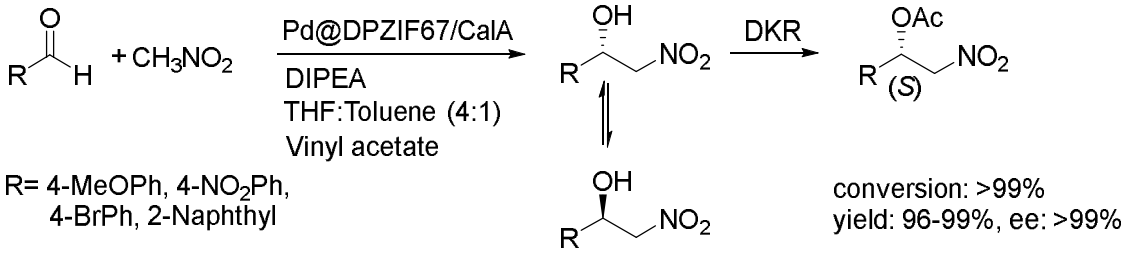
Ramstrom and coworkers have used a lipase based dynamic combinatorial resolution (DCR) approach that involved (i) triethylamine catalyzed 2-nitropropane addition to different aromatic aldehydes in the preparation of racemic β-nitroalcohols followed by (ii) *Pseudomonas cepacian* lipase catalyzed resolution using *para*-chlorophenyl acetate as an acylating agent.[50] The same group have latter developed a DKR that used a one-pot nitroaldol reaction with lipase catalyzed KR at mild conditions.[51] Similar to the DCR, a double parallel dynamic resolution has been reported to prepare enantiopure β-nitroalcohols.[52] In this approach, two parallel dynamic systems were prepared by the addition of 2-nitropropane and 1-butanethiol to three different aromatic aldehydes in the presence of the base trimethylamine. This has produced two simultaneous dynamic equilibrium systems between the aldehydes and (a) racemic β-nitroalcohols, and (b) corresponding racemic hemithioacetals. *Burkholderia cepacia* (formerly *Pseudomonas cepacia*) lipase (PS-IM) and *Pseudozyma antarctica* (formerly *Candida antarctica* lipase B) were investigated in the stereoselective resolution of the double parallel dynamic system (**Scheme 1.6**). CALB did not give any product, while PS-IM gave a higher ratio of acetylated hemithioacetal in 10 to 11 days of reaction time. The PS-IM showed a high preference for the hemiacetal compared to nitroaldol. Among the three aldehydes, i.e., 3-nitrobenzaldehyde, 2-chlorobenzaldehyde, and 2,4-dichlorobenzaldehyde used in this study, the lipase could produce the nitroaldol product of only 3-nitrobenzaldehyde, probably due to the less preference of the enzyme towards the *ortho* substituted substrates.



Scheme 1.6: *Burkholderia cepacia* catalyzed double parallel dynamic resolution in the enantioselective synthesis of β-nitroalcohol esters.

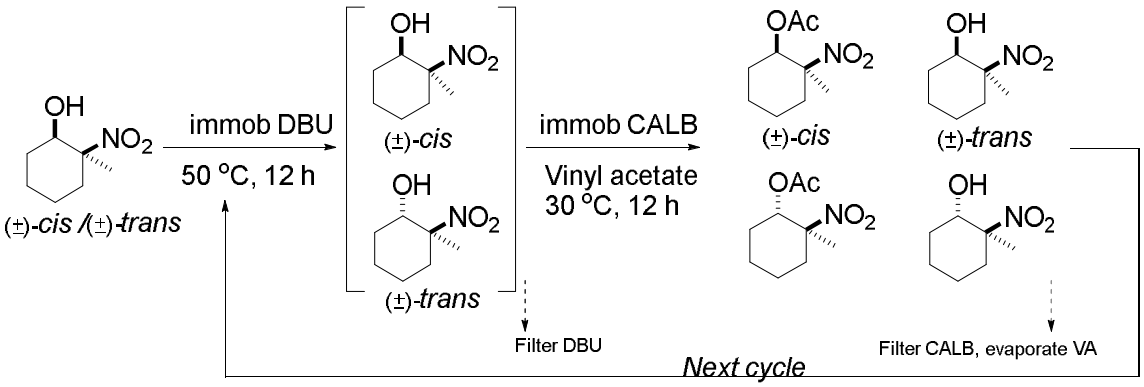
A recent multi-step chemo-biocatalytic DKR process involves conversion of aldehydes into (*S*)-β-nitroalcohol esters.[53] The cascade is a combination of three reactions, nitroaldol, KR, and racemization (**Scheme 1.7**). Dutta et al. have designed and synthesized multimodal catalytic nanoreactors (MCNRs) to achieve this cascade reaction in a one-pot system. The MCNR, Pd@DPZIF67/CalA had an assembly of three catalysts, i.e., (a) a mesoporous metal organic framework (MOF), (b) *Candida antarctica* lipase A (CalA), and (c) metal nanocrystals to carry out racemic β-nitroalcohol synthesis, KR, and racemization respectively. Optimization of the cascade starting with *p*-anisaldehyde and nitromethane showed >97% yield and >99% ee of the corresponding (*S*)-acetyl nitroalcohol in THF: toluene (4:1) at room temperature with vinyl acetate as the acyl donor and in the presence of 0.1 mol % of *N*,*N*-diisopropylethylamine in 20 h (**Scheme 1.7**). Four different aromatic aldehydes tested in the cascade have shown very high conversion and % ee of their corresponding (*S*)-β-nitroalcohol acetyl derivatives (>99% conversion and >99% ee). The Pd@DPZIF67/CalA was tested for recyclability, and the catalyst showed >89% residual activity with 86% yield and >80% ee of the product after five successive

cycles of reuse. However, in the consecutive cycles, the reaction time increased from 20 to 35 h.



Scheme 1.7: One-pot DKR based chemo-enzymatic cascade using *Candida antarctica* lipase A in the synthesis of (*S*)-β-nitroalcohol esters.

The one-pot two-step DKR of 2-methyl-2-nitrocyclohexanol using 1,8-Diazabicyclo[5.4.0]undec-7-ene (DBU) catalyzed intramolecular nitroaldol (Henry) reaction followed by immobilized CALB catalyzed KR to produce (1*R*,2*S*)-*cis*-2-methyl-2-nitrocyclohexyl acetate and (1*R*,2*R*)-*trans*-2-methyl-2-nitrocyclohexyl acetate in 97 and 96% ee with 18 and 53% conversion respectively. While the acetates had 49.3% de (*trans*), corresponding alcohols had 21.4% de (*trans*) (**Scheme 1.8**) [54].



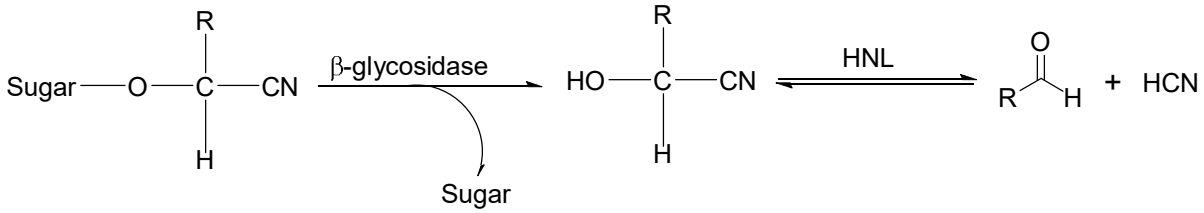
Scheme 1.8: One-pot DKR with repeated interconversion and lipase based KR.

1.2.2.3. Direct C–C bond formation

Stereoselective direct C–C bond formation between an electrophilic carbonyl carbon and nucleophilic nitroalkane, also known as Henry reaction, is one of the most important transformation for the synthesis of chiral β- nitroalcohols. It is mostly catalyzed by a few hydroxynitrile lyases (HNLs).

1.2.2.3.1. Hydroxynitrile lyase (HNL)

Hydroxynitrile lyases (HNL), belong to E.C. 4.1.2.X, X = 10, 11, 46 and 47. Most of the known HNLs are from higher plants, although they are also found in some arthropods, bacteria, ferns, lichens and fungi. In nature HNLs catalyze the cleavage of cynohydrins that are resulted due to the hydrolysis of cyanogenic glycosides by a glycosidase (**Scheme 1.9**).[55] This process of decomposition of cyanohydrin to a carbonyl compound and HCN is known as cyanogenesis, which plants use to protect them from herbivores and pathogens.[55]



Scheme 1.9: catabolism of cyanogen glycoside to carbonyl compound and HCN

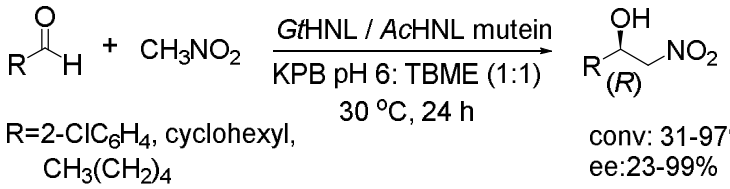
Based on the stereoselectivity in the synthesis of cyanohydrins, HNLs can be categorized as (*R*)-, and (*S*)-selective HNLs. Prominent examples of (*R*)-selective HNLs are from *Arabidopsis thaliana* (*At*HNL), *Prunus amygdalus* (*Pa*HNL), *Linum usitatissimum* (*Lu*HNL), *Chamberlinius hualienensis* (*Chua*HNL), *Parafontaria tonominea* (*Pton*HNL), *Prunus serotine* (*Ps*HNL),[56] *Prunus amygdalus turcomanica* (*Pat*HNL),[57] *Prunus mume* (*Pm*HNL),[58-59] *Amygdalus pedunculata* Pall (*AP*HNL),[60] *Passiflora edulis* (*Pe*HNL),[61-63] *Prunus communis* (*Pc*HNL),[64] wild apricot i.e. *Prunus armeniaca* L. (*Pars*HNL),[65-67] *Prunus serotina* var. capulli), peach (*Prunus persica*) HNL, *Acidobacterium capsulatum* ATCC 51196 (*Ac*HNL) and *Granulicella tundricula* (*Gt*HNL),[68] etc. Similarly (*S*)- selective HNLs are reported with *Baliospermum montanum* (*Bm*HNL),[69] *Hevea brasiliensis* (*Hb*HNL), *Manihot esculenta* (*Me*HNL) and *Sorghum bicolor* (*Sb*HNL), etc. Based on the presence of co-factor HNLs may be classified into (a) with FAD: *Pa*HNL and other *Prunus* sp. HNLs, and (b) without FAD: *At*HNL, *Phlebodium aureum* HNL (*Fa*HNL), *Lu*HNL, *Passiflora edulis* HNL (*Pe*HNL), *Xylella fastidiosa* HNL (*Xf*HNL), *Sorghum bicolor* HNL (*Sb*HNL), *Ximenia americana* HNL (*Xa*HNL), *Hb*HNL, *Me*HNL and *Bm*HNL.

Apart from the cleavage of cyanohydrins in higher plants as described earlier, HNLs also catalyse the reverse reaction i.e., the synthesis of optically pure cyanohydrins, an important class of organic molecules having a lot of industrial significance. The asymmetric biocatalytic synthesis of chiral cyanohydrins using HNLs is a very cost effective, easy and eco-friendly process.[55,70-74] HNLs catalyze the asymmetric synthesis of chiral α-cyanohydrins using HCN and aldehydes as substrates.[75-76] Enantiopure cyanohydrins formed by this process are valuable chiral intermediates of pharmaceuticals, agrochemicals, and fine chemicals.[55,74,77]

1.2.2.3.2. HNLs and other enzyme catalyzed synthesis of optically pure β-nitroalcohols
Purkarthofer et al. reported the first biocatalytic enantioselective nitroaldol synthesis using *Hb*HNL, an (*S*)-selective HNL.[78] Further study on the *Hb*HNL catalyzed nitroaldol reaction was performed by Griengl and coworkers.[79] Exploiting the (*R*)-selectivity of *At*HNL, Fuhshuku and Asano have synthesized a series of (*R*)-β-nitro alcohols.[80] Both the *Hb*HNL and *At*HNL nitroaldol syntheses were elaborated by Milner et al.[81]

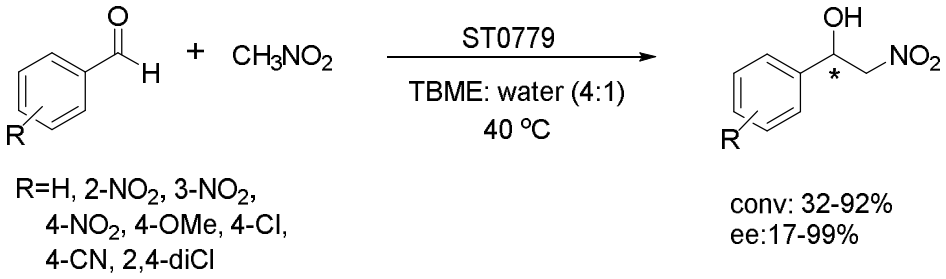
Subsequently two metal dependent cupin fold containing bacterial HNLs *Ac*HNL and *Gt*HNL were reported in the stereoselective synthesis of (*R*)-NPE.[68] While wild-type of *Ac*HNL showed moderate enantioselectivity (79% ee) and poor yield (37%), *Gt*HNL did not catalyze the reaction at all, despite its 77% sequence identity with *Ac*HNL and several identical active site residues, i.e., A40, V42, and Q110.[82] The *Gt*HNL and *Ac*HNL muteins (A40H, A40R, and A40H-V42T-Q110H) created earlier to improve the activity of cyanohydrin synthesis were tested for the synthesis of (*R*)-NPE. The *Ac*HNL muteins have shown 66–74% conversion and 93–97% ee of (*R*)-NPE in a 24 h reaction time. In 2 to 4 h, up to >99% ee of the product was achieved, but the % conversion was affected, i.e., 11–72%. Long reaction time (24 h) increased

the yield but decreased the % ee of the product. Among the three *Ac*HNL muteins, A40H showed the highest conversion of 74%, with 97% ee of the (*R*)-NPE. Similar to *Ac*HNL, all three *Gt*HNL muteins gave the highest conversion in case of 24 h biotransformation, compared to the 2 or 4 h reaction. The *Gt*HNL muteins produced 15–75% conversion and 94–98% ee of the (*R*)-NPE in 24 h. In a study to find out the importance of metal ions in *Gt*HNL, the bound Mn was replaced with Ni, Co, Fe, and Zn. *Gt*HNL-A40H-V42T-Q110H with Fe and Co showed higher % conversion to (*R*)-NPE than the Mn counterpart in 4 h, while the % ee remained high (>97%). Two *Gt*HNL (A40R, and A40H/A42T/Q110H) and three *Ac*HNL muteins (A40H, A40R, and A40H/A42T/Q110H) were tested toward the enantioselective addition of nitromethane to 2-chlorobenzaldehyde, cyclohexanecarboxaldehyde and hexanal (**Scheme 1.10**). For 2-chloro benzaldehyde, *Ac*HNL-A40H and A40R gave 89–95% conversion with 80–83% ee of the corresponding (*R*)-β-nitroalcohol, which was comparatively better than the results by other *Ac*HNL and *Gt*HNL variants. In the case of cyclohexanecarboxaldehyde the triple variants of both *Ac*HNL and *Gt*HNL showed 80–86% conversion and 96.9–98% ee of the product. Similarly, for hexanal, both the triple variants gave 93.7–95% conversion and >99% ee of the corresponding (*R*)-β-nitroalcohol.



Scheme 1.10: Enantioselective nitroaldol catalyzed by *Gt*HNL and *Ac*HNL muteins

Yu et al. studied the catalytic ability of several hydrolases (cloned and purified enzymes) and two commercial lipases for promiscuous nitroaldol reaction.[83] Among the seven biocatalysts evaluated, an acyl peptide releasing enzyme from *Sulfolobus tokodaii* (ST0779) gave the highest yield (92%) and 94% ee of the nitroaldol product in the condensation of 4-nitro benzaldehyde and nitromethane (**Scheme 1.11**). Several important biocatalytic parameters of the ST0779 catalyzed nitroadol condensation, i.e., the solvent system, temperature, % water content, reaction time, and the ratio of the two substrates, were optimized to achieve the maximum yield and enantioselectivity of the product. The optimized parameters include MTBE as the best organic solvent, at 40 °C, 15% (v/v) water content, 36 h reaction time, and 10 : 1 ratio of nitromethane to 4-nitrobenzaldehyde. ST0779 has provided 89–92% yield with 93–99% ee of β-nitroalcohols in the case of the benzaldehyde derivatives carrying electron withdrawing groups, i.e., 2-NO_2, 3-NO_2, 4-NO_2, and 4-CN in 18–24 h reaction time. Other substrates tested showed only 32–45% yields, with 17–94% ee in 60–90 h reaction time (**Scheme 1.11**). Although ST0779 has successfully helped synthesize a number of chiral β-nitroalcohols, the absolute configuration of the products was not clearly mentioned. From the HPLC profile of the products, it could be interpreted that the enantiopreference of the catalyst varies with the electronic effects of the substituents on the benzaldehyde ring.



Scheme 1.11: Enantioselective nitroaldol catalyzed by acyl peptide releasing enzyme from *Sulfolobus tokodaii* (ST0799)

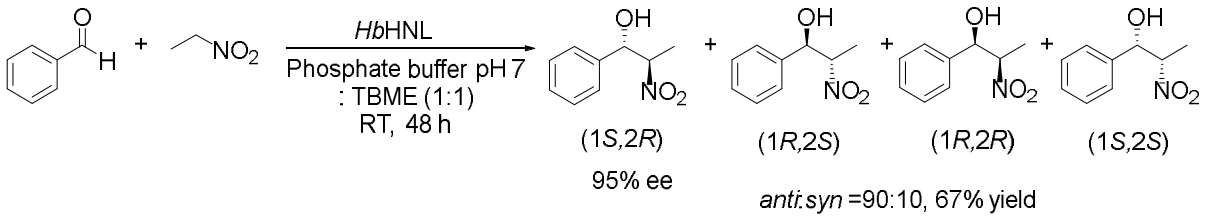
Yu et al. have used porcine pancreas lipase (PPL) among the biocatalysts screened for the stereoselective nitroaldol synthesis and further investigated it based on the reasonable activity and enantioselectivity of the product obtained with it.[83] PPL was also tested against the eight aromatic aldehydes in the nitroaldol reaction that are used with ST0779. Unlike ST0779, PPL showed low yield and enantioselectivity for all substrates except 4-cyanobenzaldehyde (71% yield, 93% ee).

Devamani et al. have explored the catalytic promiscuity of several ancestral enzymes.[84] They hypothesized that ancestral enzymes are more promiscuous than their modern successors. To investigate their hypothesis, they reconstructed ancestral enzymes by predicting the sequences of four of them at different branch points during the esterase evolution to HNLs. They have tested the ancestral enzymes and the modern HNLs, i.e., *Hb*HNL and *Me*HNL, and a modern esterase *At*EST (*Arabidopsis thaliana*) for different promiscuous reactions, including retro-Henry reaction and Henry reaction. The *At*EST described here as an esterase by Devamani et al. is the same enzyme that shows HNL activity, reported by Andexer et al. earlier.[85] Among the fourteen enzymes examined, only six showed promiscuous Henry reaction in the synthesis of chiral NPE (**Table 1.1**). Except *Me*HNL, all others have shown high conversion and enantioselectivity in the NPE synthesis. HNL1-NJ and HNL1 have shown higher % conversion (up to 98) and ee (up to 96) than *Hb*HNL in the (*S*)-NPE synthesis. Only *At*EST showed (*R*)-selectivity, while all other HNLs showed (*S*)-selectivity in the Henry reaction.

Table 1.1: Modern HNLs and their ancestral enzymes in the stereoselective Henry reaction in the synthesis of chiral NPE

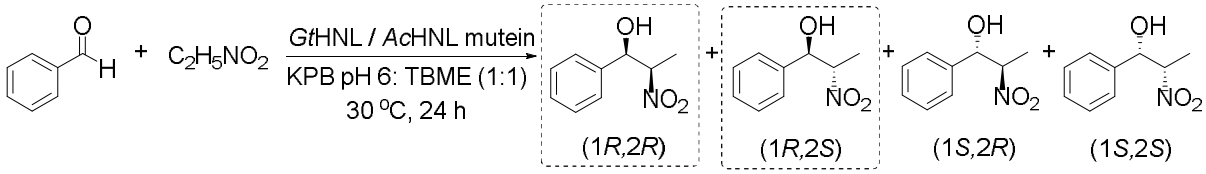
Entry	Enzyme	Conv., % ee	major enantiomer
1	*Hb*HNL	63, 92	*S*
2	*Me*HNL	76, 5	*S*
3	HNL1-ML	85, 83	*S*
4	HNL1-NJ	98, 95	*S*
5	HNL1	91, 96	*S*
6	*At*EST	96, 88	*R*

To date, there are only two reports that showcased the effectiveness of HNL in the distereoselective β-nitroalcohol synthesis via Henry reaction. *Hb*HNL catalyzed nitroethane addition to benzaldehyde has produced a mixture of diastereomers of 2-nitro-1-phenylpropanol (NPP) in 67% yield, wherein the *anti* stereoisomer (*1S,2R*)- was found in 80% de with 95% ee (**Scheme 1.12**) [78].



Scheme 1.12: *Hb*HNL catalyzed diastereoselective Henry reaction

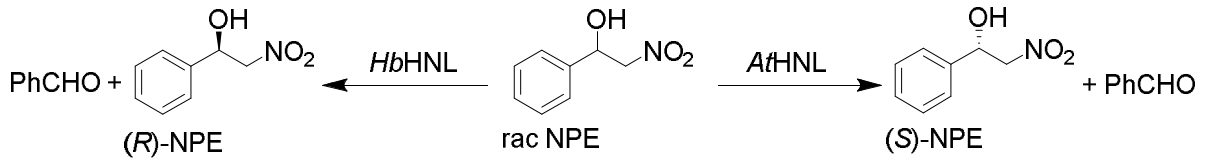
Two variants of *Gt*HNL (A40R, and A40H-A42T-Q110H) and three of *Ac*HNL (A40H, A40R, and A40H-A42T-Q110H) were reported in the diastereoselective synthesis of NPP, wherein the *anti* product, i.e., (*1R,2S*)- was majorly found (**Scheme 1.13**). [68]



Scheme 1.13: *Gt*HNL and *Ac*HNL muteins catalyzed diastereoselective Henry reaction

1.2.2.4. Stereoselective cleavage of racemic β-nitroalcohols (retro-Henry reaction)

Two HNLs are reported to catalyze reversible Henry reaction, i.e., stereoselective cleavage of one enantiomer of a racemic β-nitroalcohol based on the stereopreference of the HNL. This results in the production of an aldehyde as the cleavage product, and the complementary enantiomer of the racemic β-nitroalcohol remains unreacted. This method is also known as the asymmetric retro-Henry reaction. (**Scheme 1.14**)



Scheme 1.14: Retro-Henry reaction by *Hb*HNL and *At*HNL produces (*R*)- and (*S*)-NPE respectively, while Henry reaction by them is shown in grey.

Thus, along with this approach, an HNL can be used to synthesize both (*R*)- and (*S*)-β-nitroalcohols. Eventually, the substrate scope of the HNL is extended to synthesize enantiocomplementary β-nitroalcohols. For example, the substrate selectivity of *At*HNL can be used to synthesize (*S*)-β-nitroalcohols, while *Hb*HNL can be used to synthesize (*R*)-β-nitroalcohols in the retro-Henry approach. Importantly, a HNL shows higher specific activity for C–C bond cleavage than a C–C bond formation. In the case of cleavage and synthesis of β-nitroalcohols by *At*HNL and *Hb*HNL, specific activity of both the enzymes are found to be more for retro-Henry reaction than for synthesis of Henry products.[80,86] However, the retro-Henry approach has multiple limitations. They are (i) maximum of 50% yield, (ii) one of the products, i.e., the aldehyde is often an inhibitor of the HNL, which can also denature the enzyme,[87] (iii) the starting substrate is not commercially available, its preparation requires an additional reaction, and (iv) loss of 50% of the product. The first biocatalytic retro-Henry reaction using *Hb*HNL[87] was elaborated elsewhere.[81] Although it was tested with the only substrate NPE, this methodology can be used to synthesize other (*R*)-β-nitroalcohols. Langermann et al. have engineered *Hb*HNL to enhance its substrate preference for cyanohydrin

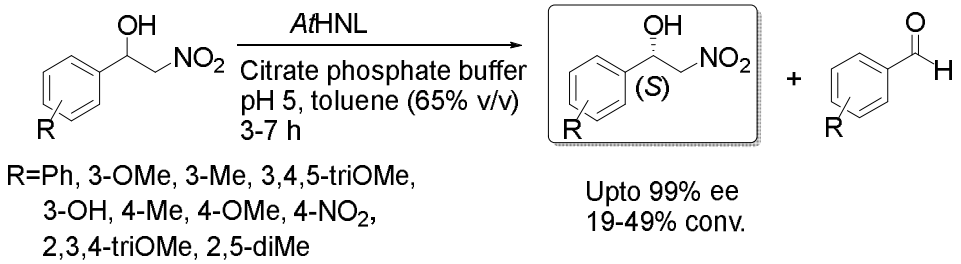
synthesis but simultaneously tested the variants for retro-Henry reaction.[88] Several variants have shown higher specific activity in the corresponding spectrophotometric assay. The best variant with the triple substitution L121Y-F125T-L146M, showed a specific activity of 0.71 Umg^{-1} toward the cleavage of racemic NPE, which is ~5.5 fold higher than the wild-type (0.13 Umg^{-1}) and k_{cat} 3.3 times higher than the wild-type. The *Hb*HNL variants, however, were neither tested for stereoselective nitroaldol synthesis nor in the retro-Henry approach in the preparation of chiral β-nitroalcohols. Their biocatalytic potential and substrate selectivity remains unexplored, especially in the synthesis of chiral β-nitroalcohols. Devamani et al. have also investigated the ancestral enzymes for promiscuous retro-Henry reaction.[84] As described in section 2.3, the same set of six enzymes showed retro-Henry activity in the cleavage of NPE (**Table 1.2**).

Table 1.2: HNLs including their ancestral enzymes in the stereoselective cleavage of NPE

Entry	Enzyme	Rate of cleavage (min^{-1})	% ee (preferred enantiomer)
1	*Hb*HNL	7.2±0.3	49, *S*
2	*Me*HNL	0.3	1.1, *S*
3	HNL1-ML	3.4±0.4	5.6, *S*
4	HNL1-NJ	9.6±0.6	32, *S*
5	HNL1	14±1	32, *S*
6	*At*EST	4.6±3	13, *R*

Three ancestral HNLs, HNL1-ML, HNL1-NJ, and HNL1 were effective towards retro-Henry reaction, while two of them HNL1-NJ, and HNL1 had a higher cleavage rate of NPE than *Hb*HNL. The % ee of the cleavage products was not high for all the six enzymes. Except for *At*EST, other enzymes were (*S*)-selective.

Rao et al. have synthesized ten aromatic (*S*)-β-nitroalcohols using *At*HNL catalyzed retro-Henry reaction with optimized biocatalytic reaction conditions (**Scheme 1.15**).[89] At least half a dozen aromatic (*S*)-β-nitroalcohols were prepared in up to 99% ee and 47% conversion and *E* value up to 84. Among the different racemic aromatic β-nitroalcohols tested, reasonable % ee was obtained with substrates having substituents at either *meta*, or *para,* or both positions of the aromatic ring. However, it was difficult to equate the % ee of *At*HNL catalyzed retro-Henry reaction with the effect of the nature of substituents in the aromatic rings or their positions because four more substrates with a single or multiple substituents in the phenyl ring showed very poor optical yield in the retro-Henry approach. Substrates with *ortho* substituents did not result in the production of a good % ee of products. Nevertheless, a preparative scale synthesis of (*S*)-NPE was reported that supports the synthetic feasibility of this approach.

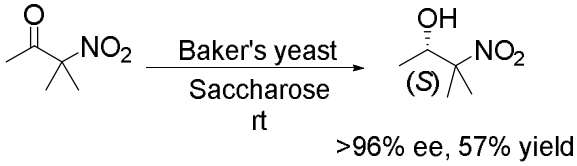


Scheme 1.15: *At*HNL catalyzed synthesis of (*S*)-β-nitroalcohols by retro-Henry approach.

Recently we have shown celite immobilized *At*HNL catalyzed retro-Henry reaction and produced a dozen of (*S*)-β-nitroalcohols under optimized conditions.[90] Racemic NPE and its two analogous, with *meta* methoxy and *meta* methyl substituents in the aromatic ring, showed excellent enantioselectivity (97-98.5% ee), and 45-48% conversion in the retro-Henry reaction. Three other NPE analogous with *para* fluoro, *meta* chloro, and *para* methyl substituents in the aromatic ring produced corresponding (*S*)-β-nitroalcohols in 68–75% ee and 44–54% conversion. Four more substrates having single or multiple substituents in the *ortho*, *meta*, and *para* positions of the phenyl ring showed poor optical yield. The *para* allyloxy-NPE and racemic β-nitroalcohol of cinnamaldehyde showed poor % ee of the corresponding product in the celite-*At*HNL catalyzed retro-Henry reaction.

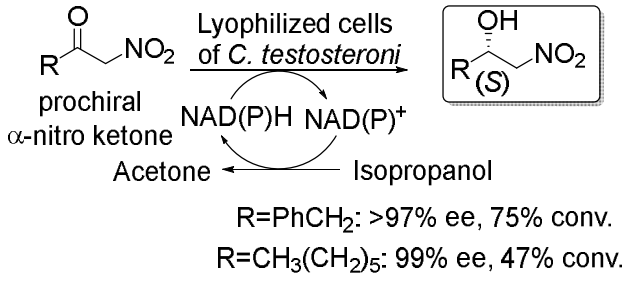
1.2.2.5. Biocatalytic asymmetric reduction

Asymmetric reduction of prochiral α-nitro ketones by whole cells and purified alcohol dehydrogenases produces chiral β-nitroalcohols. The first example is the asymmetric reduction of 3-methyl-3-nitro-2-butanone by baker's yeast in the presence of saccharose at room temperature that produced the (*S*)-enantiomer of 3-methyl-3-nitro-2-butanol in >96% ee, and 57% yield (**Scheme 1.16**).[91]



Scheme 1.16: Baker's yeast catalyzed asymmetric reduction of an α-nitro ketone

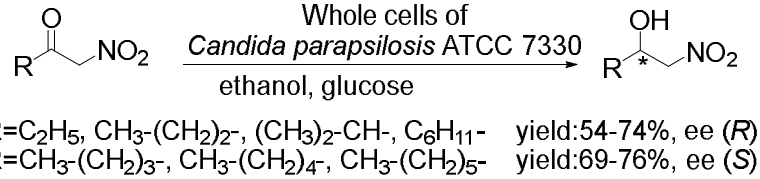
Asymmetric reduction of two α-nitro ketones by lyophilized cells of the bacterium *Comamonas testosteroni* DSM 1455 has produced their corresponding (*S*)-β-nitroalcohols in the presence of 20% (v/v) of 2-propanol as a hydrogen donor (**Scheme 1.17**).[92] Here the alcohol dehydrogenase has shown anti-Prelog preference. Both the substrates have shown very high stereoselectivity; for example, the β-nitroalcohol of aliphatic α-nitro ketone was obtained in >99% ee and 47% conversion by GC while the one corresponds to an aromatic ketone in >97% ee and 75% conversion by HPLC. However, the reduction of the aliphatic substrate took 48 h compared to 24 h for the aromatic one.



Scheme 1.17: Alcohol dehydrogenase catalyzed asymmetric reduction of α-nitro ketones.

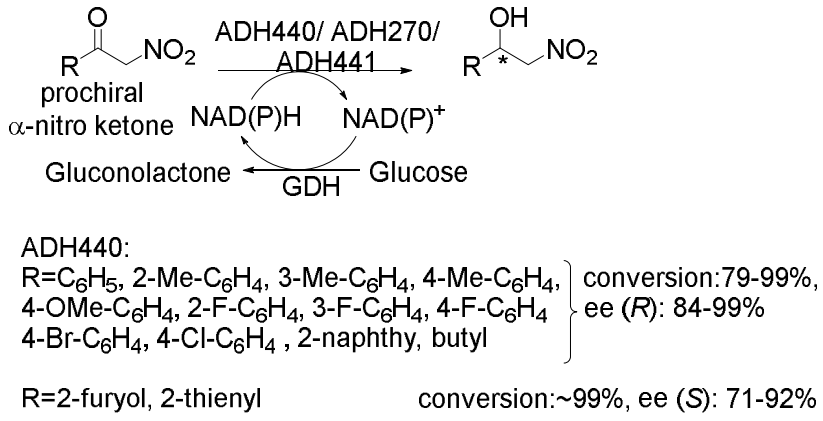
Venkataraman and Chadha showed an asymmetric reduction of aliphatic α-nitro ketones by whole cells of *Candida parapsilosis* ATCC 7330 using ethanol as co-solvent and glucose as co-substrate, in the synthesis of aliphatic β-nitroalcohols (**Scheme 1.18**).[93-94] The biocatalyst was very selective for keto reduction than the nitro group; however, it showed diverse

enantiopreference toward the seven aliphatic α-nitro ketones reduced by it. Four substrates with short alkyl chains attached to the keto carbon were reduced to their corresponding (*R*)-β-nitroalcohols in 8.2 to 79.5% ee and 54 to 74% yield, while three others with long carbon chain produced their (*S*)-enantiomers in 59 to 81% ee and 69 to 76% yield.



Scheme 1.18: *Candida parapsilosis* ATCC7330 catalyzed asymmetric reduction of aliphatic α-nitro ketones.

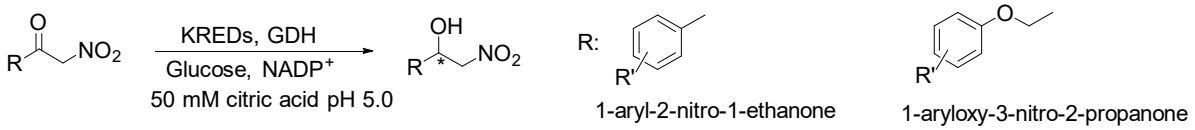
Screening of eighteen commercially available alcohol dehydrogenases for asymmetric reduction of α-nitro acetophenone gave successful results with eight of them.[95] The best three of the eight were used in the asymmetric reduction of fifteen α-nitroketones along with glucose dehydrogenase from *Bacillus megaterium* for NAD(P)H regeneration. Among the three dehydrogenases, ADH440 has mostly produced (*R*)-β-nitroalcohols in 79-99% conversion and 92-99% ee, while ADH270 and ADH441 have produced (*S*)-β-nitroalcohols from their corresponding α-nitro ketones. In the case of the 2-furyl and 2-thienyl α-nitro ketones, ADH440 produced their corresponding (*S*)-β-nitroalcohols, while ADH270, and 441 produced the (*R*)-β-nitroalcohols. This opposite stereoselectivity is due to the change in the priority of the substituents attached to the chiral center because of the presence of the heteroaromatic ring. Inverse enantioselectivity was observed in the asymmetric reduction of *ortho* fluro derivative (R= *o*-F-C6H4-), and 1-nitro-butan-2-one (R=Et, **Scheme 1.19**) by ADH441, and 270 respectively, where the corresponding (*R*)-β-nitroalcohols were formed.



Scheme 1.19: Alcohol dehydrogenase catalyzed reduction of prochiral α-nitro ketones.

Ketoreductases (KREDs) were used in the asymmetric reduction of class I (1-aryl-2-nitro-1-ethanone) and class II α-nitro ketones (1-aryloxy-3-nitro-2-propanone) (**Scheme 1.20**).[96] Evaluation of 13 KREDs in the reduction of α-nitro acetophenone uncovered (*R*)-selectivity with RasADH from *Ralstonia* species, while YGL039w showed (*S*)-selectivity. YGL039w showed (*S*)-selectivity for all tested substrates except for 1-naphthyl, benzyl, and phenethyl derivatives. It preferred *para* substituents than *ortho*, and *meta*, and electron donating groups than electron withdrawing groups in the aromatic ring. RasADH showed excellent

enantioselectivity for most of the class I substrates (up to >99% ee). It preferred *ortho* and *para* substituted 1-aryl-2-nitro-1-ethanones (except *p*-*t*Bu). Screening of KREDs against a class II α-nitro ketone model substrate, 1-benzyloxy-3-nitro-2- propanone, again identified YGL039w and RasADH as the stereocomplementary dehydrogenases that produced 96 and 58% ee of (*R*)- and (*S*)-products respectively. Further screening of KREDs against the same substrate has identified SyADH (*Sphingobium yanoikuyae* ADH) with 96% ee of the (*S*)-product. Ten class II α-nitro ketones were reduced using YGL039w and SyADH.



the % ee and conv of products by YGL039w are in blue, RasADH are in red, and SyADH are in green

For the products of 1-aryl-2-nitro-1-ethanones:

R':	H	2-Cl	2-Me	2-OMe	3-Cl
	>99%, 99% ee (*S*)	63%, 90% ee (*ND*)	31%, 74% ee (*S*)	50%, 31% ee (*S*)	73%, 29% ee (*S*)
	>99%, 98% ee (*R*)	>99%, >99% ee (*ND*)	81%, >99% ee (*R*)	79%, 84% ee (*R*)	72%, 96% ee (*R*)

R':	3-Me	3-OMe	3-CF_3	4-Cl	4-Me
	95%, 93% ee (*S*)	73%, 92% ee (*S*)	87%, 92% ee (*S*)	>99%, 98% ee (*S*)	96%, 96% ee (*S*)
	94%, 91% ee (*R*)	59%, 79% ee (*R*)	>99%, 85% ee (*R*)	98%, 98% ee (*R*)	>99%, 86% ee (*R*)

R':	4-OMe	4-CF_3	4-F	4-Br	4-$NHCOCH_3$
	96%,>99% ee (*S*)	43%, 72% ee (*S*)	93%, 68% ee (*S*)	76%, 96% ee (*S*)	55%, 96% ee (*S*)
	>99%, 99% ee (*R*)	85%, 98% ee (*R*)	85%, 96% ee (*R*)	86%, 98% ee (*R*)	99%, 89% ee (*R*)

R':	4-NO_2	4-(*tert*-butyl)	2,4-*di*Cl	3,4-*di*Cl
	62%, 77% ee (*S*)	35%, 66% ee (*S*)	80%, 32% ee (*S*)	45%, 82% ee (*S*)
	88%, 98% ee (*R*)	31%, >99% ee (*R*)	>99%, 99% ee (*R*)	55%, 92% ee (*R*)

R:	1-Naphthyl	2-Naphthyl	Benzyl	Phenethyl
	18%, 37% ee (*R*)	74%, 99% ee (*S*)	82%, 83% ee (*R*)	48%, 6% ee (*R*)
	37%, 92% ee (*R*)	86%, 96% ee (*R*)	65%, 17% ee (*S*)	64%, 90% ee (*R*)

For the products of 1-aryloxy-3-nitro-2-propanones:

R':	H	2-Me	2-OMe	3-Me	4-Me
	>99%, 96% ee (*R*)	90%, 94% ee (*R*)	64%, 98% ee (*R*)	83%, 85% ee (*R*)	75%, 99% ee (*R*)
	75%, 96% ee (*S*)	80%, 57% ee (*S*)	>99%, 97% ee (*S*)	>99%, 77% ee (*S*)	95%, 86% ee (*S*)

R':	4-OMe	4-F	4-Cl	4-NO_2	R = 1-Naphthyl
	>99%, 98% ee (*R*)	83%, 95% ee (*R*)	83%, 92% ee (*R*)	93%, 55% ee (*R*)	49%, 98% ee (*R*)
	>99%, 97% ee (*S*)	88%, 79% ee (*S*)	77%, 94% ee (*S*)	74%, >99% ee (*S*)	21%, 93% ee (*S*)

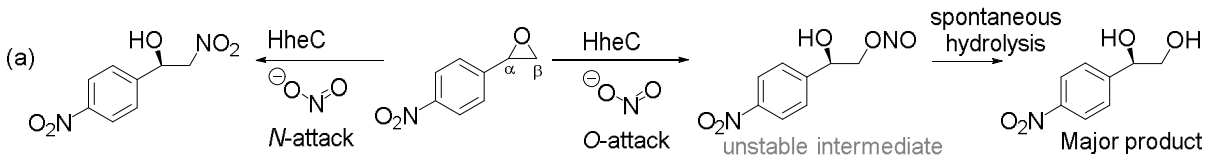
Scheme 1.20: KREDs catalyzed reduction of α-nitro ketones (1-aryl-2-nitro-1-ethanone, and 1-aryloxy-3-nitro-2-propanone).

As the phenyl ring was not directly connected to the carbonyl group in these substrates, hence steric hindrance and electronic effects were less important for class II α-nitro ketones than the class I. Most of the substrates were converted to their corresponding products with good to excellent conversion (up to >99%) and excellent ee (up to >99%), except the naphthyl derivative one.

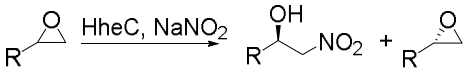
1.2.2.6. Stereooselective epoxide ring opening

Halohydrin dehalogenases catalyze the dehalogenation of vicinal halohydrins to produce the corresponding epoxides. They also catalyze the reverse reaction, i.e., ring opening of epoxide

by a nucleophile such as nitrite, cyanide, or azide to produce corresponding β-substituted alcohols. A halohydrin dehalogenase (HheC) from the bacterium *Agrobacterium radiobacter* AD1 catalyzes both the ring closure of halohydrin to epoxide and enantioselective nucleophilic ring opening of the epoxide.[97] HheC accepts nitrite as a nucleophile in the ring opening reaction and shows β-regioselectivity, i.e., nucleophile attacks at the terminal carbon of the oxirane ring. However, in the oxygen vs. nitrogen selectivity in the nitrite attack, the enzyme produces a vicinal diol due to oxygen attack, as the major product (**Scheme 1.21a**). In the case of *p*-nitrostyrene oxide ring opening, corresponding nirite ester, an unstable intermediate was formed by oxygen attack, which subsequently hydrolyzed spontaneously to its 1,2-diol. Simultaneously, β-regioselective nitrite attack happens through the nitrogen of the nitrite to produce the minor enantiopure β-nitroalcohol (**Scheme 1.21a**). The ratio of 1,2-diol and β-nitroalcohol was 4:1. This is a kinetic resolution, where the (*R*)-epoxide undergoes ring opening to produce the corresponding β-nitroalcohol, while the (*S*)-epoxide remains unreactive. Six aromatic epoxides were tested for the nitrite-mediated ring opening by wild type HheC, and its W249F variant. All of them showed β-regioselectivity, and except 2-((4-nitrophenoxy)methyl)oxirane, the other five showed (*R*)-selectivity in the halohydrin dehalogenase catalyzed kinetic resolution. The reverse enantioselectivity in the case of 2-((4 nitrophenoxy)methyl)oxirane is not due to the opposite enantio preference by the enzyme, rather due to change in the priority of the substituents around the chiral center. The enantioselectivity, *E* of HheC wild-type, and its W249F variant in the KR based enantioselective ring opening of all the substrates are shown in **Scheme 1.21b**. The wild-type enzyme showed good to excellent enantioselectivity for the first three substrates. The mutein has shown higher enantioselectivity in the KR compared to the WT enzyme in the case of all the substrates, except 2-((4-nitrophenoxy)methyl)oxirane.



(b)

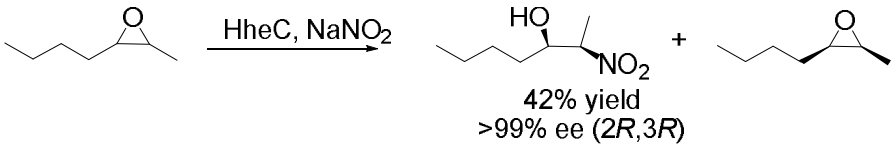


		4-NO_2-C_6H_4	3-Cl-C_6H_4	4-NO_2-C_6H_4-OCH_2	C_6H_5	4-Cl-C_6H_4	4-Me-C_6H_4
WT	*E*:	200	55	45	5	12	5
W249F	*E*:	>200	100	28	40	90	193

Scheme 1.21: Halohydrin dehalogenase catalyzed regio and enantioselective ring opening of epoxide by nitrite in the synthesis of chiral β-nitroalcohols, along with *E* values.

In another study HheC catalyzed nitrite mediated ring opening of an aliphatic epoxide 1,2-epoxybutane showed only 26% conversion, and 96% ee of (*R*)-1-nitro-butan-2-ol with *E*=28, and 97% β-regioselectivity (terminal position).[98]

This synthesis approach was also used for the diastereoselective β-nitroalcohol production. The halohydrin dehalogenase (HheC) catalyzed regio and enantioselective ring opening of epoxide by nitrite was tested with 2,3-epoxyheptane, which showed high regioselectivity in the nitrite attack to the sterically less crowded position to produce (2*R*,3*R*)-2-nitroheptan-3-ol in >99% ee and 42% yield (**Scheme 1.22**) [98].



Scheme 1.22: Halohydrin dehalogenase catalyzed ring opening by nitrite in the synthesis of β-nitroalcohol diastereomer.

1.3. Outline of the thesis

The current era is demanding for greener synthetic methods for industrially important fine chemicals and chiral intermediates. Exploring the diverse selectivity (chemo, regio, and stereo) of the natural enzymes and the tailor made enzymes have provided greener routes for numerous asymmetric syntheses, including the chiral β-nitroalcohols. Having elaborated the significance of enantioenriched β-nitroalcohols and their applications, and discussed about the six different biocatalytic approaches for the asymmetric synthesis of chiral β-nitroalcohols, it was realized that the best biocatalytic approach would be the HNL catalyzed Henry reaction because of its own advantages. Further, the substrates used in this process are widely available and economical. Though HNLs are pretty efficient in catalyzing this carboligation reaction between a carbonyl and cyanide, they have several limitations towards the asymmetric nitroaldol reaction. Substrate (aldehyde) inhibition, unavailability of significant number of HNLs with promiscuous (nitroaldolase) activity, poor % conversion, and stereoselectivity are among the major ones. To overcome these limitations, we envisioned a bi-enzymatic cascade approach using primary aromatic alcohols as the starting materials which are oxidized by horse liver alcohol dehydrogenase (HLADH) to their corresponding aldehydes, while these in-situ generated aldehydes are converted into enantiocomplementary (*R*)- or (*S*)- β-nitroalcohols by using (*R*)-selective *At*HNL or (*S*)-selective *Bm*HNL respectively in a one-pot enzyme cascade. The primary alcohols work as surrogate molecules in this cascade to overcome the aldehyde inhibition. Like the enantioselective β-nitroalcohol synthesis, Henry reaction can also be employed to synthesize β-nitroalcohol diastereomers, which find large synthetic applications. Despite the importance of the products and the transformation, HNL catalyzed diastereoselective Henry reaction remains poorly studied. So far only two (*R*)-selective HNLs, *Ac*HNL and *Gt*HNL, and one (*S*)-selective HNL, *Hb*HNL are known to show this activity using one aldehyde (benzaldehyde) and one nucleophile (nitroethane). Our study of wild type *At*HNL toward the diastereoselective β-nitroalcohol synthesis did not show significant activity. Screening of in-house *At*HNL libraries has identified several variants towards this promiscuous activity. We focussed on exploring the substrate scope, nucleophile promiscuity, stability, reusability, and the enhanced catalytic activity of these *At*HNL muteins towards synthesizing a wide range of different β-nitroalcohol diastereomers. Subsequently, we investigated *Bm*HNL in the diastereoselective synthesis of β-nitroalcohols using several aldehydes and nucleophiles. The entire study represented in the thesis with major objectives framed as follows.

1.4. Objectives

To develop a one-pot enzyme cascade system for synthesizing enantiocomplementary chiral β-nitroalcohols starting from aromatic primary alcohols.

To explore the applications of *At*HNL variants in the diastereoselective synthesis of (*R*)-β-nitroalcohols.

To investigate the catalytic potential of wild type *Bm*HNL in the Henry reaction towards synthesizing optically active β-nitroalcohols with two chiral centers.

1.5. References:

1. D.H.S. Rao, A. Chatterjee, and S.K. Padhi, *Org. Biomol. Chem.* 2021, **19 (2)**, 322–337.

2. D. Seebach, E. Colvin, F. Lehr and T. Weller, *Chimia (Aarau).*, 1979, **33**, 1–18.

3. D. J. Ager, I. Prakash and D. R. Schaad, *Chem. Rev.*, 1996, **96**, 835–875.

4. J. Burés, C. Lsart and J. Vllarrasa, *Org. Lett.*, 2009, **11**, 4414–4417.

5. J. I. Oshida, M. Okamoto, S. Azuma and T. Tanaka, *Tetrahedron: Asymmetry*, 1997, **8**, 2579–2584.

6. S. P. Rosini G, Ballini R and Petrini M, *Synthesis*, 1985, 585.

7. W. Ai, R. Shi, L. Zhu, D. Jiang, X. Ma, J. Yuan and Z. Wang, *RSC Adv.*, 2015, **5**, 24044–24048.

8. S. C. Bobzin and D. J. Faulkner, *J. Org. Chem.*, 1991, **56**, 4403–4407.

9. M. J. Cheng, K. H. Lee, I. L. Tsai and I. S. Chen, *Bioorganic Med. Chem.*, 2005, **13**, 5915–5920.

10. F. Porciatti, E. Cerbai, I. Masini and A. Mugelli, *Arch. Int. Pharmacodyn. Ther.*, 1989, **299**, 200–209.

11. M. Dukes and L. H. Smith, *J. Med. Chem.*, 1971, **14**, 326–328.

12. T. Nyronen, M. Pihlavisto, J. M. Peltonen, A. M. Hoffren, M. Varis, T. Salminen, S. Wurster, A. Marjamäki, L. Kanerva, E. Katainen, L. Laaksonen, J. M. Savola, M. Scheinin and M. S. Johnson, *Mol. Pharmacol.*, 2001, **59**, 1343–1354.

13. T. Taggart, P. Sutton and R. Donaldson, *Clin. Sci.*, 1985, **69**, 631–636.

14. E. J. Martin, *Drug Intell. Clin. Pharm.*, 1980, **14**, 86–95.

15. A. Shoeb, R. S. Kapil and S. P. Popli, *Phytochemistry*, 1973, **12**, 2071–2072.

16. J. E. Pessin, W. Gitomer, Y. Oka, C. L. Oppenheimer and M. P. Czech, *J. Biol. Chem.*, 1983, **258**, 7386–7394.

17. P. A. Procopiou, V. J. Barrett, N. J. Bevan, K. Biggadike, P. C. Box, P. R. Butchers, D. M. Coe, R. Conroy, A. Emmons, A. J. Ford, D. S. Holmes, H. Horsley, F. Kerr, A. M. Li-Kwai-Cheung, B. E. Looker, I. S. Mann, I. M. McLay, V. S. Morrison, P. J. Mutch, C. E. Smith and P. Tomlin, *J. Med. Chem.*, 2010, **53**, 4522–4530.

18. L. Almirante and W. Murmann, *J. Med. Chem.*, 1966, **9(5)**, 650–653.

19. H. Yokoyama, T. Yanagisawa, and N. Taira, *Cardiovasc. Pharmacol.*, 1988, **12**, 323.

20. R. Cuadros, E. Montejo De Garcini, F. Wandosell, G. Faircloth, J. M. Fernandez-Sousa and J. Avila, *Cancer Lett.*, 2000, **152**, 23–29.

21. P. M. Koskinen and A. M. P. Koskinen, *Synthesis*, 1998, 1075–1091.

22. N. F. Albertson, F. C. McKay, H. E. Lape, J. O. Hoppe, W. H. Selberis and A. Arnold, *J. Med. Chem.*, 1970, **13**, 132–134.

23. O. M. Jones, J. M. Thompson, A. F. Brading and N. J. McC. Mortensen, *Br. J. Surg.*, 2003, **90**, 872–876.

24. A. A. Yunis, *Annu. Rev. Pharmacol. Toxicol.*, 1988, **28**, 83–100.

25. K. Hashimoto, N. Kumagai and M. Shibasaki, *Org. Lett.*, 2014, **16**, 3496–3499.

26. G. Bosica and K. Polidano, *J. Chem.* 2017, 1–10.

27. M. Phukan, K. J. Borah, and R. Borah, *Green Chem. Lett. Rev.* 2009, **2 (4)**, 249–253.

28. R. Ballini and G. Bosica, *J. Org. Chem.* 1997, **62 (2)**, 425–427.

29. Y. Xiong, F. Wang, X. Huang, Y. Wen, and X. Feng, *Chem. - A Eur. J.* 2007, **13 (3)**, 829–833.

30. G. Blay, L. R. Domingo, V. Hernández-Olmos, J. R. Pedro, *Chem. - A Eur. J.* 2008, **14 (15)**, 4725–4730.

31. K. Xu, G. Lai, Z. Zha, S. Pan, H. Chen, and Z. Wang, *Chem. - A Eur. J.* 2012, **18 (39)**, 12357–12362.

32. J. D. White and S. Shaw, *Org. Lett.* 2012, **14 (24)**, 6270–6273.

33. T. Arai, M. Watanabe, A. Fujiwara, N. Yokoyama, and A. Yanagisawa, *Angew. Chemie - Int. Ed.* 2006, **45 (36)**, 5978–5981.

34. Y. Sohtome, Y. Hashimoto, and K. Nagasawa, *Adv. Synth. Catal.* 2005, **347 (11–13)**, 1643–1648.

35. Y. Shi, Y. Li, J. Sun, Q. Lai, C. Wei, Z. Gong, Q. Gu, and Z. Song, *Appl. Organomet. Chem.* 2015, **29 (10)**, 661–667.

36. L. Filippova, Y. Stenstrom, and T. V. Hansen, *Molecules* 2015, **20 (4)**, 6224–6236.

37. T. Marcelli, R. N. S. Van Der Haas, J. H. Van Maarseveen, and H. Hiemstra, *Angew. Chemie - Int. Ed.* 2006, **45 (6)**, 929–931.

38. H. Sasai, T. Suzuki, N. Itoh, and M. Shibasaki, *Appl. Organomet. Chem.* 1995, **9 (5–6)**, 421–426.

39. Y. Alvarez-Casao, E. Marques-Lopez, and R. P. Herrera, *Symmetry (Basel).* 2011, **3 (2)**, 220–245.

40. T. Kitayama, *Tetrahedron*, 1996, **52**, 6139–6148.

41. T. Kitayama, T. Rokutanzono, R. Nagao, Y. Kubo, M. Takatani, K. Nakamura and T. Okamoto, *J. Mol. Catal. B: Enzym.*, 1999, **7**, 291–297.

42. M. J. Sorgedrager, R. Malpique, F. Van Rantwijk and R. A. Sheldon, *Tetrahedron: Asymmetry*, 2004, **15**, 1295–1299.

43. J. C. Borah, J. Boruwa, B. Kalita, A. K. Hazarika and N. C. Barua, *Indian J. Chem., Sect. B: Org. Chem. Incl. Med. Chem.*, 2005, **44**, 1961–1965.

44. F. Xu, J. Wang, B. Liu, Q. Wu and X. Lin, *Green Chem.*, 2011, **13**, 2359.

45. N. Li, S. Bin Hu and G. Y. Feng, *Biotechnol. Lett.*, 2012, **34**, 153–158.

48. S. E. Milner, M. Brossat, T. S. Moody, C. J. Elcoate, S. E. Lawrence, and A. R. Maguire, *Tetrahedron: Asymmetry*, 2010, **21(8)**, 1011-1016.

49. D. Kuhbeck, J. Mayr, M. Haring, M. Hofmann, F. Quignard and D. Díaz Díaz, *New J.Chem.*, 2015, **39**, 2306–2315.

50. P. Vongvilai, M. Angelin, R. Larsson and O. Ramstrom, *Angew. Chem. Int. Ed.*, 2007, **46**, 948–950.

51. P. Vongvilai, R. Larsson and O. Ramstrom, *Adv. Synth. Catal.*, 2008, **350**, 448–452.

52. Y. Zhang, L. Hu and O. Ramstrom, *Chem. Commun.*, 2013, **49**, 1805–1807.

53. S. Dutta, N. Kumari, S. Dubbu, S. W. Jang, A. Kumar, H. Ohtsu, J. Kim, S. H. Cho, M. Kawano and I. S. Lee, *Angew. Chem. Int. Ed.*, 2020, **132**, 3444–3450.

54. Foley, and M. Aoife, *Tetrahedron,* 2018, **74(13)**, 1435-1443.

55. M. Dadashipour and Y. Asano, *ACS Catal.*, 2011, **1**, 1121–1149.

56. I. P. Cheng and J. E. Poulton, *Plant Cell Physiol.* 1993, **34**, 1139–1143.

57. D. Alagoz, S. S. Tukel and D. Yildirim, *J. Mol. Catal. B Enzym.*, 2014, **101**, 40–46.

58. S. Nanda, Y. Kato and Y. Asano, *Tetrahedron*, 2005, **61**, 10908–10916.

59. S. Nanda, Y. Kato and Y. Asano, *Tetrahedron: Asymmetry*, 2006, **17**, 735–741.

60. L. Yao, H. Li, J. Yang, C. Li and Y. Shen, *Int. J. Biol. Macromol.*, 2018, **118,** 189–194.

61. F. Motojima, A. Nuylert and Y. Asano, *FEBS J.*, 2018, **285,** 313–324.

62. T. Ueatrongchit, K. Tamura, T. Ohmiya, A. H-Kittikun and Y. Asano, *Enzyme Microb.Technol.*, 2010, **46**, 456–465.

63. A. Nuylert, Y. Ishida and Y. Asano, *ChemBioChem*., 2017, **18**, 257–265.

64. Y. C. Zheng, J. H. Xu, H. Wang, G. Q. Lin, R. Hong and H. L. Yu, *Adv. Synth. Catal.*, 2017 **359**, 1185–1193.

65. R. Bhunya, T. Mahapatra, and S. Nanda, *Tetrahedron: Asymmetry*, 2009, **20,** 1526–1530.

66. M. Asif and T.C. Bhalla, *Catal Lett.*, 2016, **146**, 1118–1127.

67. M. Asif and T.C. Bhalla, *Catal. Lett.*, 2017, **147**, 1592–1597.

68. M. Bekerle-Bogner, M. Gruber-Khadjawi, H. Wiltsche, R. Wiedner, H. Schwab and K. Steiner, *ChemCatChem*, 2016, **8**, 2214–2216.

69. M. Dadashipour, M. Yamazaki, K. Momonoi, K. Tamura, K.I. Fuhshuku, Y. Kanase, E. Uchimura, G. Kaiyun and Y. Asano, *J. Biotechnol.*, 2011, **153**, 100–110.

70. T. Purkarthofer, W. Skranc, C. Schuster and H. Griengel, *Appl. Microbiol. Biotechnol.*, 2007, **76**, 309–320.

71. D. V. Johnson, A. A. Z. Mackova and H. Griengel, *Curr Opin Chem Biol.*, 2000, **4**, 103–109.

72. J. N. Andexer, J. V. Langermann, U. Kragl and M. Pohl, *Trends Biotechnol.*, 2009, **27**, 599–607.

73. M. Sharma, N. N. Sharma and T. C. Bhalla, *Enzyme Microb. Technol.*, 2005, **37**, 279–294.

74. P. Bracco, H. Busch, J. V. Langermann and U. Hanefeld, *Org. Biomol. Chem.*, 2016, **14**, 6375–6389.

75. S. K. Padhi, *ChemBioChem*, 2017, **18**, 152–160.

76. M. A. Kassim and K. Rumboldt, *Biotechnol. Lett.*, 2014, **36**, 223-228.

77. M. Brovetto, D. Gamenara, P. S. Mendez and G. A. Seoane, *Chem. Rev.*, 2011, **111**, 4346-4403.

78. T. Purkarthofer, K. Gruber, M. Gruber-Khadjawi, K. Waich, W. Skranc, D. Mink and H. Griengl, *Angew. Chemie - Int. Ed.*, 2006, **45**, 3454–3456.

79. M. Gruber-Khadjawi, T. Purkarthofer, W. Skranc and H. Griengl, *Adv. Synth. Catal.*, 2007, **349**, 1445–1450.

80. K. I. Fuhshuku and Y. Asano, *J. Biotechnol.*, 2011, **153**, 153–159.

81. S. E. Milner, T. S. Moody and A. R. Maguire, *European J. Org. Chem.*, 2012, **16**, 3059–3067.

82. R. Wiedner, B. Kothbauer, T. Pavkov-Keller, M. Gruber-Khadjawi, K. Gruber, H. Schwab and K. Steiner, *ChemCatChem*, 2015, **7**, 325–332.

83. X. Yu, B. Pérez, Z. Zhang, R. Gao and Z. Guo, *Green Chem.*, 2016, **18**, 2753–2761.

84. T. Devamani, A. M. Rauwerdink, M. Lunzer, B. J. Jones, J. L. Mooney, M. A. O. Tan, Z. J. Zhang, J. H. Xu, A. M. Dean and R. J. Kazlauskas, *J. Am. Chem. Soc.*, 2016, **138**, 1046–1056.

85. J. Andexer, J. Von Langermann, A. Mell, M. Bocola, U. Kragl, T. Eggert and M. Pohl, *Angew. Chemie - Int. Ed.*, 2007, **46**, 8679–8681.

86. R. Yuryev, T. Purkarthofer, M. Gruber, H. Griengl and A. Liese, *Biocatal. Biotransformation*, 2010, **28**, 348–356.

87. R. Yuryev, S. Briechle, M. Gruber-Khadjawi, H. Griengl and A. Liese, *ChemCatChem*, 2010, **2**, 981–986.

88. J. Von Langermann, D. M. Nedrud and R. J. Kazlauskas, *ChemBioChem*, 2014, **15**, 1931–1938.

89. D. H. S. Rao and S. K. Padhi, *ChemBioChem*, 2019, **20**, 371–378.

90. D. H. S. Rao, Kummari. Shivani, S. K. Padhi, *Appl. Biochem. Biotechnol.*, 2020, **193**, 560-576.

91. T. Fujisawa, H. Hayashi and Y. Kishioka, *Chem. Lett.*, 1987, **16**, 129–132.

92. S. R. Wallner, I. Lavandera, S. F. Mayer, R. Öhrlein, A. Hafner, K. Edegger, K. Faber and W. Kroutil, *J. Mol. Catal. B: Enzym.*, 2008, **55**, 126–129.

93. S. Venkataraman and A. Chadha, *RSC Adv.*, 2015, **5**, 73807–73813.

94. A. Chadha, S. Venkataraman, R. Preetha and S. K. Padhi, *Bioorg. Chem.*, 2016, **68**, 187–213.

95. F. Tentori, E. Brenna, D. Colombo, M. Crotti, F. G. Gatti, M. G. Chiara and G. Pedrocchi-Fantoni, *Catalysts*, 2018, **8**, 308.

96. Z. Wang, X. Wu, Z. Li, Z. Huang and F. Chen, *Org. Biomol. Chem.*, 2019, **17**, 3575– 3580.

97. Hasnaoui, J. H. Lutje Spelberg, E. De Vries, L. Tang, B. Hauer and D. B. Janssen, *Tetrahedron: Asymmetry*, 2005, **16**, 1685–1692.

98. G. Hasnaoui-Dijoux, M. M. Elenkov, J. H. Lutje Spelberg, B. Hauer and D. B. Janssen, *ChemBioChem,*2008, **9**, 1048–1051.

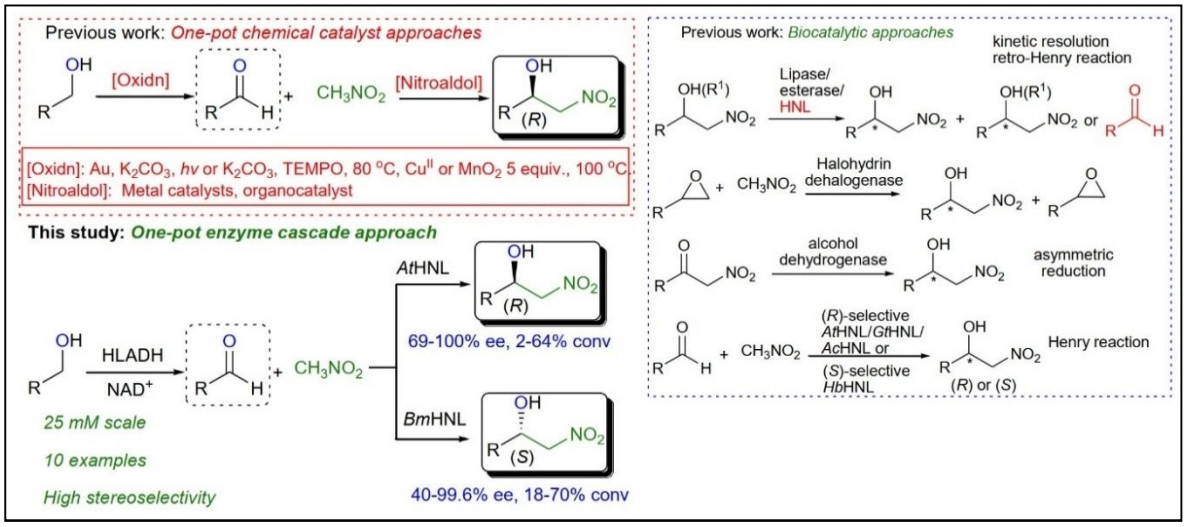
Chapter 2

One-pot enzyme cascade in the synthesis of enantiocomplementary chiral β-nitroalcohols starting from aromatic primary alcohols

2.1. Introduction

Enantioenriched β-nitroalcohols represent versatile precursors and central chiral intermediates used in the synthesis of a large number of pharmaceuticals and biologically active molecules (Figure 2.1).[1–8] Conventional chemical approaches in the enantioselective synthesis of β-nitroalcohols from simple and readily available primary alcohols involve a two-step process of oxidation followed by a nitroaldol reaction. Herrera et al. synthesized several aromatic (*S*)-β-nitroalcohols by MnO_2 catalyzed oxidation of benzylic alcohols followed by trifunctional squaramide catalysed nitroaldol reaction.[9] Gold nanoparticles immobilized in porphyrin-containing homochiral covalent organic framework were used in the photothermal conversion of primary alcohols into (*R*)-β-nitroalcohols.[10] Maria et al. used K_2CO_3 and TEMPO to oxidize alcohols and a Cu(II) complex to catalyze the nitroaldol reaction.[11] Alternative to these chemical approaches (Scheme 2.1), biocatalytic syntheses have gained impetus in preparing versatile chiral β-nitroalcohols in recent years. Biocatalytic synthesis of chiral β-nitroalcohols is carried out using three major approaches: kinetic resolution, asymmetric reduction, and Henry reaction (Scheme 2.1). Lipase, esterase, halohydrin dehalogenase, and HNL catalyzed retro-Henry reaction are primarily used in the kinetic resolution of a racemic β-nitroalcohol or an epoxide.[12–16] Alcohol dehydrogenase catalyzed asymmetric reduction[17–20] and HNL catalyzed asymmetric nitroaldol reaction[21–25] are the other two routes. Both kinetic resolution and asymmetric reduction require an additional step of substrate preparation, while the former could provide a maximum 50% theoretical yield. Dynamic kinetic resolution overcomes the yield limitation, however, it is not purely biocatalytic. It uses lipase-catalyzed kinetic resolution combined with a chemical catalyst in the racemization of the less reactive enantiomer.[26–28] The Henry reaction is an atom economy and efficient approach to prepare β-nitroalcohols that involves C–C bond formation between an aldehyde and a nitroalkane.[29] Three (*R*)-selective HNLs, *At*HNL, *Granulicella tundricola* (*Gt*HNL), and *Acidobacterium capsulatum* (*Ac*HNL) have been reported for the promiscuous Henry reaction, while *Hevea brasiliensis* HNL (*Hb*HNL) is the only (*S*)-selective one known so far.[21–24] Yu et al. reported about an acyl-peptide releasing enzyme from *Sulfolobus tokodaii* (ST0779) that catalyzed the enantioselective synthesis of β-nitroalcohols. However, the catalyst does not show uniform enantiopreference; rather, its enantioselectivity varies with the electronic effects of the substituents on the benzaldehyde ring.[30] Further, the transformation was carried out on a 0.1 mM scale using 20 mg of the purified enzyme at 40 °C. A major limitation of the biocatalytic Henry reaction is it uses reactive aldehydes. Benzaldehyde at high concentrations is known to inhibit HNLs.[31,32] Aldehydes could form Schiff-base with lysine residues in the enzyme and potentially decrease enzyme activity by causing partial denaturation that limits the high-yield product formation. Reactions involving aldehydes as starting substrates often require in situ preparation due to their instability.[33,34] Further, free aldehydes are prone to undergo aerobic oxidation and other side reactions. Considering the limitations in the use of aldehydes as starting substrates in chemical as well as in the biocatalytic synthesis of chiral β-nitroalcohols, there is a need to use an alternate starting substrate. Alcohols are the reduced form of aldehydes and can be used as surrogate molecules for the corresponding aldehydes. Therefore, developing

a sustainable, environment-friendly, and atom-economy approach for the stereoselective synthesis of β-nitroalcohols starting from simple alcohols would be highly beneficial. Biocatalysis provides green and sustainable technology in synthesizing diverse chemical structural units with high selectivity.[35] Especially remarkable advances have been achieved in enzyme cascade catalysis in the stereoselective synthesis of a diverse range of chiral intermediates.[36–42] Biocatalytic cascades have several advantages, such as intermediate purification becomes inessential, reduction of waste and production cost, improvement in product yield, etc. However, the development of stereocomplementary selective synthetic transformations yet remains a challenge in biocatalytic cascade processes. We have developed a one-pot enzyme cascade for the sustainable conversion of primary alcohols into enantiopure β-nitroalcohols. The enzyme cascade consists of horse liver alcohol dehydrogenase (HLADH) catalyzed oxidation of benzylic alcohols to their corresponding aldehydes with concurrent Henry reaction by *At*HNL in the stereoselective synthesis of (*R*)-β-nitroalcohols (Scheme 2.1). To synthesize the opposite stereoisomer, we exploited the synthetic potential of *Bm*HNL, another natural HNL with complementary stereoselectivity, whose catalytic ability in promiscuous stereoselective Henry reaction was not proved earlier. This method functionalizes the sp^3 C–H bond of inexpensive, stable, readily available benzylic alcohols to produce value-added chiral intermediates in one pot. The cascade is successful in asymmetrization of primary alcohols to produce both the enantiomers of β- nitroalcohols.



Scheme 2.1: Chemical (top left), biocatalytic (right), and current method (bottom left) of syntheses of enantiopure β-nitroalcohols.

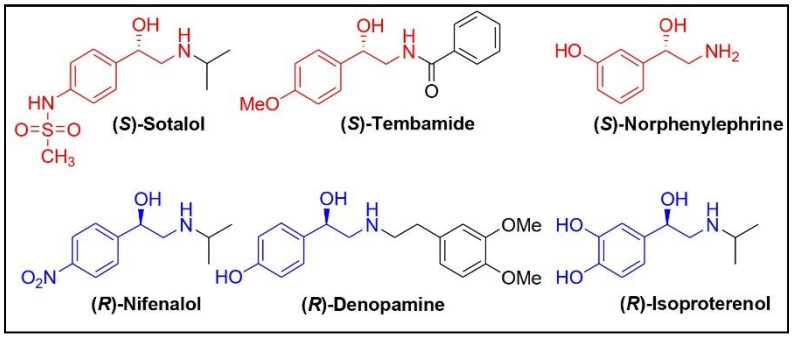


Figure 2.1: Representative examples of enantiopure aromatic β-nitroalcohols as chiral intermediates of some pharmaceuticals and biologically active molecules (the reduced forms of β-nitroalcohols are shown in color)

2.2. Objectives

1. To study the inhibition effect of the enzymes used in the cascade.

2. To address the pH hurdle of the enzymes of the HLADH-*At*HNL cascade.

3. To optimize the reaction conditions of the HLADH-*At*HNL cascade.

4. To unravel the substrate scope of HLADH-*At*HNL cascade in the stereoselective syntheses of diverse (*R*)-β-nitroalcohols.

5. To study the promiscuous activity of *Bm*HNL and optimization of different biocatalytic parameters in the stereoselective nitroaldol reactions.

6. To explore the substrate scope of HLADH-*Bm*HNL cascade in the stereoselective syntheses of diverse (*S*)-β-nitroalcohols.

2.3. Materials and methods

2.3.1. Chemicals and materials

The recombinant *At*HNL gene in pET28a plasmid was synthesized and purchased from Abgenex Pvt. Ltd, India. *Bm*HNL cloning and expression detail have been described earlier.[43] HLADH (LOC100034242, an alcohol dehydrogenase-E-isoenzyme of *Equus caballus*) synthetic gene cloned into pET14b at *BamH*I and *Sal*I restriction sites was procured and further used. Culture media, kanamycin, and ampicillin were purchased from HiMedia Laboratory Pvt. Ltd, India. Isopropyl-β-D-1-thiogalactopyranoside was purchased from BR-BIOCHEM Pvt. Ltd, and SRL India. Aldehydes, nitromethane, and mandelonitrile were purchased from Sigma Aldrich, AVRA, SRL, TCI, and Alfa-Aesar. HPLC grade solvents were obtained from RANKEM, Molychem, FINAR, and SRL, India. Chemicals purchased were used without purification.

2.3.2. Heterologous expression, purification, and assay of enzymes

2.3.2.1. Heterologous expression, purification, and assay of HLADH

An overnight 30 mL of Luria Bertani culture of *E. coli* BL21 (DE3) harboring the recombinant plasmid pET14b-HLADH with 100 µg/mL ampicillin was transferred to a 3 L LB culture having 100 µg/mL ampicillin. The cells were grown at 37 °C, 200 rpm, until OD_{600} reached 0.5 to 0.8. The culture was induced with 1 mM IPTG at 25 °C for 24 h. Cells were harvested by centrifuging at 8000 rpm for 12 minutes, and the cell pellet was suspended in 50 mM Tris-HCl buffer pH 8.8. The cell suspension was sonicated, and the crude cell extract was centrifuged at 10,000 rpm. The protein was purified with a Ni–NTA agarose column using binding buffer 20 mM imidazole, 300 mM NaCl, and 50 mM Tris – HCl buffer pH 8.8 as a binding buffer and 50 mM imidazole, 300 mM NaCl, and 50 mM Tris-HCL buffer pH 8.8 as wash buffer. The protein was eluted using 500 mM imidazole, 300 mM NaCl, and 50 mM Tris-HCL buffer pH 8.8, and the eluent was dialyzed in 50 mM Tris-HCl buffer pH 8.8 three times.

The HLADH assay was carried out in a 96 well plate and in triplicates. Each reaction well of total 200 µL was comprised of 158 µL of water, Tris-HCl buffer pH 8.8 (1 M, 10 µL), purified HLADH (0.025 mg/mL, 20 µL), ethanol (100 mM, 10 µL), and freshly prepared NAD^+ (100 mM, 2 µL). In the control experiment, purified HLADH was replaced with 50 mM Tris-HCl

buffer pH 8.8, keeping other reaction components similar. The molar extinction coefficient for NADH was taken as 6220 M^{-1} cm^{-1}. HLADH activity was determined by monitoring the continuous formation of NADH at 340 nm. One unit of HLADH activity is defined as 1 µmol of NADH formed per minute in the reaction system.

2.3.2.2. Heterologous expression, purification, and assay of *At*HNL

*At*HNL protein expression and purification were performed according to the protocol described earlier.[23,14] *At*HNL activity was measured by a spectrophotometric assay that monitored the formation of benzaldehyde from racemic mandelonitrile at 280 nm. The reaction was performed in a 96 well microtiter plate. Each well of the plate consisted of 160 µL of 50 mM citrate phosphate buffer, pH 5.5, 20 µL of purified *At*HNL (0.075 mg/mL), and 20 µL of 67 mM mandelonitrile solution prepared in 5 mM citrate phosphate buffer, pH 3.15. The activity was calculated using the molar extinction coefficient of benzaldehyde (1380 M^{-1} cm^{-1}). One unit of HNL activity is defined as the amount of enzyme that produces 1 µmol of benzaldehyde from mandelonitrile per minute. All measurements were performed in triplicates. The control experiment had all the reaction components except the enzyme, replaced by its corresponding buffer. One unit of *At*HNL activity is defined as 1 µmol of benzaldehyde formed per minute in the reaction medium.[23,14]

2.3.2.3. Heterologous expression, purification, and assay of *Bm*HNL

E.coli BL21 (DE3) cells carrying pCold1-*Bm*HNL plasmid were inoculated into sterile Luria Bertani broth comprised of 100 µg/mL ampicillin antibiotic and incubated at 37 °C for 12 to 16 h at 180 rpm. A 1% (v/v) of this cultured inoculum was used for secondary culture and incubated at 37 °C until OD_{600} reached 0.5 to 0.8. After getting the appropriate cell density, the culture was incubated at 4 °C for 2 hours to induce a cold shock. The *Bm*HNL protein expression was then induced with 1 mM IPTG, and the culture was incubated at 18 °C for 24 h at 180 rpm. Cells were harvested by centrifuging at 8000 rpm for 12 minutes, and the cell pellet was suspended in 20 mM potassium phosphate buffer pH 7.0 (KPB). The cells were sonicated, and crude cell extract was purified by Ni-NTA affinity chromatography, where three purification buffers were used. They are binding buffer (20 mM imidazole + 20 mM KPB + 300 mM NaCl), wash buffer (50 mM imidazole + 20 mM KPB + 300 mM NaCl), and elution buffer (500 mM imidazole + 20 mM KPB + 300 mM NaCl). After purification, the eluent was dialyzed thrice in 20 mM KPB pH 7. *Bm*HNL's specific activity determination also measured benzaldehyde formation similar to the *At*HNL assay in a 96 well plate using 1 mg/mL of enzyme concentration.[44]

2.3.3. Kinetics and inhibition studies

2.3.3.1. Steady-state kinetics of HLADH

Steady-state kinetics of HLADH was performed using the NADH assay described in 2.3.2.1 above where benzyl alcohol was used as the substrate and varied its concentration from 0.005 to 20 mM. The reaction was monitored for 1 minute. Absorbance of control was subtracted from the enzymatic reaction. Best fit of the data to Michaelis-Menten equation was done using the Solver function of Microsoft excel.

2.3.3.2. Inhibition of HLADH by benzaldehyde

The inhibitory effect of benzaldehyde on HLADH was studied by incubating the enzyme (0.025 mg/mL) with 0, 1, 5, 25, and 50 mM of benzaldehyde for 3 h at 30 °C, and immediately kept in ice for 10 to 15 minutes.[34] Subsequently, when it came to room temperature, HLADH kinetics was done with different benzyl alcohol concentrations, keeping NAD^+ concentration constant (1 mM), as per the HLADH assay described earlier. The detailed reaction protocol was as follows. For each benzaldehyde concentration, the reaction mixture consisted of 50 mM Tris-HCl buffer pH 8.8, purified HLADH 0.5 µg, 1 mM NAD^+, a varied concentration of benzyl alcohol, and the final volume was adjusted to 200 µL. In case of no benzaldehyde, the benzyl alcohol concentration was 0.01 to 20 mM. For 1 mM benzaldehyde, the benzyl alcohol concentration was 0.01 to 40 mM. For 5 mM benzaldehyde, the benzyl alcohol concentration was 0.05 to 40 mM. The benzyl alcohol concentration was 0.1 to 200 mM in the case of 25 mM benzaldehyde, and for 50 mM benzaldehyde, the benzyl alcohol concentration was 10 to 200 mM. The data was used to plot the MM curve.

2.3.3.3. Inhibitory effects of benzyl alcohol and benzaldehyde on *At*HNL

The inhibitory effect of benzyl alcohol on *At*HNL's activity was determined. The *At*HNL in 0.075 mg/mL was then incubated with 0, 1, 5, 25, and 50 mM benzyl alcohol. Each reaction well contained 160 µL of 50 mM citrate-phosphate buffer pH 5.5, 20 µL 0.075 mg/mL purified *At*HNL protein, and 20 µL of 67 mM racemic mandelonitrile solution. In the control reaction, all reactants were added except purified *At*HNL was replaced by 20 mM KPB pH 7.0. The inhibitory effect of benzaldehyde on *At*HNL was also measured using a similar protocol as above. In this case, 0, 1, 5, 25, and 50 mM of benzaldehyde were used instead of benzyl alcohol. Further, the assay used 20 µL of 75 mM racemic mandelonitrile solution instead of 67 mM stock solution. Prior to its use in the experiment, the *At*HNL was kept for 3 h at 30 °C in different concentrations of benzyl alcohol or benzaldehyde, followed by an ice incubation of 10 to 15 minutes.

2.3.3.4. Inhibitory effects of benzyl alcohol and benzaldehyde on *Bm*HNL

The experimental protocol of 2.3.3.3. was used here to study the inhibitory effects of benzyl alcohol and benzaldehyde on *Bm*HNL. All the reaction conditions remained the same, except the concentration of *Bm*HNL was 1 mg/mL, unlike 0.075 mg/mL.

2.3.4. Optimization of reaction conditions of HLADH-*At*HNL cascade

Fifteen different reaction parameters of this enzymatic cascade were optimized. Each of them is elaborated below. Before carrying out every optimization reaction, the specific activity of the enzyme used was determined using ethanol oxidation assay for HLADH and mandelonitrile cleavage assay for *At*HNL, as described above.

2.3.4.1. Optimization of buffer system and its pH

Two different buffer systems, KPB and acetate buffer, and three different pH 6.0, 6.5, and 7.0, were selected for this optimization study. Acetone and benzyl alcohol stock were made in *n*-butyl acetate. $ZnCl_2$ and NAD^+ stocks were made in autoclaved double distilled water. The reaction mixture contained 580 µL *n*-butyl acetate, 1 U of HLADH in 50 mM Tris-HCl buffer pH 8.8, 80 U of *At*HNL in 20 mM KPB pH 7, 50 mM of different buffers, 1 mM NAD^+ (100 mM, 10 µL), 150 mM acetone (3 M, 50 µL), 0.91 M nitromethane (50 µL), 0.1 mM $ZnCl_2$ (10 mM, 10 µL), and 20 mM benzyl alcohol (1 M, 20 µL). The control experiment replaced HLADH and *At*HNL enzymes with a corresponding equal volume of 50 mM Tris-HCl buffer

and 20 mM KPB, respectively. The total reaction volume was made up to 1 mL by adding autoclaved double distilled water. This reaction mixture was incubated at 30 °C and 1,200 rpm in a thermoshaker. A 50 µL of an aliquot of this reaction was mixed with 350 µL of hexane: 2-propanol (93:7). The mixture was vortexed vigorously, followed by dried over sodium sulfate to remove any aqueous contamination, then centrifuged at 15000*g* for 5 min at 4 °C. A 20 µL of this sample was analyzed in HPLC using the CHIRALPACK® IB column. HPLC conditions: *n*-hexane: 2-propanol = 93:7 (v/v), flow rate: 1 mL/min, and absorbance: 210 nm. The retention times of benzaldehyde, benzyl alcohol, (*R*)-2-nitro-1-phenylethanol (NPE), and (*S*)-NPE are 4.95, 8.78, 15.37, and 18.02 min, respectively.

2.3.4.2 Screening for cofactor recycling agent

Two carbonyl compounds, acetaldehyde and acetone, were selected as cofactor recycling agents for screening. Acetaldehyde stock was made in *n*-butyl acetate. The reaction mixture contained 580 µL *n*-butyl acetate, 5 U of HLADH in 50 mM Tris-HCl buffer pH 8.8, 200 U of *At*HNL in 20 mM KPB pH 7.0, 50 mM KPB pH 6.0 (1 M, 50 µL), 1 mM NAD^+ (100 mM, 10 µL), 150 mM acetone/ acetaldehyde (3 M, 50 µL), 0.91 M nitromethane (50 µL), 0.1 mM zinc chloride (10 mM, 10 µL), and 20 mM benzyl alcohol (1 M, 20 µL). The total reaction volume was made up to 1 mL by adding autoclaved double distilled water. Aliquot extraction and HPLC analysis were done according to the previously described method.

2.3.4.3. Optimization of *At*HNL content

Four enzyme concentrations ranging from 400 to 1000 U were chosen for this optimization study. The detailed reaction conditions were as follows 580 µL *n*-butyl acetate, 5 U of HLADH in 50 mM Tris-HCl buffer pH 8.8, four different concentrations of *At*HNL (400, 600, 800, and 1000 U in 20 mM KPB pH 7.0), 50 mM KPB pH 6.0, 1 mM NAD^+ (100 mM, 10 µL), 150 mM acetaldehyde, 0.91 M nitromethane, 0.1 mM $ZnCl_2$, 20 mM benzyl alcohol, and remaining volume was adjusted with double distilled water to get total 1 mL. In the case of lower *At*HNL contents, 20 mM KPB pH 7.0 was used to adjust the remaining volume equivalent to the case of 1000 U *At*HNL. Aliquot extraction and HPLC analysis were done according to the previously described method.

2.3.4.4. Optimization of cofactor (NAD^+) concentration

In this study, eight different NAD^+ concentrations (0.2 to 3 mM) were used. The reaction mixture contained 580 µL *n*-butyl acetate, 5 U of HLADH in 50 mM Tris-HCl buffer pH 8.8, 800 U of *At*HNL in 20 mM KPB pH 7.0, 50 mM KPB pH 6.0, eight different NAD^+ concentrations 0.2, 0.5, 0.8, 1.0, 1.5, 2.0, 2.5, and 3.0 mM NAD^+ (stock 100 mM), 150 mM acetaldehyde, 0.91 M nitromethane, 0.1 mM $ZnCl_2$, 20 mM benzyl alcohol, and remaining volume was adjusted with autoclaved double distilled water to get total 1 mL. Aliquot extraction and HPLC analysis were done according to the previously described method.

2.3.4.5. Optimization of HLADH content

HLADH enzyme content was optimized by varying its amount from 1 to 5 U, keeping other reaction parameters constant. The detailed reaction conditions were as follows: 580 µL *n*-butyl acetate, five different HLADH amounts i.e., 0.5, 1, 2, 3, 4, and 5 U of HLADH in 50 mM Tris-HCl buffer pH 8.8, 800 U of *At*HNL in 20 mM KPB pH 7.0, 50 mM KPB pH 6.0, 0.8 mM NAD^+, 150 mM acetaldehyde, 0.91 M nitromethane, 0.1 mM $ZnCl_2$, 20 mM benzyl alcohol, and remaining volume was adjusted with double distilled water to get total 1 mL. For lower

HLADH contents, 50 mM Tris-HCl buffer pH 8.8 was used to adjust the remaining volume equivalent to the case of 5 U of HLADH. Aliquot extraction and HPLC analysis were done according to the previously described method.

2.3.4.6. Optimization of concentration of KPB pH 6.0

Four different concentrations, i.e., 50, 100, 150, and 200 mM of KPB pH 6.0, were taken for this study. Reaction conditions: 580 µL *n*-butyl acetate, 2 U of HLADH in 50 mM Tris-HCl buffer pH 8.8, 800 U of *At*HNL in 20 mM KPB pH 7.0, four different concentrations of KPB (pH 6) 50, 100, 150, and 200 mM (stock 1 M), 0.8 mM NAD^+, 150 mM acetaldehyde, 0.91 M nitromethane, 0.1 mM $ZnCl_2$, 20 mM benzyl alcohol, and remaining volume was adjusted with double distilled water to get total 1 mL. Aliquot extraction and HPLC analysis remained the same as described previously.

2.3.4.7. Optimization of nitromethane concentration

Five different nitromethane concentrations ranging from 0.5 to 2.5 M, were selected for this optimization study. We used 50 µL/mL of reaction volume equivalent to 0.91 M of nitromethane in the preceding experiments. The reaction mixture contained 580 µL *n*-butyl acetate, 2 U of HLADH in 50 mM Tris-HCl buffer pH 8.8, 800 U of *At*HNL in 20 mM KPB pH 7.0, 100 mM KPB pH 6.0, 0.8 mM NAD^+, 150 mM acetaldehyde, five different nitromethane concentrations 0.5, 0.91, 1.5, 2 and 2.5 M, 0.1 mM $ZnCl_2$, 20 mM benzyl alcohol, and remaining volume was adjusted with double distilled water to get total 1 mL. Aliquot extraction and HPLC analysis were done according to the previously described method.

2.3.4.8. Optimization of the biphasic system

We selected five different organic solvents to evaluate them in the biphasic system in the cascade. They were diethyl ether (log_p = 0.89), TBME (log_p = 0.94), DIPE (log_p = 1.52), *n*-butyl acetate (log_p = 1.78), and toluene (log_p = 2.73). The reaction conditions used are: 580 µL of different organic solvents, 2 U of HLADH in 50 mM Tris-HCl buffer pH 8.8, 800 U of *At*HNL in 20 mM KPB pH 7.0, 100 mM KPB pH 6.0, 0.8 mM NAD^+, 150 mM acetaldehyde, 1.5 M nitromethane, 0.1 mM $ZnCl_2$, 20 mM benzyl alcohol, and remaining volume was adjusted with double distilled water to get total 1 mL. Aliquot extraction and HPLC analysis were done according to the previously described method.

2.3.4.9. Optimization of organic solvent content

Five different % v/v of *n*-butyl acetate ranging from 45 to 65 were taken for this optimization study. The detailed reaction condition used are as follows. To five different organic solvent v/v ratios, i.e., 65% (580 µL), 60% (530 µL), 55% (480 µL), 50% (430 µL), and 45% (380 µL), were added to a mixture of 2 U of HLADH in 50 mM Tris-HCl buffer pH 8.8, 800 U of *At*HNL in 20 mM KPB pH 7.0, 100 mM KPB pH 6.0, 0.8 mM NAD^+, 150 mM acetaldehyde, 1.5 M nitromethane, 0.1 mM $ZnCl_2$, 20 mM benzyl alcohol, and. The total volume was adjusted to 1 mL by adding remaining volume of double distilled. Aliquot extraction and HPLC analysis were done according to the previously described method.

2.3.4.10. Intermittent addition of benzyl alcohol and HLADH

In the HLADH-*At*HNL cascade study, we observed that HLADH catalyzed benzaldehyde formation rate is much higher than the rate of *At*HNL catalyzed synthesis of (*R*)-NPE. We assumed that if benzaldehyde formation can be controlled, it would increase *At*HNL's

efficiency in the formation of (*R*)-NPE by minimizing inhibition of the HNL caused by benzaldehyde. We anticipated that benzaldehyde accumulation in the reaction could be minimized by slow addition (at specific time intervals) of either HLADH or benzyl alcohol, which may result in controlled production of benzaldehyde. To decrease the benzaldehyde production rate, we introduced HLADH (enzyme) and benzyl alcohol (substrate) intermittently into the reaction system at different time points, keeping all the reactants constant. The reaction conditions of 2.3.4.9 were adopted using 50% *n*-butyl acetate. Aliquot extraction and HPLC analysis were done according to the previously described method. Three different addition strategies were adopted as follows (Table 2.1).

Table 2.1: Details of intermittent addition of HLADH and benzyl alcohol in the cascade

Time (h)	Intermittent HLADH with 20 µmol benzyl alcohol	Intermittent benzyl alcohol with 2 U of HLADH	Intermittent combination
0	0.25 U HLADH	2.5 µmol benzyl alcohol	2.5 µmol benzyl alcohol + 0.25 U HLADH
0.5	0.25 U HLADH	2.5 µmol benzyl alcohol	2.5 µmol benzyl alcohol + 0.25 U HLADH
1	0.25 U HLADH	2.5 µmol benzyl alcohol	2.5 µmol benzyl alcohol + 0.25 U HLADH
1.5	0.25 U HLADH	2.5 µmol benzyl alcohol	2.5 µmol benzyl alcohol + 0.25 U HLADH
2	0.25 U HLADH	2.5 µmol benzyl alcohol	2.5 µmol benzyl alcohol + 0.25 U HLADH
2.5	0.25 U HLADH	2.5 µmol benzyl alcohol	2.5 µmol benzyl alcohol + 0.25 U HLADH
3	0.25 U HLADH	2.5 µmol benzyl alcohol	2.5 µmol benzyl alcohol + 0.25 U HLADH
3.5	0.25 U HLADH	2.5 µmol benzyl alcohol	2.5 µmol benzyl alcohol + 0.25 U HLADH

2.3.4.11. Optimization of substrate concentration

Failed with the above approach to control benzaldehyde accumulation, we planned to study the effect of the amount of benzyl alcohol on the cascade. Six different benzyl alcohol concentrations ranging from 15 to 40 mM were selected for this study. Here, along with benzyl alcohol, the concentration of HLADH, benzyl alcohol, NAD^+, and acetaldehyde were altered by maintaining their uniform ratio (Table 2.2). The components that remained common to all these experiments in this optimization study were: 800 U of *At*HNL, 83 µL of nitromethane, 100 mM pH 6.0 KPB (1.25 M, 80 µL), and 10 µL of 10 mM $ZnCl_2$. The total reaction volume was made up to 1 mL by adding autoclaved double distilled water. The reaction conditions, aliquot extraction, and HPLC analysis were done according to the previously described method.

Table 2.2: Detail of reaction conditions used for this optimization study

benzyl alcohol (mM)	*n*-butyl acetate (µL)	HLADH (U)	100 mM NAD^+ (µL)	3 M acetaldehyde (µL)	1 M benzyl alcohol (µL)
15	447.5	1.5	6	37.5	15

20	430	2	8	50	20
25	412.5	2.5	10	62.5	25
30	395	3	12	75	30
35	377.5	3.5	14	87.5	35
40	360	4	16	100	40

2.3.4.12. Optimization of protein stabilizer

Benzaldehyde's destabilizing effect on *Hb*HNL structure[45] has motivated us to study the impact of protein stabilizers on this cascade. Our recent study revealed that glycerol could stabilize *Bm*HNL and improve its enantioselectivity in mandelonitrile synthesis.[46] Guterl et al. found two protein stabilizers, sucrose and sorbitol, which increased the half-life of *At*HNL by 24 to 36 fold when incubated at room temperature compared to the non-stabilizer condition.[47] We thus investigated the effect of the same two protein stabilizers in our cascade by adding them in 100 mg/mL. The reaction mixture consisted of 413 µL of different organic solvents, 2.5 U of HLADH in 50 mM Tris-HCl buffer pH 8.8, 800 U of *At*HNL in 20 mM KPB pH 7.0, 100 mM KPB pH 6.0, 1 mM NAD^+, 187.5 mM acetaldehyde, 1.5 M nitromethane, 0.1 mM $ZnCl_2$, 25 mM benzyl alcohol, 100 mg/mL of sucrose (0.8 gm/mL, 125 µL) or sorbitol and remaining volume was adjusted with double distilled water to get total 1 mL. Aliquot extraction and HPLC analysis were done according to the previously described method.

2.3.4.13. Optimization of cofactor recycling agent (acetaldehyde) concentration

The cofactor recycling agent acetaldehyde plays an indirect but important role in product synthesis, and hence, its concentration was optimized. The reaction mixture contained 2.5 U of HLADH in 50 mM Tris-HCl buffer pH 8.8, 800 U of *At*HNL in 20 mM KPB pH 7.0, 100 mM KPB pH 6.0, 1 mM NAD^+, 187.5 mM acetaldehyde, 1.5 M nitromethane, 0.1 mM $ZnCl_2$, 100 mg/mL of sorbitol, 25 mM benzyl alcohol, five different acetaldehyde concentrations ranging from 75 to 187.5 mM in different volumes of *n*-butyl acetate and remaining volume was adjusted with double distilled water to get total 1 mL. For 75, 100, 125, 150, and 187.5 mM acetaldehyde, 450, 442, 433, 425, and 413 µL of *n*-butyl acetate were taken, respectively. Aliquot extraction, and HPLC analysis were done according to the previously described method.

2.3.4.14. Optimization of reaction time

The reaction time of the HLADH-*At*HNL cascade was optimized by monitoring the reaction at four different time points from 2 to 8 h. The reaction mixture contained 433 µL of *n*-butyl acetate, 2.5 U of HLADH in 50 mM Tris-HCl buffer pH 8.8, 800 U of *At*HNL in 20 mM KPB pH 7.0, 100 mM KPB pH 6.0, 1 mM NAD_+, 125 mM acetaldehyde, 1.5 M nitromethane, 0.1 mM $ZnCl_2$, 100 mg/mL sorbitol, 25 mM benzyl alcohol, and the rest volume up to 1 mL is autoclaved double distilled water. Aliquot extraction, and HPLC analysis were done according to the previously described method.

2.3.4.15. Optimization of sorbitol concentration

To determine the minimum concentration of stabilizer that could be effective in the stereoselective synthesis by the cascade, we varied the sorbitol concentration from 10 to 200 mg/mL. The reaction mixture composed of 433 µL of *n*-butyl acetate, 2.5 U of HLADH in 50 mM Tris-HCl buffer pH 8.8, 800 U of *At*HNL in 20 mM KPB pH 7.0, 100 mM KPB pH 6.0,

1 mM NAD^+, 125 mM acetaldehyde, 1.5 M nitromethane, 0.1 mM $ZnCl_2$, a varied concentration of sorbitol (10, 25, 50, 100, 150, and 200 mg/mL), 25 mM benzyl alcohol, and the remaining volume of autoclaved double distilled water up to 1 mL.

2.3.5. Synthesis of racemic β-nitro alcohols

Ten racemic β-nitro alcohols were synthesized. A mixture of nitroalkane (10 mmol), aldehyde (1 mmol), and $Ba(OH)_2$ (5 mol%) in H_2O (3 mL) was taken in a round bottom flask and stirred at room temperature for 30 to 60 minutes.[48] The reaction mixture was then extracted thrice with ethyl acetate. The combined organic layer was dried over anhydrous Na_2SO_4 and concentrated in vacuo. After silica gel column purification, the purified racemic β-nitroalcohols were characterized by ^1H and ^{13}C-NMR.

2.3.6. HLADH-*At*HNL cascade catalyzed enantioselective synthesis of different (*R*)-β-nitroalcohols

A typical reaction mixture contained 433 µL of *n*-butyl acetate, 2.5 U of HLADH in 50 mM Tris-HCl buffer pH 8.8, 800 U of *At*HNL in 20 mM KPB pH 7, 100 mM of KPB pH 6 (1.25 M, 80 µL), 1 mM NAD^+ (100 mM, 10 µL), 125 mM acetaldehyde (3 M, 42 µL), 1.5 M nitromethane (83 µL), 0.1 mM zinc chloride (10 mM, 10 µL), 25 mg/mL sorbitol (0.8 gm/mL) and 25 mM different benzylic alcohols (1 M, 25 µL). The total reaction volume was made up to 1 mL by adding autoclaved double distilled water. This reaction mixture was incubated at 30 °C and 1,200 rpm in a Thermo shaker. Aliquot extraction and HPLC analysis were done according to the previously described method. Using these optimized reaction conditions, ten different benzylic types of alcohols were converted to their corresponding (*R*)-β-nitroalcohols.

$$\%\ \text{ee of (R) product} = \frac{[(\text{Area of (R) product} - \text{Area of (R) control}) - (\text{Area of (S) product} - \text{Area of (S) control})]}{[(\text{Area of (R) product} - \text{Area of (R) control}) + (\text{Area of (S) product} - \text{Area of (S) control})]}$$

$$\%\ \text{ee of (S) product} = \frac{[(\text{Area of (S) product} - \text{Area of (S) control}) - (\text{Area of (R) product} - \text{Area of (R) control})]}{[(\text{Area of (S) product} - \text{Area of (S) control}) + (\text{Area of (R) product} - \text{Area of (R) control})]}$$

The % conversions of the enzymatic products were calculated using the conversion factor determined by taking an equimolar amount of alcohol, aldehyde, and racemic β-nitroalcohol. For each substrate, the cascade biocatalysis was done twice.

2.3.7. Optimization of reaction parameters of *Bm*HNL catalyzed nitroaldol reaction

As *Bm*HNL was not reported as a catalyst earlier in nitroaldol reaction, hence prior to use it in the cascade, a few crucial parameters were optimized using benzaldehyde to (*S*)-NPE synthesis as the model reaction.

2.3.7.1. Optimization of *Bm*HNL enzyme content using benzaldehyde as the substrate

The content of purified *Bm*HNL used in the reaction was optimized. Nine *Bm*HNL concentrations were chosen, ranging from 2 to 100 U. The total reaction mixture contained 475 µL *n*-butyl acetate, 2, 5, 10, 15, 23, 40, 60, 80, and 100 U of *Bm*HNL in 20 mM KPB pH 7.0, 100 mM KPB pH 6.0 (1.25 M, 80 µL), 1.5 M nitromethane (83 µL), 25 mM benzaldehyde (1 M, 25 µL), and 50 mg/mL glycerol (40 µL). In the case of lower *Bm*HNL contents, 20 mM KPB pH 7 was used to adjust the remaining volume equivalent to the case of 100 U of *Bm*HNL. The total reaction volume was made up to 1 mL by adding autoclaved double distilled water.

This reaction mixture was incubated at 30 °C and 1,200 rpm in a thermoshaker. Aliquot extraction and HPLC analysis were done, as mentioned in 2.3.4.1.

2.3.7.2. Optimization of buffer system and its pH

Three buffers were selected for this optimization study. The reaction mixture contained 475 µL *n*-butyl acetate, 5 U *Bm*HNL in 20 mM KPB pH 7.0, 100 mM of different buffers [citrate phosphate buffer (CPB), Tris-HCl buffer, and phosphate buffer, pH ranged from 4.5 to 8, 100 µL of 1 M stock], 1.5 M nitromethane, 25 mM benzaldehyde, 50 mg/mL glycerol, and the remaining volume of autoclaved double distilled water to a total reaction volume of 1 mL. Aliquot extraction and HPLC analysis were done according to the previously described method.

2.3.7.3. Optimization of organic solvent

Five organic solvents were considered for this study. The reaction mixture contained 475 µL of different organic solvents (toluene, *n*-butyl acetate, DIPE, TBME, and *di*-ethyl ether), 5 U *Bm*HNL in 20 mM KPB pH 7.0, 100 mM CPB pH 5.5, 1.5 M nitromethane, 25 mM benzaldehyde, 50 mg/mL glycerol, and the remaining volume of autoclaved double distilled water to a total reaction volume of 1 mL. A separate experiment was also carried out with only buffer (without any organic solvent). Aliquot extraction and HPLC analysis were done according to the previously described method.

2.3.7.4. Optimization of protein stabilizer or reaction additive

In this experiment, ten different sugars and polyols were tested. Reaction conditions: 475 µL of TBME, 5 U *Bm*HNL in 20 mM KPB pH 7.0, 100 mM CPB pH 5.5, 1.5 M nitromethane, 25 mM benzaldehyde, 50 mg of different additives (glycerol, raffinose, mannitol, glucose, arabinose, maltose, galactose, sucrose, lactose, and sorbitol), and the remaining volume of autoclaved double distilled water to a total reaction volume of 1 mL. Aliquot extraction and HPLC analysis were done according to the previously described method.

2.3.7.5. Optimization of substrate

Six different substituted benzaldehydes were investigated for this nitroaldol reaction, replacing normal benzaldehyde as the substrate while keeping the previous reaction conditions with 50 mg/mL sorbitol. Reaction conditions: 475 µL of TBME, 5 U *Bm*HNL in 20 mM KPB pH 7.0, 100 mM CPB pH 5.5, 1.5 M nitromethane, 25 mM of different aldehydes (3,4 dichlorobenzaldehyde, 3,5-dimethoxybenzaldehyde, 2,3,4-trimethoxybenzaldehyde, 3,4,5-trimethoxybenzaldehyde, 4-allyloxybenzaldehyde, and 4-benzyloxybenzaldehyde), 50 mg of sorbitol, and the remaining volume of autoclaved double distilled water to a total reaction volume of 1 mL. Aliquot extraction and HPLC analysis were done according to the previously described method.

2.3.7.6. Optimization of *Bm*HNL content using 3,5-dimethoxybenzaldehyde as the substrate

In this experiment, five different *Bm*HNL concentrations were used. The total reaction mixture contained 475 µL TBME, different concentrations of *Bm*HNL (5, 10, 20, 30, and 40 U), 100 mM CPB pH 5.5, 1.5 M nitromethane, 25 mM 3,5-dimethoxy benzaldehyde, 50 mg/mL sorbitol, and the remaining volume of autoclaved double distilled water to a total reaction volume of 1 mL. In the case of lower *Bm*HNL contents, 20 mM KPB pH 7 was used to adjust

the remaining volume equivalent to the case of 40 U of *Bm*HNL. Aliquot extraction and HPLC analysis were done according to the previously described method.

2.3.8. Optimization of HLADH content in the HLADH-*Bm*HNL cascade using 3,5-dimethoxybenzyl alcohol as the substrate

In this experiment, three biocatalytic conditions were investigated. They were (a) 10 U HLADH with 1 mM NAD^+, (b) 10 U HLADH with 4 mM NAD^+, and (c) 20 U HLADH with 1 mM NAD^+. In each of these reactions, the composition was 358 µL TBME, different concentrations of HLADH, 30 U *Bm*HNL, 100 mM CPB pH 5.5, 1.5 M nitromethane, 25 mM 3,5-dimethoxybenzyl alcohol, 50 mg/mL sorbitol, different concentrations of NAD^+, 0.1 mM $ZnCl_2$, and 125 mM acetaldehyde. For lower HLADH and NAD^+ concentrations, 50 mM Tris-HCl buffer pH 8.8 and double distilled water were used to adjust the remaining volume equivalent to the case of 20 U of HLADH and 4 mM NAD^+. The remaining volume of the reaction mixture was filled with autoclaved double distilled water to get a total reaction volume of 1 mL. Aliquot extraction and HPLC analysis were done according to the previously described method.

2.3.9. HLADH-*Bm*HNL cascade catalyzed enantioselective synthesis of different (*S*)-β-nitroalcohols

The reaction mixture contained 358 µL TBME, 2.5 or 10 U of HLADH, 5 or 30 U of *Bm*HNL, 100 mM CPB pH 5.5 (2 M, 50 µL), 1.5 M nitromethane (83 µL), 25 mM different substrates (250 mM, 100 µL), 50 mg/mL sorbitol (0.86 gm/mL, 58 µL), 1 mM of NAD^+ (100 mM, 10 µL), 0.1 mM $ZnCl_2$ (10 mM, 10 µL), 125 mM acetaldehyde (3 M, 42 µL), and the remaining volume of autoclaved double distilled water to a total reaction volume of 1 mL. For benzyl alcohol, 2.5 U of HLADH and 5 U of *Bm*HNL were used, whereas, for the remaining nine substrates, 10 U of HLADH and 30 U of *Bm*HNL were used. Except for these two different enzyme ratios, other reaction conditions were the same for all the ten benzylic type alcohols investigated in this study. Aliquoting procedure and product analysis were done according to the previously described method (Table 2.3).

2.4. Results

2.4.1. NMR characterization of racemic β-nitroalcohols

Racemic standards corresponding to enzymatic reaction products were prepared as described above. All the products of this study are known compounds. Their NMR spectral data (both ^1H and ^{13}C) were in agreement with reported values.[20,23,49-51]

^1H and ^{13}C NMR characterization of β-nitro alcohols **1**-**10** (figure 2.2.1-2.2.10).

2-Nitro-1-phenylethanol[1] (9H), 1

^1H NMR (400 MHz, $CDCl_3$): δ 2.01 (1H, s), 4.51 (1H, dd, J = 3.2, 13.2 Hz), 4.62 (1H, dd, J = 9.6, 13.2 Hz), 5.45 (1H, dd, J = 2.8, 9.6 Hz), 7.28-7.44 (5H, m); ^{13}C NMR (100 MHz, $CDCl_3$) δ 70.9, 81.2, 125.9 (X2), 128.9, 128.9 (X2), 138.3.

1-(3-Methoxylphenyl)-2-nitroethanol[1] (11H), 2

^1H NMR (500 MHz, $CDCl_3$) δ 3.45 (1H, brs), 3.80 (3H, s), 4.49 (1H, dd, J = 3, 13.5 Hz), 4.58 (1H, dd, J = 9.5, 13.0 Hz), 5.39 (1H, dd, J = 2.5, 9.5 Hz), 6.88 (1H, ddd, J = 0.5, 2.5, 8.0 Hz),

6.93-6.95 (2H, m), 7.31 (1H, dd, *J* = 1.0, 8.5 Hz); ^{13}C NMR (125 MHz, $CDCl_3$) δ 55.3, 70.8, 81.2, 111.5, 114.3, 118.1, 130.0, 139.9, 159.9.

1-(3,5-Dimethoxyphenyl)-2-nitroethanol [14] (13H), 3

^{1}H NMR (500 MHz, $CDCl_3$): δ 3.80 (6H, s), 4.48-4.61 (2H, m), 5.37-5.40 (1H, dd, *J* = 2.5, 9.5 Hz), 6.43-6.44 (1H, t, *J* = 2.5), 6.54-6.55 (2H, d, *J* = 2.0 Hz) ^{13}C NMR (125 MHz, $CDCl_3$) δ 55.4, 71.0, 81.2, 100.6, 103.8, 140.6, 161.2.

1-(2-Chlorophenyl)-2-nitroethanol[16] (8H), 4

^{1}H NMR (500 MHz, $CDCl_3$): δ 4.44-4.49 (1H, m), 4.66-4.70 (1H, dd, *J* = 2.5, 14 Hz), 5.84-5.87 (1H, m), 7.28-7.40 (3H, m), 7.66-7.68 (1H, dd, *J* = 1.5, 7.5 Hz) ^{13}C NMR (125 MHz, $CDCl_3$) δ 67.8, 79.3, 127.5, 127.6, 129.7, 129.2, 131.4, 135.5

1-(3-Chlorophenyl)-2-nitroethanol[14] (8H), 5

^{1}H NMR (500 MHz, $CDCl_3$): δ 3.17 (1H, brs), 4.50-4.60 (2H, m), 5.43-5.46 (1H, dd, *J* = 3.5, 9.5 Hz), 7.27-7.29 (1H, m), 7.34-7.35 (2H, m), 7.430-7.437(1H, m); ^{13}C NMR (120 MHz, $CDCl_3$) δ 70.2, 80.9, 124, 126.2, 129 (X2),130.3, 135, 140.1.

1-(4-Chlorophenyl)-2-nitroethanol[14] (8H), 6

^{1}H NMR (400 MHz, $CDCl_3$): δ 3.04 (1H, brs), 4.48-4.61 (2H, m), 5.44-5.47 (1H, dd, *J* = 3.2, 9.2 Hz), 7.34-7.41 (4H, m); ^{13}C NMR (100 MHz, $CDCl_3$) δ 70.3, 80.9, 127.3, 129.2, 134.8, 136.5.

1-(3, 4-Dichlorophenyl)-2-nitroethanol[15] (7H), 7

^{1}H NMR (500 Hz, $CDCl_3$): δ 3.28 (1H, brs), 4.49-4.59 (2H, m), 5.43-5.45 (1H, dd, *J* = 2, 9 Hz), 7.23-7.28 (1H, m), 7.47-7.49 (1H, d, *J* = 8.0 Hz), 7.53-7.54 (1H, d, *J* = 1.5 Hz).^{13}C NMR (125 MHz, $CDCl_3$) δ 69.72, 80.77, 125.22, 128.07, 131.0, 133.03, 133.26, 138.24.

1-(3-Nitrophenyl)-2-nitroethanol[14] (8H), 8

^{1}H NMR (500 Hz, $CDCl_3$): δ 3.39 (1H, s), 4.59-4.67 (2H, m), 5.62-5.64(1H, dd, *J* = 4 Hz), 7.61-7.64 (1H, t, *J* = 8), 7.78-7.80 (1H, d, *J* = 8 Hz), 8.21-8.23 (1H, m), 8.32-8.33 (1H, t, *J* = 2)^{13}C NMR (125 MHz, $CDCl_3$) δ 69.8, 80.6, 121.1, 123.8, 130.1, 132.0, 140.2, 148.5.

1-(4-Nitrophenyl)-2-nitroethanol[13] (8H), 9

^{1}H NMR (500 MHz, CDCl3) δ 3.51 (1H, d, *J* = 7, 14 Hz), 4.56-4.64 (2H, m), 5.63 (1H, dd, *J* = 5, 10 Hz), 7.65 (2H, d, *J* = 10 Hz), 8.29 (2H, d, *J* = 9 Hz); δ 69.6, 80.1, 124.3 (2X), 126.6 (2X), 145.1, 148.1.

1-(4-Benzyloxyphenyl)-2-nitroethanol[14] (15H), 10

^{1}H NMR (500 Hz, $CDCl_3$): δ 2.8 (1H, brs), 4.47-4.63 (2H, m), 5.0 (2H, s), 5.39-5.42 (1H, dd, *J* =3, 10), 7.01-7.02 (2H, d, *J* = 8.5 Hz), 7.28-7.46 (7H, m). ^{13}C NMR (125 MHz, $CDCl_3$) δ 70.1, 70.6, 81.2, 115.3, 127.3, 127.4, 128.1, 128.6, 130.5, 136.6, 159.2.

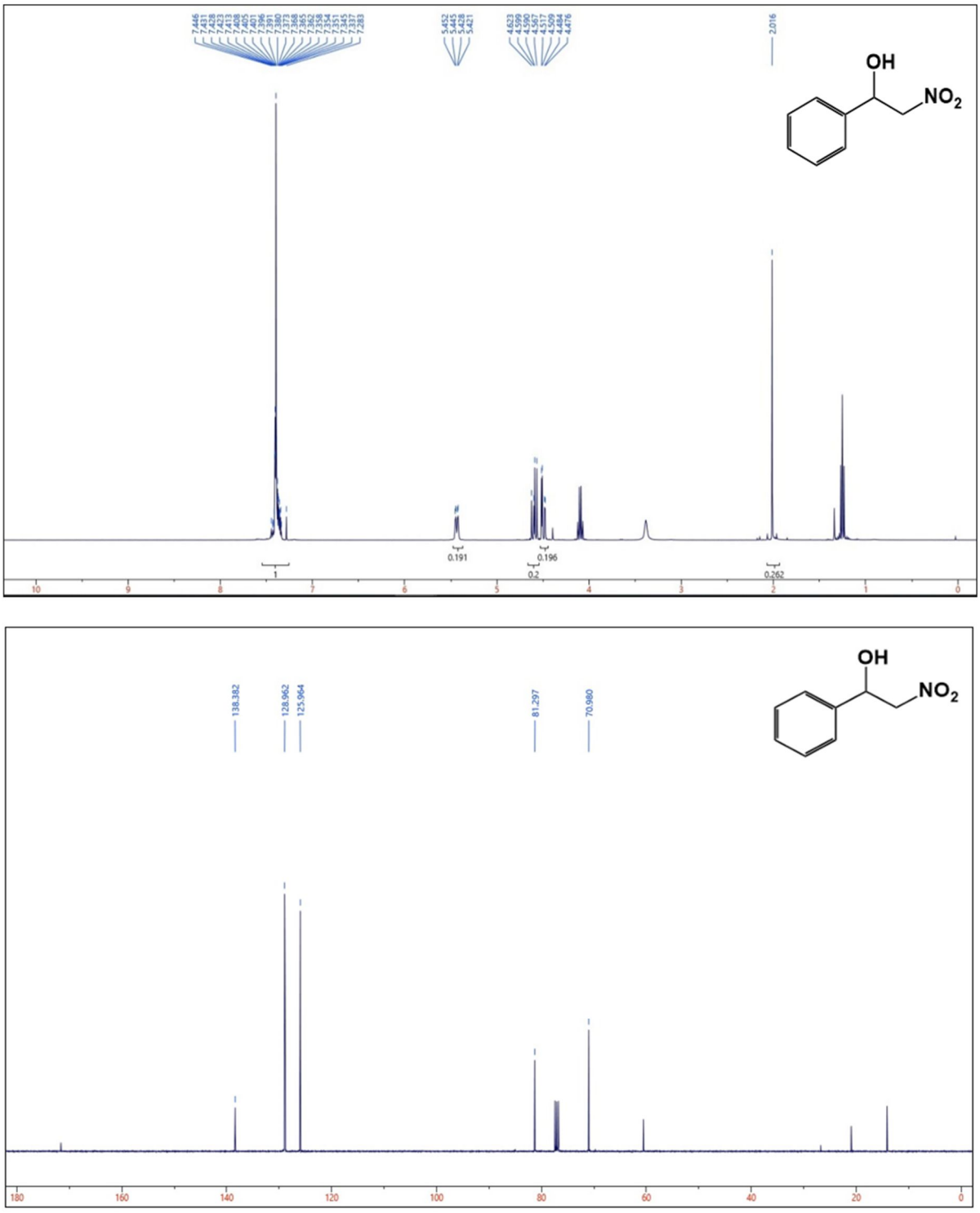


Figure 2.2.1: ^{1}H NMR and ^{13}C NMR spectra of 2-nitro-1-phenyl ethanol

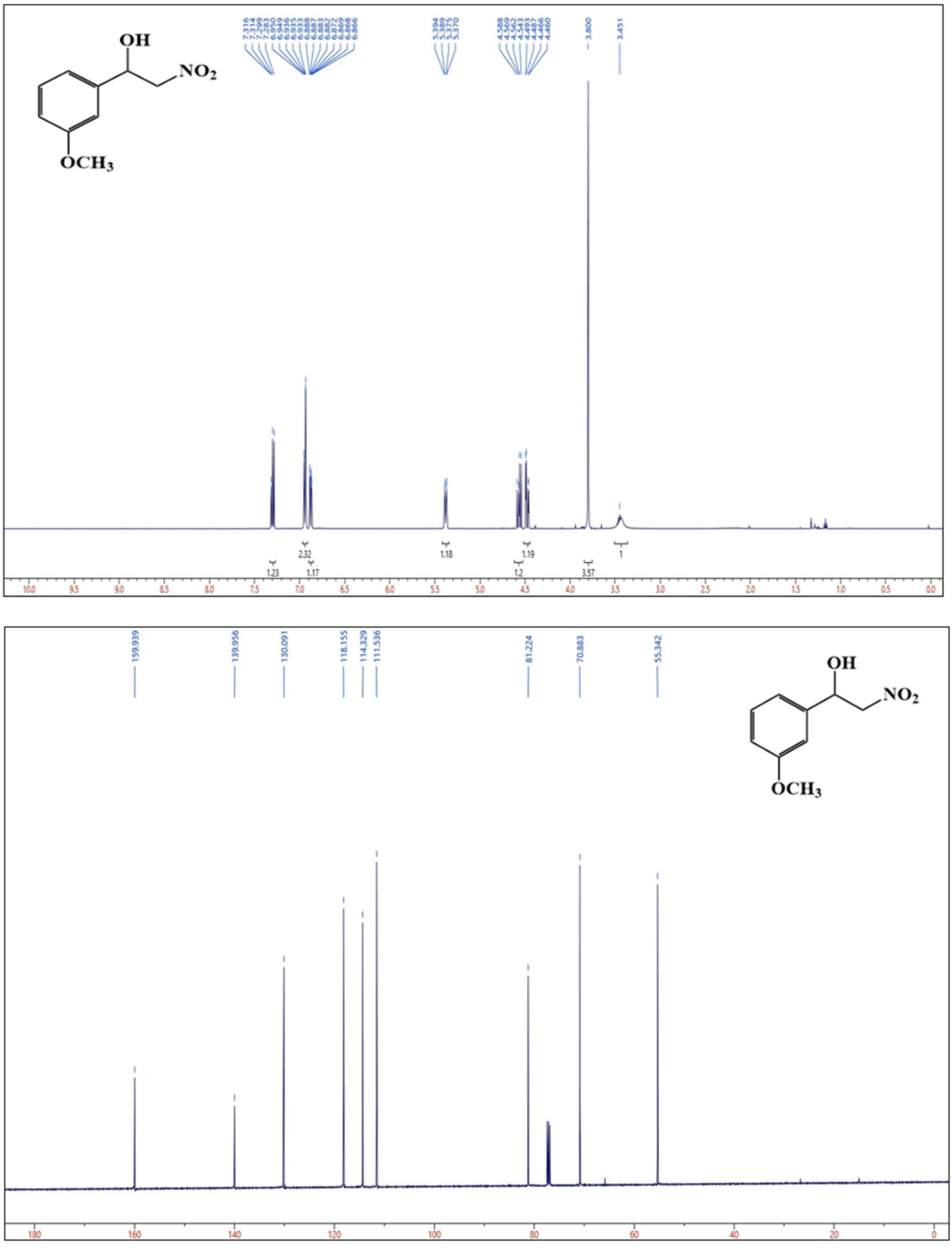


Figure 2.2.2: ^{1}H NMR and ^{13}C NMR spectra of 1-(3-methoxylphenyl)-2-nitroethanol.

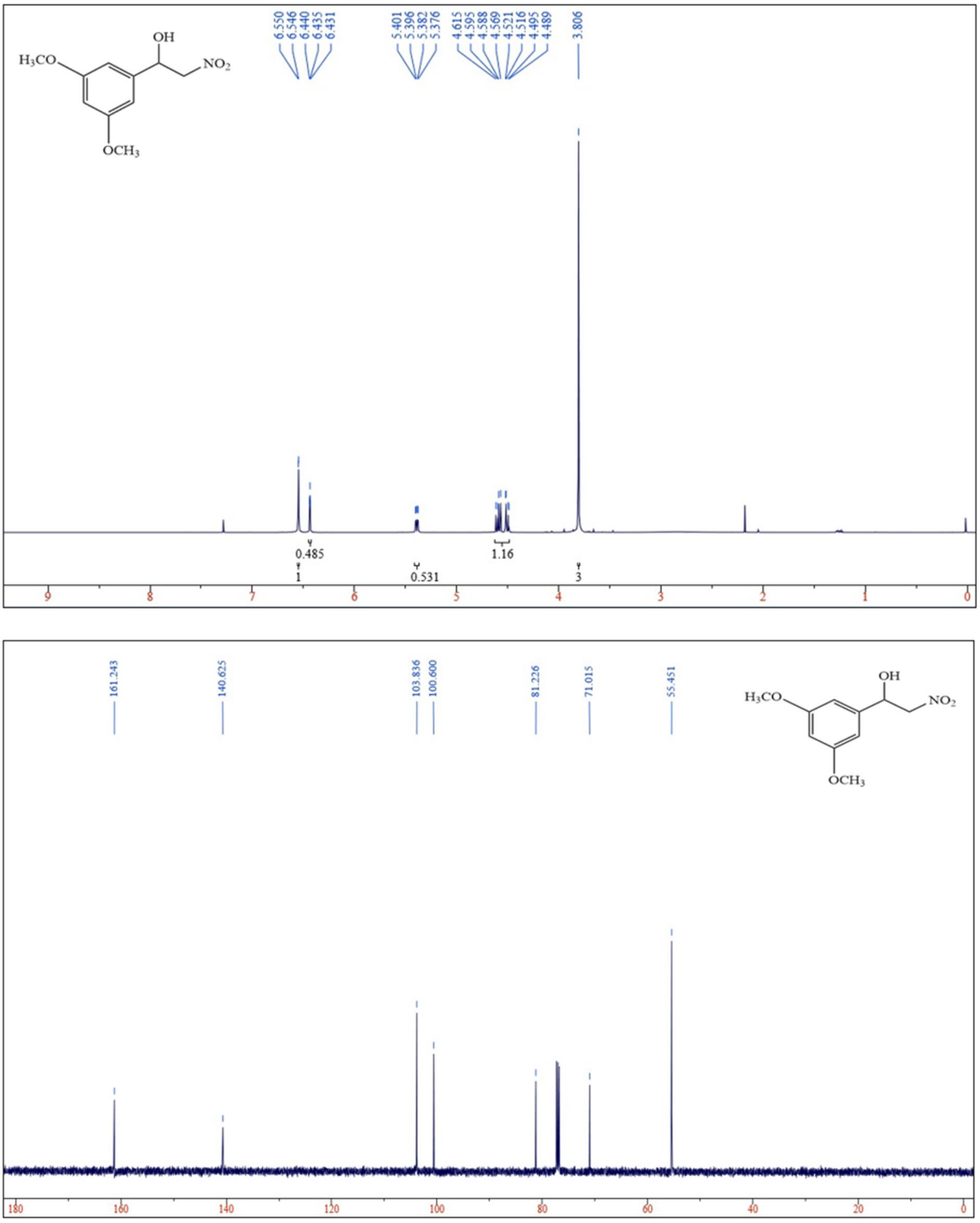


Figure 2.2.3: ^{1}H NMR and ^{13}C NMR spectra of 1-(3,5-dimethoxyphenyl)-2-nitroethanol

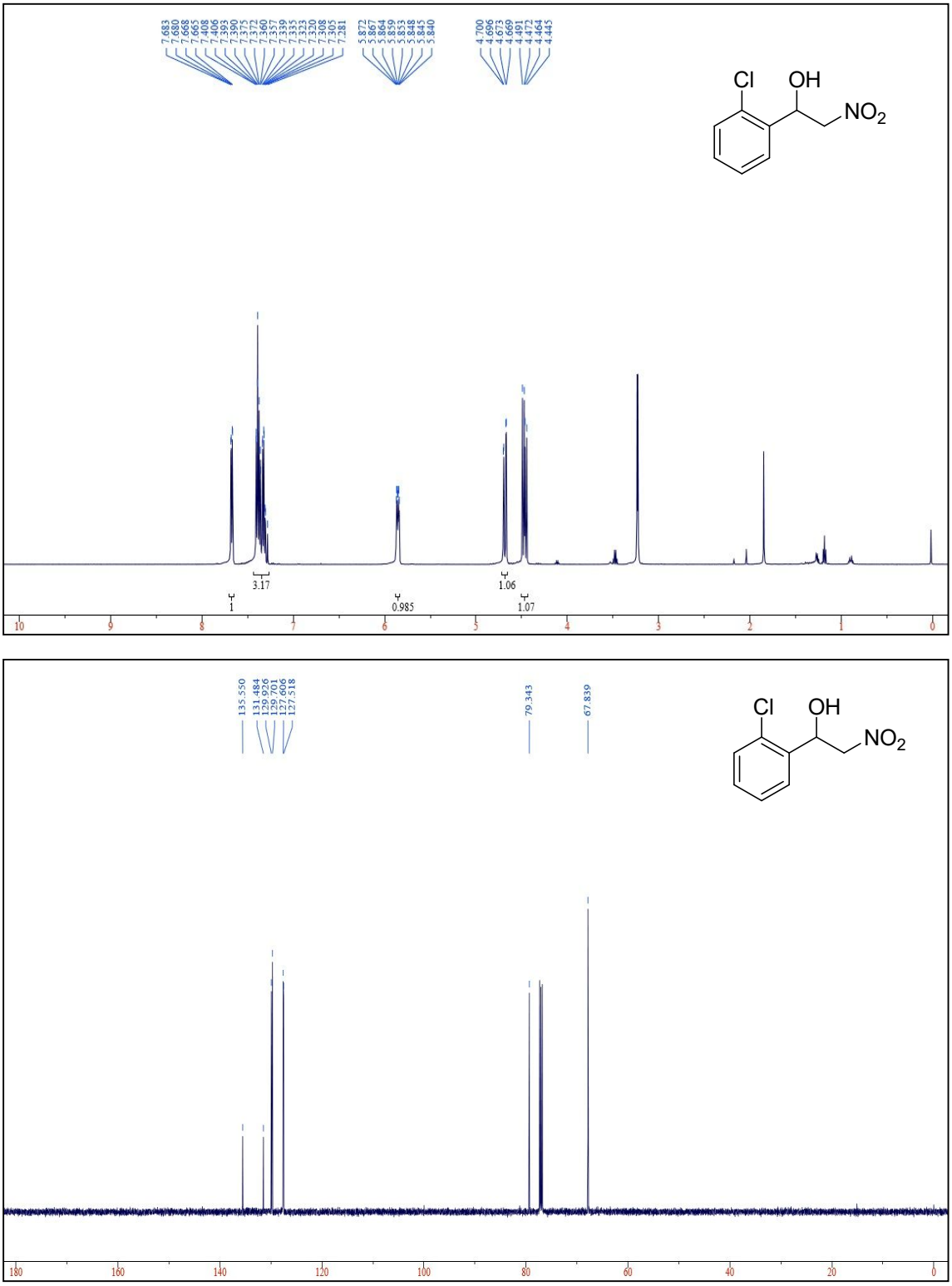
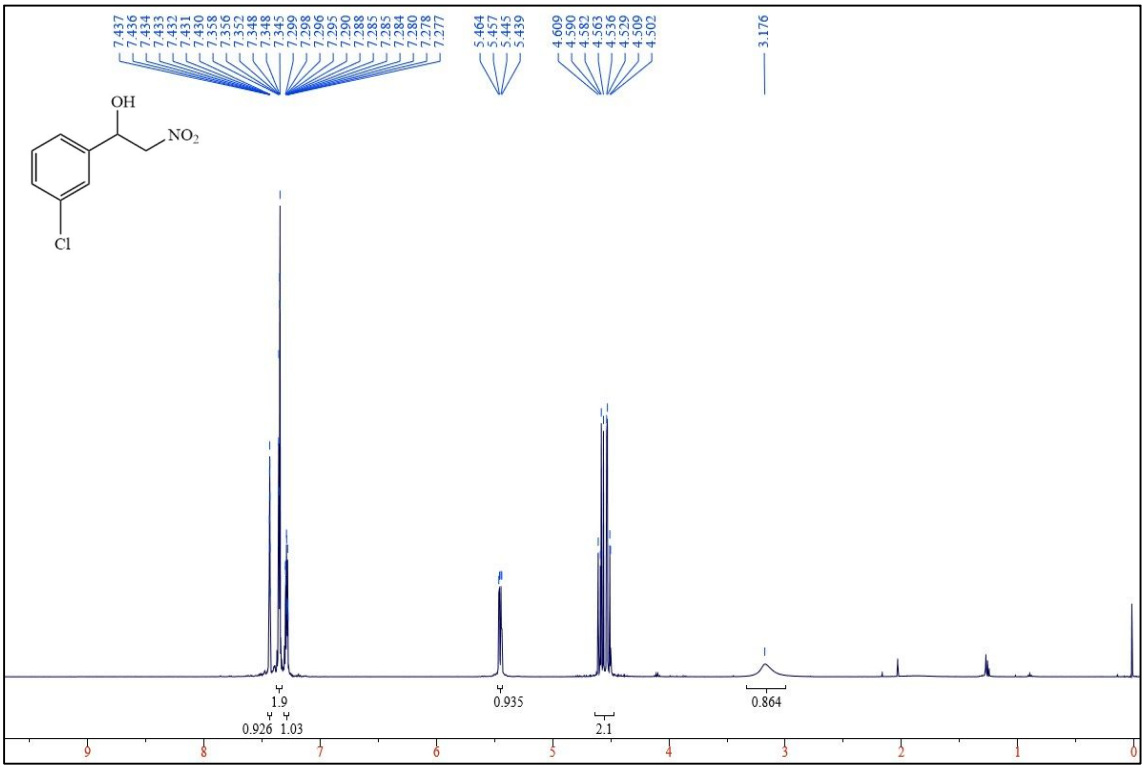


Figure 2.2.4: ^{1}H and ^{13}C NMR spectra of 1-(2-chlorophenyl)-2-nitroethanol



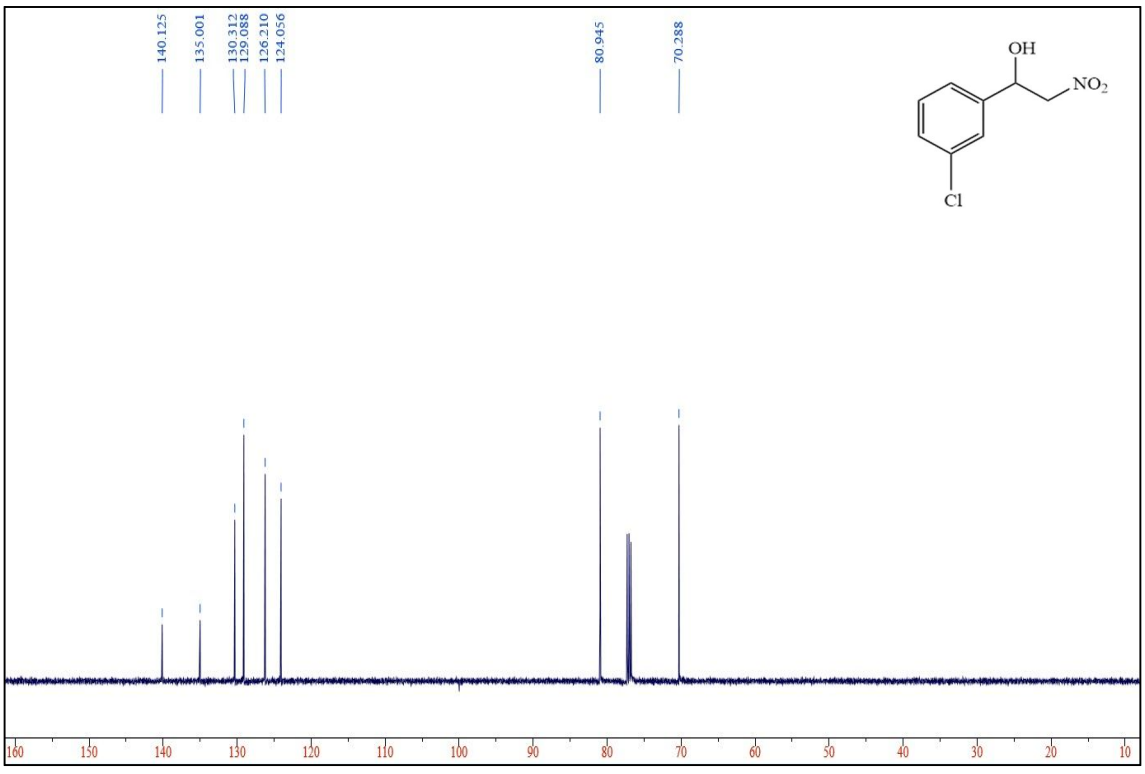


Figure 2.2.5: ^{1}H and ^{13}C NMR spectra of 1-(3-chlorophenyl)-2-nitroethanol

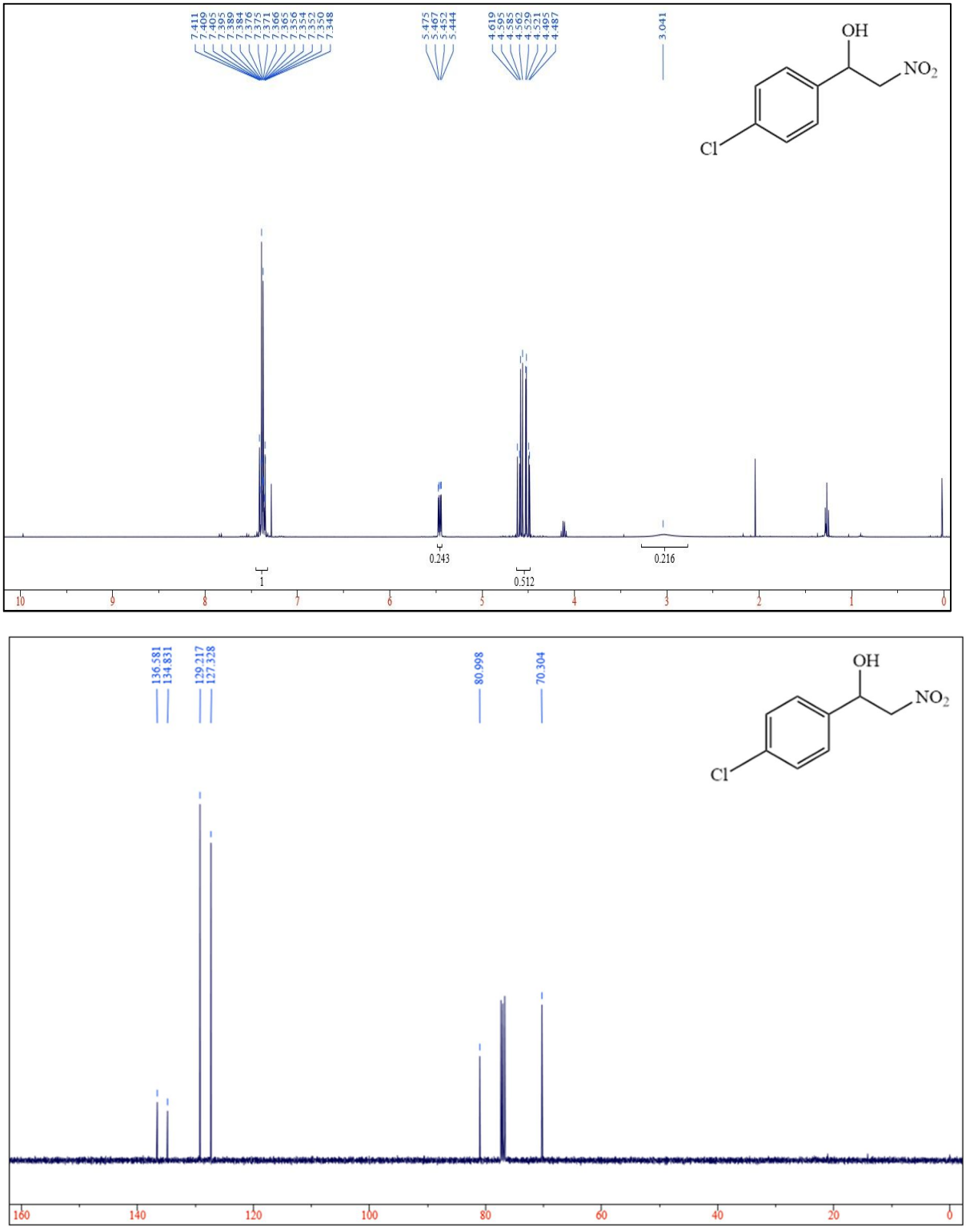


Figure 2.2.6: ^{1}H NMR and ^{13}C NMR spectra of 1-(4-chlorophenyl)-2-nitroethanol

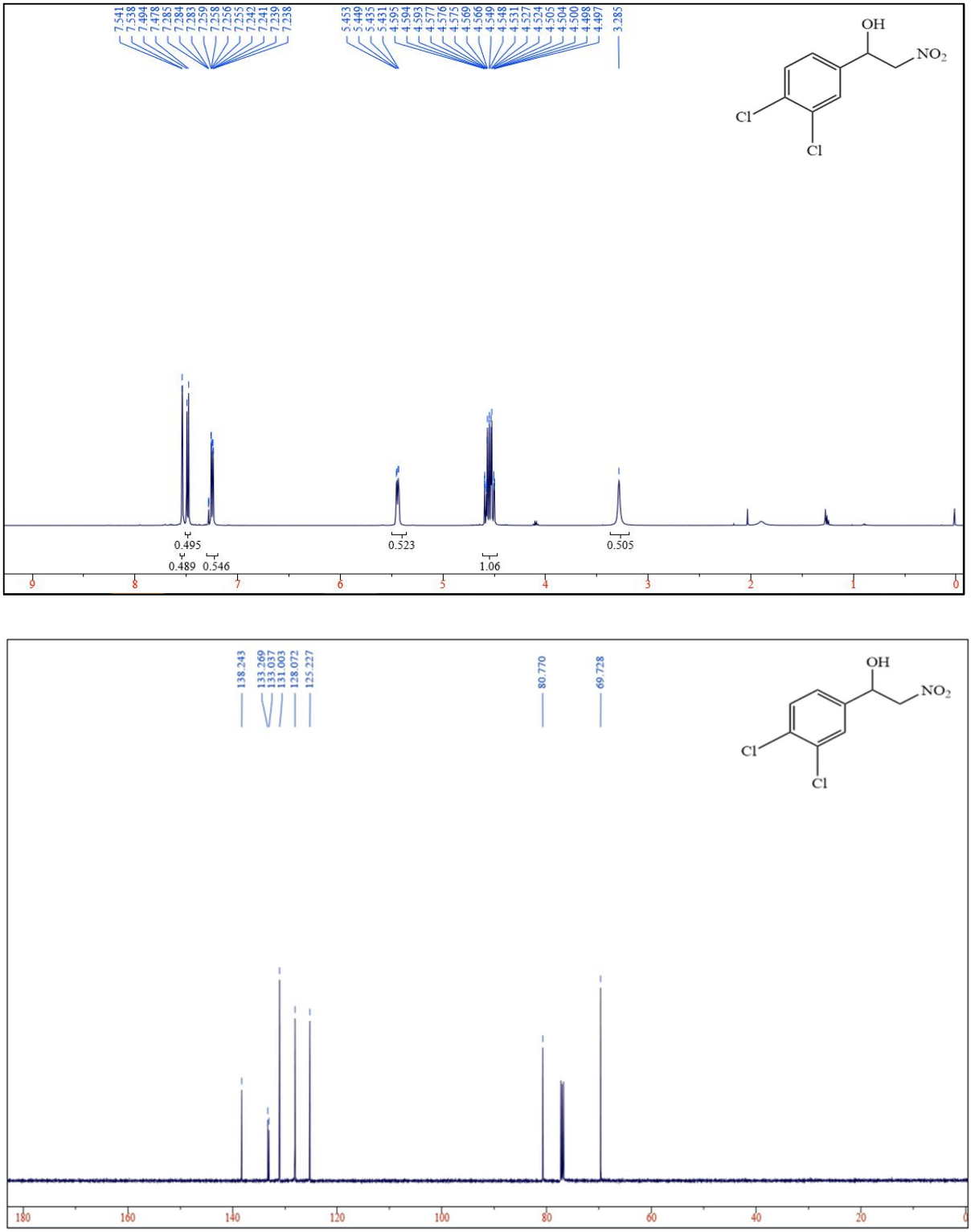


Figure 2.2.7: ^{1}H NMR and ^{13}C NMR spectra of 1-(3,4-dichlorophenyl)-2-nitroethanol

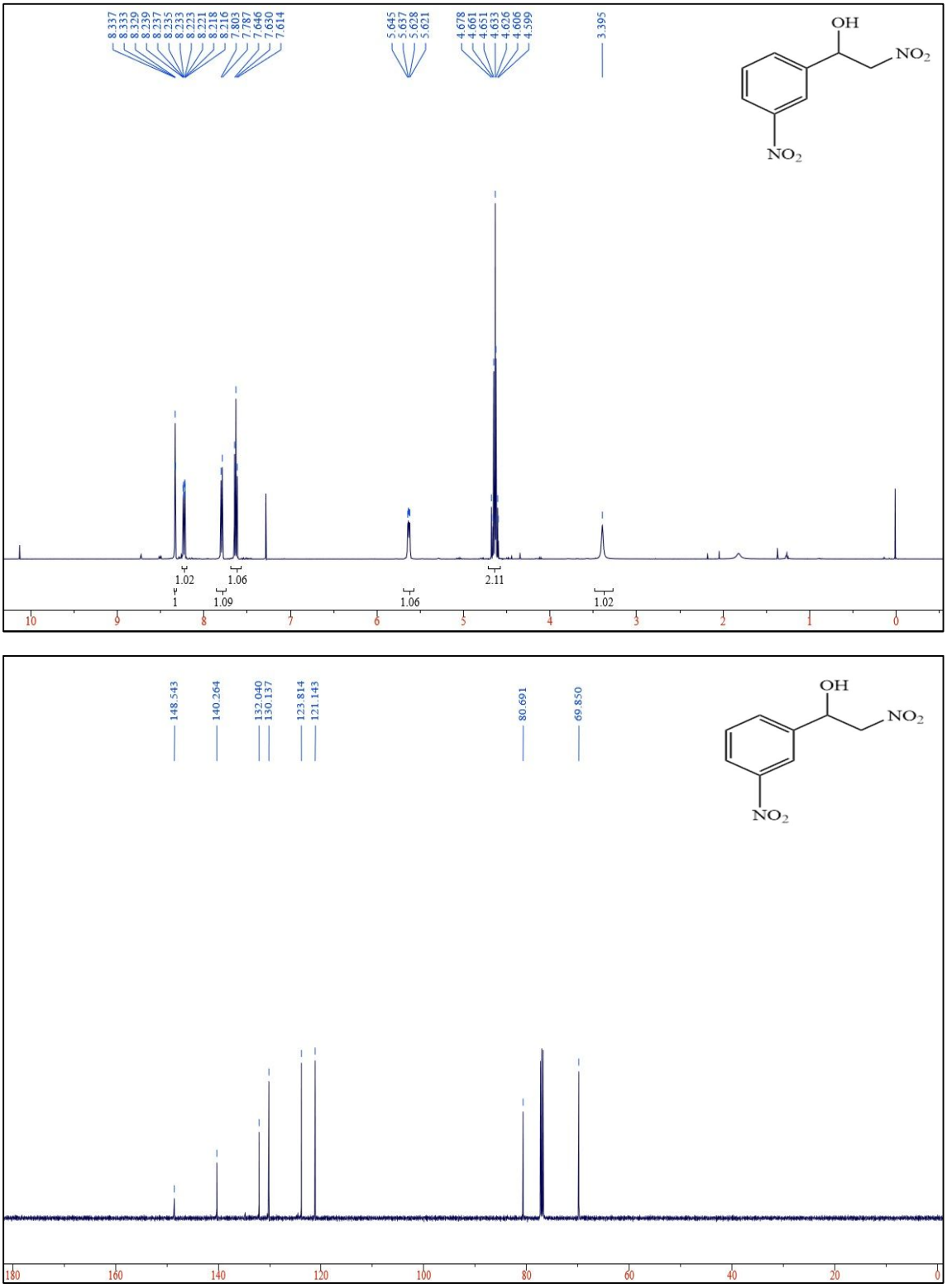


Figure 2.2.8: ^{1}H NMR and ^{13}C NMR spectra of 1-(3-nitrophenyl)-2-nitroethanol

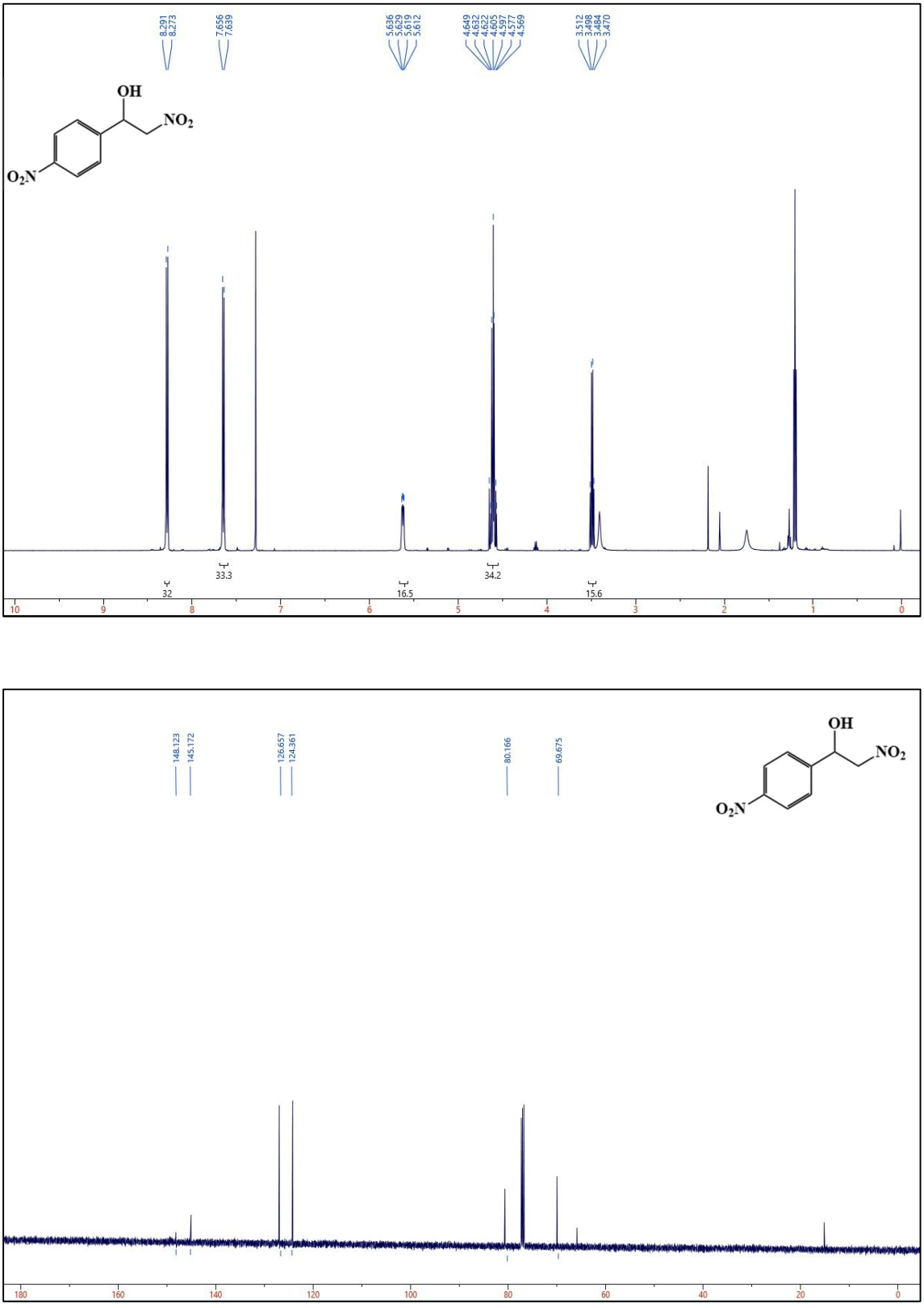


Figure 2.2.9: ^{1}H NMR and ^{13}C NMR spectra of 1-(4-nitrophenyl)-2-nitroethanol

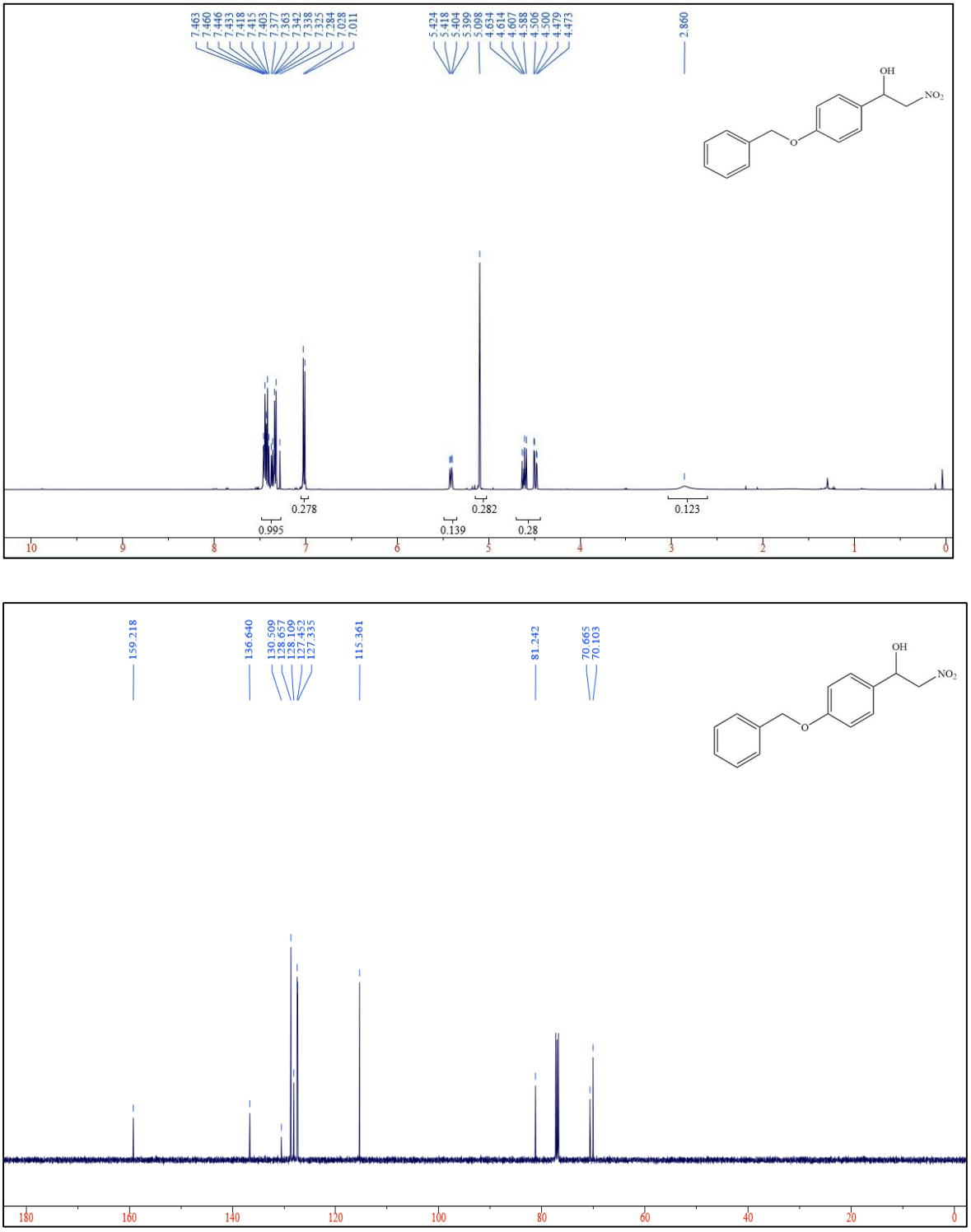


Figure 2.2.10: ^{1}H NMR and ^{13}C NMR spectra of 1-(4-benzoloxyphenyl)-2-nitroethanol

2.4.2. HPLC conditions for chiral resolution of racemic β-nitroalcohols

Table 2.3: HPLC conditions for chiral resolution of racemic β-nitroalcohols

Racemic β-nitroalcohols with different substituents in the aromatic ring of NPE	HPLC conditions			
	Wavelength	Flow rate	Chiral column used	Hexane: Isopropanol
H	210 nm	1 mL/min	Chiralpak - IB	93:7
3-methoxy			Chiralpak - IB	93:7
3,5-dimethoxy			Lux Amylose-1	96:4 or 98:2 for 10 min, followed by 96:4
2,3,4-trimethoxy			Lux Amylose-1	98:2
2-chloro			Chiralpak - IB	97:3
3-chloro			Chiralpak - IB	94:6
4-chloro			Chiralpak - IB	94:6
3,4-dichloro			Chiralpak - IB	93:7
3-nitro			Chiralpak - IB	95:5
4-nitro			Chiralpak - IB	93:7
4-benzyloxy			Chiralpak - IB	93:7

2.4.3. SDS-PAGE of purified HLADH, *At*HNL, and *Bm*HNL enzymes and their specific activity determination

HLADH, *At*HNL, and *Bm*HNL purified as described in section 2.3.2 above were characterized by SDS-PAGE (Figure 2.3). All the components such as pellet, supernatant, eluents, and pure protein were analyzed by 12% SDS-PAGE and stained by Coomassie Brilliant Blue R-250. A clear band at ~42 kDa (Figure 2.3A), 28 kDa (Figure 2.3B), and 29 kDa (Figure 2.3C) indicated the good expression and purity of the purified HLADH, *At*HNL, and *Bm*HNL respectively.

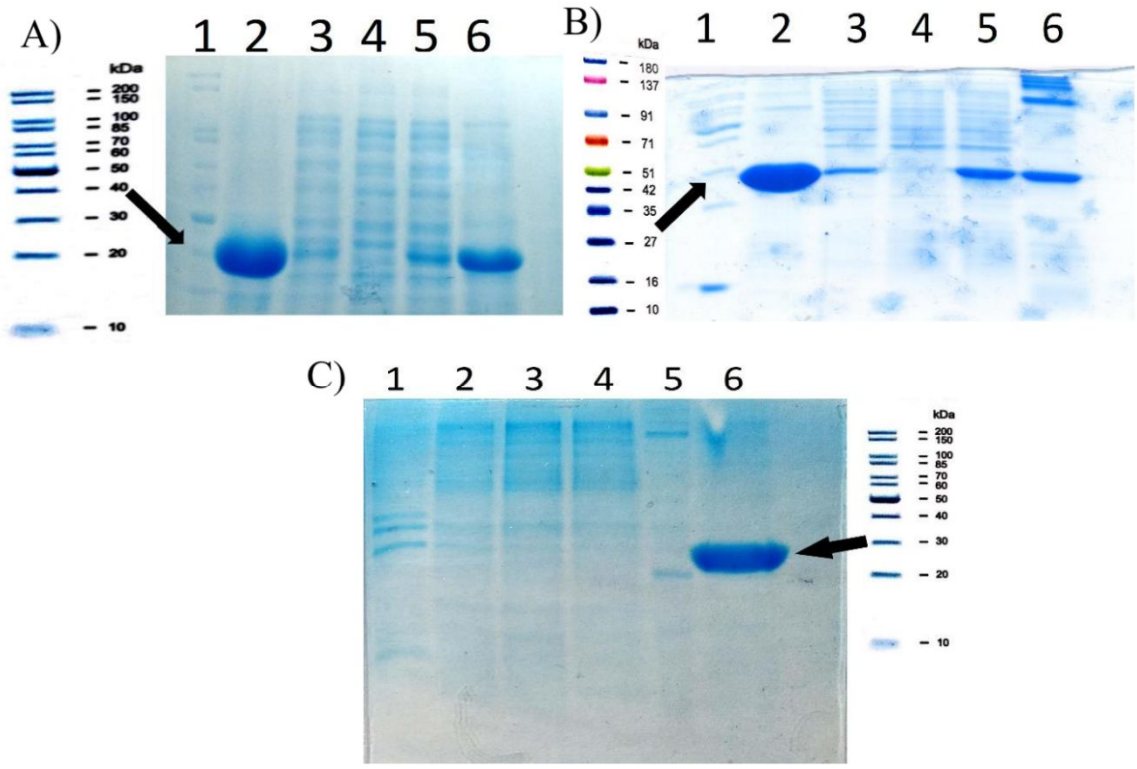


Figure 2.3: SDS-PAGE of purified HLADH, *At*HNL, and *Bm*HNL protein. (A) SDS-PAGE analysis of purified HLADH. Lane 1: ladder, 2: pure HLADH protein, 3: wash fraction, 4: flow through, 5: sonicated supernatant, and 6: sonicated pellet. (B) SDS PAGE analysis of purified *At*HNL. Lane 1: ladder, 2: pure *At*HNL protein, 3: wash fraction, 4: flow through, 5: sonicated supernatant, and 6: sonicated pellet. (C) SDS PAGE analysis of purified *Bm*HNL. Lane 1: sonicated pellet, 2: sonicated supernatant, 3: flow through, 4: wash fraction, 5: ladder, and 6: pure *Bm*HNL protein.

The specific activity of purified HLADH, *At*HNL, and *Bm*HNL was found to be 5.12±0.41, 151.98±7.85, and 14.03±0.56 U/mg respectively.

2.4.4. Kinetics and inhibition studies

2.4.4.1. Steady-state kinetics of HLADH

Steady-state kinetics of HLADH was performed using the NADH assay as described in 2.3.3.1 above. From the Michaelis–Menten plot (Figure 2.4), the kinetic parameters were found as $K_{M:}$ 0.0186 mM, and $V_{max:}$ 2.351 U/mg.

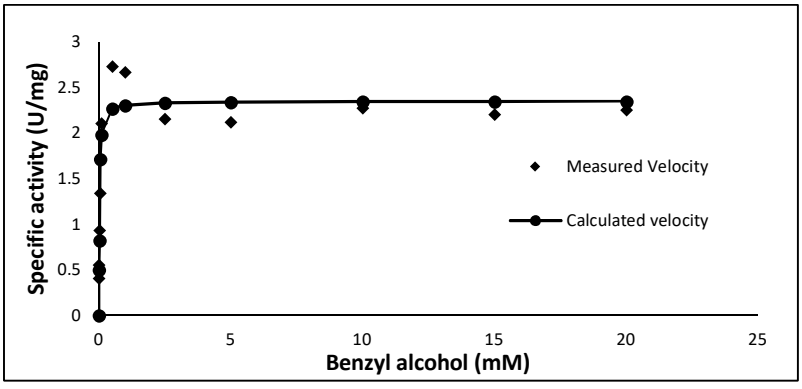


Figure 2.4: Michaelis–Menten kinetics of HLADH for benzyl alcohol oxidation.

2.4.4.2. Inhibition of HLADH by benzaldehyde

The inhibitory effect of benzaldehyde on HLADH was studied following the protocol described in 2.3.3.2 above. Analysis of the data suggests that in the presence of higher concentrations of benzaldehyde, the decrease in the V_{max} of HLADH was not significant; however, the K_M of the enzyme has increased drastically (Figure 2.5). This is an indication of competitive inhibition. Moreover, The K_i of HLADH for benzaldehyde and the K_M for benzyl alcohol were found to be 0.01 mM and 0.0073 mM, respectively.

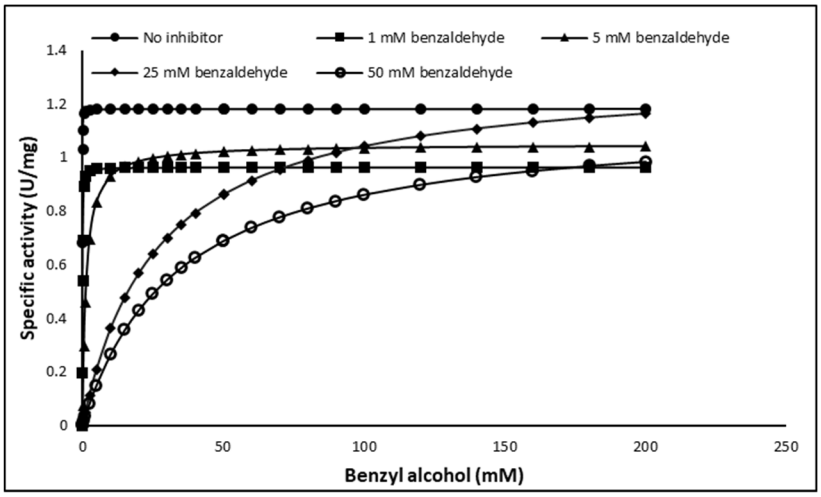


Figure 2.5: Michaelis–Menten kinetics of HLADH using benzyl alcohol oxidation assay shows inhibitory effect by benzaldehyde.

2.4.4.3. Inhibitory effects of benzyl alcohol and benzaldehyde on *At*HNL

This study was carried out following the protocol explained in 2.3.3.3. We did not find a significant decrease in the *At*HNL's activity with the increasing inhibitor concentration. (Figure 2.6) Even in the presence of 50 mM benzyl alcohol, *At*HNL has shown 185 U/mg of activity vs. 200 U/mg in the absence of benzyl alcohol. This suggests that excess benzyl alcohol can be taken as a substrate in the cascade, which causes minimum loss of *At*HNL's activity. Whereas, benzaldehyde in contrast, showed a drastic decrease in the *At*HNL specific activity with increasing concentration. In the presence of 50 mM benzaldehyde, *At*HNL's specific activity came down to 29 U/mg. This clearly indicates that benzaldehyde is a potent inhibitor of *At*HNL and it retards the enzymatic activity at higher concentrations.

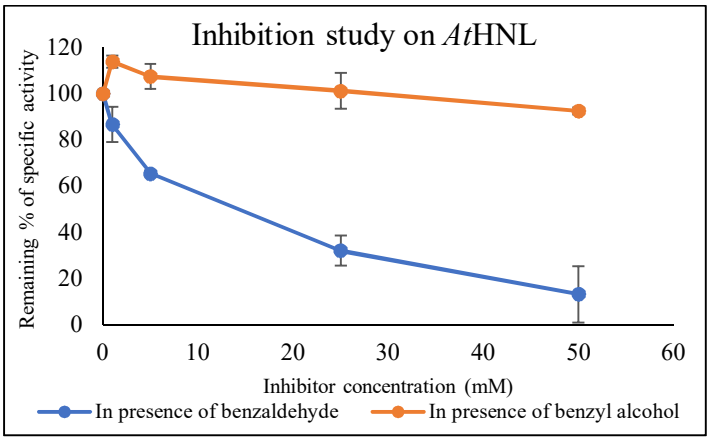


Figure 2.6: Inhibitory effect of benzyl alcohol and benzaldehyde on the specific activity of *At*HNL determined using mandelonitrile cleavage assay.

2.4.4.4. Inhibitory effects of benzyl alcohol and benzaldehyde on *Bm*HNL

This inhibition study was carried out following the protocol described in 2.3.3.4 above. Similar to the *At*HNL, an almost identical result was found in the case of *Bm*HNL. With the increasing benzyl alcohol concentration the specific activity of *Bm*HNL did not decrease at all up to 50 mM, in contrast a steady fall in the activity was observed when benzaldehyde was used as the inhibitor in the experiment. In presence of 50 mM benzaldehyde, the specific activity reduced to only 32% compared to the no inhibitor condition. (Figure 2.7)

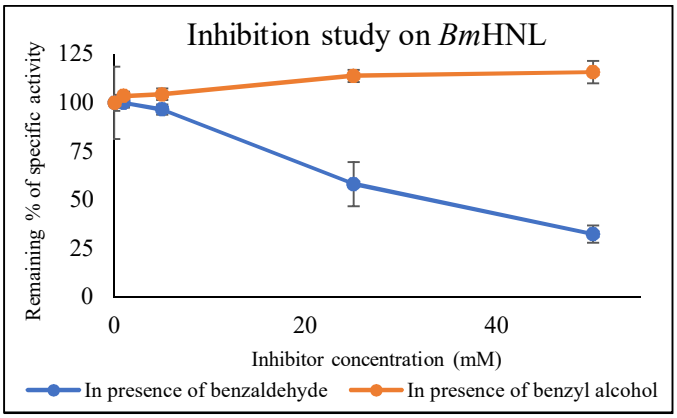


Figure 2.7: Inhibitory effect of benzyl alcohol and benzaldehyde on the specific activity of *Bm*HNL determined using mandelonitrile cleavage assay.

2.4.5. Optimization of reaction conditions of HLADH-*At*HNL cascade

2.4.5.1 Optimization of buffer system and its pH

Finding a suitable buffer and pH optima in an enzyme catalyzed reaction especially in HNL biocatalysis is essential because it effects on the enantioselectivity of the product. In this experiment KPB and acetate buffer has been used at different pH to determine the pH optima. With an increase in the pH of the KPB, both the % conversion to benzaldehyde and NPE increased, while % ee of NPE decreased, and this trend was continued from 2 to 22 h. Highest % ee (>99) of NPE was found in KPB pH 6.0 with only 3.5% conversion. (Figure 2.8)

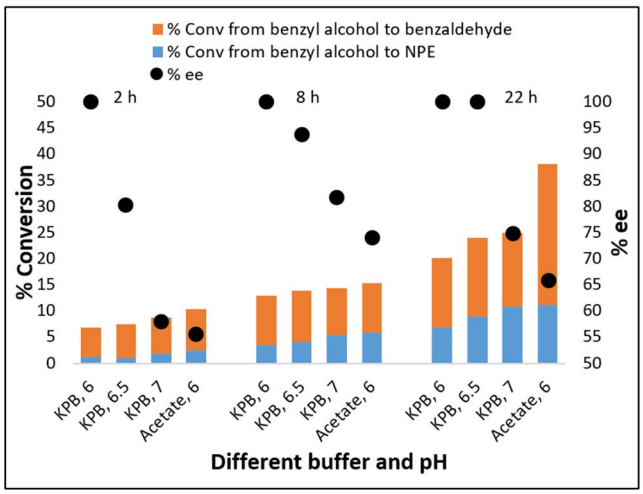


Figure 2.8: Optimization of biocatalytic conditions of the HLADH-*At*HNL cascade: different pH and buffer.

2.4.5.2. Screening of cofactor recycling agent

The first step of this cascade involves HLADH catalyzed oxidation of aromatic alcohols and this step uses NAD^+ as the cofactor. So, to avoid stoichiometric use of NAD^+ in the reaction, a suitable cofactor recycling agent is very essential. Two cofactor recycling agents have been tested here acetone and acetaldehyde. Higher % conversion to benzaldehyde and NPE was observed in the case of acetaldehyde than acetone (Figure 2.9). The formation of total benzaldehyde increased to 73.6%, while 18% conversion and 98% ee of NPE was observed in 8 h. With an increase in reaction time, the amount of total benzaldehyde production decreased, probably due to its reverse conversion to benzyl alcohol.

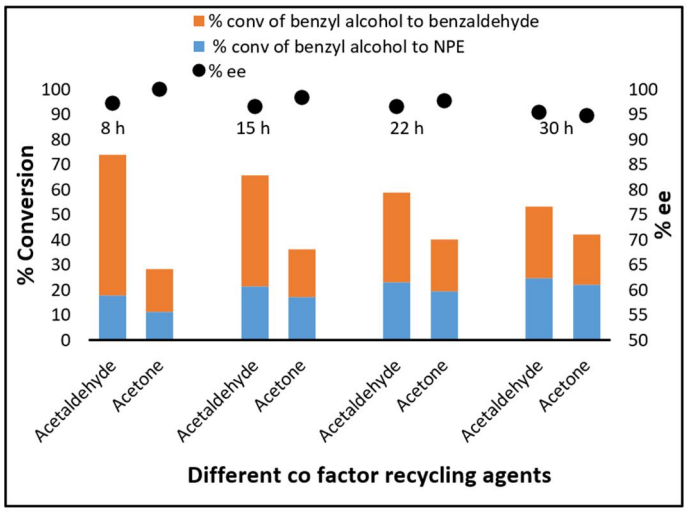


Figure 2.9: Optimization of biocatalytic conditions of the HLADH-*At*HNL cascade: different cofactor recycling agents.

2.4.5.3. Optimization of *At*HNL content

To effectively transform the benzaldehyde to (*R*)-NPE, *At*HNL amount in the cascade was varied from 400 to 1000 U. NPE production increased with an increase in the *At*HNL amount, however, a significant increase was not seen beyond 800 U (Figure 2.10). With an increase in time, total benzaldehyde content slightly decreased, probably due to the reverse action of HLADH, while the NPE amount increased marginally. With 800 U of *At*HNL, NPE production was doubled, i.e., 38.4% conversion, and >99% ee of (*R*)-NPE was observed in 8 h.

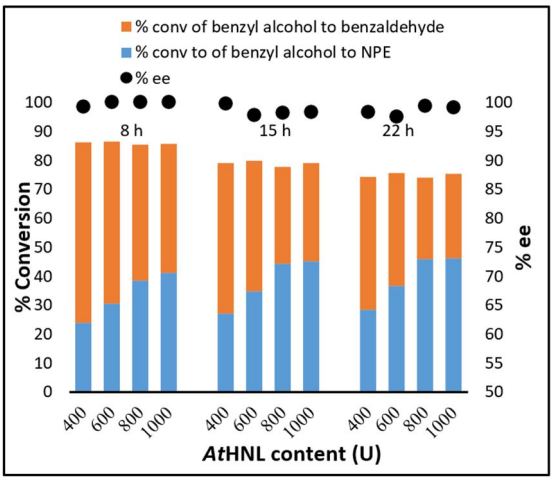


Figure 2.10: Optimization of biocatalytic conditions of the HLADH-*At*HNL cascade: *At*HNL content.

2.4.5.4. Optimization of cofactor (NAD^+) concentration

In this study, eight different NAD^+ concentrations (0.2 to 3 mM) were used. The % conversion to NPE was increased with an increase in NAD^+ concentration up to 0.8 mM (Figure 2.11). Not only at higher NAD^+ concentrations but also with longer reaction time, the benzaldehyde content started decreasing. However, such decrease was not observed in 30 minutes. This suggests that the reduced cofactor may be carrying out the reverse reaction by HLADH at longer time. So, for further optimization study, we selected 0.8 mM NAD^+, where a maximum of 40% conversion and 99.2% ee of NPE was attained.

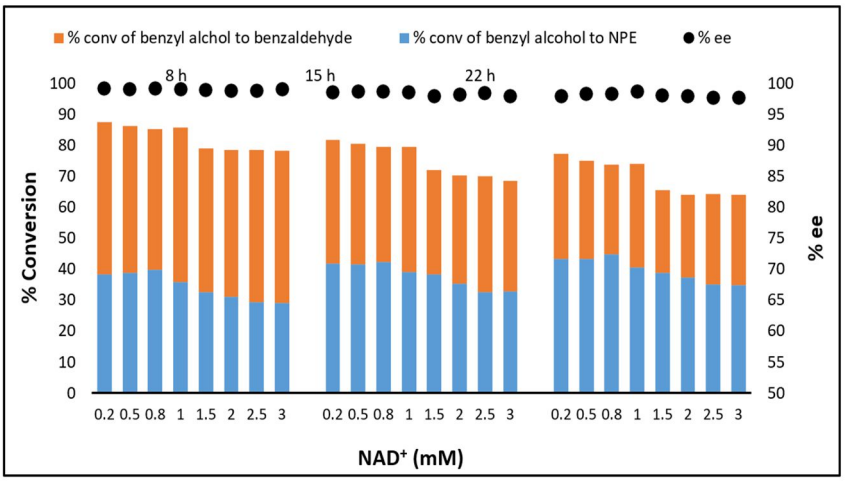


Figure 2.11: Optimization of biocatalytic conditions of the HLADH-*At*HNL cascade: NAD^+ concentration.

2.4.5.5. Optimization of HLADH content

HLADH enzyme content was optimized by varying its amount from 1 to 5 U. Optimization of HLADH amount not only increased the production of benzaldehyde to 93% (Figure 2.12), but the final product conversion also increased to 49.2%. With 2 U of HLADH, 49.2% conversion, and >99 % ee of NPE was found in 8 h. An increasing HLADH amount has resulted in a slight

decrease in benzaldehyde production, which could be due to the product inhibition, as discussed earlier.

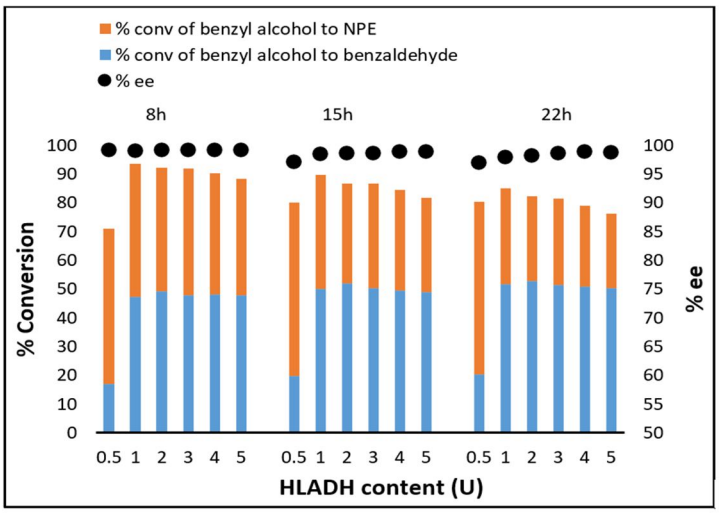


Figure 2.12: Optimization of biocatalytic conditions of the HLADH-*At*HNL cascade: HLADH amount.

2.4.5.6. Optimization of KPB concentration

KPB which was found to be the most efficient buffer to carry out this cascade its concentration was varied from 50-250 mM. This study has resulted in a marginal improvement in the conversion to NPE in 100 mM compared to 50 mM buffer, and no further increase in the conversion to the product in higher buffer concentrations was observed (Figure 2.13).

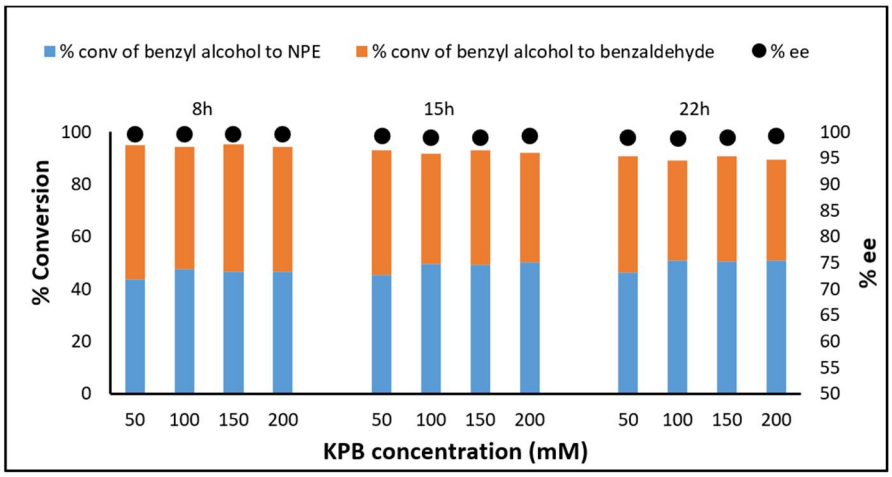


Figure 2.13: Optimization of biocatalytic conditions of the HLADH-*At*HNL cascade: KPB concentration.

2.4.5.7. Optimization of nitromethane concentration

Five different nitromethane concentrations, i.e., 0.5 to 2.5 M were selected for this optimization study. In the preceding experiments we were using 50 µL of nitromethane per mL of reaction volume (equivalent to 0.91 M of nitromethane).[23] The % conversion to NPE was increased with the increasing nitromethane concentration up to 1.5 M, and it decreased beyond that (Figure 2.14). We found 53% conversion with 99.5% ee of NPE when 1.5 M nitromethane was

used. At low nitromethane concentration (0.5 M) not only NPE formation but also total conversion to benzaldehyde is decreased. Inefficient utilization of benzaldehyde by *At*HNL, as happens in this case, could lead to the inhibition of both enzymes.

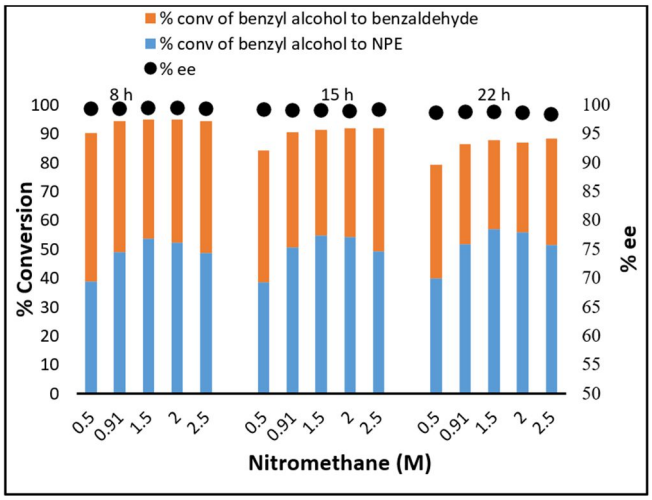


Figure 2.14: Optimization of biocatalytic conditions of the HLADH-*At*HNL cascade: nitromethane concentration.

2.4.5.8. Optimization of the biphasic system

An aqueous-organic biphasic system is often used in HNL biocatalysis to minimize the spontaneous reaction, product/substrate inhibition, and increase substrate solubility. We observed a gradual increase in the NPE production with increasing nonpolarity of the solvent ($\log^P$ values) until *n*-butyl acetate while it decreased in the case of toluene. Our investigation has successfully demonstrated the conversion of benzyl alcohol to NPE in 55% conversion and 98.4% *ee* in 50% v/v of *n*-butyl acetate.

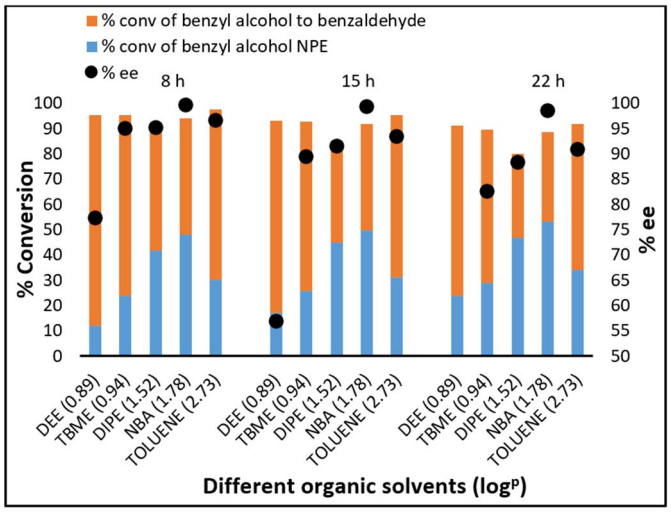


Figure 2.15: Optimization of biocatalytic conditions of the HLADH-*At*HNL cascade: organic solvent content.

2.4.5.9. Optimization of organic solvent content

Although biphasic systems are known to increase the enantioselectivity of HNLs, excess organic solvent can destabilize the protein structure. Hence a proper balance in organic solvent content is very important for the cascade. An earlier study shows that in the case of *At*HNL catalyzed (*R*)-NPE synthesis, an increase in organic solvent content has increased % ee but decreased % conversion of the product.[23] In the earlier experiments, we used 65% of *n*-butyl acetate that resulted in >99% ee of (*R*)-NPE, hence for this optimization study, we varied its content from 45 to 65%. While % ee of product decreased slightly with a decrease in *n*-butyl acetate amount from 65 to 45%, considering the highest % conversion with minimum organic solvent content, we have selected 50% *n*-butyl acetate as the optimum solvent content. We observed 55.2% conversion and 98.4% ee of NPE with 50% *n*-butyl acetate in 8 h (Figure 2.16). Asano.et al. also found this solvent ratio as the optimum condition in the enantioselective synthesis of (*R*)-NPE.[1]

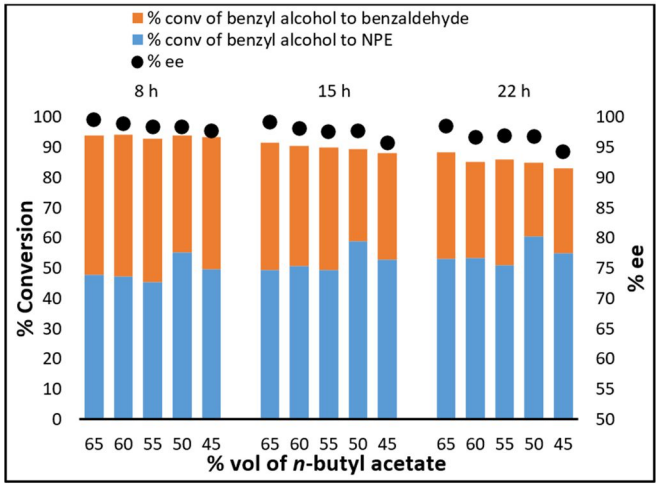


Figure 2.16: Effect of the % of organic solvent on the HLADH-*At*HNL cascade catalysis.

2.4.5.10. Intermittent addition of benzyl alcohol and HLADH

We anticipated that benzaldehyde accumulation in the reaction could be minimized by slow addition (at specific time intervals) of either HLADH or benzyl alcohol, which may result in controlled production of benzaldehyde. To decrease the benzaldehyde production rate, we introduced HLADH (enzyme) and benzyl alcohol (substrate) intermittently into the reaction system at different time points keeping all the reactant's amount constant. None of the intermittent addition techniques could increase the synthesis of (*R*)-NPE, compared to our regular approach, so we proceeded with the latter.

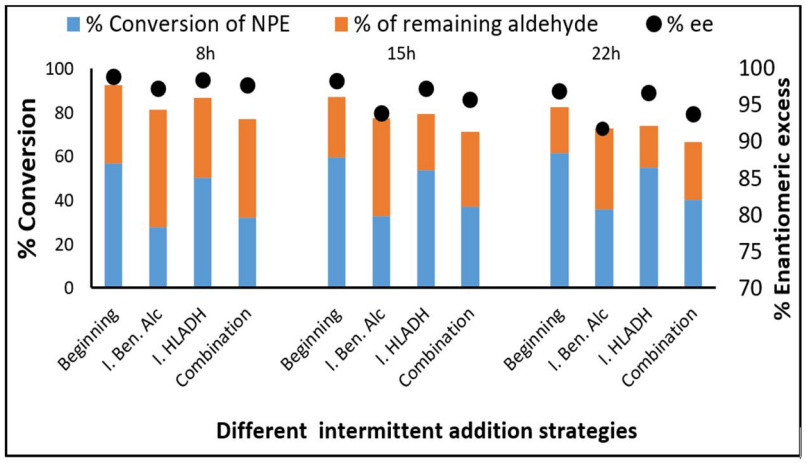


Figure 2.17: Effect of different intermittent addition strategies on the HLADH-*At*HNL cascade catalysis.

2.4.5.11. Optimization of substrate concentration

To control the benzaldehyde accumulation, we studied the effect of the amount of benzyl alcohol on the cascade. Six different benzyl alcohol concentrations ranging from 15 to 40 mM were selected for this study. In the case of 25 mM benzyl alcohol, the amount of total NPE formation increased and showed a negligible increase at higher concentrations (Figure 2.18). However, with the increasing substrate burden, the enantiopurity of the product decreased gradually, i.e., up to 95% ee. We have thus finalized to proceed with 25 mM benzyl alcohol that gave 55.1% conversion and 98.3% ee of product in 8 h.

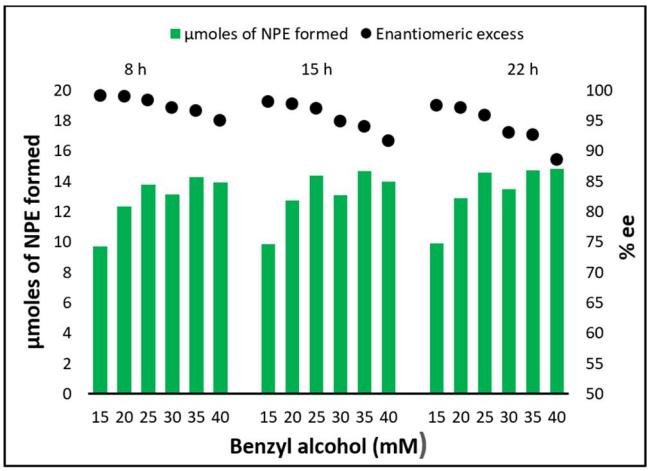


Figure 2.18: Optimization of biocatalytic conditions of the HLADH-*At*HNL cascade substrate concentration.

2.4.5.12. Optimization of protein stabilizer

We investigated the effect of two protein stabilizers, sucrose, and sorbitol, on our cascade assuming their addition might provide stability to *At*HNL structure and prevent its possible destabilization due to the accretion of benzaldehyde. Both the stabilizers have shown an increase in % conversion and % ee of NPE compared to the no stabilizer condition, while sorbitol performed better than sucrose (Figure 2.19). With sorbitol, 57.5% conversion and 99%

ee of NPE was found in 8 h. At a longer reaction time (22 h), the conversion increased further 2%, while the enantioselectivity of (*R*)-NPE was still high (97.6% ee).

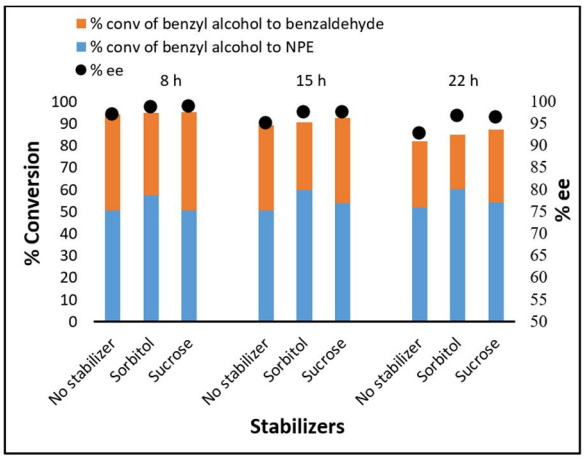


Figure 2.19: Optimization of biocatalytic conditions of the HLADH-*At*HNL cascade substrate concentration.

Our attempt to convert the remaining benzaldehyde of the cascade to NPE by adding a second dose of 800 U of *At*HNL at 4 h was unsuccessful. It has increased only 3-4% of conversion to NPE, indicating strong benzaldehyde inhibition of the enzyme (Figure 2.20).

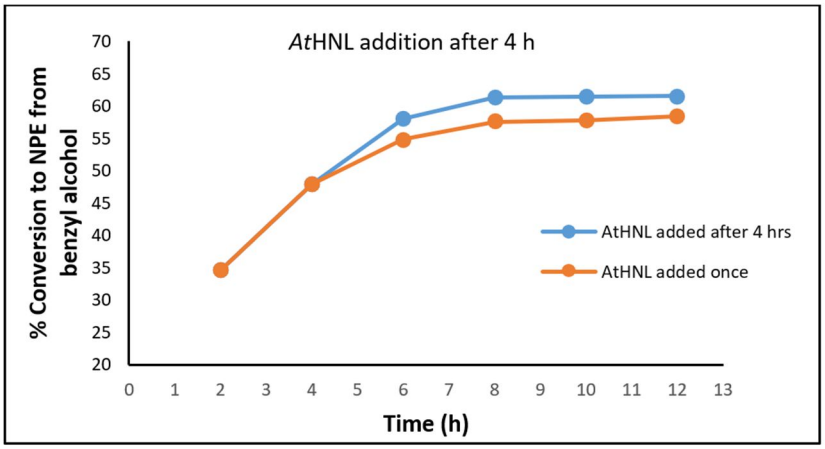


Figure 2.20: Effect of addition of extra 800 U of *At*HNL on the biocatalytic cascade after 4 h.

2.4.5.13. Optimization of cofactor recycling agent (acetaldehyde) concentration

The cofactor recycling agent acetaldehyde plays an indirect but important role in product synthesis, and hence its concentration was optimized by varying its concentration from 75-187.5 mM. A marginal increase in NPE formation was found between 100 to 150 mM acetaldehyde, in all three-time points analyzed. Increased acetaldehyde concentration would prompt more NAD^+ generation, which would drive benzaldehyde formation by HLADH and subsequently NPE formation (Figure 2.21). Up to 125 mM acetaldehyde concentration, the product conversion increased, where 61% conversion and 99% ee of NPE was found.

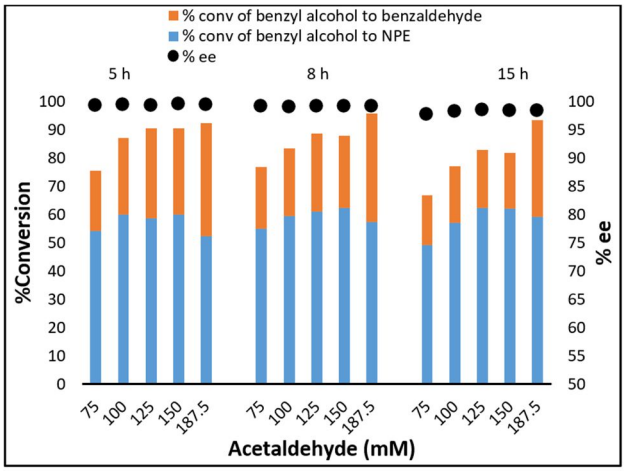


Figure 2.21: Effect of different acetaldehyde concentrations on the HLADH-*At*HNL cascade catalysis.

2.4.5.14. Optimization of reaction time

The time-course study of the cascade was performed by monitoring the reaction progress for 8 h. Almost 90% of benzyl alcohol has been converted to benzaldehyde in just 4 h, with 56.7% NPE of >99% optical purity. In another two hours, the NPE formation reached >60% with >99% ee (Figure 2.22). No further significant improvement in NPE production was seen beyond 6 h.

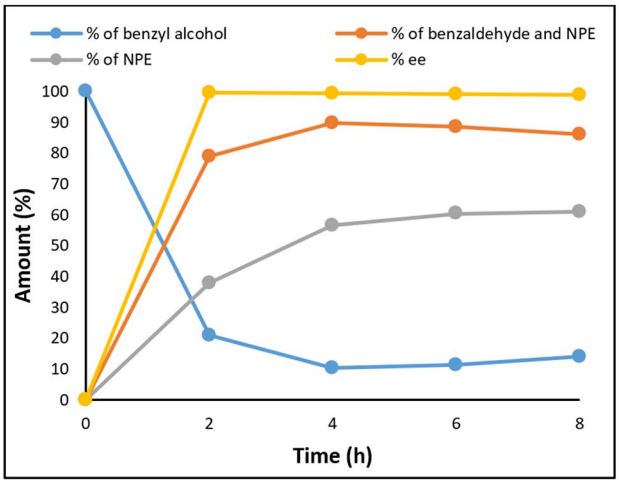


Figure 2.22: Reaction progression curve of HLADH-*At*HNL cascade.

2.4.5.15. Optimization of sorbitol concentration

To determine the minimum concentration of stabilizer that could be effective in the stereoselective synthesis by the cascade, its concentration was varied from 10 to 200 mg/mL. Consistent with our earlier study, sorbitol addition has improved product conversion. As low as 10-25 mg/mL of sorbitol addition has shown 58% of NPE with ~99% ee in 4 h, while in 6 h, the % conversion reached 63.8 with 98.2% ee (Figure 2.23).

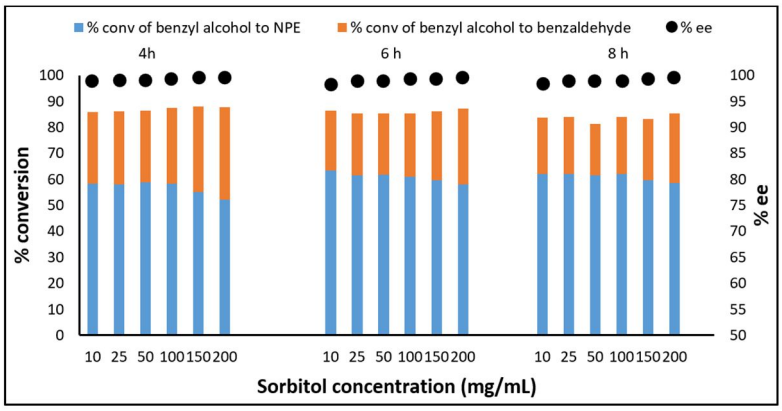


Figure 2.23: Effect of different sorbitol concentrations on the HLADH-*At*HNL cascade catalysis.

The overall optimization studies have improved the % conversion of product from 2 to 64 while the % ee of NPE was 97-99% (Figure 2.24).

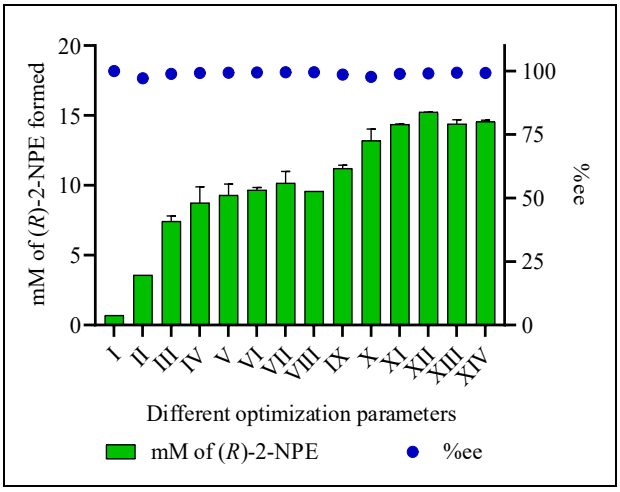
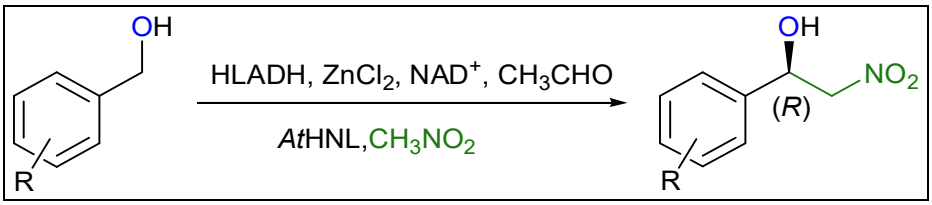


Figure 2.24: Summary of all the parameters optimized for HLADH-*At*HNL cascade to achieve maximum % conversion and % *ee* of (*R*)-NPE. I: buffer system and pH, II: different cofactor recycling agents, III: *At*HNL content, IV: NAD^+ concentration, V: HLADH content, VI: buffer concentration, VII: nitromethane concentration, VIII: different co-solvents (organic), IX: % v/v of co-solvent, X: substrate concentration, XI: protein stabilizer, XII: concentration of cofactor recycling agent, XIII: reaction time, and XIV: concentration of protein stabilizer. For I to IX, 20 mM, while for X to XIV, 25 mM of benzyl alcohol was used. I to XII are from 8 h data, while XIII and XIV are 4 h.

2.4.6. HLADH-*At*HNL cascade catalyzed enantioselective synthesis of different (*R*)-β-nitroalcohols

The substrate scope of HLADH-*At*HNL cascade was exploited to prepare a variety of aromatic (*R*)-β-nitroalcohols (figure 2.33-2.42). Using the optimized biocatalytic reaction conditions, several benzylic type alcohols having substituents at different positions in the aromatic ring were converted into their corresponding (*R*)-β-nitroalcohols. This versatile substrate set contained benzyl alcohols having both electron donating and withdrawing groups, single, double and triple substitutions in the aromatic ring, and substitutions were present at the *ortho*, *meta*, and *para* positions of the aromatic ring in different combinations. It also contained 4-

benzyloxy benzyl alcohol, which has a bulky benzyloxy group at the *para* position. Our cascade has produced (*R*)-NPE with >99% enantiopurity and 64% conversion. Not only HLADH was found to be very efficient in the oxidation of benzyl alcohol, but also *At*HNL showed very good conversion, (up to 90%) in the nitroaldol reaction of this cascade. Among the ten (*R*)-β-nitroalcohols synthesized here, four others (entries 3, 5, 6, and 7, Table 2.4) were studied earlier but our cascade has produced higher enantioselectivity (98 to >99%) in all the four cases and conversion too, except 2- chlorobenzyl alcohol. HLADH oxidation produced only 9.3% of 2-chloro benzaldehyde, which is the reason for this poor overall conversion. The remaining five (*R*)-β-nitroalcohols (entries 4, 8, 9, 10, and 11, Table 2.4) synthesized using the current enzyme cascade have not been prepared earlier by any HNL biocatalysis. With increasing the number of substitutions in the aromatic alcohol, decreasing % conversion was observed. For example, 3-methoxybenzyl alcohol, 3,5-dimethoxybenzyl alcohol, and 2,3,4-trimethoxybenzyl alcohol (not shown) produced 25, 1.4, and no conversion respectively (Table 2.4). A similar trend was found in the case of chloro substituted benzyl alcohols. 3-Chlorobenzyl alcohol, 4-chlorobenzyl alcohol, and 3,4-dichlorobenzyl alcohol produced 41.2, 26.8, and 19% conversion of corresponding NPEs. Bulky *para*- substituted 4- benzyloxybenzyl alcohol gave only 1.5% conversion. This suggests that *At*HNL's catalytic efficiency is less towards bulky substrates. HLADH also did not show similar oxidation efficiency with other alcohols to that of benzyl alcohol.



Scheme 2.2. HLADH-*At*HNL cascade catalyzed stereoselective conversion of benzylic alcohols to (*R*)-β-nitroalcohols.

Table 2.4. HLADH-*At*HNL cascade catalyzed synthesis of enantioenriched (*R*)-β-nitroalcohols from corresponding primary alcohols.[a)]

Entry	R[a)]	Time (h)	% conv. alc.to ald[b)]	% conv. ald.to BNA[c)]	% conv. alc.to BNA[d)]	% *ee*
1	H	4	90.0 ± 6.1	64.6 ± 3.9	58.2 ± 0.4	99.2 ± 0.3
2	H	6	85.3 ± 4.2	74.5 ± 3.2	63.8 ± 0.4	98.2 ± 0.3
3	3-OMe	8	59.7 ± 5.4	41.8 ± 2.1	24.9 ± 1.0	98.6 ± 1.1
4	3,5-*di*OMe	8	6.2 ± 4.5	23.5 ± 0.2	1.4 ± 1.1	>99
5	2-Cl	8	9.3 ± 0.1	82.2 ± 0.1	7.6 ± 0.1	>99
6	3-Cl	4	54.5 ± 5.0	75.8 ± 5.6	41.2 ± 0.8	99.4 ± 0.2
7	4-Cl	4	70.1 ± 6.1	38.2 ± 1.0	26.8 ± 1.6	98.0 ± 0.9
8	3,4-*di*Cl	4	33.1 ± 7.2	57.8 ± 2.2	19.0 ± 3.4	99.1 ± 0.7
9	3-NO_2	8	26.0 ± 0.8	90.3 ± 1.4	23.4 ± 0.4	95.1 ± 6.9
10	4-NO_2	8	11.0 ± 4.0	89.5 ± 14.9	9.3 ± 2.0	69.3 ± 11.7
11	4-$PhCH_2O$	8	60.0 ± 14.4	2.6 ± 1.2	1.5 ± 0.3	>99

[a)] R belongs to structure of Scheme 2.2. [b)] % conversion of alcohol to aldehyde. [c)] % conversion of aldehyde to β-nitroalcohol (BNA), [d)] % conversion of alcohol to BNA, Reaction conditions (1 mL): For HLADH-*At*HNL, 433 µL of *n*-butyl acetate, 2.5 U of HLADH, 800 U of *At*HNL, 100 mM KPB pH 6, 1 mM NAD^+, 125 mM acetaldehyde, 1.5 M nitromethane, 0.1 mM $ZnCl_2$, 25 mg/mL sorbitol, 25 mM substrate and the remaining volume of autoclaved double distilled water. This reaction mixture was incubated at 30 °C and 1,200 rpm in a thermoshaker. For every reaction two replicates were taken.

2.4.7. Optimization of reaction parameters of *Bm*HNL catalyzed nitroaldol reaction

After successfully illustrating the HLADH-*At*HNL cascade catalyzed biotransformation, we aimed to prepare stereocomplementary β-nitroalcohols by using *Bm*HNL, an (*S*)-selective hydroxynitrile lyase from *Baliospermum montanum*. So far, *Bm*HNL has not been explored for the nitroaldolase activity. To our pleasure, *Bm*HNL catalyzed this promiscuous nitroaldol reaction and subsequently, the reaction parameters of this biotransformation were optimized to achieve maximum conversion and enantiopurity of (*S*)-β-nitroalcohols.

2.4.7.1. Optimization of *Bm*HNL enzyme content using benzaldehyde as the substrate

With the increase in *Bm*HNL content, % conversion of (*S*)-NPE increased significantly but the % ee of the product decreased after 5 U of *Bm*HNL. So, for further studies 5 U of *Bm*HNL was selected, where 37% conversion with 52% ee of (*S*)-NPE was found (Figure 2.25).

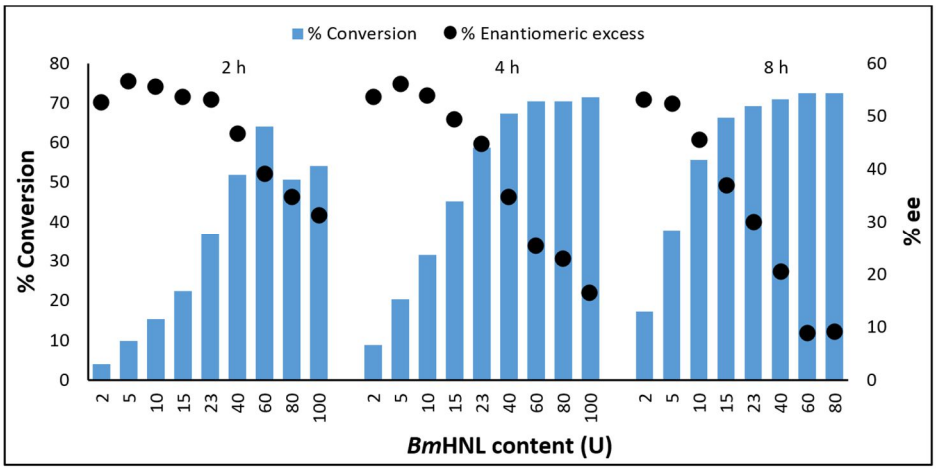


Figure 2.25: Optimization of *Bm*HNL content in the synthesis of (*S*)-NPE from benzaldehyde.

2.4.7.2. Optimization of buffer system and its pH

To further improve the enantioselectivity of the product, we investigated the effect of reaction buffer and its pH on the nitroaldol synthesis. A gradual decrease in *ee* of the product was noticed with an increase in pH of the three buffers tested [citrate phosphate buffer (CPB), Tris-HCl, and phosphate buffer]. Instead of choosing CPB pH 4.5 that gave 62% *ee*, CPB pH 5.5 was selected where 56.3% *ee* with 37.6% conversion of (*S*)-NPE was observed. This % *ee* is similar to the previous optimization experiment result, while the % conversion is more than two-fold as compared to the case of CPB pH 4.5 (Figure 2.26).

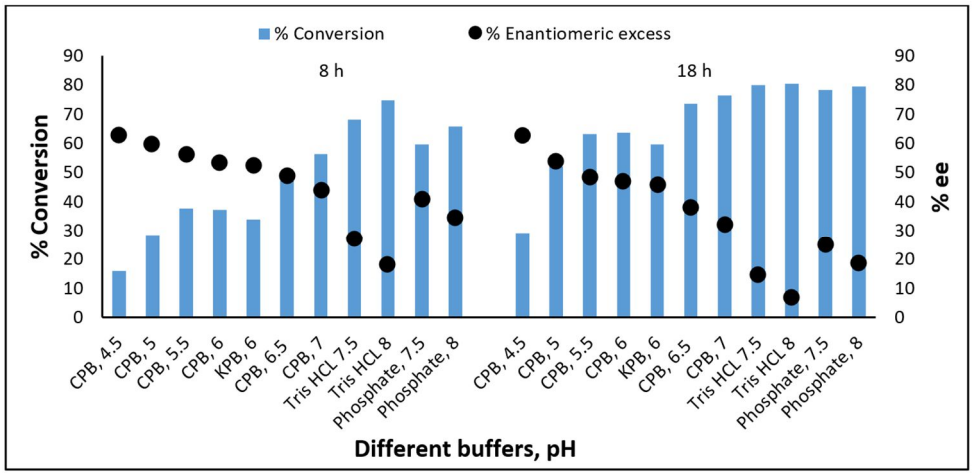


Figure 2.26: Effect of different buffers and their pH in the *Bm*HNL catalyzed synthesis of (*S*)-NPE.

2.4.7.3. Optimization of organic solvent

The significance of a biphasic system in HNL Catalyzed nitroaldol reaction has been explained earlier. Among the five organic solvents selected, i.e., *n*-butyl acetate, DIPE, TBME, toluene, and *di*-ethyl ether, increased enantioselectivity was seen with TBME and *di*-ethyl ether. We found a marginal increase in enantiopurity of (*S*)-NPE in TBME, where 60% ee and 55% conversion to the product was found in 8 h (figure 2.27).

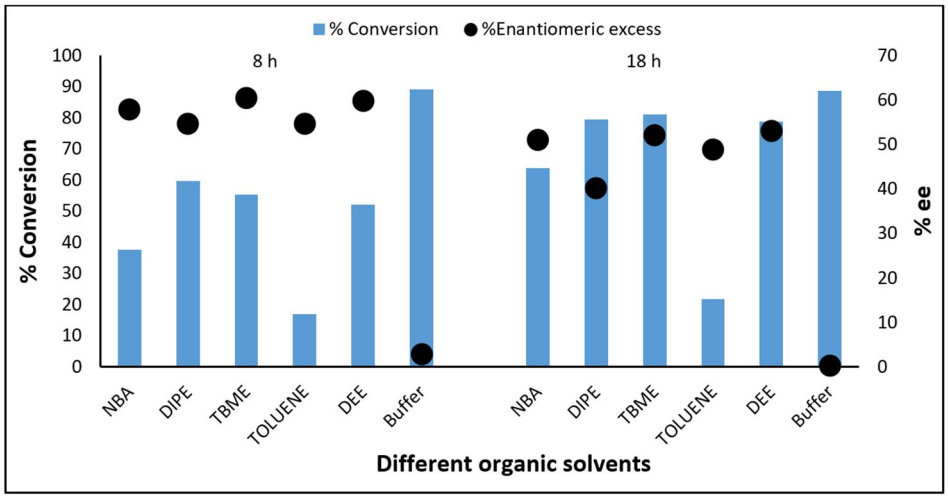


Figure 2.27: Effect of different organic solvents in the *Bm*HNL catalyzed synthesis of (*S*)-NPE.

2.4.7.4. Optimization of protein stabilizer or reaction additive

We added ten different sugars and polyols to *Bm*HNL and investigated whether their presence could increase the optical yield and conversion to (*S*)-NPE from benzaldehyde. None of them has increased the % *ee* of the product significantly; however, lactose, sucrose, and sorbitol increased the % conversion up to 60% and sorbitol was chosen for further experiments (figure 2.28).

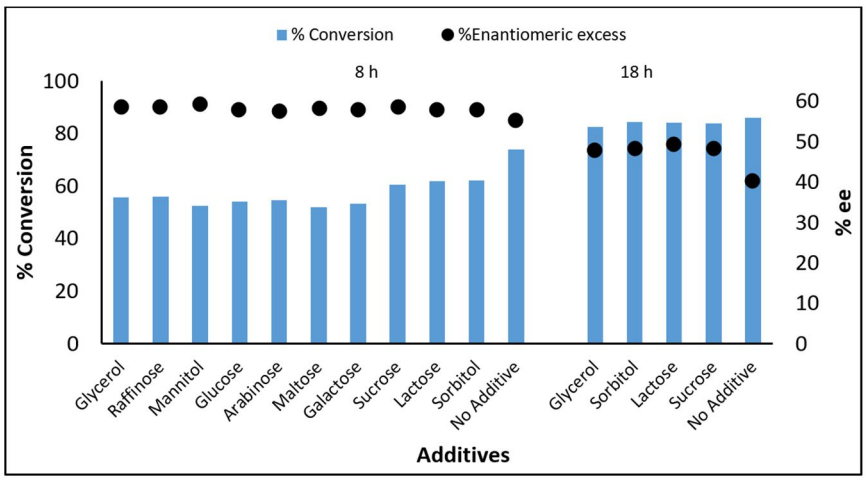


Figure 2.28: Effect of different additives in the *Bm*HNL catalyzed synthesis of (*S*)-NPE.

2.4.7.5. Optimization of substrate

Optimization of different biocatalytic conditions of the *Bm*HNL catalyzed nitroaldol reaction has provided little improvement in the % ee of (*S*)-NPE (52% to 60%). We, therefore, selected six different bulkier aromatic aldehydes, and under optimized conditions their corresponding (*S*)-β-nitroalcohols were synthesized. In the case of 3,5-dimethoxybenzaldehyde (3,5-*di*OMeBA), the corresponding (*S*)-β-nitroalcohol was produced in excellent *ee*, i.e., 98%, while the conversion was found to be 48% (figure 2.29).

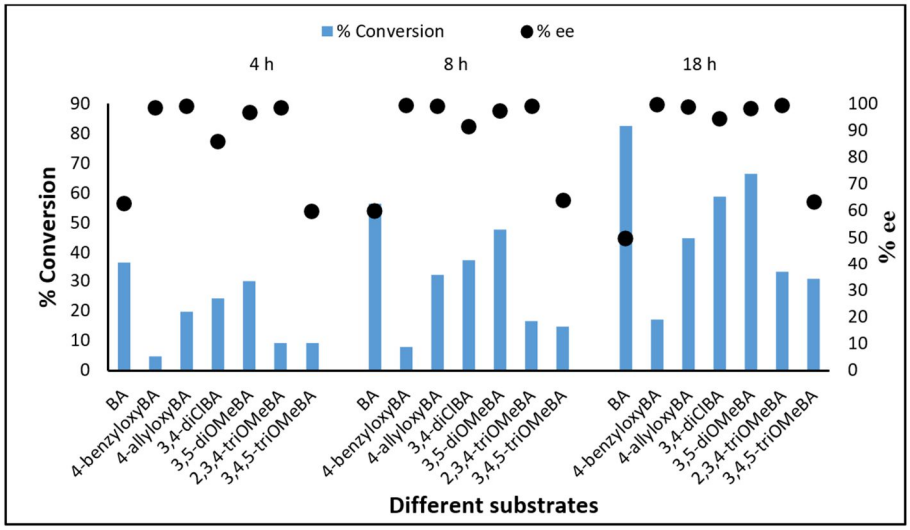


Figure 2.29: Study of different aromatic aldehydes in the *Bm*HNL catalyzed synthesis of the corresponding (*S*)-nitroaldol products.

2.4.7.6. Optimization of *Bm*HNL content using 3,5-dimethoxybenzaldehyde as the substrate

Prior to explore the HLADH-*Bm*HNL cascade, we further optimized the *Bm*HNL content in the nitroaldol reaction using 3,5-*di*OMeBA as substrate. To our pleasure, the % conversion to corresponding (*S*)-nitroaldol has increased to 77 in 8 h with 30 U of *Bm*HNL (figure 2.30). The whole optimization study is summarised in figure 2.31.

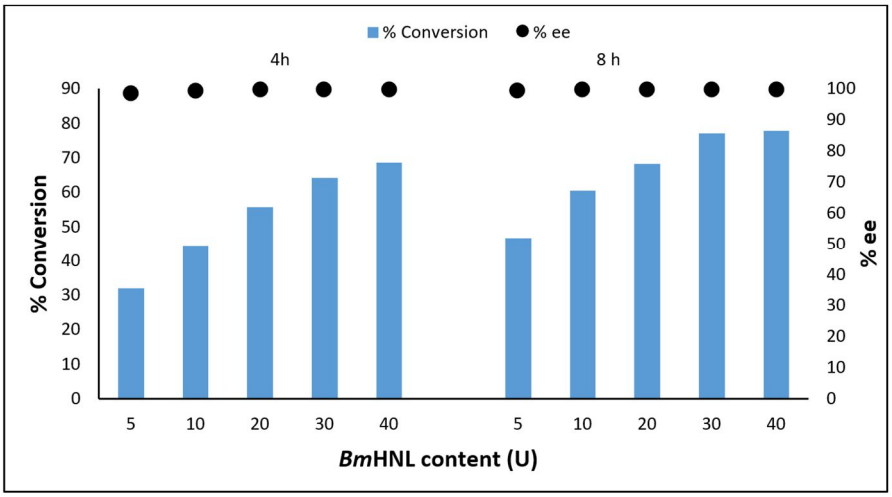


Figure 2.30: Optimization of *Bm*HNL content in the synthesis of the corresponding (*S*)-nitroaldol from 3,5-dimethoxy benzaldehyde.

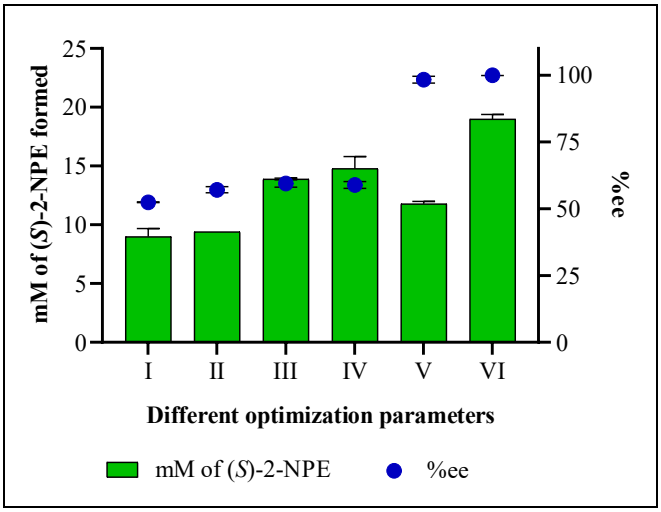


Figure 2.31: Summary of optimization of biocatalytic parameters of *Bm*HNL catalyzed nitroaldol reaction using benzaldehyde (I to IV) or 3,5-dimethoxy benzaldehyde as substrate (VI) in the synthesis of (*S*)-β-nitroalcohols. I: *Bm*HNL content, II: buffer system and pH, III: different co-solvents (organic), IV: reaction additive, V: screening of substrates, VI: *Bm*HNL content.

2.4.8. Optimization of HLADH content in the HLADH-*Bm*HNL cascade using 3,5-dimethoxybenzyl alcohol as the substrate

To carry out the HLADH-*Bm*HNL cascade, we have combined the optimal reaction conditions of HLADH catalyzed oxidation (used in the previous cascade), and *Bm*HNL catalyzed nitroaldol synthesis using 3,5-*di*OMeBA as the substrate. In this experiment, three biocatalytic conditions were investigated. They were (a) 10 U HLADH with 1 mM NAD^+, (b) 10 U HLADH with 4 mM NAD^+ and (c) 20 U HLADH with 1 mM NAD^+. However, we noticed that HLADH had shown only 6% conversion in the oxidation of 3,5-*di*OMebenzyl alcohol to its aldehyde in the HLADH-*At*HNL cascade (Table 2.4). Therefore, we have tested higher HLADH content in the cascade, and accordingly NAD^+ amount in this optimization study. A five-fold increase in the oxidation was observed with 10 U of HLADH and 1 mM NAD^+, as compared to the addition of 4 mM NAD^+. A significant increase in the oxidation was not

observed even if HLADH amount was doubled (20 U). In 24 h, with 10 U of HLADH the cascade has resulted in 41% oxidation of 3,5-*di*OMebenzyl alcohol, and corresponding (*S*)-nitroalcohol was found in 37% conversion with >99% *ee* (figure 2.32).

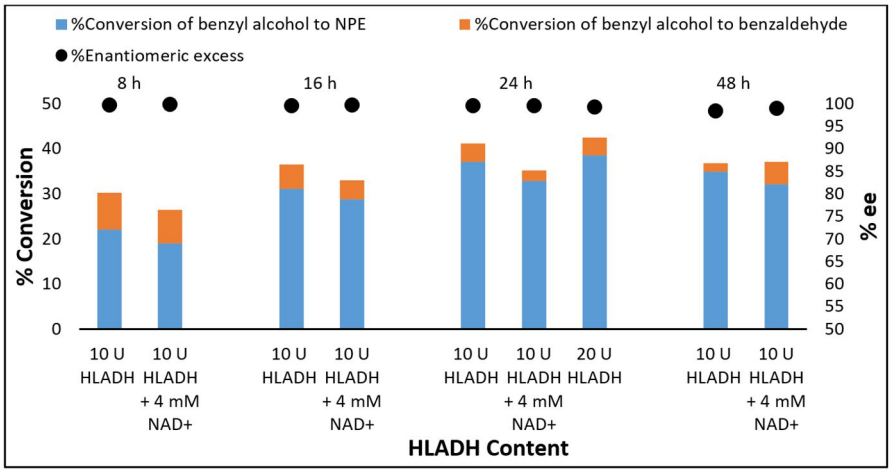
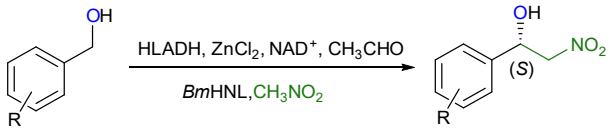


Figure 2.32: Study of the amount of HLADH in HLADH-*Bm*HNL cascade in the synthesis of (*S*)-NPE.

2.4.9. HLADH-*Bm*HNL cascade catalyzed enantioselective synthesis of different (*S*)-β-nitroalcohols

The same substrate set of Table 2.4 was used in the HLADH-*Bm*HNL cascade that resulted in the syntheses of the corresponding (*R*)-β-nitroalcohols with high enantioselectivity (up to >99%) (figure 2.33-2.42). *Bm*HNL not only showed opposite enantiopreference to *At*HNL but also better substrate preference. Unlike the previous cascade, HLADH-*Bm*HNL cascade converted most of the bulky aromatic alcohols into their corresponding (*S*)-β-nitroalcohols with high enantioselectivity. *Bm*HNL catalyzed Henry reaction in the cascade has produced 42-97% conversion of the aldehydes to their corresponding (*S*)-β-nitroalcohols. Analysis of the HLADH-*Bm*HNL cascade shows that except benzyl alcohol and 2-chlorobenzyl alcohol, the remaining eight alcohols were converted in 83-99% *ee* and 19-55% conversion. Five (*S*)-β-nitroalcohols (entries 3, 4, 8, 9, and 11, Table 2.5) were first time synthesized by HNL biocatalysis here using our enzyme cascade. Between the two cascades involving *At*HNL, and *Bm*HNL, higher % conversion was observed in the case of the latter, not only with the second step (Henry reaction) but also in the overall reaction. This higher conversion by *Bm*HNL cascade could be justified due to lesser benzaldehyde (aldehyde) inhibition than *At*HNL (Figure 2.6 and 2.7).



Scheme 2.3: HLADH-*Bm*HNL cascade catalyzed stereoselective conversion of benzylic alcohols to (*S*)-β-nitroalcohols.

Table 2.5. HLADH-*Bm*HNL cascade catalyzed synthesis of (*S*)-β-nitroalcohols from corresponding primary alcohols.[a)]

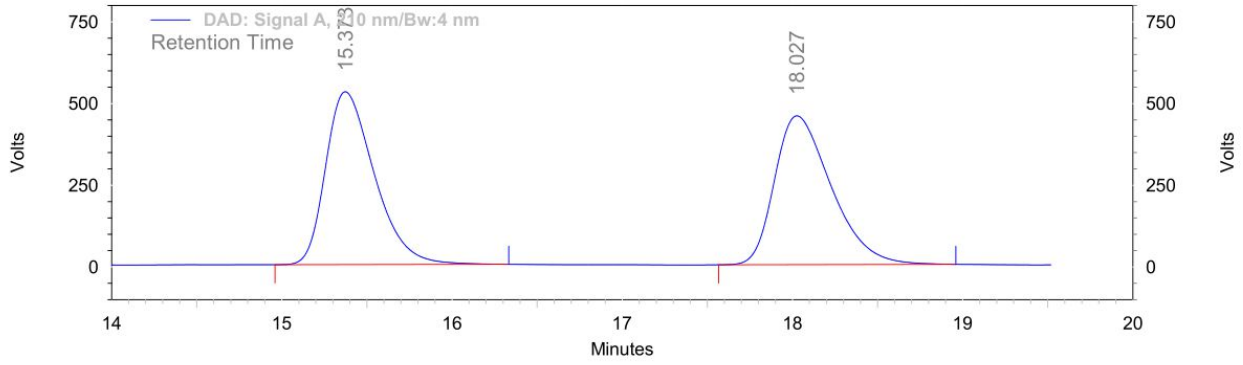
Entry	R[a)]	Time (h)	% conv. alc.to ald[b)]	% conv. ald.to BNA[c)]	% conv. alc.to BNA[d)]	% *ee*
1	H	8	85.2 ± 1	57.6 ± 5.5	49.1 ± 4.1	57.7 ± 0.8
2	H	16	83 ± 0.8	84.3 ± 1.2	70± 1.8	46.2 ± 0.5
3	3-OMe	8	66.5 ± 13.7	69.8 ± 0.7	46.4 ± 9.1	94.5 ± 0.5
4	3,5-*di*OMe	24	40.6 ± 0.7	92.9 ± 3.8	37.7 ± 0.9	>99
5	2-Cl	8	18.7 ± 2.9	96.8 ± 0.5	18.1 ± 2.7	40 ± 0.3
6	3-Cl	16	60.1 ± 6.1	91.7 ± 1.5	55.1 ± 4.6	91.8 ± 0.76
7	4-Cl	16	54.9 ± 6.6	76.3 ± 6.7	41.7 ± 1.3	94.5 ± 0.1
8	3,4-*di*Cl	24	34.8 ± 5.8	84.2 ± 11.2	28.9 ± 1	98 ± 0.7
9	3-NO_2	8	34.2 ± 10.7	95.1 ± 7.6	32.1 ± 7.6	82.6 ± 7.2
10	4-NO_2	8	38.6 ± 8.2	97.2 ± 3.8	37.7 ± 9.4	93 ± 2.2
11	4-$PhCH_2O$	24	46.4 ± 8.1	41.6 ± 0.9	19.3 ± 3.8	98.1 ± 0.8

[a)] R belongs to structure of Scheme 2.3. [b)] % conversion of alcohol to aldehyde. [c)] % conversion of aldehyde to BNA, [d)] % conversion of alcohol to BNA, Reaction conditions (1 mL): For HLADH-*Bm*HNL, 358 µL TBME, 2.5 or 10 U of HLADH, 5 or 30 U of *Bm*HNL, 100 mM CPB pH 5.5, 1.5 M nitromethane, 25 mM substrate, 50 mg/mL sorbitol, 1 mM of NAD^+, 0.1 mM $ZnCl_2$, and 125 mM acetaldehyde and the remaining volume of autoclaved double distilled water.

2.4.10. HPLC chromatograms of products of HLADH-*At*HNL and HLADH-*Bm*HNL cascade

1. HPLC chromatograms of 2-nitro-1-phenylethanol

A.

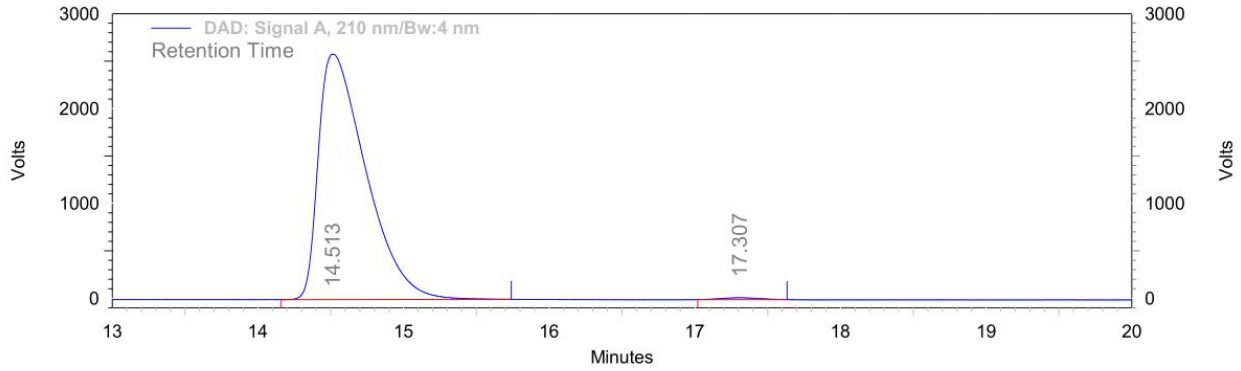


DAD: Signal A, 210 nm/Bw:4 nm
Results

Retention Time	Area	Area %	Height	Height %
15.373	22080299	49.96	1109114	53.73
18.027	22112873	50.04	955154	46.27
Totals	44193172	100.00	2064268	100.00

Retention time	15.373	18.027
Product	(*R*)-product	(*S*)-product

B.

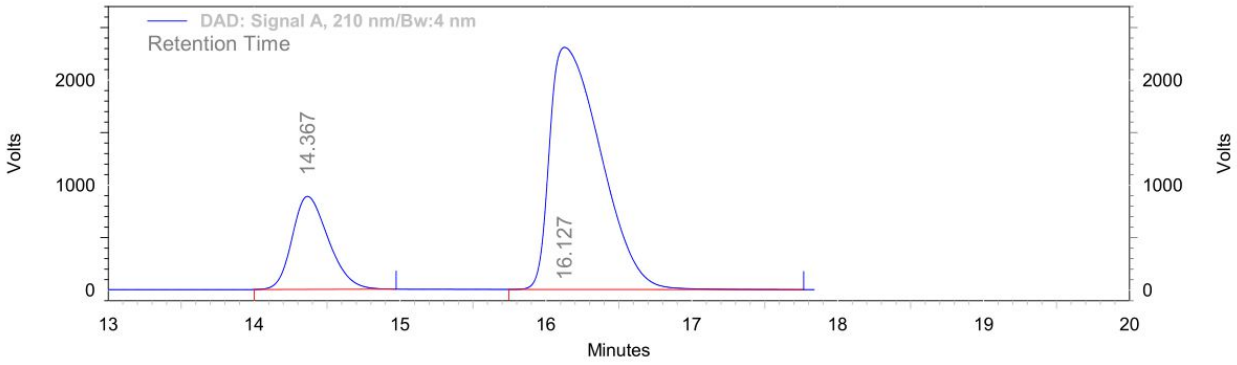


DAD: Signal A,
210 nm/Bw:4 nm
Results

Retention Time	Area	Area %	Height	Height %
14.513	123020005	99.38	5426675	99.24
17.307	761631	0.62	41357	0.76
Totals	123781636	100.00	5468032	100.00

Retention time	14.513	17.307
Product	(*R*)-product	(*S*)-product

C.



DAD: Signal A,
210 nm/Bw:4 nm
Results

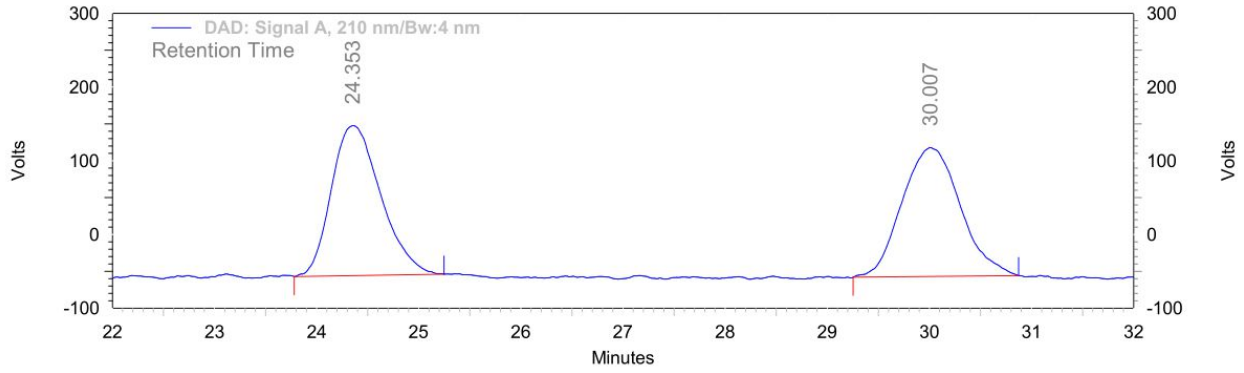
Retention Time	Area	Area %	Height	Height %
14.367	32087074	21.40	1857561	27.76
16.127	117837173	78.60	4833452	72.24
Totals	149924247	100.00	6691013	100.00

Retention time	14.367	16.127
Product	(*R*)-product	(*S*)-product

Figure 2.33: HPLC chromatograms of 2-nitro-1-phenylethanol. A. racemic standard, B. enantiopure product synthesized by HLADH-*At*HNL cascade, C. enantioenriched (*S*)-2-nitro-1-phenylethanol synthesized by HLADH-*Bm*HNL cascade.

2. HPLC chromatograms of 1-(3-methoxyphenyl)-2-nitroethanol

A.

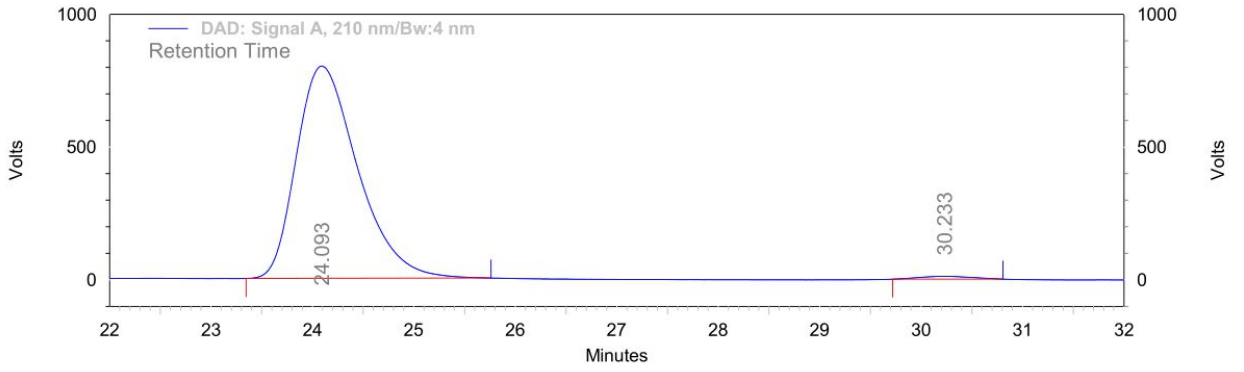


DAD: Signal A,
210 nm/Bw:4 nm
Results

Retention Time	Area	Area %	Height	Height %
24.353	14321619	49.63	427267	53.79
30.007	14535602	50.37	366995	46.21
Totals	28857221	100.00	794262	100.00

Retention time	24.353	30.007
Product	(*R*)-product	(*S*)-product

B.

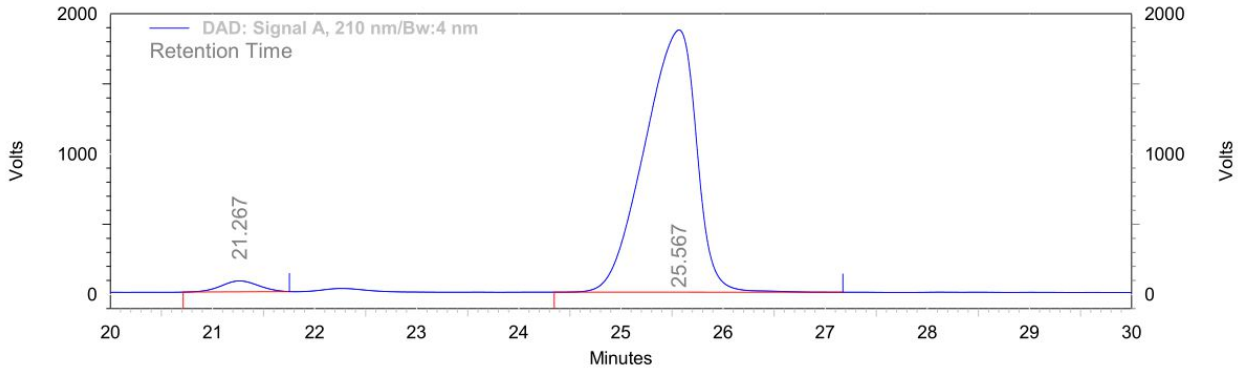


DAD: Signal A,
210 nm/Bw:4 nm
Results

Retention Time	Area	Area %	Height	Height %
24.093	70380983	98.89	1675738	98.73
30.233	789491	1.11	21629	1.27
Totals	71170474	100.00	1697367	100.00

Retention time	24.093	30.233
Product	(*R*)-product	(*S*)-product

C.



DAD: Signal A,
210 nm/Bw:4 nm
Results

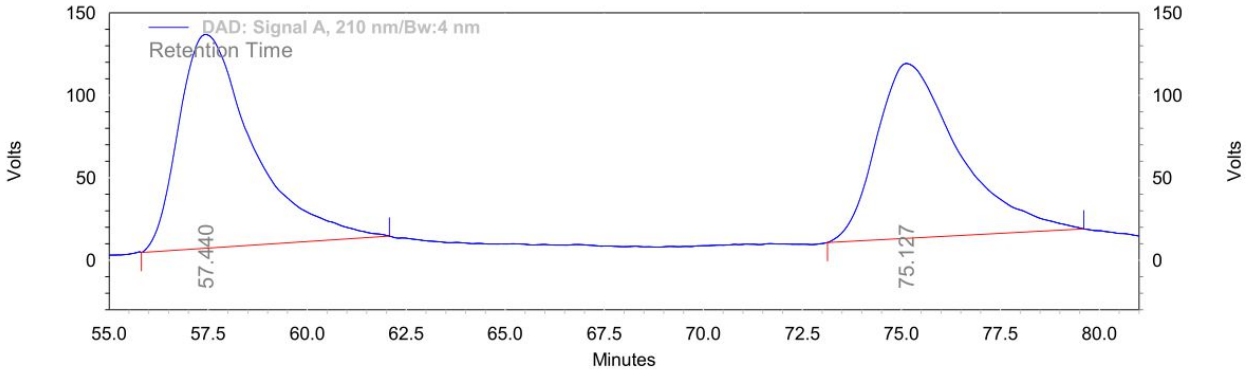
Retention Time	Area	Area %	Height	Height %
21.267	4162634	2.92	163119	4.00
25.567	138313675	97.08	3916959	96.00
Totals	142476309	100.00	4080078	100.00

Retention time	21.267	25.567
Product	(*R*)-product	(*S*)-product

Figure 2.34: HPLC chromatograms of 1-(3-methoxyphenyl)-2-nitroethanol. A. racemic standard, B. enantiopure product synthesized by HLADH-*At*HNL cascade, C. enantioenriched (*S*)- 1-(3-methoxyphenyl)-2-nitroethanol synthesized by HLADH-*Bm*HNL cascade.

3. HPLC chromatograms of 1-(3, 5-dimethoxyphenyl)-2-nitroethanol

A.

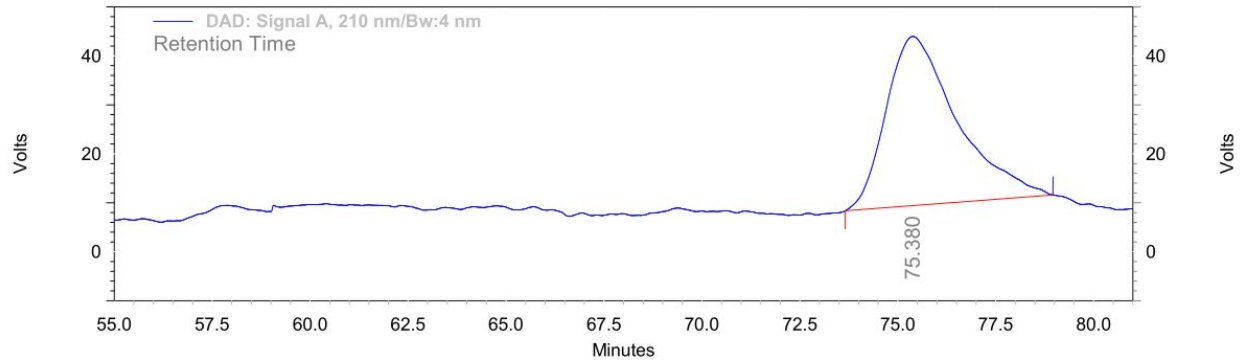


DAD: Signal A,
210 nm/Bw:4 nm
Results

Retention Time	Area	Area %	Height	Height %
57.440	35389865	52.49	271666	55.01
75.127	32029222	47.51	222219	44.99
Totals	67419087	100.00	493885	100.00

Retention time	57.440	75.127
Product	(*S*)-product	(*R*)-product

B.

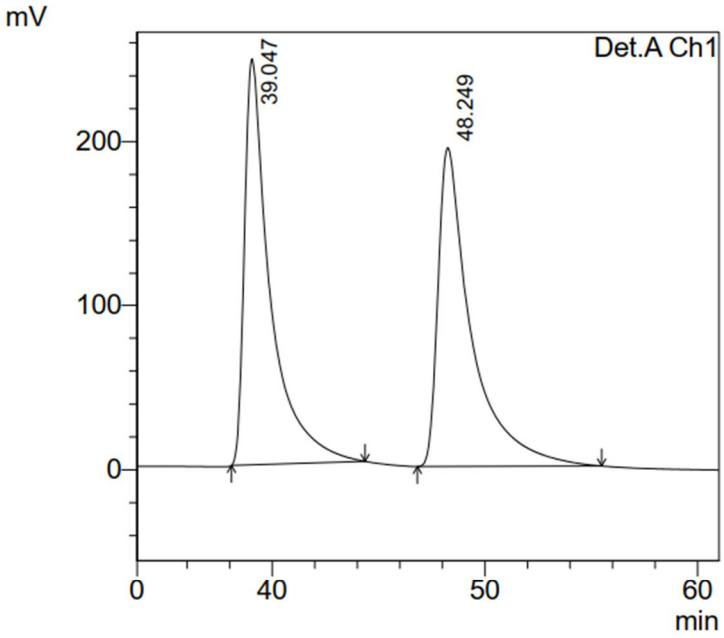


DAD: Signal A,
210 nm/Bw:4 nm
Results

Retention Time	Area	Area %	Height	Height %
75.380	9110897	100.00	72495	100.00
Totals	9110897	100.00	72495	100.00

Retention time	75.380
Product	(*R*)-product

C.



1 Det.A Ch1/210nm

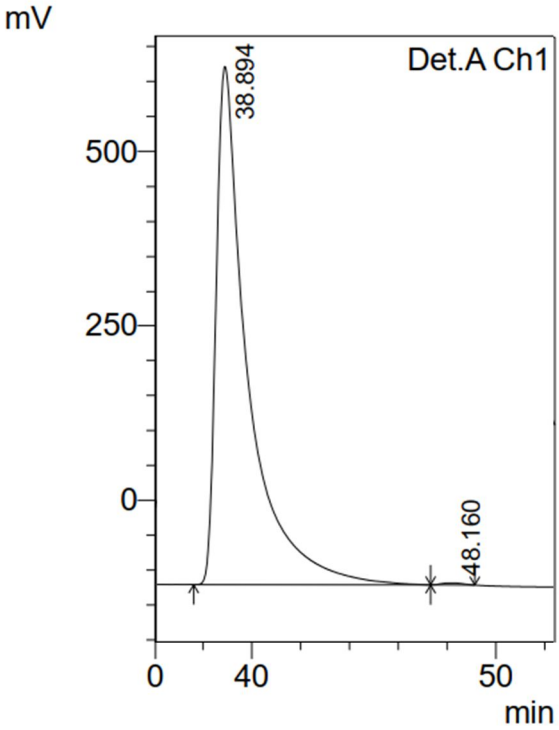
PeakTable

Detector A Ch1 210nm

Peak#	Ret. Time	Area	Height	Area %	Height %
1	39.047	20806850	247203	49.664	55.990
2	48.249	21088132	194310	50.336	44.010
Total		41894982	441513	100.000	100.000

Retention time	39.047	48.249
Product	(*S*)-product	(*R*)-product

D.



1 Det.A Ch1/210nm

PeakTable

Detector A Ch1 210nm

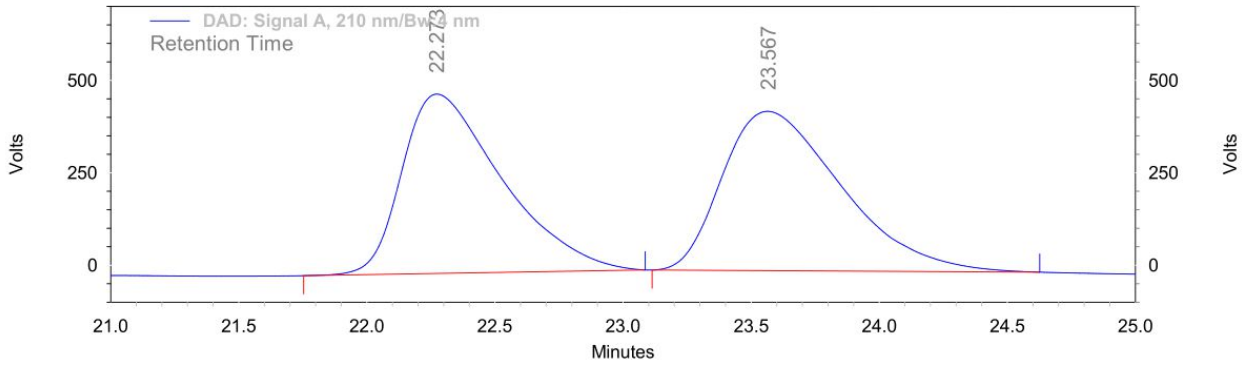
Peak#	Ret. Time	Area	Height	Area %	Height %
1	38.894	66964071	742196	99.747	99.592
2	48.160	169717	3043	0.253	0.408
Total		67133788	745239	100.000	100.000

Retention time	38.894	48.160
Product	(*S*)-product	(*R*)-product

Figure 2.35: HPLC chromatograms of 1-(3, 5-dimethoxyphenyl)-2-nitroethanol. A. racemic standard, B. enantiopure product synthesized by HLADH-*At*HNL cascade, C. racemic standard for HLADH-*Bm*HNL cascade, D. enantiopure product synthesized by HLADH-*Bm*HNL cascade.

4. HPLC chromatograms of 1-(2-chlorophenyl)-2-nitroethanol

A.

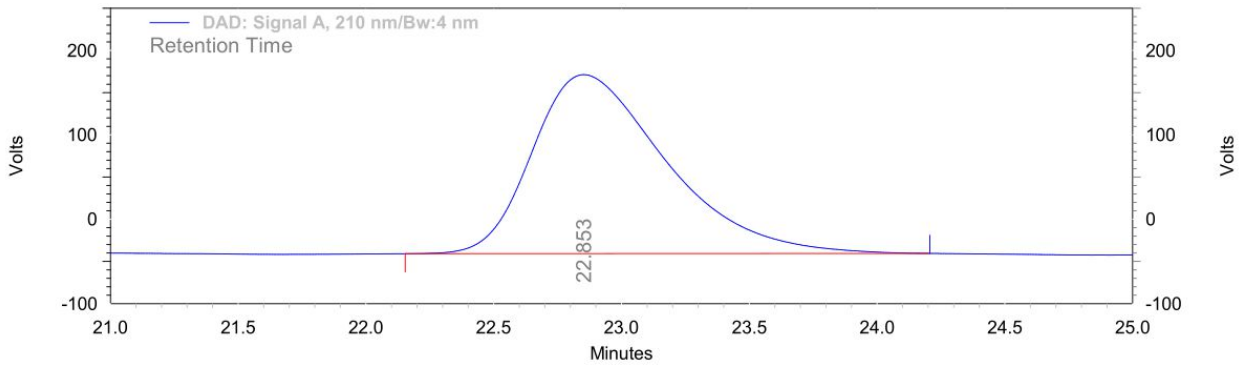


DAD: Signal A,
210 nm/Bw:4 nm
Results

Retention Time	Area	Area %	Height	Height %
22.273	27577483	48.60	1017459	52.96
23.567	29171331	51.40	903700	47.04
Totals	56748814	100.00	1921159	100.00

Retention time	22.273	23.567
Product	(*R*)-product	(*S*)-product

B.

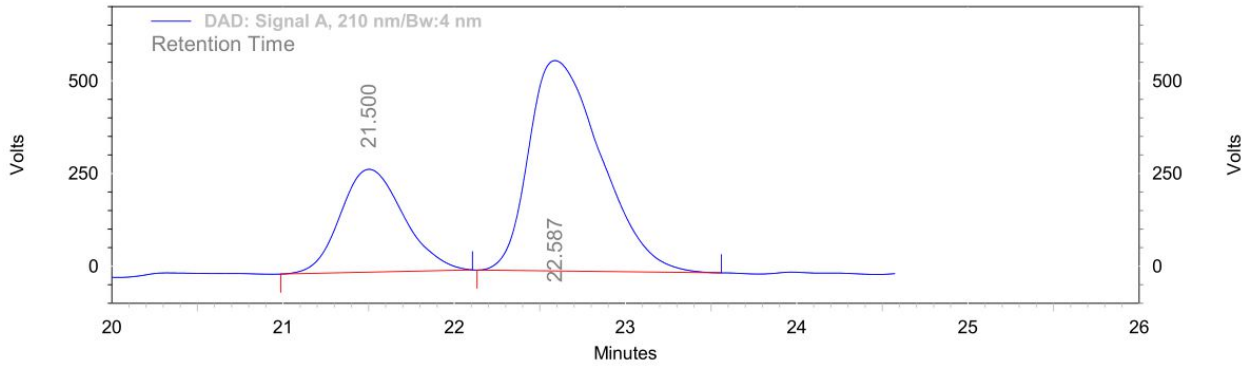


DAD: Signal A,
210 nm/Bw:4 nm
Results

Retention Time	Area	Area %	Height	Height %
22.853	16221263	100.00	444704	100.00
Totals	16221263	100.00	444704	100.00

Retention time	22.853
Product	(*R*)-product

C.



DAD: Signal A,
210 nm/Bw:4 nm
Results

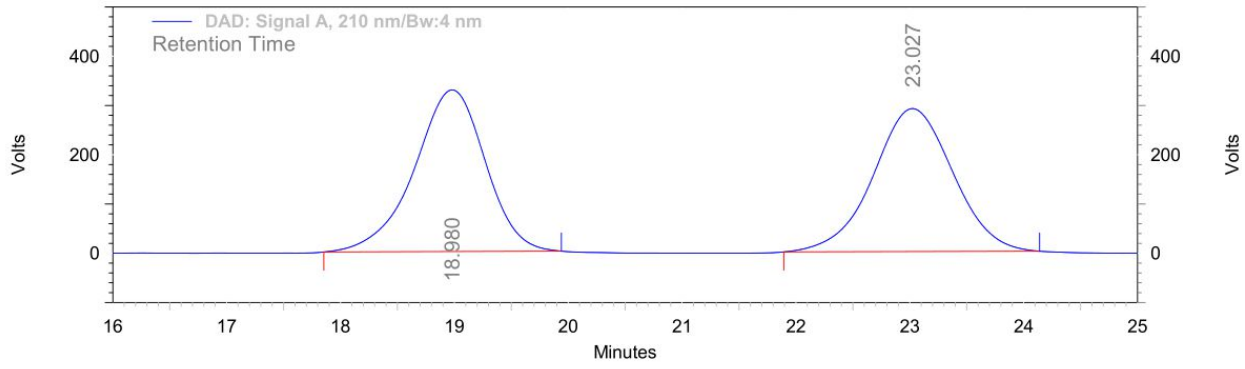
Retention Time	Area	Area %	Height	Height %
21.500	14904826	29.90	581498	32.83
22.587	34943613	70.10	1189860	67.17
Totals	49848439	100.00	1771358	100.00

Retention time	14.367	16.127
Product	(*R*)-product	(*S*)-product

Figure 2.36: HPLC chromatograms of 1-(2-chlorophenyl)-2-nitroethanol. A. racemic standard, B. enantiopure product synthesized by HLADH-*At*HNL cascade, C. enantioenriched product synthesized by HLADH-*Bm*HNL cascade

5. HPLC chromatograms of 1-(3-chlorophenyl)-2-nitroethanol

A.

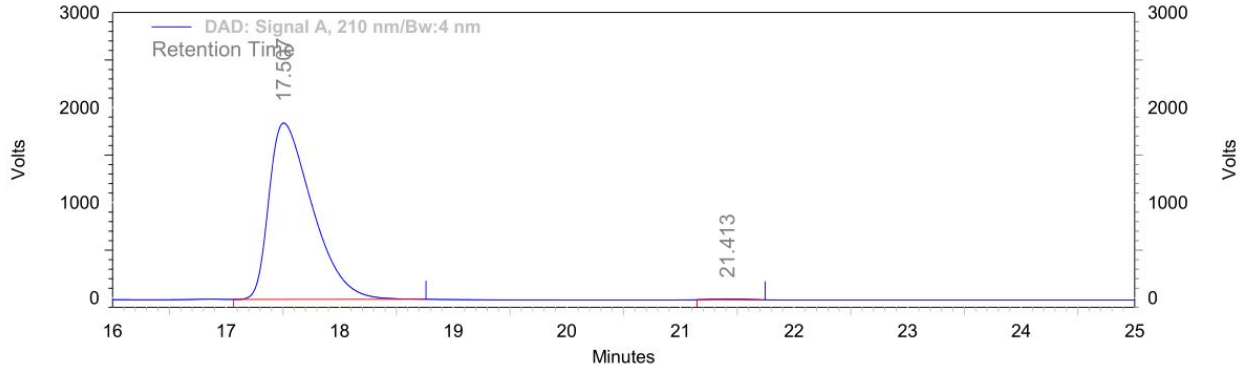


DAD: Signal A,
210 nm/Bw:4 nm
Results

Retention Time	Area	Area %	Height	Height %
18.980	29775193	50.13	688052	53.06
23.027	29618270	49.87	608747	46.94
Totals	59393463	100.00	1296799	100.00

Retention time	18.980	23.027
Product	(*R*)-product	(*S*)-product

B.

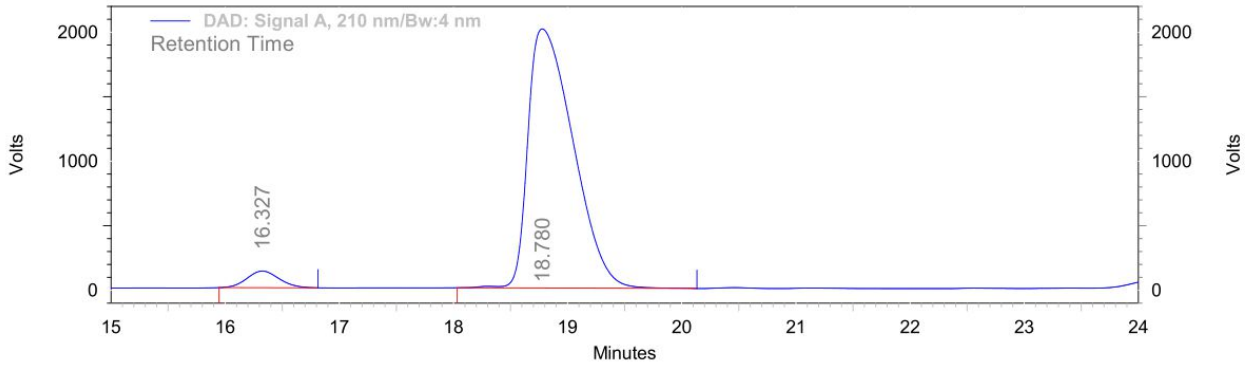


DAD: Signal A,
210 nm/Bw:4 nm
Results

Retention Time	Area	Area %	Height	Height %
17.507	103061924	99.63	3890782	99.51
21.413	386893	0.37	19177	0.49
Totals	103448817	100.00	3909959	100.00

Retention time	17.507	21.413
Product	(*R*)-product	(*S*)-product

C.



DAD: Signal A,
210 nm/Bw:4 nm
Results

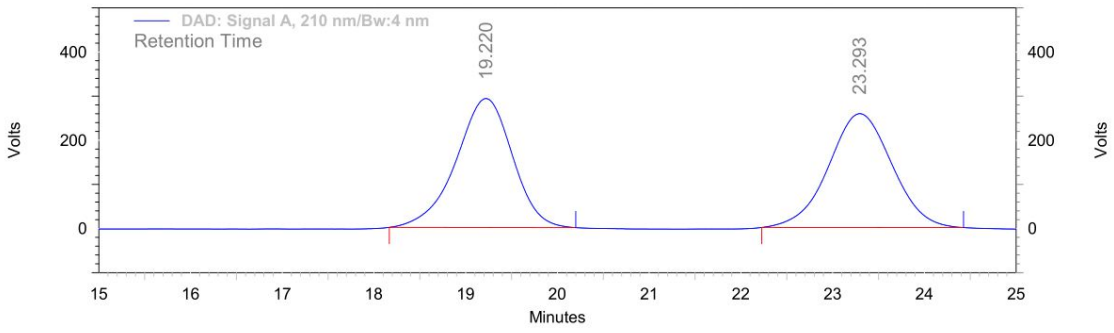
Retention Time	Area	Area %	Height	Height %
16.327	5309929	4.38	270777	6.04
18.780	115886959	95.62	4211825	93.96
Totals	121196888	100.00	4482602	100.00

Retention time	16.327	18.780
Product	(*R*)-product	(*S*)-product

Figure 2.37: HPLC chromatograms of 1-(3-chlorophenyl)-2-nitroethanol. A. racemic standard, B. enantiopure product synthesized by HLADH-*At*HNL cascade, C. enantioenriched product synthesized by HLADH-*Bm*HNL cascade.

6. HPLC chromatograms of 1-(4-chlorophenyl)-2-nitroethanol

A.

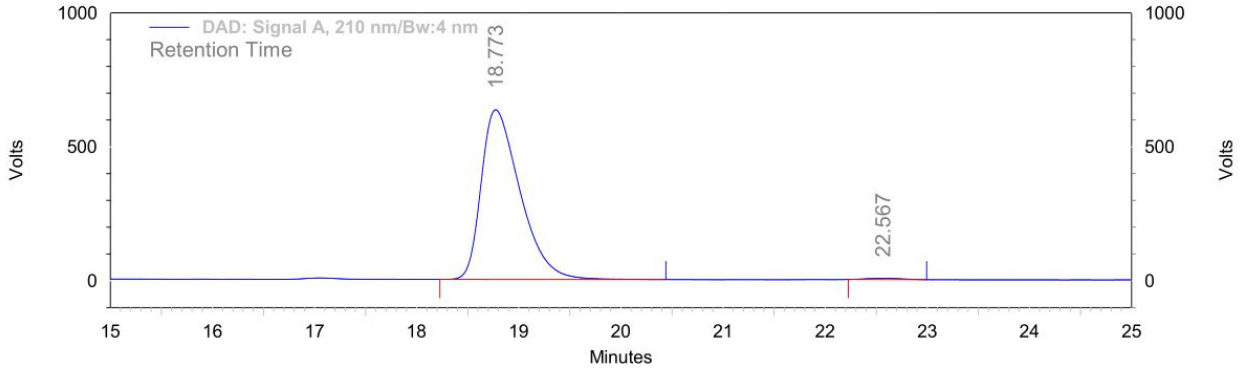


DAD: Signal A,
210 nm/Bw:4 nm
Results

Retention Time	Area	Area %	Height	Height %
19.220	26188506	50.16	612783	53.11
23.293	26019227	49.84	540993	46.89
Totals	52207733	100.00	1153776	100.00

Retention time	19.220	23.293
Product	(*R*)-product	(*S*)-product

B.

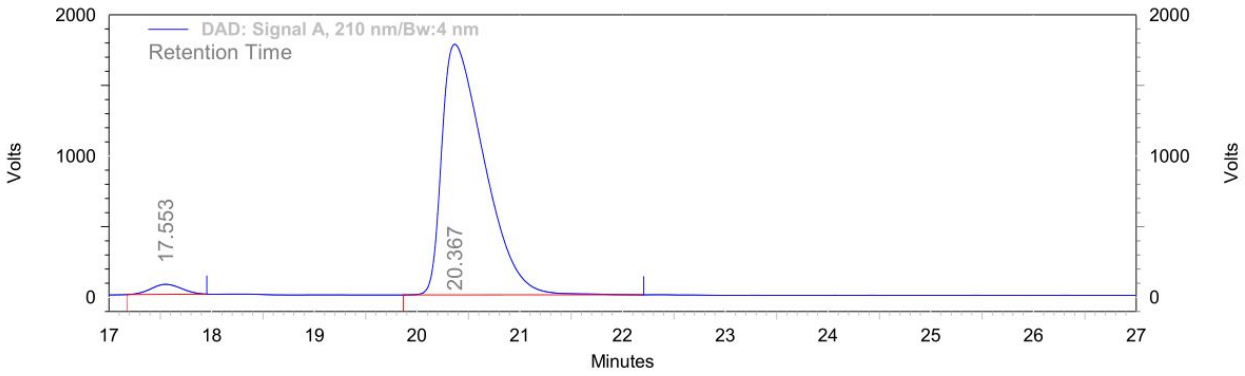


DAD: Signal A,
210 nm/Bw:4 nm
Results

Retention Time	Area	Area %	Height	Height %
18.773	35095626	99.31	1328146	99.24
22.567	245029	0.69	10140	0.76
Totals	35340655	100.00	1338286	100.00

Retention time	18.773	22.567
Product	(*R*)-product	(*S*)-product

C.



DAD: Signal A,
210 nm/Bw:4 nm
Results

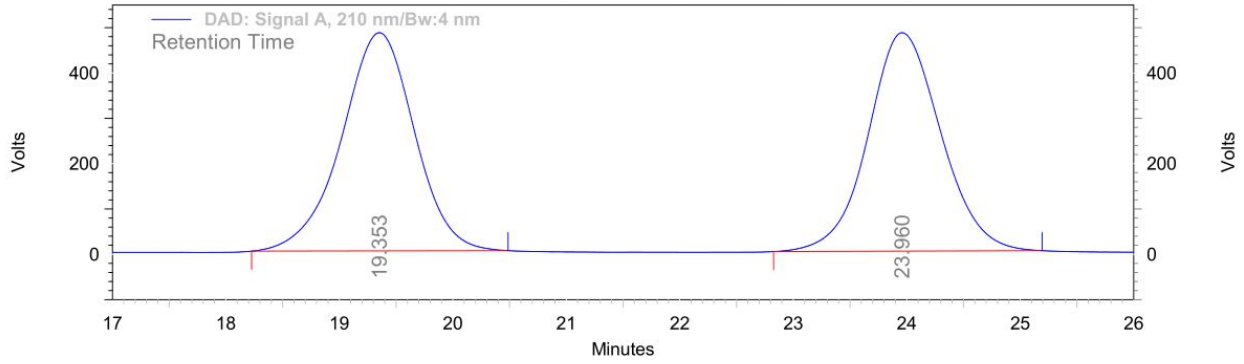
Retention Time	Area	Area %	Height	Height %
17.553	3095310	2.81	148900	3.85
20.367	106888490	97.19	3721136	96.15
Totals	109983800	100.00	3870036	100.00

Retention time	17.553	20.367
Product	(*R*)-product	(*S*)-product

Figure 2.38: HPLC chromatograms of 1-(4-chlorophenyl)-2-nitroethanol. A. racemic standard, B. enantiopure product synthesized by HLADH-*At*HNL cascade, C. enantioenriched product synthesized by HLADH-*Bm*HNL cascade.

7. HPLC chromatograms of 1-(3, 4-dichlorophenyl)-2-nitroethanol

A.

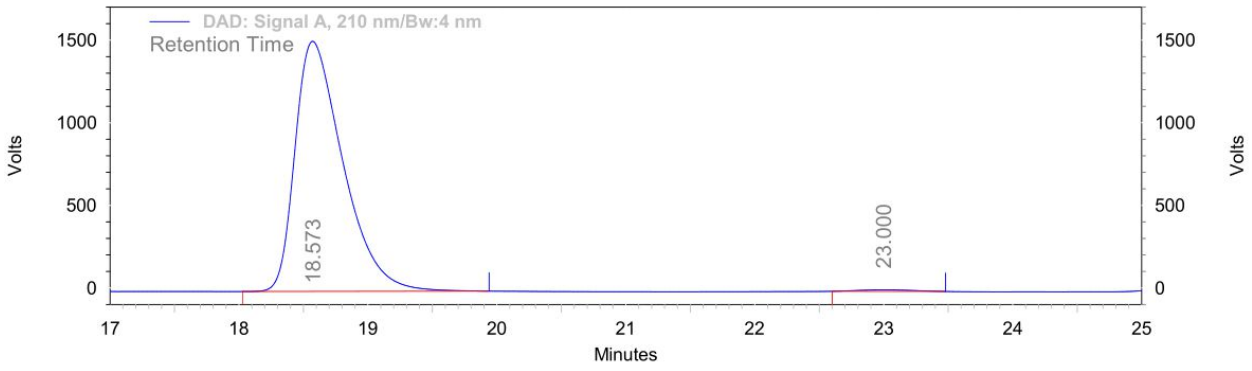


DAD: Signal A,
210 nm/Bw:4 nm
Results

Retention Time	Area	Area %	Height	Height %
19.353	44963009	49.93	1009745	49.98
23.960	45084127	50.07	1010644	50.02
Totals	90047136	100.00	2020389	100.00

Retention time	19.353	23.960
Product	(*R*)-product	(*S*)-product

B.

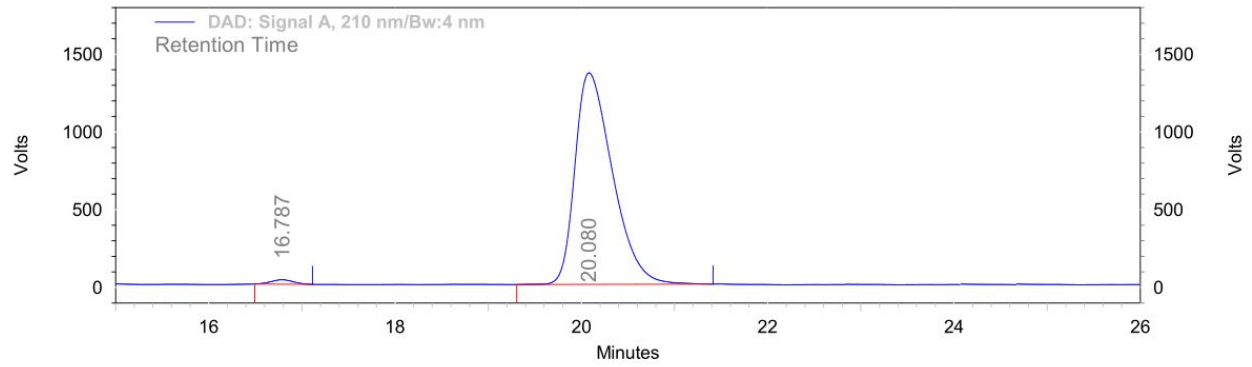


DAD: Signal A,
210 nm/Bw:4 nm
Results

Retention Time	Area	Area %	Height	Height %
18.573	81990482	99.31	3174494	99.38
23.000	568578	0.69	19794	0.62
Totals	82559060	100.00	3194288	100.00

Retention time	18.573	23
Product	(*R*)-product	(*S*)-product

C.



DAD: Signal A,
210 nm/Bw:4 nm
Results

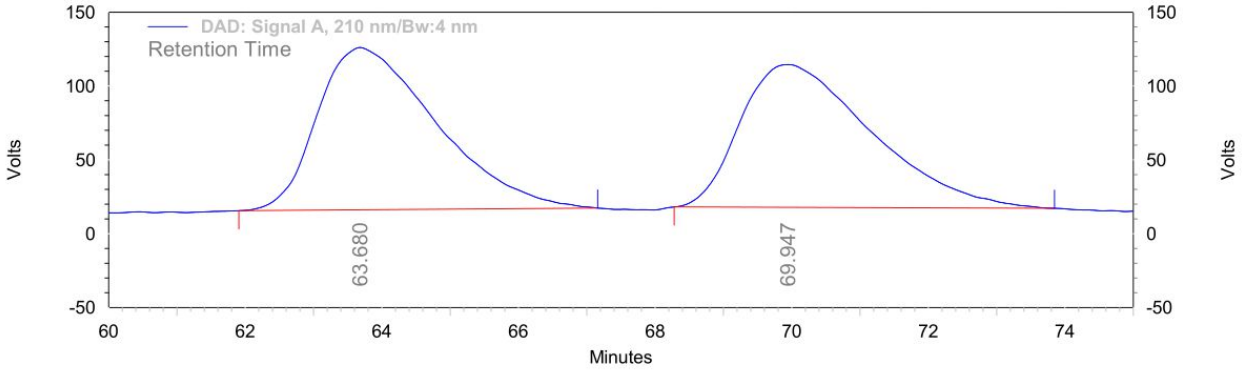
Retention Time	Area	Area %	Height	Height %
16.787	999611	1.24	59598	2.05
20.080	79893351	98.76	2853354	97.95
Totals	80892962	100.00	2912952	100.00

Retention time	16.787	20.080
Product	(*R*)-product	(*S*)-product

Figure 2.39: HPLC chromatograms of 1-(3, 4-dichlorophenyl)-2-nitroethanol. A. racemic standard, B. enantiopure product synthesized by HLADH-*At*HNL cascade, C. enantioenriched product synthesized by HLADH-*Bm*HNL cascade.

8. HPLC chromatograms of 1-(3-nitrophenyl)-2-nitroethanol

A.

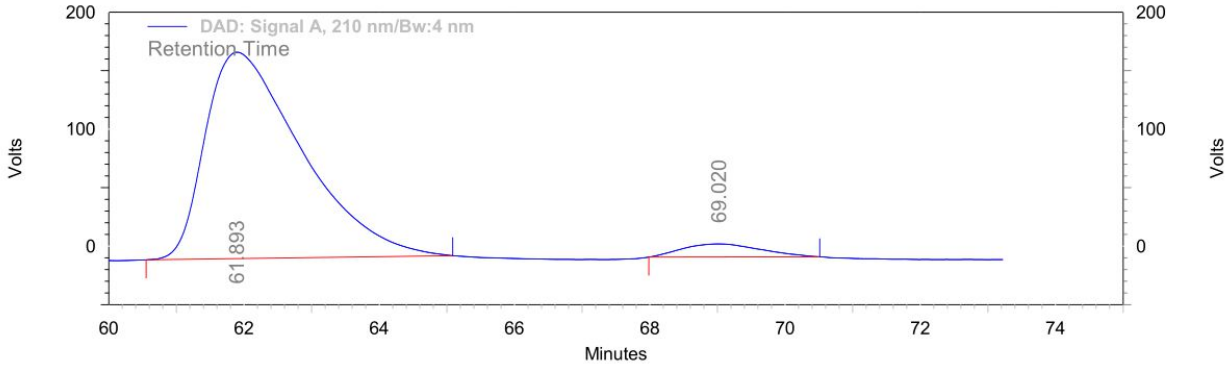


DAD: Signal A,
210 nm/Bw:4 nm
Results

Retention Time	Area	Area %	Height	Height %
63.680	27849210	50.81	230533	53.21
69.947	26963598	49.19	202752	46.79
Totals	54812808	100.00	433285	100.00

Retention time	63.680	69.947
Product	(*R*)-product	(*S*)-product

B.

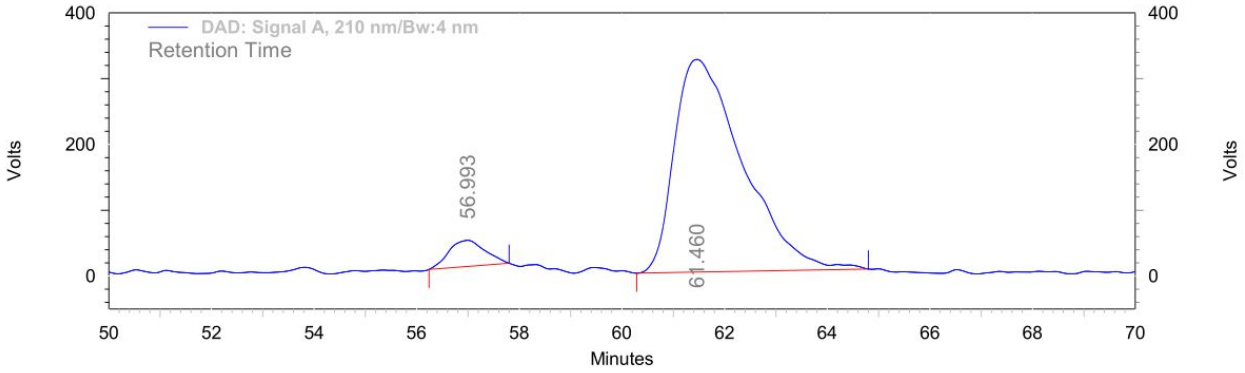


DAD: Signal A,
210 nm/Bw:4 nm
Results

Retention Time	Area	Area %	Height	Height %
61.893	36630656	95.11	369910	94.06
69.020	1883946	4.89	23344	5.94
Totals	38514602	100.00	393254	100.00

Retention time	61.893	69.020
Product	(*R*)-product	(*S*)-product

C.



DAD: Signal A,
210 nm/Bw:4 nm
Results

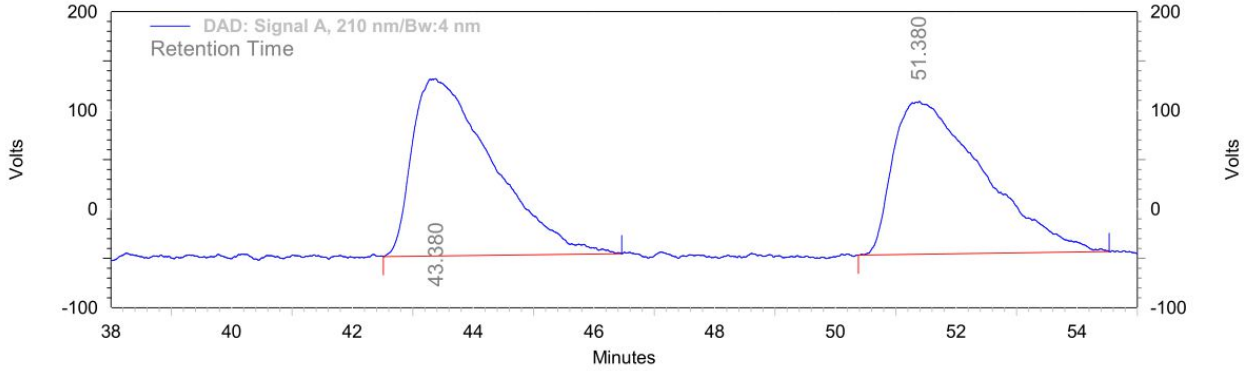
Retention Time	Area	Area %	Height	Height %
56.993	4093226	6.13	83031	10.92
61.460	62731388	93.87	677517	89.08
Totals	66824614	100.00	760548	100.00

Retention time	56.993	61.640
Product	(*R*)-product	(*S*)-product

Figure 2.40: HPLC chromatograms of 1-(3-nitrophenyl)-2-nitroethanol. A. racemic standard, B. enantioenriched product synthesized by HLADH-*At*HNL cascade, C. enantioenriched product synthesized by HLADH-*Bm*HNL cascade.

9. HPLC chromatograms of 1-(4-Nitrophenyl)-2-nitroethanol

A.

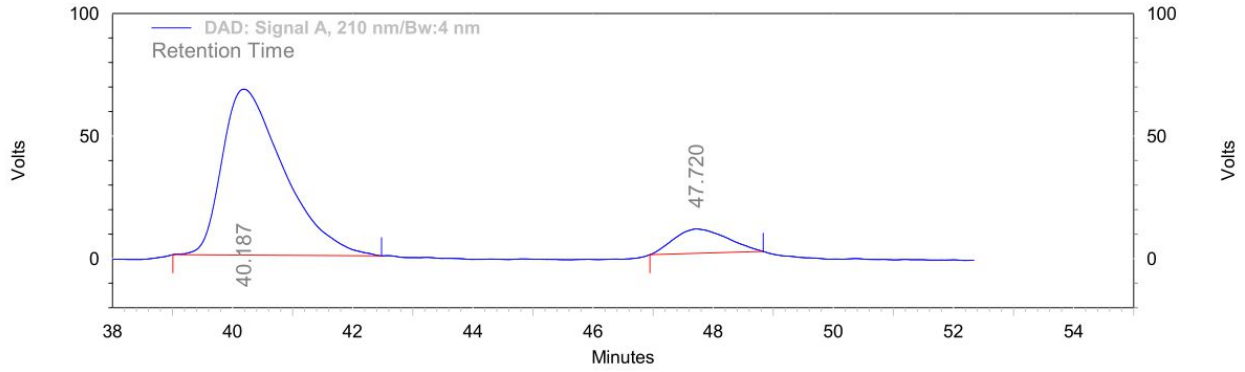


DAD: Signal A,
210 nm/Bw:4 nm
Results

Retention Time	Area	Area %	Height	Height %
43.380	34900380	50.80	376829	53.75
51.380	33805895	49.20	324205	46.25
Totals	68706275	100.00	701034	100.00

Retention time	43.38	51.38
Product	(*R*)-product	(*S*)-product

B.

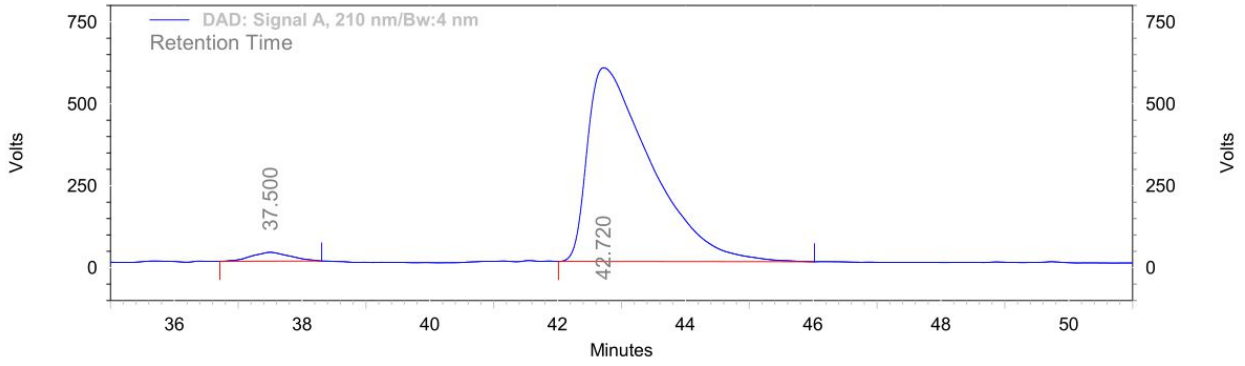


DAD: Signal A,
210 nm/Bw:4 nm
Results

Retention Time	Area	Area %	Height	Height %
40.187	10126891	88.77	141914	87.18
47.720	1280962	11.23	20871	12.82
Totals	11407853	100.00	162785	100.00

Retention time	40.187	47.720
Product	(*R*)-product	(*S*)-product

C.



DAD: Signal A,
210 nm/Bw:4 nm
Results

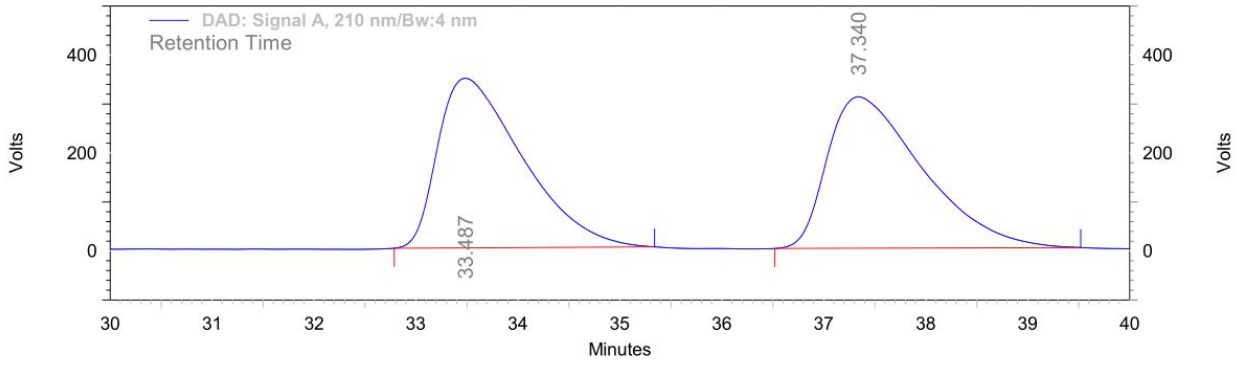
Retention Time	Area	Area %	Height	Height %
37.500	2373332	2.70	56610	4.37
42.720	85629667	97.30	1239670	95.63
Totals	88002999	100.00	1296280	100.00

Retention time	37.500	42.720
Product	(*R*)-product	(*S*)-product

Figure 2.41: HPLC chromatograms of 1-(4-nitrophenyl)-2-nitroethanol. A. racemic standard, B. enantioenriched product synthesized by HLADH-*At*HNL cascade, C. enantioenriched product synthesized by HLADH-*Bm*HNL cascade.

10. HPLC chromatograms of 1-(4-benzyloxyphenyl)-2-nitroethanol

A.

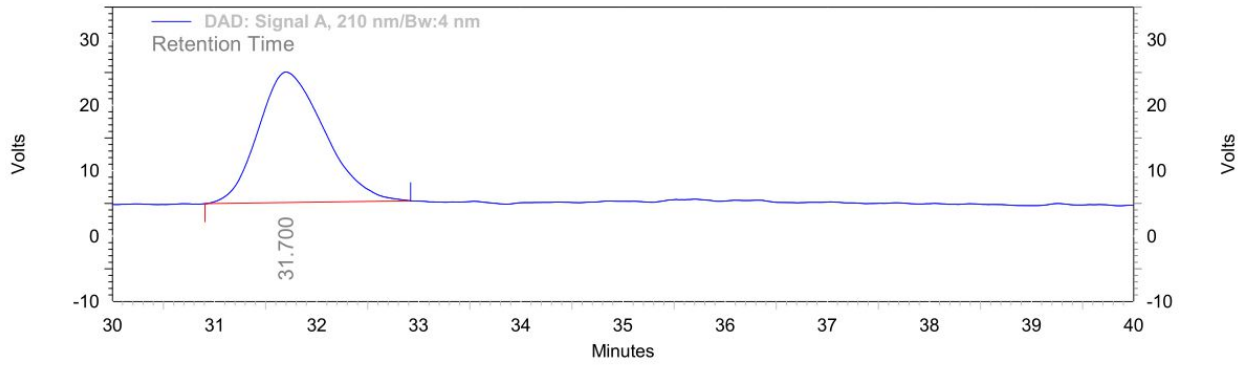


DAD: Signal A,
210 nm/Bw:4 nm
Results

Retention Time	Area	Area %	Height	Height %
33.487	41827588	49.87	725843	52.82
37.340	42043414	50.13	648355	47.18
Totals	83871002	100.00	1374198	100.00

Retention time	33.487	37.340
Product	(*R*)-product	(*S*)-product

B.



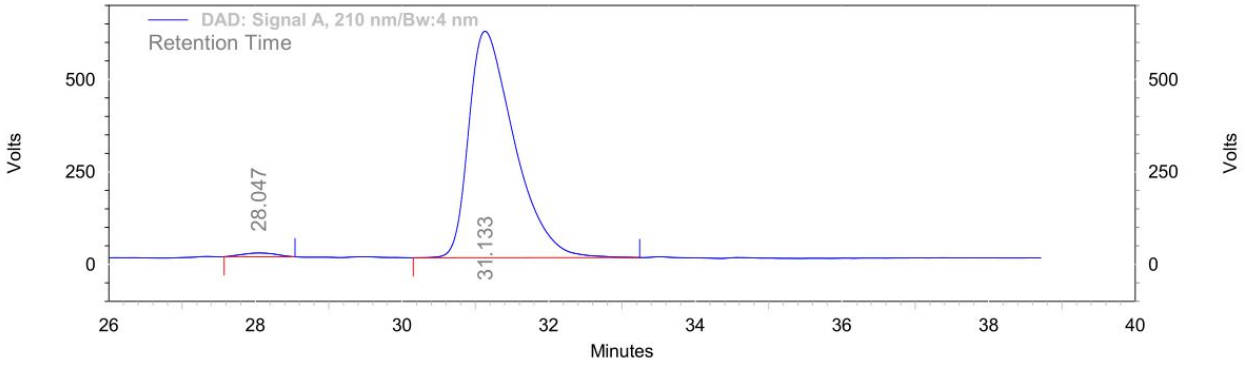
DAD: Signal A,
210 nm/Bw:4 nm
Results

Retention Time	Area	Area %	Height	Height %
31.700	1884474	100.00	41832	100.00

Totals	1884474	100.00	41832	100.00

Retention time	31.700
Product	(*R*)-product

C.



DAD: Signal A,
210 nm/Bw:4 nm
Results

Retention Time	Area	Area %	Height	Height %
28.047	692523	1.24	21313	1.63
31.133	55319952	98.76	1283902	98.37

Totals	56012475	100.00	1305215	100.00

Retention time	28.047	31.133
Product	(*R*)-product	(*S*)-product

Figure 2.42: HPLC chromatograms of 1-(4-benzyloxyphenyl)-2-nitroethanol. A. racemic standard, B. enantiopure product synthesized by HLADH-*At*HNL cascade. C. enantioenriched product synthesized by HLADH-*Bm*HNL cascade.

2.5. Discussion

2.5.1. Inhibition study of the enzymes used in the cascade

Substrate selectivity of both the enzymes reveals that HLADH oxidizes benzylic alcohols[52], and *At*HNL catalyzes nitromethane addition to aromatic aldehydes in the nitroaldol reaction.[23] Based on the substrate scope of both the enzymes, we have selected benzyl alcohol as the starting substrate, and its conversion to (*R*)-NPE was taken as the model reaction. Prior to optimizing the different reaction parameters of this cascade, we investigated the inhibitory effect of benzaldehyde on HLADH, benzyl alcohol on *At*HNL, and benzaldehyde on *At*HNL. Subsequently, the inhibitory effects of benzyl alcohol, and benzaldehyde on *Bm*HNL were studied and compared with *At*HNL. Benzaldehyde showed a competitive inhibition in the HLADH catalyzed oxidation. The K_i of HLADH for benzaldehyde and the K_M for benzyl alcohol were found to be 0.01 mM and 0.0073 mM, respectively (Figure 2.5). As the ratio between the K_i and K_M is greater than one, the reaction is assumed to proceed efficiently and would not encounter product inhibition.[53] In the case of benzyl alcohol inhibition, we found no significant decrease in the specific activity of both *At*HNL and *Bm*HNL up to 50 mM concentration (Figure 2.6, 2.7). Benzaldehyde inhibition study revealed a continuous decrease in the specific activity of both *At*HNL and *Bm*HNL with an increase in benzaldehyde concentration (Figure 2.6, 2.7). Between the two, *At*HNL was inhibited to a higher extent than *Bm*HNL. Benzaldehyde has been reported to be a strong competitive inhibitor of *Hb*HNL[31] a α/β hydrolase fold HNL with 45% identity and 67% similarity with *At*HNL[54] and decreases its half-life by destabilizing its native structure.[45] Therefore we hypothesized that instead of using the reactive benzaldehyde, its continuous regeneration by HLADH catalyzed oxidation might minimize the *At*HNL inhibition in the enzyme cascade.

2.5.2. Overcoming the pH hurdle of the HLADH-*At*HNL cascade

The first hurdle in the enzyme cascade was to find a common suitable pH, where both the enzymes could be functional. HNL catalyzed chiral β-nitroalcohol synthesis is usually carried out at pH≤7 (preferably pH 6)[23,24] to avoid the non-enzymatic synthesis of racemic β-nitroalcohol that may reduce the enantiomeric excess of the enzyme catalyzed product.[55] HLADH in contrary, has been reported to retain only 20% of its activity at pH 6.0 compared to its optimal pH 8.8.[56] An early reaction to study the HLADH catalyzed benzyl alcohol oxidation using 20 mM substrate, 1 mM NAD^+, 150 mM acetone as cofactor recycling agent in 100 mM buffer of pH ranging from 5 to 8.8 resulted in negligible (<1%) benzaldehyde formation below pH 7. Drum *et al*. made an important observation that in the presence of 0.1 mM $ZnCl_2$, HLADH retains >90% of its activity even at pH 5.5.[57] We thus included 0.1 mM $ZnCl_2$ to our previous reaction conditions and observed ~70% of the maximum HLADH activity at pH 6.

2.5.3. Reaction condition optimization of HLADH-*At*HNL cascade

To maximize the production of (*R*)-NPE, a thorough optimization study of the HLADH-*At*HNL cascade was carried out. Fourteen different reaction parameters were systematically varied to attain the optimum biocatalytic reaction conditions of this HLADH-*At*HNL cascade. Initially

2 buffers, KPB and acetate buffer were tested at different pH. When HLADH was dialysed in sodium phosphate and acetate buffer at low pH for example 5.5, enzymatic activity has decreased to 12% and 30% of its original activity, respectively. Further in case of sodium phosphate buffer the zinc content of the enzyme was found to be decreasing very rapidly (page 13 lab note book-1 reference). The hydrolysis rate of NAD^+ was also found to be 3-4 fold higher in citrate and phosphate buffer compared to acetate buffer (page 12 lab note book-1 reference). We believe, acetate buffer might have shown better results for the first reaction (benzyl alcohol to benzaldehyde) compared to the other buffers but as *At*HNL catalysed nitroaldol reaction was not efficient in acetate buffer (poor % ee), we decided to employ KPB pH 6 for further studies. The decreased % ee with an increase in pH could be due to the spontaneous reaction at high pH (Figure 2.8).[58] The first step of our cascade uses NAD^+ as the cofactor in the HLADH catalyzed oxidation of aromatic alcohols. Previously acetaldehyde and acetone have been reported to be used as the co-factor recycling agents in benzyl alcohol oxidation.[59] Additionally, in HLADH catalyzed aminoalcohol lactamization, in-situ regeneration of NAD^+ has improved the HLADH activity by more than 2.5 folds compared to the stoichiometric usage of NAD^+.[56] So, to avoid stoichiometric use of NAD^+ in the reaction, acetaldehyde and acetone were tested as the cofactor recycling agent. An aqueous-organic biphasic system is often used in HNL biocatalysis to minimize the spontaneous reaction, product/substrate inhibition, and increase substrate solubility. However, it is uncommon in HLADH catalyzed oxidation. Our investigation has successfully demonstrated the conversion of benzyl alcohol to NPE in 55% conversion and 98.4% *ee* in 50% v/v of *n*-butyl acetate. It has been reported that sugars and polyols like sucrose and sorbitol improves the half-life of *At*HNL enzyme by 24-36 fold upon incubation by providing stability to *At*HNL structure.[47] We believed the necessity of *At*HNL stabilization to account possible benzaldehyde inhibition. In presence of optimum 50 mg/mL of sorbitol (*R*)-2-NPE production increased to 58%.

2.5.4. Stereoselective syntheses of (*R*)-β-nitroalcohols by HLADH-*At*HNL cascade

To explore the substrate scope of this cascade, several benzylic type alcohols having substituents at different positions in the aromatic ring were converted into their corresponding (*R*)-β-nitroalcohols by employing the optimized biocatalytic reaction condition. Our cascade has produced (*R*)-NPE with >99% enantiopurity and 64% conversion compared to only 91% *ee* and 30% conversion by the *At*HNL catalyzed Henry reaction. Two other (*R*)- selective HNLs, *Gt*HNL, *Ac*HNL have been reported in the synthesis of (*R*)-NPE from benzaldehyde.[24] While wild type *Ac*HNL showed only 80% *ee* with ~8% conversion to (*R*) NPE, high % *ee* was achieved with the engineered enzyme, *Ac*HNL-A40H. This variant showed 74% conversion of 20 mM substrate, which is equivalent to 14.8 mM product, while our study showed 64% conversion of 25 mM substrate equivalent to 16 mM product. Among the ten other (*R*)-β-nitroalcohols synthesized here, four (entries 3, 5, 6, and 7, Table 2.4) were studied earlier using *At*HNL or engineered *Gt*HNL and *Ac*HNL catalyzed Henry reaction starting from their corresponding aldehydes.[23,24] Our cascade has produced higher enantioselectivity (98 to >99%) in all the four cases and conversion too, except 2- chlorobenzyl alcohol. HLADH oxidation produced only 9.3% of 2-chloro benzaldehyde, which is the reason for this poor overall conversion. The remaining five (*R*)-β-nitroalcohols (entries 4, 8, 9, 10, and 11, Table 2.4) synthesized using the current enzyme cascade have not been prepared earlier by any HNL biocatalysis.

2.5.5. Study of the promiscuous activity of *Bm*HNL in stereoselective nitroaldol reactions

After synthesizing an array of (*R*)- β-nitroalcohols by employing HLADH-*At*HNL cascade we planned to prepare stereocomplementary (*S*)-β-nitroalcohols by using *Bm*HNL. *Hb*HNL is the only (*S*)-selective HNL reported to have promiscuous nitroaldolase activity.[21, 22] With the growing concern to design and obtain new stereoselective biocatalysts to expand the biocatalytic toolbox, we have investigated the nitroaldolase activity of *Bm*HNL. So far, *Bm*HNL has been exploited exclusively for the synthesis of chiral cyanohydrins. [32,43,46,60,61] It is noteworthy that like *Hb*HNL, *Bm*HNL is a (*S*)-selective plant HNL. Both belongs to α/β hydrolase fold superfamily, have 56% sequence similarity, and possesses similar catalytic machinery in their active site, i.e., aspartic acid, histidine, serine, threonine and lysine. With similar catalytic machinery and structural fold, we anticipated *Bm*HNL to show nitroaldolase activity. To our pleasure, *Bm*HNL catalyzed this stereoselective nitroaldol reaction.

2.5.6. Optimization of *Bm*HNL catalysed nitroaldol reaction

To investigate the nitroaldol activity of *Bm*HNL, conversion of benzaldehyde to (*S*)-NPE was taken as the model reaction. Optimization of several parameters like enzyme content, buffers and its pH, organic solvent and different protein stabilizer provided little improvement in the % ee of (*S*)-NPE (52% to 60%). *Bm*HNL has been reported to show 54% *ee* in the synthesis of (*S*)-mandelonitrile, which demonstrates the poor preference of the enzyme for benzaldehyde.[32] On the contrary, *Bm*HNL has shown greater enantioselectivity with hydrophobic aromatic aldehydes in the synthesis of chiral cyanohydrins. [32,61] We, therefore, selected six different bulkier aromatic aldehydes and among them 3,5-dimethoxy benzaldehyde turned out to be the best. After optimizing another reaction parameter of the *Bm*HNL content, the % conversion to corresponding (*S*)-nitroaldol product has increased to 77 in 8 h with >99% ee.

2.5.7. Stereoselective syntheses of (*S*)-β-nitroalcohols by HLADH-*Bm*HNL cascade

In the HLADH-*Bm*HNL cascade, we used the same set of substrates of Table 2.4 that resulted in the syntheses of the corresponding (*R*)-β-nitroalcohols with high enantioselectivity (up to >99%). HLADH-*Bm*HNL cascade converted most of the bulky benzylic type alcohols into their corresponding (*S*)-β-nitroalcohols with high enantioselectivity. Such substrate preference of *Bm*HNL is due to its hydrophobic substrate-binding core.[32] *Bm*HNL is the second HNL (after *Hb*HNL) to show such promiscuous nitroaldol activity with (*S*)-selectivity. While *Hb*HNL has been reported to show 64-99% *ee* in the synthesis of diverse (*S*)-β-nitroalcohols, the yield was limited to 13-43%, except 4-nitrobenzaldehyde, where 57% yield with 64% *ee* was found.[22] *Bm*HNL catalyzed Henry reaction in the cascade has produced 42-97% conversion of the aldehydes to their corresponding (*S*)-β-nitroalcohols. The higher catalytic efficiency of *Bm*HNL over *Hb*HNL can be evidenced from the comparison of the two transformations with respect to the amount of enzymes used per mmol of substrate, and the time of biocatalysis in the synthesis of (*S*)-β-nitroalcohols. While *Hb*HNL used 146 mg (2 mL of 73 mg/mL) of purified enzyme per mmol of aldehyde,[22] our cascade would need 14.2 to 85.4 mg of purified *Bm*HNL per mmol of substrate. Further *Hb*HNL biocatalysis was carried out for 48 h compared to only 8-24 h by our cascade.

2.6. Conclusions

Biocatalytic asymetrization of primary alcohols in the preparation of enantiopure β-nitroalcohols was exemplified. We have demonstrated for the first time, an ADH-HNL cascade catalyzed one-pot oxidation cum asymmetric Henry reaction in the synthesis of enantiocomplementary chiral β-nitroalcohols. The HLADH-*At*HNL cascade enabled to prepare enantiopure (*R*)-β-nitroalcohols. In the presence of catalytic amount of $ZnCl_2$, HLADH could be successfully used in the cascades at pH 6, despite its pH optima of 8.8. Optimization of reaction conditions has improved the conversion from 2 to 64% in the synthesis of (*R*)-NPE. Using ten different benzylic type alcohols, each in 25 mM substrate concentration, we have illustrated the practical application of the cascade in the syntheses of the respective (*R*)-β-nitroalcohols in up to >99% *ee* and 64% conversion. Promiscuous nitroaldol activity by *Bm*HNL was reported here for the first time. Subsequently, HLADH-*Bm*HNL cascade was explored in the preparation of a broad range of enantiopure (*S*)-β-nitroalcohols. *Bm*HNL has shown 42-97% conversions in the nitroaldol reaction part of the cascade, while an overall 40-99.6% *ee* and 18-70% conversions was found in the cascade catalyzed conversion of the benzylic type alcohols to their corresponding (*S*)-β-nitroalcohols. The catalytic efficiency of *Bm*HNL in the synthesis of (*S*)-β-nitroalcohols was found to be higher than *Hb*HNL, the only (*S*)-selective HNL reported in the nitroaldol synthesis. Five (*R*)-β-nitroalcohols (entries 4, 8, 9, 10, and 11, Table 2.4) and five (*S*)-β-nitroalcohols (entries 3, 4, 8, 9, and 11, Table 2.5) were first time synthesized by HNL biocatalysis using our enzyme cascade. Both the cascades help in the reduction of aldehyde inhibition on the HNL, avoid the use of reactive aldehydes, and use inexpensive, readily available, and stable alcohols as substrates. Compared to the conventional chemical catalyst, this method demonstrated a green and sustainable approach to synthesize enantioenriched β-nitroalcohols in a one-pot system. The cascades have provided insights into the substrate selectivity of both the enzymes and stereoselectivity of the HNLs.

2.7. References

[1] M. J. Cheng, K. H. Lee, I. L. Tsai, I. S. Chen, *Bioorganic Med. Chem.* **2005**, *13*, 5915–5920.

[2] J. E. Pessin, W. Gitomer, Y. Oka, C. L. Oppenheimer, M. P. Czech, *J. Biol. Chem.* **1983**, *258*, 7386–7394.

[3] T. Taggart, P. Sutton, R. Donaldson, *Clin. Sci.* **1985**, *69*, 631–636.

[4] B. M. Trost, V. S. C. Yeh, H. Ito, N. Bremeyer, *Org. Lett.* **2002**, *4*, 2621–2623.

[5] T. Nyrönen, M. Pihlavisto, J. M. Peltonen, A. M. Hoffrén, M. Varis, T. Salminen, S. Wurster, A. Marjamäki, L. Kanerva, E. Katainen, et al., *Mol. Pharmacol.* **2001**, *59*, 1343–1354.

[6] W. M. Luigi Almirante, *J. Med. Chem* **1966**, *9*, 650–653.

[7] S. E. Milner, T. S. Moody, A. R. Maguire, *European J. Org. Chem.* **2012**, 3059–3067.

[8] D. H. S. Rao, A. Chatterjee, S. K. Padhi, *Org. Biomol. Chem.* **2021**, *19*, 322–337.

[9] J. V. Alegre-Requena, E. Marqués-López, R. P. Herrera, *Adv. Synth. Catal.* **2018**, *360*, 124–129.

[10] H. C. Ma, C. C. Zhao, G. J. Chen, Y. Bin Dong, *Nat. Commun.* **2019**, *10*, DOI 10.1038/s41467-019-11355-x.

[11] A. G. Mahmoud, M. F. C. Guedes da Silva, E. I. Śliwa, P. Smoleński, M. L. Kuznetsov, A. J. L. Pombeiro, *Chem. - An Asian J.* **2018**, *13*, 2868–2880.

[12] S. E. Milner, M. Brossat, T. S. Moody, C. J. Elcoate, S. E. Lawrence, A. R. Maguire, *Tetrahedron Asymmetry* **2010**, *21*, 1011–1016.

[13] F. Xu, J. Wang, B. Liu, Q. Wu, X. Lin, *Green Chem.* **2011**, *13*, 2359.

[14] D. H. S. Rao, S. K. Padhi, *ChemBioChem* **2019**, *20*, 371–378.

[15] D. H. S. Rao, K. Shivani, S. K. Padhi, *Appl. Biochem. Biotechnol.* **2021**, *193*, 560–576.

[16] G. Hasnaoui, J. H. Lutje Spelberg, E. De Vries, L. Tang, B. Hauer, D. B. Janssen, *Tetrahedron Asymmetry* **2005**, *16*, 1685–1692.

[17] S. Venkataraman, A. Chadha, *RSC Adv.* **2015**, *5*, 73807–73813.

[18] A. Chadha, S. Venkataraman, R. Preetha, S. K. Padhi, *Bioorg. Chem.* **2016**, *68*, 187–213.

[19] F. Tentori, E. Brenna, D. Colombo, M. Crotti, F. G. Gatti, M. G. Chiara, G. Pedrocchi-Fantoni, *Catalysts* **2018**, *8*, 308.

[20] Z. Wang, X. Wu, Z. Li, Z. Huang, F. Chen, *Org. Biomol. Chem.* **2019**, *17*, 3575–3580.

[21] T. Purkarthofer, K. Gruber, M. Gruber-Khadjawi, K. Waich, W. Skranc, D. Mink, H. Griengl, *Angew. Chemie - Int. Ed.* **2006**, *45*, 3454–3456.

[22] M. Gruber-Khadjawi, T. Purkarthofer, W. Skranc, H. Griengl, *Adv. Synth. Catal.* **2007**, *349*, 1445–1450.

[23] K. I. Fuhshuku, Y. Asano, *J. Biotechnol.* **2011**, *153*, 153–159.

[24] M. Bekerle-Bogner, M. Gruber-Khadjawi, H. Wiltsche, R. Wiedner, H. Schwab, K. Steiner, *ChemCatChem* **2016**, *8*, 2214–2216.

[25] J. Von Langermann, D. M. Nedrud, R. J. Kazlauskas, *ChemBioChem* **2014**, *15*, 1931–1938.

[26] P. Vongvilai, M. Angelin, R. Larsson, O. Ramström, *Angew. Chemie - Int. Ed.* **2007**, *46*, 948–950.

[27] Y. Zhang, L. Hu, O. Ramström, *Chem. Commun.* **2013**, *49*, 1805–1807.

[28] S. Dutta, N. Kumari, S. Dubbu, S. W. Jang, A. Kumar, H. Ohtsu, J. Kim, S. H. Cho, M. Kawano, I. S. Lee, *Angew. Chemie* **2020**, *132*, 3444–3450.

[29] Y. Alvarez-Casao, E. Marques-Lopez, R. P. Herrera, *Symmetry (Basel).* **2011**, *3*, 220–245.

[30] X. Yu, B. Pérez, Z. Zhang, R. Gao, Z. Guo, *Green Chem.* **2016**, *18*, 2753–2761.

[31] M. Bauer, H. Griengl, W. Steiner, *Biotechnol. Bioeng.* **1999**, *62*, 20–29.

[32] M. Dadashipour, M. Yamazaki, K. Momonoi, K. Tamura, K. I. Fuhshuku, Y. Kanase, E. Uchimura, G. Kaiyun, Y. Asano, *J. Biotechnol.* **2011**, *153*, 100–110.

[33] J. I. Ramsden, R. S. Heath, S. R. Derrington, S. L. Montgomery, J. Mangas-Sanchez, K. R. Mulholland, N. J. Turner, *J. Am. Chem. Soc.* **2019**, *141*, 1201–1206.

[34] S. Schmidt, T. Pedroso De Almeida, D. Rother, F. Hollmann, *Green Chem.* **2017**, *19*, 1226–1229.

[35] R. A. Sheldon, J. M. Woodley, *Chem. Rev.* **2018**, *118*, 801–838.

[36] J. H. Schrittwieser, S. Velikogne, M. Hall, W. Kroutil, *Chem. Rev.* **2018**, *118*, 270–348.

[37] F. Rudroff, M. D. Mihovilovic, H. Gröger, R. Snajdrova, H. Iding, U. T. Bornscheuer, *Nat. Catal.* **2018**, *1*, 12–22.

[38] T. W. Thorpe, S. P. France, S. Hussain, J. R. Marshall, W. Zawodny, J. Mangas-Sanchez, S. L. Montgomery, R. M. Howard, D. S. B. Daniels, R. Kumar, et al., *J. Am. Chem. Soc.* **2019**, *141*, 19208–19213.

[39] L. Biewenga, T. Saravanan, A. Kunzendorf, J. Y. Van Der Meer, T. Pijning, P. G. Tepper, R. Van Merkerk, S. J. Charnock, A. M. W. H. Thunnissen, G. J. Poelarends, *ACS Catal.* **2019**, *9*, 1503–1513.

[40] M. L. Contente, F. Paradisi, *Nat. Catal.* **2018**, *1*, 452–459.

[41] H. J. Cha, S. Y. Hwang, D. S. Lee, A. R. Kumar, Y. U. Kwon, M. Voß, E. Schuiten, U. T. Bornscheuer, F. Hollmann, D. K. Oh, et al., *Angew. Chemie - Int. Ed.* **2020**, *59*, 7024–7028.

[42] P. Gomez De Santos, S. Lazaro, J. Vinã-Gonzalez, M. D. Hoang, I. Sánchez-Moreno, A. Glieder, F. Hollmann, M. Alcalde, *ACS Catal.* **2020**, *10*, 13524–13534.

[43] N. Jangir, S. K. Padhi, *Bioorg. Chem.* **2019**, *84*, 32–40.

[44] A. Chatterjee, D. H. S. Rao, S. K. Padhi. *Adv. Synth. & Catal.* **2021**, *363* (23), 5310–5318.

[45] M. Bauer, H. Griengl, W. Steiner, *Enzyme Microb. Technol.* **1999**, *24*, 514–522.

[46] N. Jangir, Preeti, S. K. Padhi, *Process Biochem.* **2020**, *88*, 78–89.

[47] J. K. Guterl, J. N. Andexer, T. Sehl, J. von Langermann, I. Frindi-Wosch, T. Rosenkranz, J. Fitter, K. Gruber, U. Kragl, T. Eggert, et al., *J. Biotechnol.* **2009**, *141*, 166–173.

[48] M. Pandi, P. K. Chanani, S. Govindasamy, *"Applied Catal. A, Gen.* **2012**, *441–442*, 119–123.

[49] C. Vovard-Le Bray, F. Jiang, X. F. Wu, J. B. Sortais, C. Darcel, *Tetrahedron Lett.* **2010**, *51*, 4555–4557.

[50] R. Boobalan, G. H. Lee, C. Chen, *Adv. Synth. Catal.* **2012**, *354*, 2511–2520.

[51] P. Milbeo, L. Moulat, C. Didierjean, E. Aubert, J. Martinez, M. Calmès, *European J. Org. Chem.* **2018**, *2018*, 178–187.

[52] B. V. P. Robert T. Dworschack, *Biochemistry* **1977**, *16*, 2716–2725.

[53] A. Liese, M. Karutz, J. Kamphuis, C. Wandrey, U. Kragl, *Biotechnol. Bioeng.* **1996**, *51*, 544–550.

[54] J. N. Andexer, N. Staunig, T. Eggert, C. Kratky, M. Pohl, K. Gruber, *ChemBioChem* **2012**, *13(13)*, 1932-1939.

[55] R. Yuryev, S. Briechle, M. Gruber-Khadjawi, H. Griengl, A. Liese, *ChemCatChem* **2010**, *2*, 981–986.

[56] L. Huang, G. V. Sayoga, F. Hollmann, S. Kara, *ACS Catal.* **2018**, *8*, 8680–8684.

[57] D. E. Drum, T. K. Li, B. L. Vallee, *Biochemistry* **1969**, *8*, 3783–3791.

[58] R. Yuryev, S. Briechle, M. Gruber-Khadjawi, H. Griengl, A. Liese, *ChemCatChem* **2010**, *2*, 981–986.

[59] T. Orbegozo, I. Lavandera, W.M.F. Fabian, B. Mautner, J.G. de Vries c, W. Kroutil, *Tetrahedron* **2009**, *65* (34), 6805–6809.

[60] S. Nakano, M. Dadashipour, Y. Asano, *Biochim. Biophys. Acta - Proteins Proteomics* **2014**, *1844*, 2059–2067.

[61] N. Jangir, D. Sangoji, S. K. Padhi, *Biocatal. Agric. Biotechnol.* **2018**, *16*, 229–236.

Engineered *At*HNL variants catalyzed diastereoselective synthesis of β-nitroalcohols with broad substrate scope and high enantioselectivity

3.1. Introduction

Chiral β-nitroalcohols with two chiral centers are key building blocks in the synthesis of pharmaceuticals, and bioactive molecules (Figure 3.1).[1] Asymmetric synthesis of β-nitroalcohol diastereomers majorly uses chemical catalysts, especially organometallic catalysts. There exists six different biocatalytic methods for enantioselective synthesis of β-nitroalcohols, of which four have been exploited in the synthesis of β-nitroalcohol diastereomers. These methods include (a) lipase catalyzed kinetic resolution (KR), (b) chemo-enzymatic dynamic kinetic resolution (DKR) using lipase and 1,8-Diazabicyclo[5.4.0]undec-7-ene (DBU) (c) halohydrin dehalogenase catalyzed epoxide ring opening, and (d) HNL catalyzed asymmetric Henry reaction. The KR based diastereoselective synthesis of β-nitroalcohols uses biocatalytic stereoselective transesterification or hydrolysis of racemic β-nitroalcohols or esters respectively. The lipases reported towards this process are *Pseudomonas flourescens* lipase [2] and *Candida antarctica* lipase B (CALB),[3] however, the % conversions are not very efficient. Substrates used in the KR, i.e., racemic β-nitroalcohol or their esters require prior chemical synthesis. The other limitations of this approach are (i) long reaction time (60 h), (ii) very limited substrate scope, and (iii) moderate yield (highest 53%). The only DKR known for diastereoselective synthesis of β-nitroalcohol has used one substrate. Under optimized conditions, the DKR has produced (1*R*,2*S*)-*cis*-2-methyl-2-nitrocyclohexyl acetate and (1*R*,2*R*)-*trans*-2-methyl-2-nitrocyclohexyl acetate, in 97 and 96% ee, 18 and 53% conversion respectively with 49.3% de (*trans*), while corresponding alcohols had only 21.4% de (*trans*).[4] Further the DKR is a chemo-enzymatic approach, not pure biocatalytic. The epoxide ring opening by nitrite is another example of KR using halohydrin dehalogenase. It is limited by poor yield of 42%, requires additional step of substrate preparation, and has not been tested with more than one substrate.[5] HNL catalysed diastereoselective synthesis is a direct approach to synthesize β-nitroalcohol diastereomers. *Hb*HNL catalyzed diastereoselective Henry reaction is the first HNL catalyzed promiscuous reaction to synthesize β-nitroalcohol diasteromers from benzaldehyde and nitroethane. This method synthesized (1*S*,2*R*)-NPP by virtue of the (*S*)-selectivity of *Hb*HNL. Wild type (WT) *Hb*HNL was reported to show such promiscuous reaction in the conversion of (*1S,2R*)-2-NPB with 67% conversion and 95% ee, and 80% de. [6] Two (*R*)-selective bacterial hydroxynitrile lyases, *Acidobacterium capsulatum* (*Ac*HNL) and *Granulicella tundricula* (*Gt*HNL) were tested in the diastereoselective synthesis of (*1R,2S*)-2-NPP starting from benzaldehyde and nitroethane. WT *Ac*HNL produced highest activity of 77% conversion, 73% ee and 6% de of (*1R,2S*)-2-NPP.[7] The % de and % ee was improved to 27 and 88 respectively by using the engineered enzyme, *Ac*HNL-A40H, however, % conversion was compromised to 66. No mutant found to give high conversion, % ee and % de of a β-nitroalcohol diastereomer. While a few mutants produced *anti* product, i.e., (1*R*,2*S*)-2-(NPP), some gave *syn*, i.e. (1*R*,2*R*)-2-NPP major. Both of the above HNL based studies used only one substrate, which clearly exemplifies the poor substrate scope of the enzymes tested.

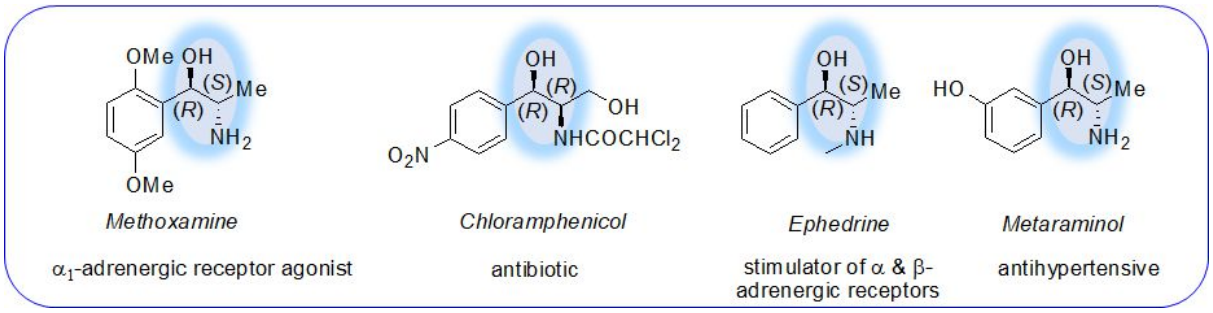


Figure 3.1: Different pharmaceutical molecules with chiral β-amino alcohol moiety that can be derived from corresponding β-nitro alcohols with two chiral centers (highlighted)

To address the limitations of biocatalytic synthesis of β-nitroalcohol diastereomers, we screened in-house libraries of *At*HNL variants towards the stereoselective Henry reaction. Our screening has uncovered two (*R*)-selective *At*HNL muteins, each with a single mutation in their amino acid sequence, towards the direct addition of nitroalkane into a carbonyl substrate in the diastereoselective synthesis of β-nitroalcohols. The engineered enzymes showed high % conversion and stereoselectivity in the addition of nitroalkane nucleophiles into the carbonyl center and produced β-nitroalcohols with two chiral centers. This process was exemplified using a number of aldehydes, including molecules that could synthesize products of pharmaceutical significance. The versatility of the biocatalysts was proved by using more than one nucleophile, especially nitroalkane in the stereoselective addition to a carbonyl center to synthesize corresponding β-nitroalcohol diastereomers. Unlike the existing HNLs, the enzymes reported here have shown high selectivity with respect to both the substrates, i.e., aldehyde, and nitroalkane. The muteins also showed high % of conversion, ee, and de, i.e., up to >99%. We observed almost >250 fold improved catalytic efficiency towards the stereoselective synthesis of (*1R,2S*)-2-NPP compared by the mutant, Y14C compared to the wild-type enzyme. Preparative scale biotransformation in the synthesis of (*1R,2S*)-2-NPP was carried out, which was later converted to *L*-norpsuedoephedrine drug intermediate via a chemical reduction method.

3.2. Objectives

1. Expression and purification of WT *At*HNL and its variants and preparation of their crude enzyme extracts.

2. Screening of *At*HNL mutant library for diastereoselective synthesis of 2-nitro-1-phenylpropan-1-ol (2-NPP).

3. Optimization of biocatalytic parameters for diastereoselective synthesis of 2-NPP by using *At*HNL-Y14C as the biocatalyst.

4. Exploring the substrate scope of Y14C in the diastereoselective Henry reaction in the synthesis of various β-nitroalcohols starting from different aromatic aldehydes and nitroethane.

5. Screening of *At*HNL mutant library for diastereoselective synthesis of 2-nitro-1-phenyl butan-1-ol (2-NPB).

6. Optimization of biocatalytic parameters for diastereoselective synthesis of 2-NPB by using *At*HNL-Y14A as the biocatalyst.

7. Exploring the substrate scope of Y14A in the diastereoselective Henry reaction in the synthesis of different β-nitroalcohols starting from dissimilar aromatic aldehydes and 1-nitropropane.

8. Gram scale synthesis of (*1R,2S*)-2-NPP by using AtHNL-Y14C crude enzyme.

9. Synthesis of L-norephedrine drug intermediate from (*1R,2S*) 2-NPP.

3.3. Materials and methods

3.3.1. Chemicals and materials

Culture media and kanamycin were purchased from HiMedia laboratory Pvt. Ltd, India. Isopropyl-β-D-1-thiogalactopyranoside (IPTG) was purchased from SRL Pvt. Ltd, India. Aldehydes, nitromethane, nitroethane, nitropropane, and mandelonitrile were purchased from Sigma Aldrich, AVRA, SRL and Alfa-Aesar. HPLC grade solvents were obtained from FINAR pvt. ltd., India. Chemicals purchased were used without purification. Silica gel 100-200 mesh used in column chromatography purifications was purchased from Molychem. Primers used in this work were synthesized by Eurofins Genomics India Pvt. Ltd., Hyderabad, India. ^{1}H- and ^{13}C-NMR spectra were recorded on a Bruker 500 MHz instrument with deuterated chloroform as solvents as specified. ^{1}H-NMR data are given as chemical shift (δ ppm), multiplicity (s = singlet, brs= broad singlet, d = doublet, t = triplet, q = quartet, m =multiplet, dd = doublet of doublet, dt = doublet of triplet, ddd = doublet of doublet of doublet), coupling constant (Hz), and integration. ^{13}C-NMR data are reported in terms of chemical shift relative to $CDCl_3$ (77.16 ppm). VCX500 ultrasonic processor was used for lysing the cells by sonication. Enzyme assay was carried out in a UV/VIS Microplate & Cuvette spectrophotometer, Multiscan Go, Thermo Fisher Scientific. TLC silica gel 60 F_{254} (Merck) plates were used to monitor organic reactions using a UV-lamp for visualization.

3.3.2. Chromatography

Analytical high-performance liquid chromatography (HPLC) along with chiral analysis was performed in an Agilent 1260 Infinity II system or LC-2080, Shimadzu system. Chiral HPLC was carried out using an Agilent 1260 Infinity II chiral HPLC system with isopropanol and hexanes as the mobile phase. Lux 5µm Amylose-1, Lux 5µm Cellulose-1, and Daicel CHIRALPAK IB columns (4.6 x 20 mm, 5 µm) were used to separate stereoisomers. For calculating the % conversion of a few substrates, Shimadzu LC-2080 HPLC was used with water and acetonitrile mixture as the mobile phase. Agilent InfinityLab Poroshell 120 EC-C18 column (4.6 x 150 mm, 4 µm) was used in the reverse phase HPLC analysis.

3.3.3. Cloning

*At*HNL (UniProt accession ID: Q9LFT6) synthetic gene, 782 bp, codon optimized for *E. coli* expression was cloned into pET28a+ vector between NcoI and XhoI restriction sites. The recombinant plasmid was procured from Abgenex Pvt. Ltd, India.

3.3.4. Preparation of *At*HNL variant library

The library of *At*HNL variants used for screening in the current study was prepared by altering at two different positions of the *At*HNL gene. Site saturation mutagenesis (SSM) was carried out at Tyr14 and Phe179 to create the corresponding libraries using protocol mentioned in our previous paper.[8] To prepare Y14C-F179L, F179L plasmid was taken as template and forward and reverse primers provided in Table 3.1 were used in the PCR. PCR conditions remained same as used earlier.[8]

Table 3.1: List of primers employed in the above work. Italicized nucleotides are the site of mutation.

Name	Sequence
Y14C- FP	GTTCATAATGCG***TGC***CACGGTGCGTGG
Y14C - RP	CCACGCACCGTG***GCA***CGCATTATGAAC

3.3.5. Expression and purification of WT *At*HNL and its variants

Expression and purification of *At*HNL were carried out using the method reported by Asano and co-workers.[9] Wild type or mutant *At*HNL plasmid transformed in *E.coli* BL21(DE3) cells was inoculated in sterile Luria Bertani broth comprised of 50 µg/mL kanamycin antibiotic, incubated at 37 °C, 180 rpm for 12 to 16 h to prepare a primary culture. A 2% (v/v) primary culture inoculum was used to prepare the secondary culture that incubated at 37 °C until OD_{600} reached 0.5 to 0.8. Protein expression was induced by adding 0.5 mM IPTG, incubated at 30°C, 180 rpm for 6 h. Cells were harvested by centrifuging at 8000 rpm for 12 minutes and the cell pellet was suspended in 20 mM potassium phosphate buffer pH 7. The cell suspension was sonicated over ice and centrifuged at 10000 rpm for 45 min. This supernatant obtained was used as crude enzyme extract during biocatalysis. The supernatant was further used in purification by Ni-NTA agarose affinity chromatography to achieve purified proteins. Protein purification was done by loading the sonicated supernatant into a Ni-NTA agarose column pre-equilibrated with twice its volume of binding buffer (20 mM imidazole, 300 mM sodium chloride, 20 mM KPB, pH 7). The column was subsequently washed with three supernatant volumes of wash buffer (50 mM imidazole, 300 mM sodium chloride, 20 mM KPB, pH 7), and finally eluted with one supernatant volume of elution buffer (500 mM imidazole, 300 mM sodium chloride, 20 mM KPB, pH 7). The eluted protein solution was dialyzed in 20 mM KPB pH 7 for 3 h, 3 times. The dialyzed protein was concentrated and used for biocatalysis. All mutants were expressed and purified using identical procedure to that of wild-type enzyme.

3.3.6. Screening of *At*HNL library for diastereoselective synthesis of 2-nitro-1-phenylpropanol (2-NPP)

E. coli BL21(DE3) cells harboring mutant *At*HNL plasmids were grown and harvested following the protocol mentioned in **3.3.5**. Harvested cells were suspended in 20 mM KPB pH

7 and sonicated over ice. Sonicated supernatant was further used as the crude enzyme for the screening study (Table 3.4). The reaction mixture for this experiment was prepared by adding 600 µL of *n*-butyl acetate, 15 mg crude mutant enzyme (450 µL, 33 mg/mL), and 50 mM KPB pH 6 (50 µL, 1.25 M). The mixture was kept at 30 °C, 1200 rpm for 5 mins to form the emulsion of enzyme and solvent. Then 20 mM (25 µL, 1M stock prepared in *n*-butyl acetate) benzaldehyde was added into it and incubated at 30 °C, 1200 rpm for 5 mins. Subsequently 1 M nitroethane (92 µL) was added into the mixture.[6] Final reaction volume was kept 1.25 mL by adding remaining amount of double distilled water. The reaction was incubated for 24 h and then analysed by chiral HPLC.

3.3.7. Optimization of biocatalytic parameters for diastereoselective synthesis of 2-NPP

To improve the catalytic activity of Y14C, various reaction conditions of the biocatalysis, i.e., buffer type, buffer pH, buffer concentration, organic solvent, nitroethane (co-substrate) concentration and enzyme content were optimized to achieve maximum % conversion, % ee and % de of the product 2-NPP.

3.3.7.1. Buffer and pH optimization: In this experiment, two buffers KPB (potassium phosphate buffer) and CPB (citrate phosphate buffer) were tested varying its pH from 5.5 to 7. Reaction mixture contained 600 µL of *n*-butyl acetate, 50 mM reaction buffer (42 µL, 1.5 M), 15 mg of crude *At*HNL-Y14C, 1 M nitroethane (91.8 µL), and 20 mM benzaldehyde solution (25 µl, 1 M). Final reaction volume was kept 1.25 mL by adding remaining amount of double distilled water. Benzaldehyde stock was prepared in *n*-butyl acetate.

3.3.7.2. Organic solvent optimization: To find out the best organic solvent for our biocatalytic Henry reaction, five different organic solvents were selected and tested. The solvents used are *n*-butyl acetate (NBA), *tert*-butyl methyl ether (TBME), diethyl ether (DEE), toluene and diisopropylether (DIPE). The reaction mixture consisted of 600 µL of different organic solvent, 50 mM CPB pH 5.5 (42 µL, 1.5 M), 15 mg of crude *At*HNL-Y14C, 1 M nitroethane (91.8 µL), and 20 mM benzaldehyde solution (25 µL, 1 M). Final reaction volume was kept 1.25 mL by adding the remaining amount of double distilled water. Benzaldehyde stock was prepared in different (corresponding) organic solvents.

3.3.7.3. Nitroethane concentration optimization: Co-substrate concentration is an important reaction parameter in HNL catalyzed Henry reaction. Six different concentrations of nitroethane were checked to obtain maximum % conversion and stereoselectivity in the Y14C catalyzed Henry reaction. The detailed reaction condition was as follows: 600 µL of TBME, 50 mM CPB pH 5.5 (42 µL, 1.5 M), 15 mg of crude *At*HNL-Y14C, 0.75 M (69 µL)/ 1 M (92 µL)/ 1.25 M (114.7 µL/ 1.5 M (138 µL)/ 1.75 M (161 µL)/ 2 M (184 µL) nitroethane, and 20 mM benzaldehyde solution (25 µL, 1 M). Final reaction volume was kept 1.25 mL by adding the remaining amount of double distilled water. Benzaldehyde stock was prepared in TBME.

3.3.7.4. Citrate phosphate buffer concentration optimization: The concentration of the buffer (CPB) used in biocatalysis was optimized. Buffer concentration was varied from 50 to 250 mM. The reaction condition used was as follows: 600 µL of TBME, CPB pH 5.5 50 mM (42 µL, 1.5 M)/ 100 mM (83 µL, 1.5 M)/ 150 mM (125 µL, 1.5 M)/ 200 mM (167 µL, 1.5 M)/

250 mM (208 µL, 1.5 M), 1.75 M (161 µL) nitroethane, 20 mM benzaldehyde solution (25 µL, 1 M), and 15 mg of crude *At*HNL-Y14C. Final reaction volume was maintained to 1.25 mL by adding the remaining amount of double distilled water. Benzaldehyde stock was prepared in TBME.

3.3.7.5. Enzyme content optimization: To optimize the amount of enzyme required to gain maximum yield, % ee and % de of the product, six different contents of the enzyme starting from 5 to 25 mg, were tested. The reaction conditions are as follows: 600 µL of TBME, CPB pH 5.5 100 mM (83 µL, 1.5 M), 5/ 10/ 15/ 20/ 25 mg of crude *At*HNL-Y14C, 1.75 M (161 µL) nitroethane, and 20 mM benzaldehyde solution (25 µL, 1 M). Final reaction volume was kept 1.25 mL by adding the remaining amount of double distilled water. Benzaldehyde stock was prepared in TBME.

3.3.8. Y14C catalyzed diastereoselective Henry reaction in the synthesis of diverse β-nitroalcohols using nitroethane as a nucleophile:

The optimised reaction conditions obtained from the above studies using benzaldehyde as the substrate was extended towards other aromatic aldehydes to synthesize their corresponding β-nitroalcohol diastereomers. A typical reaction contained 600 µL of TBME, 5 mM of different aldehydes (25 µL, 250 mM), 1.75 M nitroethane (161 µL), 100 mM CPB pH 5.5 (83 µL, 1.5M), and 3 mg of purified *At*HNL-Y14C. Different aromatic aldehyde stock solutions were made in TBME. The total reaction volume was made up to 1.25 mL by adding remaining volume of autoclaved double distilled water. This reaction mixture was incubated at 30 °C and 1,200 rpm in a Thermo shaker. A 100 µL of an aliquot of the reaction was mixed with 200 µL of hexane: 2-propanol (90:10). The mixture was vortexed vigorously, followed by dried over anhydrous sodium sulphate to remove any aqueous part, and then centrifuged at 15000*g* for 5 min at 4 °C. A 20 µL of this sample was taken and analysed in HPLC using appropriate chiral column.

3.3.9. Y14C-F179L catalyzed diastereoselective Henry reaction in the synthesis of diverse β-nitroalcohols using nitroethane as a nucleophile:

In case of the double mutant catalysed Henry reaction, the reaction mixture was composed of 600 µL TBME, 5 mM aldehyde substrate (25 µL, 250 mM), 1.75 M nitroethane (161 µL), 3 mg pure Y14C-F179L, and 100 mM CPB pH 5.5 (83 µL, 1.5 M). Benzaldehyde stock was prepared in TBME. Total reaction volume was made up to 1.25 mL by adding remaining amount of double distilled water. The reaction conditions, and product analysis remained same to the previous experiment.

3.3.10. Screening of *At*HNL library for diastereoselective synthesis of 2-nitro-1-phenyl butan-1-ol (2-NPB):

We began screening the two libraries of *At*HNL (Tyr14 and Phe179) towards the diastereoselective synthesis of 2-NPB using similar reaction conditions as mentioned in **3.3.8.**, except 1.75 M 1-nitropropane (195 µL) in place of nitroethane and fifteen mg of crude enzyme of each of the *At*HNL variants were used as the catalyst. Further among the 38 mutants, 5 of them were used in their purified form towards the synthesis of 2-NPB. The biocatalytic reaction conditions with pure enzyme was as follows: 600 µL of TBME, 1.75 M nitropropane (195 µL), 3 mg of *At*HNL mutant pure enzyme, 100 mM CPB pH 5.5 (83 µL, 1.5 M), and 5 mM

benzaldehyde (25 µL, 250 mM). The reaction volume was made up to 1.25 mL using double distilled water.

3.3.11. Optimization of biocatalytic parameters for diastereoselective synthesis of 2-NPB

3.3.11.1. Optimization of reaction time and catalyst amount: To optimize the reaction time of the biocatalytic Henry reaction, the reaction mixture was incubated for longer time periods, while aliquots were taken at different time intervals (24, 48, and 72 h). Optimization of the catalyst amount was carried out by using different amount of purified Y14A (3, 6, and 10 mg) in the biocatalysis. All other reaction conditions remained same to **3.3.10**.

3.3.11.2. Optimization of 1-nitropropane concentration: To optimize the 1-nitropropane concentration in biocatalytic Henry reaction, a range of 1-nitropropane concentrations (0.25 to 1.75 M) was used. The reaction conditions were as follows: 600 µL TBME, 0.25 to 1.75 M 1-nitropropane, 6 mg of purified Y14A, 100 mM CPB pH 5.5 (83 µL, 1.5 M), and 5 mM benzaldehyde (25 µL, 250 mM). The reaction volume was made up to 1.25 mL using double distilled water. Substrate stock preparation and other reaction parameters were kept similar to **3.3.10**. Product extraction and HPLC were done according to the previously described method.

3.3.12. Y14A catalyzed diastereoselective Henry reaction in the synthesis of diverse β-nitroalcohols using 1-nitropropane as the nucleophile:

The optimized reaction conditions obtained from **3.3.11.**, were employed in the diastereoselective Henry reaction along with other aromatic aldehydes to synthesize their corresponding β-nitroalcohol products. A typical reaction consisted of 600 µL of TBME, 5 mM different aldehyde substrate (25 µL of the 250 mM stock), 1.4 M nitropropane (156 µL), 100 mM CPB pH 5.5 (63 µL of 2 M stock), and 6 mg of purified Y14A. Substrate stock preparation and other reaction parameters were kept similar. This reaction mixture was incubated at 30 °C and 1,200 rpm in a Thermoshaker. A 100 µL of an aliquot of the reaction was mixed with 200 µL of hexane: 2-propanol (90:10). The mixture was vortexed vigorously, followed by dried over anhydrous sodium sulphate to remove any aqueous part, and then centrifuged at 15000*g* for 5 min at 4 °C. A 20 µL of this sample was taken and analysed in HPLC using appropriate chiral column.

3.3.13. Determination of kinetics parameters:

Initial reaction rate of Y14C mutant towards the synthesis of (*1R,2S*)-2-NPP was determined by measuring its activity using a normal phase chiral HPLC. Similarly the initial reaction rate of the WT *At*HNL was determined and compared with Y14C. Prior to the kinetic studies, the time period of the biocatalysis to get 10% conversion was found out. The initial reaction rates of Y14C were measured by varying the substrate concentration. A typical reaction mixture contained: 1.75 M nitroethane (161 µL), 1 to 200 mM benzaldehyde, 100 mM CPB pH 5.5 (63 µL of 2 M stock), and 1.5 mg Y14C or WT *At*HNL. Similarly, kinetic parameters were determined for the Y14A mutant for the synthesis of 1-(3-chlorophenyl)-2-nitrobutan-1-ol. The reaction condition used here is, 1.4 M 1-nitropropane (156 µL), 1 to 150 mM 3-chloro benzaldehyde, 100 mM CPB pH 5.5 (84 µL of 1.5 M stock), and 3 mg of Y14A. Substrate stock preparation was done in TBME. Total volume of organic part i.e., TBME and stock

substrate solution was kept 625 µL. Total reaction volume was made up to 1.25 mL by adding double distilled water. The time for Y14C, Y14A, and WT *At*HNL catalysed biocatalysis towards the kinetic studies was 20 mins, 1 h, and 22 h respectively. Each reaction mixture was incubated at 30 °C and 1,200 rpm in a Thermoshaker. Product extraction and HPLC were done according to previously described method in **3.3.8.**

3.3.14. The pH dependence of Y14C kinetic parameters: Probing proton donation role of Cys14 in diastereoselective nitroaldol synthesis

This experiment is designed to find out the possible proton donor role of the sulfhydryl proton of the cysteine residue at the 14th position of the Y14C. Enzyme kinetic parameters were determined for both the WT and Y14C at pH 8.2. Each of these reaction mixture was prepared by taking 1.75 M nitroethane (161 µL), 1 to 200 mM benzaldehyde, 100 mM tris-HCl buffer pH 8.2. (126 µL of 1 M stock), and 1.5 mg of Y14C or WT *At*HNL. Substrate stock preparation was done in TBME. Total volume of organic part i.e., TBME and stock substrate solution was kept 625 µL. Total reaction volume was made up to 1.25 mL by adding double distilled water. The Y14C, and WT *At*HNL biocatalysis were incubated for 20 minutes and 22 hours respectively. Each reaction mixture was incubated at 30 °C and 1,200 rpm in a Thermoshaker Product extraction and HPLC were done according to previously described method in **3.3.8.**

3.3.15. Comparison of cyanogenesis and retro-nitroaldolase activity of WT *At*HNL, Y14C, and Y14A:

The mutants showing promiscuous nitroaldolase activity were examined whether they still retain the natural cyanogenesis activity. In order to find out the answer the WT and mutants (Y14C and Y14A) were studied in the cyanogenesis and retro-nitroaldol reaction. Racemic compounds of mandelonitrile, 2-nitro-1-phenyl ethan-1-ol, 2-nitro-1-phenyl propan-1-ol and 2-nitro-1-phenyl butan-1-ol were used as the substrates for the cleavage assays. The reaction was performed in a 96 well microtiter plate. Each well of the plate consisted of 160 µL of 50 mM citrate phosphate buffer, pH 5.5, 20 µL of purified wild type or mutant *At*HNL (1 mg/mL), and 20 µL of 70 mM substrate prepared in 5 mM CPB pH 3.15. The activity was calculated by measuring the amount of benzaldehyde produced using its molar extinction coefficient (1380 M^{-1} cm^{-1}). One unit of HNL activity is defined as the amount of enzyme that produced 1 µmol of benzaldehyde from mandelonitrile per minute. All measurements were performed in triplicates. The control experiment had all the reaction components except the enzyme which was replaced by its corresponding buffer.

3.3.16. Gram scale synthesis of (*1R,2S*)-2-NPP using Y14C crude enzyme as the catalyst:

From the optimization studies, it was evident that the mutant Y14C can be efficiently used in its crude form. We aimed to carry out a large scale synthesis of the *anti* diastereoisomer, (*1R,2S*)-2-NPP using the Y14C crude cell lysates. The preparative scale synthesis included 100 mM benzaldehyde (1.05 mL) in 6.8 mL of 1.5 M CPB pH 5.5, 49.5 mL of TBME, 13 mL of nitroethane, 24 mL of *At*HNL-Y14C crude enzyme (50.8 mg/mL) as the catalyst and 6.7 mL of water. The reaction mixture was stirred at room temperature at 350 rpm, for 24 h. The

product was extracted by ethyl acetate and column purified using hexane: ethyl acetate (95:5 v/v). The purified extract was dried over sodium sulfate and later concentrated under vacuum. The purified concentrated product was analyzed in chiral HPLC, and characterized by ^{1}H and ^{13}C NMR. Total turnover number (TTN) was calculated using the following formula. $Total\ turnover\ number = \frac{\mu mol\ of\ product\ formed}{\mu mol\ of\ mutant\ enzyme\ used}$

3.3.17. Synthesis of L-norephedrine drug intermediate from (*1R,2S*)-2-NPP:

The optically pure (*1R,2S*)-2-NPP synthesized via *At*HNL-Y14C catalyzed Henry reaction was subjected to the reduction of its nitro group. The end product of this reaction is a vital drug molecule, i.e., L-norephedrine, a psychostimulant, belongs to the amphetamine family. Both the racemic and chiral 2-NPP were reduced to synthesize the drug in its racemic and enantiopure forms, respectively.[10] The reaction was carried out in the following manner. A mixture of 1 g of (*1R,2S*)-2-NPP or racemic 2-NPP, 1.65 g of zinc dust, and 1.8 mL 95% ethanol were taken and stirred in a round bottom flask. To this solution, 23.5 mL 30% (w/v) sulphuric acid was added dropwise using an additional funnel under nitrogen-purged condition. The acid was added at such a rate that the temperature of the reaction vessel remained less than 45 °C. After completion of the reaction excess amount of 50% NaOH solution was added to quench the reaction. The reaction mixture was extracted using diethyl ether, dried over anhydrous sodium sulfate, concentrated in a rotary evaporator, and further purified by silica column purification using DCM and methanol as the mobile phase. Ninhydrin staining was used to monitor the reaction progress and detection of the product. The purified product was characterized by both chiral HPLC and ^{1}H NMR. As the product did not have any *syn* diastereomer, the enantiomeric excess of the *anti*-stereoisomers was determined using reverse phase HPLC according to Kao et.al.[11] The HPLC conditions used were as follows. Column: Daicel crownpak CR(+) column, mobile phase: Perchloric acid (pH 2.0), flow rate: 0.5 mL/min, wavelength: 205 nm, and column oven temperature: 4 °C.

3.3.18. Deciphering the reaction mechanism of diastereoselective Henry reaction by selective deuteration

3.3.18.1. Synthesis of monodeuterated nitroethane by replacing a proton at its α-carbon with deuterium: In order to incorporate deuterium into the β-carbon of the nitroaldol product, monodeuterated nitroethane was required to be used as a nucleophile in the Henry reaction. We aimed to synthesize it by performing deuterium exchange at the α-carbon of nitroethane. The reaction was carried out by taking 625 µL of TBME, 125 µL of CPB (1 M, pD 5.5), 50 µL KPB (20 mM, pD 7), 161 µL nitroethane and 289 µL D_2O in a 2 mL vial, incubated at 30°C in a thermoshaker at 1200 rpm. The reaction was monitored by ^{1}H NMR and stopped at 108 h. Finally, the deuterated nitroethane was extracted by diethyl ether, concentrated by nitrogen purging and characterized by ^{1}H NMR.

3.3.18.2. Synthesis of • -deuterated-2-NPP: The diastereoselective Henry reaction for asymmetric synthesis of the β-deuterated-2-NPP was carried out using the deuterated nitroethane obtained from the previous experiment. The reaction was performed by taking 500

µL of TBME, 125 µL of CPB (1 M, pD 5.5), 3 mg of Y14C-*At*HNL in 20 mM KPB pD 7 [12], 161 µL of deuterated nitroethane, 125 µL of benzaldehyde solution (1M stock prepared in TBME) and 289 µL of D_2O in a 2 mL vial, incubated at 30°C for 7 h in a thermoshaker at 1200 rpm. Total reaction volume was 1.25 mL. After completion of the reaction the reaction mixture was extracted using diethyl ether and concentrated under vacuum. The obtained product was characterized by ^{1}H NMR and chiral HPLC.

3.3.18. Recycling *At*HNL-Y14C for the synthesis of (*1R,2S*)-2-NPP

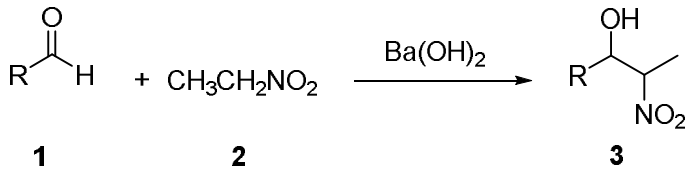
The reusability of the purified *At*HNL-Y14C for the diastereoselective Henry reaction was investigated. The biocatalytic reaction mixture contained, 500 µL of TBME, 1.75 M nitroethane (161 µL), 100 mM benzaldehyde (125 µL, 1 M), 100 mM CPB pH 5.5 (84 µL, 1.5 M), and 3 mg *At*HNL-Y14C. This reaction mixture was incubated at 30 °C and 1,200 rpm in a Thermoshaker. To test the recyclability of the enzyme, the organic layer was removed in every 16 h, and to the aqueous part (containing enzyme) a fresh 100 mM benzaldehyde, 1.75 M nitroethane, and 500 µL TBME was added followed by the reaction was continued as described above. This cycle was repeated for consecutive eight cycles.

3.3.19. Chemical synthesis of racemic β-nitroalcohol standards:

Racemic β-nitroalcohols were synthesized by the addition of aldehydes to nitroethane or 1-nitropropane in 1:10 molar ratio in the presence of 12.5-50 mol% of $Ba(OH)_2$ as a catalyst. A 3 mL of water was added for every mmol of the substrate as the reaction solvent. The reaction mixture was incubated at room temperature.[13]

3.4. Results

3.4.1. Barium hydroxide catalyzed synthesis of different racemic β-nitroalcohols starting from their corresponding aromatic aldehydes and nitroethane



Scheme 3.1. Chemical synthesis of racemic β-nitroalcohols using nitroethane as a nucleophile

Table 3.2: List of racemic β-nitroalcohols synthesized using nitroethane as nucleophile

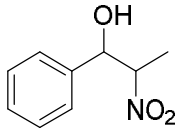
S.No.	Aldehyde	Reaction conditions				(**3**) Yield (%)
		(**1**) mmol	Catalyst mole % of aldehyde	(**2**) mmol	time (h)	
1	benzaldehyde	5	12.5	50	7	67

2	2,5-dimethoxy benzaldehyde	5	12.5	50	7.5	71
3	3-benzyloxy benzaldehyde	5	25	50	12.5	30
4	4-chloro benzaldehyde	5	12.5	50	5	68
5	4-methoxy benzaldehyde	7.5	12.5	75	7.5	39
6	2-methyl benzaldehyde	7.5	25	75	11	75
7	2-methoxy benzaldehyde	7.5	12.5	75	8.5	95
8	3-phenyl propionaldehyde	7.5	12.5	75	7	73
9	1-napthaldehyde	7.5	12.5	75	13	35
10	3-methoxy benzaldehyde	7.5	12.5	75	8	67
11	3-methyl benzaldehyde	7.5	12.5	75	10	72
12	3-chloro benzaldehyde	7.5	12.5	75	9	76
13	2-chloro benzaldehyde	7.5	12.5	75	13	58
14	4-methyl benzaldehyde	7.5	12.5	75	10	64
15	4-nitro benzaldehyde	7.5	12.5	75	6	88
16	2-bromo benzaldehyde	6	37.5	60	8	94
17	3-bromo benzaldehyde	7.5	37.5	75	8	69
18	2,3-dimethoxy benzaldehyde	7.5	37.5	75	8	85
19	2,3-dichloro benzaldehyde	7.5	37.5	75	8	96
20	2-nitro benzaldehyde	7.5	37.5	75	6	91

3.4.2. NMR characterization of nitroethane corresponding racemic β-nitroalcohols

Racemic β-nitroalcohols to be used as analytical standards to compare enzymatically synthesized products, were prepared as described above. All the products of this study are known compounds. Their NMR spectral data (both ^{1}H and ^{13}C) were in agreement with reported values. Figure 3.2 to 3.20 represents the ^{1}H NMR and ^{13}C NMR of racemic β-nitroalcohols (**3**) synthesized by chemical catalyst as given in Scheme 3.1, Table 3.22.

1. 2-Nitro-1-phenylpropan-1-ol (NPP) [14]



^{1}H NMR (500 MHz, $CDCl_3$) δ 7.44 – 7.31 (m, 10H), 5.40 (d, J = 3.5 Hz, 1H), 5.03 (d, J = 9.0 Hz, 1H), 4.81 – 4.66 (m, 2H), 2.71 (s, 1H), 2.59 (s, 1H), 1.51 (d, J = 6.8 Hz, 3H), 1.32 (dd, J = 6.8 Hz, 3H).

^{13}C NMR (101 MHz, $CDCl_3$) δ 138.56, 138.42, 129.34, 129.15, 128.87, 128.65, 127.05, 126.07, 88.54, 87.55, 76.40, 74.01, 16.59, 12.19.

Diastereomeric ratio 1:1.38 (*anti*: *syn*)

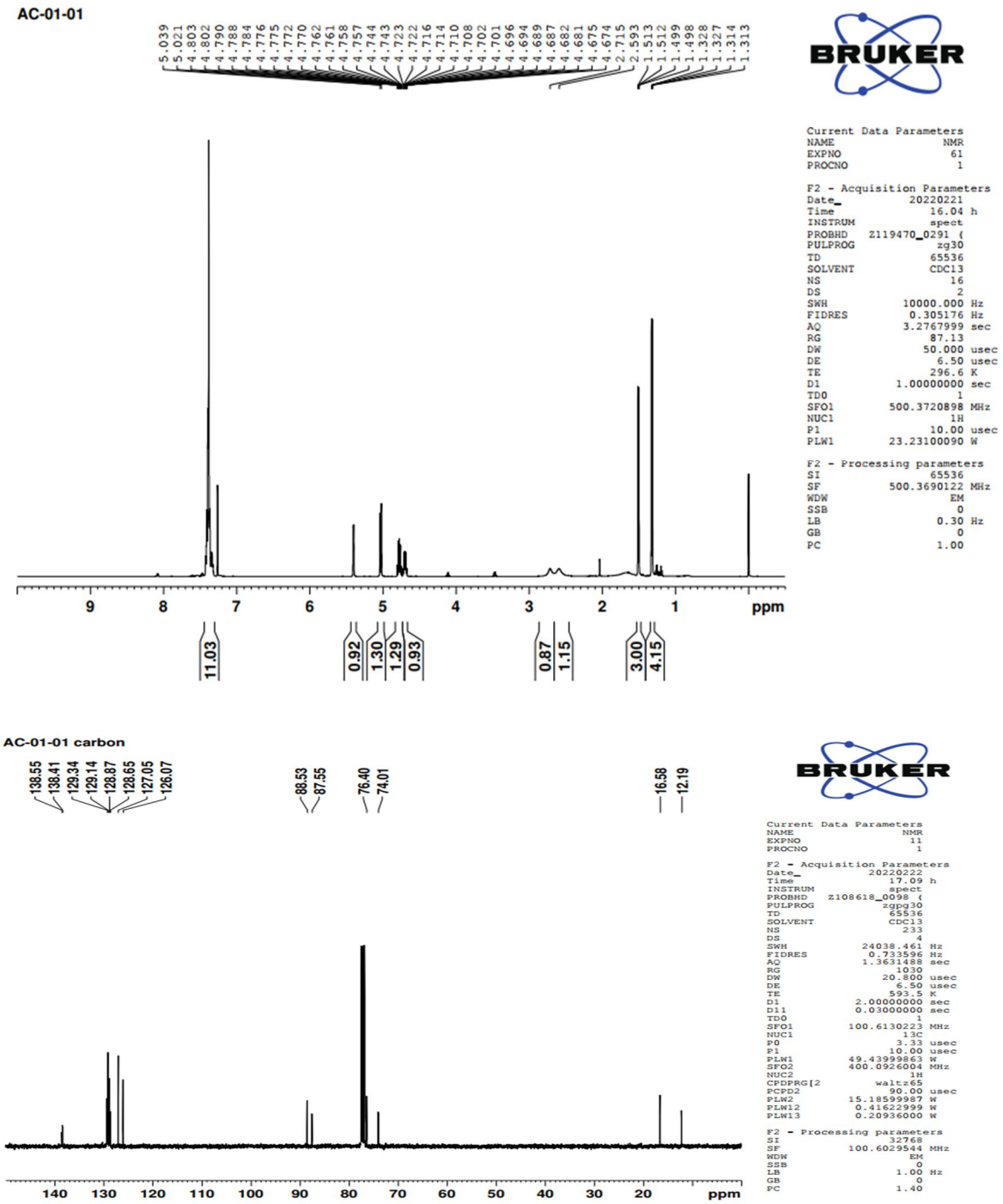
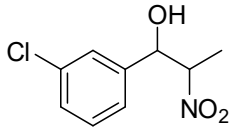


Figure 3.2: ^{1}H NMR and ^{13}C NMR spectra of 2-nitro-1-phenylpropan-1-ol.

2. 1-(3-Chlorophenyl)-2-nitropropan-1-ol [15]



^{1}H NMR (500 MHz, $CDCl_3$) δ 7.43 – 7.21 (m, 8H), 5.39 (d, *J* = 3.4 Hz, 1H), 5.01 (d, *J* = 8.9 Hz, 1H), 4.78 – 4.63 (m, 2H), 2.90 (s, 1H), 2.84 (s, 1H), 1.49 (d, *J* = 6.8 Hz, 3H), 1.34 (d, *J* = 6.9 Hz, 5H).

^{13}C NMR (101 MHz, $CDCl_3$) δ 140.60, 140.41, 135.09, 134.92, 130.41, 130.17, 129.48, 128.81, 127.22, 126.32, 125.25, 124.22, 88.23, 87.24, 75.66, 73.21, 16.53, 12.00.

Diastereomeric ratio 1:1.82 (*anti*: *syn*)

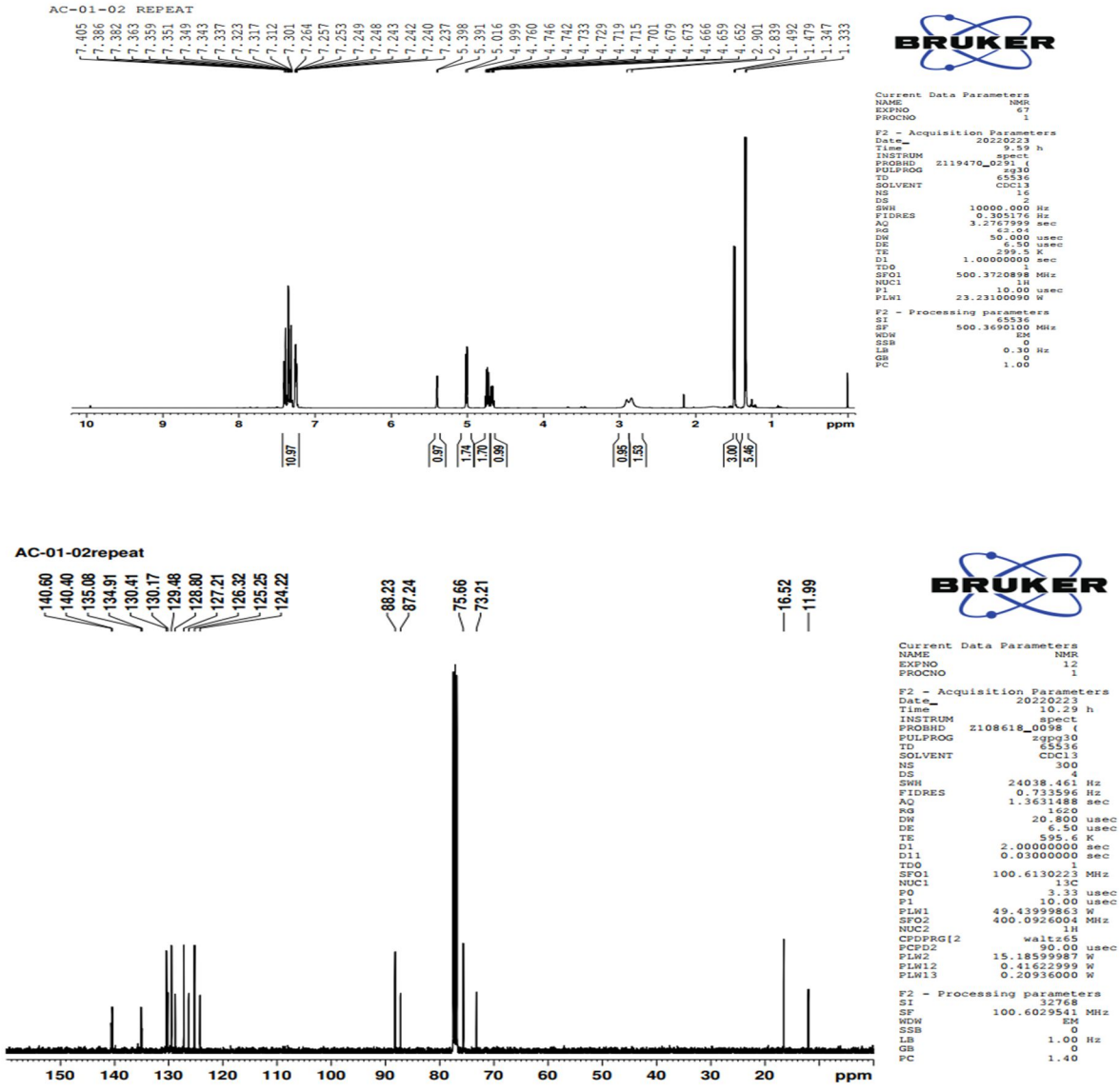
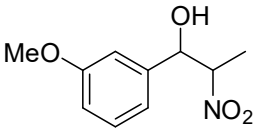


Figure 3.3: ^{1}H NMR and ^{13}C NMR spectra of 1-(3-chlorophenyl)-2-nitropropan-1-ol.

3. 1-(3-Methoxyphenyl)-2-nitropropan-1-ol [15]



^{1}H NMR (500 MHz, $CDCl_3$) δ 7.34 – 7.24 (m, 4H), 6.96 – 6.83 (m, 4H), 5.37 (d, *J* = 3.5 Hz, 1H), 4.98 (d, *J* = 9.1 Hz, 1H), 4.80 – 4.64 (m, 2H), 3.82 (s, 3H), 3.81 (s, 3H), 2.79 (s, 1H), 2.71 (s, 1H), 1.49 (d, *J* = 6.8 Hz, 3H), 1.32 (d, *J* = 6.8 Hz, 3H).

^{13}C NMR (101 MHz, $CDCl_3$) δ 160.14, 159.98, 140.26, 139.99, 130.20, 129.95, 119.34, 118.24, 114.74, 113.96, 112.46, 111.73, 88.49, 87.49, 76.33, 73.83, 55.45, 16.61, 12.13.

Diastereomeric ratio 1:3.2 (*anti*: *syn*)

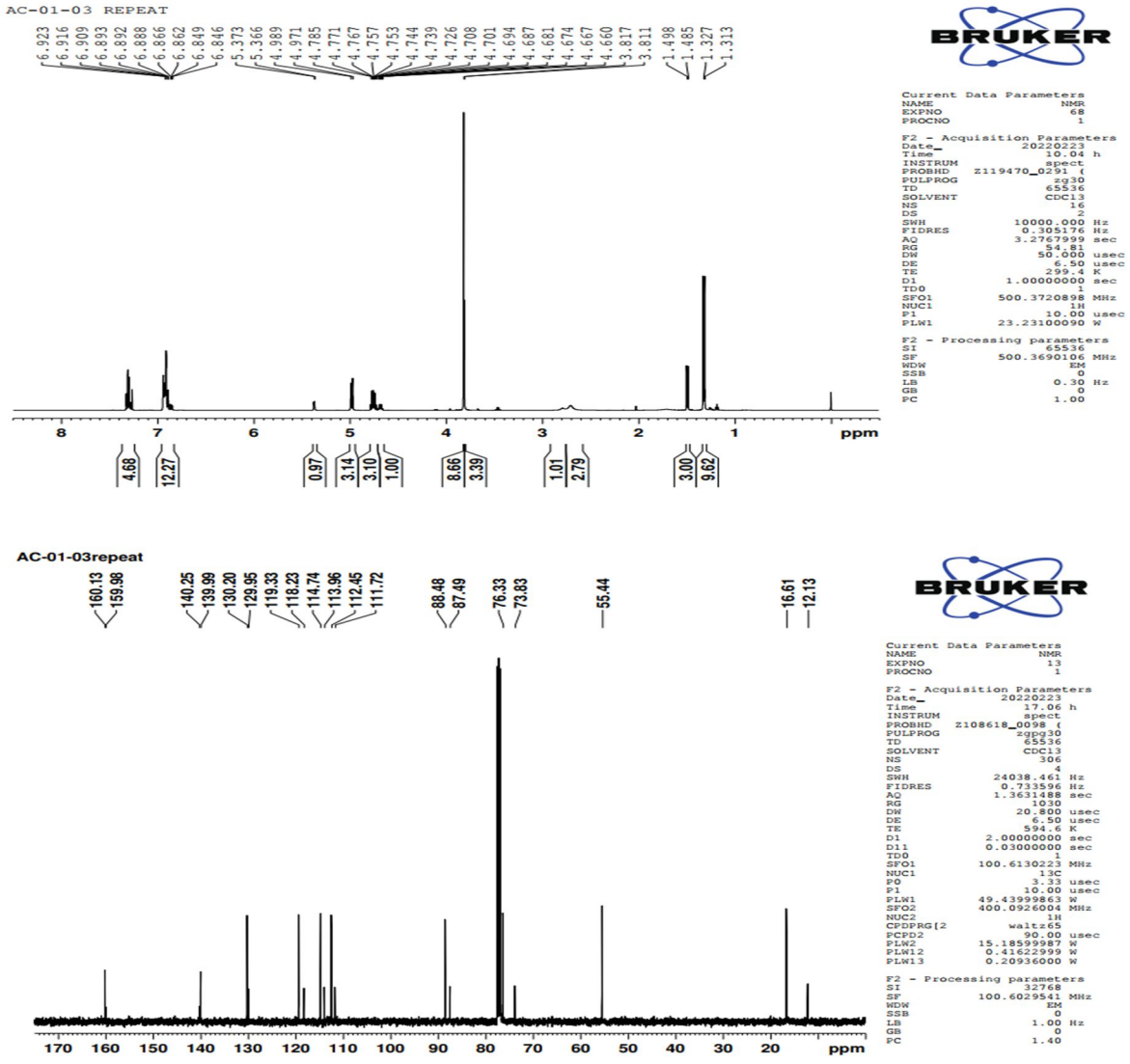
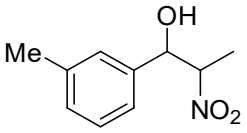


Figure 3.4: ^{1}H NMR and ^{13}C NMR spectra of 1-(3-methoxyphenyl)-2-nitropropan-1-ol.

4. 1-(3-Methylphenyl)-2-nitropropan-1-ol [15]



^{1}H NMR (500 MHz, $CDCl_3$) δ 7.31 – 7.09 (m, 8H), 5.33 (d, *J* = 3.6 Hz, 1H), 4.96 (d, *J* = 9.1 Hz, 1H), 4.80 – 4.63 (m, 2H), 2.77 (s, 1H), 2.67 (s, 1H), 2.37 (s, 3H), 2.36 (s, 3H), 1.49 (d, *J* = 6.8 Hz, 3H), 1.30 (d, *J* = 6.9 Hz, 3H).

^{13}C NMR (126 MHz, $CDCl_3$) δ 139.01, 138.66, 138.58, 138.42, 130.09, 129.40, 129.02, 128.77, 127.63, 126.71, 124.18, 123.13, 88.57, 87.61, 76.46, 74.09, 21.56, 21.51, 16.64, 12.27.

Diastereomeric ratio 1:1.7 (*anti*: *syn*)

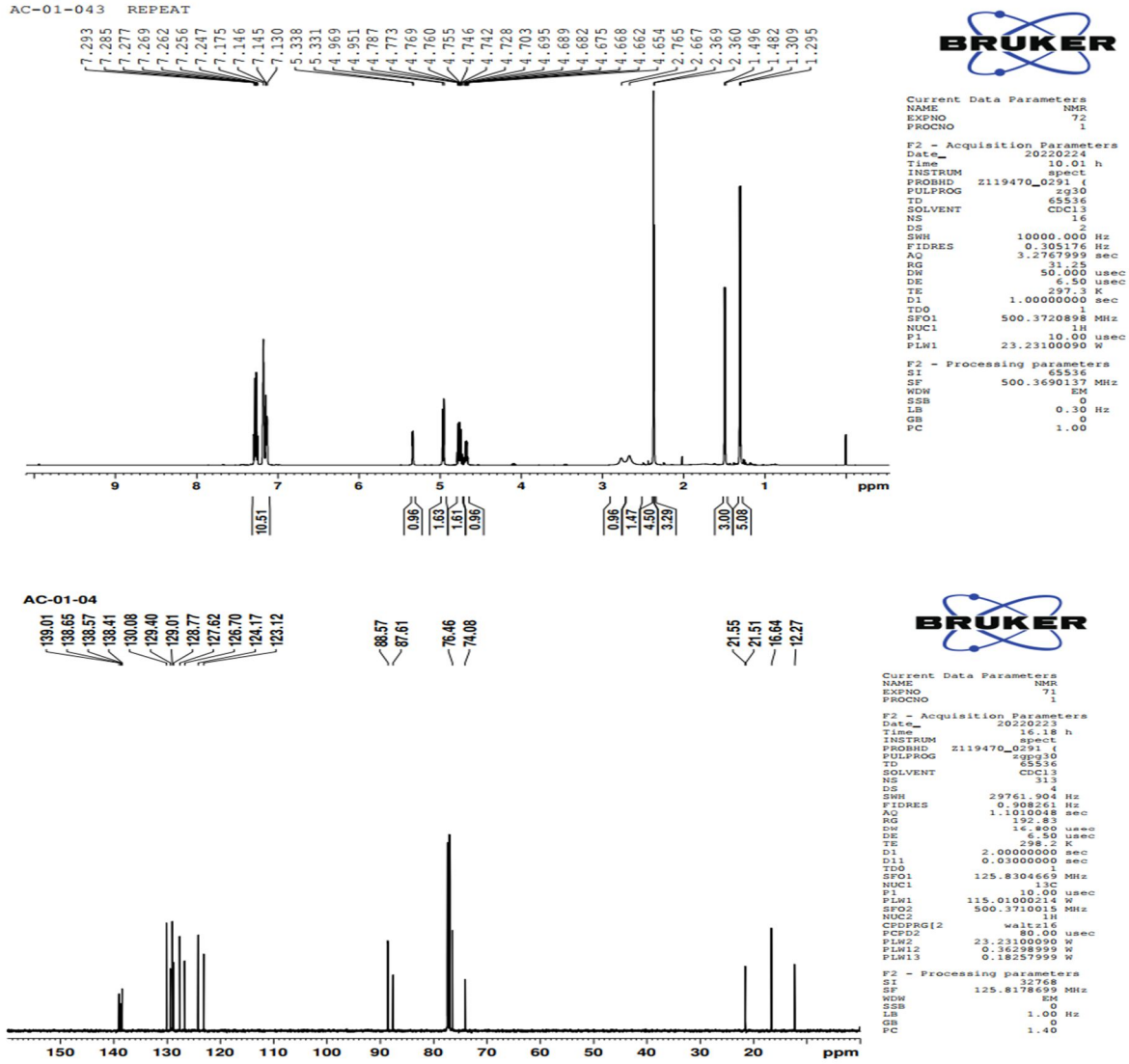
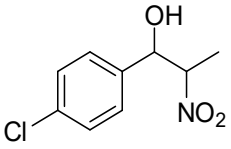


Figure 3.5: ^{1}H NMR and ^{13}C NMR spectra of 1-(3-methylphenyl)-2-nitropropan-1-ol.

5. 1-(4-Chlorophenyl)-2-nitropropan-1-ol [14]



^{1}H NMR (500 MHz, $CDCl_3$) δ 7.40 – 7.28 (m, 8H), 5.36 (d, *J* = 3.6 Hz, 1H), 5.01 (d, *J* = 8.9 Hz, 1H), 4.76 – 4.61 (m, 2H), 2.92 (s, 1H), 2.86 (s, 1H), 1.48 (d, *J* = 6.8 Hz, 3H), 1.31 (d, *J* = 6.9 Hz, 3H).

^{13}C NMR (101 MHz, $CDCl_3$) δ 137.04, 136.87, 135.14, 134.45, 129.30, 129.03, 128.39, 127.49, 88.30, 87.32, 75.60, 73.35, 16.44, 12.11.

Diastereomeric ratio 1:1.72 (*anti*: *syn*)

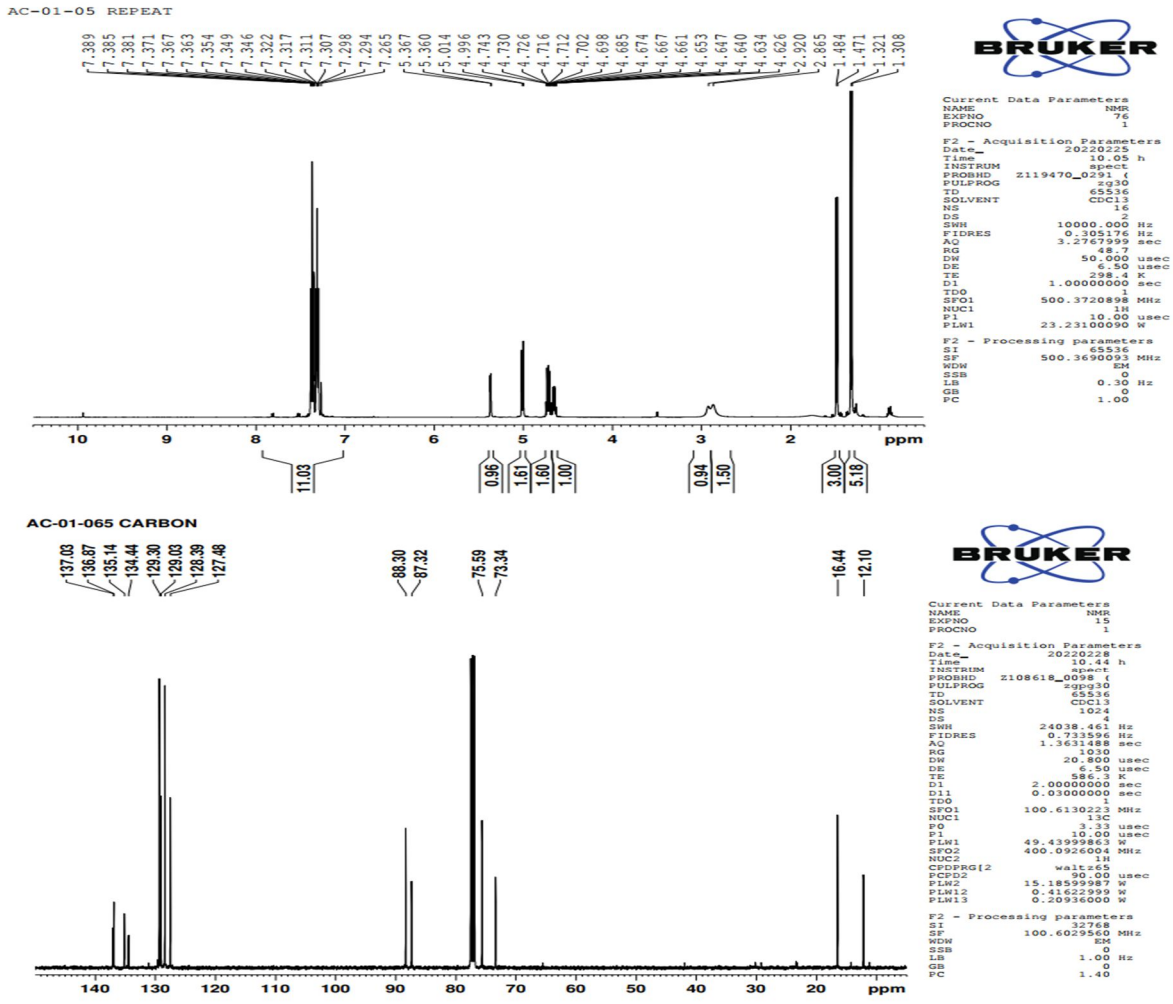
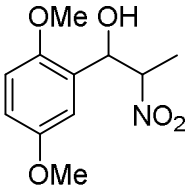


Figure 3.6: ^{1}H NMR and ^{13}C NMR spectra of 1-(4-chlorophenyl)-2-nitropropan-1-ol.

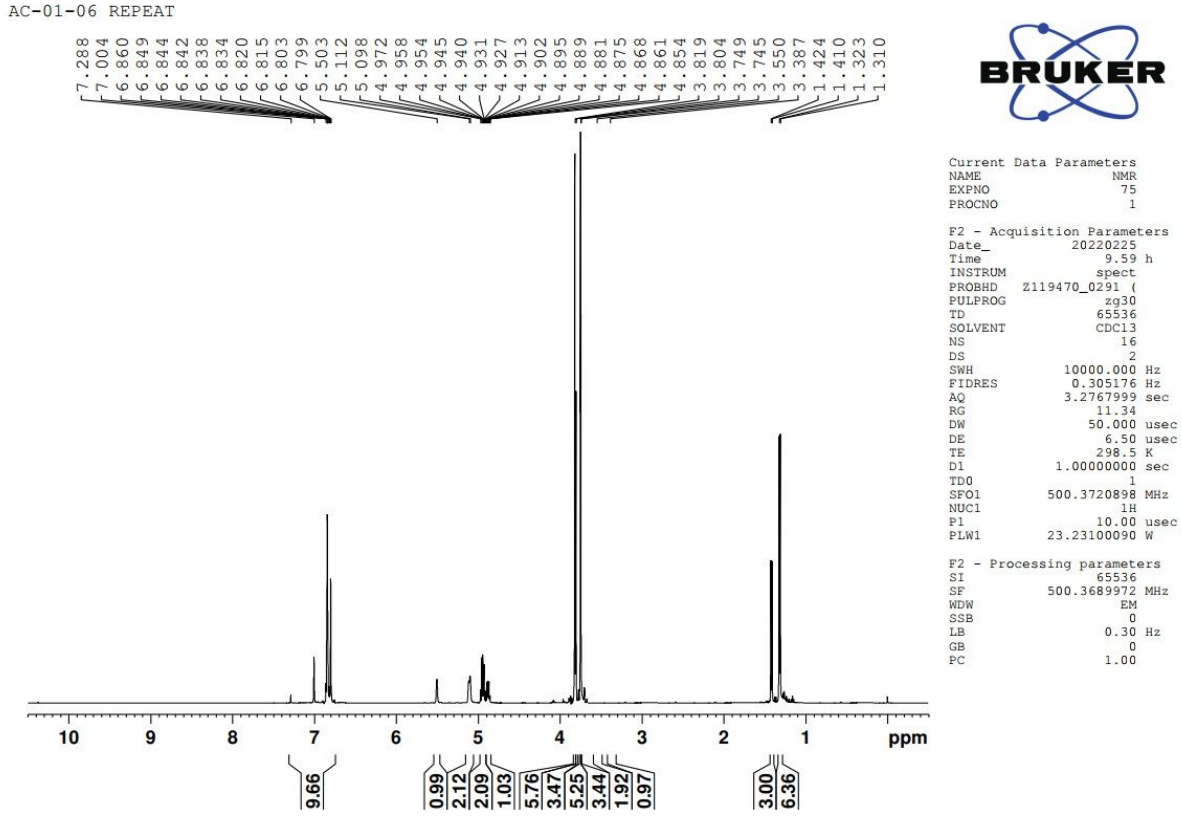
6. 1-(2,5-Dimethoxyphenyl)-2-nitropropan-1-ol [16]



^{1}H NMR (500 MHz, $CDCl_3$) δ 7.02 – 6.78 (m, 6H), 5.50 (s, 1H), 5.11 (d, *J* = 6.0 Hz, 1H), 4.99 – 4.81 (m, 2H), 3.82 (s, 3H), 3.80 (s, 3H), 3.75 (s, 3H), 3.75 (s, 3H), 3.55 (s, 1H), 3.39 (s, 1H), 1.42 (d, *J* = 6.9 Hz, 3H), 1.32 (d, *J* = 6.8 Hz, 3H).

^{13}C NMR (126 MHz, $CDCl_3$) δ 153.73, 153.72, 150.81, 149.83, 127.58, 126.95, 114.68, 114.28, 113.67, 113.56, 111.92, 111.27, 87.75, 84.85, 73.40, 70.42, 55.77, 55.70, 55.68, 16.37, 12.06.

Diastereomeric ratio 1:2.12 (*anti*: *syn*)



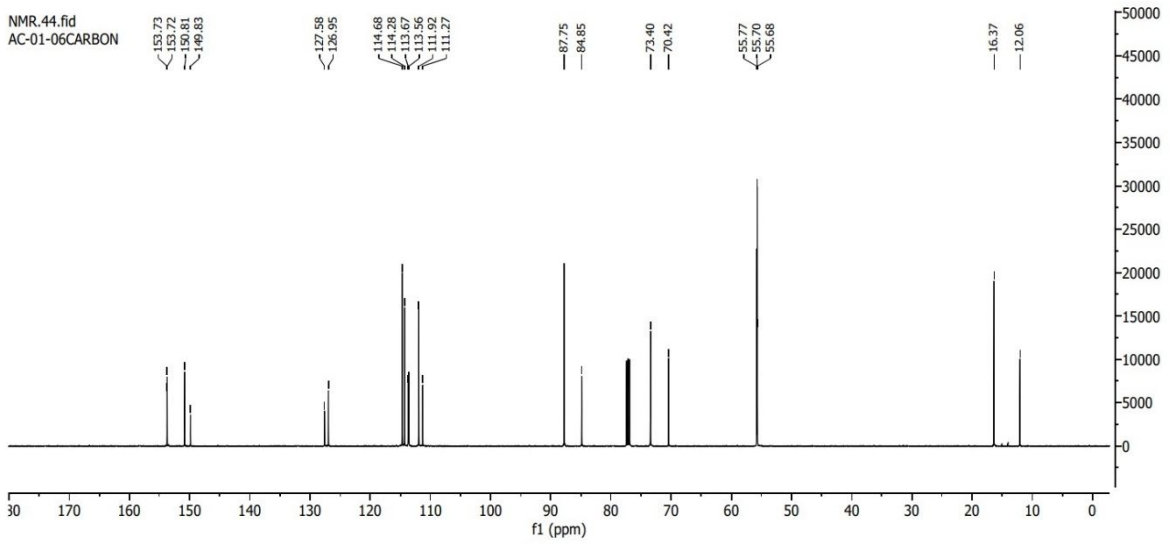
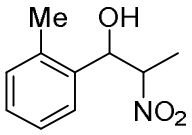


Figure 3.7: ^{1}H NMR and ^{13}C NMR spectra of 1-(2,5-dimethoxyphenyl)-2-nitropropan-1-ol.

7. 1-(2-Methylphenyl)-2-nitropropan-1-ol [14]



^{1}H NMR (500 MHz, $CDCl_3$) δ 7.97 – 7.11 (m, 8H), 5.57 (d, *J* = 3.1 Hz, 1H), 5.32 (d, *J* = 9.4 Hz, 1H), 4.87 – 4.56 (m, 2H), 2.86 (s, 2H), 2.41 (s, 3H), 2.35 (s, 3H), 1.47 (d, *J* = 6.8 Hz, 3H), 1.28 (d, *J* = 6.9 Hz, 3H).

^{13}C NMR (101 MHz, $CDCl_3$) δ 136.83, 136.68, 135.90, 134.40, 131.05, 130.76, 128.79, 128.33, 126.88, 126.64, 126.44, 126.05, 88.90, 85.41, 72.18, 70.97, 19.60, 18.85, 16.06, 11.55.

Diastereomeric ratio 1:3.36 (*anti*: *syn*)

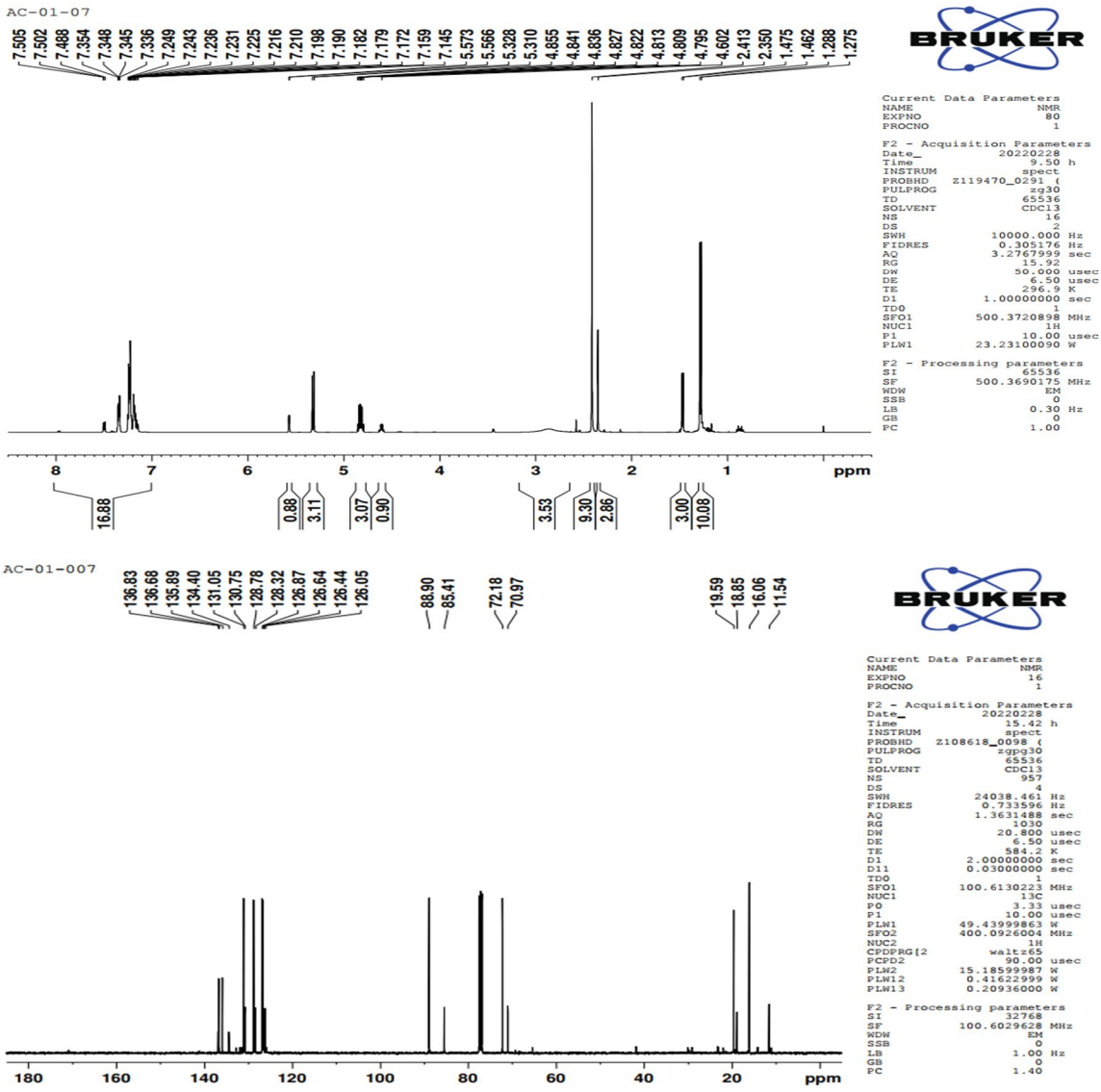
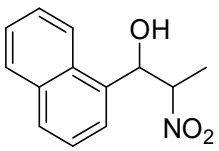


Figure 3.8: ^{1}H NMR and ^{13}C NMR spectra of 1-(2-methylphenyl)-2-nitropropan-1-ol.

8. 1-(Naphthalen-5-yl)-2-nitropropan-1-ol [15]



^{1}H NMR (500 MHz, $CDCl_3$) δ 8.31 – 7.41 (m, 14H), 6.26 (d, *J* = 2.5 Hz, 1H), 5.79 (d, *J* = 9.3 Hz, 1H), 5.12 (dq, *J* = 9.3, 6.9 Hz, 1H), 4.91 (qd, *J* = 6.7, 2.5 Hz, 1H), 2.84 (s, 1H), 1.42 (d, *J* = 6.8 Hz, 3H), 1.26 (d, *J* = 6.9 Hz, 3H).

^{13}C NMR (101 MHz, $CDCl_3$) δ 134.13, 133.97, 133.77, 130.93, 129.89, 129.44, 129.29, 129.16, 127.15, 126.95, 126.23, 126.07, 125.76, 125.52, 125.48, 124.13, 123.34, 121.89, 88.63, 85.72, 73.82, 70.99, 16.94, 11.11.

Diastereomeric ratio 1:4.66 (*anti*: *syn*)

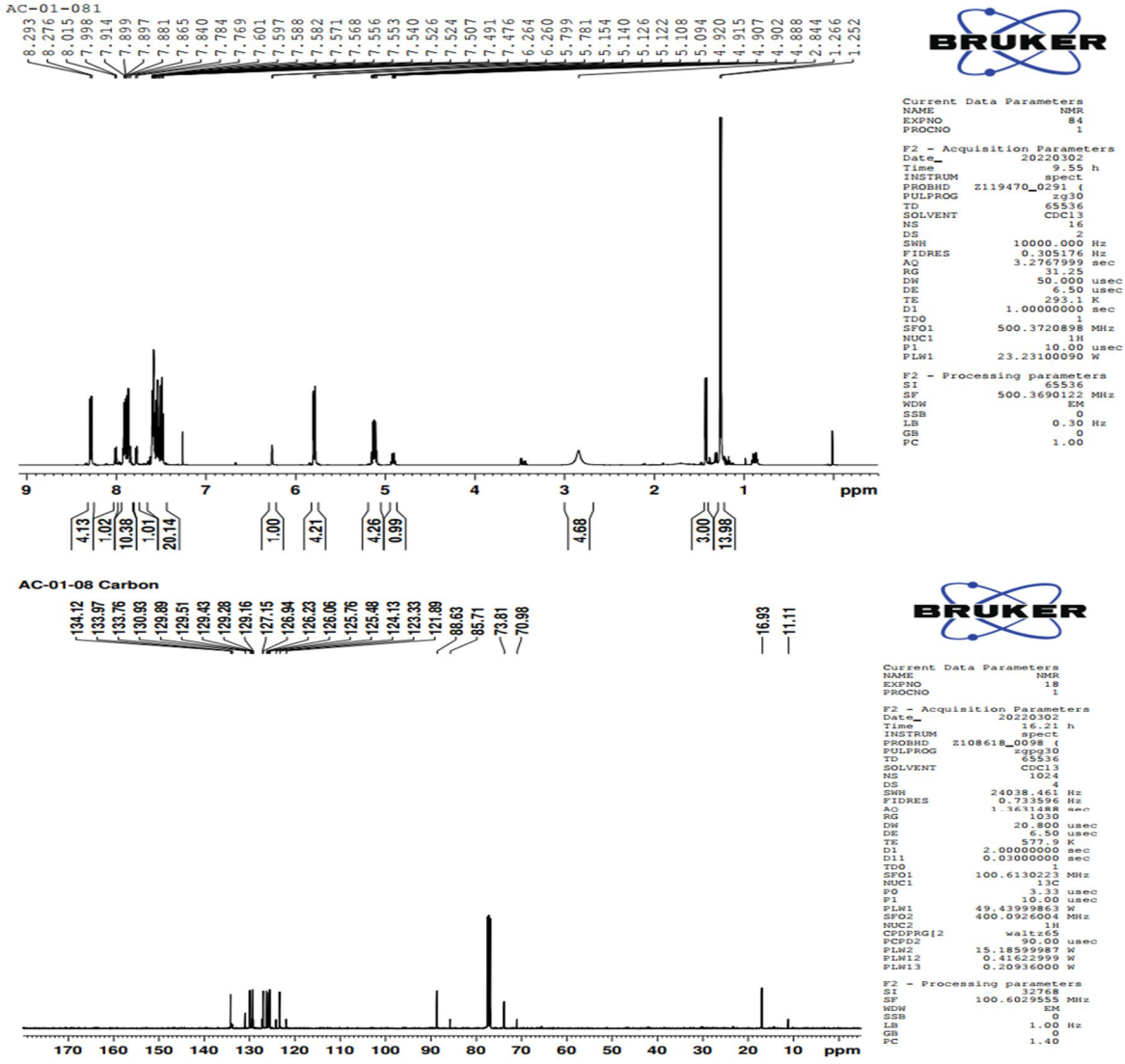
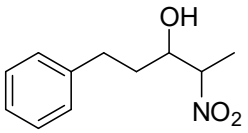


Figure 3.9: ^{1}H NMR and ^{13}C NMR spectra of 1-(naphthalen-5-yl)-2-nitropropan-1-ol.

9. 4-Nitro-1-phenylpentan-3-ol [14]



^{1}H NMR (500 MHz, $CDCl_3$) δ 7.34 – 7.14 (m, 10H), 4.58 – 4.44 (m, 2H), 4.17 (dt, *J* = 9.6, 3.3 Hz, 1H), 3.89 (ddd, *J* = 9.9, 7.0, 3.2 Hz, 1H), 2.88 (dddd, *J* = 14.3, 9.5, 7.1, 5.3 Hz, 2H), 2.70 (dddd, *J* = 20.9, 13.8, 9.1, 7.2 Hz, 2H), 2.54 (s, 2H), 1.92 – 1.63 (m, 4H), 1.53 (d, *J* = 6.8 Hz, 3H), 1.51 (d, *J* = 6.9 Hz, 3H).

^{13}C NMR (101 MHz, $CDCl_3$) δ 140.98, 140.91, 128.69, 128.52, 126.34, 87.88, 86.48, 72.21, 71.33, 34.77, 34.71, 31.99, 31.50, 16.25, 12.54.

Diastereomeric ratio 1:1.28 (*anti*: *syn*)

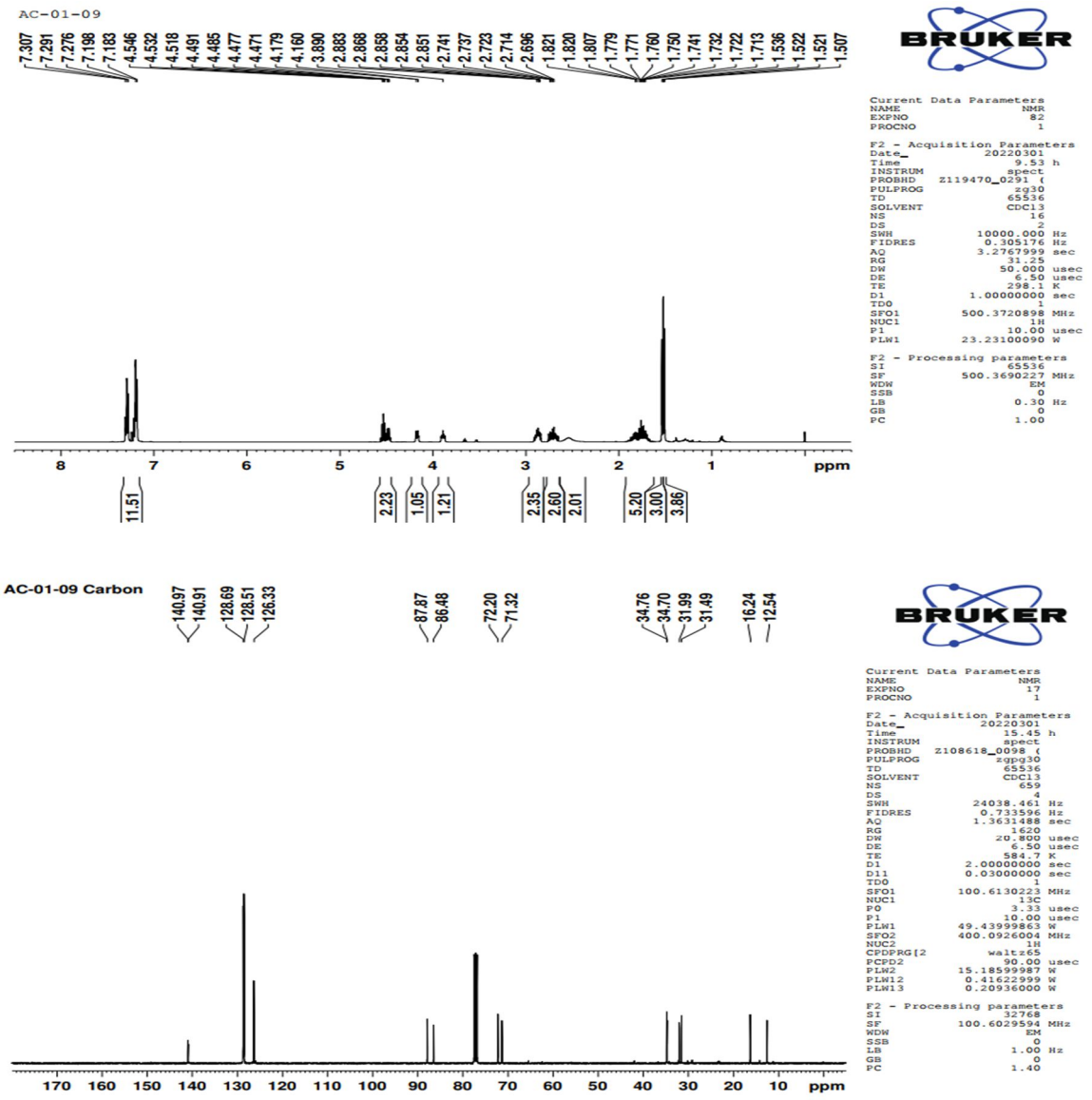
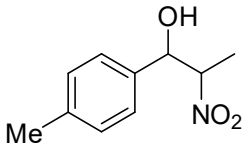


Figure 3.10: ^{1}H NMR and ^{13}C NMR spectra of 4-nitro-1-phenylpentan-3-ol.

10. 1-(4-Methylphenyl)-2-nitropropan-1-ol [15]



^{1}H NMR (500 MHz, $CDCl_3$) δ 7.34 – 7.18 (m, 8H), 5.34 (d, *J* = 3.8 Hz, 1H), 4.99 (d, *J* = 9.1 Hz, 1H), 4.81 – 4.65 (m, 2H), 2.79 (s, 1H), 2.68 (s, 1H), 2.39 (s, 3H), 2.37 (s, 3H), 1.51 (d, *J* = 6.8 Hz, 3H), 1.32 (d, *J* = 6.8 Hz, 3H).

^{13}C NMR (101 MHz, $CDCl_3$) δ 139.23, 138.46, 135.59, 135.44, 129.77, 129.49, 126.93, 125.98, 88.55, 87.61, 76.23, 74.02, 21.28, 21.23, 16.56, 12.34.

Diastereomeric ratio 1:1.45 (*anti*: *syn*)

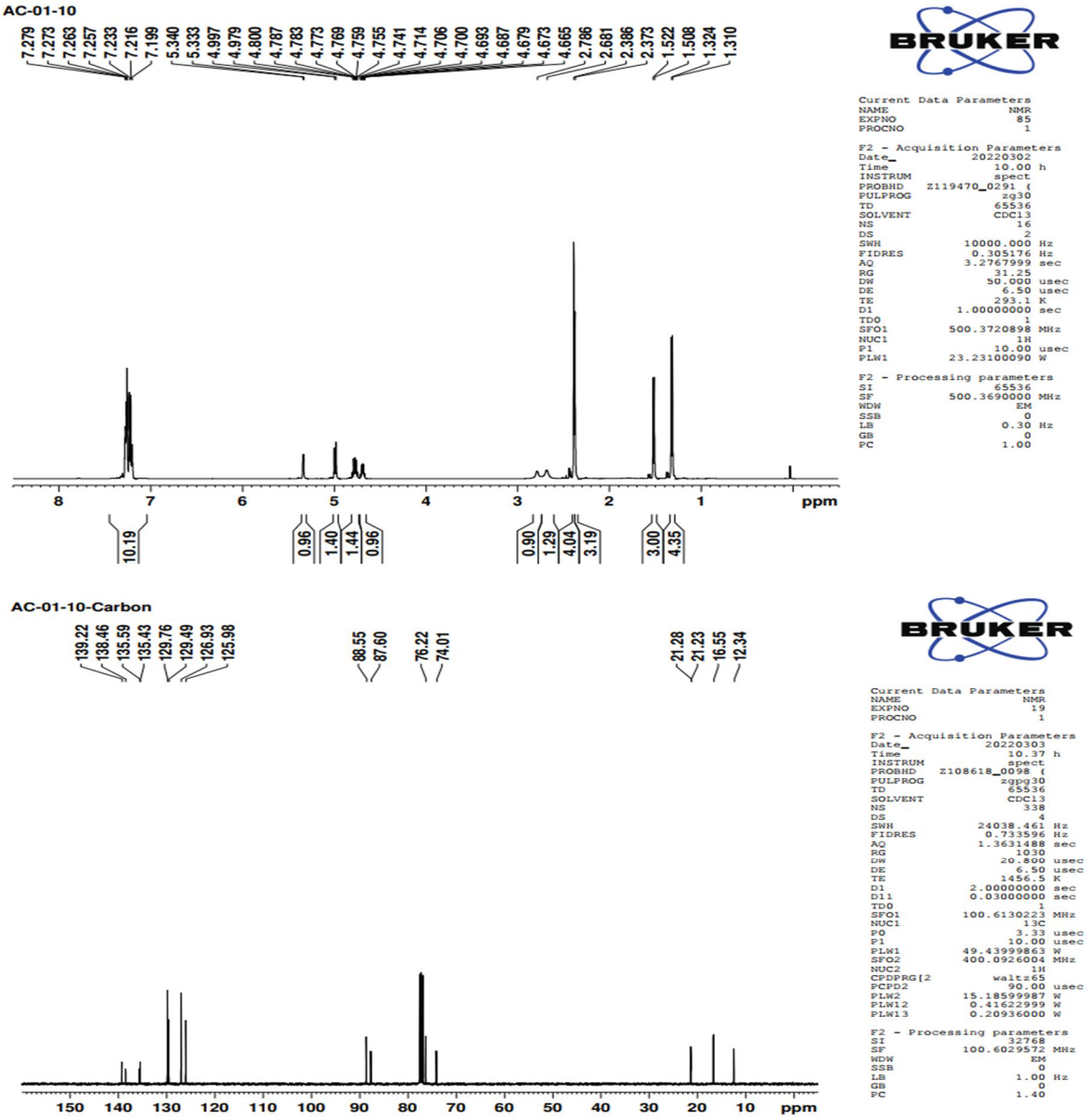
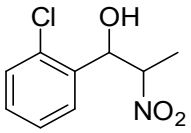


Figure 3.11: ^{1}H NMR and ^{13}C NMR spectra of 1-(4-methylphenyl)-2-nitropropan-1-ol.

11. 1-(2-Chlorophenyl)-2-nitropropan-1-ol [15]



^{1}H NMR (500 MHz, $CDCl_3$) δ 7.68 – 7.27 (m, 8H), 5.85 (s, 1H), 5.61 (d, *J* = 8.3 Hz, 1H), 4.95 – 4.79 (m, 2H), 3.06 (s, 1H), 3.02 (s, 1H), 1.46 (d, *J* = 5.1 Hz, 3H), 1.44 (d, *J* = 5.1 Hz, 3H).

^{13}C NMR (101 MHz, $CDCl_3$) δ 136.20, 135.89, 132.85, 131.54, 130.14, 129.95, 129.72, 128.34, 128.19, 127.78, 127.38, 88.19, 84.11, 71.90, 70.60, 16.09, 11.22.

Diastereomeric ratio 1.12:1 (*anti*: *syn*)

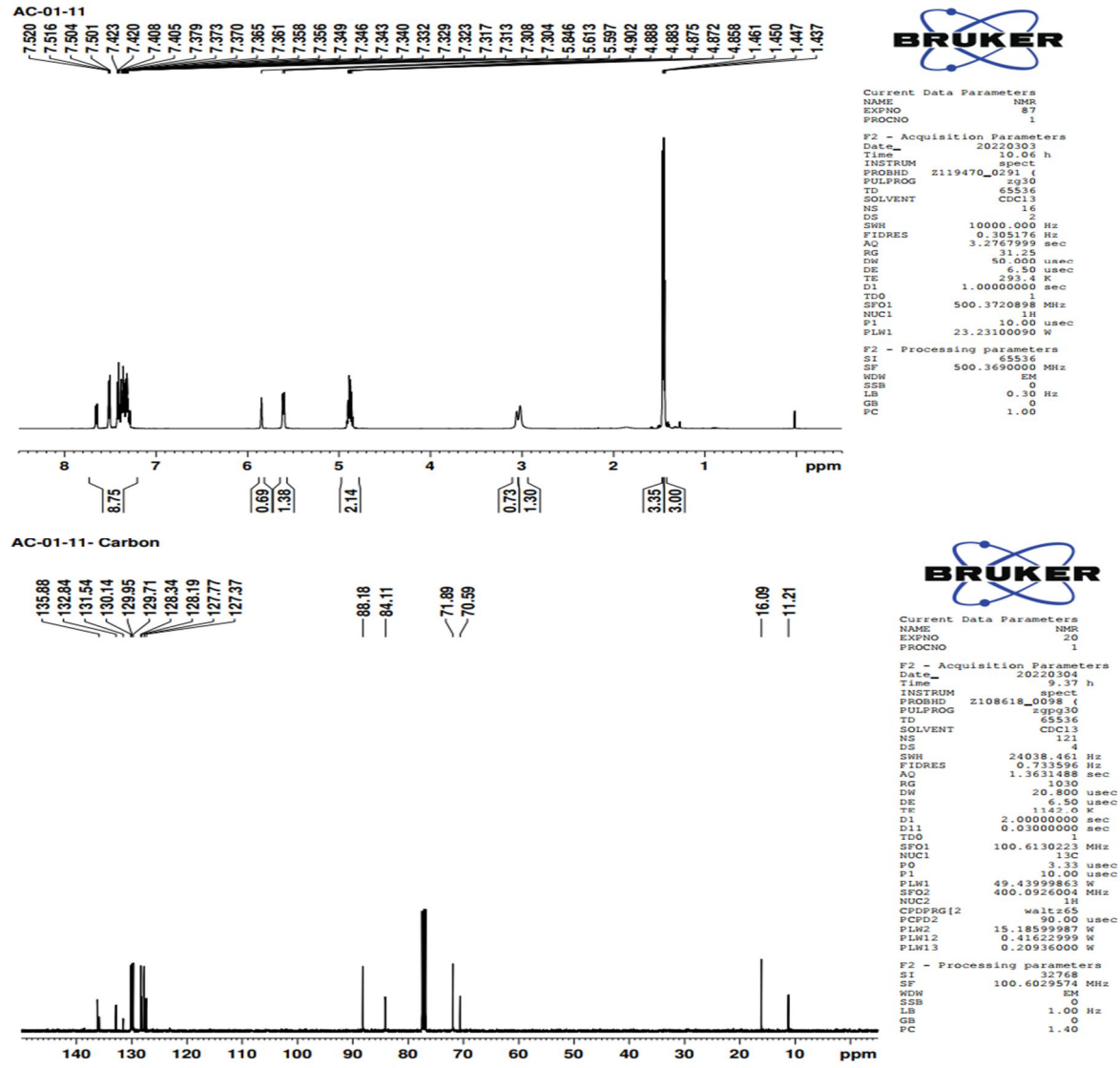
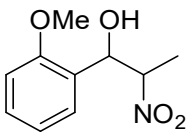


Figure 3.12: ^{1}H NMR and ^{13}C NMR spectra of 1-(2-chlorophenyl)-2-nitropropan-1-ol.

12. 1-(2-Methoxyphenyl)-2-nitropropan-1-ol [14]



^{1}H NMR (500 MHz, $CDCl_3$) δ 7.44 – 6.85 (m, 8H), 5.52 (d, *J* = 3.8 Hz, 1H), 5.13 (d, *J* = 9.0 Hz, 1H), 5.00 (dq, *J* = 9.0, 6.7 Hz, 1H), 4.89 (qd, *J* = 6.9, 3.8 Hz, 1H), 3.88 (s, 3H), 3.86 (s, 3H), 3.38 (s, 1H), 3.16 (s, 1H), 1.46 (d, *J* = 6.9 Hz, 3H), 1.32 (d, *J* = 6.8 Hz, 3H).

^{13}C NMR (101 MHz, $CDCl_3$) δ 156.80, 155.82, 130.14, 129.50, 129.03, 127.65, 126.36, 125.93, 121.25, 120.96, 111.03, 110.43, 87.72, 85.09, 74.15, 70.79, 55.49, 55.44, 16.62, 12.54.

Diastereomeric ratio 1:1.87 (*anti*: *syn*)

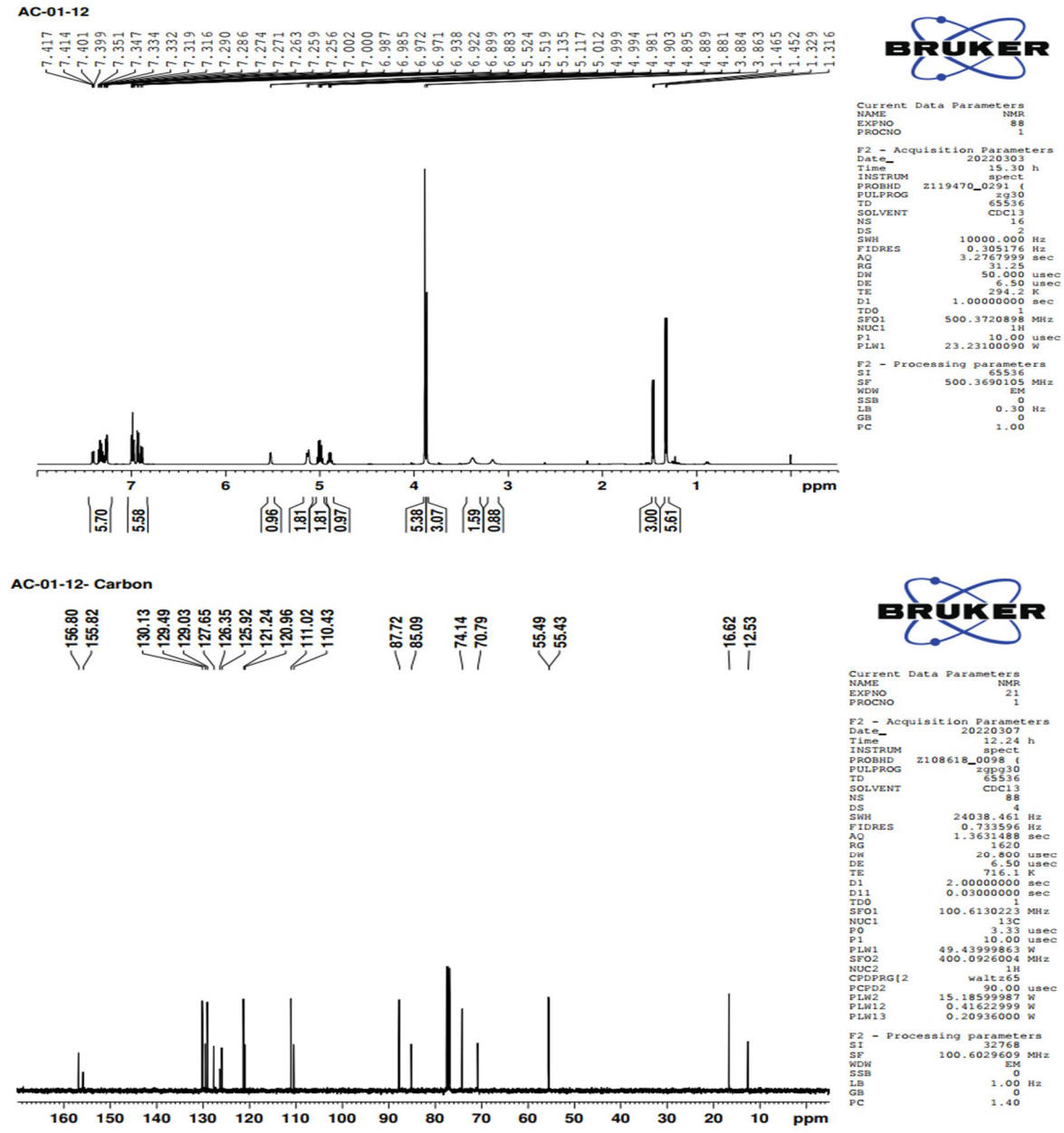
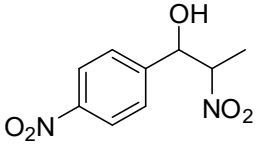


Figure 3.13: ^{1}H NMR and ^{13}C NMR spectra of 1-(2-methoxyphenyl)-2-nitropropan-1-ol.

13. 1-(4-Nitrophenyl)-2-nitropropan-1-ol [14]



^{1}H NMR (500 MHz, $CDCl_3$) δ 8.32 – 7.49 (m, 8H), 5.55 (s, 1H), 5.18 (d, J = 8.5 Hz, 1H), 4.89 – 4.63 (m, 2H), 3.13 (s, 2H), 1.48 (d, J = 6.8 Hz, 3H), 1.37 (d, J = 6.9 Hz, 3H).

^{13}C NMR (126 MHz, $CDCl_3$) δ 148.40, 148.01, 145.67, 145.40, 128.04, 127.14, 124.21, 124.05, 87.90, 86.92, 75.16, 73.02, 16.32, 11.97.

Diastereomeric ratio 1.41:1 (*anti*: *syn*)

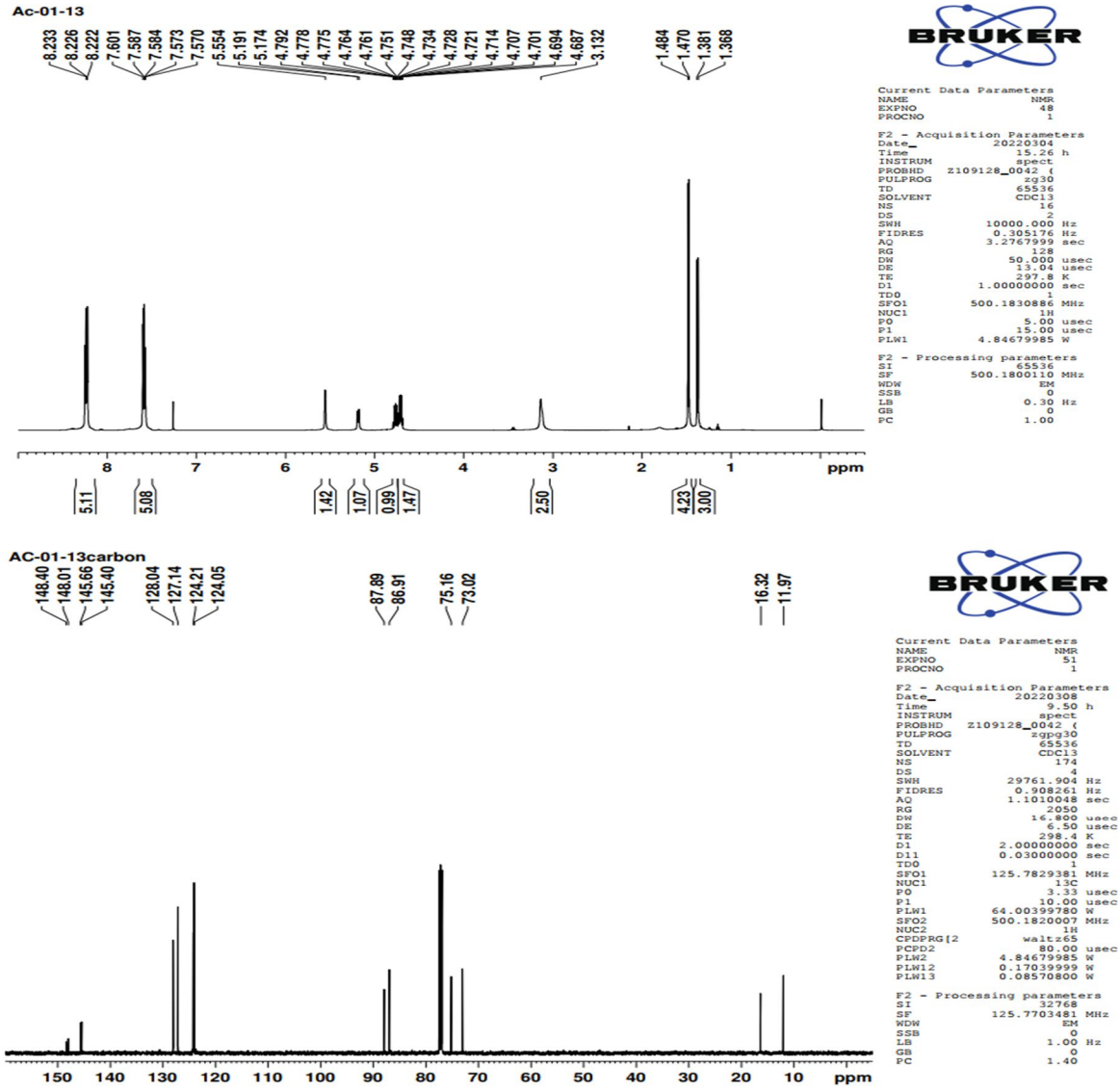
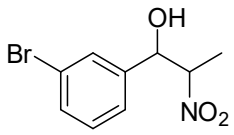


Figure 3.14: ^{1}H NMR and ^{13}C NMR spectra of 1-(4-nitrophenyl)-2-nitropropan-1-ol.

14. 1-(3-Bromophenyl)-2-nitropropan-1-ol [15]



^{1}H NMR (500 MHz, $CDCl_3$) δ 7.57 – 7.21 (m, 8H), 5.37 (s, 1H), 4.98 (d, J = 9.0 Hz, 1H), 4.76 – 4.60 (m, 2H), 3.00 (s, 1H), 2.97 (s, 1H), 1.47 (d, J = 6.9 Hz, 3H), 1.32 (d, J = 6.9 Hz, 3H).

^{13}C NMR (126 MHz, $CDCl_3$) δ 140.84, 140.61, 132.36, 131.68, 130.64, 130.41, 130.09, 129.17, 125.72, 124.69, 123.12, 122.97, 88.21, 87.20, 75.55, 73.12, 16.48, 11.94.

Diastereomeric ratio 1:2.45 (*anti*: *syn*)

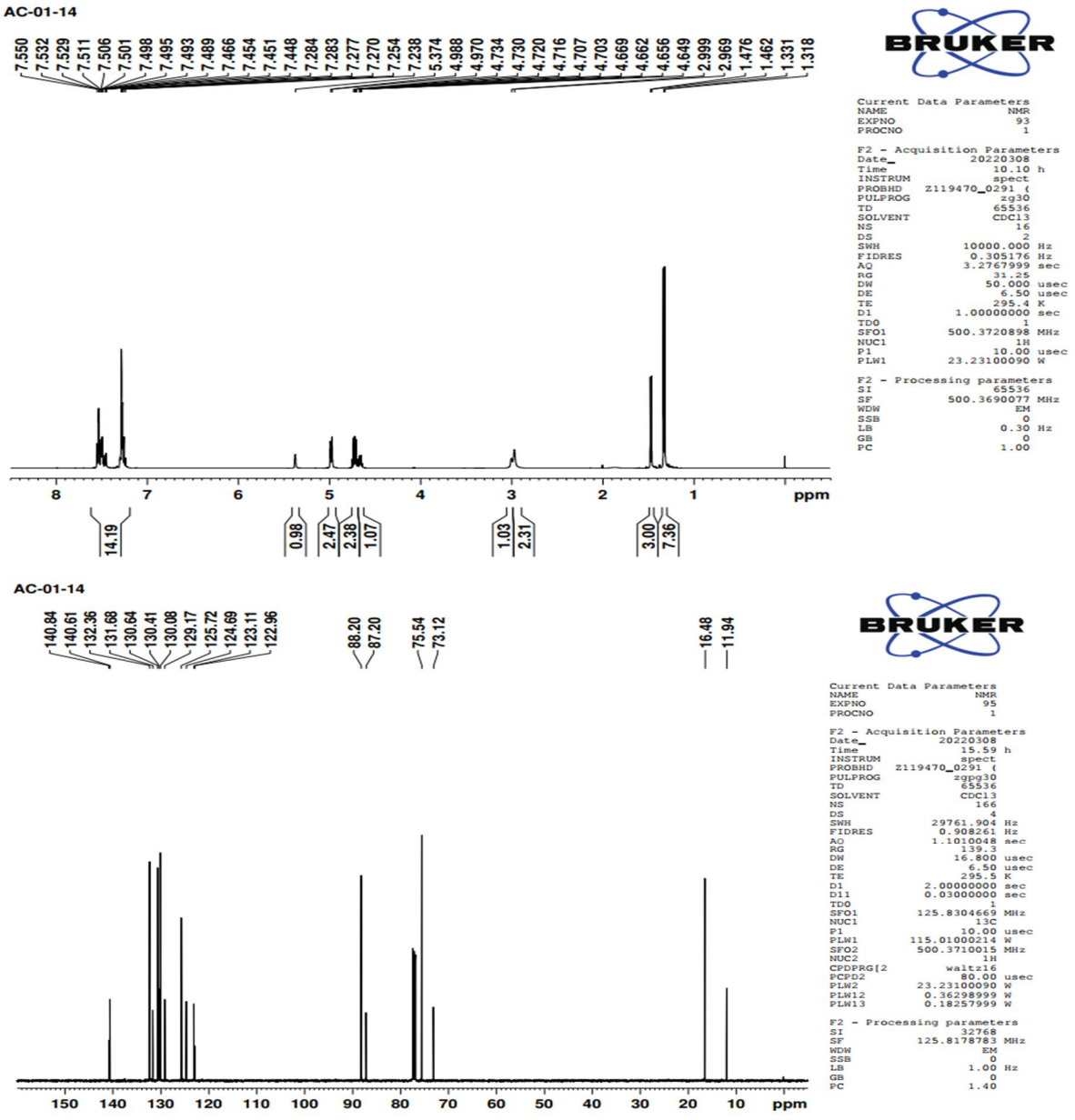
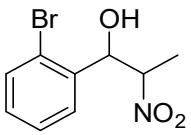


Figure 3.15: ^{1}H NMR and ^{13}C NMR spectra of 1-(3-bromophenyl)-2-nitropropan-1-ol.

15. 1-(2-Bromophenyl)-2-nitropropan-1-ol [17]



^{1}H NMR (500 MHz, $CDCl_3$) δ 7.60 – 7.05 (m, 8H), 5.69 (s, 1H), 5.48 (d, *J* = 8.3 Hz, 1H), 4.85 – 4.72 (m, 2H), 3.01 (s, 2H), 1.36 (d, *J* = 6.9 Hz, 3H), 1.33 (d, *J* = 6.9 Hz, 3H).

^{13}C NMR (101 MHz, $CDCl_3$) δ 137.85, 137.42, 133.21, 132.99, 130.42, 130.01, 128.53, 128.36, 127.91, 123.00, 121.56, 88.25, 84.08, 74.01, 72.59, 16.13, 11.04.

Diastereomeric ratio 1:1.13 (*anti*: *syn*)

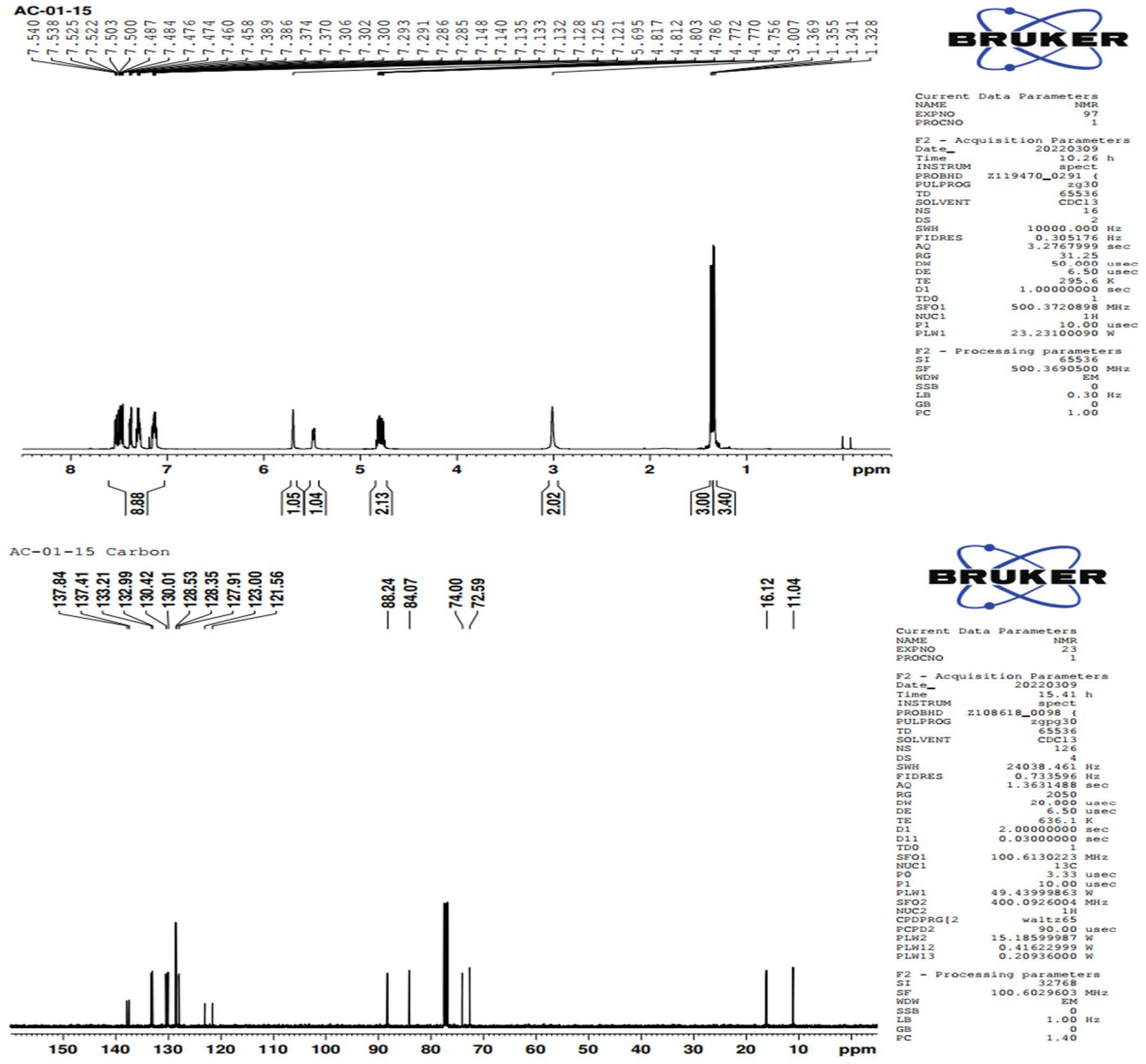
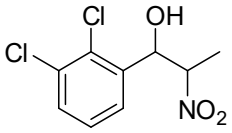


Figure 3.16: ^{1}H NMR and ^{13}C NMR spectra of 1-(2-bromophenyl)-2-nitropropan-1-ol.

16. 1-(2,3-Dichlorophenyl)-2-nitropropan-1-ol



^{1}H NMR (500 MHz, $CDCl_3$) δ 7.62 – 7.26 (m, 6H), 5.86 (s, 1H), 5.62 (dd, *J* = 8.2, 3.3 Hz, 1H), 4.95 – 4.79 (m, 2H), 3.19 (br, 2H), 1.47 (d, *J* = 7.0 Hz, 3H), 1.42 (d, *J* = 6.9 Hz, 3H).

^{13}C NMR (101 MHz, $CDCl_3$) δ 138.62, 138.30, 133.59, 133.42, 131.04, 130.86, 130.39, 129.73, 128.16, 127.83, 126.42, 87.91, 83.73, 72.21, 70.94, 16.05, 11.09.

Diastereomeric ratio 1.2:1 (*anti*: *syn*)

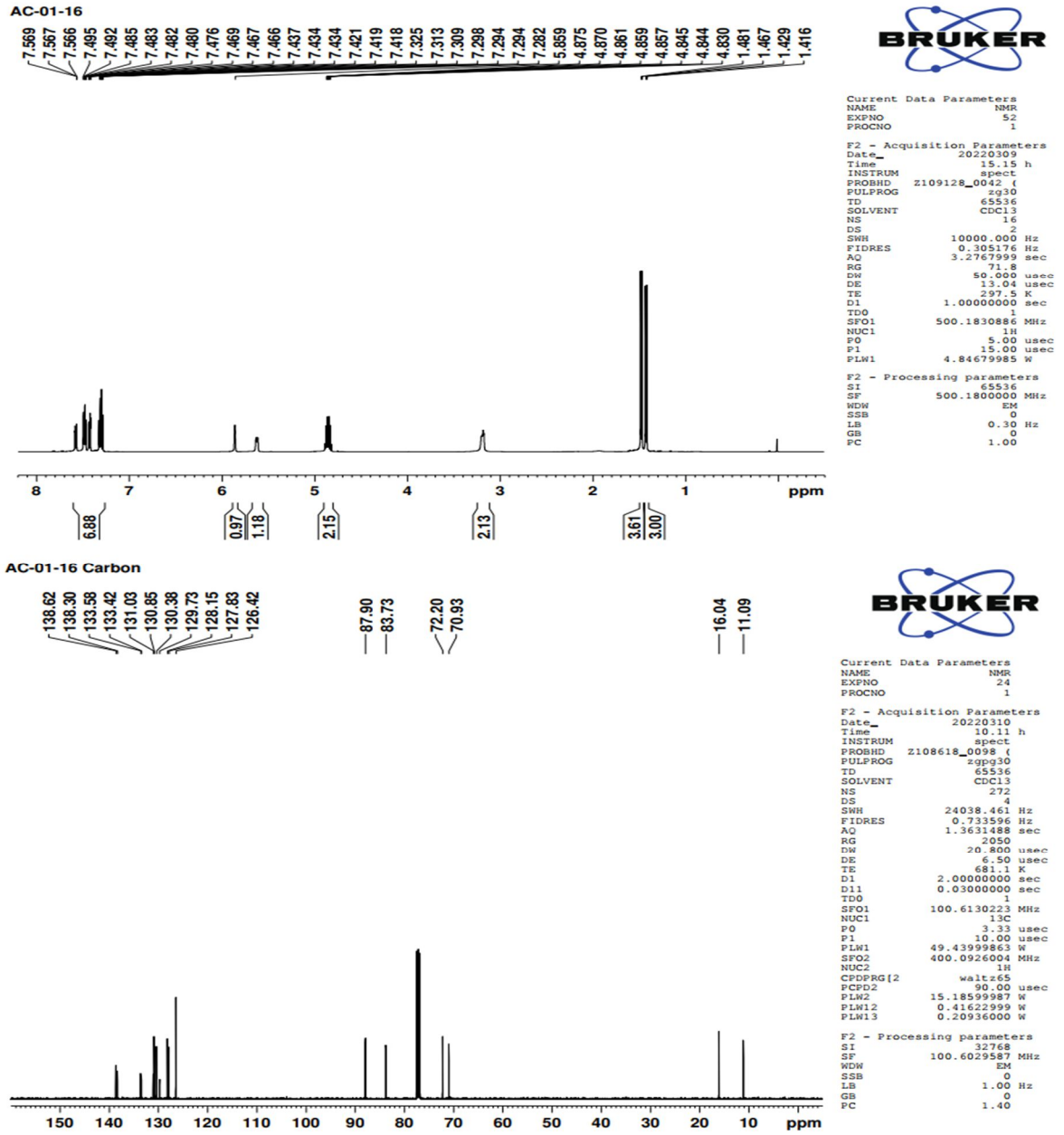
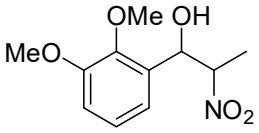


Figure 3.17: ^{1}H NMR and ^{13}C NMR spectra of 1-(2,3-dichlorophenyl)-2-nitropropan-1-ol.

17. 1-(2,3-Dimethoxyphenyl)-2-nitropropan-1-ol



^{1}H NMR (500 MHz, $CDCl_3$) δ 7.12 – 6.86 (m, 6H), 5.54 (s, 1H), 5.30 – 5.20 (m, 1H), 4.97 – 4.78 (m, 2H), 3.90 (s, 1H), 3.89 (s, 1H), 3.86 (s, 1H), 3.85 (s, 1H), 3.35 (d, *J* = 6.0 Hz, 1H), 3.32 (d, *J* = 5.2 Hz, 1H), 1.41 (d, *J* = 6.9 Hz, 3H), 1.31 (d, *J* = 6.9 Hz, 3H).

^{13}C NMR (126 MHz, $CDCl_3$) δ 152.52, 152.21, 146.57, 145.39, 131.86, 131.52, 124.52, 124.17, 119.63, 118.94, 112.90, 112.50, 88.28, 85.62, 72.17, 70.41, 61.05, 60.66, 55.73, 55.72, 16.40, 12.11.

Diastereomeric ratio 1.08:1 (*anti*: *syn*)

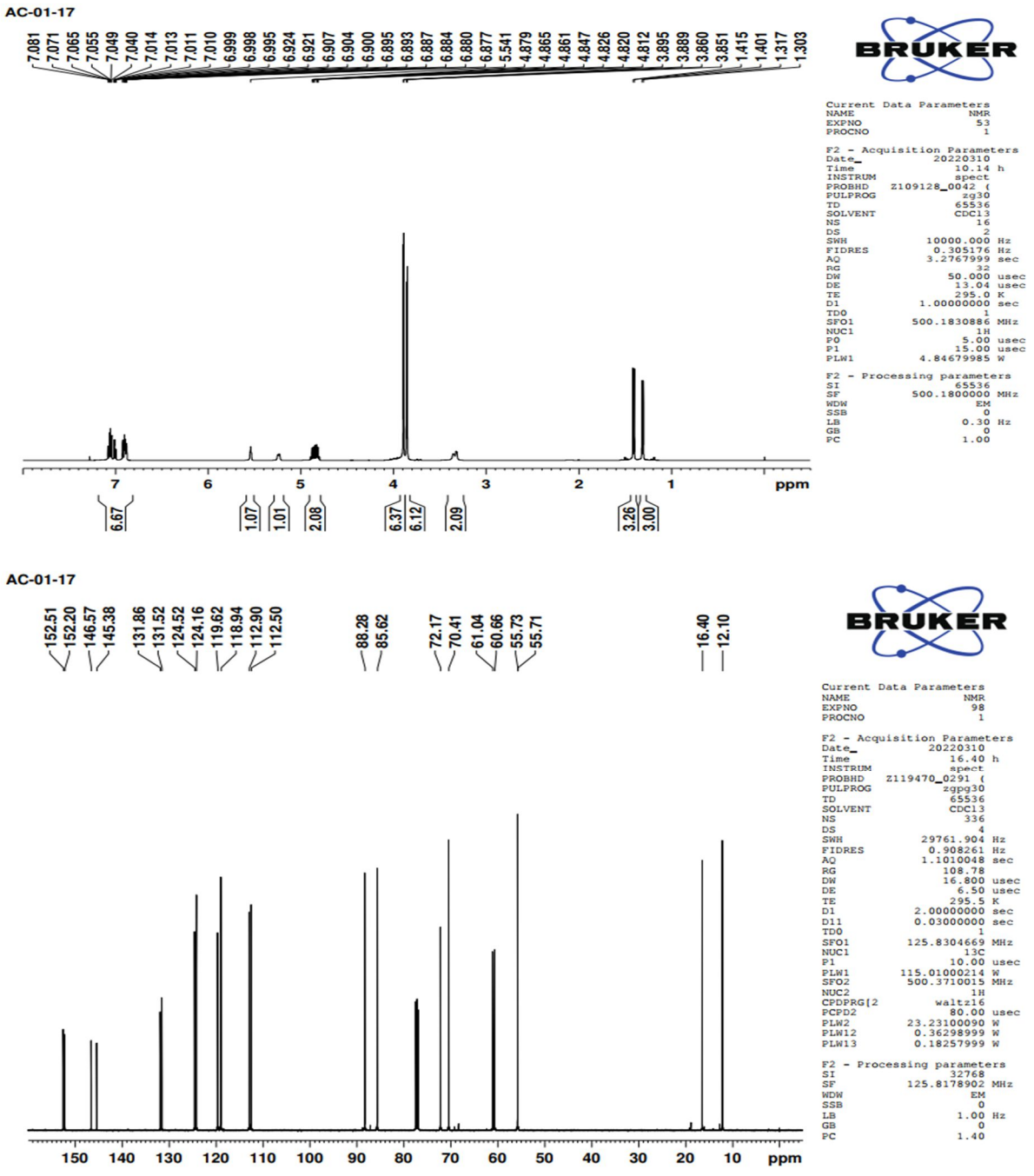
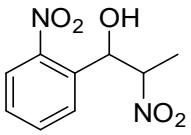


Figure 3.18: ^{1}H NMR and ^{13}C NMR spectra of 1-(2,3-dimethoxyphenyl)-2-nitropropan-1-ol.

18. 1-(2 Nitrophenyl)-2-nitropropan-1-ol [18]



^{1}H NMR (500 MHz, $CDCl_3$) δ 8.15 – 7.49 (m, 8H), 6.08 (d, *J* = 2.6 Hz, 1H), 5.70 (d, *J* = 6.6 Hz, 1H), 5.10 – 4.90 (m, 2H), 3.36 (s, 1H), 3.27 (s, 1H), 1.53 (d, *J* = 6.9 Hz, 3H), 1.51 (d, *J* = 6.9 Hz, 3H).

^{13}C NMR (101 MHz, $CDCl_3$) δ 148.16, 147.19, 134.34, 134.23, 134.16, 134.09, 129.82, 129.56, 129.42, 128.99, 125.27, 125.07, 87.67, 84.87, 70.64, 69.38, 16.45, 11.97.

Diastereomeric ratio 1:1.35 (*anti*: *syn*)

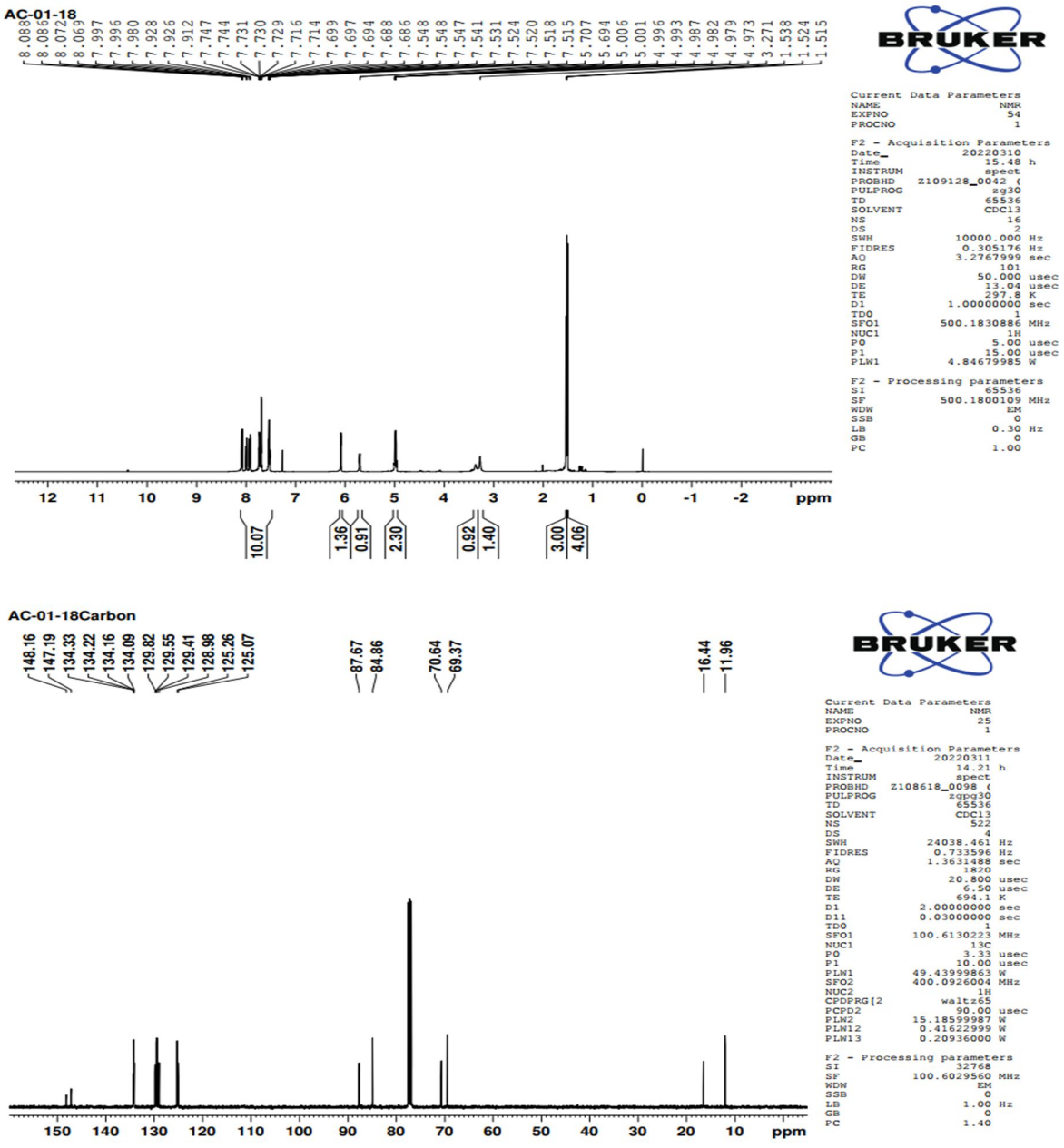
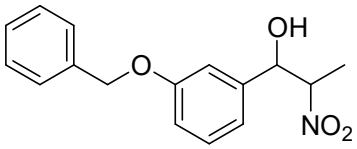


Figure 3.19: ^{1}H NMR and ^{13}C NMR spectra of 1-(2-nitrophenyl)-2-nitropropan-1-ol.

19. 1-(3-(Benzyloxy)phenyl)-2-nitropropan-1-ol [16]



^{1}H NMR (500 MHz, $CDCl_3$) δ 7.55 – 6.93 (m, 18H), 5.36 (d, *J* = 3.5 Hz, 1H), 5.09 (s, 4H), 4.97 (d, *J* = 9.1 Hz, 1H), 4.81 – 4.64 (m, 2H), 2.86 (s, 2H), 1.47 (d, *J* = 6.8 Hz, 3H), 1.31 (d, *J* = 6.9 Hz, 3H).

^{13}C NMR (101 MHz, $CDCl_3$) δ 159.14, 139.98, 136.62, 130.15, 128.69, 128.17, 127.61, 119.55, 115.63, 113.41, 88.43, 76.19, 70.12, 16.48.

Diastereomeric ratio 1:11.11 (*anti*: *syn*)

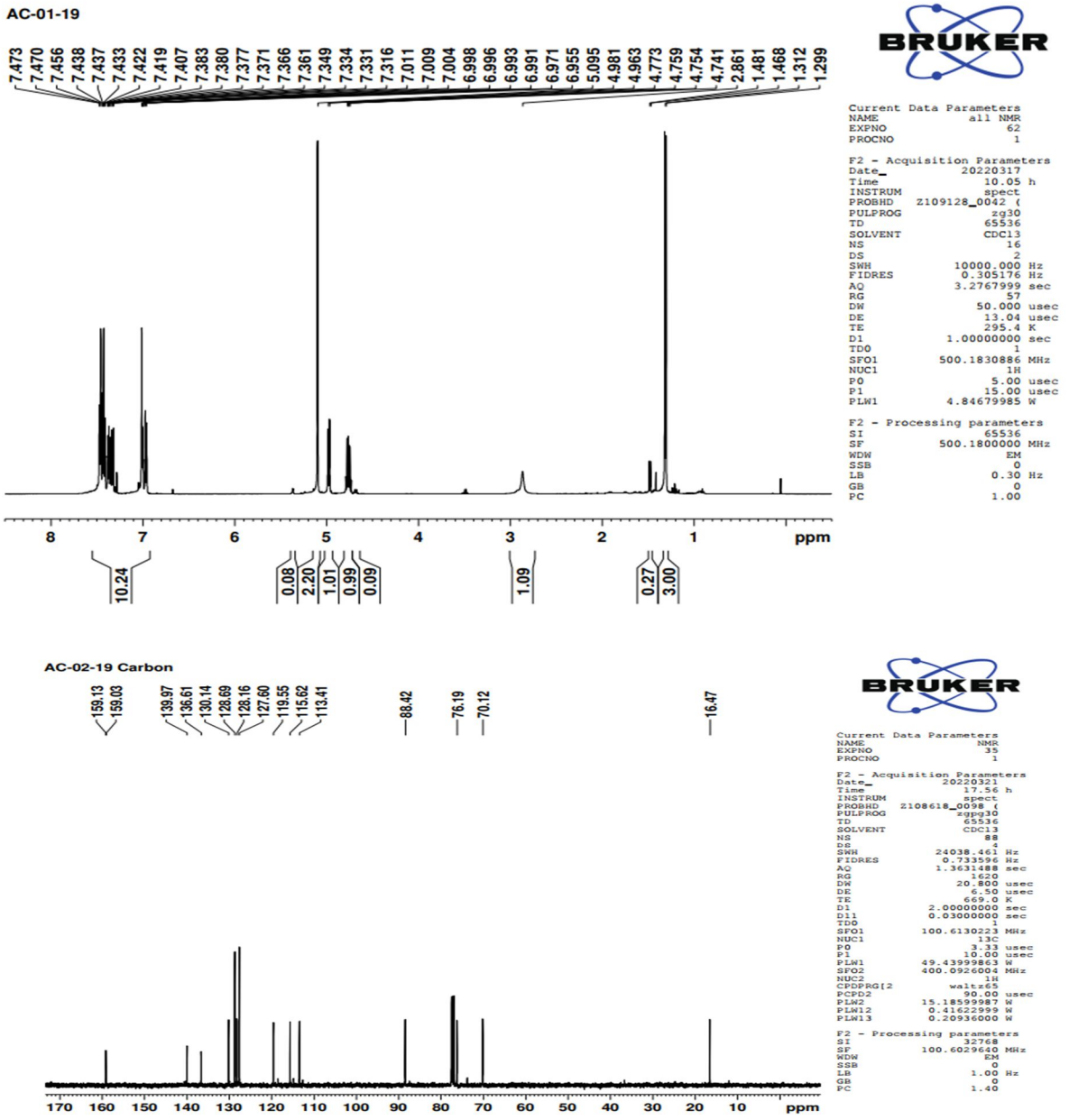
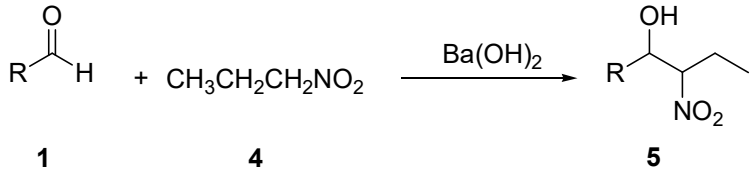


Figure 3.20: ^{1}H NMR and ^{13}C NMR spectra of 1-(3-(benzyloxy)phenyl)-2-nitropropan-1-ol.

3.4.3. Barium hydroxide catalyzed synthesis of different racemic β-nitroalcohols starting from their corresponding aromatic aldehydes and 1-nitropropane



Scheme 3.2. Chemical synthesis of racemic β-nitroalcohols using 1-nitropropane as a nucleophile

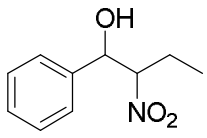
Table 3.3: List of racemic β-nitroalcohols synthesized using 1-nitropropane as nucleophile

S. No.	Aldehyde	Reaction conditions				(**5**) Yield (%)
		(**1**) mmol	Catalyst (mole % of aldehyde)	(**4**) mmol	time (h)	
1	benzaldehyde	10	25	100	11	64
2	2-furaldehyde	10	12.5	100	7.5	57
3	4-methoxy benzaldehyde	7.5	25	75	11.5	32
4	2-methoxy benzaldehyde	7.5	25	75	9	79
5	4-chloro benzaldehyde	7.5	12.5	75	8	56
6	2-methyl benzaldehyde	7.5	25	75	10	59
7	4-nitro benzaldehyde	5	18.75	50	6	59
8	4-methyl benzaldehyde	5	37.5	75	12	38
9	3-phenyl propionaldehyde	7.5	12.5	75	9	58
10	3-chloro benzaldehyde	7.5	25	75	7	67.3
11	3-methoxy benzaldehyde	7.5	25	75	8	81
12	3-methyl benzaldehyde	7.5	25	75	9	65
13	2-bromo benzaldehyde	7.5	50	75	12	82
14	3-bromo benzaldehyde	7.5	50	75	12	95
15	2,3-dichloro benzaldehyde	7.5	50	75	12	87
16	2-nitro benzaldehyde	7.5	50	75	12	95

3.4.4. NMR characterization of 1-nitropropane corresponding racemic β-nitroalcohols

Figure 3.21 to 3.34 represents the ^{1}H NMR and ^{13}C NMR of racemic β-nitroalcohols (**5**) synthesized by chemical catalyst as given in Scheme 3.2, Table 3.3.

1. 2-Nitro-1-phenylbutan-1-ol (NPB) [19]



^{1}H NMR (500 MHz, $CDCl_3$) δ 7.57 – 7.28 (m, 10H), 5.10 (d, *J* = 5.3 Hz, 1H), 4.98 (d, *J* = 9.1 Hz, 1H), 4.75 – 4.50 (m, 2H), 3.02 (s, 1H), 2.91 (s, 1H), 2.11 (m, 1H), 1.89 (m, 1H), 1.81 (m, 1H), 1.37 (m, 1H), 0.90 (t, *J* = 7.4 Hz, 3H), 0.84 (t, *J* = 7.4 Hz, 3H).

^{13}C NMR (126 MHz, $CDCl_3$) δ 138.73, 138.68, 129.17, 129.04, 128.76, 128.73, 126.97, 126.31, 95.32, 94.73, 75.55, 74.31, 23.95, 21.52, 10.40, 10.09.

Diastereomeric ratio 1:3.76 (*anti*: *syn*)

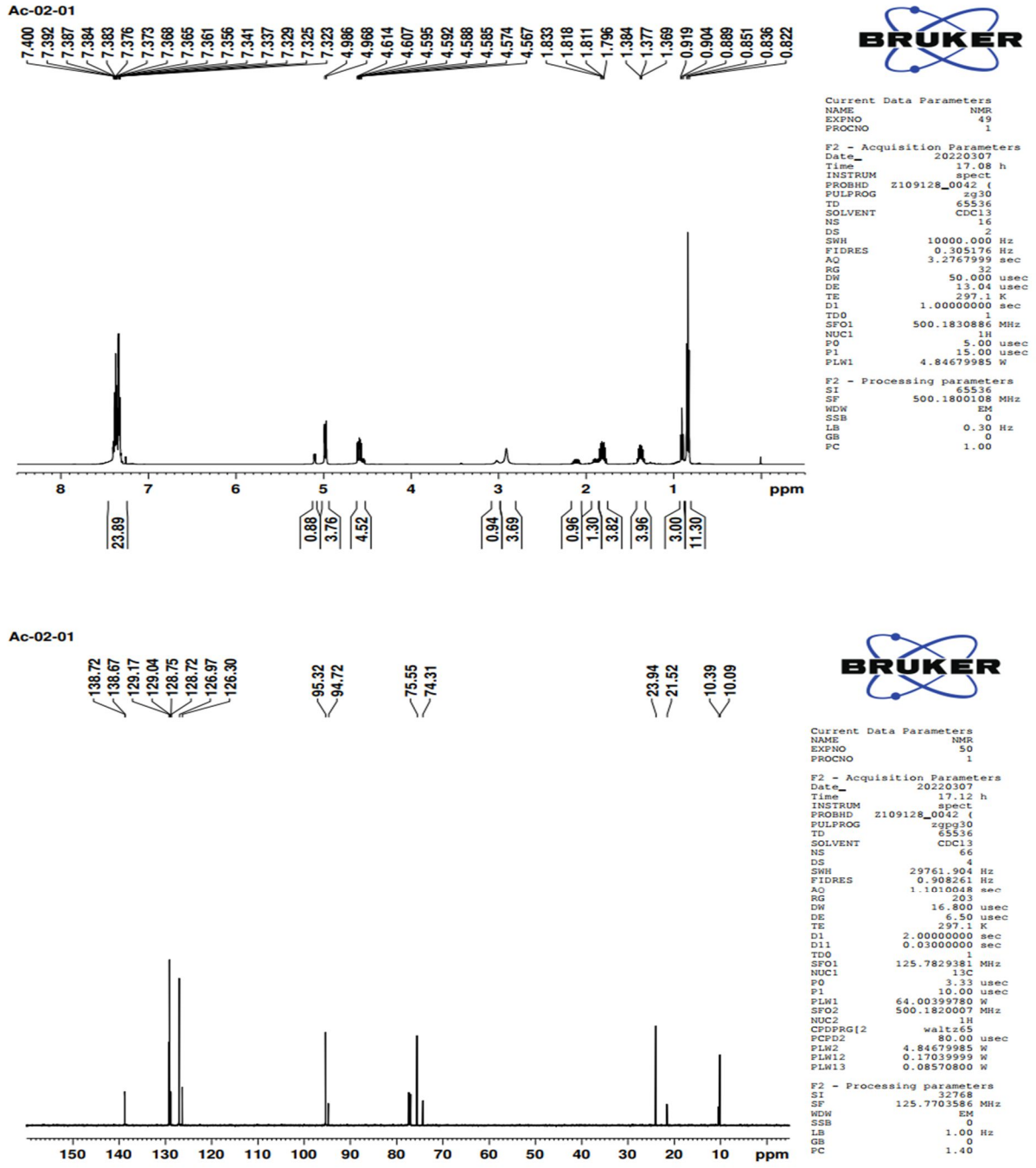
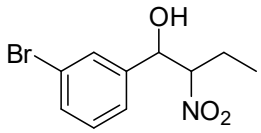


Figure 3.21: ^{1}H NMR and ^{13}C NMR spectra of 2-nitro-1-phenylbutan-1-ol.

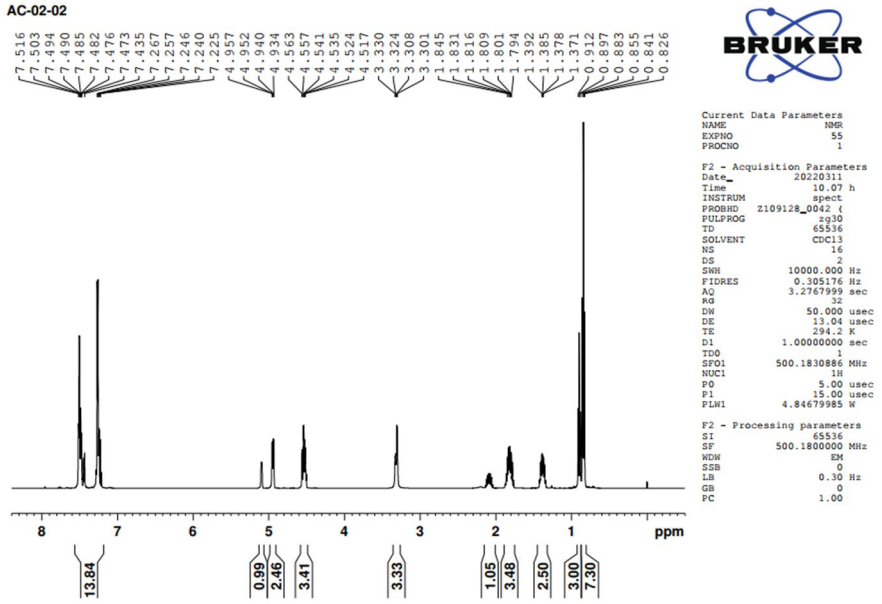
2. 1-(3-Bromophenyl)-2-nitrobutan-1-ol



^{1}H NMR (500 MHz, $CDCl_3$) δ 7.56 – 7.18 (m, 8H), 5.10 (dd, *J* = 5.1, 2.7 Hz, 1H), 4.95 (dd, *J* = 9.1, 3.3 Hz, 1H), 4.61 – 4.46 (m, 2H), 3.33 (s, 1H), 3.30 (s, 1H), 2.09 (m, 1H), 1.91 – 1.71 (m, 2H), 1.38 (m, 1H), 0.90 (t, *J* = 7.4 Hz, 3H), 0.84 (t, *J* = 7.4 Hz, 3H).

^{13}C NMR (101 MHz, $CDCl_3$) δ 140.88, 132.17, 131.73, 130.58, 130.30, 129.94, 129.32, 125.63, 124.96, 122.94, 122.74, 94.95, 94.34, 74.71, 73.44, 23.82, 21.30, 10.32, 10.02.

Diastereomeric ratio 1:2.43 (*anti*: *syn*)



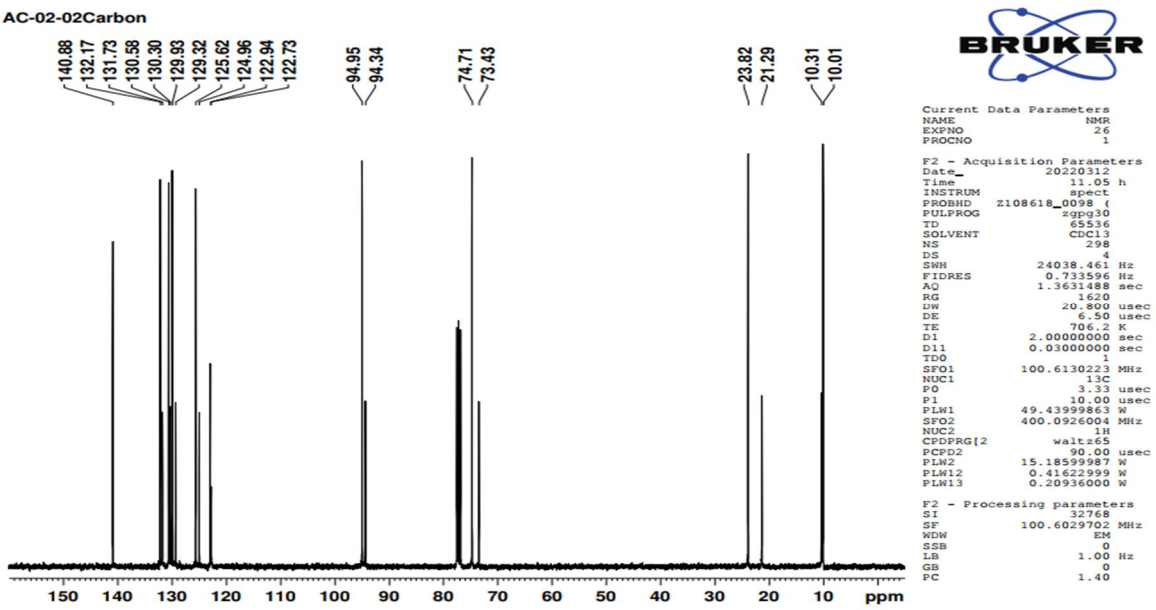
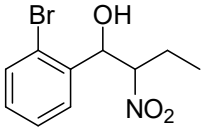


Figure 3.22: ^{1}H NMR and ^{13}C NMR spectra of 1-(3-bromophenyl)-2-nitrobutan-1-ol.

3. 1-(2-Bromophenyl)-2-nitrobutan-1-ol



^{1}H NMR (500 MHz, $CDCl_3$) δ 7.67 – 7.13 (m, 8H), 5.62 – 5.47 (m, 2H), 4.72 (m, 2H), 3.29 (d, J = 3.3 Hz, 1H), 3.14 (d, J = 5.2 Hz, 1H), 2.19 (m, 1H), 2.09 (m, 1H), 1.66 (m, 1H), 1.54 (m, 1H), 0.89 (dt, J = 11.5, 7.3 Hz, 6H).

^{13}C NMR (101 MHz, $CDCl_3$) δ 138.04, 137.18, 133.16, 133.08, 130.36, 130.07, 128.56, 128.44, 128.35, 127.87, 122.85, 121.84, 94.87, 91.48, 73.30, 72.97, 23.56, 19.62, 10.54, 10.37.

Diastereomeric ratio 1:2.41 (*anti*: *syn*)

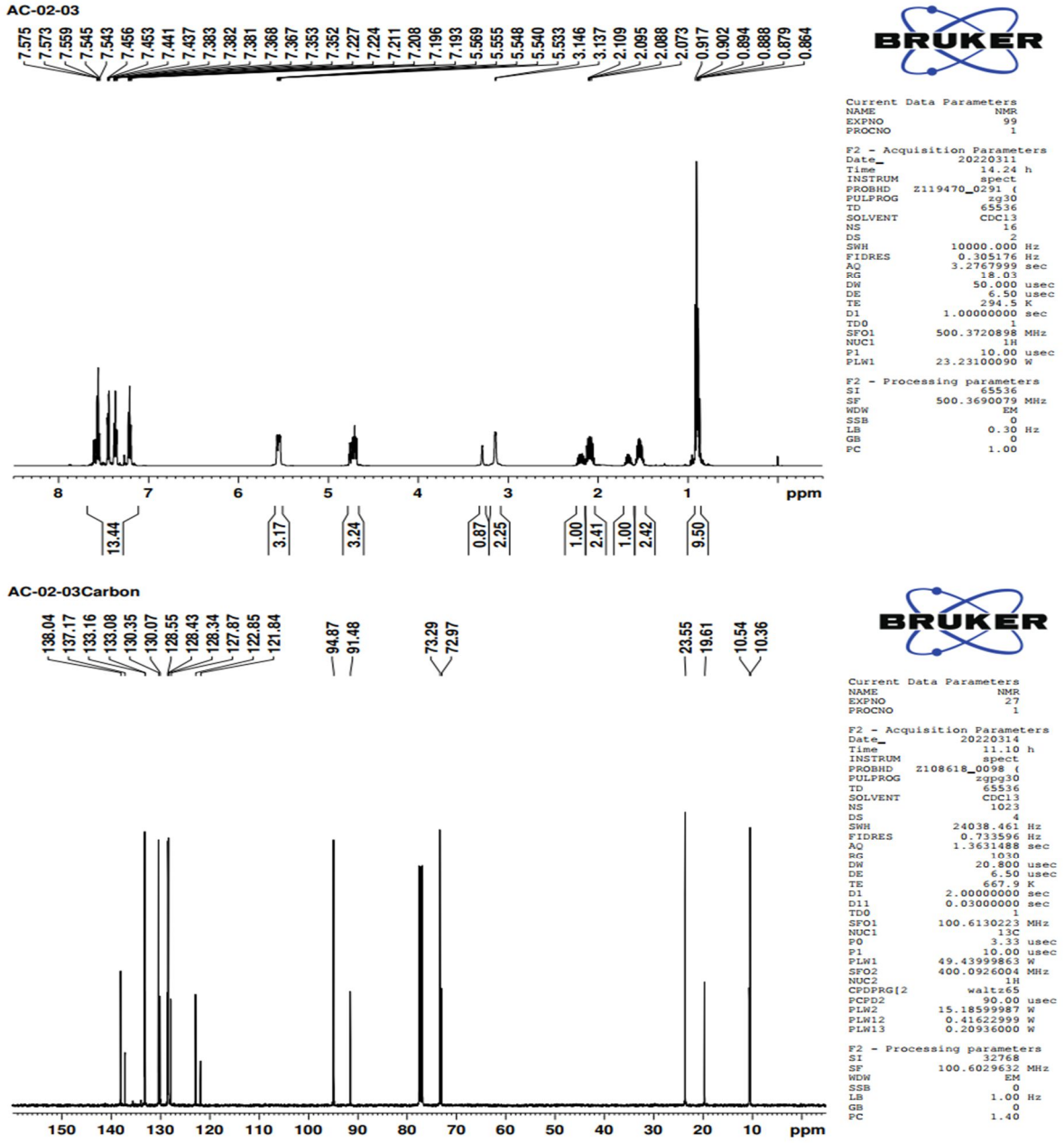
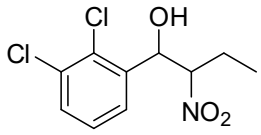


Figure 3.23: ^{1}H NMR and ^{13}C NMR spectra of 1-(2-bromophenyl)-2-nitrobutan-1-ol

4. 1-(2,3-Dichlorophenyl)-2-nitrobutan-1-ol



^{1}H NMR (500 MHz, $CDCl_3$) δ 7.60 – 7.19 (m, 6H), 5.80 – 5.53 (m, 2H), 4.88 – 4.60 (m, 2H), 3.45 (d, *J* = 3.6 Hz, 1H), 3.40 (d, *J* = 5.4 Hz, 1H), 2.13 (m, 2H), 1.57 (m, 2H), 0.89 (dt, *J* = 15.7, 7.4 Hz, 6H).

^{13}C NMR (101 MHz, $CDCl_3$) δ 138.81, 138.09, 133.45, 130.85, 130.73, 130.42, 129.96, 128.12, 127.74, 126.43, 126.33, 94.51, 91.16, 71.44, 71.33, 23.45, 19.64, 10.48, 10.28.

Diastereomeric ratio 1:2.13 (*anti*: *syn*)

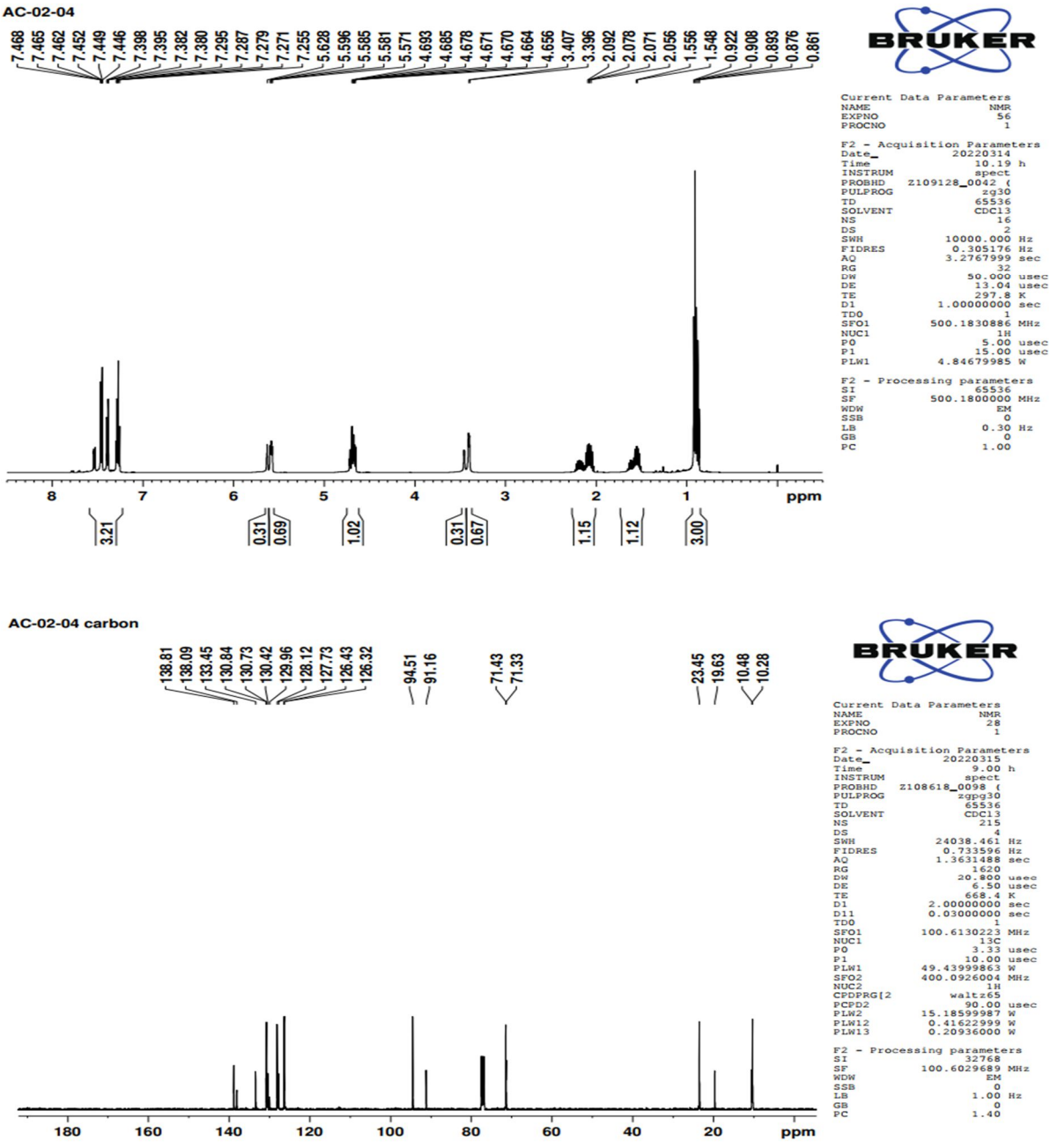
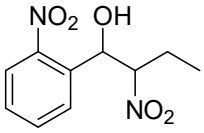


Figure 3.24: ^{1}H NMR and ^{13}C NMR spectra of 1-(2,3-dichlorophenyl)-2-nitrobutan-1-ol

5. 1-(2-Nitrorophenyl)-2-nitrobutan-1-ol [20]



^{1}H NMR (500 MHz, $CDCl_3$) δ 8.07 – 7.45 (m, 8H), 5.8 (d, *J* = 3.6 Hz, 1H), 5.68 (d, *J* = 6.5 Hz, 1H), 4.79 (m, 2H), 3.58 (s, 2H), 2.18 (m, 1H), 2.09 (m, 1H), 1.79 (m, 1H), 1.63 (m, 1H), 0.90 (dt, *J* = 15.9, 7.4 Hz, 6H).

^{13}C NMR (101 MHz, $CDCl_3$) δ 147.97, 147.39, 134.30, 134.10, 134.01, 129.72, 129.62, 129.33, 128.81, 125.26, 124.99, 94.32, 92.11, 69.90, 69.71, 23.88, 20.73, 10.41, 10.27.

Diastereomeric ratio 1:2.17 (*anti*: *syn*)

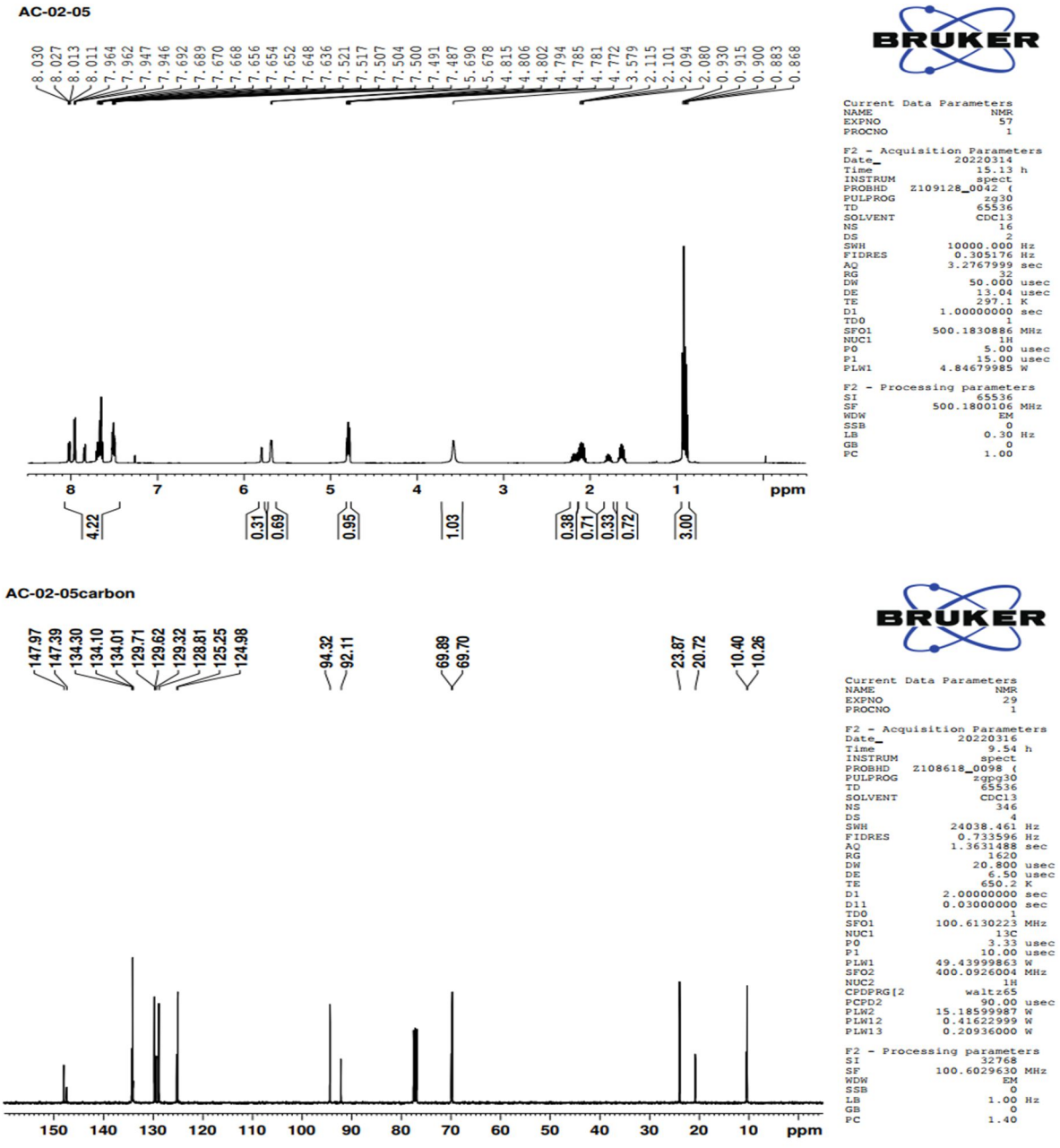
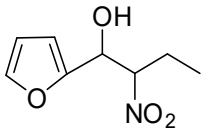


Figure 3.25: ^{1}H NMR and ^{13}C NMR spectra of 1-(2-nitrophenyl)-2-nitrobutan-1-ol

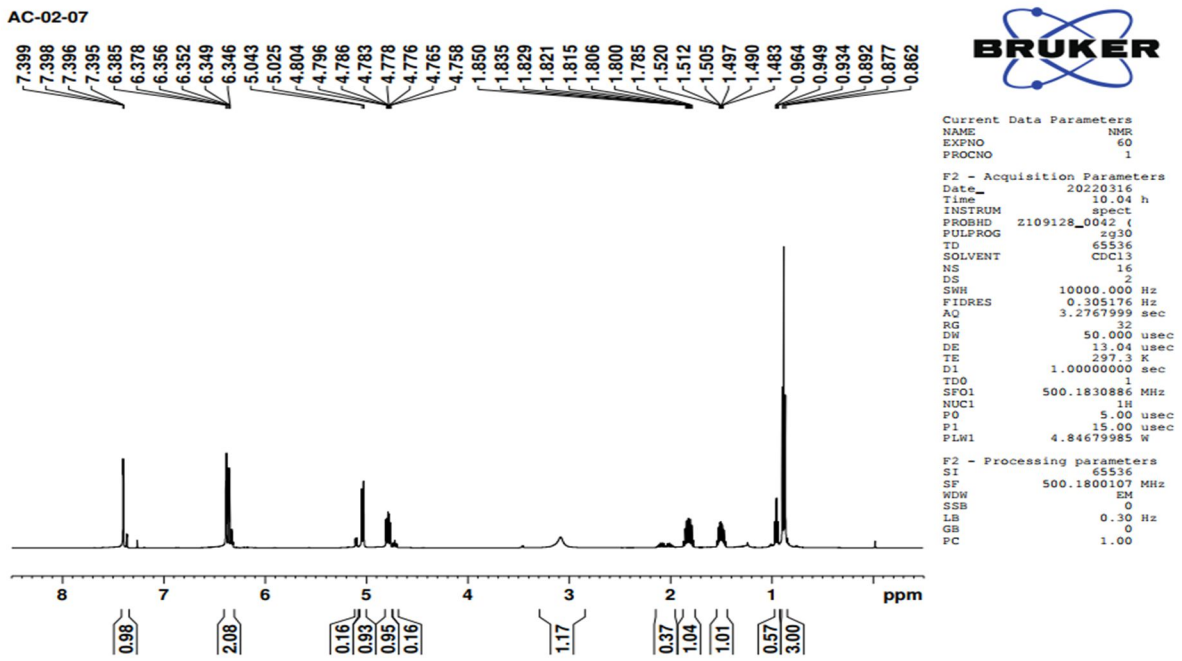
6. 1-(Furan-2-yl)-2-nitrobutan-1-ol [19]



^{1}H NMR (500 MHz, $CDCl_3$) δ 7.38 (ddd, *J* = 17.3, 1.9, 0.9 Hz, 2H), 6.53 – 6.29 (m, 4H), 5.10 (d, *J* = 6.1 Hz, 1H), 5.03 (d, *J* = 9.0 Hz, 1H), 4.78 (m, 1H), 4.72 (m, 1H), 3.08 (s, 2H), 2.18 – 1.94 (m, 2H), 1.82 (m, 1H), 1.49 (m, 1H), 0.95 (t, *J* = 7.4 Hz, 3H), 0.88 (t, *J* = 7.4 Hz, 3H).

^{13}C NMR (101 MHz, $CDCl_3$) δ 151.25, 150.95, 143.33, 142.97, 110.67, 110.58, 109.39, 108.44, 92.93, 91.92, 68.62, 68.49, 23.91, 22.45, 10.26, 9.98.

Diastereomeric ratio 1:5.23 (*anti*: *syn*)



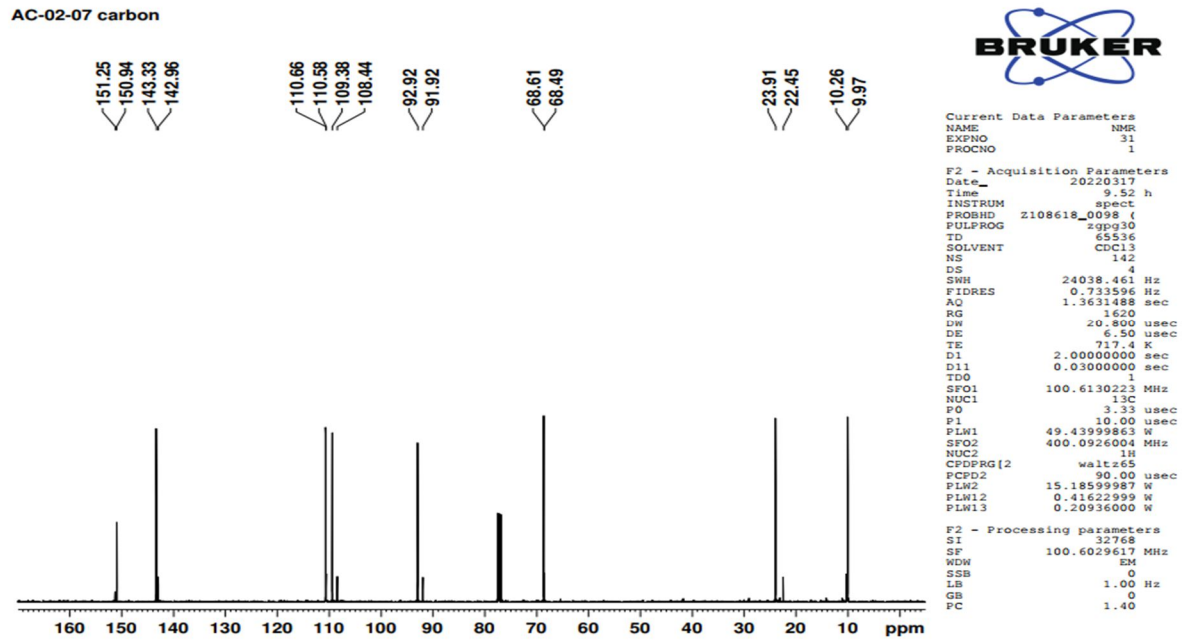
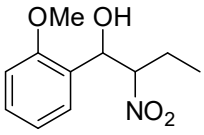


Figure 3.26: ^{1}H NMR and ^{13}C NMR spectra of 1-(furan-2-yl)-2-nitrobutan-1-ol.

7. 1-(2-Methoxyphenyl)-2-nitrobutan-1-ol[14]



^{1}H NMR (500 MHz, $CDCl_3$) δ 7.36 – 7.20 (m, 4H), 7.00 – 6.85 (m, 4H), 5.24 – 5.17 (m, 1H), 5.17 – 5.07 (m, 1H), 4.79 (m, 2H), 3.85 (s, 3H), 3.84 (s, 3H), 3.54 (s, 2H), 2.10 (m,1H), 1.97 – 1.78 (m, 2H), 1.47 – 1.32 (m, 1H), 0.89 (t, J = 7.5 Hz, 3H), 0.83 (t, J = 7.4 Hz, 3H).

^{13}C NMR (126 MHz, $CDCl_3$) δ 156.68, 156.14, 129.95, 129.58, 128.72, 128.13, 126.20, 126.09, 121.08, 120.82, 110.94, 110.62, 94.51, 92.51, 72.92, 71.92, 55.37, 55.35, 23.93, 21.53, 10.38, 10.09.

Diastereomeric ratio 1:1.38 (*anti*: *syn*)

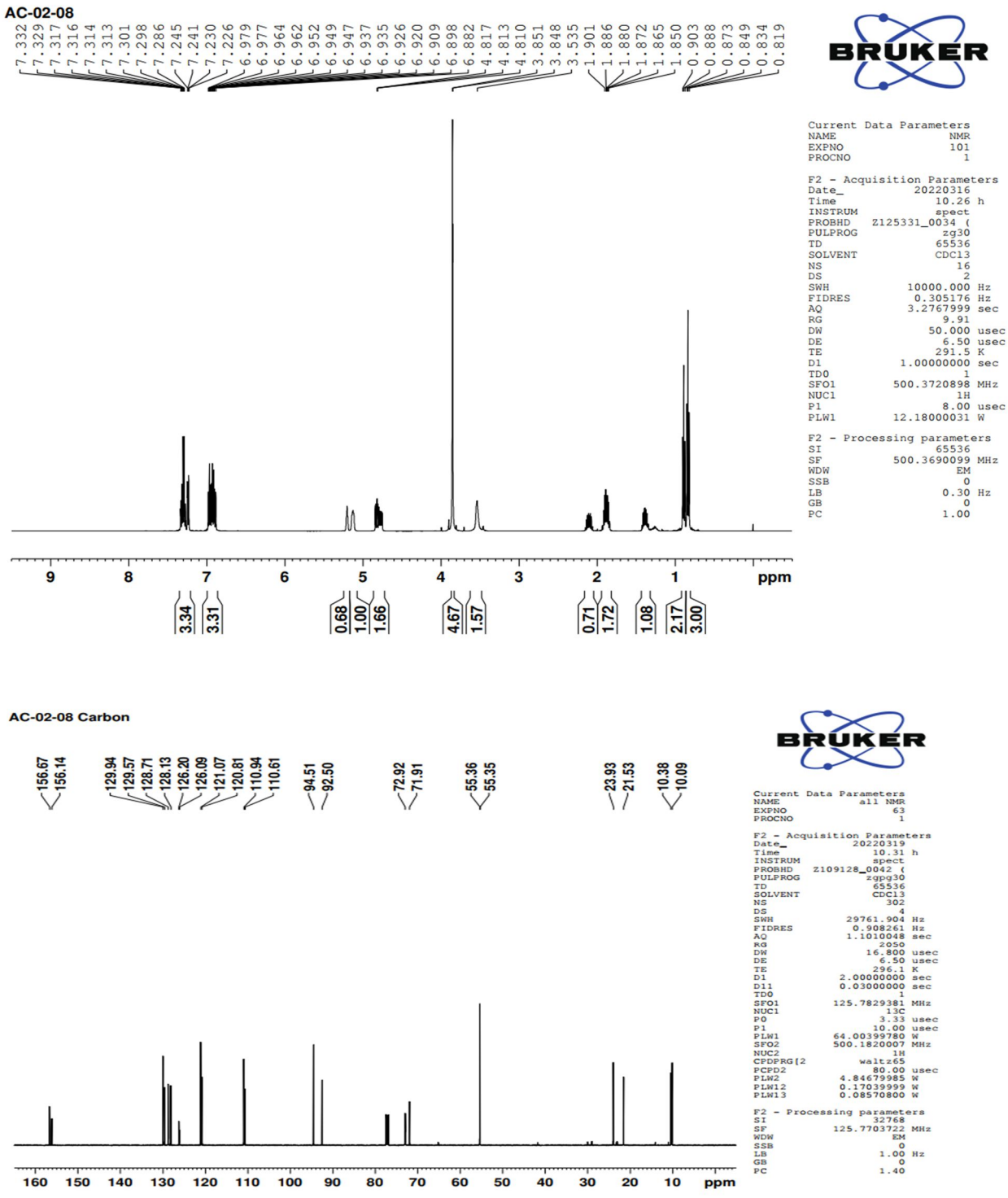
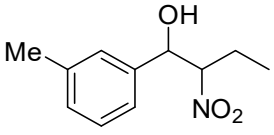


Figure 3.27: ^{1}H NMR and ^{13}C NMR spectra of 1-(2-methoxyphenyl)-2-nitrobutan-1-ol.

8. 1-(3-Methylphenyl)-2-nitrobutan-1-ol



^{1}H NMR (500 MHz, $CDCl_3$) δ 7.40 – 7.09 (m, 8H), 5.05 (d, *J* = 5.4 Hz, 1H), 4.94 (d, *J* = 9.2 Hz, 1H), 4.69 – 4.52 (m, 2H), 3.13 (s, 1H), 3.04 (s, 1H), 2.39 (s, 3H), 2.36 (s, 3H), 2.12 (m, 1H), 1.97 – 1.75 (m, 2H), 1.39 (m, 1H), 0.92 (t, *J* = 7.4 Hz, 3H), 0.85 (t, *J* = 7.4 Hz, 3H).

^{13}C NMR (101 MHz, $CDCl_3$) δ 138.74, 138.62, 138.35, 129.80, 129.38, 128.79, 128.53, 127.51, 126.90, 124.03, 123.32, 95.29, 94.65, 75.50, 74.28, 23.89, 21.55, 21.34, 10.29, 10.00.

Diastereomeric ratio 1:2.36 (*anti*: *syn*)

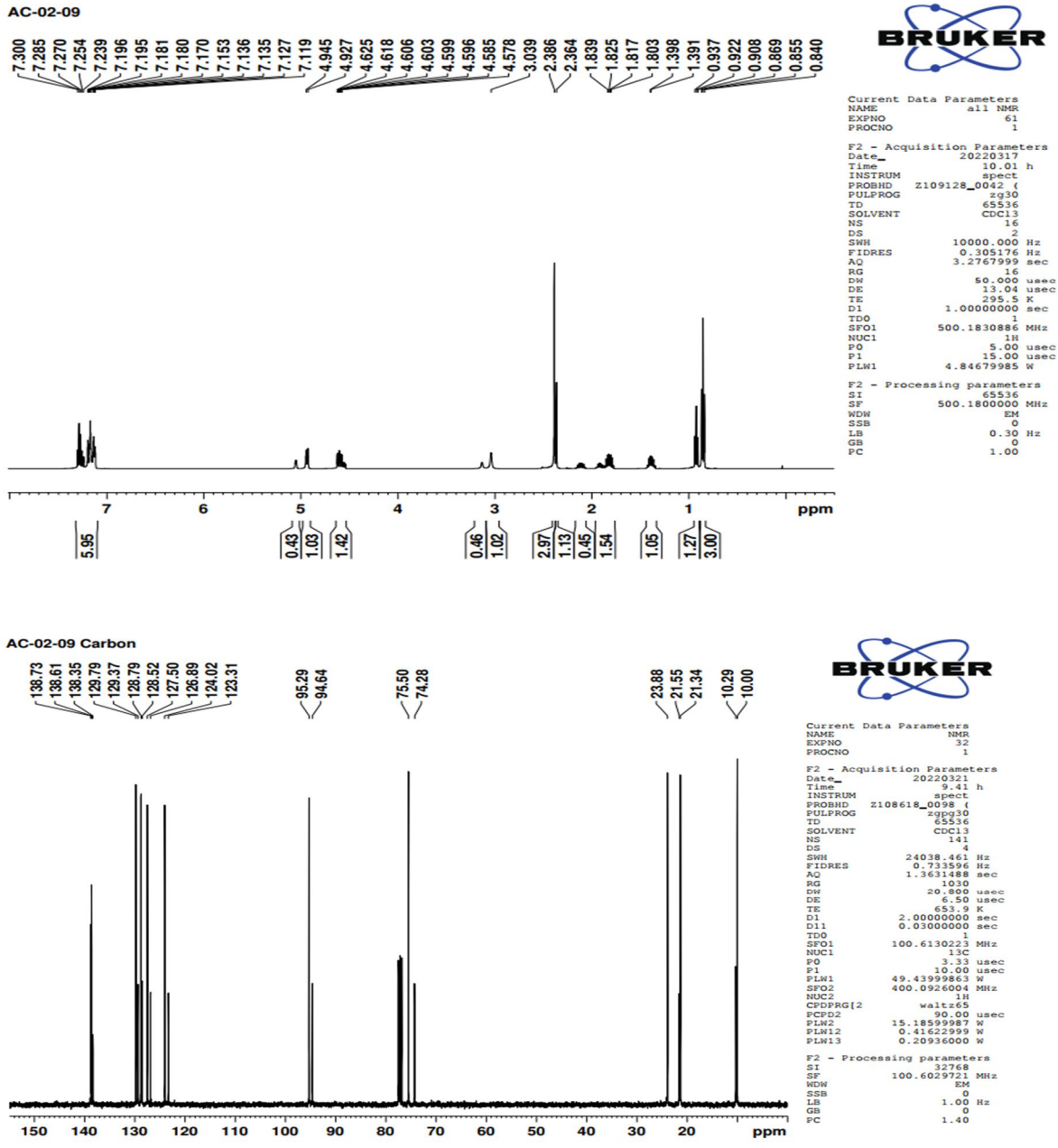
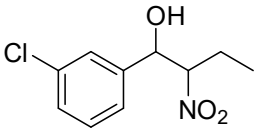


Figure 3.28: ^{1}H NMR and ^{13}C NMR spectra of 1-(3-methylphenyl)-2-nitrobutan-1-ol.

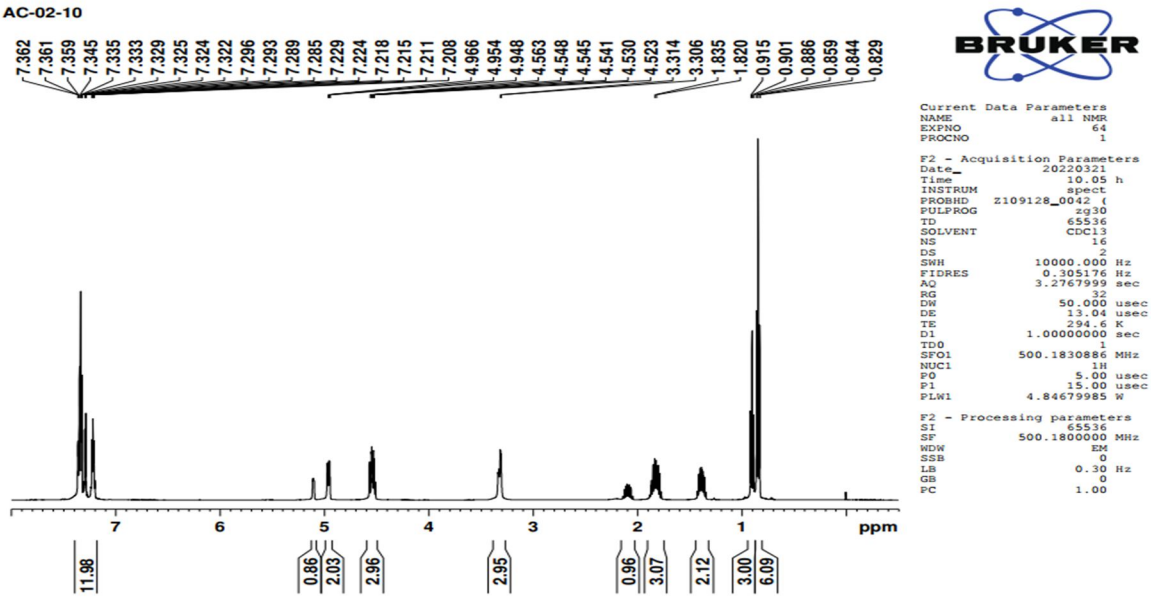
9. 1-(3-Chlorophenyl)-2-nitrobutan-1-ol



^{1}H NMR (500 MHz, $CDCl_3$) δ 7.45 – 7.16 (m, 8H), 5.10 (dd, *J* = 5.2, 2.6 Hz, 1H), 4.96 (dd, *J* = 9.1, 3.1 Hz, 1H), 4.65 – 4.47 (m, 2H), 3.33 (d, *J* = 3.5 Hz, 1H), 3.31 (d, *J* = 4.3 Hz, 1H), 2.09 (m, 1H), 1.94 – 1.73 (m, 2H), 1.38 (m, 1H), 0.90 (t, *J* = 7.4 Hz, 3H), 0.84 (t, *J* = 7.4 Hz, 3H).

^{13}C NMR (101 MHz, $CDCl_3$) δ 140.67, 134.82, 134.60, 130.33, 130.04, 129.26, 128.82, 127.06, 126.46, 125.17, 124.50, 94.99, 94.39, 74.80, 73.55, 23.84, 21.33, 10.31, 10.01.

Diastereomeric ratio 1:2.01 (*anti*: *syn*)



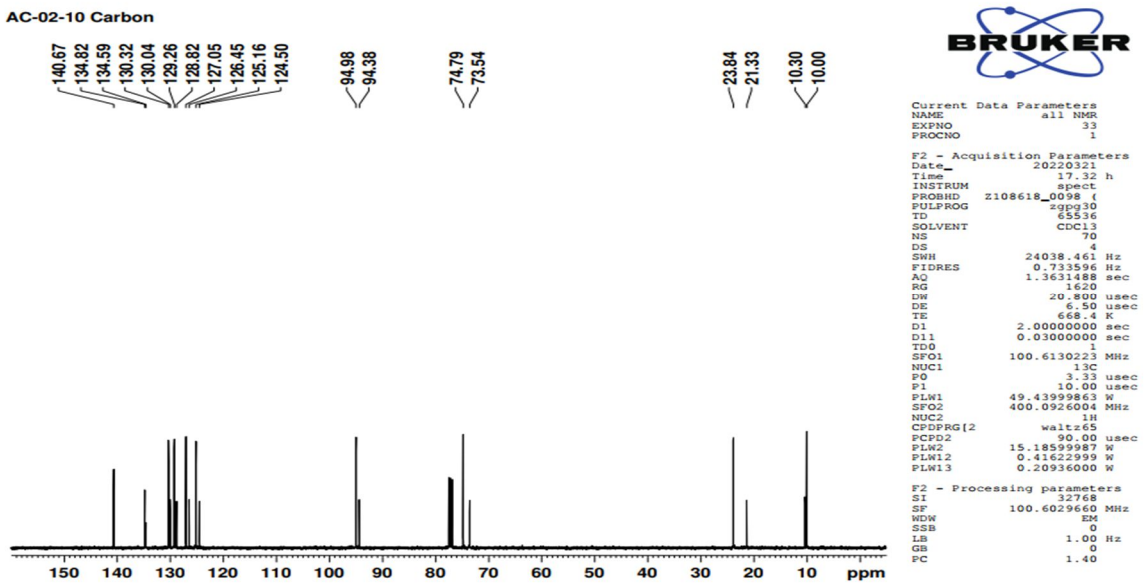
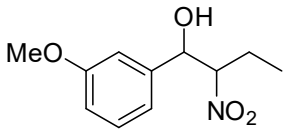


Figure 3.29: ^{1}H NMR and ^{13}C NMR spectra of 1-(3-chlorophenyl)-2-nitrobutan-1-ol.

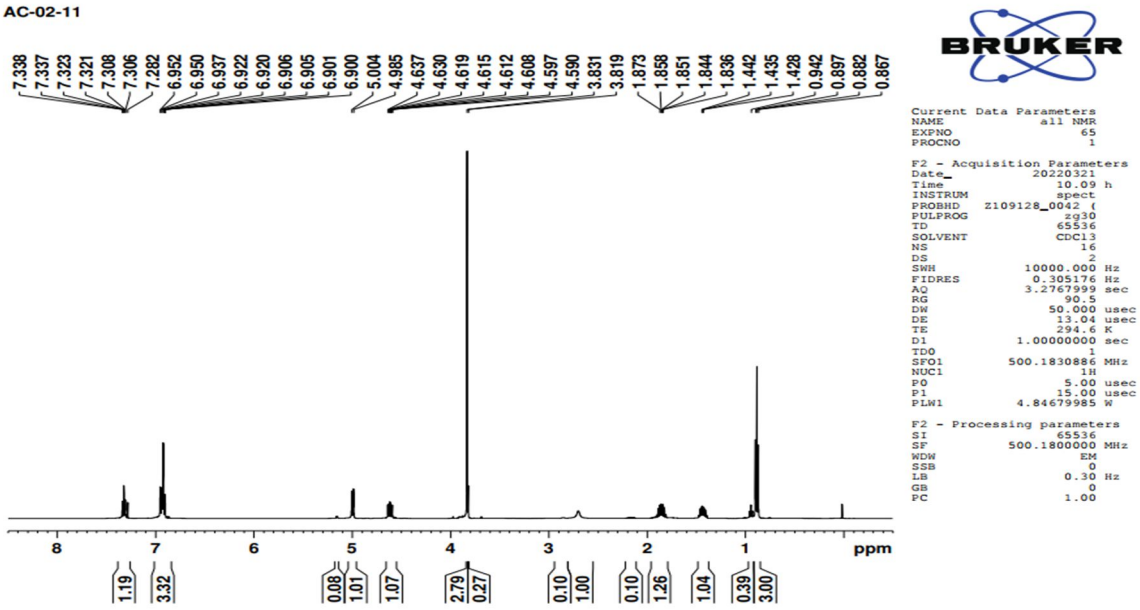
10. 1-(3-Methoxyphenyl)-2-nitrobutan-1-ol[21]



^{1}H NMR (500 MHz, $CDCl_3$) δ 7.45 – 6.85 (m, 8H), 5.15 (d, *J* = 4.9 Hz, 1H), 4.99 (d, *J* = 9.1 Hz, 1H), 4.73 – 4.54 (m, 2H), 3.83 (s, 3H), 3.82 (s, 3H), 2.85 (s, 1H), 2.70 (s, 1H), 2.16 (m, 1H), 1.85 (m, 2H), 1.43 (m, 1H), 0.94 (t, *J* = 7.4 Hz, 3H), 0.88 (t, *J* = 7.4 Hz, 3H).

^{13}C NMR (101 MHz, $CDCl_3$) δ 160.13, 140.34, 130.21, 119.28, 114.69, 112.44, 95.31, 75.61, 55.45, 24.06, 10.20.

Diastereomeric ratio 1:7.70 (*anti*: *syn*)



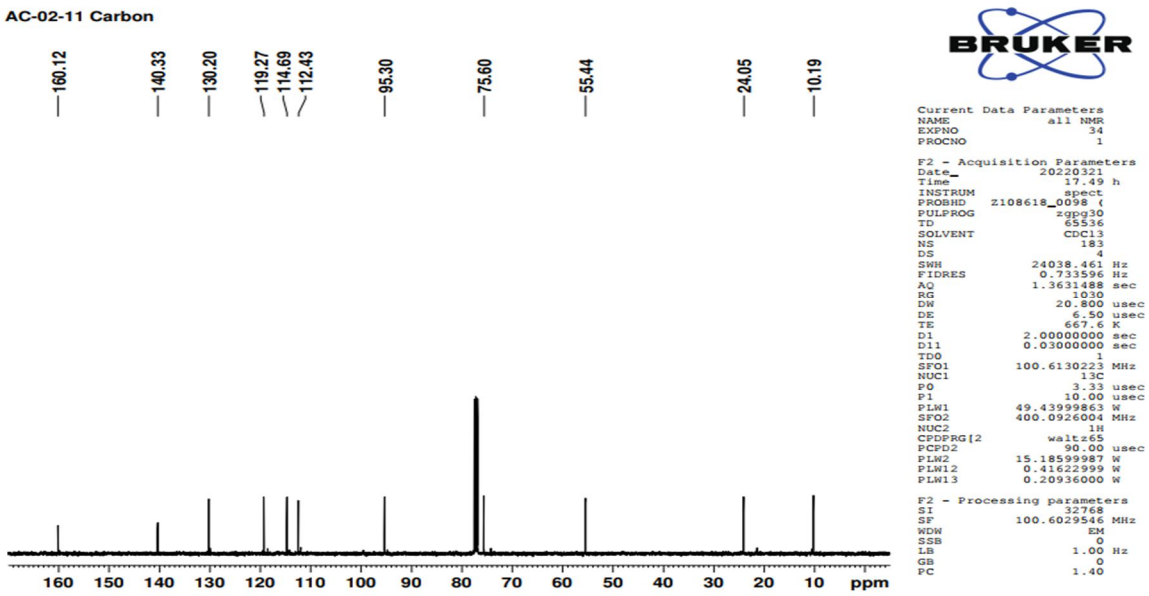
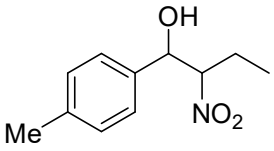


Figure 3.30: ^{1}H NMR and ^{13}C NMR spectra of 1-(3-methoxyphenyl)-2-nitrobutan-1-ol.

11. 1-(4-Methylphenyl)-2-nitrobutan-1-ol[19]



^{1}H NMR (500 MHz, $CDCl_3$) δ 7.27 – 7.14 (m, 8H), 5.04 (d, J = 5.6 Hz, 1H), 4.95 (d, J = 9.2 Hz, 1H), 4.64 – 4.50 (m, 2H), 3.12 (s, 1H), 3.03 (s, 1H), 2.38 (s, 3H), 2.35 (s, 3H), 2.10 (m, 1H), 1.93 (m, 1H), 1.81 (m, 1H), 1.38 (m, 1H), 0.92 (t, J = 7.4 Hz, 3H), 0.85 (t, J = 7.4 Hz, 3H).

^{13}C NMR (101 MHz, $CDCl_3$) δ 139.09, 138.57, 135.77, 135.72, 129.71, 129.43, 126.88, 126.23, 95.39, 94.80, 75.42, 74.27, 23.98, 21.71, 21.22, 21.19, 10.40, 10.10.

Diastereomeric ratio 1:2.34 (*anti*: *syn*)

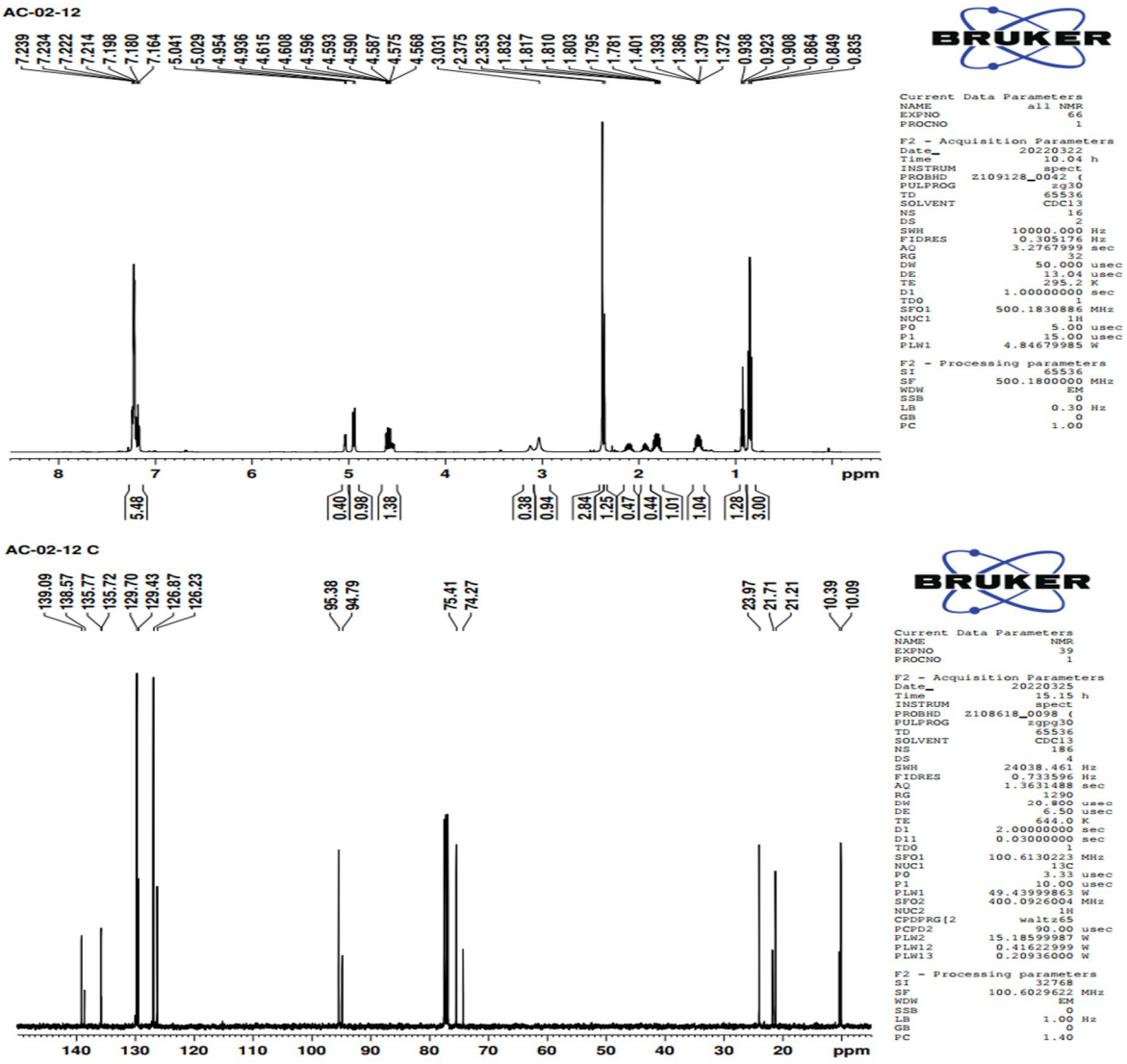
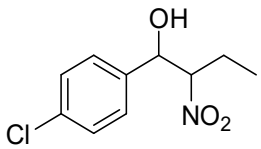


Figure 3.31: ^{1}H NMR and ^{13}C NMR spectra of 1-(4-methylphenyl)-2-nitrobutan-1-ol.

12. 1-(4-Chlorophenyl)-2-nitrobutan-1-ol[14]



^{1}H NMR (500 MHz, $CDCl_3$) δ 7.41 – 7.21 (m, 8H), 5.08 (d, J = 5.3 Hz, 1H), 4.96 (d, J = 9.1 Hz, 1H), 4.59 – 4.46 (m, 2H), 3.33 (s, 2H), 2.08 (m, 1H), 1.91 – 1.72 (m, 2H), 1.36 (m, 1H), 0.90 (t, J = 7.4 Hz, 3H), 0.84 (t, J = 7.4 Hz, 3H).

^{13}C NMR (101 MHz, $CDCl_3$) δ 137.17, 134.89, 134.44, 129.16, 128.87, 128.34, 127.73, 95.11, 94.50, 74.76, 73.62, 23.84, 21.53, 10.32, 10.02.

Diastereomeric ratio 1:3.47 (*anti*: *syn*)

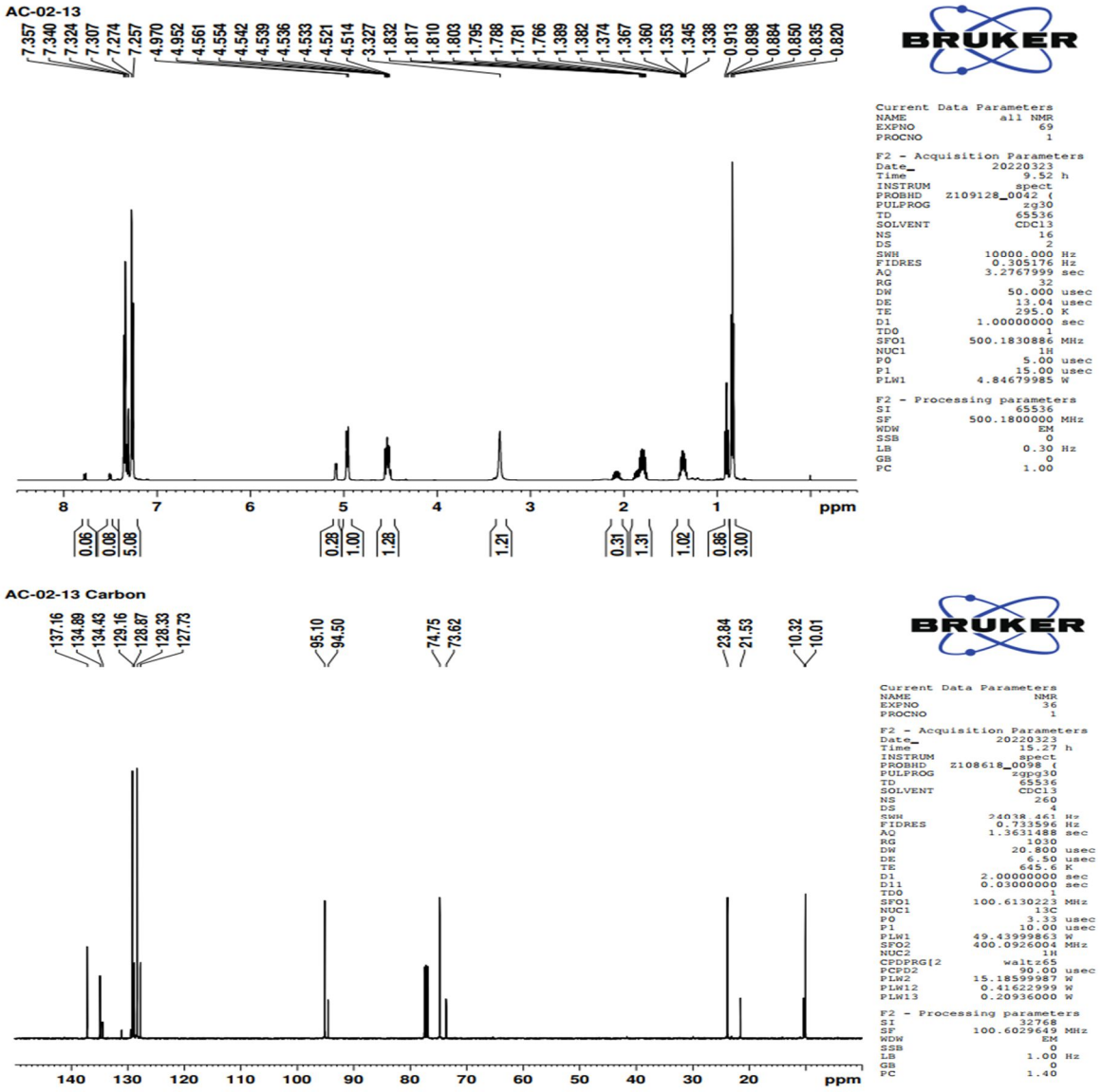
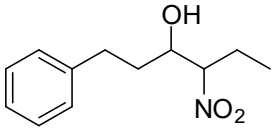


Figure 3.32: ^{1}H NMR and ^{13}C NMR spectra of 1-(4-chlorophenyl)-2-nitrobutan-1-ol.

13. 4-Nitro-1-phenylhexan-3-ol[14]



^{1}H NMR (500 MHz, $CDCl_3$) δ 7.40 – 7.29 (m, 4H), 7.27 – 7.18 (m, 6H), 4.41 (m, , 2H), 4.05 (m, 1H), 3.92 (m, 1H), 2.91 (m, 2H), 2.74 (m, 2H), 2.52 (s, 1H), 2.42 (s, 1H), 2.09 (m, 2H), 1.94 – 1.72 (m, 6H), 0.99 (q, J = 7.4 Hz, 6H).

^{13}C NMR (101 MHz, $CDCl_3$) δ 140.87, 128.66, 128.48, 126.31, 94.40, 93.90, 71.40, 71.05, 35.25, 34.75, 31.84, 31.55, 23.95, 21.57, 10.57, 10.19.

Diastereomeric ratio 1:1.5 (*anti*: *syn*)

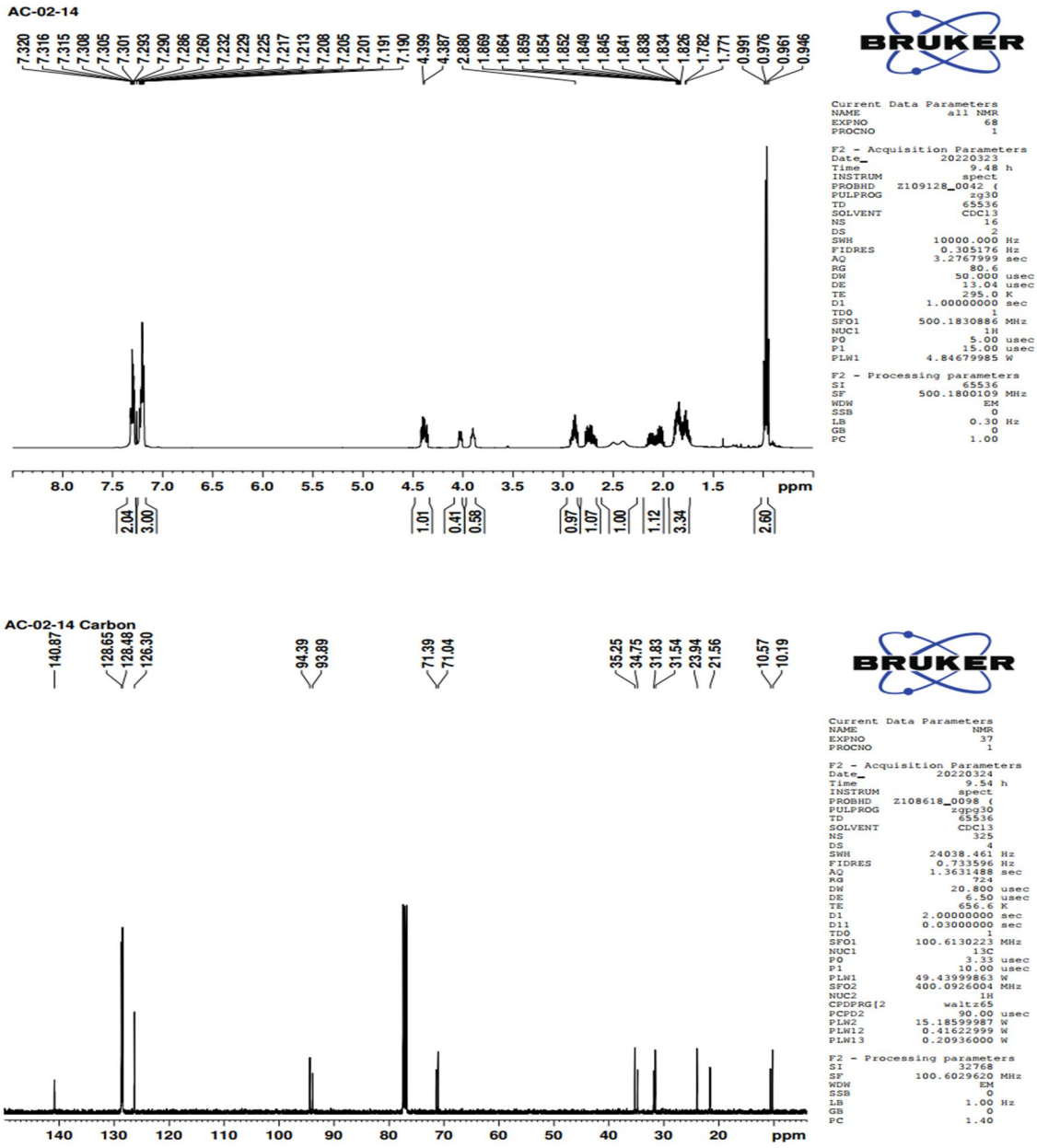
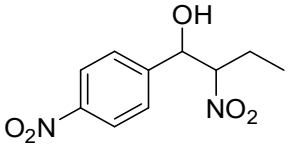


Figure 3.33: ^{1}H NMR and ^{13}C NMR spectra of 4-nitro-1-phenylhexan-3-ol.

14. 1-(4-Nitrophenyl)-2-nitrobutan-1-ol[14]



^{1}H NMR (500 MHz, $CDCl_3$) δ 8.31 – 8.19 (d, 4H), 7.65 – 7.54 (d, 4H), 5.32 (d, *J* = 4.6 Hz, 1H), 5.17 (d, *J* = 8.4 Hz, 1H), 4.70 – 4.52 (m, 2H), 3.18 (s, 1H), 3.10 (s, 1H), 2.16 (m, 1H), 2.00 – 1.65 (m, 2H), 1.46 (m, 1H), 0.97 – 0.87 (m, 6H).

^{13}C NMR (101 MHz, $CDCl_3$) δ 148.36, 148.08, 145.76, 145.70, 127.96, 127.38, 124.25, 124.03, 94.69, 94.24, 74.43, 73.36, 23.96, 21.32, 10.45, 10.18.

Diastereomeric ratio 1:4.94 (*anti*: *syn*)

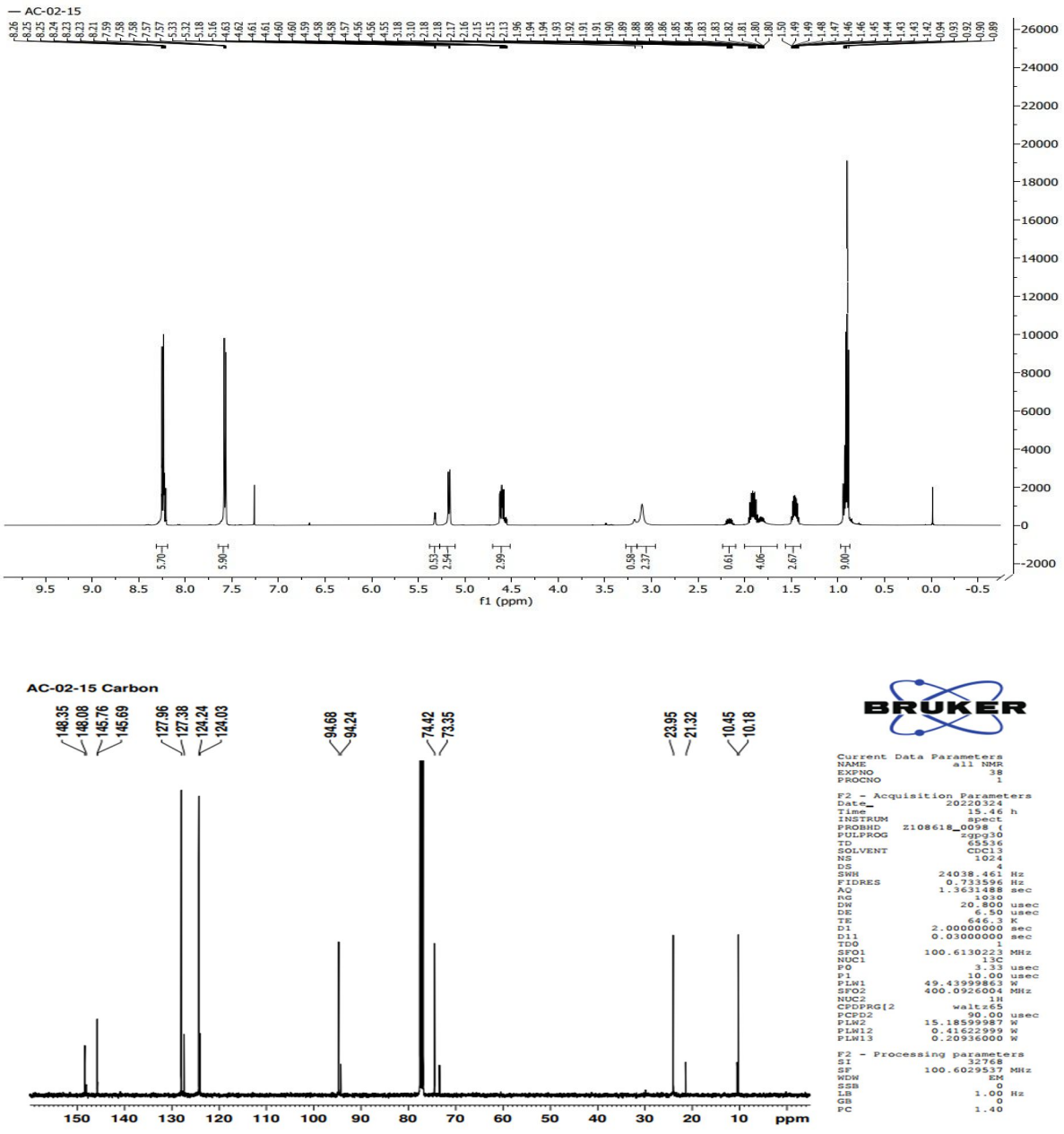


Figure 3.34: ^{1}H NMR and ^{13}C NMR spectra of 1-(4-nitrophenyl)-2-nitrobutan-1-ol.

3.4.5. Screening of *At*HNL mutant libraries towards the promiscuous nitroaldol reaction to synthesize 2-nitro-1-phenyl propanol (2-NPP)

WT *At*HNL is known for enantioselective synthesis of (*R*)-2-nitro 1-phenylethanol (2-NPE) via C–C bond formation between nitromethane and benzaldehyde.[9] However, when nitromethane was replaced by nitroethane as a nucleophile, WT *At*HNL failed to show stereoselectivity towards the diastereoselective synthesis of 2-NPP. To find an efficient mutant that can catalyze this promiscuous reaction, two in-house site saturation libraries of *At*HNL created at positions Y14 and F179 [8] were screened. The screening involved testing the crude cell lysates of the mutants towards stereoselective addition of nitroethane to benzaldehyde measured by a HPLC-based method. In the Y14 series, four mutants (Y14C, Y14D, Y14G, and Y14H) showed stereoselectivity towards the synthesis of (*1R,2S*)-2-NPP. The ee of the *anti*-isomeric products obtained by them were 96, 53, 36.6, and 54.5% respectively (Figure 3.35, Table 3.4). The % conversion of the product was also found to be highest, i.e., 58% with Y14C. Unlike the Y14 series, only one variant in the F179 series displayed stereoselectivity towards (*1R,2S*)-2-NPP synthesis. The F179L showed 46.3% enantiomeric excess with 28% conversion.

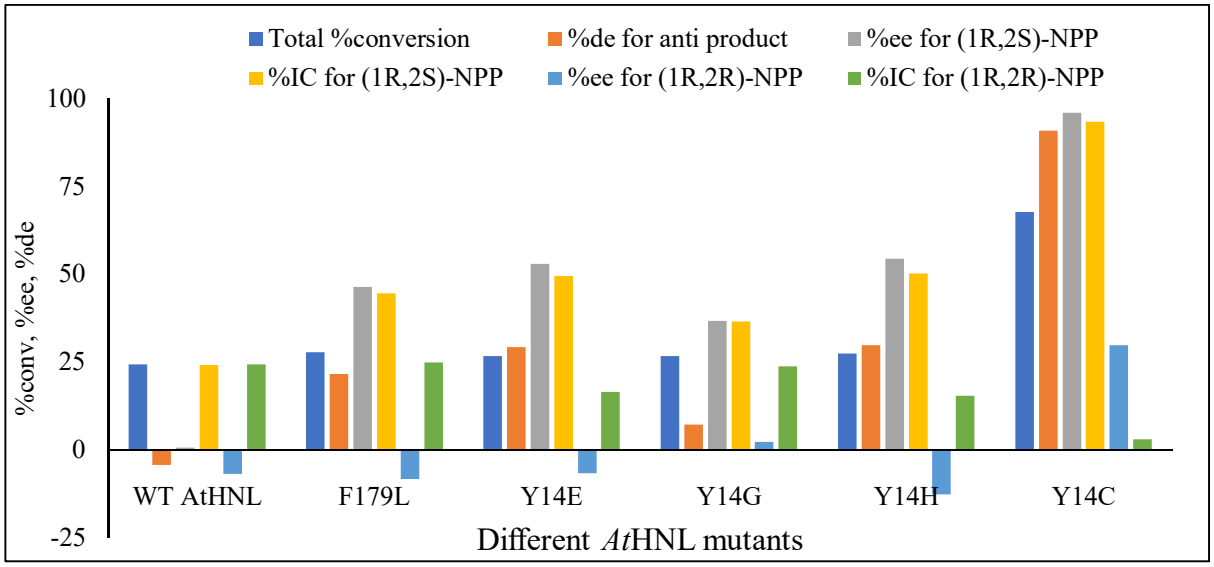


Figure 3.35: Summary of screening of F179L and *At*HNL-Y14 series towards the diastereoselective synthesis of 2-NPP.

Table 3.4: Screening of Y14C and F179L *At*HNL library for the diastereoselective synthesis of 2-NPP

S. No.	Enzyme (variant)	Total % conversion	% ee for (*1R,2S*)-2-NPP	% de for *anti* 2-NPP	Isomeric content for (1*R*,2*S*)-2-NPP
1	WT *At*HNL	24.35	0.50	–4.33	24.04
2	Y14A	23.6	1.8	–8.6	23.3
3	Y14C	58.3	95.9	90.8	93.4
4	Y14D	25.2	–0.3	–6.6	23.3
5	Y14E	26.7	52.9	29.2	49.4
6	Y14F	21.3	2.9	–9.4	23.3
7	Y14G	26.6	36.7	7.1	36.6
8	Y14H	27.4	54.5	29.8	50.1
9	Y14I	19.8	3.2	1.6	26.2
10	Y14K	23.8	3.3	–5.8	24.3

11	Y14L	23.6	0.5	–2.7	24.5
12	Y14M	25.5	0.7	–8.6	23.0
13	Y14N	27.3	3.5	–4.9	24.6
14	Y14P	25.9	–0.6	–6.4	23.2
15	Y14Q	24.7	1.7	–8.1	23.4
16	Y14R	25.9	0.6	–7.5	23.3
17	F179L	27.8	46.3	21.6	44.5
18	Y14S	18.0	–4.2	-8.0	22.0
19	Y14T	27.5	–2.5	–12.7	21.3
20	Y14V	18.9	–0.2	–0.6	24.8
21	Y14W	22.0	–1.9	–12.8	21.4
22	F179A	19.1	–4.9	–10.0	21.4
23	F179C	18.3	–2.2	–8.7	22.3
24	F179D	25.9	–4.7	–5.1	22.6
25	F179E	21.7	–17.1	–13.7	17.9
26	F179G	21.2	–1.3	–12.3	21.6
27	F179H	21.6	–5.4	–12.1	20.8
28	F179I	21.1	–2.6	–11.5	21.6
29	F179K	26.2	–4.6	–14.1	20.5
30	F179N	15.1	–2.1	–8.2	22.5
31	F179P	23.8	–3.1	–14.0	20.8
32	F179R	18.3	–5.0	–6.7	22.2
33	F179T	24.0	–1.3	–9.4	22.4
34	F179W	19.3	–4.9	–14.3	20.4
35	F179Y	22.5	–1.0	–12.2	21.7
36	F179Q	16.0	0.8	–6.8	23.5
37	F179V	18.3	–0.2	–10.4	22.3
38	F179M	21.1	0.4	–11.8	22.1
39	F179S	22.6	3.6	–13.3	22.5

3.4.6. Optimization of reaction conditions towards the stereoselective synthesis of (*1R,2S*)-2-NPP using *At*HNL-Y14C crude enzyme

Reaction parameters often play an important role in biocatalysis to obtain high stereoseletivity and yield of products. Biocatalytic Henry reaction requires optimization of key parameters such as buffer and pH, organic solvent, enzyme content, and substrate/nitroethane concentration, which could potentially influence the reaction results. A thorough optimization study was conducted to maximize the production of (*1R,2S*)-2-NPP. Five different reaction parameters as described below, were systematically varied to attain the optimum biocatalytic reaction conditions for this reaction. After optimizing these parameters, the desired product was synthesized in 81% conversion with 97% ee and 95% de.

3.4.6.1. Buffer and pH optimization: We began the optimization experiment by testing two different buffers, potassium phosphate buffer (KPB) and citrate phosphate buffer (CPB) in the pH range of 5.5 to 7. With increasing pH, the % ee of the *anti*-isomer of 2-NPP decreased in case of both buffers. The Y14C mutant could produce highest 58.5% conversion with 95.3%

ee and 90% de in CPB pH 5.5, and hence this buffer was chosen for further studies (Figure 3.36).

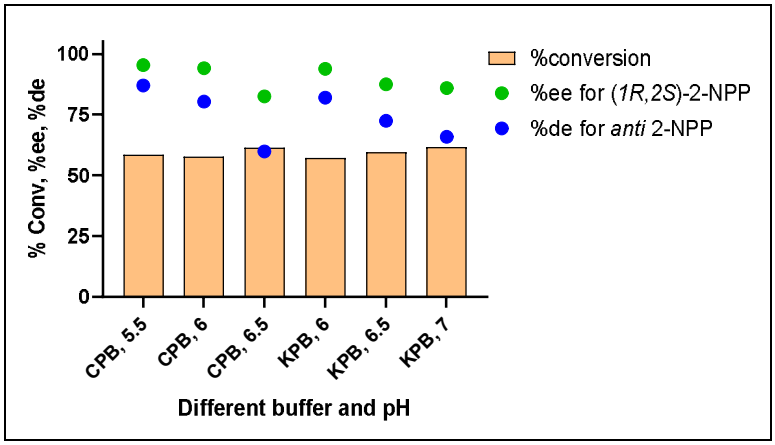


Figure 3.36: Effect of different pH and buffer in *At*HNL-Y14C catalyzed diastereoselective synthesis of 2-NPP.

3.4.6.2. Organic solvent optimization: HNL catalysed Henry reaction uses a biphasic reaction system consisting of nonpolar organic solvent and aqueous buffer.[9] We therefore selected five organic solvents based on an earlier study.[9] Among the five, TBME gave the best results in terms of % conversion and % ee in the synthesis of 2-NPP. TBME showed a 17% increment in conversion compared to NBA. (Figure 3.37)

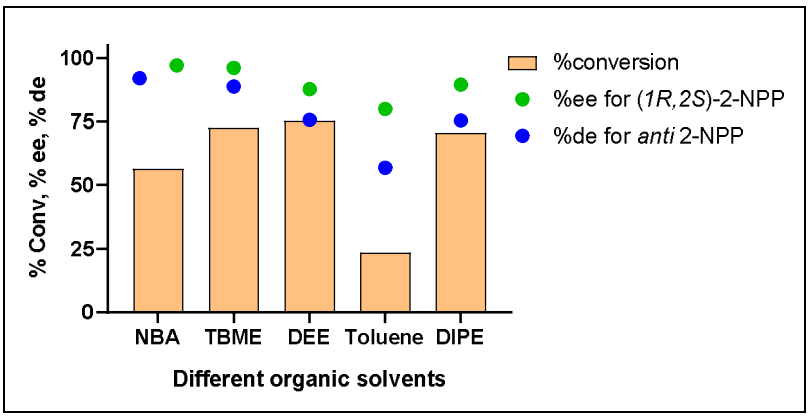


Figure 3.37: Effect of different organic solvents in a biphasic medium in *At*HNL-Y14C catalyzed diastereoselective synthesis of 2-NPP.

3.4.6.3. Nitroethane concentration optimization: Nitroethane functions as the co-substrate in this diastereoselective biocatalysis whose addition to the primary substrate benzaldehyde results in the synthesis of (*1R,2S*)-2-NPP. Optimisation of nitroethane concentration remains important to shift the reaction equilibrium right, to enhance the product formation. We varied nitroethane concentration from 0.75 to 2 M in the diastereoselective Henry reaction. *At*HNL-Y14C showed increased activity and enantioselectivity with increasing nitroethane concentration up to 1.75 M and slightly decreased in 2 M nitroethane. At 1.75 M, it showed 78% conversion with 95.4% ee and 94% de of 2-NPP. (Figure 3.38)

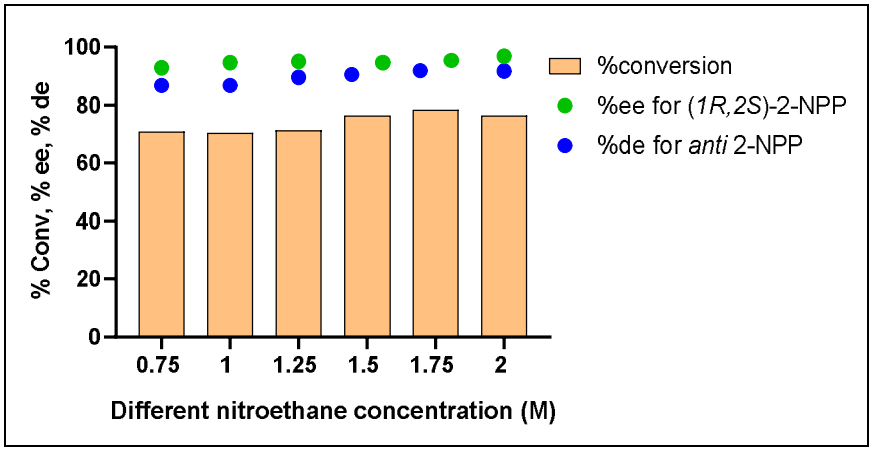


Figure 3.38: Optimization of *At*HNL-Y14C catalyzed diastereoselective synthesis of 2-NPP by varying nitroethane concentration.

3.4.6.4. Reaction buffer concentration optimization: CPB having found to be the suitable buffer to catalyse this diastereoselective reaction, its concentration was optimized. A range of buffer concentrations from 50 to 250 mM was tested for this experiment. The *At*HNL-Y14C showed a slight decrease in % conversion with the increasing buffer concentration, while % ee of the product increased. In case of 100 mM CPB, the highest (97.6%) enantiomeric excess was observed. At this concentration, the % conversion reached 77.8%. (Figure 3.39)

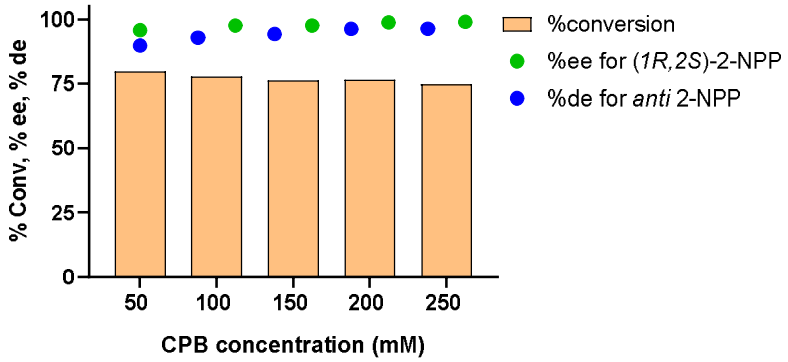


Figure 3.39: Optimization of *At*HNL-Y14C catalyzed diastereoselective synthesis of 2-NPP by varying CPB concentration.

3.4.6.5. Enzyme content optimization: To further improve the conversion of product, enzyme amount in the biocatalysis was optimized. An increase in enzyme amount has shown increasing activity up to 15 mg, beyond that the % conversion and % ee remained the same. (Figure 3.40) Hence 15 mg of crude *At*HNL-Y14C was selected to be used for further experiments.

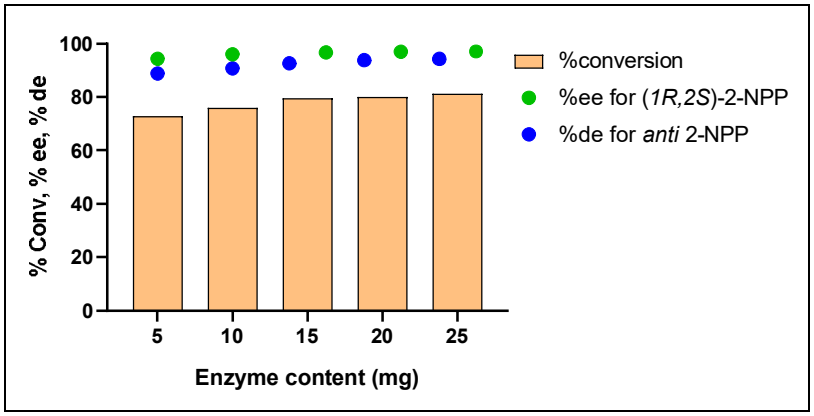


Figure 3.40: Effect of amount of enzyme on *At*HNL-Y14C catalyzed diastereoselective synthesis of 2-NPP.

The overall optimization studies have improved the % conversion of product from 57 to 80 while the % ee and % de improved to 97 and 93 respectively (Figure 3.41).

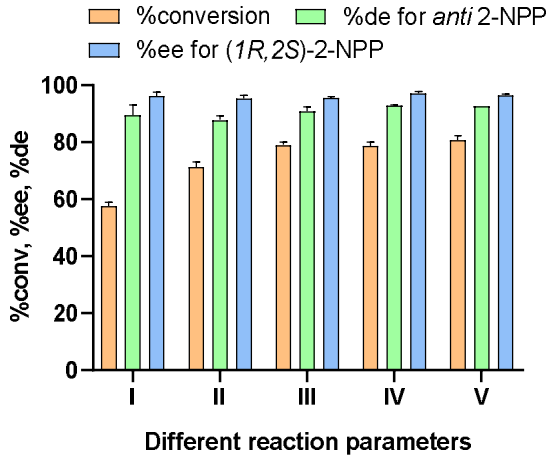


Figure 3.41: Summary of optimization of biocatalytic parameters of Y14C catalysed diastereoselective nitroaldol reaction using benzaldehyde and nitroethane as the substrate in synthesizing (*1R,2S*)-2-NPP. I: buffer system and pH, II: organic solvent, III: nitroethane concentration, IV: CPB concentration, V: enzyme content. The % conversion, % ee, and % de are mean of two data ± standard deviation.

3.4.7. SDS-PAGE of purified *At*HNL mutants selected from screening study

*At*HNL variants selected based on screening were purified as described in section **3.3.5.** above. They were characterized by SDS-PAGE (Figure 3.42). The purified protein fractions were analyzed by 12% SDS-PAGE and stained using Coomassie Brilliant Blue R-250. A clear band at ~28 kDa indicated the good expression and purity of the corresponding enzymes.

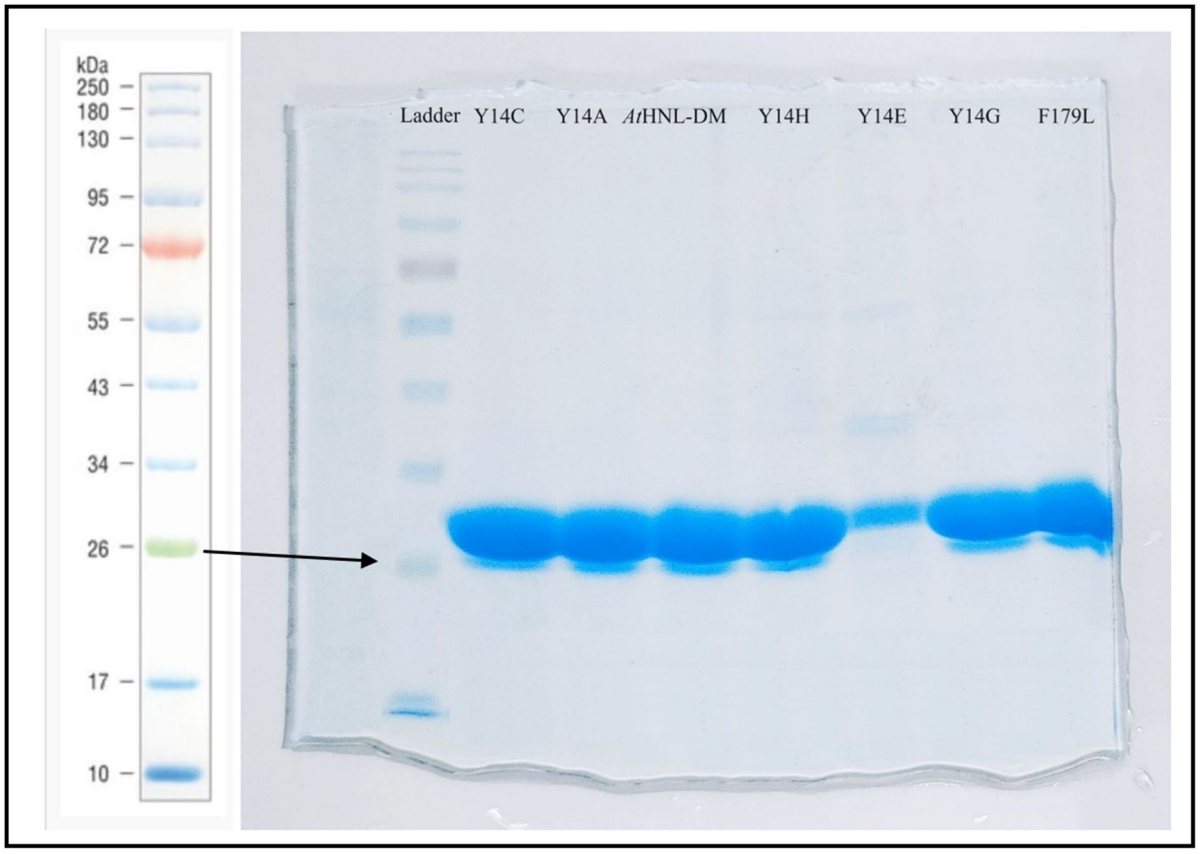
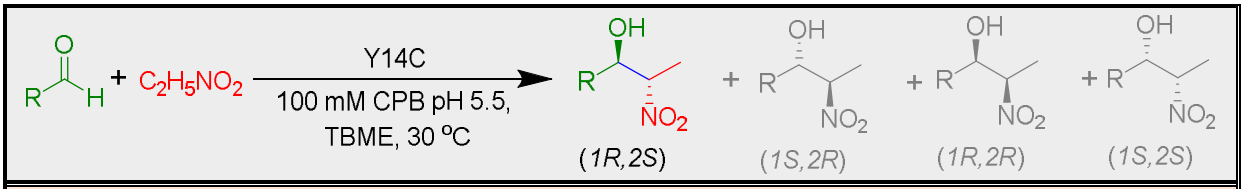


Figure 3.42: SDS-PAGE of purified *At*HNL variant proteins. Lane 1: ladder, 2: Y14C, 3: Y14A, 4: Y14H, 5: Y14E 6: Y14G and 7: F179L.

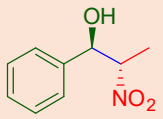
3.4.8. Substrate scope of *At*HNL-Y14C catalyzed diastereoselective synthesis of *anti* β-nitroalcohols using nitroethane as the co-substrate

Using the optimized biocatalytic reaction conditions, nineteen aromatic aldehydes having substituents at different positions of the aromatic ring were converted into their corresponding β-nitroalcohol diastereomers majorly producing the (*1R,2S*)-stereoisomer. This versatile substrate set contained both electron-donating and withdrawing groups, single and double substitutions, and substitutions were present at the *ortho*, *meta*, and *para* positions of the aromatic ring in different combinations (Figure 3.43). The Y14C displayed up to >99% conversion, >99% ee, and >99% de in the synthesis of *anti* diastereomers of β-nitroalcohols dominated by the (*1R,2S*) stereoisomer (Figure 3.43). None of these nineteen substrates used here except benzaldehyde were studied earlier by HNL catalyzed diastereoselective Henry reaction (Figure 3.43). Most of the substrates used here were transformed to their (*1R,2S*)-β-nitroalcohol product with high stereoselectivity. The Y14C exhibited higher preference towards *meta* and *ortho*-substituted aldehydes than *para*-substituted ones, irrespective of the electronic nature of the substitution attached to the benzene ring. For example, aldehydes having electron donating groups like 3-methoxy or 3-methylbenzaldehyde showed 74 and 73% conversion with 98.2 and 98.6% ee respectively, while 3-chloro benzaldehyde possessing electron withdrawing group also showed very good conversion of 93% with >99% ee. An almost similar phenomenon was encountered for *ortho* substituted aldehydes, except 2-methylbenzaldehyde where it showed poor conversion of only 38%. When these functional groups were placed in the *para* position for example with 4-chloro, 4-methyl, and 4-

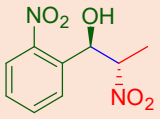
methoxybenzaldehyde, Y14C showed 35.5, 27.4, and no conversion respectively. Though excellent conversion of 93% was observed with 4-nitrobenzaldehyde, the % ee was very poor, only 17%. The mutant Y14C was also evaluated for diastereoselective Henry reaction with sterically challenged aldehydes. With 1-napthaldehyde, 3-benzyloxybenzaldehyde, and 2,5-dimethoxybenzaldehyde, the % conversions were only 54, 40, and 18.5 respectively, which demonstrates moderate catalytic activity by the variant towards bulky substrates. An increase in the number of carbons in the alkyl chain of the aldehyde affected the catalytic efficiency of Y14C severely. In case of 3-phenylpropionaldehyde, which carries two more carbons in the alkyl chain, only 5% conversion of the product was seen with 41% ee (Figure 3.61-3.79).



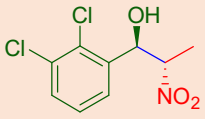
Product obtained with excellent bioconversion



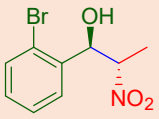
>99% ee, >99% de
79.1% conv, >99% IC



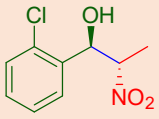
95.2% ee, 74.7% de
>99% conv, 85.3% IC



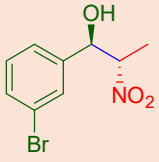
98.5% ee, 95.4% de
97.3% conv, 97% IC



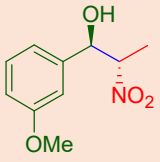
97.8% ee, 92.5% de
>99% conv, 95.2% IC



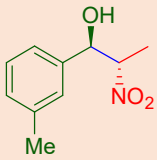
98.6% ee, 88.7% de
97.5% conv, 93.7% IC



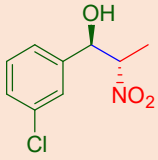
>99% ee, 98.4% de
83.6% conv, 98.9% IC



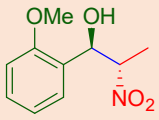
98.4% ee, 98% de
73.9% conv, 98.2% IC



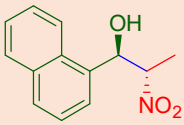
98.6% ee, >99% de
73% conv, >99% IC



>99% ee, >99% de
92.9% conv, >99% IC



98.2% ee, 75.9% de
89.7% conv, 87.2% IC



92.3% ee, 73.4% de
54.1% conv, 83.3 % IC

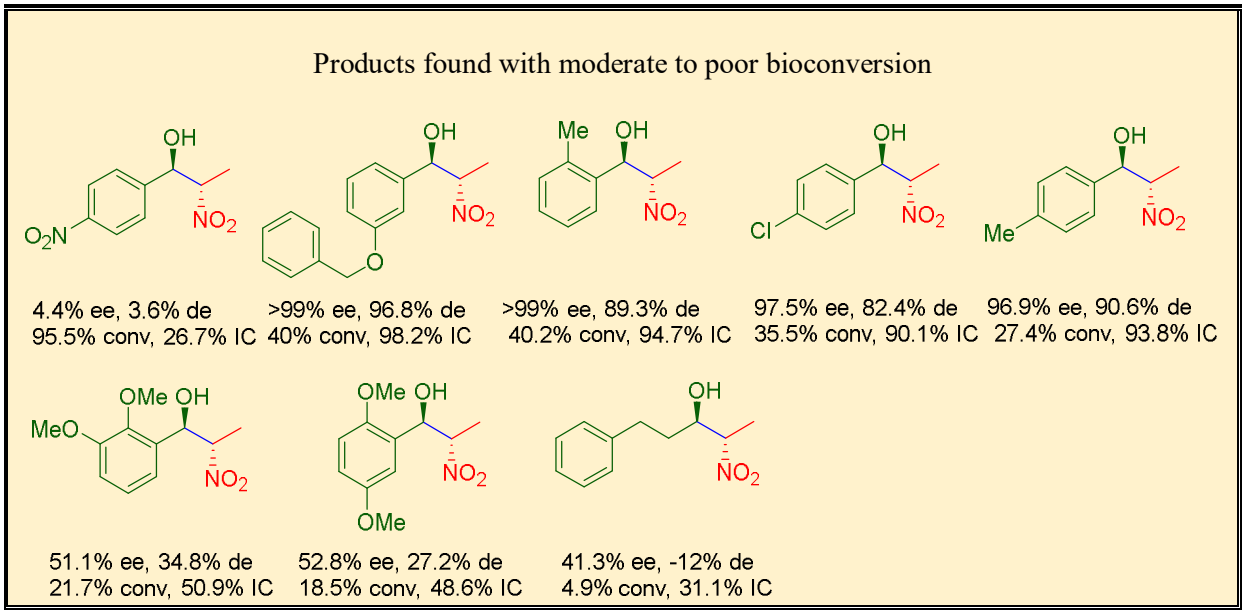
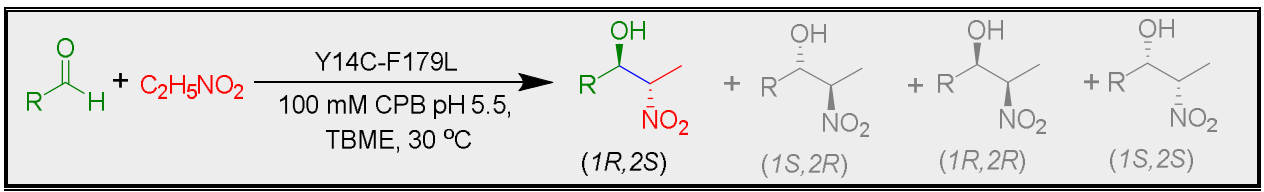


Figure 3.43: Y14C catalyzed stereoselective synthesis of (*1R,2S*) isomers of different β-nitroalcohols from their corresponding aldehydes and nitroethane.

3.4.9. Evaluation of *At*HNL double variants in the diastereoselective Henry reaction using aldehydes that were poorly accepted by Y14C

While most of the aldehydes (Figure 3.44) could be efficiently converted by Y14C into their corresponding β-nitroalcohol diastereomers, eight of them resulted in 40% or less conversion ≤ 40% with poor stereoselectivity. Based on the screening results (Table 3.4), F179L and Y14C were found to be the best mutants in their respective mutant libraries. Thus, we created the double variant Y14C-F179L, and tested it against poorly accepted substrates for efficient catalysis. Although the double mutant demonstrated excellent stereoselectivity in case of few substrates as compared to Y14C, no significant improvement in % conversion was observed for most substrates (Figure 3.44). A few other substrates like 2-methyl benzaldehyde, 2,5-dimethoxy, and 2,3-dimethoxy benzaldehyde lead to only 13, 10, and 14% conversion, respectively by the Y14C-F179L as compared to 38, 29, and 22% conversion by Y14C. The double mutant could not improve stereoselectivity in case of 4-nitrobenzaldehyde. Therefore the double mutant was not studied for further experiments.



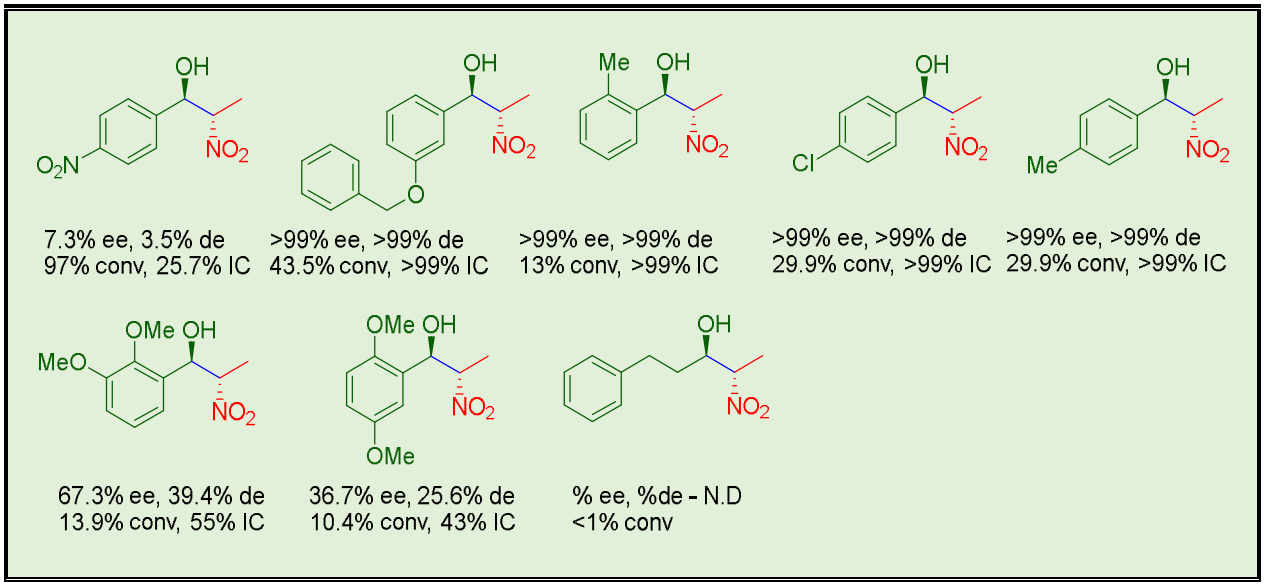


Figure 3.44: *At*HNL-Y14C-F179L catalysed stereoselective synthesis of (*1R,2S*) isomers of different β-nitroalcohols from their corresponding aldehydes and nitroethane.

3.4.10. Screening of *At*HNL mutant libraries towards the stereoselective synthesis of 2-nitro-1-phenyl butanol (2-NPB) via Henry reaction between benzaldehyde and 1-nitropropane

After successfully adding nitroethane to an array of aromatic aldehydes, another bulkier nitroalkane, 1-nitropropane, was tested as a nucleophile for the nitroaldol reaction. 1-Nitroalkane has never been studied with any HNL in stereoselective Henry reaction. Our initial experiment of 1-nitropropane addition to benzaldehyde using crude WT *At*HNL resulted in no product formation. We therefore began screening our in-house Y14 and F179 mutant libraries towards Henry reaction using their crude cell lysates. Among the Y14 series of mutants, five of them, Y14A, Y14C, Y14L, Y14N, and Y14S showed improved activity compared to the WT. In contrast, none of the mutants in the F179 series catalyzed this promiscuous reaction. The % conversion to 2-NPB by Y14A, Y14C, Y14L, Y14N, and Y14S were found to be 6.2, 7.3, 10.9, 3.6, and 3.3 respectively vs. only 0.7% conversion by the wild type (Table 3.5). As the % conversion by these mutants was very poor with the crude cell lysates, their purified enzymes were used for further evaluation. With purified enzyme, the % conversion increased up to 8 times compared to the crude enzyme. All five *At*HNL mutants showed stereopreference for the (*1R,2S*) isomer of the product with >99% ee and >99% de. Y14A, Y14C, Y14L, Y14N, and Y14S showed 37.1, 28.6, 31, 20, and 24% conversion in the synthesis of 2-NPB (Figure 3.45). Y14A having highest activity was selected for the synthesis of (*1R,2S*)-2-NPB and subsequent studies.

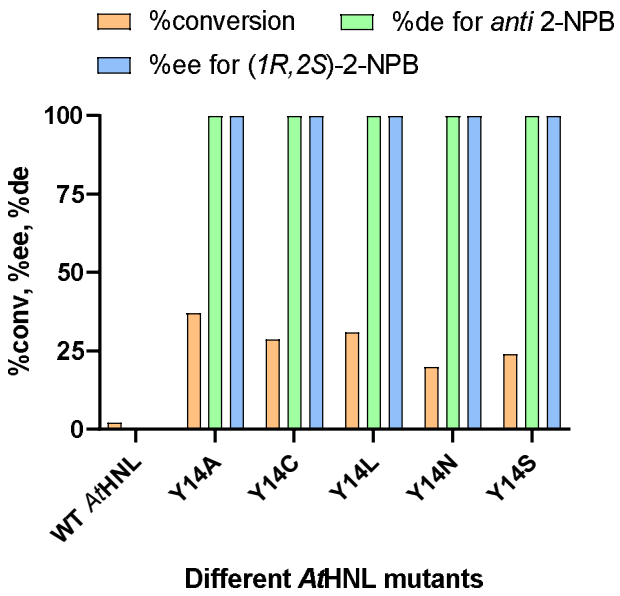


Figure 3.45: Purified *At*HNL mutants screening towards the diastereoselective synthesis of 2-NPB.

Table 3.5: Screening of Y14C and F179L *At*HNL libraries towards the diastereoselective synthesis of 2-NPB (N.D – not detected)

S. No.	Enzyme (variant)	Total % conversion	%ee for (*1R,2S*)-2-NPB	%de for *anti* 2-NPB	%IC for (1*R,2S*)-2-NPB
1	WT *At*HNL	0.7	N.D		
2	Y14A	6.2	86.9	61.1	75.3
3	Y14C	7.3	97.4	81.7	89.7
4	Y14D	1.7	N.D		
5	Y14E	1.0	N.D		
6	Y14F	1.2	N.D		
7	Y14G	0.9	N.D		
8	Y14H	0.7	N.D		
9	Y14I	1.2	N.D		
10	Y14K	1.3	N.D		
11	Y14L	10.9	98	81.6	89.9
12	Y14M	1.3	N.D		
13	Y14N	3.6	>99	37.5	68.7
14	Y14P	0.9	N.D		
15	Y14Q	1.2	N.D		
16	Y14R	0.9	N.D		
17	Y14S	3.3	>99	46.2	73.1
18	Y14T	0.9	N.D		
19	Y14V	0.9	N.D		
20	Y14W	2.0	N.D		
21	F179A	1.1	N.D		
22	F179C	1.3	N.D		
23	F179D	1.0	N.D		

24	F179E	1.0	N.D
25	F179G	1.3	N.D
26	F179H	1.6	N.D
27	F179I	1.1	N.D
28	F179K	0.8	N.D
29	F179L	0.8	N.D
30	F179M	1.0	N.D
31	F179N	1.0	N.D
32	F179P	1.2	N.D
33	F179Q	0.7	N.D
34	F179R	1.2	N.D
35	F179S	1.2	N.D
36	F179T	1.3	N.D
37	F179V	1.3	N.D
38	F179W	1.2	N.D
39	F179Y	1.2	N.D

3.4.11. Optimization of reaction conditions towards the stereoselective synthesis of (*1R,2S*)-2-NPB using *At*HNL-Y14A

3.4.11.1. Optimization of reaction time and catalyst amount:

The amount of purified enzyme and reaction time was optimized to improve the % conversion of 2-NPB. With the increasing amount of enzyme, Y14A showed enhanced % conversion up to 6 mg and a further increase in the enzyme content to 10 mg did not produce any significant increase in the % conversion. In 72 h, 6 mg of pure Y14A showed 59% conversion with >99% ee and >99% de (Figure 3.46).

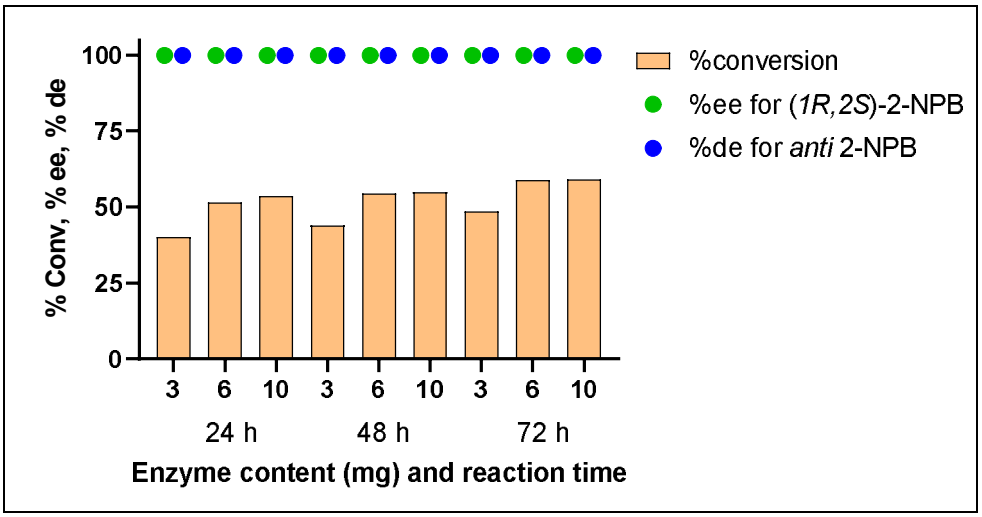


Figure 3.46: Optimization of biocatalytic conditions for the *At*HNL-Y14A: enzyme content and reaction time.

3.4.11.2. Optimization of 1-nitropropane concentration: In our previous experiments with nitroethane, we observed a 9% increase in the % conversion when its concentration was optimized, and hence the nitroethane concentration used there (1.75 M) was taken to set up the initial biocatalysis reaction with 1-nitropropane. To optimize 1-nitropropane concentration, we

choose five different concentrations 0.25, 0.6, 1, 1.4, and 1.75 M in this study. With increasing 1-nitropropane concentration *At*HNL-Y14A showed increased % conversion up to 1.4 M, beyond that it didn't increase further. The Y14A showed 48.4% conversion to (*1R,2S*)-NPB with >99% ee and >99% de after 24 h in this 1-nitropropane concentration (Figure 3.47).

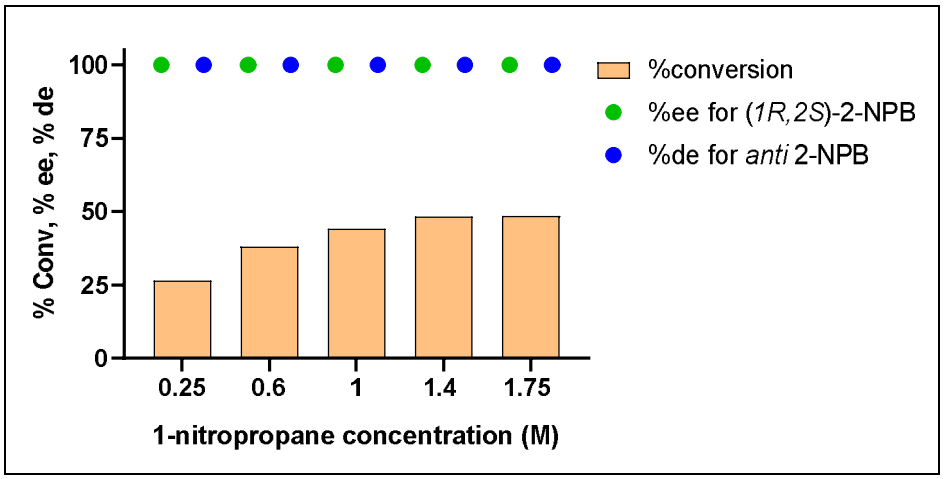


Figure 3.47: Optimization of biocatalytic conditions for the *At*HNL-Y14A: 1-nitropropane concentration.

After the optimization of the four parameters, *At*HNL-Y14A showed 50% conversion with >99% ee and de in the synthesis of (1*R*,2*S*)-2-NPB. The summary of the optimization study is presented in (Figure 3.48).

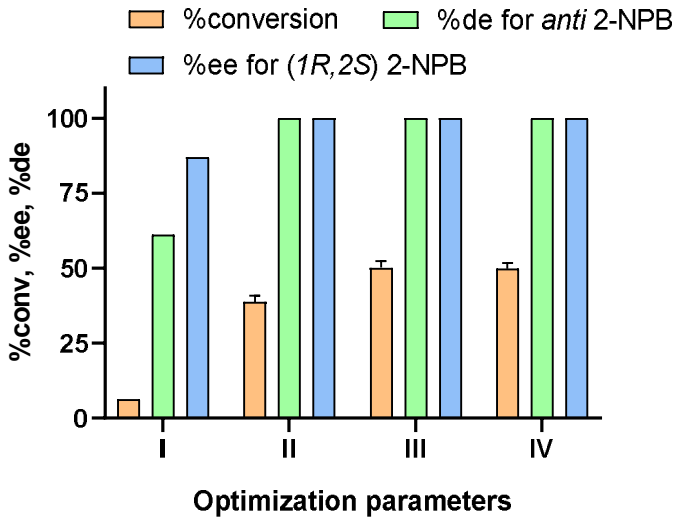


Figure 3.48: Summary of optimization of biocatalytic parameters of Y14A catalyzed nitroaldol reaction using benzaldehyde and 1-nitropropane as the substrate in synthesizing (*1R,2S*)-2-NPB. I: reaction with crude enzyme, II: reaction with purified enzyme, III: enzyme content, IV: 1-nitropropane concentration. The % conversion, % ee, and % de are mean of two data ± standard deviation.

3.4.12. Substrate scope of *At*HNL-Y14A catalyzed diastereoselective synthesis of *anti* β-nitroalcohols using 1-nitropropane as the co-substrate

The synthetic scope and substrate selectivity of *At*HNL-Y14A towards the diastereoselective synthesis was evaluated by selecting fourteen different aromatic aldehydes to obtain their corresponding nitrophenyl butanol derivatives (Figure 3.49). Like the Y14C, Y14A also displayed excellent stereoselectivity in synthesizing the desired products for most of the tested substrates, where up to 90% conversion, >99% ee and de was achieved. Only in the case of five substrates poor (<30%) conversion was observed. Except for 4-nitrobenzaldehyde and 3-phenyl propionaldehyde, which showed very poor stereoselectivity and no activity respectively, all other substrates showed excellent stereoselectivity from 93 to >99% ee and up to 75% conversion. (figure 3.80-3.92)

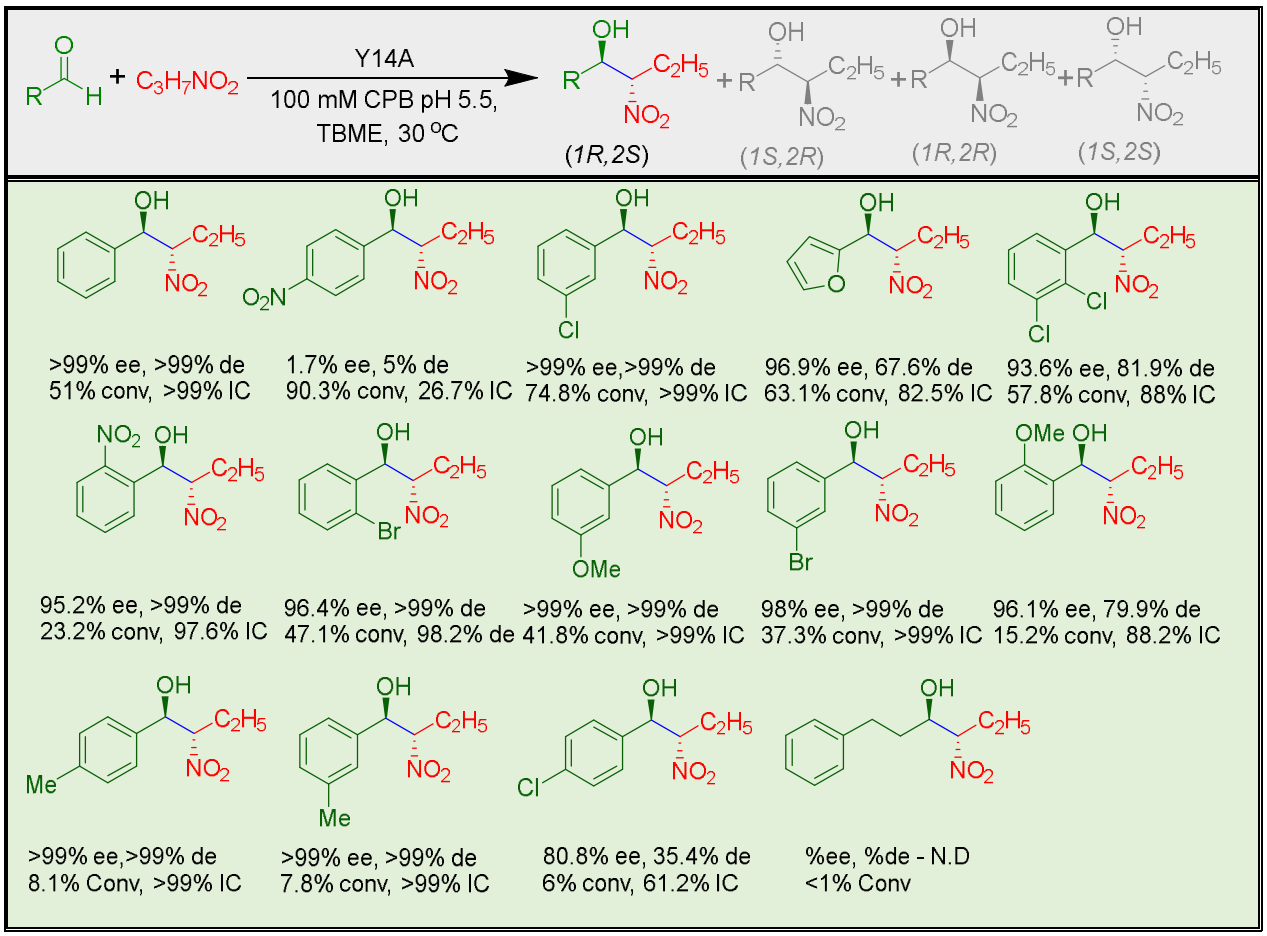


Figure 3.49: Stereoselective synthesis of (*1R,2S*) isomers of different β-nitroalcohols from their corresponding aldehyde substrates and 1-nitropropane by Y14A mutein. Reaction conditions – TBME 600 µL, 5 mM aldehyde substrate (25 µl, 250 mM), 1.4 M 1-nitropropane (156 µL), 6 mg pure Y14A enzyme, 100 mM CPB pH 5.5 (83 µL, 1.5 M). Benzaldehyde stock was prepared in TBME. Total reaction volume was made up to 1.25 mL by adding remaining amount of double distilled water.

3.4.13. Determination of the kinetic parameters of Y14C and Y14A towards the diastereoselective Henry reaction

The steady-state kinetic parameters of Y14C towards the synthesis of (*1R,2S*)-2-NPP were determined by measuring the initial velocities against different concentrations of benzaldehyde. The K_M and V_{max} of Y14C were found to be 25.1 mM and 0.4 µmol/min

respectively (Figure 3.50). Catalytic efficiency (k_{cat}/K_M) of Y14C was calculated to be 0.3 $mM^{-1}min^{-1}$, while WT *At*HNL showed a k_{cat}/K_M of only 0.00116 $mM^{-1}min^{-1}$. The Y14C is found to have 259 times higher catalytic efficiency than the WT. Similarly, the kinetic parameters were determined for *At*HNL-Y14A using 3-chlorobenzaldehyde, which showed the best result among the fourteen substrates used earlier towards diastereoselective Henry reaction. The kinetic parameters were calculated for the synthesis of (*1R,2S*)-1-(3-chlorophenyl)-2-nitrobutan-1-ol. The V_{max} of Y14A was almost similar to Y14C, however, its K_M was found to be poor, i.e., 40 mM. The catalytic efficiency (k_{cat}/K_M) of Y14A was found to be 0.09 $mM^{-1}min^{-1}$. It is almost 3.5 times less than the catalytic efficiency of Y14C towards the synthesis of 2-NPP. This explains the overall reduced % conversion to β-nitroalcohols corresponding to 1-nitropropane compared to nitroethane.

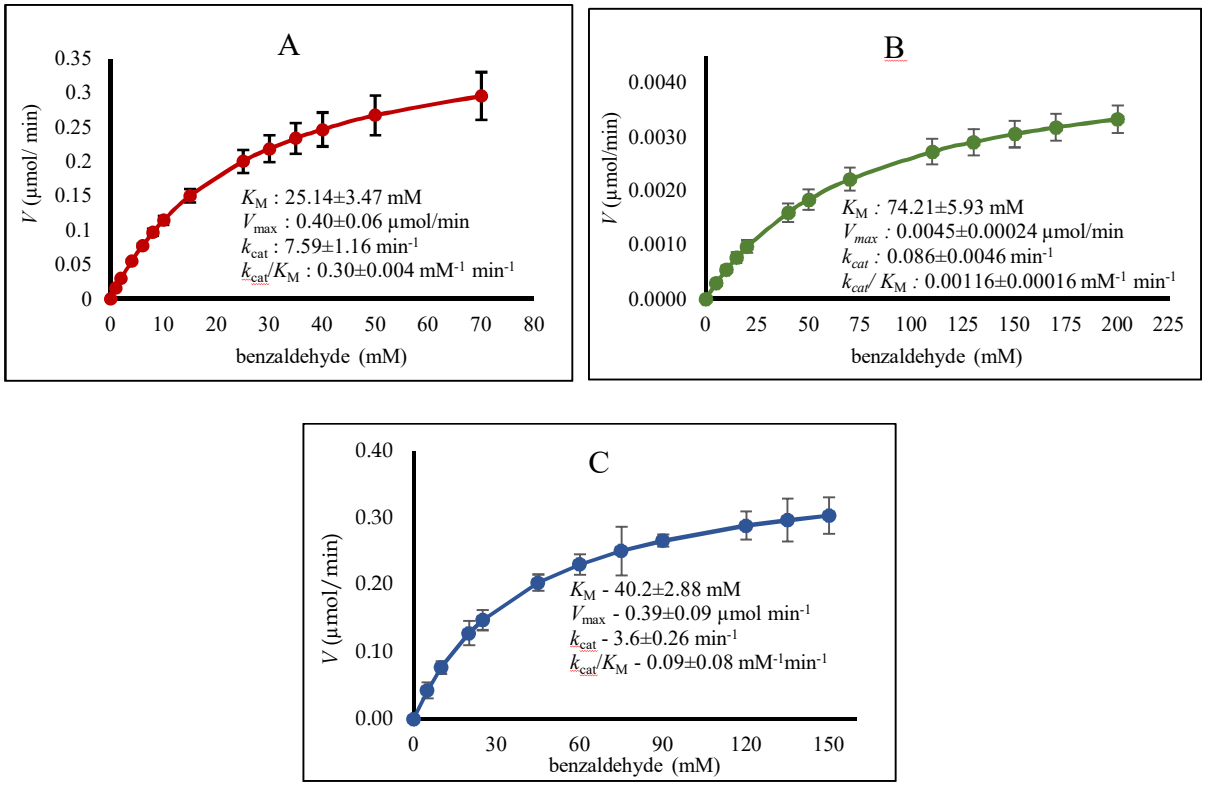


Figure 3.50: Michaelis-Menten plots of *At*HNL A. Y14C, B. WT and C. Y14A towards diastereoselective synthesis of β-nitroalcohol.

3.4.14. pH dependence of Y14C kinetic parameters: probing proton donation role of Cys14 in diastereoselective nitroaldol synthesis

This experiment was carried out to determine the role of the cysteine residue present at the 14th position of the Y14C variant, especially to find out the involvement of the sulfhydryl proton in catalysis. To carry out this experiment, enzyme kinetic parameters were determined at pH 8.2, where the sulfhydryl group of cysteine residue would undergo deprotonation. The same experiment was repeated with the WT too. At pH 8.2, the K_M of *At*HNL-Y14C increased more than two times and reached 56.9 mM compared to only 25.1 mM at pH 5.5, whereas WT *At*HNL hardly showed any change in K_M (Figure 3.51). This implies that the sulfhydryl proton of the cysteine residue in the 14th position of the amino acid chain is crucial and might be

helping the enzyme to bind with its substrate/transition state/product through hydrogen bonding or any other ionic interaction which hampered due to the deprotonation of sulfhydryl proton at a higher pH. WT *Hb*HNL the only HNL reported showing efficient diastereoselective activity also possesses cysteine as the 14th residue in its amino acid chain.[22]

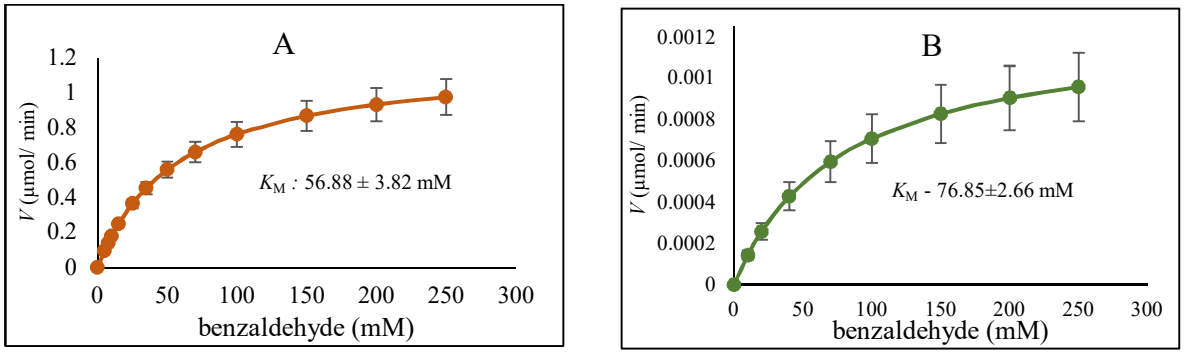


Figure 3.51: Michaelis-Menten plots of *At*HNL A. Y14C and B. WT at pH 8.2 towards diastereoselective synthesis of β-nitroalcohol.

3.4.15. Comparison of cyanogenesis and retro-nitroaldolase activity of *At*HNL WT, Y14C, and Y14A

The two variants, Y14C and Y14A, which showed improved activity in the promiscuous stereoselective Henry reaction with nitroethane and 1-nitropropane respectively were used along with the WT in their purified form to measure their cleavage activity. In the cyanogenesis of mandelonitrile, Y14C and Y14A showed a specific activity of 94.3 and 76 U/mg respectively as compared to 68 U/mg by the WT *At*HNL (Figure 3.52). Next, we selected three different racemic β- nitroalcohols, 2-NPE, 2-NPP, and 2-NPB for retro-nitroaldol reaction by these three enzymes. WT *At*HNL showed almost similar retro-nitroaldolase activity towards all the three β-nitroalcohols that suggests its poor preference for different nitroalkanes. To our pleasure, Y14C and Y14A showed almost 7 and 2.3 times more specific activity than the WT towards 2-NPP and 2-NPB respectively. This enhanced activity proves the preference of Y14C and Y14A towards 2-NPP and 2-NPB respectively. This result is in accordance with the nitroaldolase activity of the mutants. However, both Y14C and Y14A showed similar poor activity like the WT towards the cleavage of 2-NPE suggesting that they are not the best mutants for 2-NPE cleavage. A proof towards this comes from a recent study of our group [23] about screening the Y14 and F179 libraries for enantioselecive synthesis of 2-NPE, which revealed F179N with highest catalytic activity. Another important observation comes from Figure 3.52 is higher catalytic activity for 2-NPP cleavage than 2-NPB cleavage. The same trend was noticed in the synthesis reaction and in the kinetic studies. Overall, this study reveals two single mutations with not only gained promiscuous Henry reaction activity for nitroethane and 1-nitropropane but also improved their natural cyanogenesis activity.

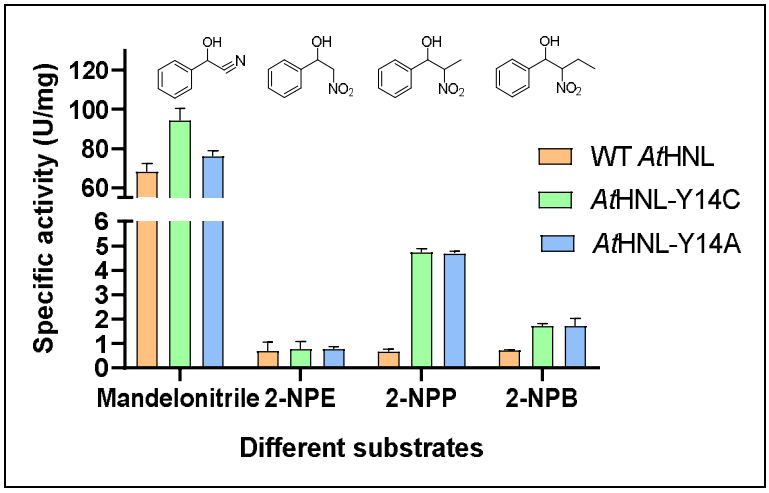


Figure 3.52: Comparison of cyanogenesis and retro-nitroaldolase activity of WT *At*HNL, Y14C, Y14A by spectrophotometric cleavage assay.

3.4.16. Gram scale synthesis of (*1R,2S*)-2-NPP by using Y14C crude enzyme as the catalyst

The optimization studies showed that the mutant Y14C can be efficiently used in its crude form. We aimed to carry out a large scale synthesis of the *anti* diastereoisomer, (*1R,2S*)-2-NPP using the Y14C crude cell lysates. This preparative scale synthesis was carried out using 10.1 mmol (100 mM in 101 ml) of benzaldehyde in the presence of 1.6 µmol of enzyme (total crude enzyme used was 1219 mg, with a fold purification of 27 ±2.5, resulting in a total pure enzyme quantity of 45 mg, with a molecular weight of 28 kDa). The isolated yield of the final product (*1R,2S*)-1a was 55%, with 98% *ee* and >99% *de*, leading to 5555 µmol of total product. This resulted in a TTN of 5555/1.6 = 3472, which, to the best of our knowledge, stands as the highest TTN value ever reported for the biocatalytic synthesis of (*1R,2S*)-2-NPP (Figure 3.53). Not only does our *At*HNL-Y14C approach outperform in terms of TTN, but it also showcased a significantly higher substrate to catalyst ratio. Our approach utilized a ratio of 10100/1.6 = 6312.5. The synthesized product after silica column purification was analysed through chiral HPLC and ^{1}H and ^{13}NMR (figure 3.54, 3.93).

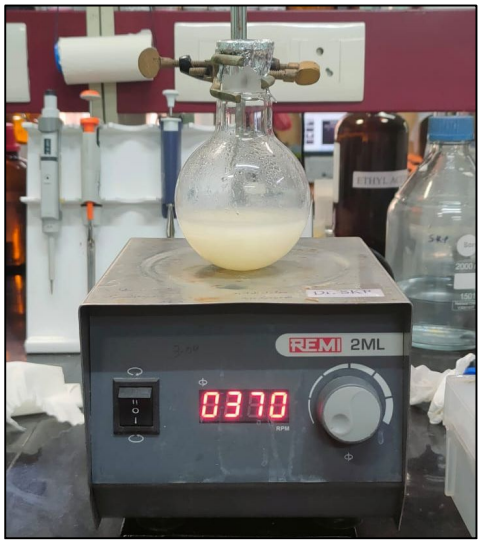
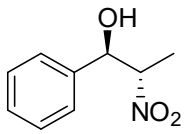


Figure 3.53: Reaction setup for the gram scale synthesis of (*1R,2S*)-2-NPP using Y14C crude enzyme.

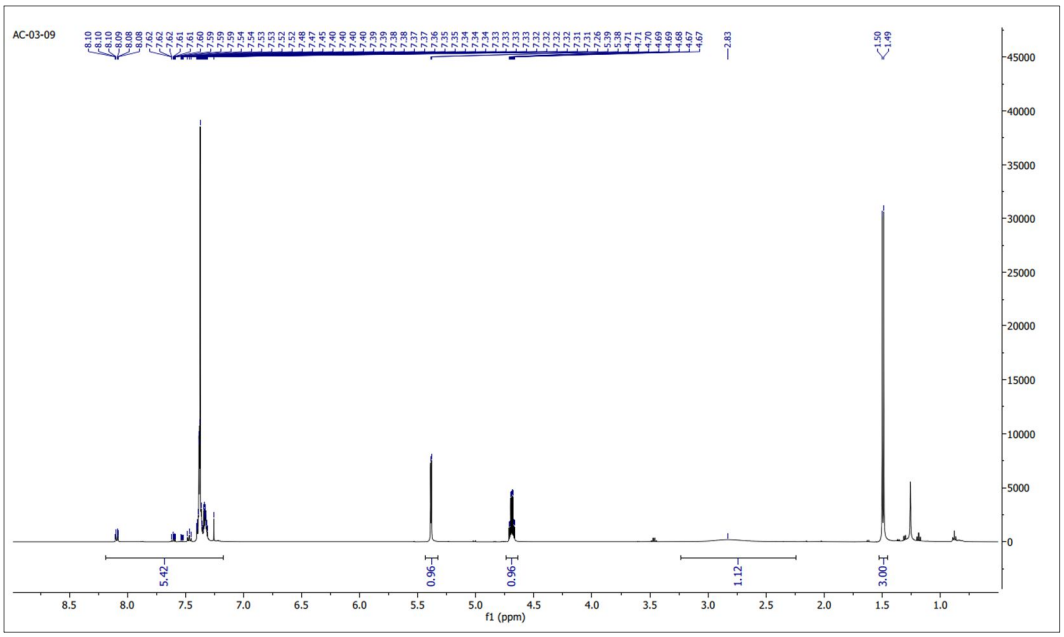
3.4.17. NMR characterization of (*1R,2S*)-2-NPP synthesized in gram scale using *At*HNL-Y14C crude enzyme

(*1R,2S*)-2-nitro-1-phenylpropan-1-ol (NPP)[14]



^{1}H NMR (500 MHz, $CDCl_3$) δ 8.19 – 7.18 (m, 5H), 5.39 (d, *J* = 3.6 Hz, 1H), 4.69 (m, 1H), 2.83 (s, 1H), 1.49 (d, *J* = 6.8 Hz, 3H).

^{13}C NMR (126 MHz, $CDCl_3$) δ 138.58, 128.87, 128.65, 126.08, 87.57, 74.04, 12.19.



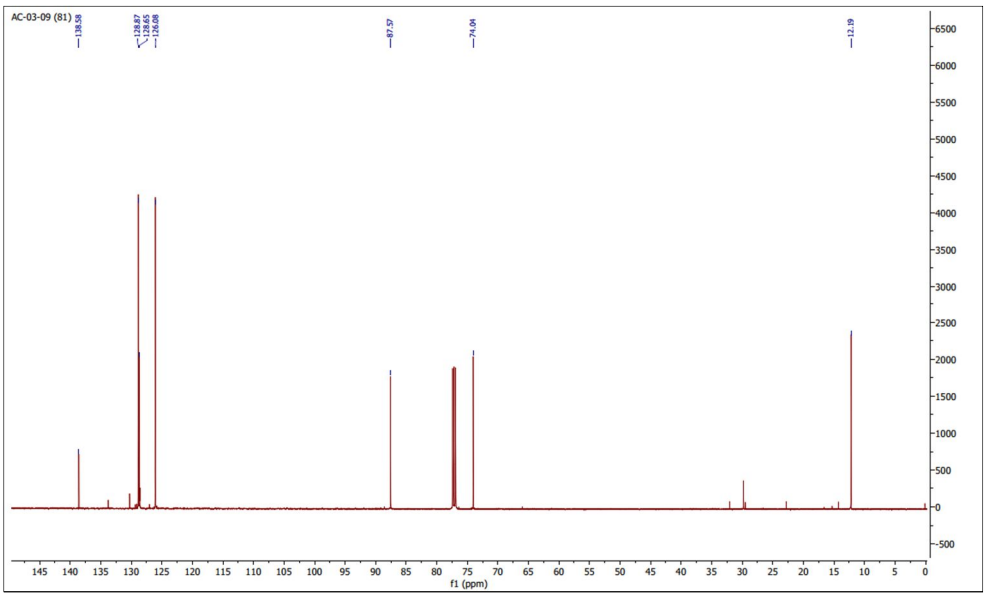


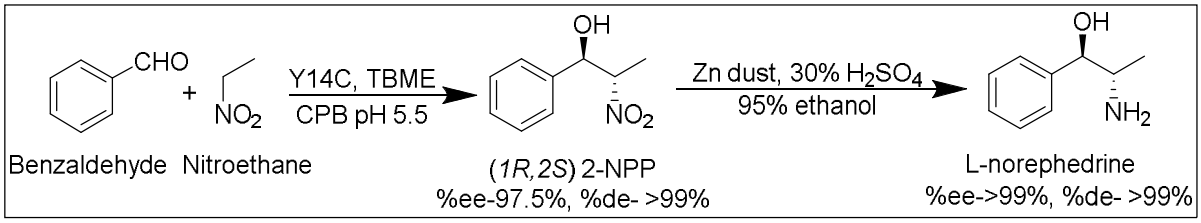
Figure 3.54: ^{1}H NMR and ^{13}C NMR spectra of (*1R,2S*)-2-nitro-1-phenylpropan-1-ol synthesized using *At*HNL-Y14C.

3.4.18. Synthesis of L-norephedrine from (*1R,2S*)-2-NPP

The enantiopure (*1R,2S*)-2-NPP synthesized through Y14C-*At*HNL catalyzed Henry reaction was subjected to reduction of its nitro group to synthesize its corresponding • -aminoalcohol. The reduced product is a vital drug molecule, i.e., L-norephedrine, a psychostimulant from the amphetamine family. A 1 g of enantiopure (*1R,2S*)-2-NPP was transformed into the final β-amino alcohol with 68% yield (Scheme 3.3, Figure 3.55). Reaction progression and product formation were monitored by ninhydrin staining.[10] The staring material, i.e., purified β-nitroalcohol did not have *syn* enantiomers, confirmed by both chiral HPLC and ^{1}H NMR (Figure 3.56, 3.57, 3.94). The ^{1}H NMR of purified β-amino alcohol also showed the absence of *syn* stereoisomers, with de of >99% *anti*. Reverse phase HPLC was carried out to determine the enantiomeric excess between the *anti*-isomers according to Kao et al. In HPLC analysis, no traces of (*1S,2R*) stereoisomer was found, which confirms that the compound's % ee is >99%.[11]



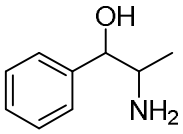
Figure 3.55: Reaction setup for the gram scale synthesis of (*1R,2S*)-2-amino phenyl propanol (2-APP).



Scheme 3.3: Chemo-enzymatic synthesis of L-norephedrine starting from benzaldehyde.

3.4.19. NMR characterization of racemic and (*1R,2S*)-2-amino-1-phenylpropan-1-ol

Racemic 2-amino-1-phenylpropan-1-ol[24]



^{1}H NMR (500 MHz, $CDCl_3$) δ 7.37 – 7.27 (m, 9H), 7.25 – 7.17 (m, 1H), 5.06 (d, *J* = 7.6 Hz, 1H), 4.55 (d, *J* = 4.7 Hz, 1H), 3.88 (dq, *J* = 7.7, 6.7 Hz, 1H), 3.22 (qd, *J* = 6.5, 4.7 Hz, 1H), 1.97 (s, 6H), 0.97 (d, *J* = 6.5 Hz, 3H), 0.72 (d, *J* = 6.7 Hz, 3H).

^{13}C NMR (101 MHz, $CDCl_3$) δ 141.72, 140.61, 128.38, 128.20, 127.66, 126.75, 126.69, 77.92, 77.37, 52.22, 18.34, 16.74.

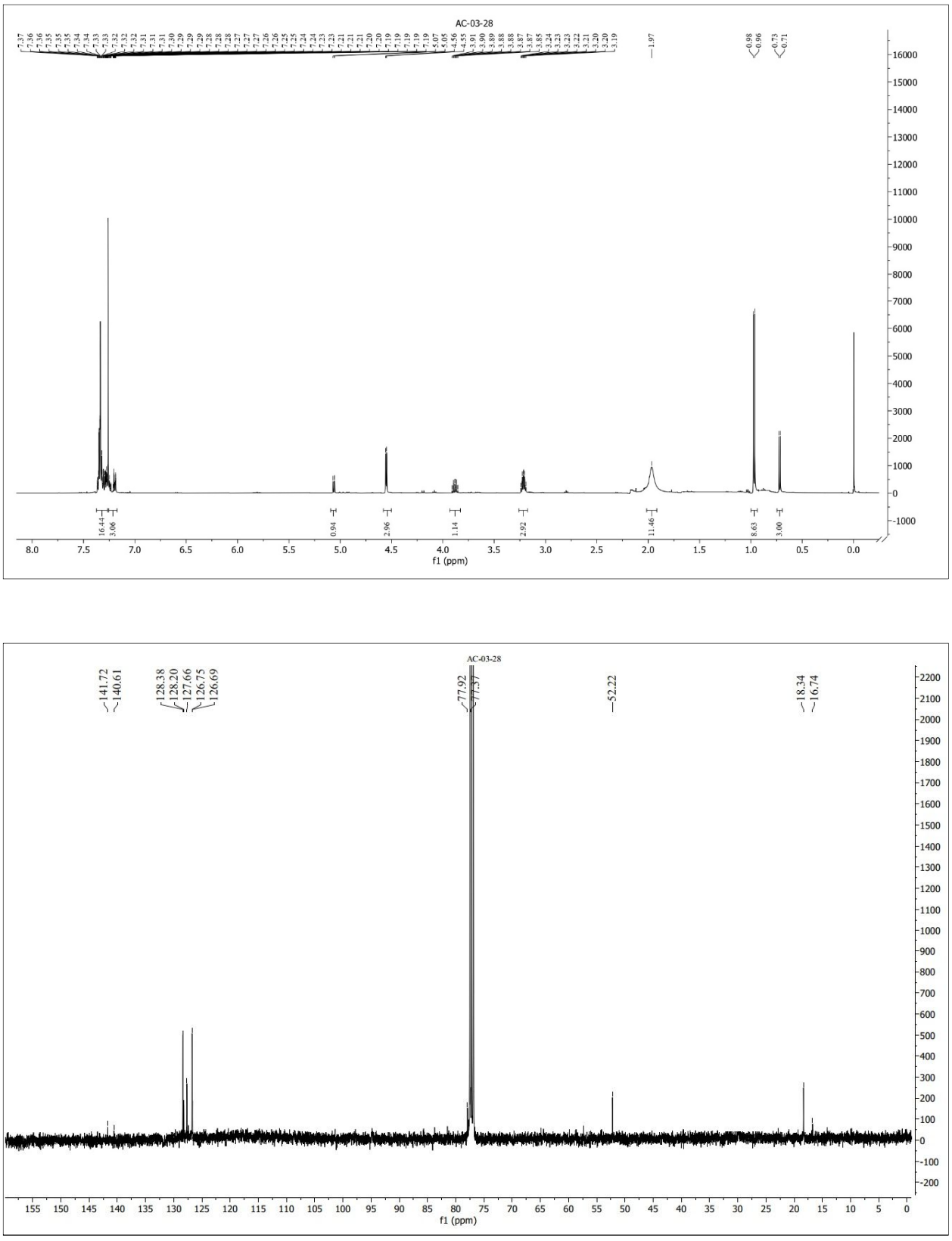
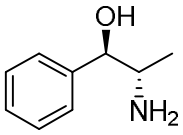


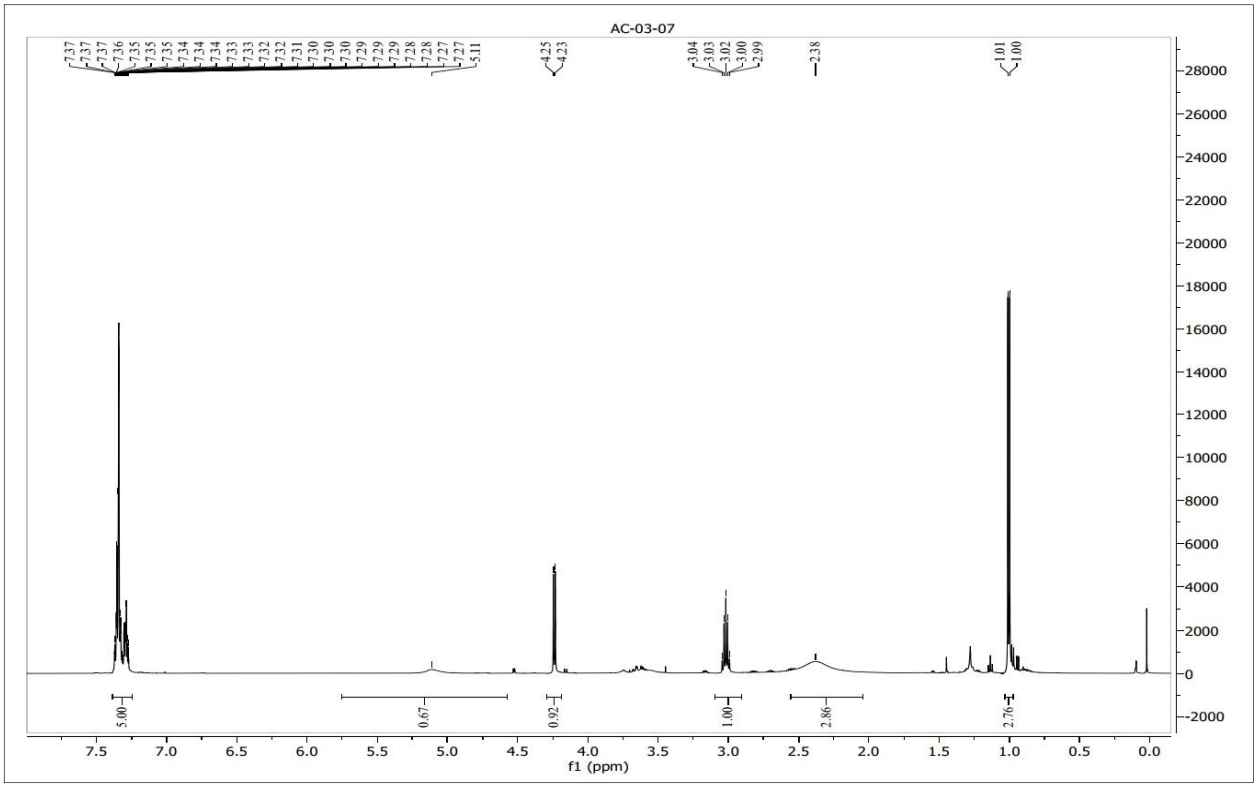
Figure 3.56: ^{1}H NMR and ^{13}C NMR spectra of racemic 2-amino-1-phenylpropan-1-ol.

(*1R,2S*)-2-amino-1-phenylpropan-1-ol[24]



^{1}H NMR (500 MHz, $CDCl_3$) δ 7.39 – 7.24 (m, 5H), 5.11 (s, 1H), 4.24 (d, *J* = 6.7 Hz, 1H), 3.02 (p, *J* = 6.5 Hz, 1H), 2.38 (s, 3H), 1.00 (d, *J* = 6.4 Hz, 3H).

^{13}C NMR (101 MHz, $CDCl_3$) δ 142.85, 128.42, 127.69, 126.70, 78.84, 53.06, 20.52.



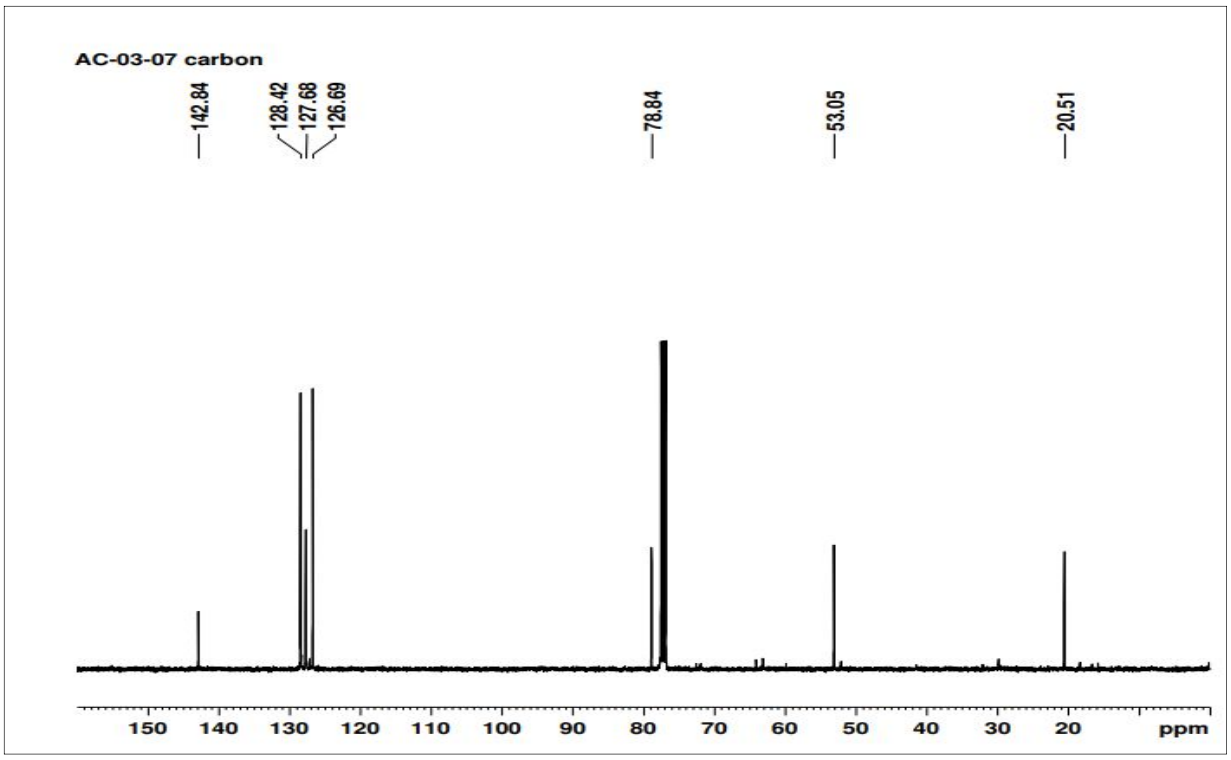


Figure 3.57: ^{1}H NMR and ^{13}C NMR spectra of (*1R,2S*)-2-amino-1-phenylpropan-1-ol.

3.4.20. Deciphering the reaction mechanism of diastereoselective Henry reaction by selective deuteration at the • -carbon of the nitroaldol product

In order to incorporate deuterium into the β-carbon of the nitroaldol product, it was necessary to use deuterated nitroethane as a nucleophile in the diastereoselective Henry reaction. We prepared deuterated nitroethane by exchanging the α-carbon of nitroethane with deuterium. ^{1}H NMR was used to monitor this exchange process. ^{1}H NMR spectra of nitroethane has two sets of signals. They appear as a quartet for –C*H*$_2$ protons at C_1 and a triplet for the –C*H*$_3$ protons at C_2, giving a C_1:C_2 proton ratio of 2:3. A single deuterium exchange to CH_3-CHD-NO_2, would decrease this ratio to 1:3, and a change in the coupling pattern to provide a doublet for the protons at C_2. If both protons of C_1 are replaced with deuterium, i.e., CH_3-CD_2-NO_2, the ratio becomes 0:3 and the C_2 protons would form a singlet. Our study of deuterium exchange of nitroethane at different time points illustrates a change in coupling pattern for the C_2 protons (1.55 ppm) and the C_1:C_2 proton ratio to 1:3 over a period of 108 h (Figure 3.58). However, we observed an interesting phenomena that in case of the control experiment, where deuterated Y14C-*At*HNL was replaced with 20 mM KPB pD 7, nitroethane was deuterated at C_1 (Figure 3.58). As CH_3-CHD-NO_2 was obtained irrespective of the use of Y14C or KPB pD 7 in 108 h, it suggests that nitroethane's deprotonation is not catalyzed by the biocatalyst and rather it happened due to the buffer used in the biocatalysis. The carbon numbering of CH_3-CHD-NO_2 in Figure 3.58 is referred to Scheme 3.4.

The deuterated nitroethane synthesized above was used in diastereoselective Henry reaction along with benzaldehyde. After seven hours, the product was analyzed by both chiral HPLC (figure 3.95) and ^{1}H NMR which confirmed the presence of deuterated NPP (Figure 3.59). Signal for the -OH proton at 2.71 ppm has disappeared indicating the proton exchanged with deuterium. Analysis of the ^{1}H NMR signal of the other four types of protons, except the

aromatic and the –OH, suggested the presence of *anti* conformations of both $C_6H_5CH(OD)CD(NO_2)CH_3$ and $C_6H_5CH(OD)CH(NO_2)CH_3$. The –C*H*(OD)- proton appeared at 5.4 ppm as a mixture of a singlet and a doublet in the ratio of 1.17:1. At 4.72 ppm a multiplet was found accounting for the -C*H*$(NO_2)CH_3$, while no signal appeared for -C*D*$(NO_2)CH_3$. The methyl protons of -$CH(NO_2)CH_3$ and -$CD(NO_2)CH_3$ provided a doublet and singlet respectively at 1.55 pm (*anti*) accounting for three protons in the ratio of 1:1.24. The synthesis of $C_6H_5CH(OD)CD(NO_2)CH_3$ along with $C_6H_5CH(OD)CH(NO_2)CH_3$ by the Y14C was unexpected for us. The former cannot be obtained due to a non-enzymatic (only by buffer) reaction which gives a mixture of *syn* and *anti* products (Figure 3.59B, 3rd NMR). It is noteworthy that CH_3-CHD-NO_2 used in here was a product of buffer catalyzed reaction, and hence is racemic. We hypothesized that the racemic CH_3-CHD-NO_2 would provide both deuterated and undeuterated *anti* products as depicted in Figure 3.59A. Both the (*R*) and (*S*) CH_3-CHD-NO_2 are expected to have specific conformation inside the Y14C by virtue of interactions of their –NO_2 and –CH_3 with in the enzyme. Therefore both the enantiomers are expected to create different anions with and without deuterium. A *si* face attack of the anions on the benzaldehyde sp^2 carbon would produce a mixture of $C_6H_5CH(OD)CD(NO_2)CH_3$ along with $C_6H_5CH(OD)CH(NO_2)CH_3$. Synthesis of both *anti* products supports the *anti* selectivity of Y14C in the diastereoselective Henry reaction.

The proton ratio of $C_6H_5CH(OD)CD(NO_2)CH_3$: $C_6H_5CH(OD)CH(NO_2)CH_3$ was found to be from 1.17:1 to 1.24:1 depending on the set of protons compared. A possible explanation for this ratio could be due to primary kinetic isotope effect (KIE). A plausible Henry reaction mechanism would involve three steps, (a) deprotonation of nitroalkane, (b) C–C bond formation between nitroalkane anion and electrophilic carbonyl center, and (c) protonation of the alkoxide anion of the β-nitroalcohol. We observed a 108 h reaction for the deuterium exchange to obtain CH_3-CHD-NO_2 from nitroethane, while a 7 h for the biocatalytic diastereoselective β-nitroalcohol synthesis, which suggests that the dissociation of nitroalkane is the slowest step. KIE would be involved in case of the first step, i.e. deprotonation of (*S*)-CH_3-CHD-NO_2 vs. dedueteration of (*R*)- CH_3-CHD-NO_2 (Figure 3.59A), while it cannot be associated in the second and third step of the mechanism. The proton ratio of the deuterated: undeuterated product coincides with the explanation of primary kinetic isotope effect. Although we do not have direct experimental evidence to prove that deprotonation or dedeuteration is the rate limiting step, based on the KIE observed we predict that the first step is the rate limiting step in our diastereoselective Henry reaction.

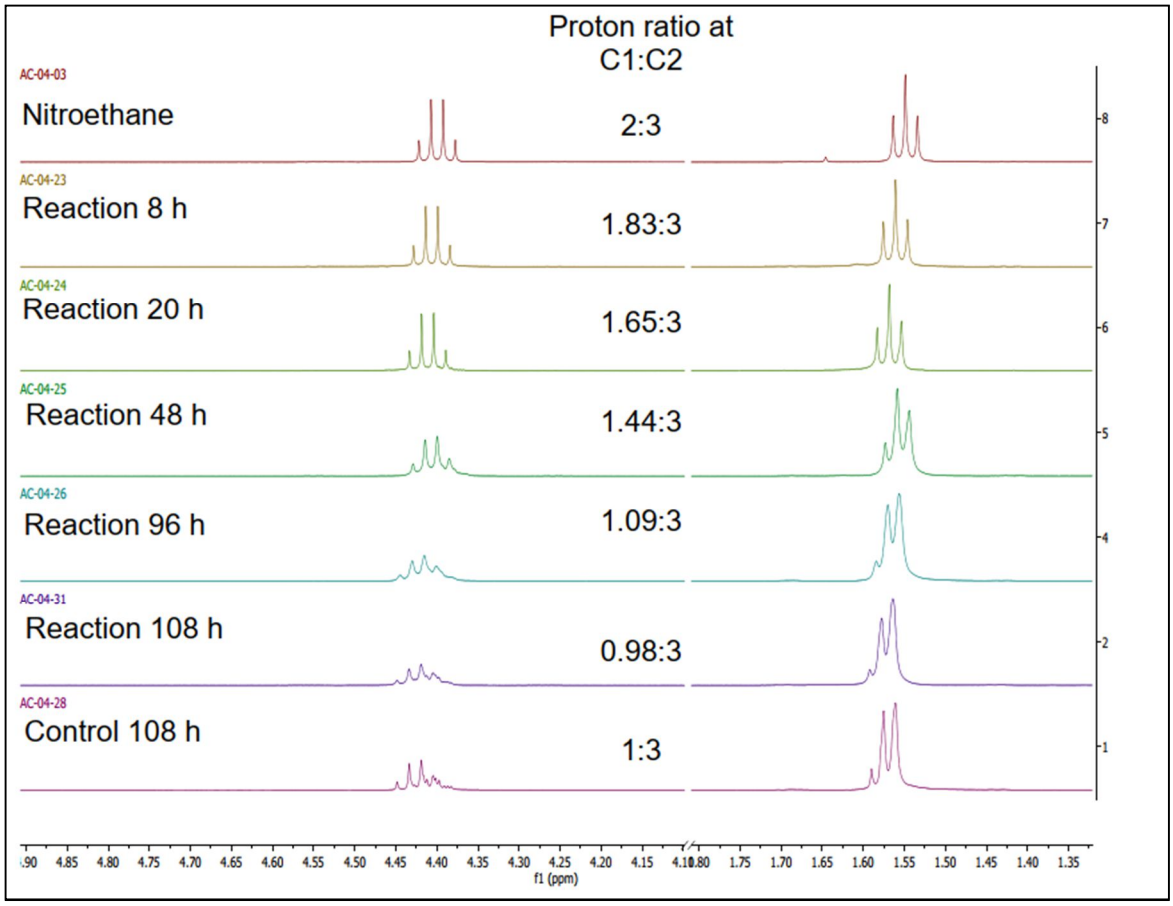
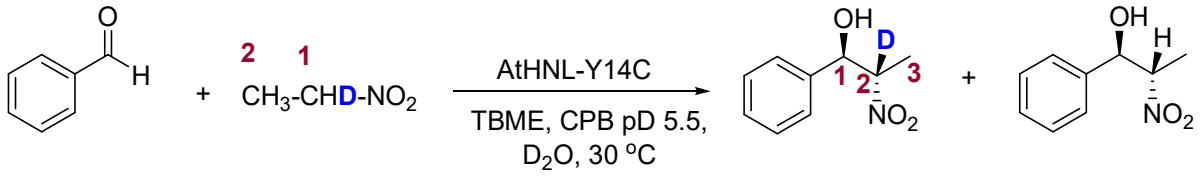
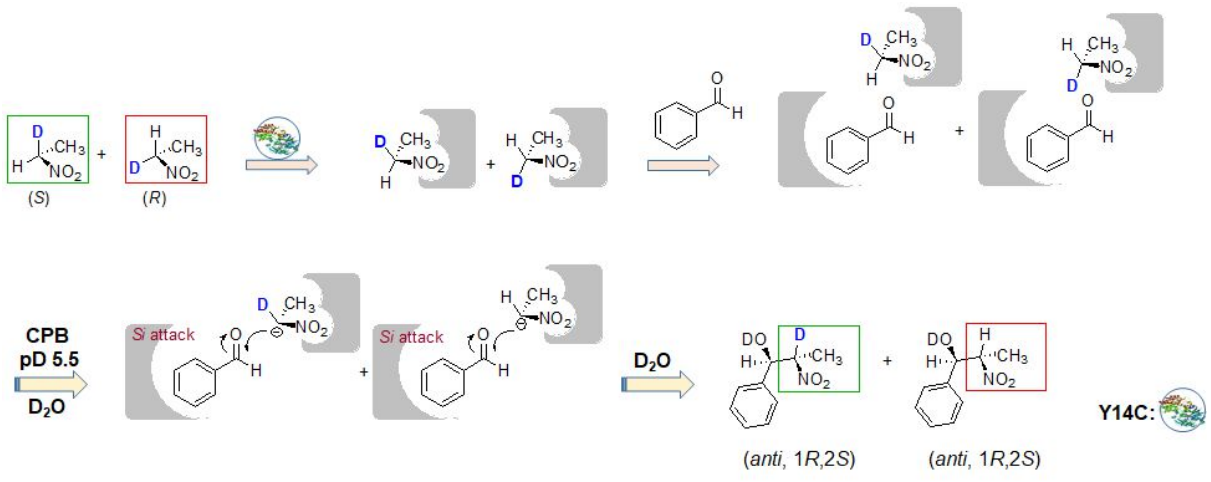


Figure 3.58: Deuterium exchange at the C_1 of nitroethane at different time points.



Scheme 3.4: *At*HNL-Y14C catalyzed diastereoselective synthesis deuterated 2-NPP

(A)



(B)

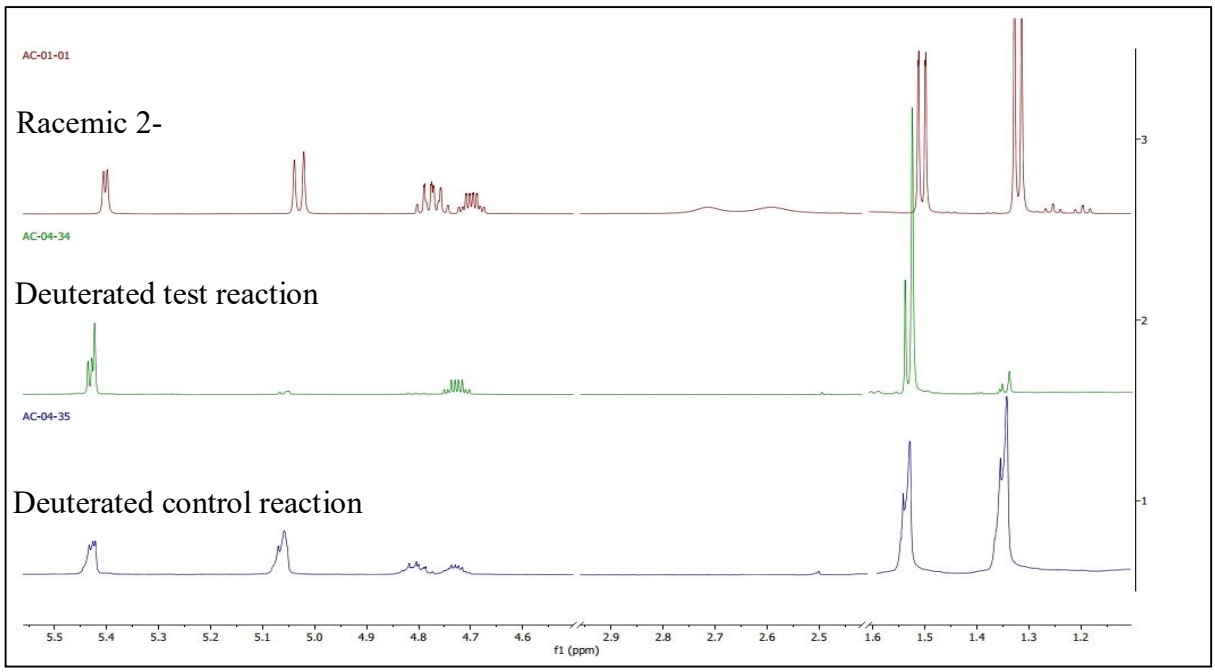


Figure 3.59: Deuterium exchange at the • -carbon of 2-NPP.

3.4.21. Recycling *At*HNL-Y14C for the synthesis of (*1R,2S*)-2-NPP

The reusability of the *At*HNL-Y14C was investigated for the production of (*1R,2S*)-2-NPP in a biphasic reaction system. The purified Y14C mutein was recycled for eight cycles of diastereoselective nitroaldol reaction in the presence of 100 mM of benzaldehyde and checked for its remaining activity after each cycle (Figure 3.60). It was observed that up to third cycle Y14C could retain 83% of its activity with >95% ee and >90% de, which gradually decreased fourth cycle onwards. It confirms that this enzyme is stable even without immobilization and can be recycled for minimum 3 cycles in presence of 100 mM of benzaldehyde.

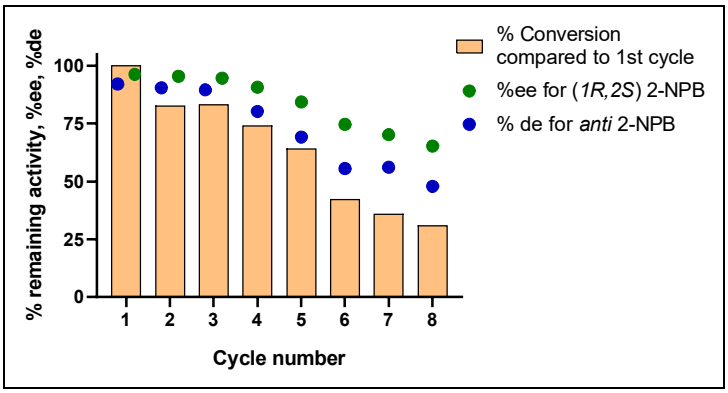
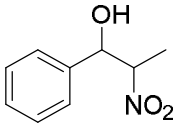


Figure 3.60: Reusability of *At*HNL-Y14C to synthesize (*1R,2S*)-2-NPP.

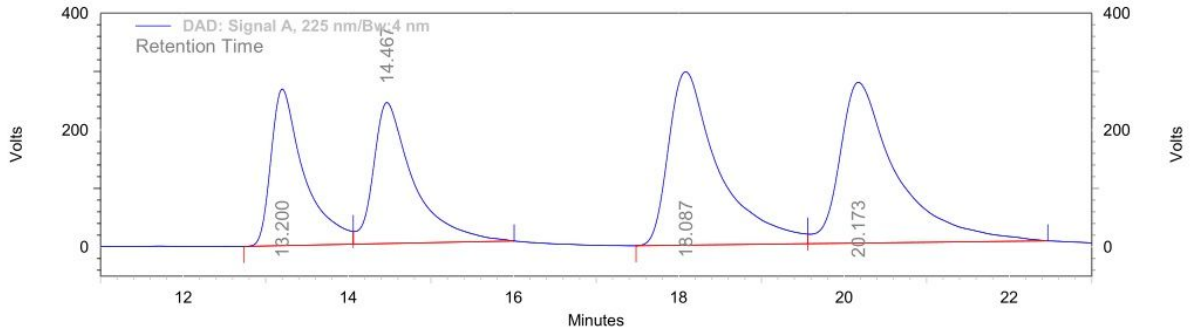
3.4.22. HPLC conditions and HPLC traces of racemic standard β-nitroalcohols and enantiopure product synthesized by *At*HNL-Y14C mutant enzyme

1. 2-nitro-1-phenylpropan-1-ol (NPP)



For % Conversion, % Enantiomeric excess, % Diastereomeric excess, % Isomeric content				Absolute conformation determination
Hexane: IPA	wavelength	Column	Flow rate	Assigned by comparison with the reported literature[25]
95:5 for 6 mins, 96:4 afterward	225 nm	Lux 5µm amylose 1	1 mL/min	

A)

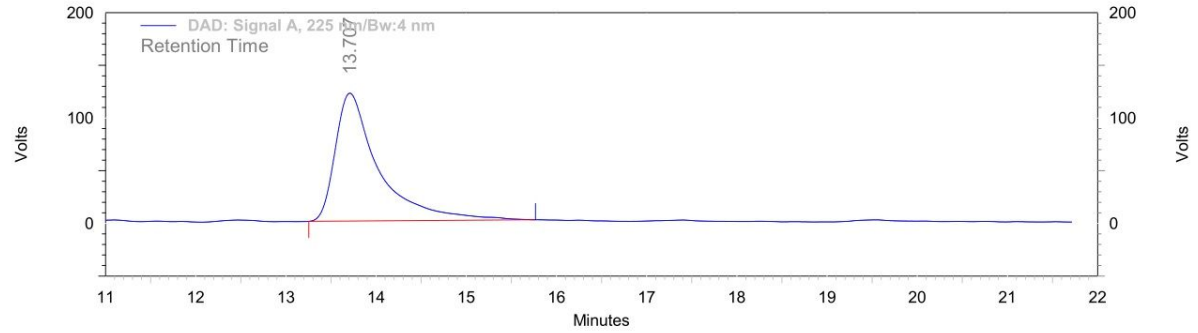


DAD: Signal A, 225 nm/Bw:4 nm
Results

Retention Time	Area	Area %	Height	Height %
13.200	15795092	18.18	561702	24.79
14.467	17125432	19.71	505579	22.32
18.087	26362942	30.35	621480	27.43
20.173	27591883	31.76	576632	25.45
Totals	86875349	100.00	2265393	100.00

Retention time	13.2	14.467	18.087	20.173
product	(*1S,2R*)	(*1R,2S*)	(*1S,2S*)	(*1R,2R*)

B)



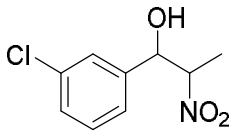
DAD: Signal A,
225 nm/Bw:4 nm
Results

Retention Time	Area	Area %	Height	Height %
13.707	8488559	100.00	254518	100.00
Totals	8488559	100.00	254518	100.00

Retention time	13.707
product	(*1R,2S*)

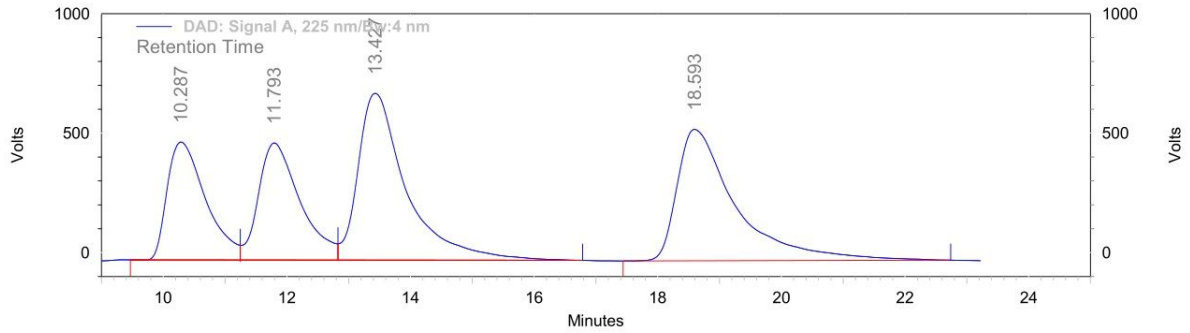
Figure 3.61: HPLC chromatograms of 2-nitro-1-phenylpropan-1-ol. A. racemic standard, B. enantiopure product synthesized by *At*HNL-Y14C mutant enzyme.

2. 1-(3-chlorophenyl)-2-nitropropan-1-ol



For % Conversion				Absolute conformation determination
Water: acetonitrile	wavelength	Column	Flowrate	Assigned by comparison with the reported literature[15]
80:20	222 nm	C_{18}	1 mL/min	
For % Enantiomeric excess, % Diastereomeric excess, % Isomeric content				
Hexane: IPA	wavelength	Column	Flowrate	
93:7	225 nm	Lux 5µm amylose 1	1 mL/min	

A)

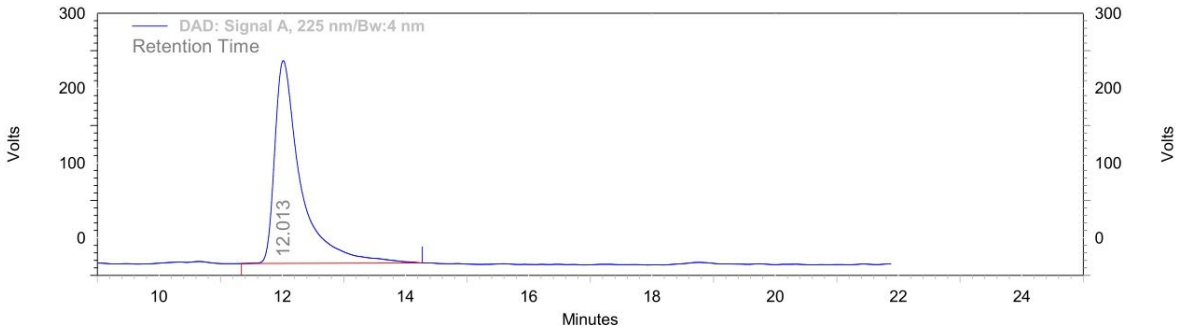


DAD: Signal A,
225 nm/Bw:4 nm
Results

Retention Time	Area	Area %	Height	Height %
10.287	44767727	18.05	1034580	22.11
11.793	48078930	19.39	1027392	21.96
13.427	79231420	31.95	1463289	31.28
18.593	75942902	30.62	1152971	24.65
Totals	248020979	100.00	4678232	100.00

Retention time	10.287	11.793	13.427	18.593
product	(*1S,2R*)	(*1R,2S*)	(*1S,2S*)	(*1R,2R*)

B)



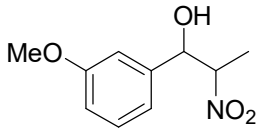
DAD: Signal A,
225 nm/Bw:4 nm
Results

Retention Time	Area	Area %	Height	Height %
12.013	16633445	100.00	567681	100.00
Totals	16633445	100.00	567681	100.00

Retention time	12.013
product	(*1R,2S*)

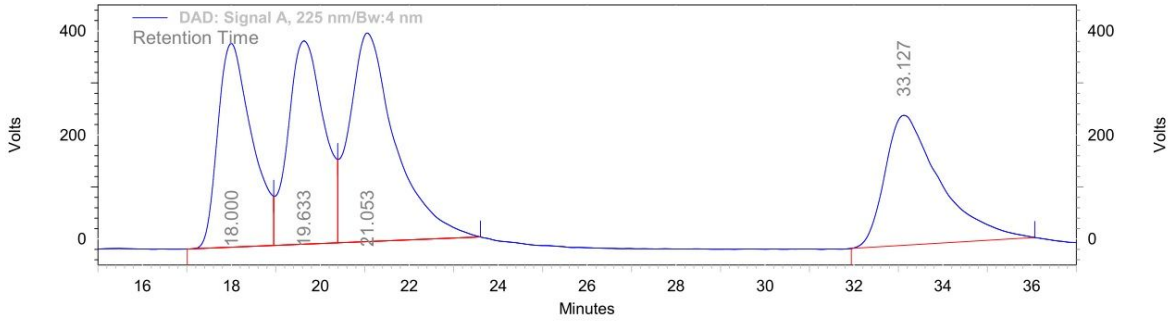
Figure 3.62: HPLC chromatograms of 1-(3-chlorophenyl)-2-nitropropan-1-ol. A. racemic standard, B. enantiopure product synthesized by *At*HNL-Y14C mutant enzyme.

3. 1-(3-methoxyphenyl)-2-nitropropan-1-ol



For % Conversion				Absolute conformation determination
Water: acetonitrile	wavelength	Column	Flowrate	Assigned by analogy with the absolute configuration of compound 1-(2-methoxyphenyl)-2-nitropropan-1-ol
80:20	222 nm	C_{18}	1 mL/min	
For % Enantiomeric excess, % Diastereomeric excess, % Isomeric content				
Hexane: IPA	wavelength	Column	Flowrate	
95:5	225 nm	Lux 5µm amylose 1	1 mL/min	

A)

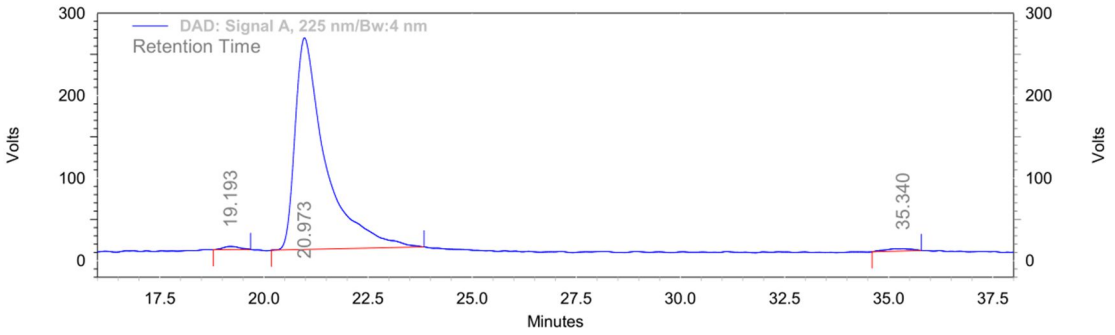


DAD: Signal A, 225 nm/Bw:4 nm
Results

Retention Time	Area	Area %	Height	Height %
18.000	43819856	22.38	821429	27.32
19.633	46223955	23.61	819757	27.27
21.053	60778842	31.05	841081	27.98
33.127	44944970	22.96	524027	17.43
Totals	195767623	100.00	3006294	100.00

Retention time	18	19.633	21.053	33.127
product	(*1S,2R*)	(*1R,2S*)	(*1S,2S*)	(*1R,2R*)

B)



DAD: Signal A,
225 nm/Bw:4 nm
Results

Retention Time	Area	Area %	Height	Height %
19.193	223507	0.81	8020	1.45
20.973	27236735	98.22	537805	97.54
35.340	270867	0.98	5551	1.01
Totals	27731109	100.00	551376	100.00

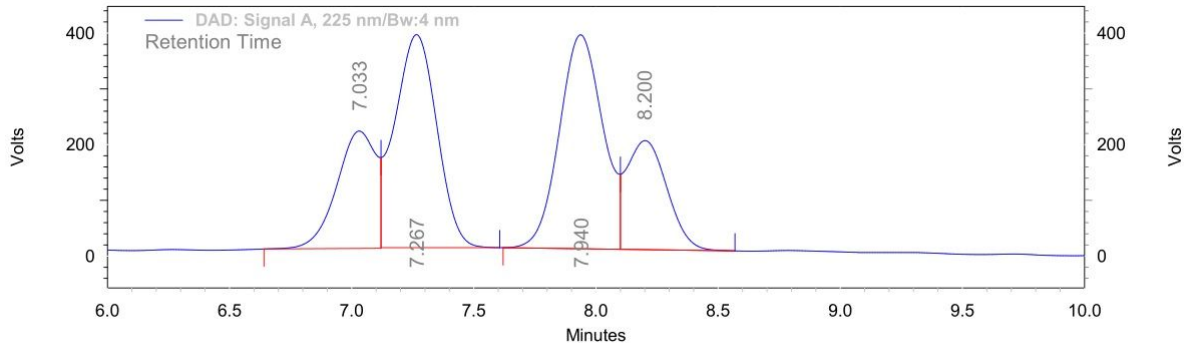
Retention time	19.193	20.973	35.34
product	(*1S,2R*)	(*1R,2S*)	(*1R,2R*)

Figure 3.63: HPLC chromatograms of 1-(3-methoxyphenyl)-2-nitropropan-1-ol. A. racemic standard, B. enantiopure product synthesized by *At*HNL-Y14C mutant enzyme.

4. 1-(3-methylphenyl)-2-nitropropan-1-ol

For % Conversion				Absolute conformation determination
Hexane: IPA	wavelength	Column	Flowrate	Assigned by analogy with the absolute configuration of compound 1-(3-(benzyloxy)phenyl)-2-nitropropan-1-ol
95:5	225 nm	Lux 5µm amylose 1	1 mL/min	
For % Enantiomeric excess, % Diastereomeric excess, % Isomeric content				
Hexane: IPA	wavelength	Column	Flowrate	
85:15	225 nm	Lux 5µm cellulose 1	1 mL/min	

A)

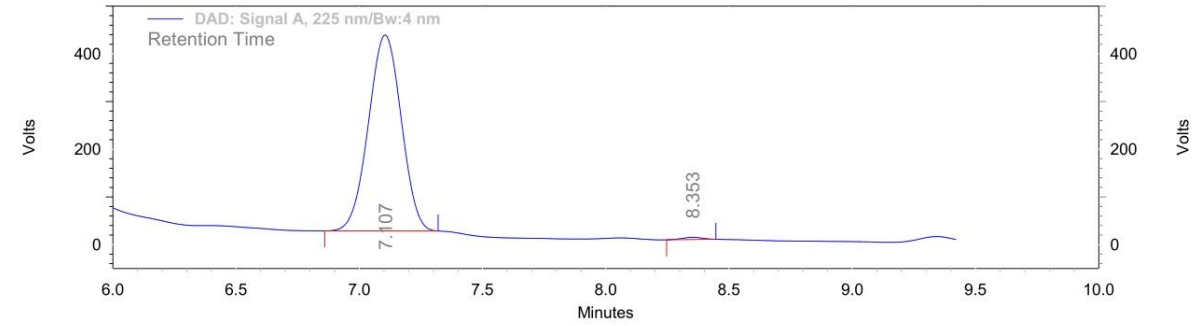


DAD: Signal A,
225 nm/Bw:4 nm
Results

Retention Time	Area	Area %	Height	Height %
7.033	4920535	16.81	441600	17.96
7.267	9632471	32.92	801837	32.61
7.940	9988062	34.13	804770	32.73
8.200	4723217	16.14	410521	16.70
Totals	29264285	100.00	2458728	100.00

Retention time	8.2	7.033	7.940	7.267
product	(*1S,2R*)	(*1R,2S*)	(*1S,2S*)	(*1R,2R*)

B)



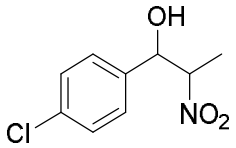
DAD: Signal A,
225 nm/Bw:4 nm
Results

Retention Time	Area	Area %	Height	Height %
7.107	7986210	99.32	861247	98.87
8.353	54612	0.68	9869	1.13
Totals	8040822	100.00	871116	100.00

Retention time	8.353	7.107
product	(*1S,2R*)	(*1R,2S*)

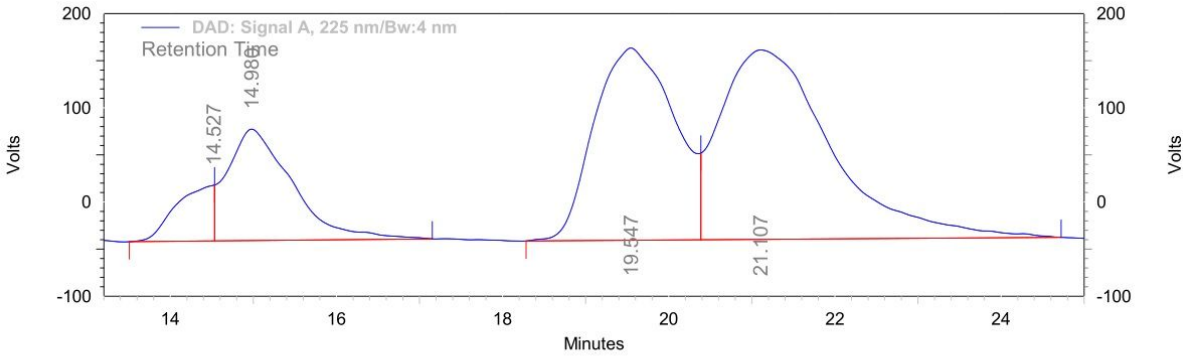
Figure 3.64: HPLC chromatograms of 1-(3-methylphenyl)-2-nitropropanol. A. racemic standard, B. enantiopure product synthesized by *At*HNL-Y14C mutant enzyme.

5. 1-(4-chlorophenyl)-2-nitropropan-1-ol



For % Conversion				Absolute conformation determination
Water: acetonitrile	wavelength	Column	Flowrate	Assigned by comparison with the reported literature[14]
60:40	222 nm	C_{18}	1 mL/min	
For % Enantiomeric excess, % Diastereomeric excess, % Isomeric content				
Hexane: IPA	wavelength	Column	Flowrate	
95:5	225 nm	Lux 5µm amylose 1	1 mL/min	

A)

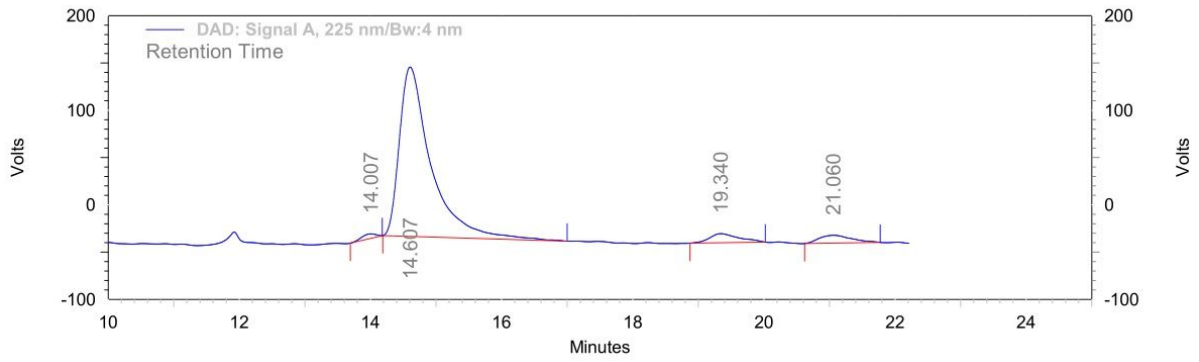


DAD: Signal A, 225 nm/Bw:4 nm
Results

Retention Time	Area	Area %	Height	Height %
14.527	3870370	4.54	124127	10.16
14.980	13417168	15.74	248069	20.30
19.547	28762585	33.73	427918	35.02
21.107	39215122	45.99	421716	34.52
Totals	85265245	100.00	1221830	100.00

Retention time	14.527	14.98	21.107	19.54
product	(*1S,2R*)	(*1R,2S*)	(*1S,2S*)	(*1R,2R*)

B)



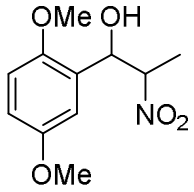
DAD: Signal A, 225 nm/Bw:4 nm Results

Retention Time	Area	Area %	Height	Height %
14.007	160382	1.15	9955	2.35
14.607	12535641	90.05	375602	88.78
19.340	630093	4.53	20178	4.77
21.060	594733	4.27	17312	4.09
Totals	13920849	100.00	423047	100.00

Retention time	14.007	14.607	21.06	19.34
product	(*1S,2R*)	(*1R,2S*)	(*1S,2S*)	(*1R,2R*)

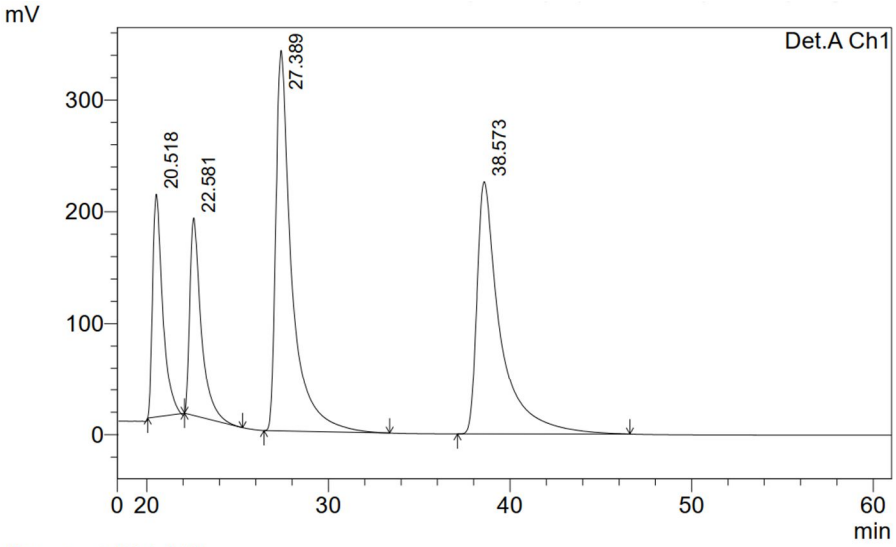
Figure 3.65: HPLC chromatograms of 1-(4-chlorophenyl)-2-nitropropan-1-ol. A. racemic standard, B. enantiopure product synthesized by *At*HNL-Y14C mutant enzyme.

6. 1-(2,5-dimethoxyphenyl)-2-nitropropan-1-ol



For % Conversion, % Enantiomeric excess, % Diastereomeric excess, % Isomeric content				Absolute conformation determination
Hexane: IPA	wavelength	Column	Flowrate	Assigned by comparison with the reported literature[16]
95:5 for 10 mins, 90:10 afterward	225 nm	Lux 5µm amylose 1	1 mL/min	

A)

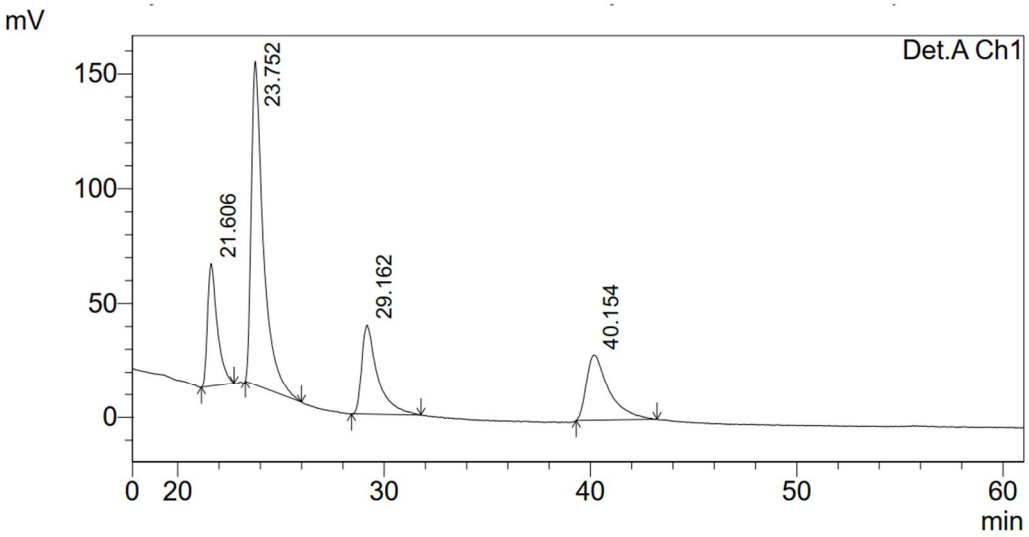


Detector A Ch1 210nm

Peak#	Ret. Time	Area	Height	Area %	Height %
1	20.518	7737754	200047	13.678	21.172
2	22.581	7733024	177477	13.670	18.783
3	27.389	20864001	341027	36.882	36.093
4	38.573	20234266	226308	35.769	23.952
Total		56569045	944859	100.000	100.000

Retention time	20.518	22.581	27.389	38.573
product	(*1S,2R*)	(*1R,2S*)	(*1S,2S*)	(*1R,2R*)

B)



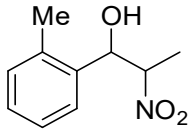
Detector A Ch1 210nm

Peak#	Ret. Time	Area	Height	Area %	Height %
1	21.606	1769970	53583	15.019	20.404
2	23.752	5726757	141062	48.593	53.716
3	29.162	2099561	39174	17.815	14.917
4	40.154	2188886	28787	18.573	10.962
Total		11785174	262606	100.000	100.000

Retention time	21.606	23.752	29.162	40.154
product	(*1S,2R*)	(*1R,2S*)	(*1S,2S*)	(*1R,2R*)

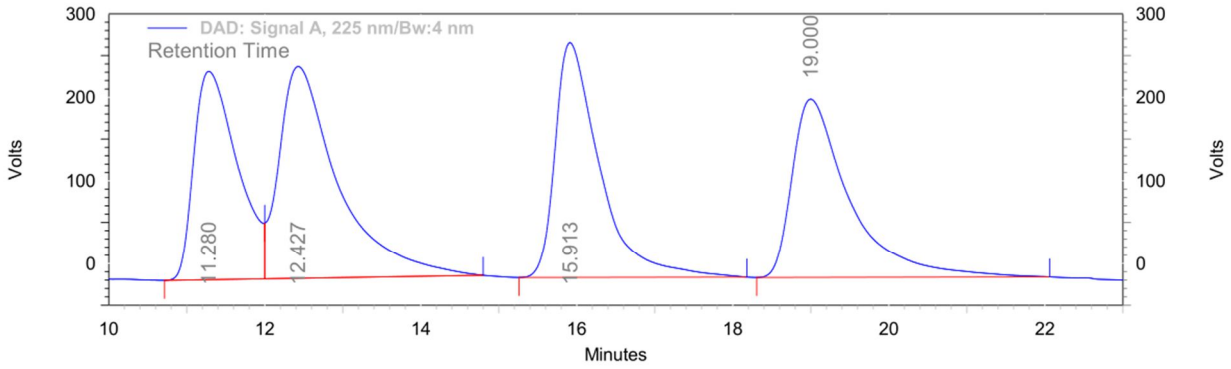
Figure 3.66: HPLC chromatograms of 1-(2,5-Dimethoxyphenyl)-2-nitropropan-1-ol. A. racemic standard, B. enantiopure product synthesized by *At*HNL-Y14C mutant enzyme.

7. 1-(2-methylphenyl)-2-nitropropan-1-ol



For % Conversion, % Enantiomeric excess, % Diastereomeric excess, % Isomeric content				Absolute conformation determination
Hexane: IPA	wavelength	Column	Flowrate	Assigned by comparison with the reported literature[14]
95:5	225 nm	Lux 5µm amylose 1	1 mL/min	

A)

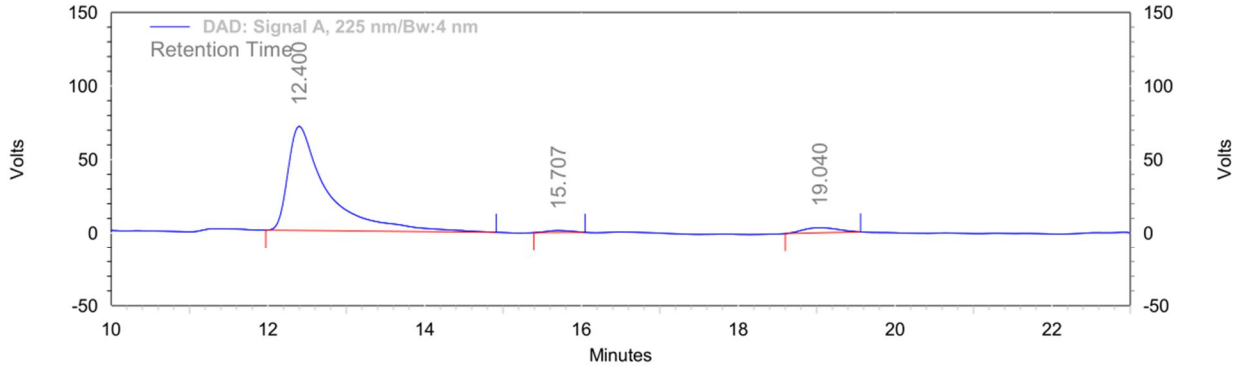


DAD: Signal A, 225 nm/Bw:4 nm
Results

Retention Time	Area	Area %	Height	Height %
11.280	20445139	21.47	525136	25.01
12.427	28120286	29.53	533782	25.42
15.913	23554630	24.74	591404	28.16
19.000	23096154	24.26	449664	21.41
Totals	95216209	100.00	2099986	100.00

Retention time	11.28	12.427	15.913	19
product	(*1S,2R*)	(*1R,2S*)	(*1S,2S*)	(*1R,2R*)

B)



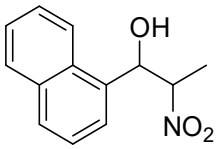
DAD: Signal A, 225 nm/Bw:4 nm Results

Retention Time	Area	Area %	Height	Height %
12.400	5118798	94.66	148260	93.66
15.707	62364	1.15	2867	1.81
19.040	226155	4.18	7172	4.53
Totals	5407317	100.00	158299	100.00

Retention time	12.4	15.707	19.04
product	(*1R,2S*)	(*1S,2S*)	(*1R,2R*)

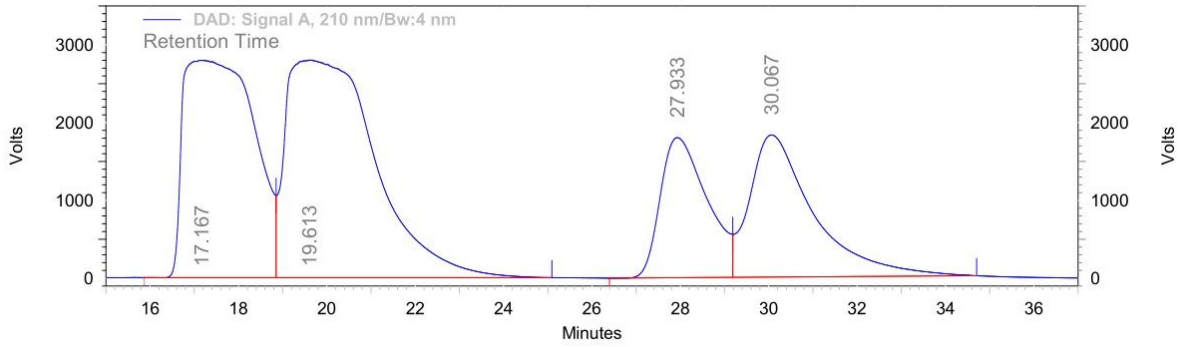
Figure 3.67: HPLC chromatograms of 1-(2-methylphenyl)-2-nitropropan-1-ol. A. racemic standard, B. enantiopure product synthesized by *At*HNL-Y14C mutant enzyme.

8. 1-(naphthalen-1-yl)-2-nitropropan-1-ol



For % Conversion				Absolute conformation determination
From standard curve				Assigned by comparison with the reported literature[15]
For % Enantiomeric excess, % Diastereomeric excess, % Isomeric content				
Hexane: IPA	wavelength	Column	Flowrate	
90:10	210 nm	Lux 5µm amylose 1	0.5 mL/min	

A)

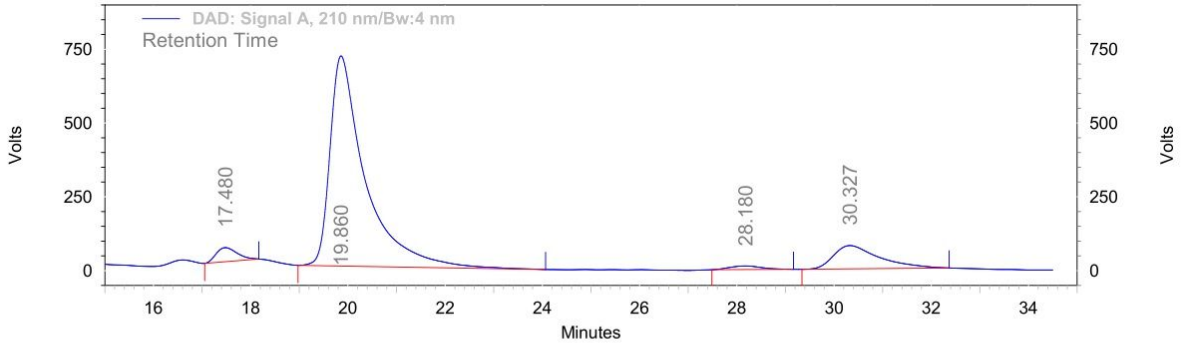


DAD: Signal A,
210 nm/Bw:4 nm
Results

Retention Time	Area	Area %	Height	Height %
17.167	653223027	30.43	5862531	30.31
19.613	830979730	38.71	5867952	30.34
27.933	277629494	12.93	3775579	19.52
30.067	384832144	17.93	3832821	19.82
Totals	2146664395	100.00	19338883	100.00

Retention time	17.167	19.613	27.933	30.067
product	(*1S,2R*)	(*1R,2S*)	(*1S,2S*)	(*1R,2R*)

B)



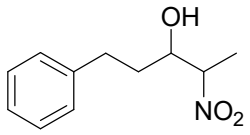
DAD: Signal A,
210 nm/Bw:4 nm
Results

Retention Time	Area	Area %	Height	Height %
17.480	3014925	3.35	99872	5.60
19.860	75085787	83.35	1492511	83.67
28.180	1159581	1.29	25658	1.44
30.327	10825173	12.02	165726	9.29
Totals	90085466	100.00	1783767	100.00

Retention time	17.48	19.86	28.18	30.327
product	(*1S,2R*)	(*1R,2S*)	(*1S,2S*)	(*1R,2R*)

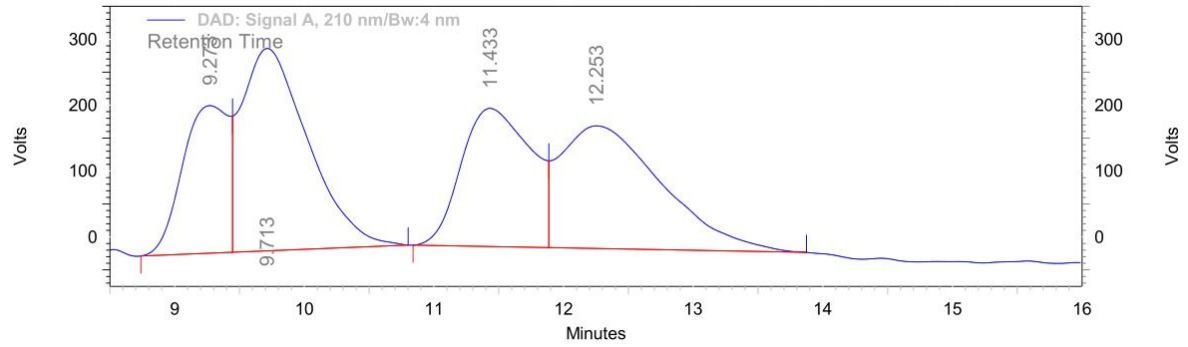
Figure 3.68: HPLC chromatograms of 1-(naphthalen-1-yl)-2-nitropropan-1-ol. A. racemic standard, B. enantiopure product synthesized by *At*HNL-Y14C mutant enzyme.

9. 4-nitro-1-phenylpentan-3-ol



For % Conversion, % Enantiomeric excess, % Diastereomeric excess, % Isomeric content				Absolute conformation determination
Hexane: IPA	wavelength	Column	Flowrate	Assigned by comparison with the reported literature[19]
90:10	210 nm	Lux 5µm amylose 1	1 mL/min	

A)

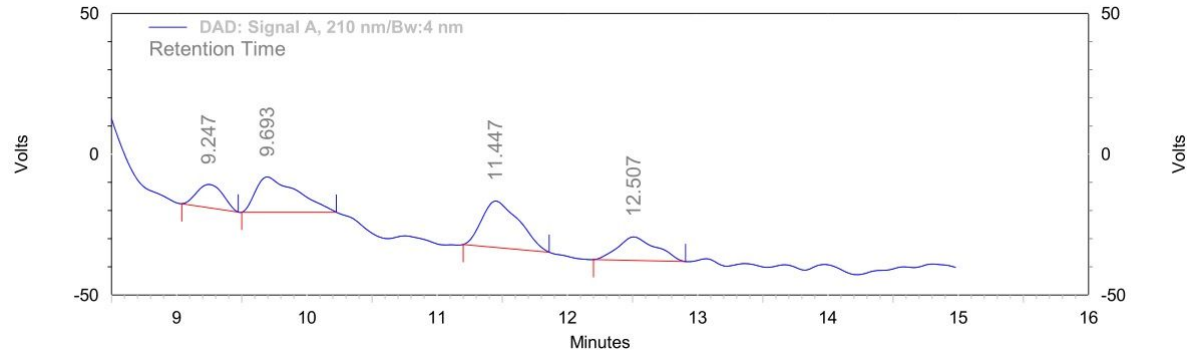


DAD: Signal A, 210 nm/Bw:4 nm
Results

Retention Time	Area	Area %	Height	Height %
9.273	11596841	16.03	469502	24.16
9.713	22979665	31.76	643951	33.14
11.433	16505377	22.81	439698	22.63
12.253	21270926	29.40	390255	20.08
Totals	72352809	100.00	1943406	100.00

Retention time	9.273	9.713	11.433	12.253
product	(*1S,2R*)	(*1R,2S*)	(*1S,2S*)	(*1R,2R*)

B)



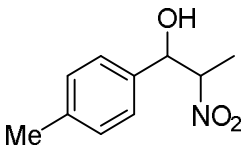
DAD: Signal A,
210 nm/Bw:4 nm
Results

Retention Time	Area	Area %	Height	Height %
9.247	243019	12.94	17327	18.12
9.693	584417	31.12	26274	27.47
11.447	690757	36.79	34527	36.10
12.507	359616	19.15	17515	18.31
Totals	1877809	100.00	95643	100.00

Retention time	9.247	9.693	11.447	12.507
product	(*1S,2R*)	(*1R,2S*)	(*1R,2R*)	(*1S,2S*)

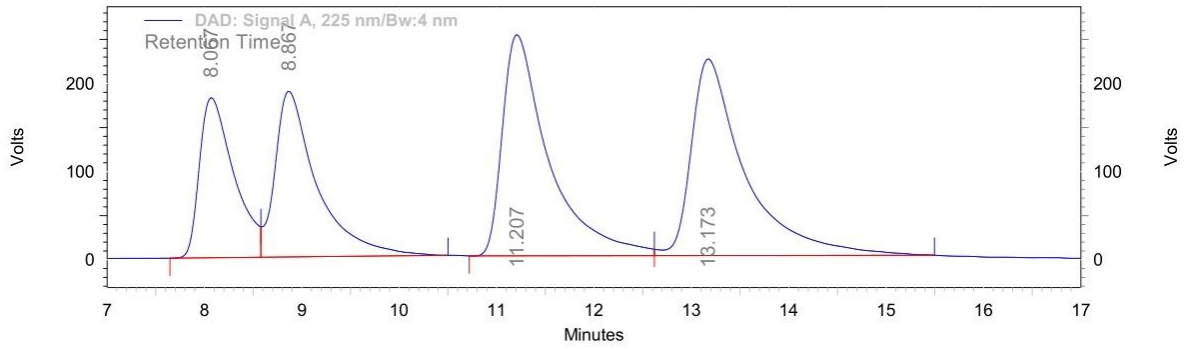
Figure 3.69: HPLC chromatograms of 4-nitro-1-phenylpentan-3-ol. A. racemic standard, B. enantiopure product synthesized by *At*HNL-Y14C mutant enzyme.

10. 1-(4-methylphenyl)-2-nitropropan-1-ol



For % Conversion				Absolute conformation determination
Water: acetonitrile	wavelength	Column	Flowrate	Assigned by analogy with the absolute configuration of compound 1-(2-methylphenyl)-2-nitropropan-1-ol
70:30	222 nm	C_{18}	1 mL/min	
For % Enantiomeric excess, % Diastereomeric excess, % Isomeric content				
Hexane: IPA	wavelength	Column	Flowrate	
90:10	225 nm	Lux 5µm amylose 1	1 mL/min	

A)

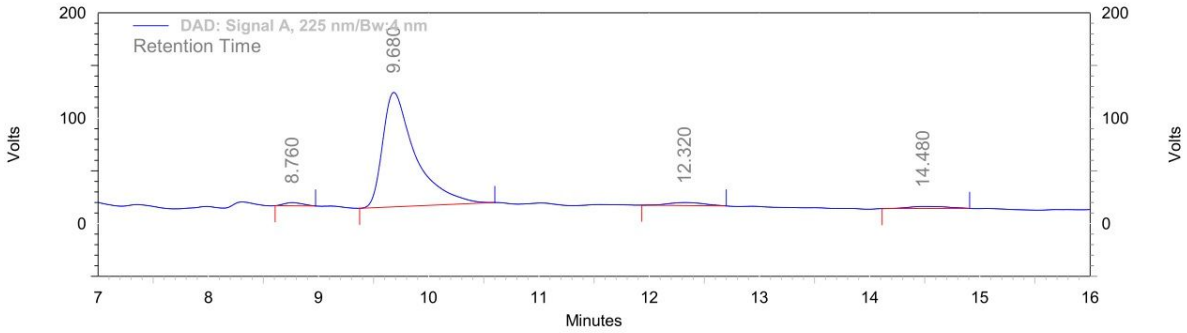


DAD: Signal A,
225 nm/Bw:4 nm
Results

Retention Time	Area	Area %	Height	Height %
8.067	9352700	16.56	380569	21.52
8.867	11744219	20.80	394110	22.28
11.207	17446689	30.90	526034	29.74
13.173	17926331	31.74	467827	26.45
Totals	56469939	100.00	1768540	100.00

Retention time	8.067	8.867	11.207	13.173
product	(*1S,2R*)	(*1R,2S*)	(*1S,2S*)	(*1R,2R*)

B)



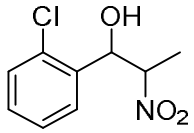
DAD: Signal A,
225 nm/Bw:4 nm
Results

Retention Time	Area	Area %	Height	Height %
8.760	73543	1.47	6250	2.56
9.680	4690499	93.81	227606	93.39
12.320	134582	2.69	5841	2.40
14.480	101545	2.03	4019	1.65
Totals	5000169	100.00	243716	100.00

Retention time	8.76	9.680	12.32	14.48
product	(*1S,2R*)	(*1R,2S*)	(*1S,2S*)	(*1R,2R*)

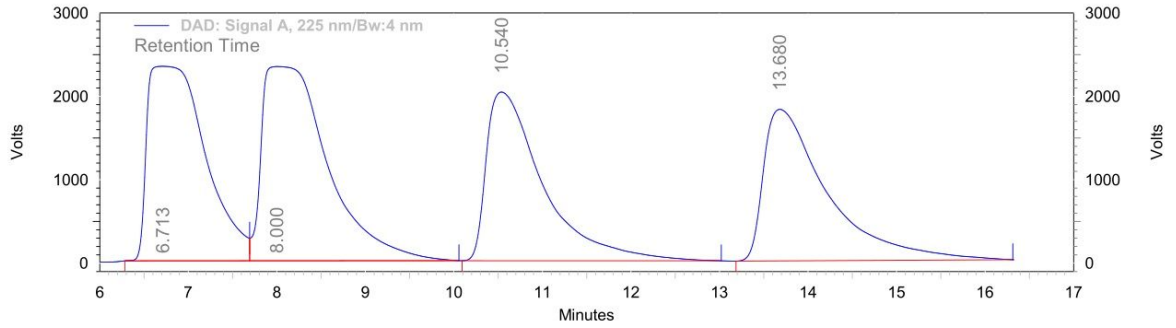
Figure 3.70: HPLC chromatograms of 1-(4-methylphenyl)-2-nitropropanol. A. racemic standard, B. enantiopure product synthesized by *At*HNL-Y14C mutant enzyme.

11. 1-(2-chlorophenyl)-2-nitropropan-1-ol



% Conversion, % Enantiomeric excess, % Diastereomeric excess, % Isomeric content				Absolute conformation determination
Hexane: IPA	wavelength	Column	Flowrate	Assigned by comparison with the reported literature[15]
90:10	225 nm	Lux 5µm amylose 1	1 mL/min	

A)

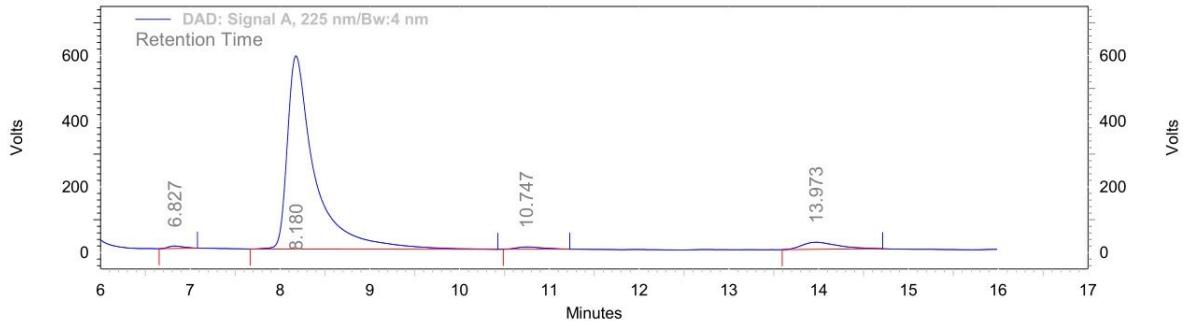


DAD: Signal A, 225 nm/Bw:4 nm
Results

Retention Time	Area	Area %	Height	Height %
6.713	222738764	26.06	4889094	27.43
8.000	252695631	29.57	4882619	27.40
10.540	188229089	22.02	4239058	23.79
13.680	191022457	22.35	3809950	21.38
Totals	854685941	100.00	17820721	100.00

Retention time	6.713	8	10.540	13.680
product	(*1S,2R*)	(*1R,2S*)	(*1S,2S*)	(*1R,2R*)

B)



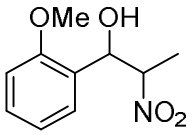
DAD: Signal A,
225 nm/Bw:4 nm
Results

Retention Time	Area	Area %	Height	Height %
6.827	188211	0.67	15782	1.20
8.180	26222644	93.67	1234417	94.22
10.747	307948	1.10	14512	1.11
13.973	1275221	4.56	45472	3.47
Totals	27994024	100.00	1310183	100.00

Retention time	6.827	8.18	10.747	13.973
product	(*1S,2R*)	(*1R,2S*)	(*1S,2S*)	(*1R,2R*)

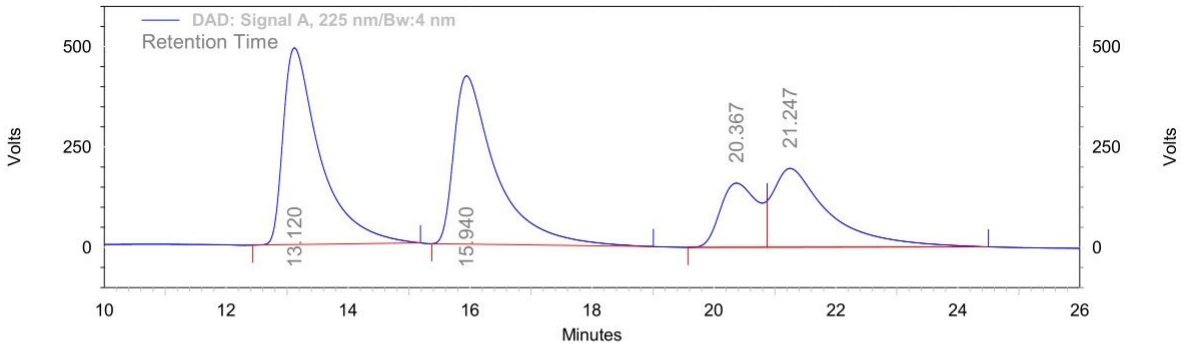
Figure 3.71: HPLC chromatograms of 1-(2-chlorophenyl)-2-nitropropan-1-ol. A. racemic standard, B. enantiopure product synthesized by *At*HNL-Y14C mutant enzyme.

12. 1-(2-methoxyphenyl)-2-nitropropan-1-ol



For % Conversion				Absolute conformation determination
Water: acetonitrile	wavelength	Column	Flowrate	Assigned by comparison with the reported literature[14]
70:30	222 nm	C_{18}	1 mL/min	
For % Enantiomeric excess, % Diastereomeric excess, % Isomeric content				
Hexane: IPA	wavelength	Column	Flowrate	
90:10	225 nm	Lux 5µm amylose 1	0.6 mL/min	

A)

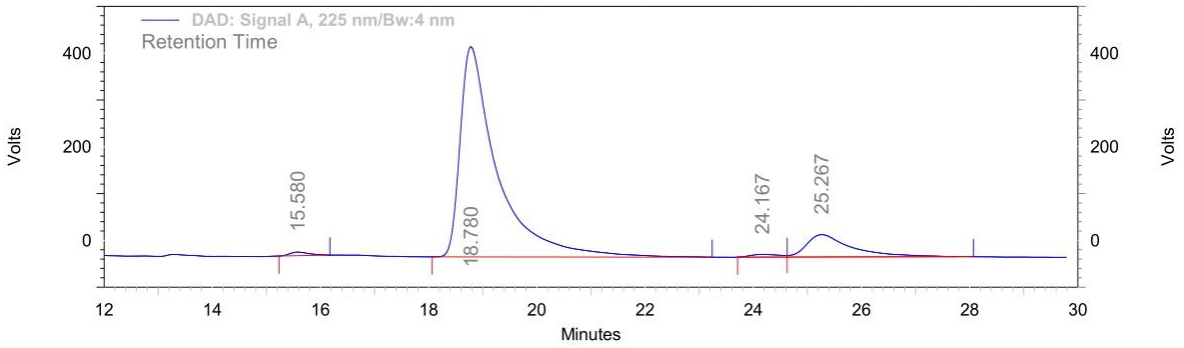


DAD: Signal A,
225 nm/Bw:4 nm
Results

Retention Time	Area	Area %	Height	Height %
13.120	43178691	34.30	1026853	38.72
15.940	42145045	33.48	878373	33.13
20.367	14417246	11.45	335056	12.64
21.247	26148837	20.77	411395	15.51
Totals	125889819	100.00	2651677	100.00

Retention time	13.12	15.94	20.367	21.247
product	(*1S,2R*)	(*1R,2S*)	(*1S,2S*)	(*1R,2R*)

B)



DAD: Signal A,
225 nm/Bw:4 nm
Results

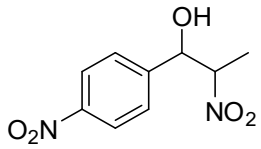
Retention Time	Area	Area %	Height	Height %
15.580	403191	0.78	16117	1.51
18.780	44849097	87.16	941249	87.99
24.167	441794	0.86	12273	1.15
25.267	5759882	11.19	100071	9.35
Totals	51453964	100.00	1069710	100.00

Retention time	15.58	18.78	24.167	25.267

product	(*1S,2R*)	(*1R,2S*)	(*1S,2S*)	(*1R,2R*)

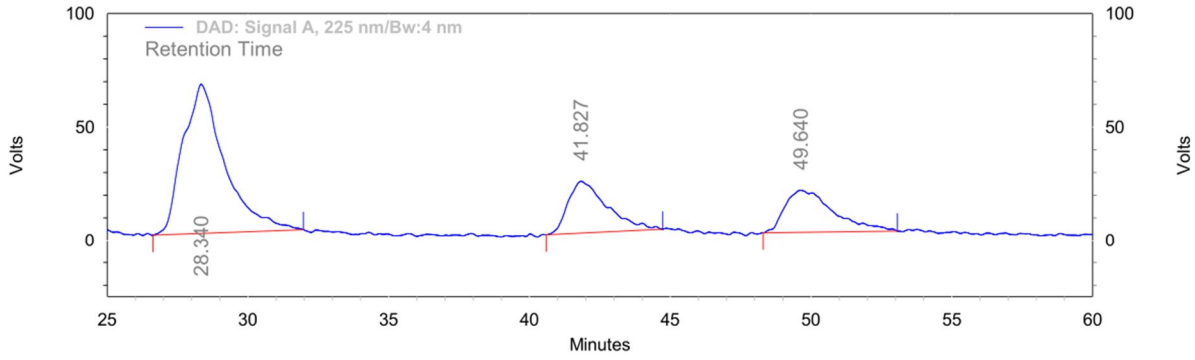
Figure 3.72: HPLC chromatograms of 1-(2-methoxyphenyl)-2-nitropropan-1-ol. A. racemic standard, B. enantiopure product synthesized by *At*HNL-Y14C mutant enzyme.

13. 1-(4-nitrophenyl)-2-nitropropan-1-ol



For % Conversion, % Enantiomeric excess of syn products, % Diastereomeric excess, % Isomeric content				Absolute conformation determination
Hexane: IPA	wavelength	Column	Flowrate	Assigned by comparison with the reported literature[14]
93:7	225 nm	Lux 5µm amylose 1	1 mL/min	
For % Enantiomeric excess of anti products				
Hexane: IPA	wavelength	Column	Flowrate	
96:4	225 nm	CHIRALPAK IB	1 mL/min	

A)

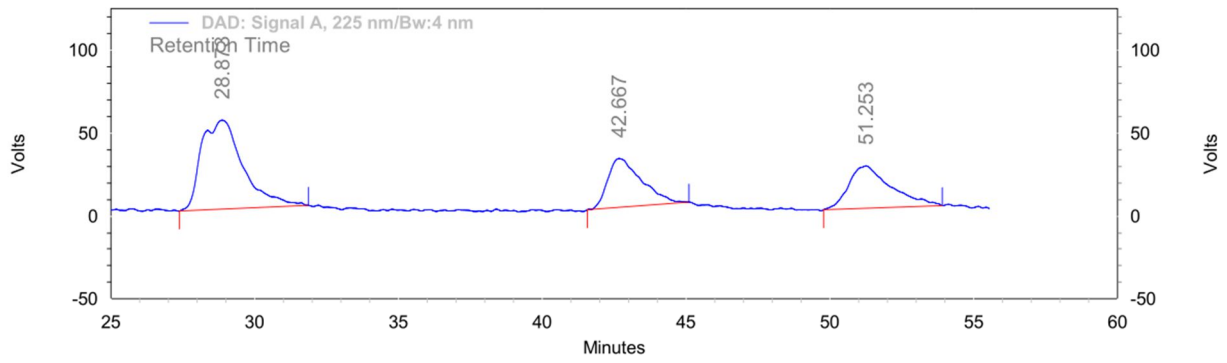


DAD: Signal A, 225 nm/Bw:4 nm
Results

Retention Time	Area	Area %	Height	Height %
28.340	14192792	60.49	137738	61.41
41.827	4600806	19.61	47778	21.30
49.640	4667858	19.90	38765	17.28
Totals	23461456	100.00	224281	100.00

Retention time	28.34	41.827	49.64
product	(*1S,2R*) +(*1R,2S*)	(*1R,2R*)	(*1S,2S*)

B)

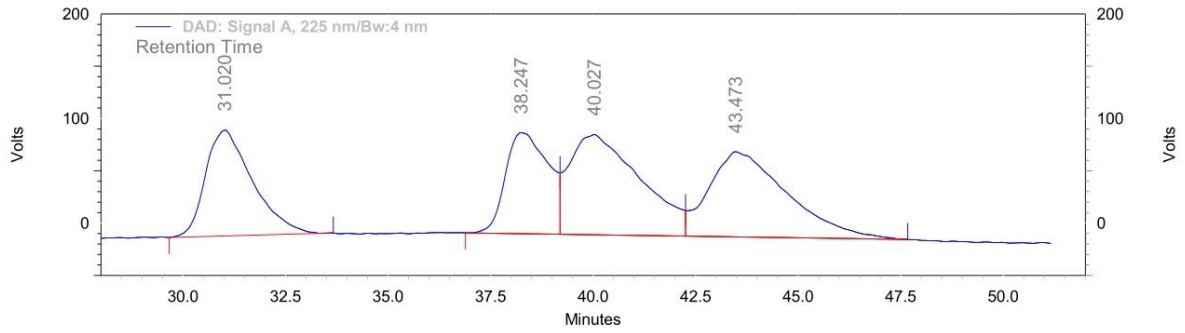


DAD: Signal A,
225 nm/Bw:4 nm
Results

Retention Time	Area	Area %	Height	Height %
28.873	11276824	51.81	112019	49.39
42.667	5029829	23.11	61477	27.10
51.253	5459954	25.08	53315	23.51
Totals	21766607	100.00	226811	100.00

Retention time	28.873	42.667	51.253
product	(*1S,2R*) +(*1R,2S*)	(*1R,2R*)	(*1S,2S*)

C)

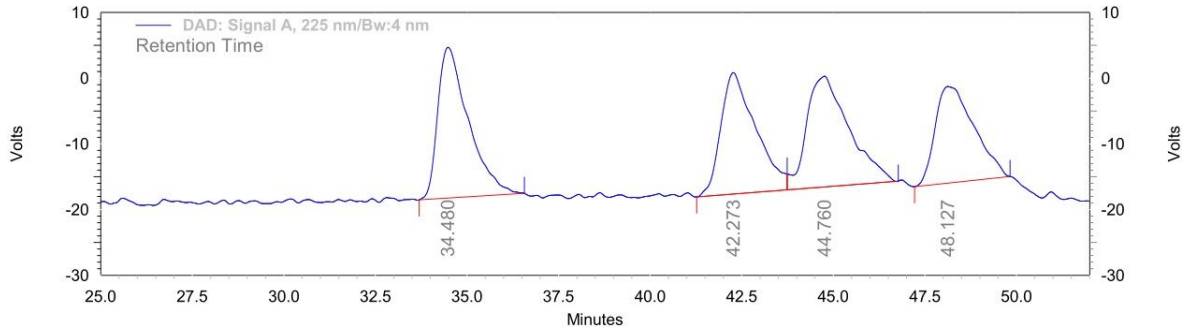


DAD: Signal A,
225 nm/Bw:4 nm
Results

Retention Time	Area	Area %	Height	Height %
31.020	16884143	21.52	212068	26.97
38.247	14692461	18.73	202506	25.76
40.027	24231844	30.89	200951	25.56
43.473	22648743	28.87	170732	21.71
Totals	78457191	100.00	786257	100.00

Retention time	38.24	31.02	40.027	43.473
product	(*1S,2R*)	(*1R,2S*)	(*1S,2S*) / (*1R,2R*)	(*1S,2S*) / (*1R,2R*)

D)



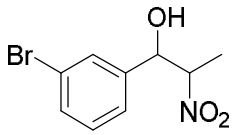
DAD: Signal A, 225 nm/Bw:4 nm
Results

Retention Time	Area	Area %	Height	Height %
34.480	2799299	26.70	48074	31.42
42.273	2565755	24.47	38735	25.32
44.760	2847954	27.16	35339	23.10
48.127	2272293	21.67	30851	20.16
Totals	10485301	100.00	152999	100.00

Retention time	42.273	34.48	44.76	48.127
product	(*1S,2R*)	(*1R,2S*)	(*1S,2S*) / (*1R,2R*)	(*1S,2S*) / (*1R,2R*)

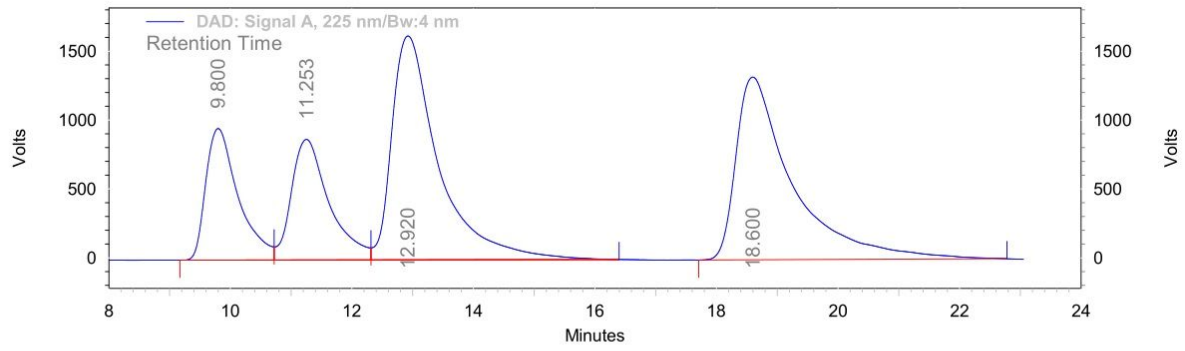
Figure 3.73: HPLC chromatograms of 1-(4-nitrophenyl)-2-nitropropan-1-ol. A. racemic standard in Lux amylose 1, B. enantiopure product in Lux amylose 1, C. racemic standard in CHIRALPAK IB, D) enantiopure product in CHIRALPAK IB synthesized by *At*HNL-Y14C mutant enzyme.

14. 1-(3-bromophenyl)-2-nitropropan-1-ol



For % Conversion				Absolute conformation determination
Water: acetonitrile	wavelength	Column	Flowrate	Assigned by comparison with the reported literature[14]
75:25	222 nm	C_{18}	1 mL/min	
For % Enantiomeric excess, % Diastereomeric excess, % Isomeric content				
Hexane: IPA	wavelength	Column	Flowrate	
93:7	225 nm	Lux 5µm amylose 1	1 mL/min	

A)

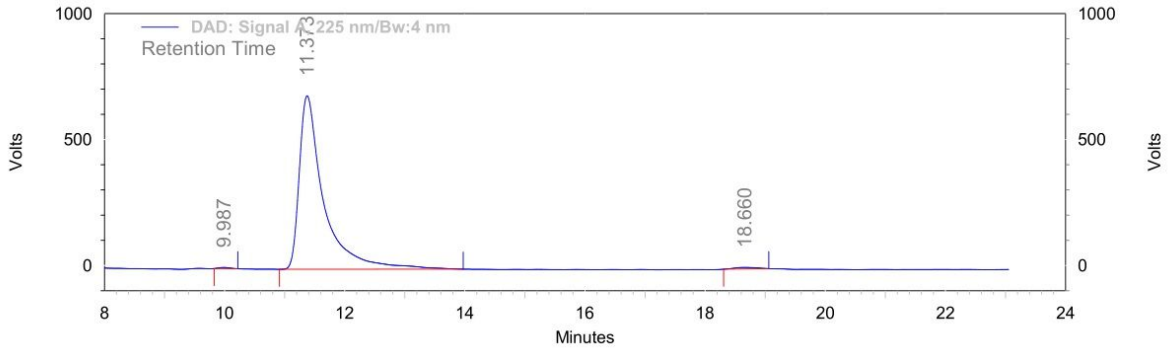


DAD: Signal A,
225 nm/Bw:4 nm
Results

Retention Time	Area	Area %	Height	Height %
9.800	74406413	14.44	2002531	19.97
11.253	79317546	15.39	1835824	18.31
12.920	181947384	35.31	3407644	33.98
18.600	179593926	34.85	2781067	27.74
Totals	515265269	100.00	10027066	100.00

Retention time	9.8	11.253	12.92	18.6
product	(*1S,2R*)	(*1R,2S*)	(*1S,2S*)	(*1R,2R*)

B)



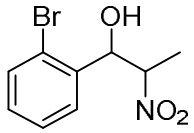
DAD: Signal A,
225 nm/Bw:4 nm
Results

Retention Time	Area	Area %	Height	Height %
9.987	121012	0.29	9433	0.64
11.373	40829401	98.92	1444049	98.50
18.660	323284	0.78	12524	0.85
Totals	41273697	100.00	1466006	100.00

Retention time	9.987	11.373	18.66
product	(*1S,2R*)	(*1R,2S*)	(*1R,2R*)

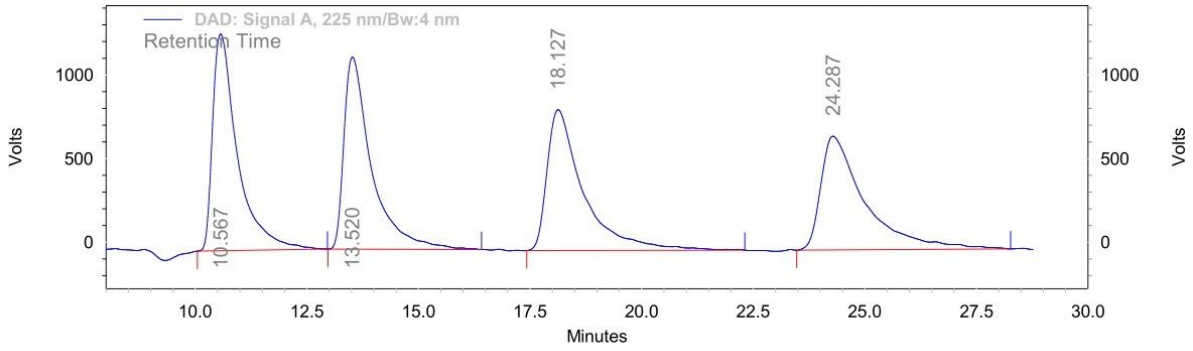
Figure 3.74: HPLC chromatograms of 1-(3-bromophenyl)-2-nitropropan-1-ol. A. racemic standard, B. enantiopure product synthesized by *At*HNL-Y14C mutant enzyme.

15. 1-(2-bromophenyl)-2-nitropropan-1-ol



For % Conversion, % Enantiomeric excess, % Diastereomeric excess, % Isomeric content				Absolute conformation determination
Hexane: IPA	wavelength	Column	Flowrate	Assigned by comparison with the reported literature[17]
93:7	225 nm	Lux 5µm amylose 1	1 mL/min	

A)

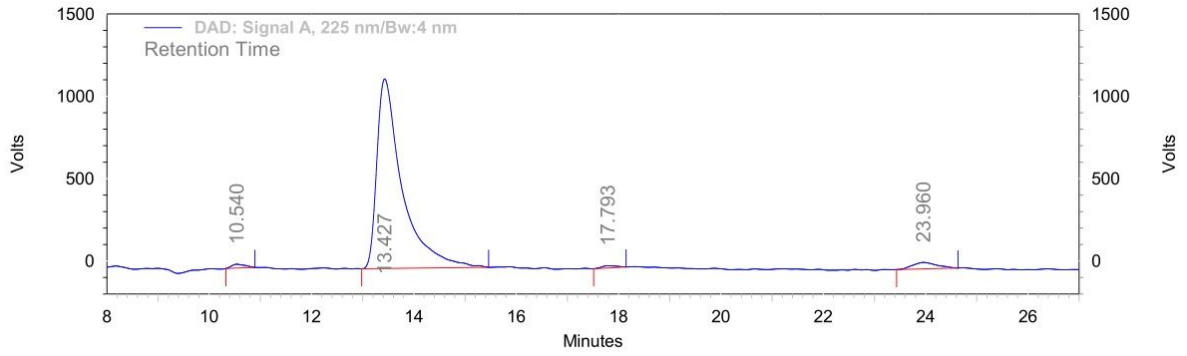


DAD: Signal A, 225 nm/Bw:4 nm
Results

Retention Time	Area	Area %	Height	Height %
10.567	105091058	25.88	2717416	32.68
13.520	103207390	25.41	2408059	28.96
18.127	99673687	24.54	1764573	21.22
24.287	98118267	24.16	1426338	17.15
Totals	406090402	100.00	8316386	100.00

Retention time	10.567	13.52	18.127	24.287
product	(*1S,2R*)	(*1R,2S*)	(*1S,2S*)	(*1R,2R*)

B)



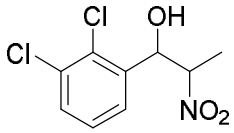
DAD: Signal A,
225 nm/Bw:4 nm
Results

Retention Time	Area	Area %	Height	Height %
10.540	901941	1.04	48859	1.90
13.427	82904443	95.22	2413514	93.80
17.793	557362	0.64	27883	1.08
23.960	2706608	3.11	82891	3.22
Totals	87070354	100.00	2573147	100.00

Retention time	10.54	13.427	17.793	23.96
product	(*1S,2R*)	(*1R,2S*)	(*1S,2S*)	(*1R,2R*)

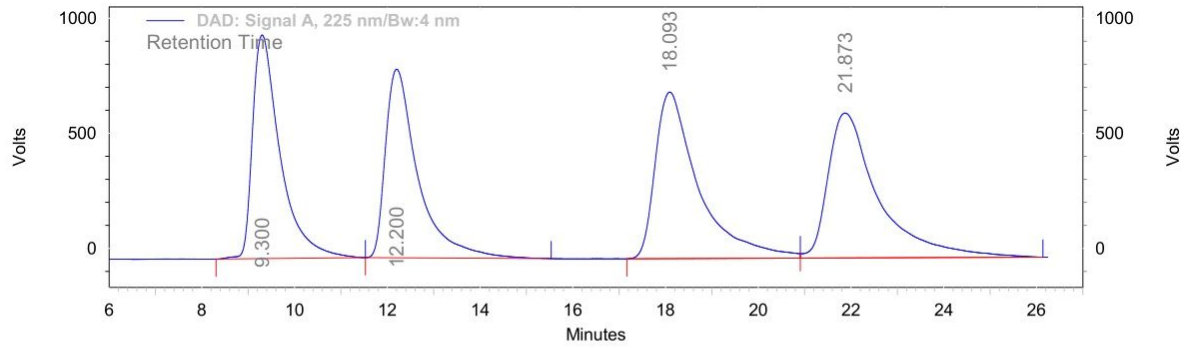
Figure 3.75: HPLC chromatograms of 1-(2-bromophenyl)-2-nitropropan-1-ol. A. racemic standard, B. enantiopure product synthesized by *At*HNL-Y14C mutant enzyme.

16. 1-(2,3-dichlorophenyl)-2-nitropropan-1-ol



For % Conversion, % Enantiomeric excess, % Diastereomeric excess, % Isomeric content				Absolute conformation determination
Hexane: IPA	wavelength	Column	Flowrate	Assigned by analogy with the absolute configuration of compound 1-(2-chlorophenyl)-2-nitropropan-1-ol
95:5	225 nm	Lux 5µm amylose 1	1 mL/min	

A)

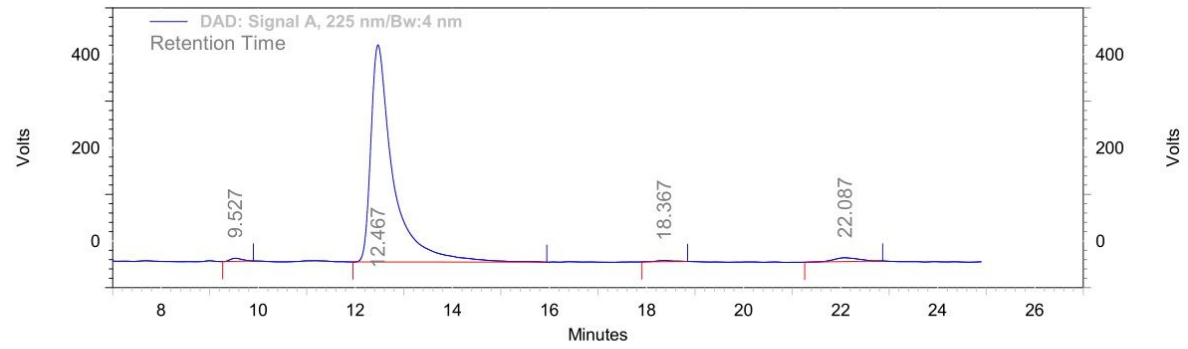


DAD: Signal A,
225 nm/Bw:4 nm
Results

Retention Time	Area	Area %	Height	Height %
9.300	84239109	23.04	2037308	30.90
12.200	83407382	22.81	1718599	26.07
18.093	98415882	26.92	1517694	23.02
21.873	99557404	27.23	1319847	20.02
Totals	365619777	100.00	6593448	100.00

Retention time	9.3	12.2	18.093	21.873
product	(*1S,2R*)	(*1R,2S*)	(*1S,2S*)	(*1R,2R*)

B)



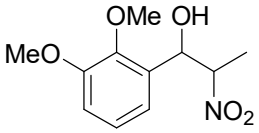
DAD: Signal A,
225 nm/Bw:4 nm
Results

Retention Time	Area	Area %	Height	Height %
9.527	240420	0.75	13802	1.36
12.467	31176020	96.97	976577	96.44
18.367	125055	0.39	5211	0.51
22.087	607321	1.89	17074	1.69
Totals	32148816	100.00	1012664	100.00

Retention time	9.527	12.467	18.367	22.087
product	(*1S,2R*)	(*1R,2S*)	(*1S,2S*)	(*1R,2R*)

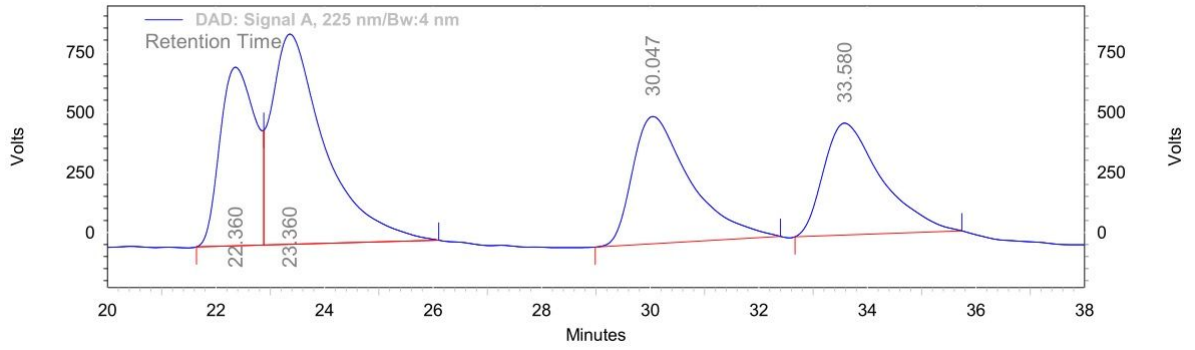
Figure 3.76: HPLC chromatograms of 1-(2,3-dichlorophenyl)-2-nitropropan-1-ol. A. racemic standard, B. enantiopure product synthesized by *At*HNL-Y14C mutant enzyme.

17. 1-(2,3-dimethoxyphenyl)-2-nitropropan-1-ol



For % Conversion				Absolute conformation determination
Water: acetonitrile	wavelength	Column	Flowrate	Assigned by analogy with the absolute configuration of compound 1-(2,5-dimethoxyphenyl)-2-nitropropan-1-ol
85:15	222 nm	C_{18}	1 mL/min	
For % Enantiomeric excess, % Diastereomeric excess, % Isomeric content				
Hexane: IPA	wavelength	Column	Flowrate	
93:7	225 nm	Lux 5µm amylose 1	0.5 mL/min	

A)

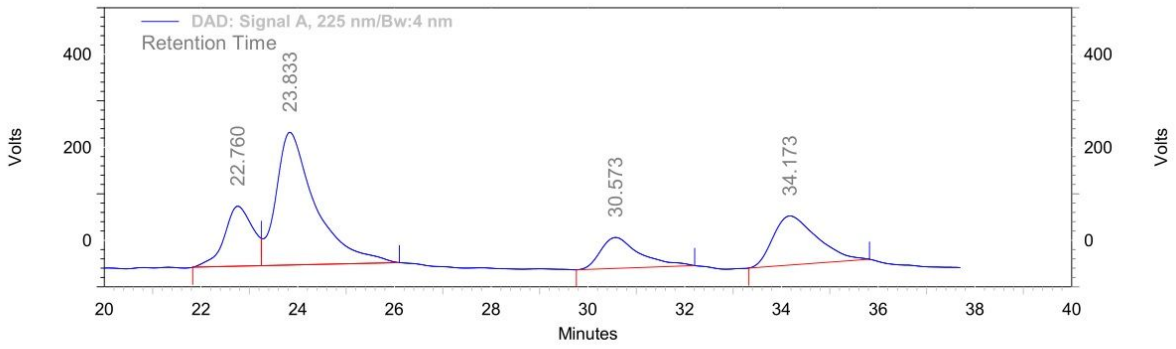


DAD: Signal A, 225 nm/Bw:4 nm
Results

Retention Time	Area	Area %	Height	Height %
22.360	70389397	20.14	1556827	28.44
23.360	125139700	35.81	1832352	33.47
30.047	81664690	23.37	1109441	20.27
33.580	72287828	20.68	975258	17.82
Totals	349481615	100.00	5473878	100.00

Retention time	22.36	23.36	30.047	33.58
product	(*1S,2R*)	(*1R,2S*)	(*1S,2S*)	(*1R,2R*)

B)



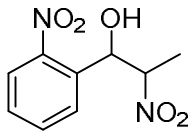
DAD: Signal A,
225 nm/Bw:4 nm
Results

Retention Time	Area	Area %	Height	Height %
22.760	11022895	16.49	270523	22.00
23.833	34024734	50.92	598365	48.65
30.573	7845944	11.74	139491	11.34
34.173	13932299	20.85	221454	18.01
Totals	66825872	100.00	1229833	100.00

Retention time	22.76	23.833	30.573	34.173
product	(*1S,2R*)	(*1R,2S*)	(*1S,2S*)	(*1R,2R*)

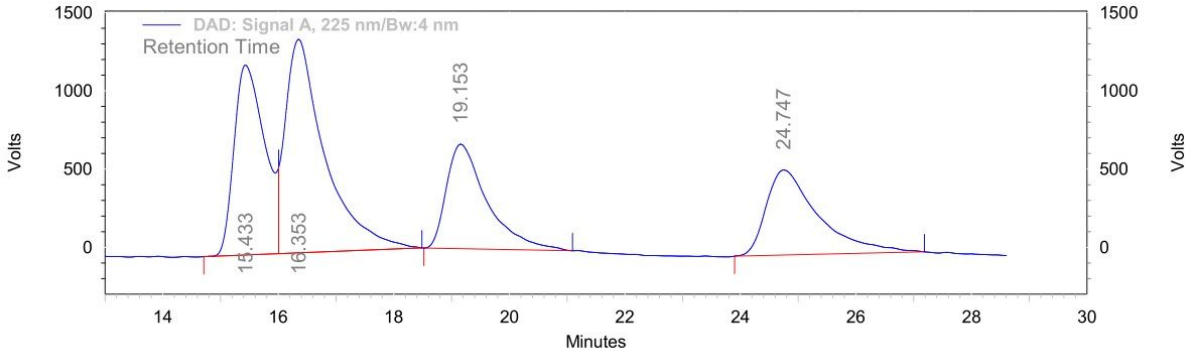
Figure 3.77: HPLC chromatograms of 1-(2,3-dimethoxyphenyl)-2-nitropropan-1-ol. A. racemic standard, B. enantiopure product synthesized by *At*HNL-Y14C mutant enzyme.

18. 1-(2-nitrophenyl)-2-nitropropan-1-ol



For % Conversion, % Enantiomeric excess, % Diastereomeric excess, % Isomeric content				Absolute conformation determination
Hexane: IPA	wavelength	Column	Flowrate	Assigned by comparison with the reported literature[18]
90:10	225 nm	Lux 5µm amylose 1	1 mL/min	

A)

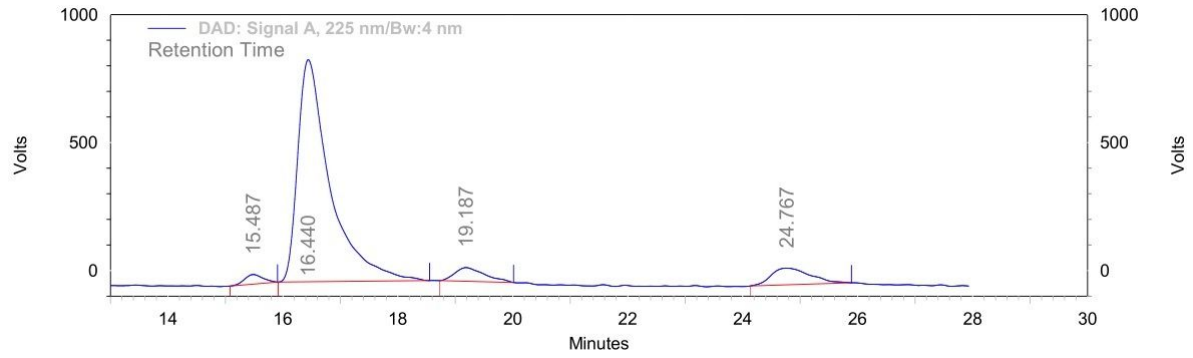


DAD: Signal A,
225 nm/Bw:4 nm
Results

Retention Time	Area	Area %	Height	Height %
15.433	94524019	25.57	2543372	32.02
16.353	135622763	36.69	2859369	36.00
19.153	68212253	18.45	1399980	17.63
24.747	71257830	19.28	1139122	14.34
Totals	369616865	100.00	7941843	100.00

Retention time	15.433	16.353	19.153	24.747
product	(*1S,2R*)	(*1R,2S*)	(*1S,2S*)	(*1R,2R*)

B)



DAD: Signal A,
225 nm/Bw:4 nm
Results

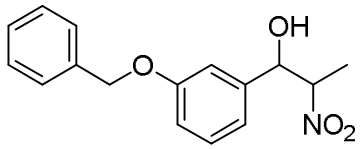
Retention Time	Area	Area %	Height	Height %
15.487	1741327	2.09	78460	3.66
16.440	71096772	85.28	1819234	84.76
19.187	4066380	4.88	112152	5.23
24.767	6462659	7.75	136401	6.36
Totals	83367138	100.00	2146247	100.00

Retention time	15.487	16.44	19.187	24.767

product	(*1S,2R*)	(*1R,2S*)	(*1S,2S*)	(*1R,2R*)

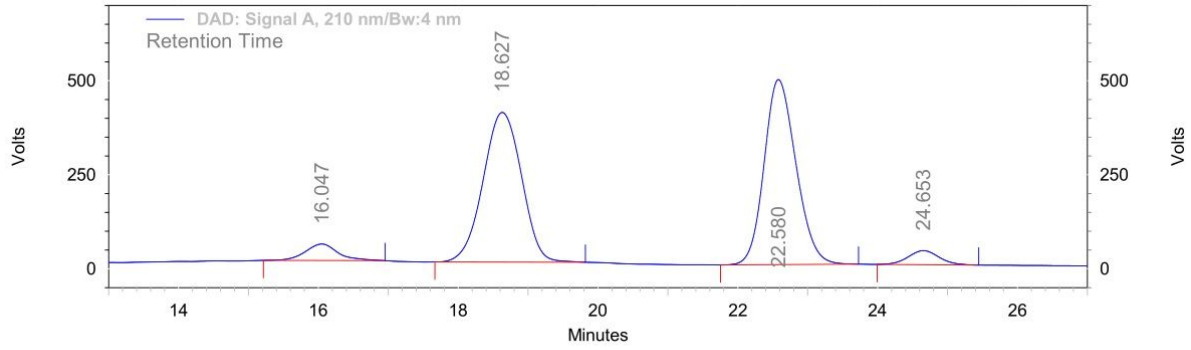
Figure 3.78: HPLC chromatograms of 1-(2-nitrophenyl)-2-nitropropanol. A. racemic standard, B. enantiopure product synthesized by *At*HNL-Y14C mutant enzyme.

19. 1-(3-(benzyloxy)phenyl)-2-nitropropan-1-ol



For % Conversion, % Enantiomeric excess, % Diastereomeric excess, % Isomeric content				Absolute conformation determination
Hexane: IPA	wavelength	Column	Flowrate	Assigned by comparison with the reported literature[16]
90:10	210 nm	CHIRALPAK IB	0.8 mL/min	

A)

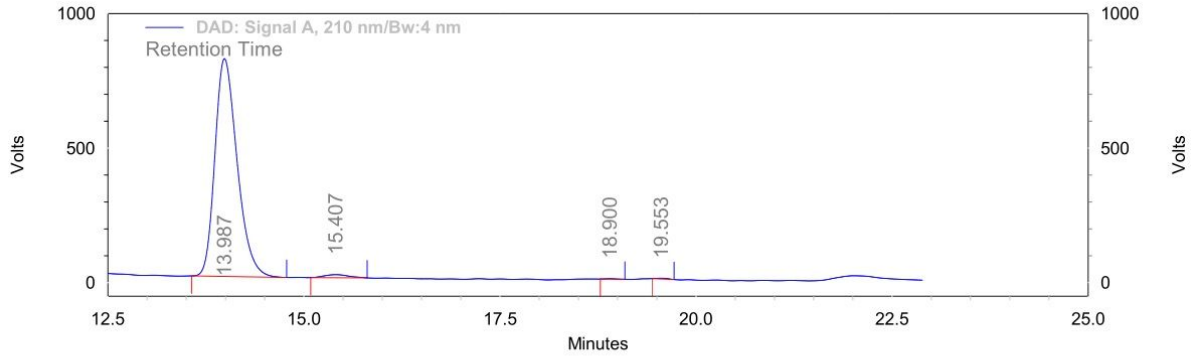


DAD: Signal A, 210 nm/Bw:4 nm
Results

Retention Time	Area	Area %	Height	Height %
16.047	3000371	4.29	91835	4.51
18.627	31893531	45.57	833993	40.98
22.580	32681935	46.69	1031266	50.67
24.653	2416183	3.45	78243	3.84
Totals	69992020	100.00	2035337	100.00

Retention time	24.563	16.047	22.580	18.627
product	(*1S,2R*)	(*1R,2S*)	(*1S,2S*)	(*1R,2R*)

B)



DAD: Signal A, 210 nm/Bw:4 nm Results

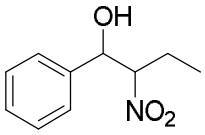
Retention Time	Area	Area %	Height	Height %
13.987	33498881	98.23	1697335	98.11
15.407	513500	1.51	23646	1.37
18.900	27614	0.08	3094	0.18
19.553	63728	0.19	6021	0.35
Totals	34103723	100.00	1730096	100.00

Retention time	19.553	13.987	18.9	15.407
product	(*1S,2R*)	(*1R,2S*)	(*1S,2S*)	(*1R,2R*)

Figure 3.79: HPLC chromatograms of 1-(3-(benzyloxy)phenyl)-2-nitropropan-1-ol. A. racemic standard, B. enantiopure product synthesized by *At*HNL-Y14C mutant enzyme.

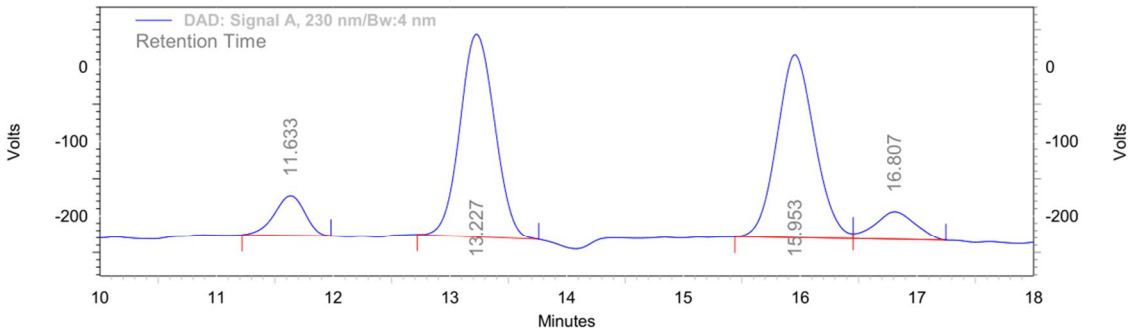
3.4.23. HPLC conditions and HPLC traces of racemic standard β-nitroalcohols and enantiopure product synthesized by *At*HNL-Y14A mutant enzyme

1. 2-nitro-1-phenylbutan-1-ol (NPB)



For % Conversion				Absolute conformation determination
Water: acetonitrile	wavelength	Column	Flowrate	Assigned by comparison with the reported literature[26]
80:20	222 nm	C_{18}	1 mL/min	
For % Enantiomeric excess, % Diastereomeric excess, % Isomeric content				
Hexane: IPA	wavelength	Column	Flowrate	
90:10	230 nm	Lux 5µm cellulose 1	0.9 mL/min	

A)

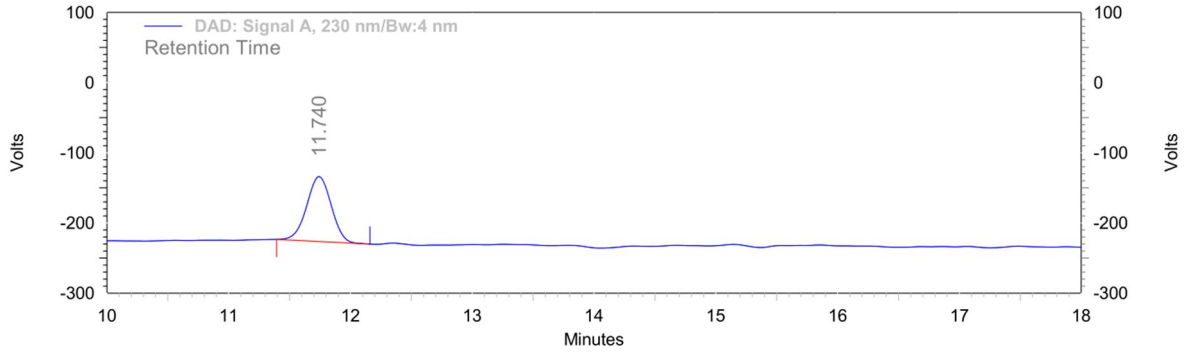


DAD: Signal A,
230 nm/Bw:4 nm
Results

Retention Time	Area	Area %	Height	Height %
11.633	2052710	7.49	112670	8.81
13.227	11821643	43.11	571485	44.69
15.953	11639602	42.45	515829	40.34
16.807	1905197	6.95	78861	6.17
Totals	27419152	100.00	1278845	100.00

Retention time	16.807	11.633	15.953	13.227
product	(*1S,2R*)	(*1R,2S*)	(*1S,2S*)	(*1R,2R*)

B)



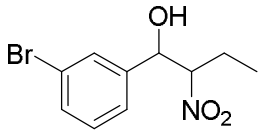
DAD: Signal A,
230 nm/Bw:4 nm
Results

Retention Time	Area	Area %	Height	Height %
11.740	2722175	100.00	193892	100.00
Totals	2722175	100.00	193892	100.00

Retention time	11.74
product	(*1R,2S*)

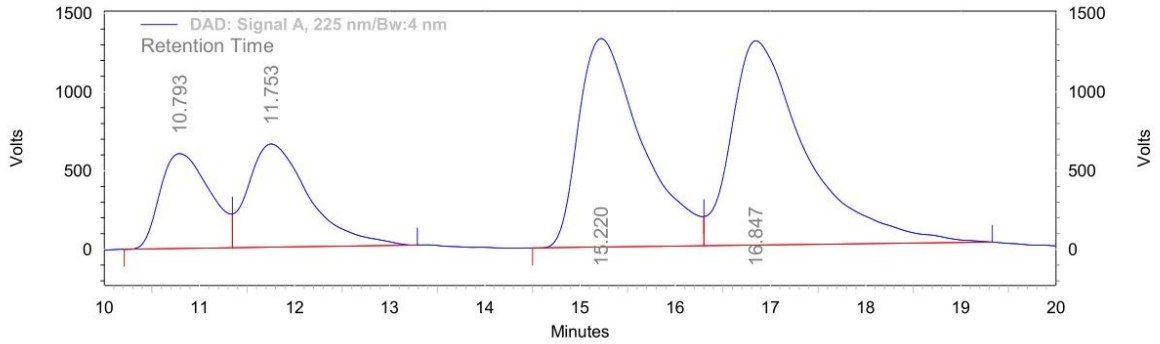
Figure 3.80: HPLC chromatograms of 2-nitro 1-phenyl butanol. A. racemic standard, B. enantiopure product synthesized by *At*HNL-Y14A mutant enzyme.

2. 1-(3-Bromophenyl)-2-nitrobutan-1-ol



For % Conversion				Absolute conformation determination
Water: acetonitrile	wavelength	Column	Flowrate	Assigned by analogy with the absolute configuration of compound 1-(3-bromophenyl)-2-nitropropan-1-ol
65:35	222 nm	C_{18}	1 mL/min	
For % Enantiomeric excess, % Diastereomeric excess, % Isomeric content				
Hexane: IPA	wavelength	Column	Flowrate	
93:7	225 nm	Lux 5µm amylose 1	1 mL/min	

A)

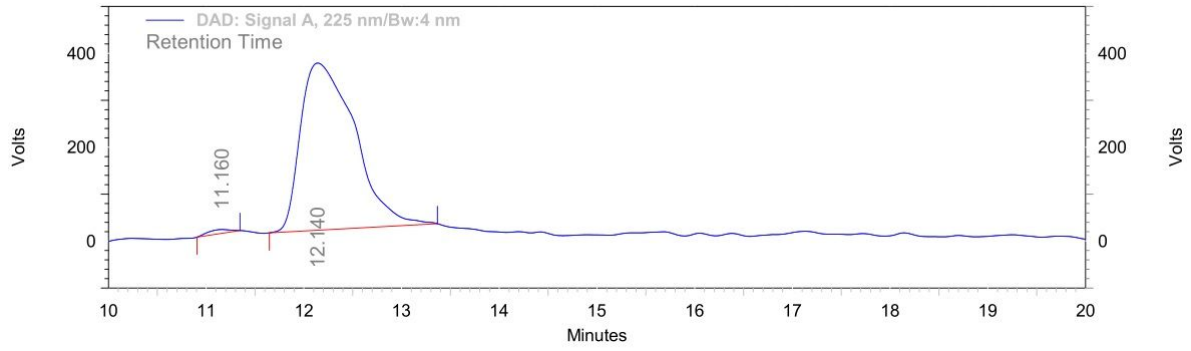


DAD: Signal A, 225 nm/Bw:4 nm
Results

Retention Time	Area	Area %	Height	Height %
10.793	46156558	11.94	1264281	15.53
11.753	61345139	15.87	1374987	16.89
15.220	129109632	33.40	2778687	34.13
16.847	149899568	38.78	2722731	33.45
Totals	386510897	100.00	8140686	100.00

Retention time	10.793	11.753	15.22	16.847
product	(*1S,2R*)	(*1R,2S*)	(*1S,2S*)	(*1R,2R*)

B)



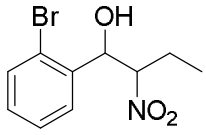
DAD: Signal A,
225 nm/Bw:4 nm
Results

Retention Time	Area	Area %	Height	Height %
11.160	288784	0.99	16943	2.22
12.140	28749252	99.01	746717	97.78
Totals	29038036	100.00	763660	100.00

Retention time	11.16	12.14
product	(*1S,2R*)	(*1R,2S*)

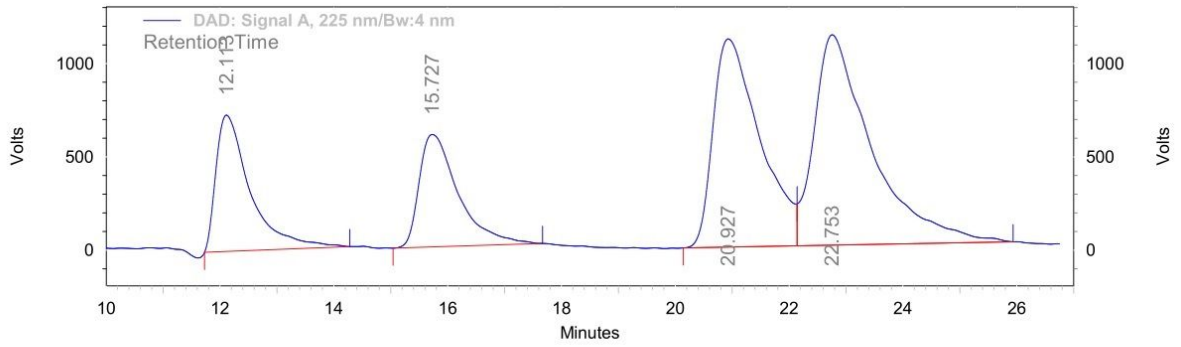
Figure 3.81: HPLC chromatograms of 1-(3-bromophenyl)-2-nitrobutan-1-ol. A. racemic standard, B. enantiopure product synthesized by *At*HNL-Y14A mutant enzyme.

3. 1-(2-bromophenyl)-2-nitrobutan-1-ol



For % Conversion, % Enantiomeric excess, % Diastereomeric excess, % Isomeric content				Absolute conformation determination
Hexane: IPA	wavelength	Column	Flowrate	Assigned by analogy with the absolute configuration of compound 1-(2-bromophenyl)-2-nitropropanol
95:5	210 nm	Lux 5µm amylose 1	1 mL/min	

A)

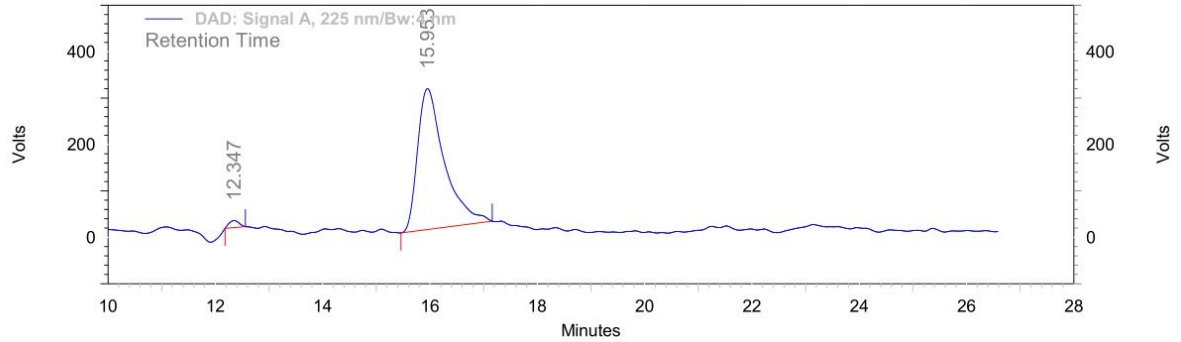


DAD: Signal A,
225 nm/Bw:4 nm
Results

Retention Time	Area	Area %	Height	Height %
12.113	64103981	15.11	1532212	20.43
15.727	60250615	14.20	1263525	16.84
20.927	133897034	31.56	2340538	31.20
22.753	166020897	39.13	2364993	31.53
Totals	424272527	100.00	7501268	100.00

Retention time	12.113	15.727	20.927	22.753
product	(*1S,2R*)	(*1R,2S*)	(*1S,2S*)	(*1R,2R*)

B)



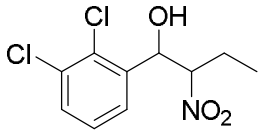
DAD: Signal A,
225 nm/Bw:4 nm
Results

Retention Time	Area	Area %	Height	Height %
12.347	410588	1.82	31911	4.78
15.953	22104992	98.18	636349	95.22
Totals	22515580	100.00	668260	100.00

Retention time	12.347	15.953
product	(*1S,2R*)	(*1R,2S*)

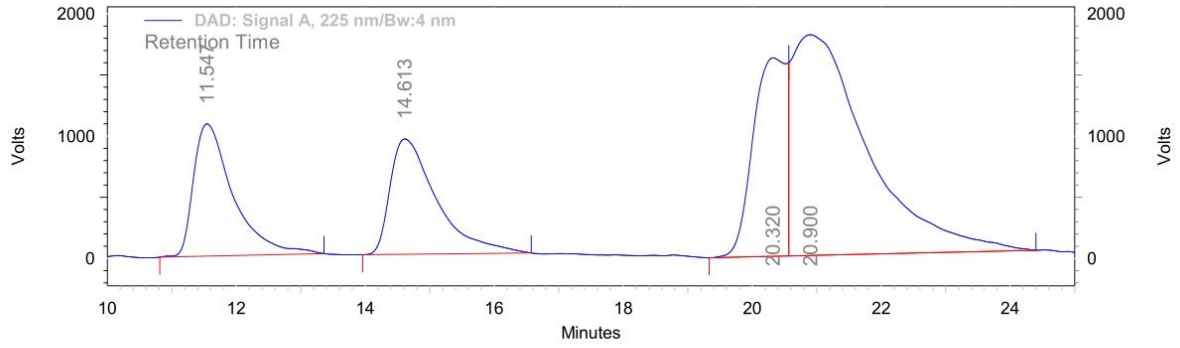
Figure 3.82: HPLC chromatograms of 1-(2-bromophenyl)-2-nitro butanol. A. racemic standard, B. enantiopure product synthesized by *At*HNL-Y14A mutant enzyme.

4. 1-(2,3-dichlorophenyl)-2-nitrobutan-1-ol



For % Conversion				Absolute conformation determination
Water: acetonitrile	wavelength	Column	Flowrate	Assigned by analogy with the absolute configuration of compound 1-(2-chlorophenyl)-2-nitropropanol
65:35	222 nm	C_{18}	1 mL/min	
For % Enantiomeric excess, % Diastereomeric excess, % Isomeric content				
Hexane: IPA	wavelength	Column	Flowrate	
95:5	225 nm	Lux 5µm amylose 1	1 mL/min	

A)

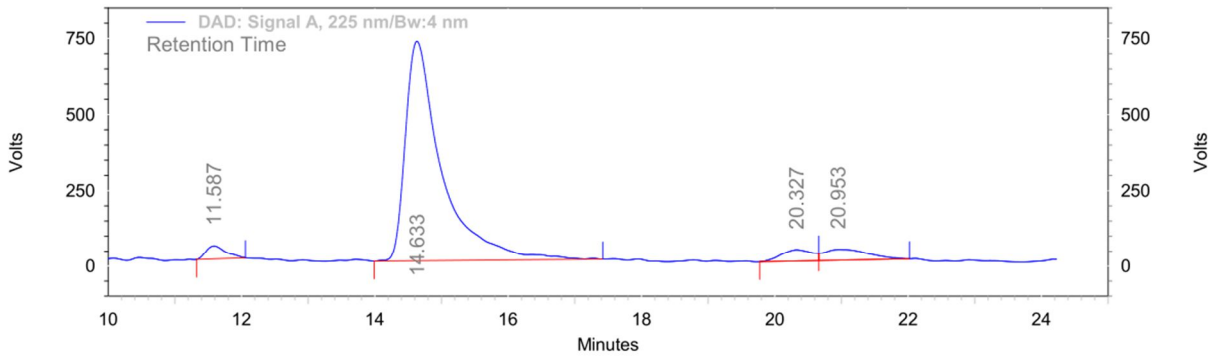


DAD: Signal A, 225 nm/Bw:4 nm
Results

Retention Time	Area	Area %	Height	Height %
11.547	96538767	15.42	2267146	19.83
14.613	98948996	15.80	1978405	17.30
20.320	121986452	19.48	3402722	29.76
20.900	308623717	49.29	3785371	33.11
Totals	626097932	100.00	11433644	100.00

Retention time	11.547	14.613	20.32	20.9
product	(*1S,2R*)	(*1R,2S*)	(*1S,2S*)	(*1R,2R*)

B)



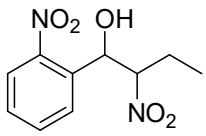
DAD: Signal A,
225 nm/Bw:4 nm
Results

Retention Time	Area	Area %	Height	Height %
11.587	1925378	2.92	92695	5.24
14.633	57719760	87.68	1517741	85.83
20.327	2625587	3.99	81168	4.59
20.953	3557402	5.40	76807	4.34
Totals	65828127	100.00	1768411	100.00

Retention time	11.587	14.633	20.327	20.953
product	(*1S,2R*)	(*1R,2S*)	(*1S,2S*)	(*1R,2R*)

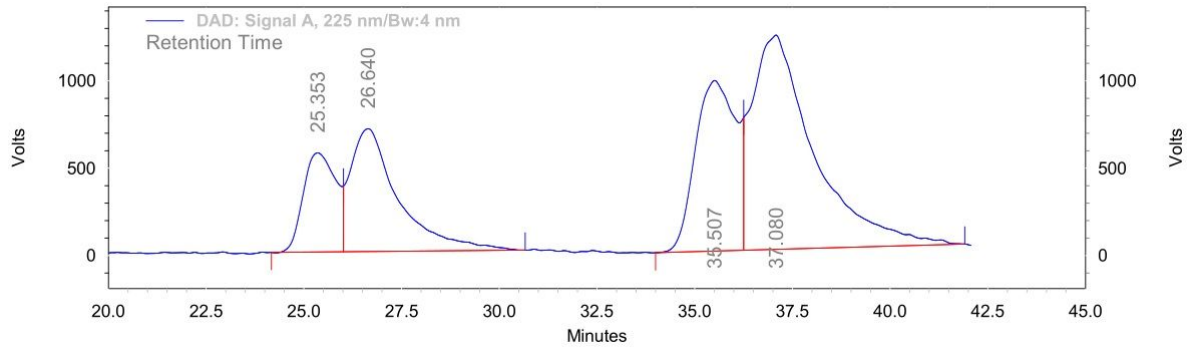
Figure 3.83: HPLC chromatograms of 1-(2,3-dichlorophenyl)-2-nitrobutan-1-ol. A. racemic standard, B. enantiopure product synthesized by *At*HNL-Y14A mutant enzyme.

5. 1-(2-nitrophenyl)-2-nitrobutan-1-ol



For % Conversion, % Enantiomeric excess, % Diastereomeric excess, % Isomeric content				Absolute conformation determination
Hexane: IPA	wavelength	Column	Flowrate	Assigned by analogy with the absolute configuration of compound 1-(2-nitrophenyl)-2-nitropropan-1-ol
95:5	225 nm	Lux 5µm amylose 1	1 mL/min	

A)

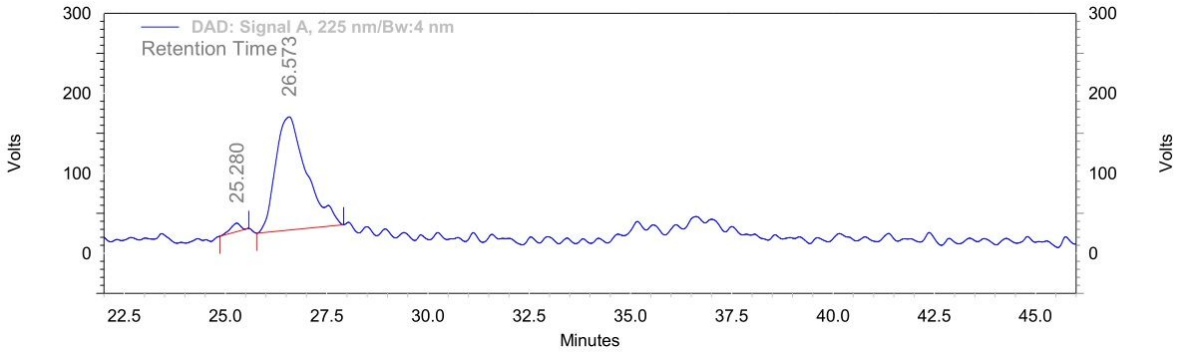


DAD: Signal A,
225 nm/Bw:4 nm
Results

Retention Time	Area	Area %	Height	Height %
25.353	69294142	11.05	1189773	16.34
26.640	125520274	20.01	1474659	20.25
35.507	148650637	23.70	2046996	28.11
37.080	283788196	45.24	2570789	35.30
Totals	627253249	100.00	7282217	100.00

Retention time	25.353	26.64	35.507	37.08
product	(*1S,2R*)	(*1R,2S*)	(*1S,2S*)	(*1R,2R*)

B)



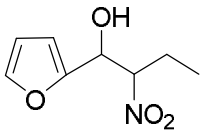
DAD: Signal A,
225 nm/Bw:4 nm
Results

Retention Time	Area	Area %	Height	Height %
25.280	385348	2.38	22151	6.95
26.573	15834631	97.62	296713	93.05
Totals	16219979	100.00	318864	100.00

Retention time	25.28	26.573
product	(*1S,2R*)	(*1R,2S*)

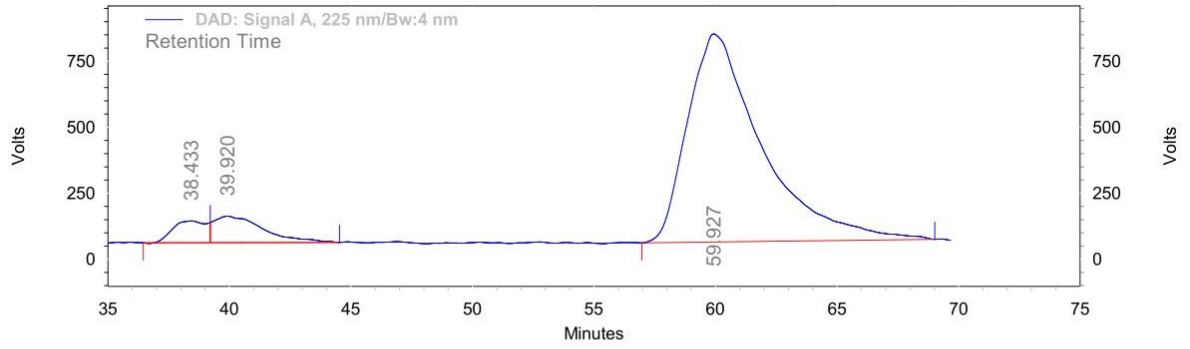
Figure 3.84: HPLC chromatograms of 1-(2-nitrophenyl)-2-nitrobutan-1-ol. A. racemic standard, B. enantiopure product synthesized by *At*HNL-Y14A mutant enzyme.

6. 1-(furan-2-yl)-2-nitrobutan-1-ol



For % Conversion, % Enantiomeric excess of anti, % Diastereomeric excess, % Isomeric content				Absolute conformation determination
Hexane: IPA	wavelength	Column	Flowrate	Assigned by comparison with the reported literature[19]
97:3	210 nm	Lux 5µm amylose 1	0.5 mL/min	

A)

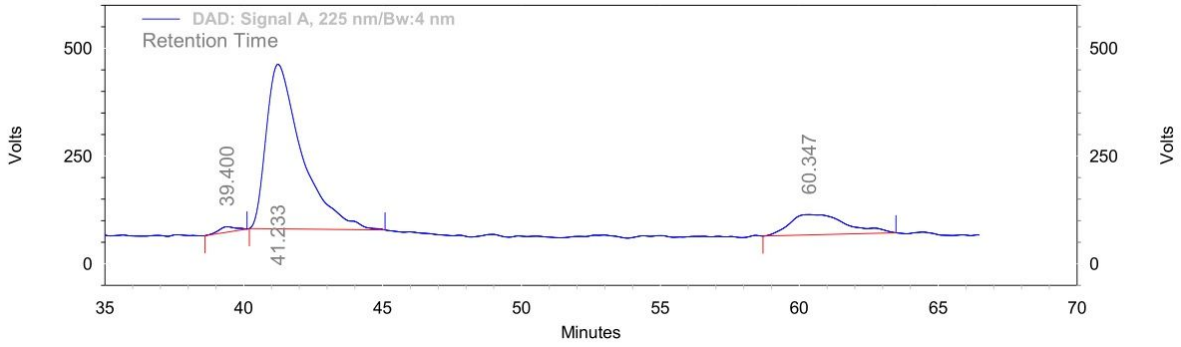


DAD: Signal A, 225 nm/Bw:4 nm
Results

Retention Time	Area	Area %	Height	Height %
38.433	16571226	4.17	173097	8.50
39.920	29813836	7.50	210502	10.34
59.927	351158091	88.33	1652657	81.16
Totals	397543153	100.00	2036256	100.00

Retention time	38.433	39.92	59.927
product	(*1S,2R*)	(*1R,2S*)	(*1S,2S*) + (*1R,2R*)

B)



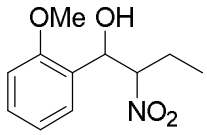
DAD: Signal A,
225 nm/Bw:4 nm
Results

Retention Time	Area	Area %	Height	Height %
39.400	1115921	1.29	26586	2.87
41.233	71474526	82.52	801182	86.46
60.347	14026030	16.19	98846	10.67
Totals	86616477	100.00	926614	100.00

Retention time	39.4	41.347	60.347
product	(*1S,2R*)	(*1R,2S*)	(*1S,2S*) + (*1R,2R*)

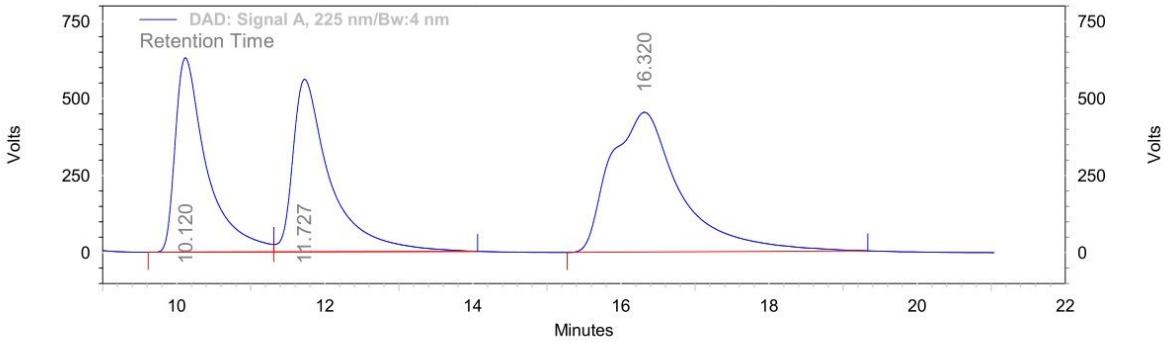
Figure 3.85: HPLC chromatograms of 2-nitro 1-fural butanol. A. racemic standard, B. enantiopure product synthesized by *At*HNL-Y14A mutant enzyme.

7. 1-(2-methoxyphenyl)-2-nitrobutan-1-ol



For % Conversion				Absolute conformation determination
Water: acetonitrile	wavelength	Column	Flowrate	Assigned by comparison with the reported literature[20]
75:25	222 nm	C_{18}	1 mL/min	
For % Enantiomeric excess, % Diastereomeric excess, % Isomeric content				
Hexane: IPA	wavelength	Column	Flowrate	
90:10	225 nm	Lux 5µm amylose 1	1 mL/min	

A)



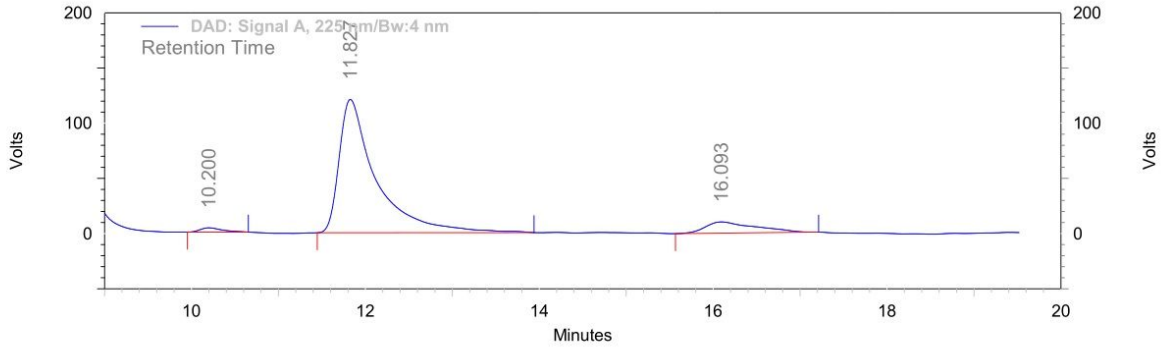
DAD: Signal A,
225 nm/Bw:4 nm
Results

Retention Time	Area	Area %	Height	Height %
10.120	39148091	27.44	1320676	38.34
11.727	41148712	28.84	1173218	34.06
16.320	62379279	43.72	950487	27.60

Totals	142676082	100.00	3444381	100.00

Retention time	10.12	11.727	16.32
product	(*1S,2R*)	(*1R,2S*)	(*1S,2S*) + (*1R,2R*)

B)



DAD: Signal A,
225 nm/Bw:4 nm
Results

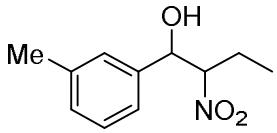
Retention Time	Area	Area %	Height	Height %
10.200	144258	1.70	8175	2.89
11.827	7468609	88.22	253290	89.55
16.093	853006	10.08	21376	7.56

Totals	8465873	100.00	282841	100.00

Retention time	10.2	11.827	16.093
product	(*1S,2R*)	(*1R,2S*)	(*1S,2S*) + (*1R,2R*)

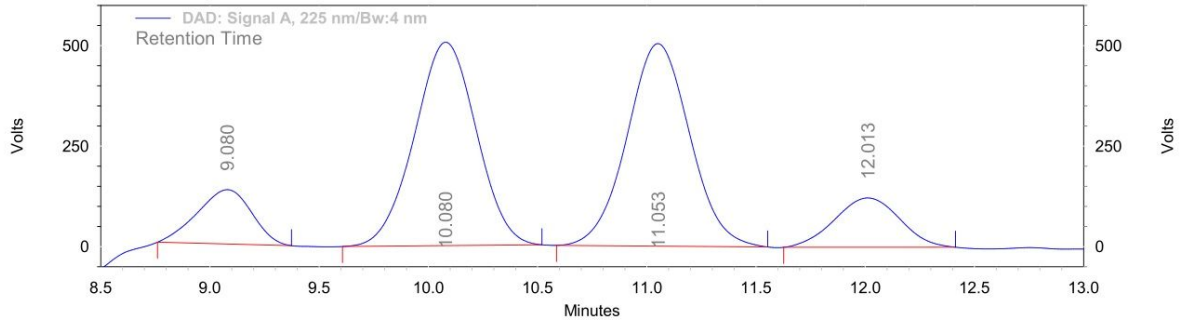
Figure 3.86: HPLC chromatograms of 1-(2-methoxyphenyl)-2-nitrobutan-1-ol. A. racemic standard, B. enantiopure product synthesized by *At*HNL-Y14A mutant enzyme.

8. 1-(3-methylphenyl)-2-nitrobutan-1-ol



For % Conversion				Absolute conformation determination
Water: acetonitrile	wavelength	Column	Flowrate	Assigned by analogy with the absolute configuration of compound 1-(3-benzyloxyphenyl)-2-nitropropan-1-ol
70:30	222 nm	C_{18}	1 mL/min	
For % Enantiomeric excess, % Diastereomeric excess, % Isomeric content				
Hexane: IPA	wavelength	Column	Flowrate	
90:10	225 nm	Lux 5µm cellulose 1	1 mL/min	

A)

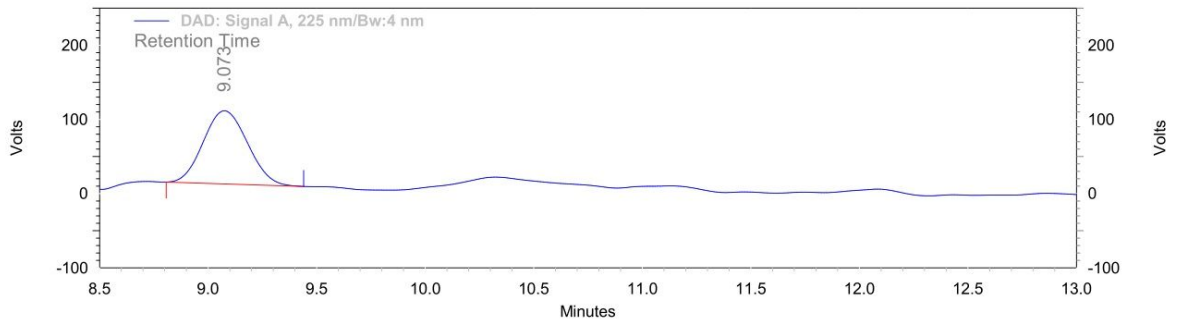


DAD: Signal A, 225 nm/Bw:4 nm
Results

Retention Time	Area	Area %	Height	Height %
9.080	4906691	9.38	283397	10.66
10.080	20936548	40.02	1061379	39.93
11.053	21131028	40.40	1056358	39.74
12.013	5335307	10.20	257222	9.68
Totals	52309574	100.00	2658356	100.00

Retention time	12.013	9.080	11.053	10.08
product	(*1S,2R*)	(*1R,2S*)	(*1S,2S*)	(*1R,2R*)

B)



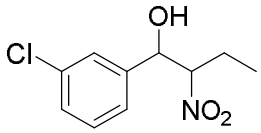
DAD: Signal A, 225 nm/Bw:4 nm
Results

Retention Time	Area	Area %	Height	Height %
9.073	2929205	100.00	206788	100.00
Totals	2929205	100.00	206788	100.00

Retention time	9.073
product	(*1R,2S*)

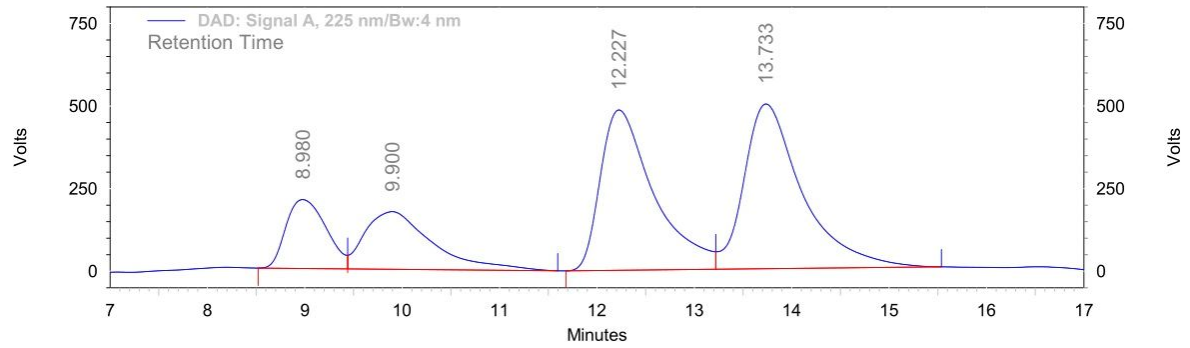
Figure 3.87: HPLC chromatograms of 1-(3-methylphenyl)-2-nitrobutan-1-ol. A. racemic standard, B. enantiopure product synthesized by *At*HNL-Y14A mutant enzyme.

9. 1-(3-chlorophenyl)-2-nitrobutan-1-ol



For % Conversion				Absolute conformation determination
Water: acetonitrile	wavelength	Column	Flowrate	Assigned by analogy with the absolute configuration of compound 1-(3-chlorophenyl)-2-nitropropan-1-ol
60:40	222 nm	C_{18}	1 mL/min	
For % Enantiomeric excess, % Diastereomeric excess, % Isomeric content				
Hexane: IPA	wavelength	Column	Flowrate	
93:7	225 nm	Lux 5µm amylose 1	1 mL/min	

A)



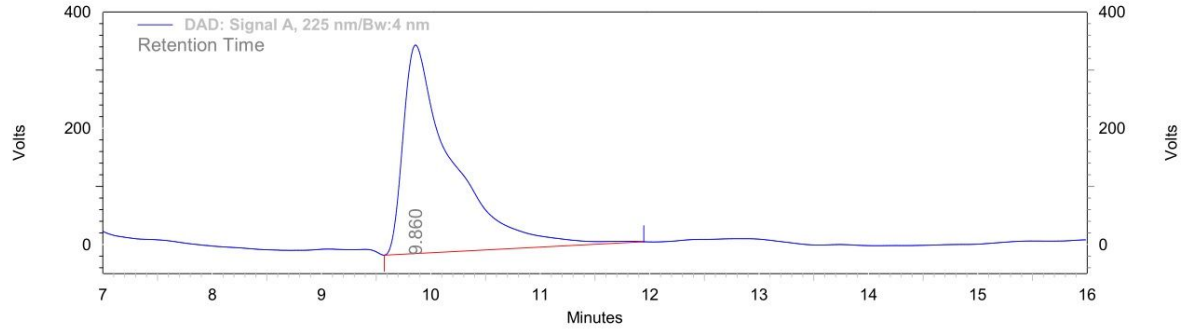
DAD: Signal A,
225 nm/Bw:4 nm
Results

Retention Time	Area	Area %	Height	Height %
8.980	12558851	11.15	437300	15.25
9.900	17613854	15.64	365863	12.76
12.227	38903880	34.55	1018012	35.51
13.733	43538244	38.66	1045952	36.48

Totals				
	112614829	100.00	2867127	100.00

Retention time	8.980	9.9	12.227	13.733
product	(*1S,2R*)	(*1R,2S*)	(*1S,2S*)	(*1R,2R*)

B)



DAD: Signal A,
225 nm/Bw:4 nm
Results

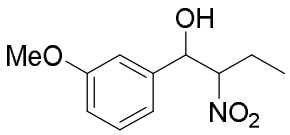
Retention Time	Area	Area %	Height	Height %
9.860	23540360	100.00	752095	100.00

Totals				
	23540360	100.00	752095	100.00

Retention time	9.86
product	(*1R,2S*)

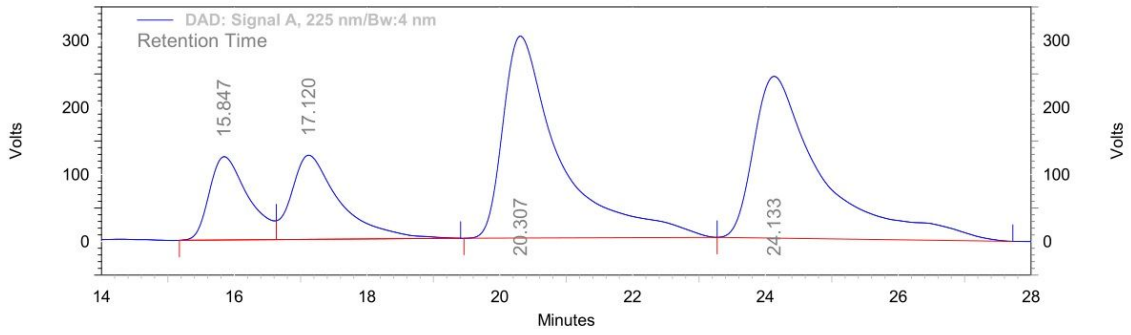
Figure 3.88: HPLC chromatograms of 1-(3-chlorophenyl)-2-nitrobutan-1-ol. A. racemic standard, B. enantiopure product synthesized by *At*HNL-Y14A mutant enzyme.

10. 1-(3-methoxyphenyl)-2-nitrobutan-1-ol



For % Conversion				Absolute conformation determination
Water: acetonitrile	wavelength	Column	Flowrate	Assigned by analogy with the absolute configuration of compound 1-(2-methoxyphenyl)-2-nitropropan-1-ol
70:30	222 nm	C_{18}	1 mL/min	
For % Enantiomeric excess, % Diastereomeric excess, % Isomeric content				
Hexane: IPA	wavelength	Column	Flowrate	
93:7	225 nm	Lux 5µm amylose 1	1 mL/min	

A)

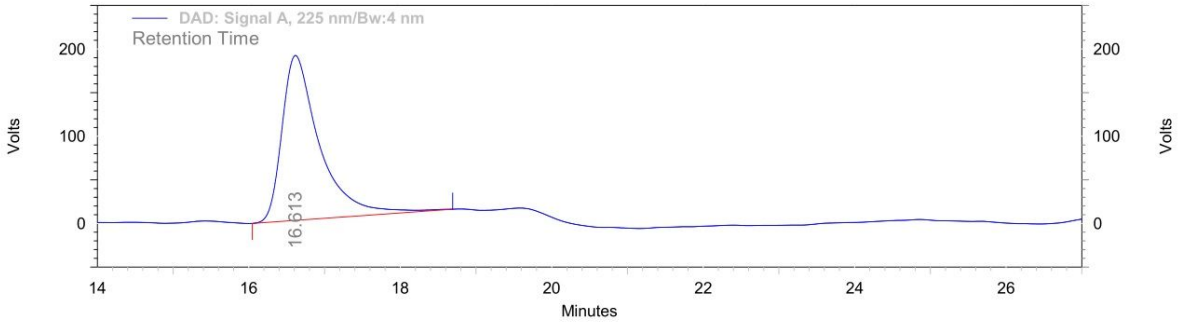


DAD: Signal A, 225 nm/Bw:4 nm
Results

Retention Time	Area	Area %	Height	Height %
15.847	10622166	10.86	260540	15.68
17.120	13284957	13.58	263261	15.85
20.307	37748917	38.58	631541	38.01
24.133	36193749	36.99	505988	30.46
Totals	97849789	100.00	1661330	100.00

Retention time	15.847	17.12	20.307	24.133
product	(*1S,2R*)	(*1R,2S*)	(*1S,2S*)	(*1R,2R*)

B)



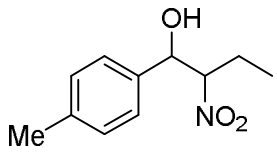
DAD: Signal A,
225 nm/Bw:4 nm
Results

Retention Time	Area	Area %	Height	Height %
16.613	13638240	100.00	396446	100.00
Totals	13638240	100.00	396446	100.00

Retention time	16.613
product	(*1R,2S*)

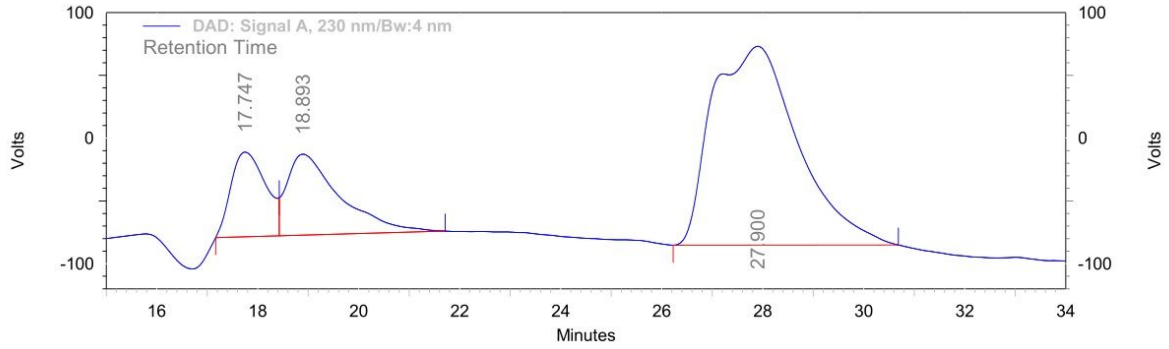
Figure 3.89: HPLC chromatograms of 1-(3-methoxyphenyl)-2-nitrobutan-1-ol. A. racemic standard, B. enantiopure product synthesized by *At*HNL-Y14A mutant enzyme.

11. 1-(4-methylphenyl)-2-nitrobutan-1-ol



For % Conversion				Absolute conformation determination
Water: acetonitrile	wavelength	Column	Flowrate	Assigned by comparison with the reported literature[19]
70:30	222 nm	C_{18}	1 mL/min	
For % Enantiomeric excess, % Diastereomeric excess, % Isomeric content				
Hexane: IPA	wavelength	Column	Flowrate	
96:4	230 nm	Lux 5µm amylose 1	1 mL/min	

A)



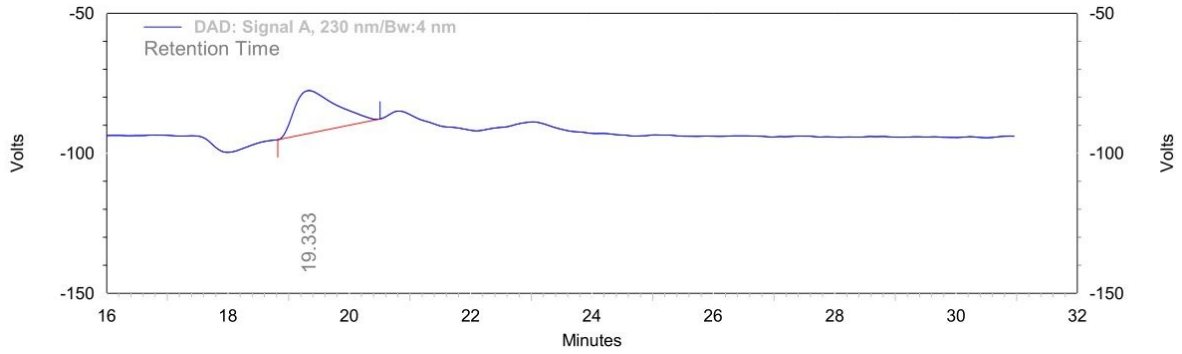
DAD: Signal A,
230 nm/Bw:4 nm
Results

Retention Time	Area	Area %	Height	Height %
17.747	6796281	12.17	141309	23.23
18.893	9865555	17.66	135138	22.21
27.900	39194536	70.17	331972	54.56

Totals	55856372	100.00	608419	100.00

Retention time	17.747	18.893	27.9
product	(*1S,2R*)	(*1R,2S*)	(*1S,2S*) + (*1R,2R*)

B)



DAD: Signal A,
230 nm/Bw:4 nm
Results

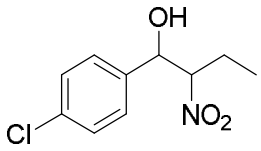
Retention Time	Area	Area %	Height	Height %
19.333	1528941	100.00	32062	100.00

Totals	1528941	100.00	32062	100.00

Retention time	19.333
product	(*1R,2S*)

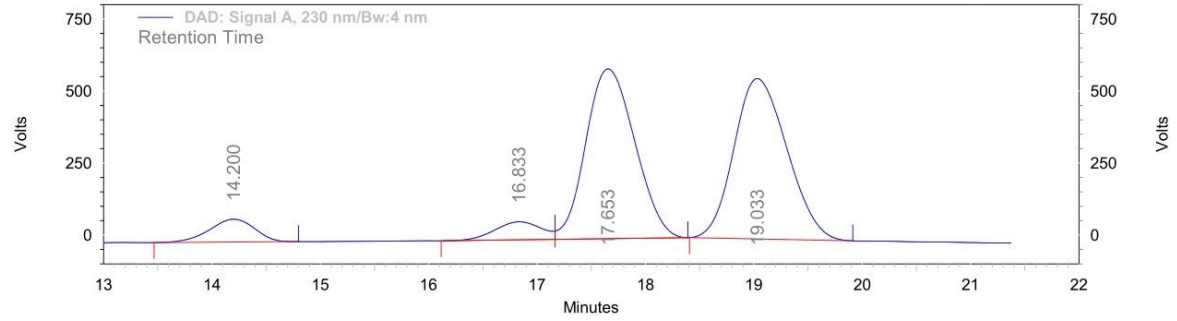
Figure 3.90: HPLC chromatograms of 1-(4-methylphenyl)-2-nitrobutan-1-ol. A. racemic standard, B. enantiopure product synthesized by *At*HNL-Y14A mutant enzyme.

12. 1-(4-chlorophenyl)-2-nitrobutan-1-ol



For % Conversion				Absolute conformation determination
Water: acetonitrile	wavelength	Column	Flowrate	Assigned by analogy with the absolute configuration of compound 1-(4-nitrophenyl)-2-nitrobutan-1-ol
70:30	222 nm	C_{18}	1 mL/min	
For % Enantiomeric excess, % Diastereomeric excess, % Isomeric content				
Hexane: IPA	wavelength	Column	Flowrate	
93:7	230 nm	Lux 5µm cellulose 1	1 mL/min	

A)

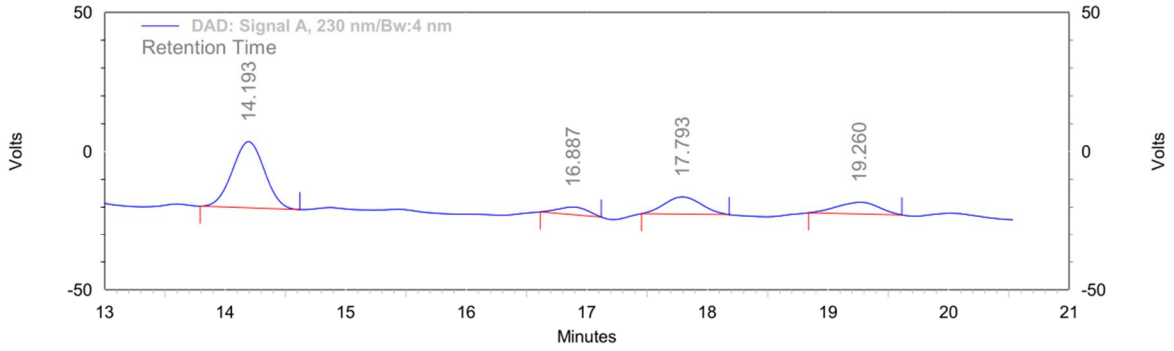


DAD: Signal A, 230 nm/Bw:4 nm
Results

Retention Time	Area	Area %	Height	Height %
14.200	4843759	5.54	165951	6.14
16.833	3923754	4.49	131265	4.86
17.653	38898210	44.47	1236272	45.76
19.033	39803276	45.51	1167902	43.23
Totals	87468999	100.00	2701390	100.00

Retention time	16.833	14.2	17.653	19.033
product	(*1S,2R*)	(*1R,2S*)	(*1S,2S*) / (*1R,2R*)	(*1S,2S*) / (*1R,2R*)

B)



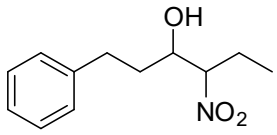
DAD: Signal A,
230 nm/Bw:4 nm
Results

Retention Time	Area	Area %	Height	Height %
14.193	924884	61.21	49860	64.45
16.887	98051	6.49	5727	7.40
17.793	275670	18.25	12970	16.77
19.260	212300	14.05	8806	11.38
Totals	1510905	100.00	77363	100.00

Retention time	16.877	14.193	17.793	19.260
product	(*1S,2R*)	(*1R,2S*)	(*1S,2S*) / (*1R,2R*)	(*1S,2S*) / (*1R,2R*)

Figure 3.91: HPLC chromatograms of 1-(4-chlorophenyl)-2-nitrobutan-1-ol. A. racemic standard, B. enantiopure product synthesized by *At*HNL-Y14A mutant enzyme.

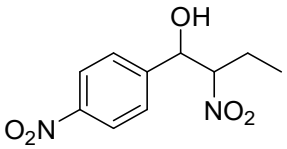
13. 4-nitro-1-phenylhexan-3-ol



For % Conversion				Absolute conformation determination
Water: acetonitrile	wavelength	Column	Flowrate	Assigned by comparison with the reported literature[19]
60:40	222 nm	C_{18}	1 mL/min	
For % Enantiomeric excess of syn , % Diastereomeric excess, % Isomeric content				
Hexane: IPA	wavelength	Column	Flowrate	
90:10	210 nm	Lux 5µm amylose 1	1 mL/min	
For % Enantiomeric excess of anti				
Hexane: IPA	wavelength	Column	Flowrate	

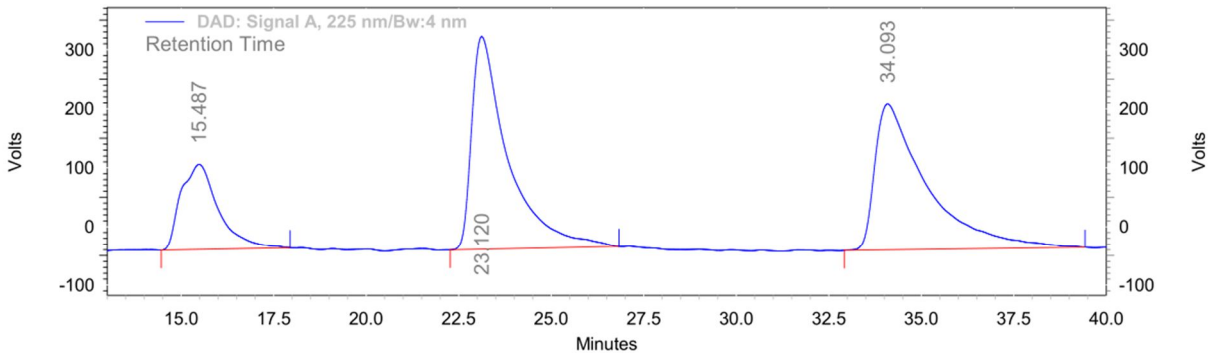
98:2	210 nm	Lux 5µm amylose 1	1 mL/min	

14. 1-(4-nitrophenyl)-2-nitrobutan-1-ol



For % Conversion, % Enantiomeric excess of syn, % Diastereomeric excess, % Isomeric content				Absolute conformation determination
Hexane: IPA	wavelength	Column	Flowrate	Assigned by comparison with the reported literature[27]
90:10	225 nm	Lux 5µm amylose 1	1 mL/min	
For % Enantiomeric excess of anti				
Hexane: IPA	wavelength	Column	Flowrate	
90:10	225 nm	Lux 5µm cellulose 1	1 mL/min	

A)

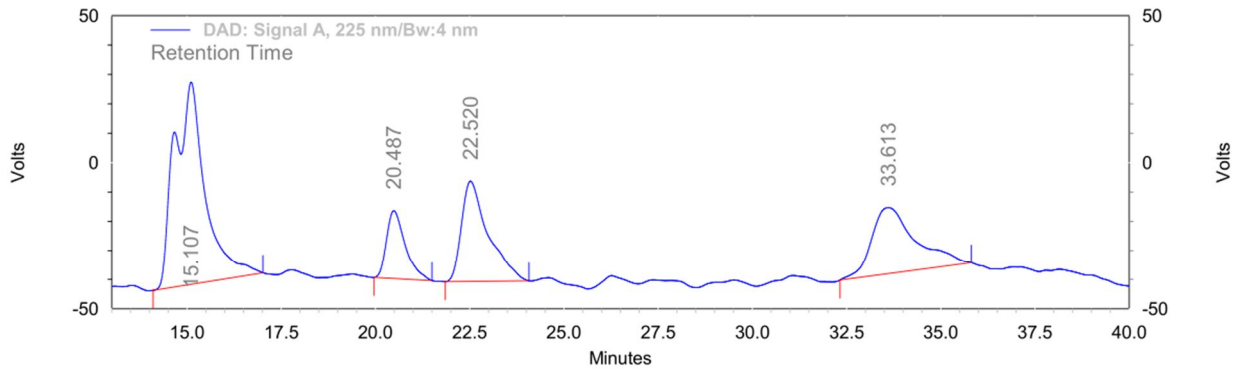


DAD: Signal A, 225 nm/Bw:4 nm
Results

Retention Time	Area	Area %	Height	Height %
15.487	21540139	17.34	304724	19.24
23.120	51748362	41.65	758037	47.87
34.093	50960114	41.01	520928	32.89
Totals	124248615	100.00	1583689	100.00

Retention time	15.487	34.093	23.12
product	(*1S,2R*) + (*1R,2S*)	(*1S,2S*)	(*1R,2R*)

B)

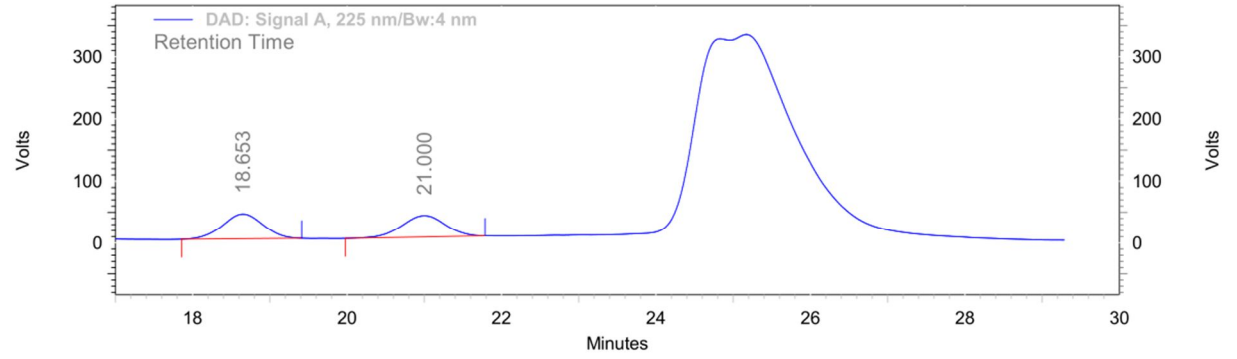


DAD: Signal A,
225 nm/Bw:4 nm
Results

Retention Time	Area	Area %	Height	Height %
15.107	8222976	47.35	144770	46.18
20.487	1699134	9.79	48993	15.63
22.520	3560472	20.50	72091	23.00
33.613	3881971	22.36	47641	15.20
Totals	17364553	100.00	313495	100.00

Retention time	15.107	20.487	33.613	22.52
product	(*1S,2R*) + (*1R,2S*)	Aldehyde substrate	(*1S,2S*)	(*1R,2R*)

C)

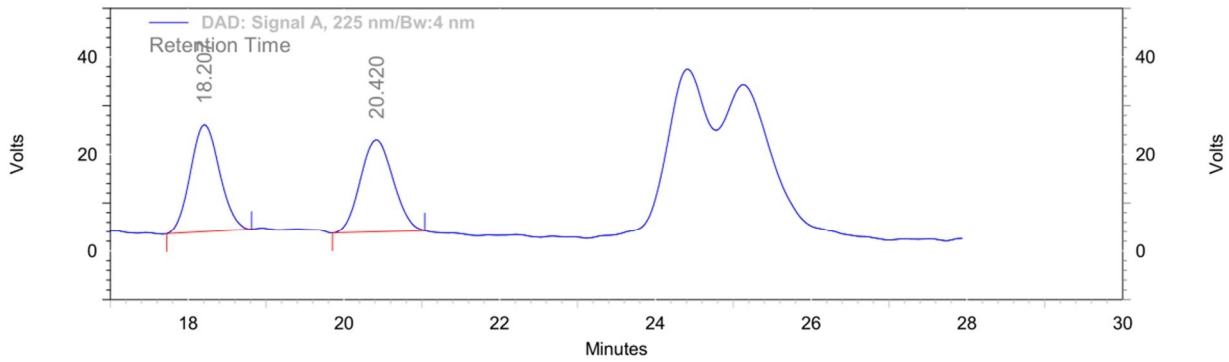


DAD: Signal A,
225 nm/Bw:4 nm
Results

Retention Time	Area	Area %	Height	Height %
18.653	3095774	51.81	84555	53.60
21.000	2879600	48.19	73185	46.40
Totals	5975374	100.00	157740	100.00

Retention time	21	18.563
product	(*1S,2R*)	(*1R,2S*)

D)



DAD: Signal A,
225 nm/Bw:4 nm
Results

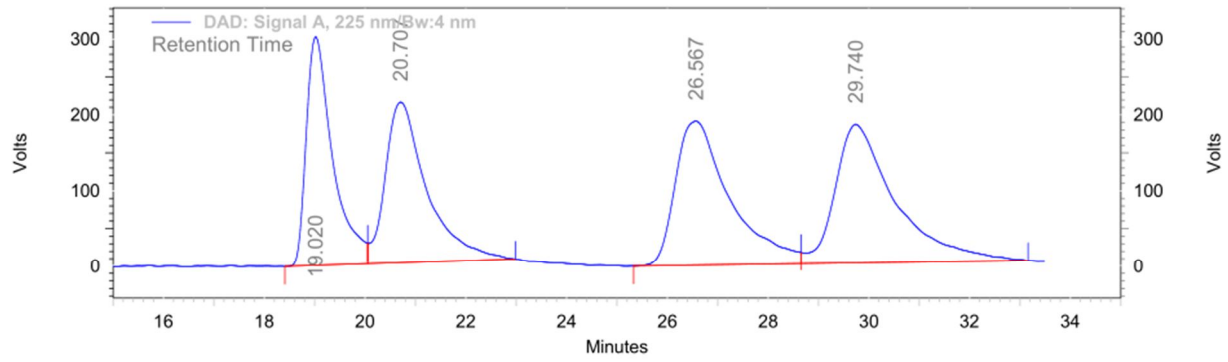
Retention Time	Area	Area %	Height	Height %
18.207	1212481	50.84	46282	53.74
20.420	1172211	49.16	39842	46.26
Totals	2384692	100.00	86124	100.00

Retention time	20.42	18.207
product	(*1S,2R*)	(*1R,2S*)

Figure 3.92: HPLC chromatograms of 1-(4-nitrophenyl)-2-nitrobutanol. A. racemic standard in Lux amylose 1, B. enantiopure product in Lux amylose 1, C. racemic standard in Lux cellulose 1, D) enantiopure product in Lux cellulose 1 synthesized by *At*HNL-Y14C mutant enzyme

3.4.24. HPLC traces of (*1R,2S*)-2-NPP synthesized in gram scale by using *At*HNL-Y14C crude enzyme

A)



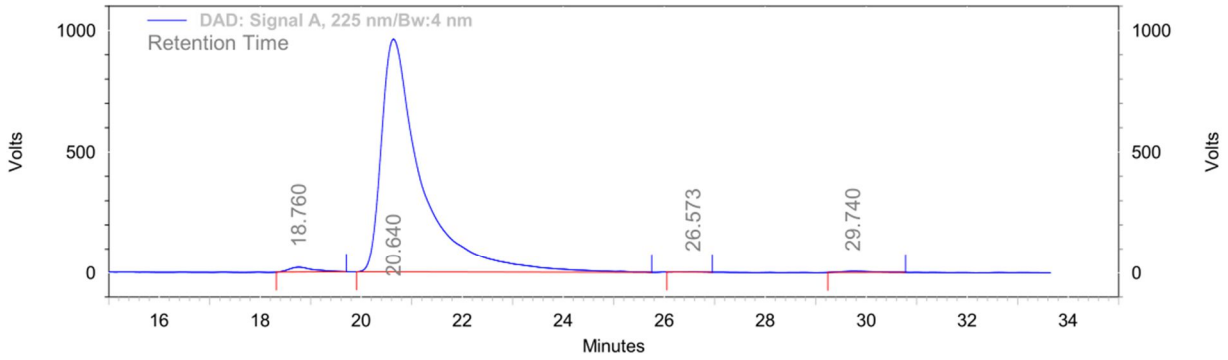
DAD: Signal A,
225 nm/Bw:4 nm
Results

Retention Time	Area	Area %	Height	Height %
19.020	23162296	20.95	633680	34.00
20.707	25536652	23.09	445440	23.90
26.567	30028170	27.16	399917	21.46
29.740	31850151	28.80	384781	20.64

Totals	110577269	100.00	1863818	100.00

Retention time	19.02	20.707	26.567	29.74
product	(*1S,2R*)	(*1R,2S*)	(*1S,2S*)	(*1R,2R*)

B)



DAD: Signal A,
225 nm/Bw:4 nm
Results

Retention Time	Area	Area %	Height	Height %
18.760	1424686	1.26	42136	2.04
20.640	111150818	98.25	2014592	97.31
26.573	96289	0.09	3477	0.17
29.740	456044	0.40	10111	0.49

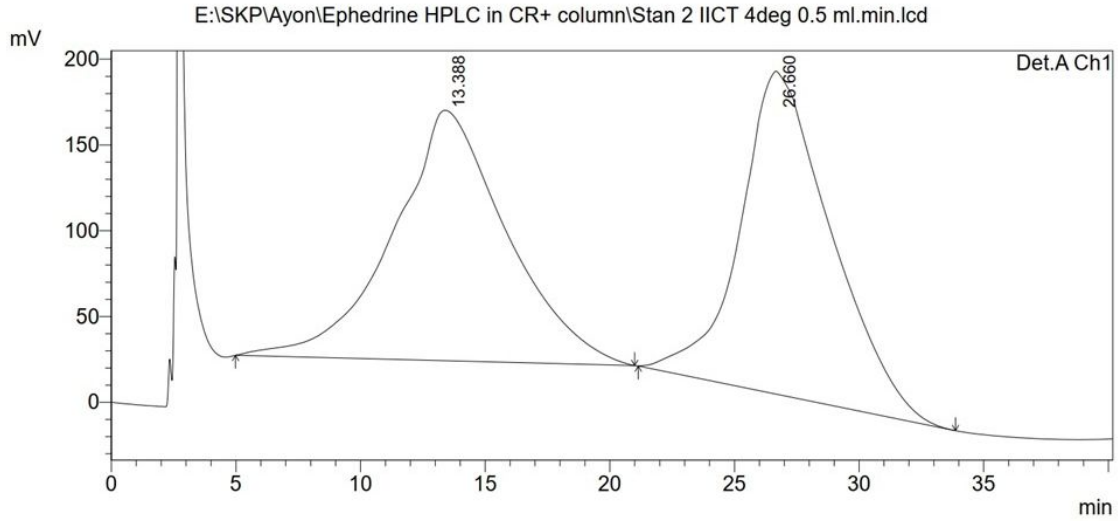
Totals	113127837	100.00	2070316	100.00

Retention time	18.76	20.64	26.573	29.74
product	(*1S,2R*)	(*1R,2S*)	(*1S,2S*)	(*1R,2R*)

Figure 3.93: HPLC chromatograms of biocatalytically synthesized (*1R,2S*)-2-nitro-1-phenyl propanol. A. racemic standard, B. *At*HNL-Y14C synthesized product in gram-scale.

3.4.25. HPLC traces of racemic and (*1R,2S*)-2-amino 1-phenylpropan-1-ol (2-APP)

A)

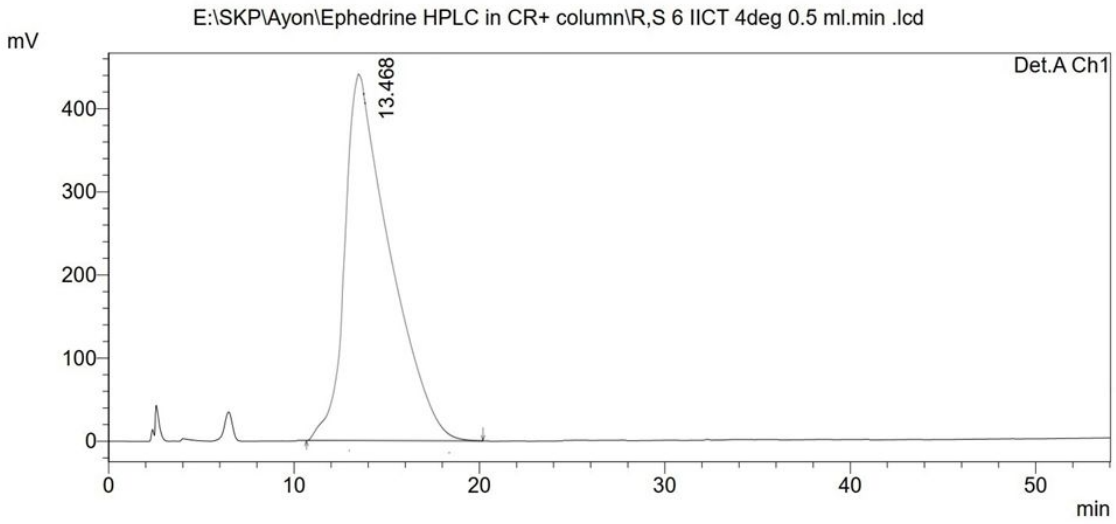


Detector A Ch1 205nm

Peak#	Ret. Time	Area	Height	Area %	Height %
1	13.388	46435233	145992	49.115	43.689
2	26.660	48108878	188169	50.885	56.311
Total		94544111	334161	100.000	100.000

Retention time	26.66	13.388
product	(*1S,2R*)-2-APP	(*1R,2S*)-2-APP

B)



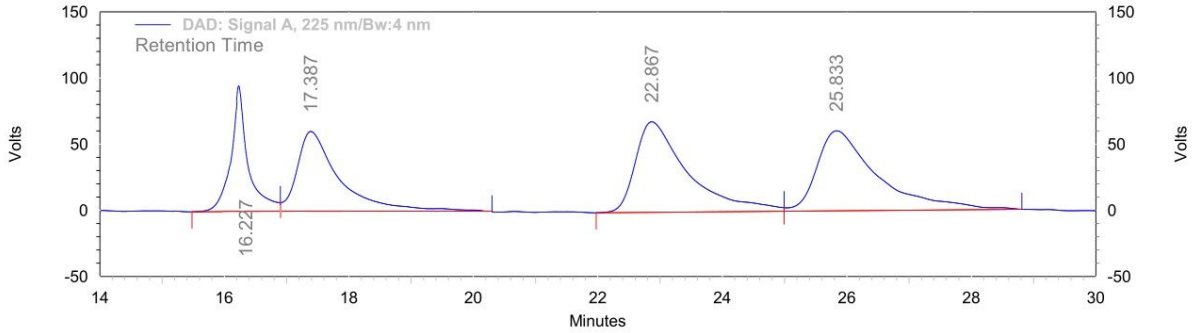
Peak#	Ret. Time	Area	Height	Area %	Height %
1	13.468	135345934	440867	100.000	100.000
Total		135345934	440867	100.000	100.000

Retention time	13.468
product	(*1R,2S*)-2-APP

Figure 3.94: HPLC chromatograms of 1-(2-aminophenyl)-2-nitropropanol. A. racemic standard, B. enantiopure product synthesized by chemoenzymatic cascade.

3.4.26. HPLC traces of racemic 2-NPP and deuteriated β-nitroalcohol product

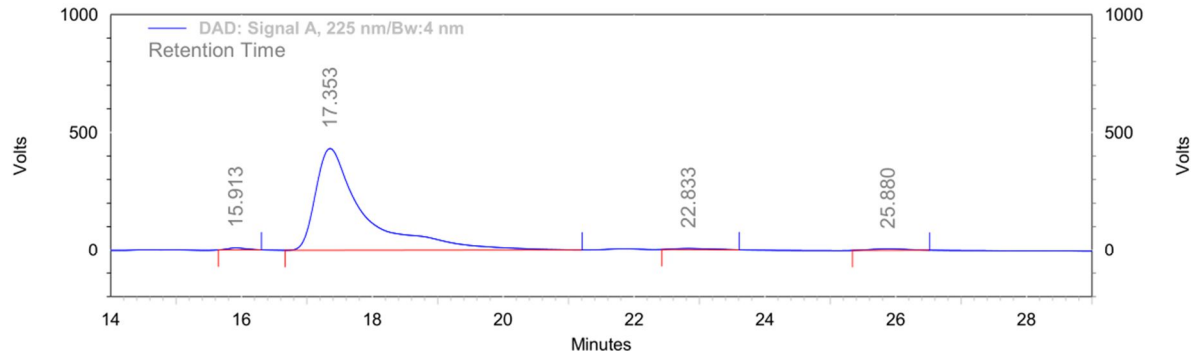
A)



DAD: Signal A,
225 nm/Bw:4 nm
Results

Retention Time	Area	Area %	Height	Height %
16.227	5136598	18.18	200079	33.44
17.387	6222688	22.03	127958	21.39
22.867	8338896	29.52	143432	23.97
25.833	8550824	30.27	126837	21.20
Totals	28249006	100.00	598306	100.00

B)



DAD: Signal A,
225 nm/Bw:4 nm
Results

Retention Time	Area	Area %	Height	Height %
15.913	346012	0.72	17602	1.86
17.353	46657066	97.44	904568	95.71
22.833	407652	0.85	10456	1.11
25.880	472116	0.99	12464	1.32
Totals	47882846	100.00	945090	100.00

Figure 3.95: HPLC chromatograms of racemic 2-NPP and deuteriated β-nitroalcohol product.

3.5. Discussion

3.5.1. Screening of *At*HNL mutant library towards promiscuous nitroaldol reaction to synthesize 2-NPP

WT *At*HNL is known to catalyze the addition of nitromethane to benzaldehyde via a C–C bond formation reaction and synthesize (*R*)-2-nitro 1-phenyl ethanol (2-NPE) in its enantiopure form.[9] However, it failed to show such stereoselective property when nitroethane was used in place of nitromethane as a nucleophile. So, to find an efficient mutant that can catalyze this promiscuous reaction, two in-house site saturation libraries of *At*HNL created at positions Y14 and F179 [8] were screened for this promiscuous reaction. In Y14 series, four mutants (Y14C, Y14D, Y14G, and Y14H) and from the F179 series only F179L showed streoselective synthesis of (*1R,2S*) isomer of the product. Two other (*R*)-selective HNLs *Gt*HNL and *Ac*HNL have been reported in the synthesis of this same isomer from benzaldehyde.[7] WT *Ac*HNL showed very poor diastereomeric excess of 6% with 73% ee and 77% conversion of (*1R,2S*)-NPP. The % diastereomeric excess and % ee were improved to 27 and 88 respectively by using the engineered enzyme, *Ac*HNL-A40H, while % conversion was compromised to 66%. Among the wild type HNLs, *Hb*HNL was reported to show such promiscuous reaction, however with opposite stereoselectivity. WT *Hb*HNL has been reported to synthesize (*1S,2R*)-2-NPP with 67% conversion, 95% ee, and 80% de.[6] The stereopreference of *At*HNL and *Hb*HNL are opposite, however both belongs to α/β hydrolase fold, have similar3D structure, reaction mechanism and share high sequence similarity. Apparently the corresponding position of Tyr14 and Phe179 of *At*HNL are Cys and Leu in *Hb*HNL respectively. Therefore presence of Cys at 14th position and Leu at 179 are logical for the diastereoselective activity of *At*HNL.[6]

3.5.2. Optimization of reaction conditions towards *At*HNL-Y14C catalyzed stereoselective synthesis of (*1R,2S*)-2-NPP

In the case of *Hb*HNL catalyzed 2-NPP synthesis KPB pH 7 was used as the reaction buffer, [6] while KPB pH 6.0 was favored for the *Ac*HNL and *Gt*HNL catalyzed study.[7] With increasing pH, the % ee of the Y14C catalyzed synthesis of (*1R,2S*) *anti* isomer decreased in both buffers. In CPB pH 5.5, the conversion was 58.5% with 95.3% ee and 90% de. Lower pH usually minimizes the non-enzymatic reaction and helps to increase stereoselectivity. Biphasic reaction system consisting of nonpolar organic solvent and aqueous buffer has been reported to improve substrate solubility into the reaction mixture and also helps to avoid substrate inhibition of enzymes.[28,29] Early studies of *Hb*HNL[6], *Ac*HNL, and *Gt*HNL mutants[7] catalyzed diastereoselective Henry reaction used *tert*-butyl methyl ether (TBME) as the organic solvent for 2-NPP synthesis. WT *At*HNL used *n*-butyl acetate (NBA) after an optimization study for the synthesis of 2-NPE. [9] In this optimization study, among the five solvents tested, TBME gave the best result in terms of % conversion and % ee and showed a 17% increment in conversion compared to NBA. Nitroethane, the second substrate of the Henry reaction was used in 1 M in case of (*R*)-selective *Ac*HNL and *Gt*HNL catalyzed diastereoselective reactions.[7] Here *At*HNL-Y14C showed increased activity and enantioselectivity with increasing nitroethane concentration up to 1.75 M. It gave 78% conversion with 95.4% ee and 94% de of (*1R,2S*)-2-NPP. After optimizing these parameters, the desired product was synthesized in 81% conversion with 97% ee and 95% de.

3.5.3. *At*HNL-Y14C catalyzed diastereoselective synthesis of *anti* stereoisomers of different β-nitroalcohols using nitroethane as the co-substrate

Using the optimized biocatalytic reaction conditions, nineteen aromatic aldehydes having substituents at different positions in the aromatic ring were converted into their corresponding (*1R,2S*) *anti*-diastereomer of β-nitroalcohols. Two other (*R*)-selective HNLs *Gt*HNL and *Ac*HNL have been reported in the synthesis of the same isomer from benzaldehyde.[7] WT *Ac*HNL showed very poor diastereomeric excess of 6% with 73% ee and 77% conversion of

(*1R,2S*)-NPP. This poor diastereomeric excess and % ee was improved to 27 and 88 respectively by using the engineered enzyme, *Ac*HNL-A40H, however % conversion was decreased to 66%. WT *Hb*HNL was reported to show such promiscuous reaction in the conversion of (*1S,2R*)-2-NPP with 67% conversion and 95% ee, and 80% de. [6] None of the nineteen substrates used here (Figure 3.43) except benzaldehyde were studied earlier by HNL-catalyzed diastereoselective Henry reaction. Among the other biocatalytic approaches, the only one reported is *Pseudomonas flourescens* lipase employed kinetic resolution to produce 1-(4-chlorophenyl)-2-nitropropanol in 77% conversion and without any mention of stereoselectivity.[2] Satisfyingly, the Y14C variant displayed up to >99% of conversion, ee and de in the synthesis of (*1R,2S*) stereoisomer of the β-nitroalcohol products (Figure 3.43).

3.5.4. Gram scale synthesis of (*1R,2S*)-2-NPP by using Y14C crude enzyme as the catalyst

Here preparative scale synthesis of the *anti* diastereoisomer (*1R,2S*)-2-NPP was carried out using the Y14C crude cell lysates. This is the first report where large scale synthesis of (*1R,2S*)-2-NPP was executed by biocatalytic route. The best report to date to synthesize this molecule on an analytical scale was through *Gt*HNL A40H/V42T/Q110H synthesizing the same compound, did not calculate TTN.[7] However, it achieved a maximum conversion of 78% of 20 µmol of benzaldehyde, yielding 15.6 µmol of product, using 10 mg of purified enzyme, equivalent to 0.67 µmol of enzyme (*Gt*HNL molecular weight: 15 kDa). This resulted in a TTN of 15.6/0.67 = 23.3, whereas our engineered enzyme showed a TTN of 3470, almost 149-fold higher than the former. Additionally, *Gt*HNL A40H/V42T/Q110H catalyzed reaction showed a substrate to catalyst ratio of only 29.85 (20/0.67), which is 211-fold lower than our *At*HNL-Y14C (6250) approach.

3.5.5. Recycling *At*HNL-Y14C for the synthesis of (*1R,2S*)-2-NPP

The reusability of the *At*HNL-Y14C was investigated for the production of (*1R,2S*)-2-NPP. The purified Y14C mutein was recycled for eight cycles of nitroaldol reaction in the presence of 100 mM of benzaldehyde and it was observed that up to third cycle Y14C could retain 83% of its activity with >95% ee and >90% de. A similar study was carried out by Nuylert et.al., where reusability of a C-terminal truncated residue of *Pe*HNL (*Pe*HNLΔ_{107}) was checked and found to be active up to four cycles without any decrease in the activity. [30]

3.6. Conclusions

Arabidopsis thaliana hydroxynitrile lyase catalyzed diastereoselective Henry reactions involving aldehydes and either nitroethane or 1-nitropropane as nucleophile are investigated. As WT *At*HNL was unable to catalyze the reaction, two in-house site saturation library of *At*HNL created at positions Y14 and F179 were screened using benzaldehyde with nitroethane or 1-nitropropane. The screening has successfully identified Y14C as the best variant to catalyze the nitroaldol reaction for stereoselective addition of nitroethane and Y14A for 1-nitropropane addition to benzaldehyde. Both the variants preferentially produced the (*1R,2S*) *anti* diastereomers of the desired nitroaldol products. Several reaction parameters towards the Y14C catalyzed nitroethane addition to benzaldehyde, or Y14A catalyzed 1-nitropropane addition to benzaldehyde were optimized to improve the yield, % ee and % de of the products. Synthetic scope of Y14C was exemplified by synthesizing nineteen different (*1R,2S*)-β-nitroalcohols with % conversion, % ee, and % de up to >99%, from their corresponding

aldehydes and nitroethane. Similarly, Y14A could be used to synthesize fourteen different (*1R,2S*)-β-nitroalcohols with up to 90% conversion, up to >99% ee, and up to >99% de from their corresponding aldehydes and 1-nitropropane. The Y14C has shown a k_{cat}/K_M of 0.3 $mM^{-1}.min^{-1}$ in the synthesis of (*1R,2S*)-2-NPP, which is almost 259 times higher than the wild-type enzyme. Similarly for Y14A catalyzed synthesis of (*1R,2S*)-1-(3-chlorophenyl)-2-nitro butanol, k_{cat}/K_M was found to be 0.09 $mM^{-1}.min^{-1}$ while wild type did not catalyze it. Gram scale synthesis of (*1R,2S*)-2-NPP was carried out using Y14C crude enzyme. The synthesized product showed excellent stereoselectivity of 97.5% ee with >99% de and a TTN of 3,438, which is >100 times than the earlier reported biocatalyst, AcHNL-A40H. The enantiopure (*1R,2S*)-2-NPP synthesized, was converted to a value-added drug intermediate, L-norpsuedoephedrine with >99% ee and de, by reducing the β-nitroalcohol into β-amino alcohol.

3.7. References

1. D.H.S. Rao, A. Chatterjee, and S.K. Padhi, *Org. Biomol. Chem.* 2021, **19**, 322–337.

2) J. C. Borah, J. Boruwa, B. Kalita, A. K. Hazarika and N. C. Barua, *Indian J. Chem., Sect. B: Org. Chem. Incl. Med. Chem.*, 2005, **44**, 1961–1965.

3) S. E. Milner, M. Brossat, T. S. Moody, C. J. Elcoate, S. E. Lawrence, and A. R. Maguire, *Tetrahedron: Asymmetry*, 2010, **21**, 1011-1016.

4) Foley, and M. Aoife, *Tetrahedron,* 2018, **74**, 1435-1443.

5) G. Hasnaoui-Dijoux, M. M. Elenkov, J. H. Lutje Spelberg, B. Hauer and D. B. Janssen, *ChemBioChem,*2008, **9**, 1048–1051.

6) T. Purkarthofer, K. Gruber, M. Gruber-Khadjawi, K. Waich, W. Skranc, D. Mink and H. Griengl, *Angew. Chemie - Int. Ed.*, 2006, **45**, 3454–3456.

7) M. Bekerle-Bogner, M. Gruber-Khadjawi, H. Wiltsche, R. Wiedner, H. Schwab and K. Steiner, *ChemCatChem*, 2016, **8**, 2214–2216.

8) B. Vishnu Priya, D. H. Sreenivasa Rao, R. Gilani, S. Lata, N. Rai, M. Akif and S. Kumar Padhi, *Bioorg. Chem.*, 2022, **120**, 105594.

9) K. I. Fuhshuku and Y. Asano, *J. Biotechnol.*, 2011, **153**, 153–159.

10) F. W. Hoover and H. B. Hass, *J. Org. Chem.*, 1947, **12**, 506-509.

11) Kao, Chao-Hung, and Jian-Sin Lin. "Biosynthesis methods of norephedrine with specific optical activities." U.S. Patent Application No. 13/475,007.

12) Doyon, J. Tyler, and A. R. Buller, *JACS*, 2022, **144**, 7327-7336.

13) M. Pandi, P. K. Chanani and S. Govindasamy, *Appl. Catal. A: Gen.*, 2012, **441**, 119-123.

14) G. Blay, L.R. Domingo, V. Hernández-Olmos and J. R. Pedro, *Chem. Eur. J.*, 2008, **14**, 4725 – 4730.

15) H. Mei, X. Xiao, X. Zhao, B. Fang, X. Liu, L. Lin and X. Feng, *J. Org. Chem.*, 2015, **80**, 2272-2280.

16) S. Rossi, R. Porta, D. Brenna, A. Puglisi and M. Benaglia, *Angew. Chem. Int. Ed.*, 2017, **56**, 4290 –4294.

17) R. Boobalan, G.H. Lee and C. Chen, *Adv. Synth. Catal.*, 2012, **354**, 2511-2520.

18) T. Arai, A. Joko, and K. Sato, *Synlett*, 2015, **26**, 209-214.

19) Y. Zhou, J. Dong, F. Zhang, and Y. Gong, *J. Org. Chem.*, 2011, **76**, 588–600.

20) A. Toussaint and A. Pfaltz, A., *Eur. J. Org. Chem.*, 2008, 4591–4597.

21) E. Chinnaraja, R. Arunachalam, and P.S. Subramanian, *ChemistrySelect*, 2016, **1**, 5331 – 5338.

22) J. K. Guterl, J. N. Andexer, T. Sehl, J. v. Langermann, I. Frindi-Wosch, T. Rosenkranz, J. Fitter, K. Gruber, U. Kragl, T. Eggert and M. Pohl, *J. biotechnol.*, 2009, **141**, 166-173.

23) B.V. Priya, D.H.S. Rao, A. Chatterjee, and S.K. Padhi, *Chem. Comm.*, 2023, **59**, 12274-12277.

24) T. Sehl, H.C. Hailes, J.M. Ward, R. Wardenga, E. von Lieres, H. Offermann, R. Westphal, M. Pohl and D. Rother, *Angew. Chem. Int. Ed.*, 2013, **52**, 6772 –6775.

25) M. Gruber-Khadjawi, T. Purkarthofer, W. Skranc and H. Griengl, *Adv. Synth. Catal*., **349**, 1445-1450.

26) J. Kaldun, F. Prause, D. Scharnagel, F. Freitag and M. Breuning, *ChemCatChem*, 2016, **8**, 1846-1856.

27) R. Kowalczyk and J. Skarżewski, *Tetrahedron: Asymmetry*, 2009, **20**, 2467-2473.

28) D. Costes, E. Wehtje and P. Adlercreutz, *Enzyme and microbial technology,* 1999, **25**, 384-391.

29) H. Griengl, A. Hickel, D.V. Johnson, Schmidt, C. Kratky and H. Schwab, *Chem. Comm.*, 1997, **20**, 1933-1940.

30) A. Nuylert, F. Motojima, C. Khanongnuch, T. Hongpattarakere and Y. Asano, *ChemBioChem*, 2020, **21**, 181-189.

Chapter 4

Diastereoselective synthesis of different β-nitroalcohols by using *Bm*HNL as the biocatalyst

4.1. Introduction:

Basic introduction of diastereoselective synthesis of β-nitroalcohols is provided in section 3.1 of chapter 3. In this chapter we will be discussing about the diastereoselective synthesis of (*S*)-β-nitroalcohols . Here, we tried to uncover the catalytic potential of wild-type *Bm*HNL in the diastereoselective synthesis of optically active β-nitroalcohols, which remains unexplored so far. To date, *Hb*HNL is the only (*S*)-selective HNL known to catalyze promiscuous Henry reaction until recently, we reported the same by *Bm*HNL.[1] The diastereoselective Henry reaction by *Hb*HNL produced (*1S,2R*)-2-NPP with 67% yield, 95% ee and 80% de starting from benzaldehyde and nitroethane.[2] *Bm*HNL and *Hb*HNL belong to the α/β hydrolase fold superfamily and share 56% sequence similarity. They also possess similar catalytic machinery of Asp-His-Ser-Lys-Thr in the active site.[3] Hence, we hypothesized that *Bm*HNL may catalyze the diastereoselective Henry reaction similar to *Hb*HNL. This enzyme not only showcased broad substrate selectivity it also showed co-substrate promiscuity when both nitroethane and 1-nitropropane were tested as nucleophilic co-substrates. Total thirty three different β-nitroalcohols in their (*1S,2R*) stereoisomeric form have been synthesised using this biocatalyst with excellent % conversion and stereoselectivity (up to >99% conversion, up to 99% ee, and up to 94% de). This robust enzyme was found to be extremely stable in the reaction medium and retained >85% of its activity even after incubating for 2 months. After observing its long stability, it was successfully recycled for 20 cycles without any decrease in % ee of (*1S,2R*)-2-NPP while a TTN of 37,170 was observed. Here *Bm*HNL has also been used for the synthesis of (*1S,2S*) stereoisomer of half a dozen β-nitroalcohol diastereomers, which has not been reported yet by any biocatalytic approach. Through this method we successfully synthesized (*1S,2S*)-2-NPP the β- nitroalcohol precursor form of cathine, a well-known appetite suppressor.[4]

4.2. Objectives

1. Expression and purification of *Bm*HNL and preparation of crude enzyme extracts.

2. Optimization of biocatalytic parameters for diastereoselective synthesis of 2-NPP by using *Bm*HNL crude enzyme.

3. Exploring the substrate scope of *Bm*HNL in the diastereoselective synthesis of different β-nitroalcohols starting from various aromatic aldehydes and nitroethane.

4. Optimization of biocatalytic parameters for diastereoselective synthesis of 2-nitro-1-phenyl butan-1-ol (2-NPB) using *Bm*HNL.

5. Exploring the substrate scope of *Bm*HNL in the diastereoselective synthesis of different β-nitroalcohols starting from various aromatic aldehydes and 1-nitropropane.

6. Determination of *Bm*HNL's stability in the reaction medium and recycling of the enzyme.

7. Gram scale synthesis of (*1S,2R*)-2-NPP using *Bm*HNL recycling approach.

8. Determination of the kinetic parameters of *Bm*HNL towards the diastereoselective Henry reaction.

9. Synthesis of different *syn* (*1S,2S*)-diastereomers of β-nitroalcohols from their corresponding aldehydes and nitroethane.

4.3. Materials and methods

4.3.1. Chemicals and materials

Culture media and ampicillin were purchased from HiMedia laboratory Pvt. Ltd, India. Isopropyl-β-D-1-thiogalactopyranoside (IPTG) was purchased from SRL Pvt. Ltd, India. Aldehydes, nitromethane, nitroethane, 1-nitropropane, and mandelonitrile were purchased from Sigma Aldrich, AVRA, SRL, Alfa-Aesar and TCI. Deuterated solvents such as chloroform was purchased from Sigma Aldrich. HPLC grade solvents were obtained from FINAR pvt. ltd., India. All buffer salts were procured from SRL. Chemicals purchased were used without further purification. Silica gel 100-200 mesh used in column chromatography purifications was purchased from Molychem. ^{1}H- and ^{13}C-NMR spectra were recorded on a Bruker instrument with deuterated chloroform as solvents. ^{1}H-NMR data are given as chemical shift (δ ppm), multiplicity (s = singlet, brs = broad singlet d = doublet, t = triplet, q = quartet, m =multiplet, dd = doublet of doublet, dt = doublet of triplet, dq = doublet of quartet, qd = quartet of doublet, ddd = doublet of doublet of doublet, dddd = doublet of doublet of doublet of doublet, coupling constant (Hz), and integration. ^{13}C-NMR data are reported in terms of chemical shift relative to $CDCl_3$ (77.16 ppm). VCX500 ultrasonic processor was used for lysing the cells by sonication. Enzyme assay was carried out in a UV/Vis Microplate reader, Multiscan Go, Thermo Fisher Scientific. TLC silica gel 60 F_{254} plates from Merck were used to monitor organic reactions using a UV-lamp for visualization.

4.3.2. Chromatography

Analytical high performance liquid chromatography (HPLC) along with chiral analysis was performed in an Agilent 1260 Infinity II system or LC-2080 using isopropanol and hexane as the mobile phase. Lux 5µm Amylose-1, Lux 5µm Cellulose-1, and Daicel CHIRALPAK IB columns (4.6 x 20 mm, 5 µm) were used to separate stereoisomers. Shimadzu LC-2080 HPLC in reverse phase was used to calculate the % conversion of several substrates. The Agilent InfinityLab Poroshell 120 EC-C18 (4.6 x 150 mm, 4 µm) was used as the reverse phase column and water and acetonitrile as the mobile phase.

4.3.3. Cloning

*Bm*HNL (LOCUS: AB505969) synthetic gene cloned into pUC57 was procured from Gene Script, USA. It was sub-cloned into pCold1 plasmid at *BamH*I and *Sal*I and transformed into BL21 DE3 cells for subsequent use.

4.3.4. Expression, crude enzyme preparation, and purification of *Bm*HNL and preparation of extracts

Expression and purification of *Bm*HNL were carried out using our previously optimized method.[3] *E.coli* BL21(DE3) cells transformed with *BmHNL* plasmid were inoculated in sterile LB broth comprised of 100 µg/mL ampicillin and incubated at 37 °C, 180 rpm for 12-16 h to prepare primary culture. A 2% (v/v) primary culture inoculum was further used to prepare the secondary culture and incubated at 37 °C until $O.D_{600}$ reaches 0.5 – 0.8. Then cells were subjected to a cold shock by incubating them at 4 °C for 2 h and induced by 1 mM IPTG followed by incubated at 18 °C, 180 rpm for 24 h. Cells were harvested by centrifuging at 8000 rpm for 12 minutes, and the cell pellet was suspended in 20 mM potassium phosphate buffer (KPB) pH 7. Suspended cells were sonicated over ice and centrifuged at 10000 rpm for 45 min. This supernatant was used as crude enzyme extract or purified by Ni-NTA agarose affinity chromatography. Protein purification was done by loading the sonicated supernatant into a Ni-NTA agarose column pre-equilibrated with twice its volume of binding buffer (20 mM imidazole, 300 mM sodium chloride, 20 mM KPB, pH 7). The column was subsequently washed with three supernatant volumes of wash buffer (50 mM imidazole, 300 mM sodium chloride, 20 mM KPB, pH 7), and finally eluted with one supernatant volume of elution buffer (500 mM imidazole, 300 mM sodium chloride, 20 mM KPB, pH 7). The elution was dialyzed in 20 mM KPB pH 7 for 3 h, three times. The dialyzed protein was concentrated and used for biocatalysis.

4.3.5. Assessing the effectiveness of purified wild-type *Bm*HNL in the stereoselective synthesis of 2-nitro-1-phenylpropanol (2-NPP), using benzaldehyde as the substrate and nitroethane as the nitroalkane.

Initially *Bm*HNL was tested for its promiscuous diastereoselective Henry activity using benaldehyde and nitroethane as the substrate and nucleophile respectively. The reaction condition used was, 600 µL of *n*-butyl acetate, 50 mM KPB (50 µL, 1.25 M), 15 mg of crude *Bm*HNL, 1 M nitroethane (92 µL), and 20 mM benzaldehyde solution (25 µL, 1 M). Final reaction volume was maintained 1.25 mL by adding remaining amount of double-distilled water. Benzaldehyde stock was prepared in *n*-butyl acetate. This reaction mixture was incubated at 30 °C and 1,200 rpm in a thermoshaker. A 100 µL reaction aliquot was diluted in 200 µL of hexane: 2-propanol (90:10). The diluted reaction aliquot was vortexed vigorously and dried over anhydrous sodium sulphate to remove any aqueous part, and then centrifuged at 15000*g* for 5 min at 4 °C. A 20 µL of this sample was taken and analysed in HPLC using appropriate chiral column.

4.3.6. Optimization of biocatalytic parameters for diastereoselective synthesis of 2-NPP

To improve the catalytic activity of BmHNL for the synthesis of (1S,2R)-2-NPP, various reaction conditions like buffer type, buffer pH, buffer concentration, organic solvent, nitroethane (cosubstrate) concentration, and enzyme content were optimized.

4.3.6.1 Buffer and pH optimization

In this experiment, two buffers KPB and citrate phosphate buffer (CPB) were tested varying their pH from 5.5 to 7. Reaction condition was as follows, 600 µL *n*-butyl acetate, 50 mM reaction buffer (42 µL, 1.5 M), 15 mg of crude *Bm*HNL, 1 M nitroethane (92 µL), and 20 mM

benzaldehyde solution (25 µL, 1 M). Final reaction volume was maintained to 1.25 mL by adding remaining amount of double-distilled water. Benzaldehyde stock was prepared in *n*-butyl acetate. Remaining reaction parameters were kept similar as mentioned in section 4.3.5.

4.3.6.2. Organic solvent optimization

For organic solvent optimization experiment, different organic solvents like *n*-butyl acetate (NBA), *tert*-butyl methyl ether (TBME), diethyl ether (DEE), toluene and di-isopropyl ether (DIPE) were tested. Reaction composition was, 600 µL of different organic solvent, 50 mM CPB pH 5.5 (42 µL, 1.5 M), 15 mg of crude *Bm*HNL, 1 M nitroethane (92 µL), and 20 mM benzaldehyde solution (25 µL, 1 M). Final reaction volume was maintained to 1.25 ml by adding the remaining amount of double-distilled water. Benzaldehyde stock was prepared in corresponding organic solvent used. The remaining reaction parameters were kept similar as mentioned in section 4.3.5.

4.3.6.3. Nitroethane concentration optimization

Co-substrate concentration is an important reaction parameter in HNL catalyzed Henry reaction. Six different concentrations of nitroethane were tested to improve the % conversion and stereoselectivity of *Bm*HNL. The detailed reaction condition was, 600 µL TBME, 50 mM CPB pH 5.5 (42 µL, 1.5 M), 15 mg of crude *Bm*HNL, 0.75 M (69 µL)/ 1 M (92 µL)/ 1.25 M (114.7 µL)/ 1.5 M (138 µL)/ 1.75 M (161 µL)/ 2 M (184 µL) nitroethane, and 20 mM benzaldehyde solution (25 µL, 1 M). The final reaction volume was maintained at 1.25 mL by adding the remaining amount of double-distilled water. Benzaldehyde stock was prepared in TBME. Remaining reaction parameters were kept similar as mentioned in section 4.3.5.

4.3.6.4. Citrate phosphate buffer concentration optimization

The concentration of reaction buffer i.e., CPB was optimized in this experiment. Buffer concentration was varied from 50 to 250 mM. The reaction condition was, 600 µL TBME, 50 mM CPB pH 5.5 (42 µL, 1.5 M)/ 100 mM (83 µL, 1.5 M)/ 150 mM (125 µL, 1.5 M)/ 200 mM (167 µL, 1.5 M)/ 250 mM (208 µL, 1.5 M), 1.75 M (16L µL) nitroethane, 20 mM benzaldehyde solution (25 µL, 1 M), and 15 mg of crude *Bm*HNL. Final reaction volume was maintained to 1.25 mL by adding the remaining amount of double-distilled water. Benzaldehyde stock was prepared in TBME. The remaining reaction parameters were kept similar as mentioned in section 4.3.5.

4.3.6.5. Enzyme content optimization

To optimize the amount of enzyme required to improve the yield and stereselectivity of the product, six different enzyme amounts were taken into consideration starting from 5 to 25 mg. The reaction composition was, 600 µL TBME, CPB pH 5.5 100 mM (83 µL, 1.5 M), 5 / 10 /, 15 / 20 / 25 mg of crude *Bm*HNL, 1.75 M (161 µL) nitroethane, and 20 mM benzaldehyde solution (25 µL, 1 M). Final reaction volume was maintained to 1.25 ml by adding the remaining amount of double-distilled water. Benzaldehyde stock was prepared in TBME. Remaining reaction parameters were kept similar as mentioned in section 4.3.5.

4.3.6.7. Determining the tolerable substrate loading

To determine the tolerable substrate loading in our biotransformation, we varied the substrate concentration from 20 to 150 mM. The reaction condition was similar to the previous

experiment, except in the case of higher substrate concentrations TBME amount was varied to maintain the total volume of TBME and substrate stock to 625 µL.

4.3.7. Biocatalytic diastereoselective Henry reaction in the synthesis of different β-nitroalcohols starting from their corresponding aldehydes using nitroethane as the nucleophile

The optimized reaction conditions achieved from the above study was extended towards other aromatic aldehydes to synthesize their corresponding chiral β-nitroalcohols. A typical reaction contained 600 µL TBME, 5 mM different aldehyde substrate (25 µL, 250 mM), 1.75 M nitroethane (161 µL), 100 mM CPB pH 5.5 (83 µL, 1.5 M), and 1 mg purified *Bm*HNL. Aldehyde stock solutions were made in TBME separately. The total reaction volume was made up to 1.25 mL by adding the remaining volume of autoclaved double distilled water. Remaining reaction parameters were kept similar as mentioned in section 4.3.5.

4.3.8. Assessing the effectiveness of purified wild-type *Bm*HNL in the stereoselective synthesis of 2-nitro-1-phenylbutanol (2-NPB), using benzaldehyde and 1-nitropropane

After successfully adding nitroethane as the nucleophile with an array of aromatic aldehydes, we checked the catalytic potential of *Bm*HNL towards accepting a bulkier nucleophile, 1-nitropropane in the diastereoselective Henry reaction. The optimized reaction conditions used in 4.3.7. was adopted here. The reaction condition used was, 600 µL TBME, 100 mM CPB pH 5.5 (83 µL, 1.5 M), 1 mg of purified *Bm*HNL, 1.75 M 1-nitropropane (195 µL), and 5 mM benzaldehyde solution (25 µL, 250 mM). Final reaction volume was maintained 1.25 mL by adding remaining amount of double-distilled water. Benzaldehyde stock was prepared in TBME. This reaction mixture was incubated at 30 °C and 1,200 rpm in a thermoshaker. A 100 µL reaction aliquot was diluted in 200 µL of hexane: 2-propanol (90:10). The diluted reaction aliquot was vortexed vigorously and dried over anhydrous sodium sulphate to remove any aqueous part, and then centrifuged at 15000*g* for 5 min at 4 °C. A 20 µL of this sample was taken and analysed in HPLC using appropriate chiral column.

4.3.9. Optimization of biocatalytic parameters for diastereoselective synthesis of 2-nitro 1-phenyl butanol (2-NPB)

4.3.9.1. Optimization of reaction time and catalyst amount: Different amounts of BmHNL were used and incubated for longer periods to optimize the reaction time and catalyst amount. Purified *Bm*HNL, 1 / 2.5 / 5 mg was used for this study. All other reaction conditions were the same as the previously described method in section 4.3.8.

4.3.9.2. Optimization of 1-nitropropane concentration: To optimize the 1-nitropropane concentration in biocatalytic Henry reaction a range of 1-nitropropane concentrations (0.25 - 1.75 M) were used. The reaction condition was, 600 µL TBME, 0.25-1.75 M 1-nitropropane, 1 mg purified *Bm*HNL, 100 mM CPB pH 5.5 (83 µL, 1.5 M), and 5 mM benzaldehyde (25 µL, 250 mM). The reaction volume was made up to 1.25 mL using double distilled water. Substrate stock preparation and other reaction parameters were kept similar. All other reaction conditions were the same as the previously described method in section 4.3.8.

4.3.10. Biocatalytic diastereoselective Henry reaction in the synthesis of diverse β-nitroalcohols using 1-nitropropane as the nucleophile

The optimized reaction conditions of 4.3.9. were extended towards other aromatic aldehydes to synthesize their corresponding β-nitroalcohol product. A typical reaction contained 600 µL TBME, 5 mM different aldehyde (25µL, 250 mM), 1 M nitropropane (111 µL), 100 mM CPB pH 5.5 (63 µL, 2M), and 1 mg purified *Bm*HNL. Substrate stock preparation and other reaction parameters were kept similar. Product extraction and HPLC were done according to the previously described method in the section 4.3.9 above.

4.3.11. Determination of kinetics parameters towards the synthesis of (*1S,2R*)-2-NPP

The initial reaction rate of *Bm*HNL catalysed synthesis of (*1S,2R*)-2-NPP was determined based the amount of product obtained, analysed via normal phase chiral HPLC. A preliminary set of experiments to find out the time period for 10% conversion came to be 10 minutes. Accordingly, kinetic study was performed by carrying out biocatalysis with varied substrate concentration. The reaction condition used was, 1.75 M nitroethane (161 µL), 1 to 25 mM benzaldehyde, 100 mM CPB pH 5.5 (83 µL, 1.5 M), and 0.5 mg purified *Bm*HNL. Substrate stock preparation was done in TBME. Total volume of organic solvent i.e., TBME and stock substrate solution was kept 625 µL. Total reaction volume was made up to 1.25 mL by adding double distilled water. For each substrate concentration, biocatalysis reaction was incubated for 10 mins. Product extraction and HPLC were done according to the previously described method. Solver function in Microsoft excel was used to best fit the data to Michaelis – Menten equation.

4.3.12. Evolution of promiscuous nitroaldolase activity over hydrocyanation

Here we aimed to compare *Bm*HNL's nitroaldolase activity with its natural hydrocyanation activity. Based on easy to execution, we reverse the plan and *Bm*HNL was subjected to retro-nitroaldolase vs cyanogenesis. Towards retro-nitroaldolase different β-nitroalcohols having varied alkyl carbon chain length, were used as substrates. Racemic 2-nitro 1-phenyl ethan-1-ol (2-NPE), 2-NPP, and 2-NPB were used as the β-nitroalcohols for the cleavage assay, while racemic mandelonitrile as the cyanhohydrin for cyanogenesis. This promiscuous retro-nitroaldolase activity was compared with its natural cyanogenesis activity. The detailed reaction condition was as follows, 160 µL of 50 mM CPB pH 5.5, 20 µL 70 mM substrate prepared in 5 mM CPB pH 3.15, and 20 µL purified *Bm*HNL (1 mg/mL). The activity was calculated using the molar extinction coefficient of benzaldehyde (1380 M^{-1} cm^{-1}). One unit of HNL activity is defined as the quantity of enzyme that generates 1 µmol of benzaldehyde per minute from mandelonitrile or any of the above BNA substrates used in this study. All measurements were performed in triplicates. The control experiment had all the reaction components except the enzyme which was replaced by its corresponding buffer.

4.3.13. Determination of *Bm*HNL's stability in the reaction medium and recycling of the enzyme

The stability of *Bm*HNL was tested by measuring the loss of activity at different time points, using mandelonitrile cleavage assay. The aqueous layer of the biocatalytic reaction of diastereoselective synthesis of 2-NPP, was collected after incubation for a definite time,

because the enzyme lies in the aqueous part. Specific activity of the aqueous part was calculated using mandelonitrile cleavage assay as described in the section of 4.3.12. above. A typical biocatalytic reaction mixture contained, 538 µL of TBME, 1.75 M nitroethane (161 µL), 70 mM benzaldehyde (87.5 µL, 1 M), 100 mM CPB pH 5.5 (63 µL, 2 M), and 1 mg *Bm*HNL.

The recyclability of the enzyme was tested using the same reaction condition mentioned 4.3.7. except the benzaldehyde concentration was increased to 70 mM. In every 7 h, the organic layer was removed, and a fresh 70 mM benzaldehyde, 1.75 M nitroethane, and 538 µL TBME was added to the aqueous reaction mixture. TTN calculation was done by using the following formula

$$Total\ turnover\ number = \frac{\mu mol\ of\ product\ formed}{\mu mol\ of\ BmHNL\ used}$$

4.3.14. Gram scale synthesis of (*1S,2R*)-2-NPP by recycling the *Bm*HNL

*Bm*HNL was recycled for twenty consecutive cycles in the stereoseelctive synthesis of 2-NPP. Beyond ten cycles slight but steady decrease in enzyme activity was observed, hence for gram scale synthesis the enzyme was recycled up to ten cycles. The biocatalytic reaction condition for this experiment was as follows. The reaction mixture had 12 mg purified *Bm*HNL, 100 mM CPB pH 5.5 (1.2 mL, 1.25 M), TBME 50% (7.4 mL), 70 mM benzaldehyde (108.7 µL), nitroethane 1.75 M (1.93 mL), and 2.24 mL of water (Figure 4.1). The reaction was incubated at 30° C and 1200 rpm. After every 7 h the organic layer of the reaction containing chiral product, TBME, nitroethane, and remaining benzaldehyde was collected and replaced with fresh benzaldehyde, TBME, and nitroethane.

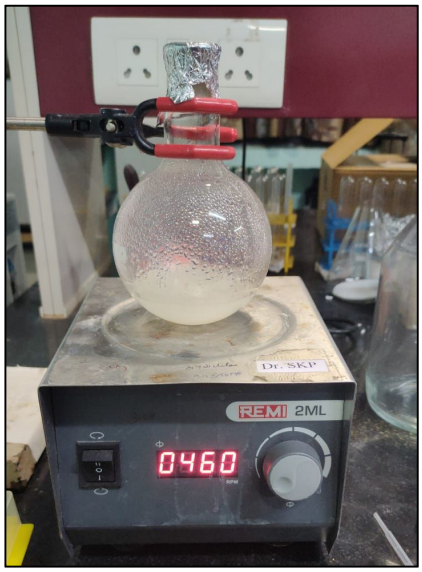


Figure 4.1: Reaction setup for the gram-scale synthesis of (*1S,2R*)-2-NPP using *Bm*HNL.

4.3.15. Conversion of *anti* (*1S,2R*)-2-NPP to *syn* (*1S,2S*)-2-NPP by *Bm*HNL

After observing the formation of (*1S,2S*)-2-NPP along with (*1S,2R*)-2-NPP, especially when the biotransformation was carried out for a longer period of time, we studied to find out the path through which (*1S,2R*)-2-NPP gets transformed into its (*1S,2S*)- stereoisomer. The experiment used (*1S,2R*)-2-NPP as the starting material. The common reaction condition used

was as follows 583 µL TBME, 5 mM (*1S,2R*) stereoisomer (150 mM, 42 µL), 100 mM CPB pH 5.5 (83µL, 1.5 M), 1 mg *Bm*HNL. (*1S,2R*)-2-NPP stock was prepared in TBME. This reaction mixture was incubated at 30 °C and 1,200 rpm in a thermoshaker. The reaction product was observed through both chiral HPLC and ^{1}H NMR. Two separate reactions were carried out, in one reaction 1.75 M nitroethane (161 µL) was added, while in the second, nitroethane was replaced with 161 µL of double distilled water.

4.3.16. Synthesis of enantiopure *syn* (*1S,2S*)-β-nitroalcohols

This experiment was carried out to synthesize the enantiopure *syn* (*1S,2S*) stereoisomers from their corresponding aldehydes. At first, *Bm*HNL catalyzed Henry reaction was performed starting from different aldehydes and nitroethane for longer time period using similar reaction condition as described in section 4.3.7 to get a mixture of (*1S,2R*)- and (*1S,2S*)-β-nitroalcohols. After completion of the reaction, the reaction mixture was extracted using TBME and concentrated under vacum. The concentrated reaction product was diluted into 625 µL TBME and was used as the substrate for *Bm*HNL catalyzed retro-Henry reaction for stereoselective cleavage of (*1S,2R*)-stereoisomer. The reaction mixture of the retro-Henry reaction was composed of 100 mM CPB pH 5.5 (83 µL, 1.5 M), 1 mg *Bm*HNL and the Henry product diluted in TBME. The total reaction volume was made up to 1.25 mL by adding the remaining volume of autoclaved double distilled water. This reaction mixture was incubated at 30 °C and 1,200 rpm in a thermoshaker. Aliquot extraction and HPLC were done according to the method described in section 4.3.7.

4.3.17. Chemical synthesis of racemic β-nitroalcohols

Racemic β-nitroalcohols were synthesized by following the same protocol mentioned in section 3.3.19 in chapter 3.

4.4. Results

4.4.1. Barium hydroxide catalyzed synthesis of different racemic β-nitroalcohols starting from their corresponding aromatic aldehydes and nitroethane or 1-nitropropane

The racemic standards used here are also used for the diastereoselective synthesis with *At*HNL mutants. Details about the reactions, molecules synthesized, and yield are already discussed in section 3.4.1. and 3.4.3. of chapter 3.

4.4.2. NMR characterization of nitroethane and 1-nitropropane corresponding racemic β-nitroalcohols

The NMR characterization of standards of racemic β-nitroalcohols resulted by addition of nitroethane to various aldehydes are provided in section 3.4.2 of chapter 3, similarly the 1-nitropropane added racemic β-nitroalcohols are given section 3.4.4 of chapter 3.

4.4.3. *Bm*HNL catalysed promiscuous diastereoselective nitroaldol reaction to synthesize 2-NPP

HNLs are a group of versatile biocatalysts that are well known for their reversible hydrocyanation activity and are used for the synthesis of enantiopure cyanohydrins from aldehydes or ketone and HCN.[5] Additionally, some of them can also catalyze the carboligation

between carbonyl substrates and nitroalkanes to produce β-nitroalcohols .[1,2,6,7] Though this promiscuous nitroaldol approach holds great synthetic applicability, to date, only *Hb*HNL is reported to catalyze the diastereoselective synthesis of (*S*)-β-nitroalcohols. It preferentially produces (*1S,2R*)-2-NPP from benzaldehyde and nitroethane. *Bm*HNL and *Hb*HNL belong to the same α/β hydrolase fold superfamily and share 56% sequence similarity. They also possess similar catalytic machinery of Asp-His-Ser-Lys-Thr in the active site.[3] Thus, it was hypothesized that *Bm*HNL may catalyze the diastereoselective Henry reaction similar to *Hb*HNL. To our surprise, crude cell lysates of *Bm*HNL catalyzed the stereoselective addition of nitroethane to benzaldehyde and synthesized (*1S,2R*)-2-NPP, the same stereoisomer produced by *Hb*HNL, with 60% conversion, 97% ee and 65% de.

4.4.4. Optimization of reaction conditions of *Bm*HNL catalyzed diastereoselective synthesis of (*1S,2R*)-2-NPP

Several important reaction parameters were optimized to improve the production of (*1S,2R*)-2-NPP with respect to % conversion and stereoselectivity.

4.4.4.1. Buffer and pH optimization: To find out a suitable buffer system to carry out this experiment, we used KPB and CPB, varying their pH from 5.5 to 7. At pH 5.5, *Bm*HNL showed 56.7% conversion with 97.4% ee, and its % de improved to 72% (Figure 4.2).

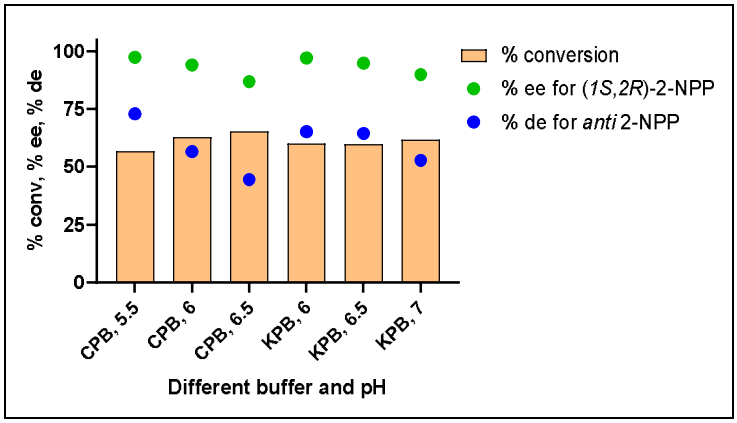


Figure 4.2: Effect of different pH and buffer on *Bm*HNL catalysed diastereoselective Henry reaction in the synthesis of 2-NPP.

4.4.4.2. Organic solvent optimization: To find a suitable organic solvent for this biphasic reaction system, five solvents, NBA, TBME, DEE, toluene and DIPE were tested. Among them, TBME provided the best results and showed a 16% improvement in % conversion compared to NBA (Figure 4.3).

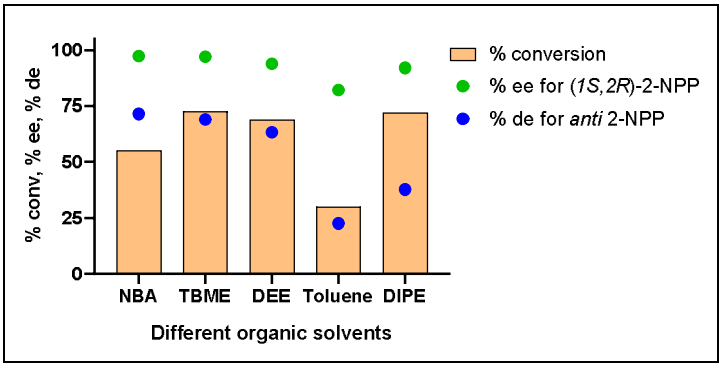


Figure 4.3: Effect of different organic solvents on *Bm*HNL catalysed diastereoselective Henry reaction in the synthesis of 2-NPP.

4.4.4.3. Nitroethane concentration optimization: Concentration of the co-substrate nitroethane was optimized in this experiment. Its concentration was varied from 0.75 to 2 M against 20 mM benzaldehyde (Figure 4.4). Catalytic activity concerning % conversion and enantioselectivity of *Bm*HNL increased with the increasing nitroethane concentration up to 1.75 M and slightly decreased further in 2 M nitroethane. The optimization study has improved % ee of 2-NPP from 97 to >99 and % de from 69 to 77.4 respectively.

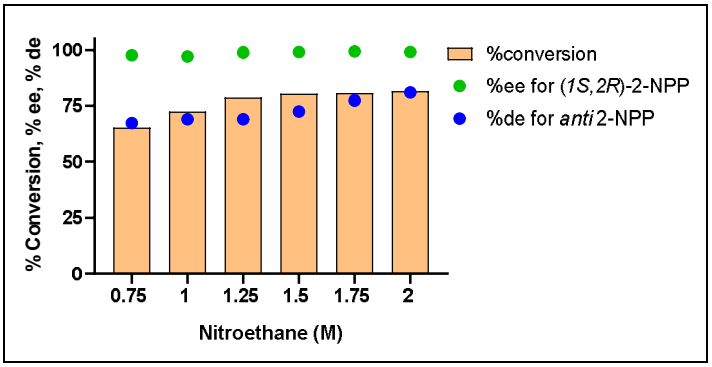


Figure 4.4: Effect of different nitroethane concentration on *Bm*HNL catalysed diastereoselective Henry reaction in the synthesis of 2-NPP.

4.4.4.4. Citrate phosphate buffer concentration optimization: Citrate phosphate buffer was found to be the most efficient buffer for this reaction, and its concentration was optimized in the subsequent experiment. With increasing buffer concentration, there was a slight improvement in % de with % conversion remained constant. *Bm*HNL showed 80% conversion in this optimized condition with >99% ee and 81.4% de (Figure 4.5).

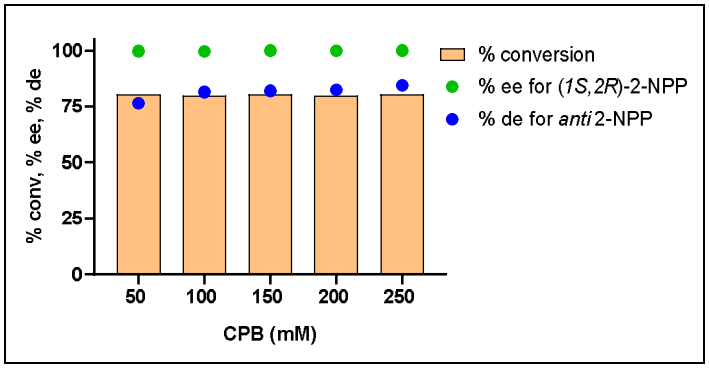


Figure 4.5: Effect of CPB concentration on *Bm*HNL catalysed diastereoselective Henry reaction in the synthesis of 2-NPP.

4.4.4.5. Optimization of *Bm*HNL amount: Since this study involves the use of the crude enzyme, the amount of enzyme was optimized by varying it from 5 to 25 mg (Figure 4.6). With an increase in enzyme amount, crude lysate of *Bm*HNL showed an increase in activity up to 10 mg, and after that, the % conversion and % ee remained the same.

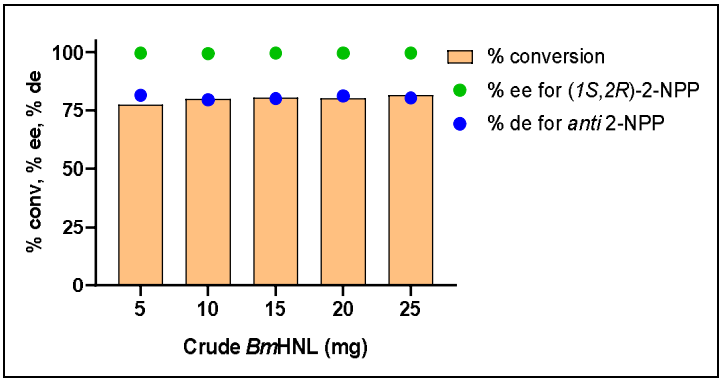


Figure 4.6: Effect of enzyme content on *Bm*HNL catalysed diastereoselective Henry reaction in the synthesis of 2-NPP.

After the optimization of the five parameters, *Bm*HNL showed 81% conversion with >99% ee and 80% de in the synthesis of (1*S*,2*R*)-2-NPP. The summary of the optimization study is presented in Figure 4.7.

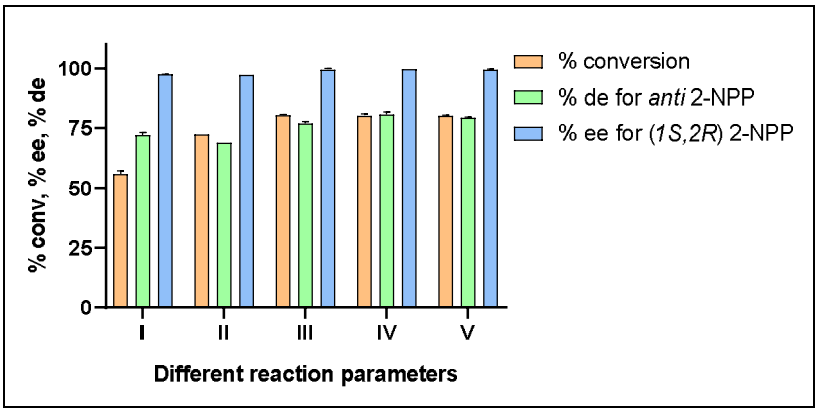


Figure 4.7: Summary of optimization of biocatalytic parameters of *Bm*HNL catalyzed nitroaldol reaction in synthesis of (*1S,2R*)-2-NPP using benzaldehyde and nitroethane. I: buffer system and pH, II: organic solvent, III: nitroethane concentration, IV: CPB concentration, V: enzyme content. The % conversion, % ee, and % de are mean of two data ± standard deviation.

4.4.4.6. Determining the tolerable substrate loading

To determine the highest substrate concentration that can be tolerated in the *Bm*HNL catalysed diastereoselective reaction, the substrate concentration was varied from 20 to 130 mM (Figure 4.8). With increasing substrate concentration, % conversion and % ee remained constant up to 70 mM, and later % conversion decreased gradually. Thus 70 mM was considered as the tolerable substrate concentration for further studies.

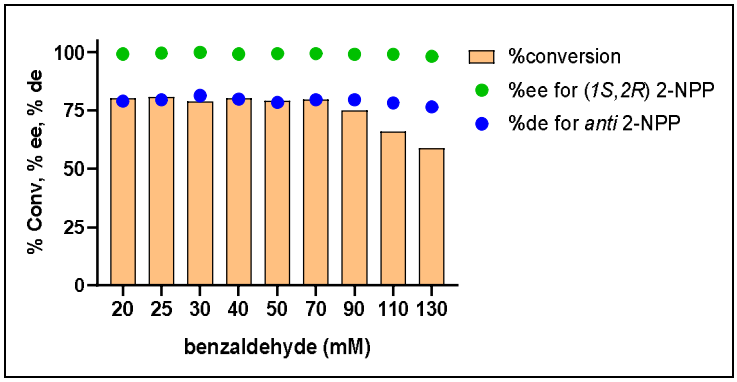


Figure 4.8: Determining the tolerable substrate concentration towards the *Bm*HNL catalyzed diastereoselective synthesis of 2-NPP.

4.4.5. SDS-PAGE of purified *Bm*HNL

Wild-type *Bm*HNL purified as described in section 4.3.4 above was characterized by SDS-PAGE (Figure 4.9). The purified protein fraction was analyzed by 12% SDS-PAGE and stained by Coomassie Brilliant Blue R-250. A clear band at around 29 kDa indicates good expression and purity of the purified *Bm*HNL enzyme.

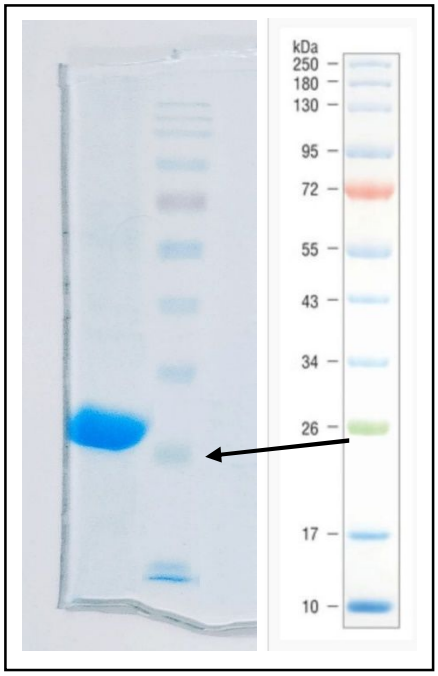


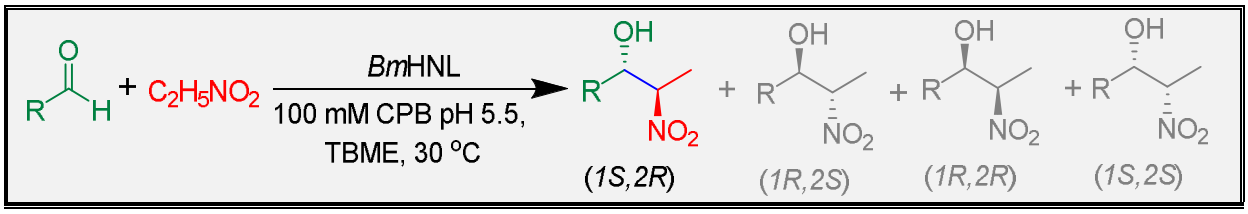
Figure 4.9: SDS-PAGE analysis of purified *Bm*HNL. Lane 1: pure *Bm*HNL, 2: ladder.

4.4.6. Purified *Bm*HNL catalyzed diastereoselective synthesis of *anti* (*1S,2R*)-stereoisomers of different β-nitroalcohols using nitroethane

Using the optimized biocatalytic reaction conditions, several aromatic aldehydes having substituents at different positions in the aromatic ring were converted into their corresponding *anti* (*1S,2R*)-diastereomers of β-nitroalcohols. This versatile substrate set contained both electron-donating and withdrawing groups, single and double substitutions in the aromatic ring, and substitutions were present at the *ortho*, *meta*, and *para* positions of the aromatic ring in different combinations. A total of nineteen substrates evaluated with *Bm*HNL for

diastereoselective synthesis resulted in up to >99% conversion with >99% ee and 92.4% de of corresponding (*1S,2R*)-β-nitroalcohols. (figure 4.23-4.41)

Among the nineteen substrates tested, *Bm*HNL could catalyze all aldehydes except 4-methoxy benzaldehyde, to synthesize their corresponding β-nitroalcohols . Irrespective of the chemical nature and position of the substituents in the aromatic part of the substrate, most of the aldehydes were tolerated by *Bm*HNL for catalysis (Figure 4.10). For example, methyl and methoxy substitutions and bromo and chloro substitutions, which are electron donating and withdrawing respectively, both showed 75->99% conversion with 98.8->99% ee except for 4-methyl benzaldehyde, where 66% conversion was observed. Aromatic aldehydes having double substitutions in their aromatic ring also exhibited very high catalytic activity. For example 2,3- dichloro, 2,3-dimethoxy, and 2,5-dimethoxybenzaldehyde showed >99, 89, and 94% conversion respectively, with >99% ee in every case. However, *Bm*HNL showed less catalytic efficiency when functional groups are introduced in the *para* position of the benzene ring. For example, 2-chloro and 3-chlorobenzaldehyde showed >99 and 93% conversion, whereas for 4-chlorobenzaldehyde, 75% conversion was found. A similar phenomenon was found in the case of 4-methyl and 4-methoxybenzaldehyde. Bulky substrates like 1-napthaldehyde and 3-benzyloxybenzaldehyde, which possess conjoint bicyclic aromatic ring and bulky benzyloxy substitution respectively, were also converted to their corresponding enantiopure (*1S,2R*)-• -nitroalcohols. While the former showed >99% conversion with >99% ee, the latter displayed 88.3% conversion with >99% ee. Even though *Bm*HNL could tolerate aromatic aldehydes with bulky substitutions attached in their benzene ring, in case of aldehydes with longer alkyl carbon chain length catalytic activity impaired severely. 3-Phenyl propionaldehyde, which possesses two extra carbons in the alkyl chain compared to benzaldehyde showed only 10% conversion with 95% ee. (figure 4.10)



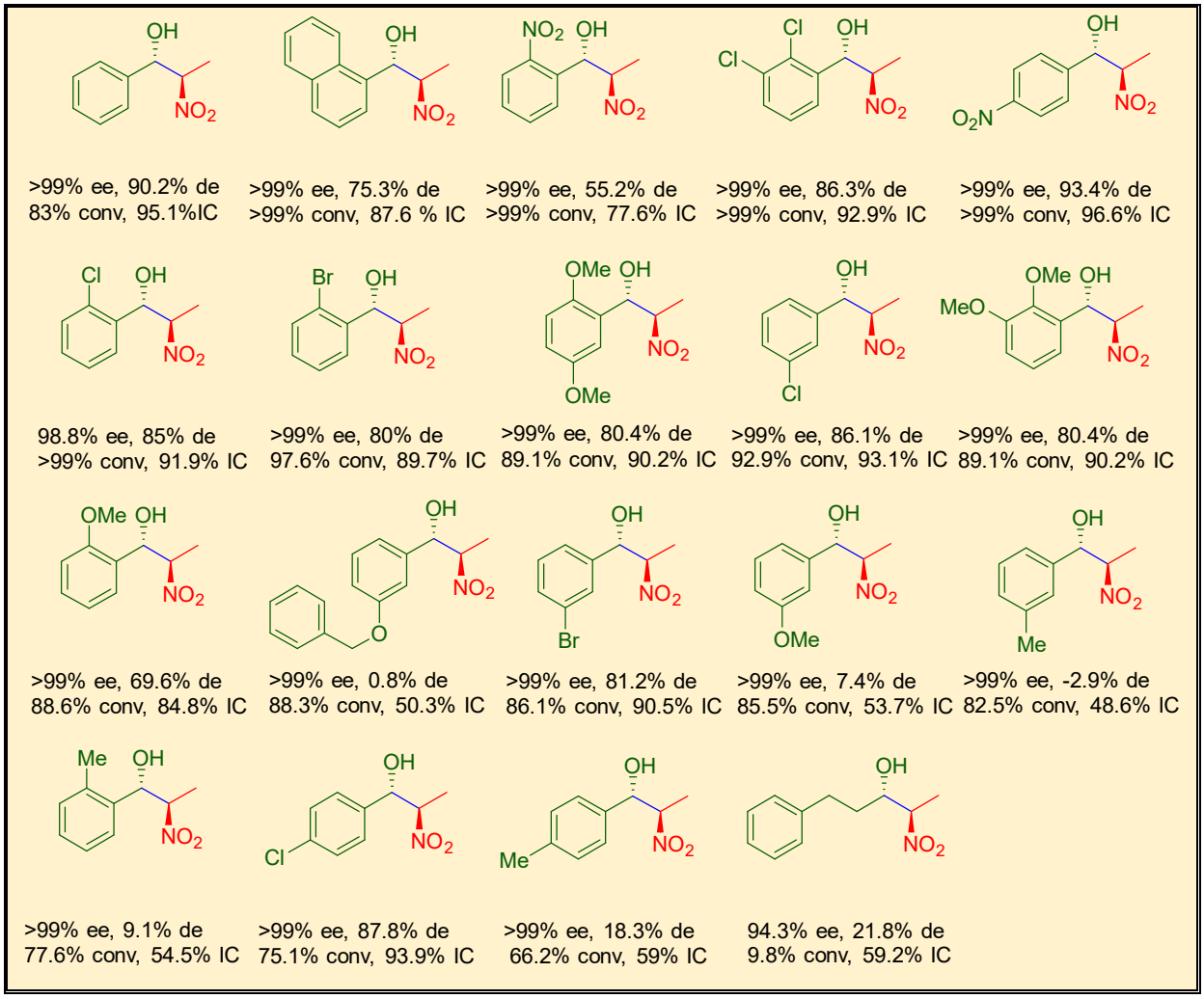


Figure 4.10: Stereoselective synthesis of *anti* (*1S,2R*)- stereoisomers of different β-nitroalcohols from their corresponding aldehydes and nitroethane by *Bm*HNL. Reaction conditions: TBME 600 µL, 5 mM aldehyde (25 µL, 250 mM), 1.75 M nitroethane (161 µL), 1 mg pure *Bm*HNL, and 100 mM CPB pH 5.5 (83 µL, 1.5 M). Benzaldehyde stock was prepared in TBME. The total reaction volume was made up to 1.25 mL by adding remaining amount of double distilled water.

4.4.7. Promiscuous nitroaldol reaction to synthesize 2-nitro-1-phenyl butanol (2-NPB) by using 1-nitropropane

After successfully synthesizing a series of enantiopure 2-nitrophenyl propanol derivatives using nitroethane, the same experiment was planned with a bulkier nucleophile, i.e., 1-nitropropane to explore *Bm*HNL's nucleophilic promiscuity. This is the first report, in parallel to our study discussed in chapter 3 of this thesis, where 1-nitropropane is used as the nucleophile in HNL catalysed Henry reaction. The optimized reaction condition obtained from the nitroethane study was employed here to conduct the preliminary experiments. However, unlike nitroethane, with 1-nitropropane crude *Bm*HNL enzyme showed very poor activity; hence the reaction was repeated with purified enzyme where a considerable better activity was observed. Purified *Bm*HNL showed 36% conversion with >99% ee and 81.3% de. To further enhance the activity, a few reaction parameters were subsequently optimized.

4.4.8. Optimization of reaction conditions towards *Bm*HNL catalysed diastereoselective synthesis of (*1S,2R*)-2-NPB

The optimized reaction condition obtained from the nitroethane study was implemented for 1-nitropropane study, with some parameters being exclusively optimized for the new co-substrate.

4.4.8.1. Optimization of reaction time and catalyst amount: The amount of purified enzyme was optimized to improve the % conversion of the synthesis of (*1S,2R*)-2-NPB. *Bm*HNL showed improved % conversion with increasing enzyme content, but failed to retain its stereoselectivity (Figure 4.11). For example, at 72 h, 1 mg of purified *Bm*HNL showed 63% conversion with >99% ee and 70% de, but use of 5 mg of enzyme produced only 10% de of 2-NPB.

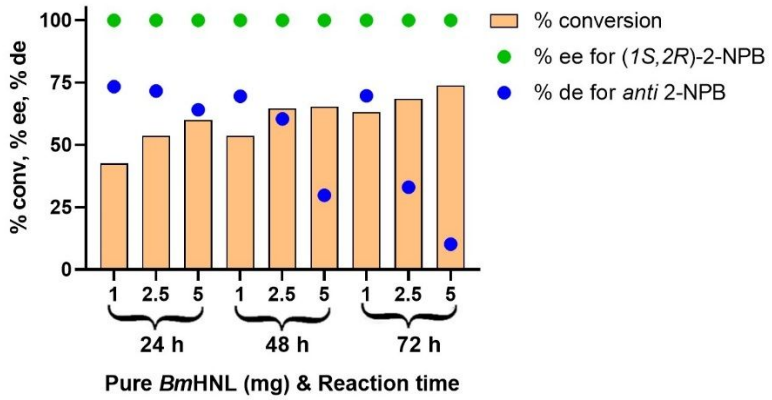


Figure 4.11: Effect of enzyme content and reaction time on *Bm*HNL catalysed diastereoselective Henry reaction in the synthesis of 2-NPB.

4.4.8.2. Optimization of 1-nitropropane concentration: In this study, 1-nitropropane concentration was optimized by varying it from 0.25 to 1.75 M. Previously 9% increase in the % conversion was observed while optimizing nitroethane concentration (Figure 4.12). BmHNL displayed increased % conversion with increasing 1-nitropropane concentration up to 1 M and then slightly decreased at higher concentrations. The % conversion increased to 39 while >99% ee and >99% de was observed at 1 M 1-nitropropane at 24 h.

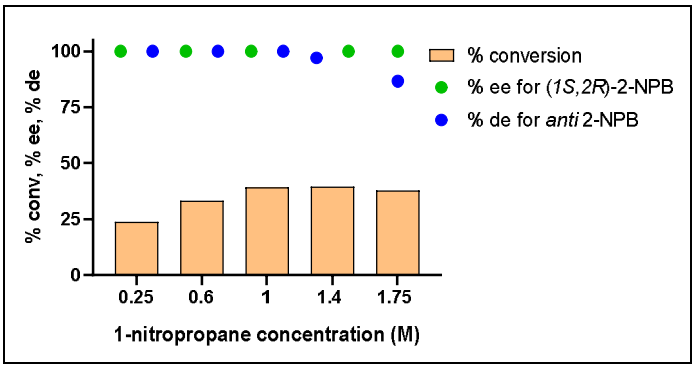


Figure 4.12: Effect of 1-nitropropane concentration on *Bm*HNL catalysed diastereoselective Henry reaction in the synthesis of 2-NPB.

After the optimization of the three parameters, *Bm*HNL showed 38% conversion with >99% ee and 90.2% de in the synthesis of (1*S*,2*R*)-2-NPB. The summary of the optimization study is presented in Figure 4.13.

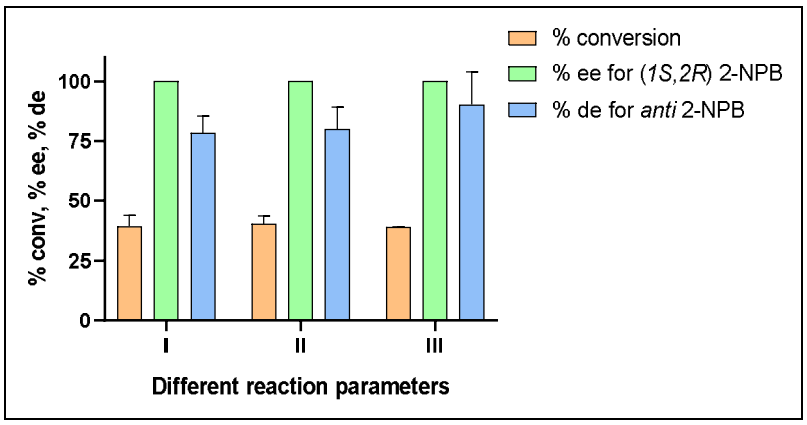
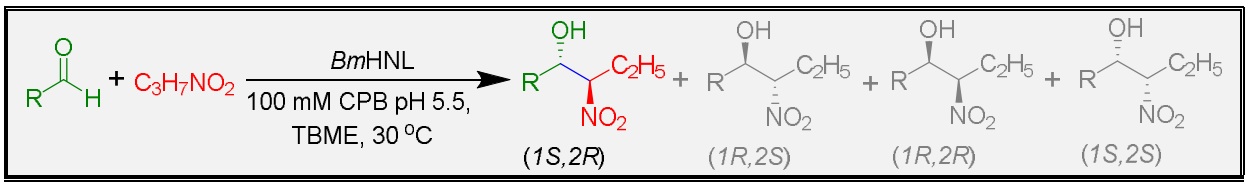


Figure 4.13: Summary of optimization of biocatalytic parameters of *Bm*HNL catalyzed nitroaldol reaction in the synthesis of (*1R,2S*)-2-NPB using benzaldehyde and 1-nitropropane. I: reaction with purified enzyme, II: reaction time and enzyme content, III: 1-nitropropane concentration. The % conversion, % ee, and % de are mean of two data ± standard deviation.

4.4.9. Purified *Bm*HNL catalyzed diastereoselective synthesis of *anti* (*1S,2R*)-stereoisomers of different β-nitroalcohols using 1-nitropropane

Fourteen aromatic aldehydes were taken for this study to synthesize their corresponding enantiopure *anti* (*1S,2R*)- stereoisomers of β-nitroalcohols using 1-nitropropane. Among them except 2-furaldehyde, all other aldehydes were tested in the nitroethane study (Figure 4.14). We observed that nitro substituted aldehydes are preferred over the other functional group substituted aldehydes and converted them to their products efficiently. For example, in case of 4-nitro and 2-nitrobenzaldehyde *Bm*HNL showed 97 and 89% conversion with 88 and >99% ee respectively. Unlike nitroethane study, in case of 1-nitropropane, we could notice a trend of preference of position of functional groups in the aromatic region of the aldehydes. For instance aldehydes having substitutions at *ortho* > *meta* > *para*, are seen in this *Bm*HNL catalysed Henry reaction. Except for 2-methoxybenzaldehyde, *ortho*-substituted 2-bromo and 2,3-dichloro benzaldehyde showed 89 and 79% conversion with 96 and 97% ee respectively. Aromatic aldehydes having *meta*-substitutions like 3-chloro, 3-methoxy, 3-bromo, and 3-methyl benzaldehydes showed 62, 53, 46, and 31% conversion with 88 - >99% ee. Lastly, substrates with *para* substitutions exhibited very minimum activity. For example, 4-chloro and 4-methyl benzaldehyde provided only 28% conversion with 96 and >99% ee. Extension in the alkyl chain in the aldehyde substrate massively reduced *Bm*HNL's efficiency, which we also found in case of nitroethane addition. 3-Phenyl propionaldehyde, which possesses two extra carbons in the alkyl chain, showed only 1% conversion in the Henry reaction. (figure 4.43-4.55)



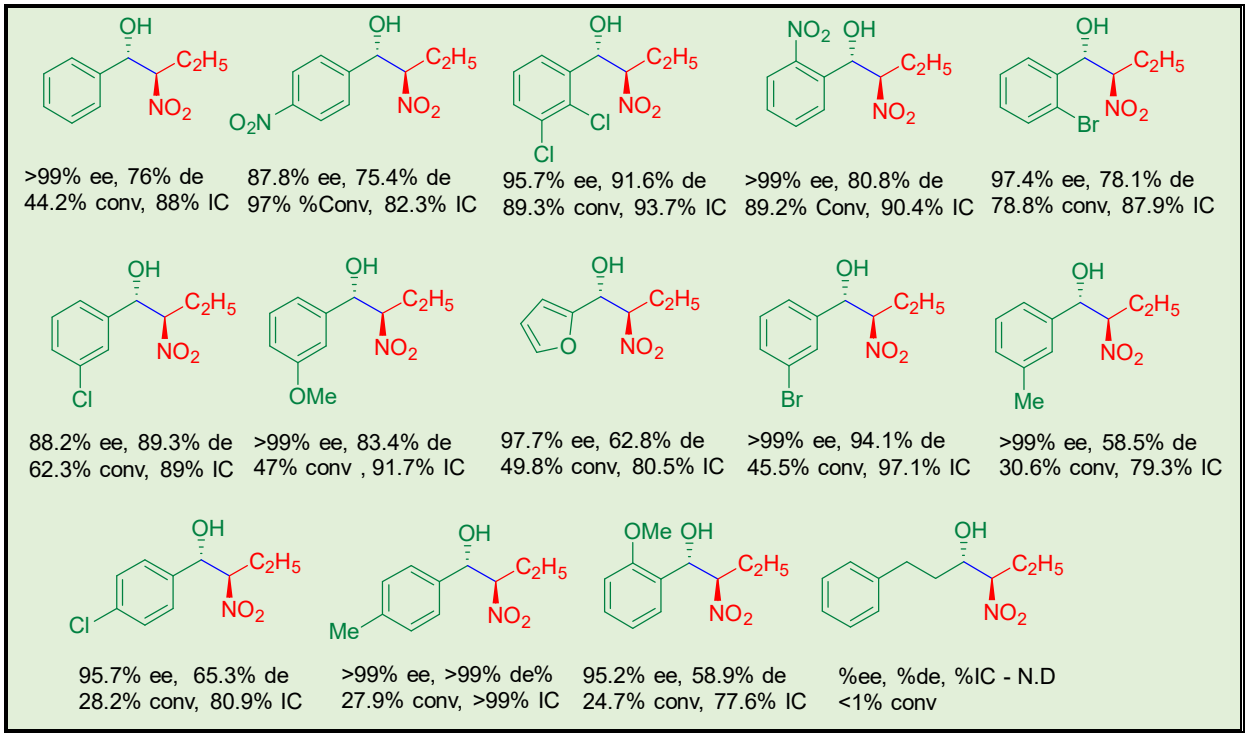


Figure 4.14: Stereoselective synthesis of *anti* (*1S,2R*)- stereoisomers of different β-nitroalcohols from their corresponding aldehydes and 1-nitropropane by *Bm*HNL. Reaction conditions: TBME 600 µL, 5 mM aldehyde (25 µL, 250 mM), 1 M 1-nitropropane (111 µL), 1 mg pure *Bm*HNL, and 100 mM CPB pH 5.5 (83 µL, 1.5 M). Benzaldehyde stock was prepared in TBME. The total reaction volume was made up to 1.25 ml by adding remaining amount of double distilled water.

4.4.10. Determination of the kinetic parameters of *Bm*HNL in the diastereoselective synthesis of 2-NPP

The steady-state kinetic parameters of *Bm*HNL towards the synthesis of (*1S,2R*)-2-NPP were determined by measuring the initial velocities against different concentrations of benzaldehyde (Figure 4.15). The K_M and V_{max} were found to be 10.3 mM and 0.46 µmol/min respectively. The catalytic efficiency (K_{cat}/K_M) was found to be 2.6 $mM^{-1}min^{-1}$. (figure 4.15)

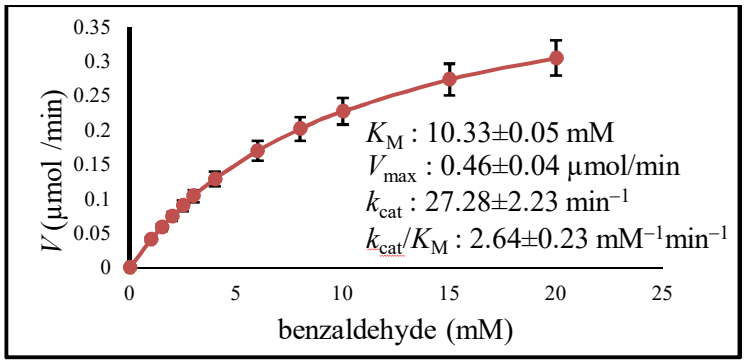


Figure 4.15: Michaelis-Menten plots of *Bm*HNL catalysed diastereoselective synthesis of (*1S,2R*)-2-NPP.

4.4.11. Comparing *Bm*HNL's hydrocyanation and nitroaldol activity by spectrophotometric cleavage assay

Here we aimed to compare *Bm*HNL's nitroaldolase activity with its natural hydrocyanation activity. Based on easy to execution, we reverse the plan and *Bm*HNL was subjected to retro-nitroaldolase vs cyanogenesis. Towards retro-nitroaldolase different β-nitroalcohols having varied alkyl carbon chain length, were used as substrates.

The impressive enantioselective and diastereoselective synthetic potential of *Bm*HNL suggests that the same active site can accommodate diverse chiral β-nitroalcohols. Here, we envisioned to compare the nitroaldolase vs. natural hydrocyanation activity of *Bm*HNL, however due to the simplicity and easy to perform, we measured retro-nitroaldolase vs. cyanogenesis activity of *Bm*HNL. Racemic mandelonirile on cyanogenesis and different β-nitroalcohols having varied alkyl carbon chain length on retro-Henry reaction produced benzaldehyde, which was used to calculate the cyanogenesis and nitroaldolase activity of *Bm*HNL. The cyanogenesis activity of was found to be 12 U/mg (Figure 4.16). However, when tested for nitroaldol reaction using different β-nitroalcohols , the same enzyme displayed less activity. Towards cleavage of racemic 2-nitro-1-phenyl ethanol (2-NPE), 2-NPP, and 2-NPB, it showed a specific activity of 1.41, 3.94, and 1.05 U/mg respectively. This data clearly indicates *Bm*HNL's preference for 2-NPP over other β-nitroalcohol substrates. This data also supports *Bm*HNL's enhanced nitroaldol synthesis activity when nitroethane was used as the nucleophilic co-substrate compared to 1-nitropropane (Figure 4.10, and Figure 4.14).

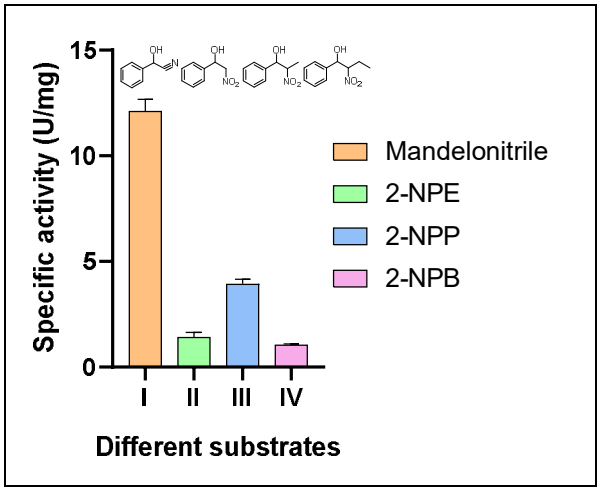


Figure 4.16. Comparing *Bm*HNL's hydrocyanation and nitroaldolase activity by spectrophotometric cleavage assay. I: Mandelonitrile, II: 2-NPE, III: 2-NPP, IV: 2-NPB.

4.4.12. Determination of *Bm*HNL's stability in the reaction medium and recycling of the enzyme

It is known that α/β hydrolase fold HNLs are known to be inhibited at higher aldehyde (especially benzaldehyde) concentrations. Here, we aimed to investigate the stability of *Bm*HNL when exposed to high aldehyde concentration for a prolonged time. In this regard, *Bm*HNL catalyzed Henry reaction was carried out in the presence of 70 mM of benzaldehyde for different time periods. We observed only a 14% loss of initial activity after incubating the

enzyme for two months, which confirms its high stability in the reaction condition (Figure 4.17A). This data inspired us to recycle the enzyme to synthesize the (1*S*,2*R*)-2-NPP. The minimum time to get the maximum % conversion was found to be 7 h. The enzyme was recycled for twenty consecutive cycles afterward. Up to ten cycles, *Bm*HNL could maintain >95% of its initial activity, afterwards a slight but steady decrease in enzyme activity was observed. However, after twenty cycles, *Bm*HNL could retain up to 82% of its activity compared to the first cycle. Throughout these twenty cycles of enzyme recycling, it could maintain >99% ee towards the synthesis of (*1S,2R*)-2-NPP (Figure 4.17B). Through this approach, a total of 1.75 mmol of benzaldehyde was converted to product with an average of 72% conversion. The total amount of enzyme used in this experiment was only 1 mg (MW of *Bm*HNL 29.5 kDa) [8], and thus a total turnover number (TTN) of the biocatalyst was calculated to be 37,170.

A) B)

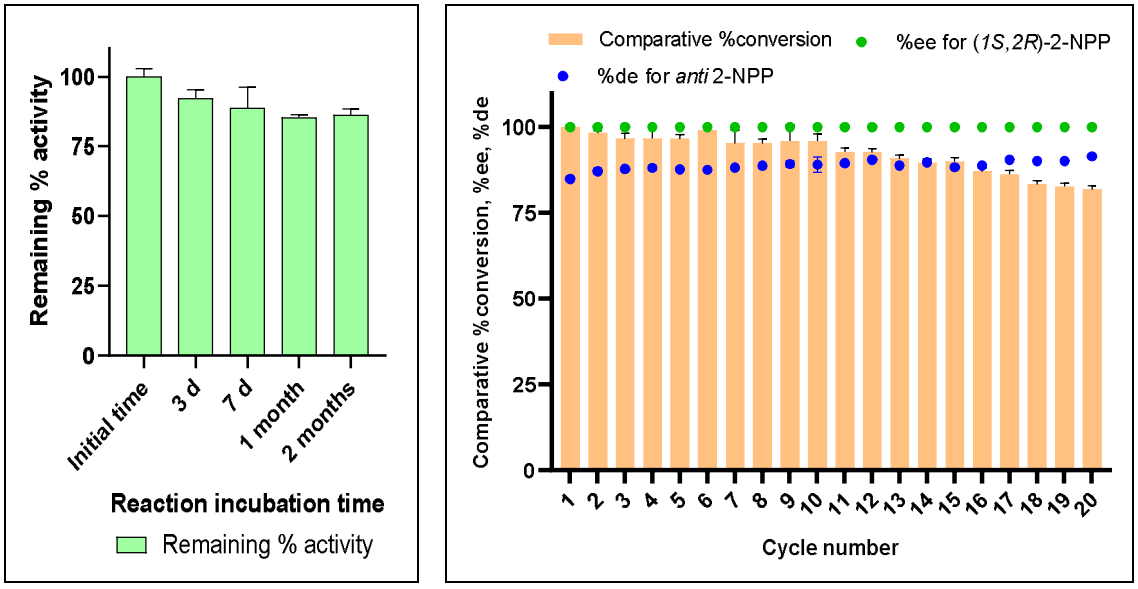


Figure 4.17: Determining *Bm*HNL's stability and recyclability in the reaction medium. (A): percentage of remaining specific activity of *Bm*HNL at different time points. (B): percentage of remaining specific activity of *Bm*HNL in the enzyme recycling experiment.

4.4.13. Gram scale synthesis of (*1S,2R*)-2-NPP by recycling the *Bm*HNL enzyme

*B*mHNL's recyclability experiment showed that the enzyme can be efficiently used up to ten cycles while retaining its % conversion and stereoselectivity. Using this recycling approach, we aimed to carry out a large scale synthesis of the *anti* (*1S,2R*)-2-NPP. We started with 153.5 U of *Bm*HNL (12 mg, 12.79 U/mg), and in each cycle of 7 h, 1.05 mmol of benzaldehyde was added into the reaction medium. Thus, total 1.11 g of benzaldehyde was converted into 0.99 g of product. The final product was obtained with >99% ee and 94% de (figure 4.42).

4.4.14. *Bm*HNL catalysed conversion of *anti* (*1S,2R*)-2-NPP to *syn* (*1S,2S*)-2-NPP

In the nitroaldol reaction between benzaldehyde and nitroethane, *Bm*HNL successfully synthesized (*1S,2R*)-2-NPP as the major product (>99% ee, 90.2% de) in a 2 h. However,

incubating the reaction beyond 2 h resulted in a gradual decrease in the % de, accompanied by the emergence of (*1S,2S*)-2-NPP, the *syn* stereoisomer, while maintaining the same % conversion. This observation confirms the specific conversion of the (*1S,2R*) stereoisomer to the (*1S,2S*), as evidenced by the high % ee of the *syn* stereoisomer (Figure 4.18). There might be two possible pathways through which this transformation can be explained. The first one is through steroinversion, and the second one is through the cleavage of (*1S,2R*) stereoisomer into benzaldehyde and then *Bm*HNL catalyzed synthesis of (*1S,2S*)- stereoisomer. To find out the actual phenomenon, pure (*1S,2R*)-2-NPP was synthesized and subjected to *Bm*HNL-catalyzed retro-Henry reaction in the absence and presence of nitroethane (Figure 4.19A, 4.19B). In absence of nitroethane, there was no increase in the (*1S,2S*), and a steady decrease in the (*1S,2R*) stereoisomer was observed, which eliminates the possibility of direct stereoinversion from (*1S,2R*) to (*1S,2S*) stereoisomer. However, in the presence of nitroethane, there was significant decrease in the amount of (*1S,2R*)-2-NPP was observed, followed by the increase in the (*1S,2S*) content. This confirms that the benzaldehyde formed due to (*1S,2R*) cleavage was converted to (*1S,2S*) stereoisomer through Henry reaction using nitroethane. It therefore clarifies that the (*1S,2S*) stereoisomer formed during the longer reaction time was synthesized through *Bm*HNL catalyzed (*1S,2R*) stereoisomer cleavage along with concomitant Henry reaction. This phenomenon was observed through both chiral HPLC and ^{1}H NMR (Figure 4.20).

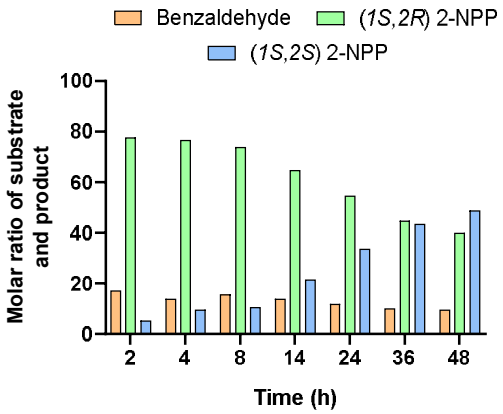


Figure 4.18: Conversion of (*1S,2R*)-2-NPP in to (*1S,2S*)-2-NPP with increase of time.

A) B)

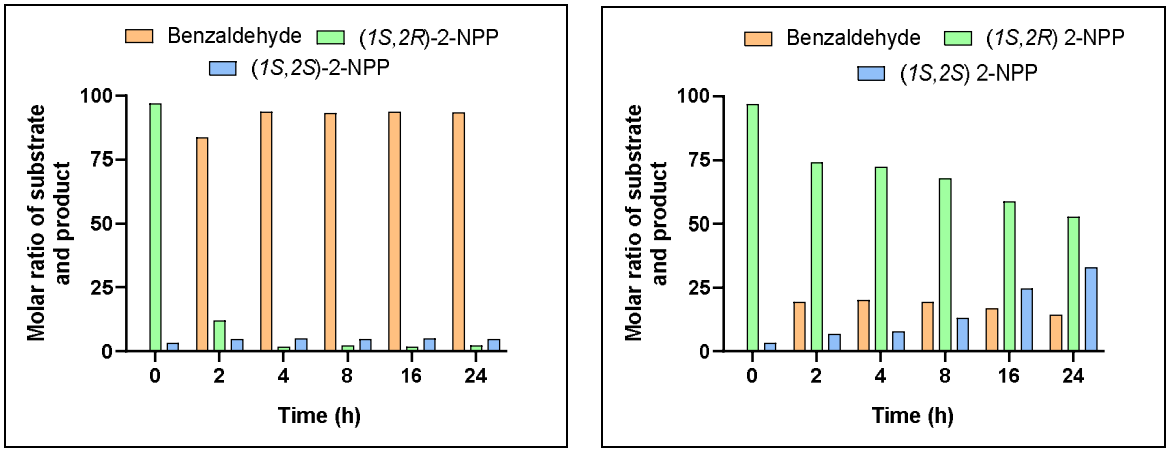


Figure 4.19: *Bm*HNL catalyzed cleavage of (*1S,2R*) 2-NPP in (A) absence and (B) presence of nitroethane.

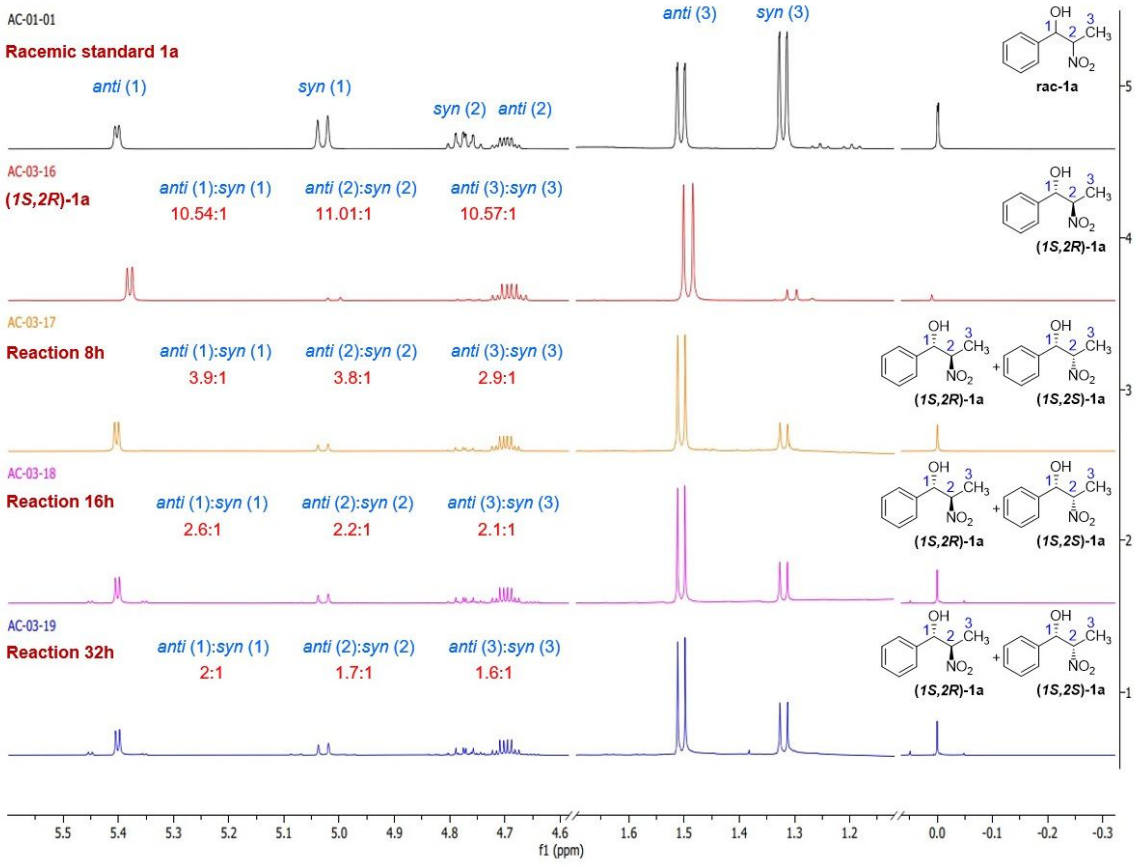
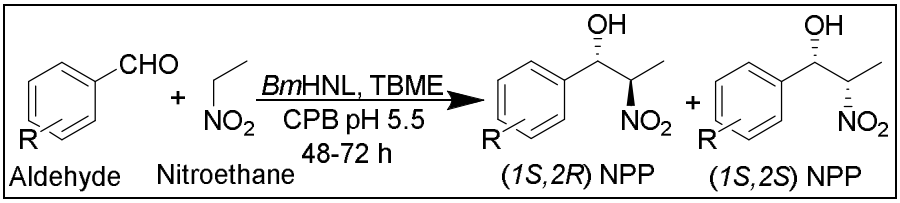


Figure 4.20: ^{1}H NMR chromatograms showing transformation of (*1S,2R*)-2-NPP to (*1S,2S*)-2-NPP over the time.

4.4.15. *Bm*HNL catalysed diastereoselective synthesis resulting a mixture of *anti* (*1S,2R*)- and *syn* (*1S,2S*)-β-nitroalcohols

Among the nineteen aromatic aldehydes used in the synthesis of their nitroethane corresponding (*1S,2R*)-β-nitroalcohols, ten of them showed ≥20% isomeric content (IC) for the (*1S,2S*) stereoisomer when the reaction mixture was incubated for 24 h. Having seen a potential to synthesize *syn* (*1S,2S*) products, we selected these ten substrate and studied further. The

optimized reaction conditions used for synthesizing (*1S,2R*) stereoisomers were kept used here, except the biotransformations were incubated for a longer time (Scheme 4.1). Among the substrates used, aromatic aldehydes having single methyl and methoxy substitution showed >60% IC for the (*1S,2S*)-stereoisomer with % conversion ranging from 79-94 and % ee from 98 to >99. Benzaldehyde and 3-benzyloxy benzaldehyde showed 87-88% conversion with 51 to 59% IC, and 94 - >99% ee of their (*1S,2S*)-stereoisomer, respectively. The remaining three substrates, 2-nitro benzaldehyde, 2,3-dimethoxy benzaldehyde, and 2,5-dimethoxy benzaldehyde, showed poor % IC ranging from 36-41 (Table 4.1).



Scheme 4.1: *Bm*HNL catalyzed synthesis of both diastereomers, (*1S,2R*)- and (*1S,2S*)-β-nitroalcohols.

Table 4.1: *Bm*HNL catalyzed synthesis of both diastereomers, *anti* (*1S,2R*)- and *syn* (*1S,2S*)-β-nitroalcohols

Substrate	Time (h)	Total % conversion	% ee of (1*S*,2*R*)	% ee of (1*S*,2*S*)	% de of *syn* product	IC of (1*S*,2*R*)	IC of (1*S*,2*S*)
2-nitro benzaldehyde	72	>99	>99	91.2	−24.4	62.2	36.2
3-benzyloxy benzaldehyde	72	87.8	>99	>99	2.7	48.4	51.2
3-methoxy benzaldehyde	48	94	>99	>99	24.2	37.9	62.1
benzaldehyde	72	87.4	87.7	94	10.1	35.9	59.1
2,5-dimethoxy benzaldehyde	72	93.7	99.5	>99	−20.9	60.3	39.6
2-methyl benzaldehyde	72	82.4	98.6	>99	21.8	38.8	60.9
4-methyl benzaldehyde	72	79	98.3	97.5	29.1	35.1	63.7
3-methyl benzaldehyde	48	85.3	>99	>99	27.2	36.4	63.6
2,3-dimethoxy benzaldehyde	72	93	>99	98	−16.7	58.3	41.2
2-methoxy benzaldehyde	72	81.6	98.7	97.9	27.6	35.9	63.1

4.4.16. Synthesis of enantiopure *syn* (*1S,2S*)-β-nitroalcohols

By extending the reaction incubation time, we could successfully synthesize the (*1S,2S*) stereoisomer as the major product for most of the aldehyde tested. However, along with the (*1S,2S*) stereoisomer, the synthesized product also contained its (*1S,2R*) form. In the previous experiment (Figure 4.19), we observed *Bm*HNL selectively cleaved the (*1S,2R*) isomer, leaving the (*1S,2S*) stereoisomer as such in the retro-Henry reaction. So, to cleave this remaining (*1S,2R*) form and to improve the overall % de of the final product, same *Bm*HNL was employed. The (*1S,2R*)- and (*1S,2S*)- mixtures of different β- nitroalcohols thus obtained were subjected to *Bm*HNL catalyzed cleavage (Figure 4.21). Eventually, pure (*1S,2S*) stereoisomers of β-nitroalcohols were synthesized from their corresponding aldehydes via our two-step process. Among the ten substrates, *Bm*HNL could successfully cleave six (*1S,2R*)-β-nitroalcohols, while it could not cleave four of them resulted from 2-nitro benzaldehyde, 3-benzyloxy benzaldehyde, 2,3-dimethoxy benzaldehyde and 2,5-dimethoxy benzaldehyde (Figure 4.21). Overall, our approach could synthesize six (*1S,2S*)-β- nitroalcohols in up to 59%

conversion, >99% ee and 94% de (figure 4.56-4.61). The ^{1}H NMR of the enantiopure (*1S,2S*)-2-NPP, which is an intermediate drug precursor of cathine, an appetite suppressor[4] is depicted in Figure 4.22.

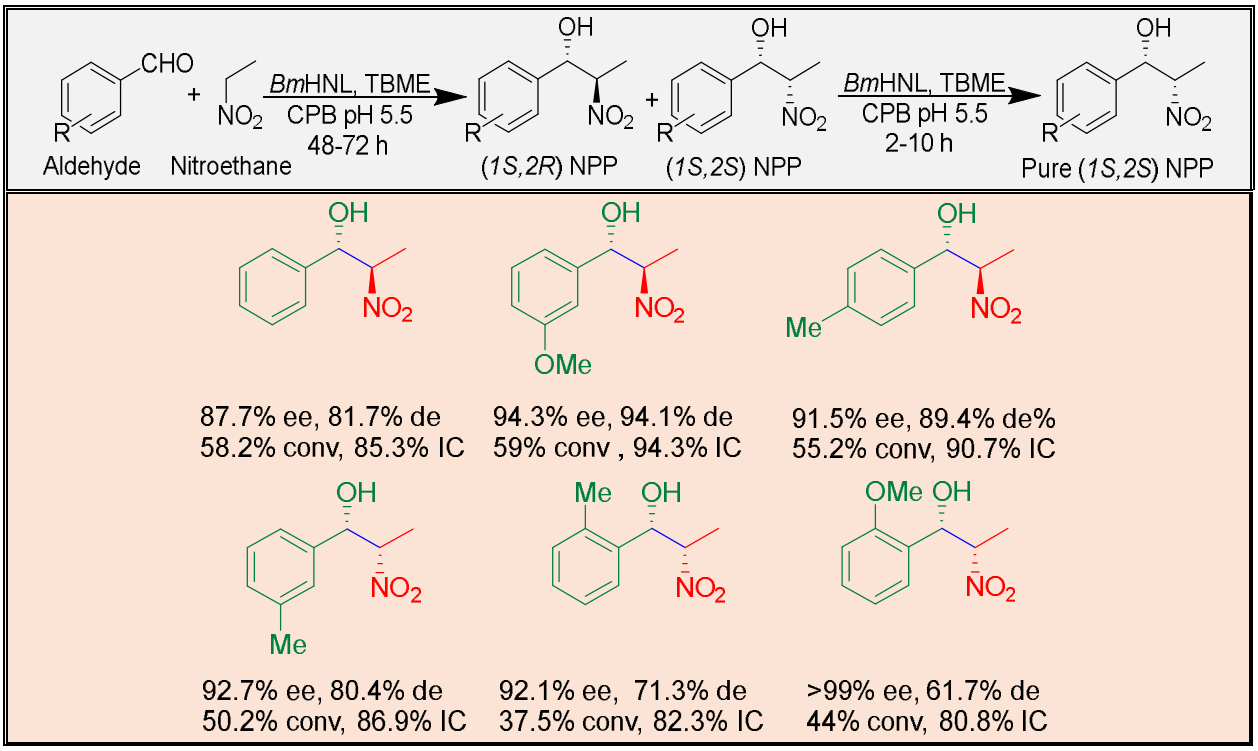


Figure 4.21: Synthesis of different (*1S,2S*)- β-nitroalcohols from corresponding achiral aromatic aldehydes.

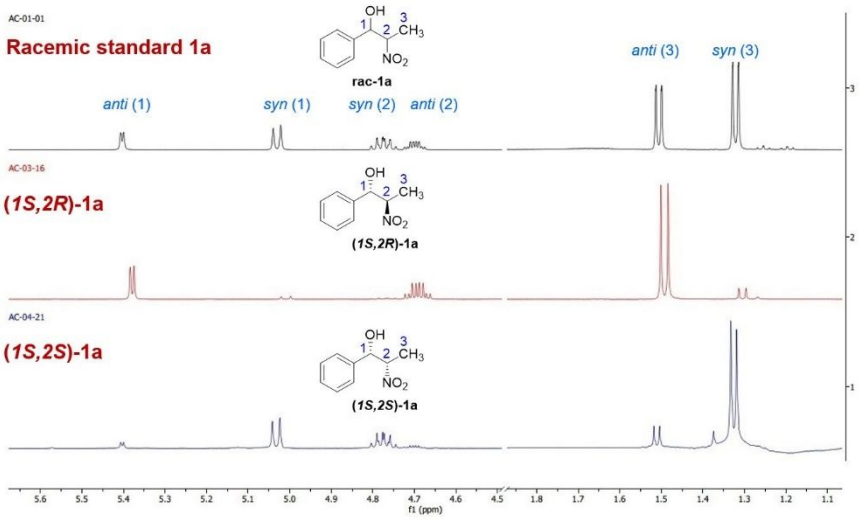


Figure 4.22: ^{1}H NMR depicting the formation of (*1S,2S*)-2-NPP. ^{1}H NMR of racemic and (*1S,2R*)-2-NPP are included for comparison.

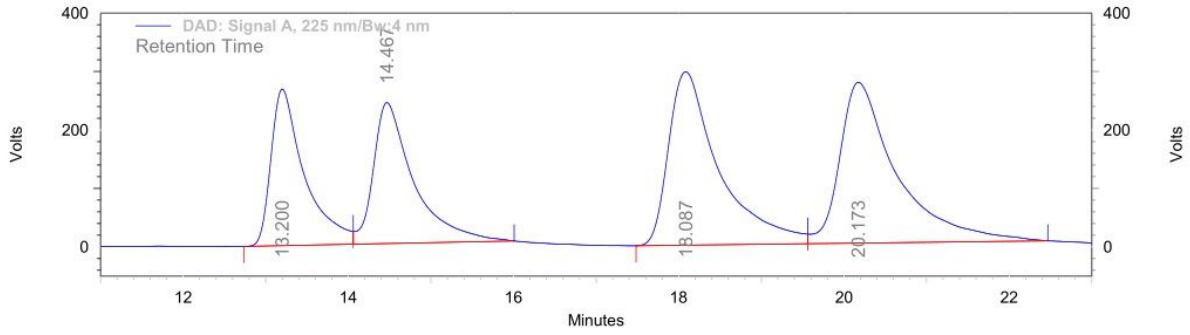
4.4.17. HPLC conditions for the chiral resolution of chemically synthesized standard racemic β-nitroalcohols

For chiral resolution of racemic β-nitroalcohols and the corresponding HPLC chromatograms please refer to section 3.4.22 of chapter 3.

4.4.18. HPLC chromatograms of biocatalytically synthesized (*1S,2R*)-nitrophenyl propanol derivatives starting from different aromatic aldehydes and nitroethane

1) HPLC chromatograms of 2-nitro 1-phenylpropan-1-ol

A)

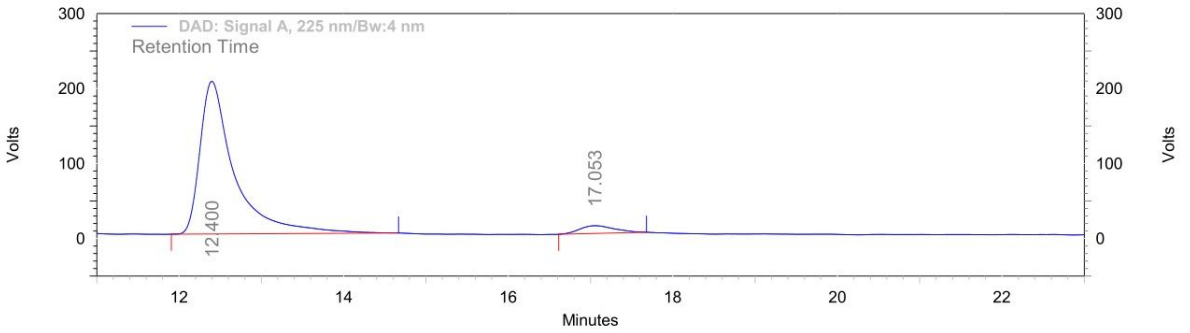


DAD: Signal A, 225 nm/Bw:4 nm
Results

Retention Time	Area	Area %	Height	Height %
13.200	15795092	18.18	561702	24.79
14.467	17125432	19.71	505579	22.32
18.087	26362942	30.35	621480	27.43
20.173	27591883	31.76	576632	25.45
Totals	86875349	100.00	2265393	100.00

Retention time	13.2	14.467	18.087	20.173
product	(*1S,2R*)	(*1R,2S*)	(*1S,2S*)	(*1R,2R*)

B)



DAD: Signal A,
225 nm/Bw:4 nm
Results

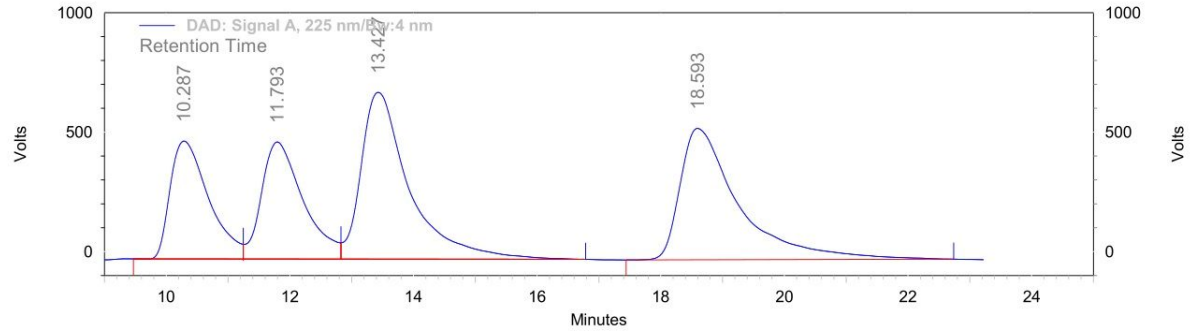
Retention Time	Area	Area %	Height	Height %
12.400	12354087	95.12	426743	95.20
17.053	633455	4.88	21537	4.80
Totals	12987542	100.00	448280	100.00

Retention time	12.4	17.053
product	(*1S,2R*)	(*1S,2S*)

Figure 4.23: HPLC chromatograms of 2-nitro 1-phenylpropan-1-ol. A. racemic standard, B. *Bm*HNL catalyzed synthesis of diastereomers.

2) HPLC chromatograms of 1-(3-chlorophenyl)-2-nitropropan-1-ol

A)

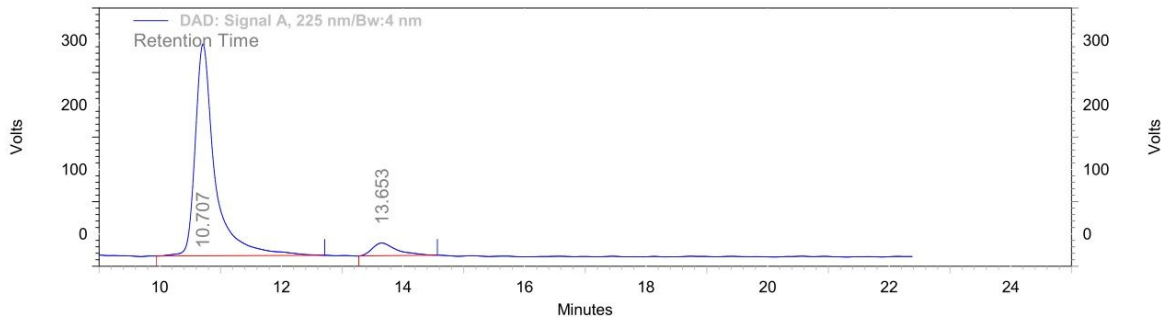


DAD: Signal A,
225 nm/Bw:4 nm
Results

Retention Time	Area	Area %	Height	Height %
10.287	44767727	18.05	1034580	22.11
11.793	48078930	19.39	1027392	21.96
13.427	79231420	31.95	1463289	31.28
18.593	75942902	30.62	1152971	24.65
Totals	248020979	100.00	4678232	100.00

Retention time	10.287	11.793	13.427	18.593
product	(*1S,2R*)	(*1R,2S*)	(*1S,2S*)	(*1R,2R*)

B)



DAD: Signal A,
225 nm/Bw:4 nm
Results

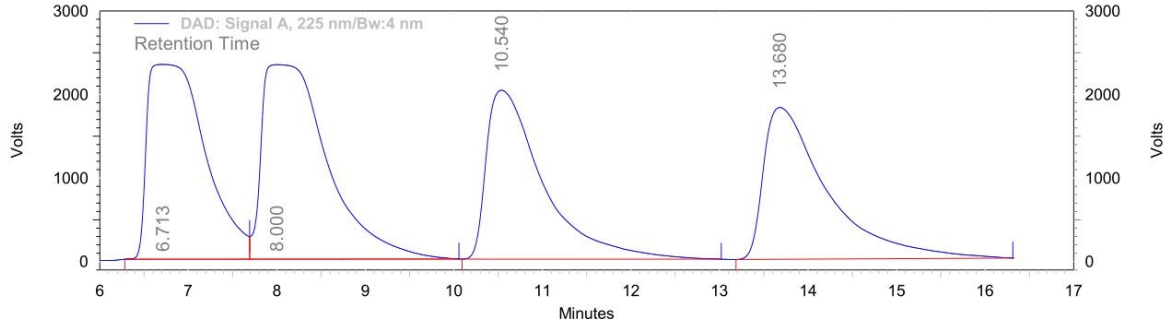
Retention Time	Area	Area %	Height	Height %
10.707	15554183	93.07	688152	94.34
13.653	1157407	6.93	41267	5.66
Totals	16711590	100.00	729419	100.00

Retention time	10.707	13.653
product	(*1S,2R*)	(*1S,2S*)

Figure 4.24: HPLC chromatograms of 1-(3-chlorophenyl)-2-nitropropan-1-ol. A. racemic standard, B. *Bm*HNL catalyzed synthesis of diastereomers.

3) HPLC chromatograms of 1-(2-chlorophenyl)-2-nitropropan-1-ol

A)

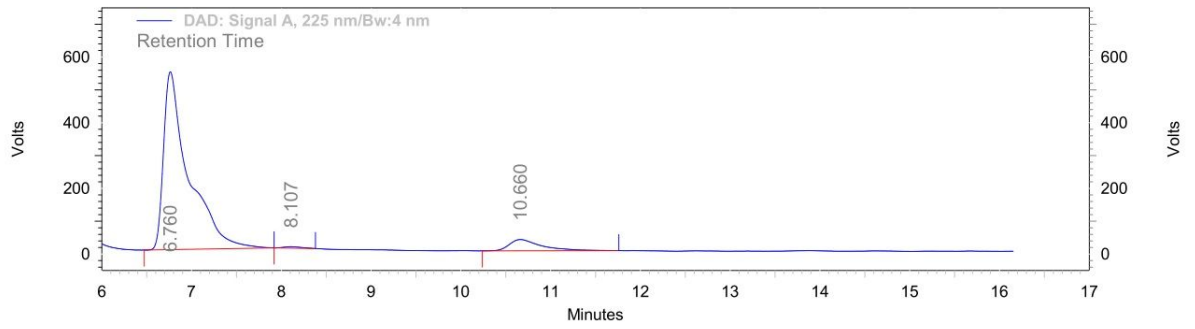


DAD: Signal A,
225 nm/Bw:4 nm
Results

Retention Time	Area	Area %	Height	Height %
6.713	222738764	26.06	4889094	27.43
8.000	252695631	29.57	4882619	27.40
10.540	188229089	22.02	4239058	23.79
13.680	191022457	22.35	3809950	21.38
Totals	854685941	100.00	17820721	100.00

Retention time	6.713	8	10.540	13.680
product	(*1S,2R*)	(*1R,2S*)	(*1S,2S*)	(*1R,2R*)

B)



DAD: Signal A,
225 nm/Bw:4 nm
Results

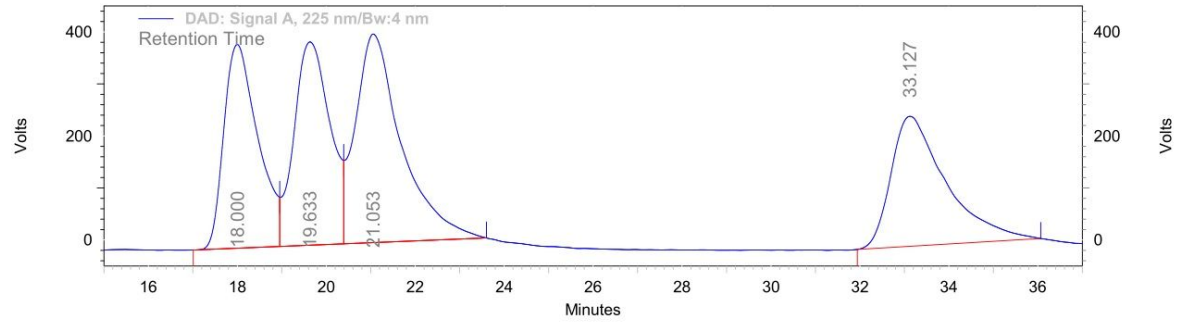
Retention Time	Area	Area %	Height	Height %
6.760	22079348	91.95	1136491	93.32
8.107	127198	0.53	9108	0.75
10.660	1805775	7.52	72245	5.93
Totals	24012321	100.00	1217844	100.00

Retention time	6.76	8.107	10.66
product	(*1S,2R*)	(*1R,2S*)	(*1S,2S*)

Figure 4.25: HPLC chromatograms of 1-(2-chlorophenyl)-2-nitropropan-1-ol. A. racemic standard, B. *Bm*HNL catalyzed synthesis of diastereomers.

4) HPLC chromatograms of 1-(3-methoxyphenyl)-2-nitropropanol

A)

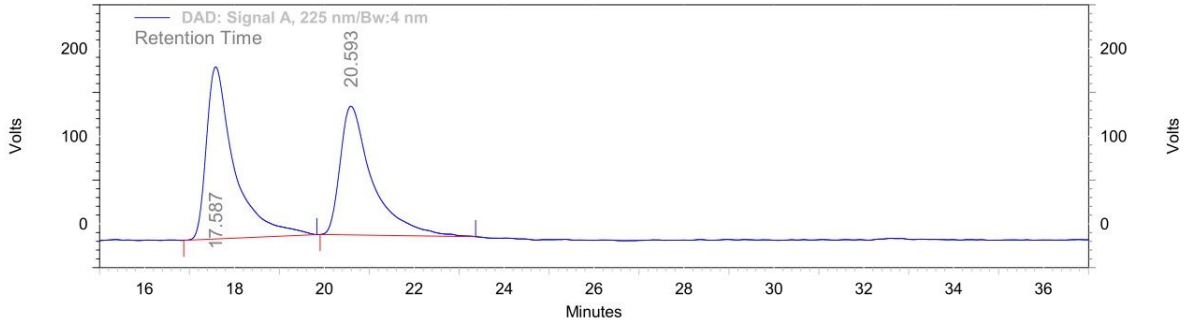


DAD: Signal A,
225 nm/Bw:4 nm
Results

Retention Time	Area	Area %	Height	Height %
18.000	43819856	22.38	821429	27.32
19.633	46223955	23.61	819757	27.27
21.053	60778842	31.05	841081	27.98
33.127	44944970	22.96	524027	17.43
Totals	195767623	100.00	3006294	100.00

Retention time	18	19.633	21.053	33.127
product	(*1S,2R*)	(*1R,2S*)	(*1S,2S*)	(*1R,2R*)

B)



DAD: Signal A,
225 nm/Bw:4 nm
Results

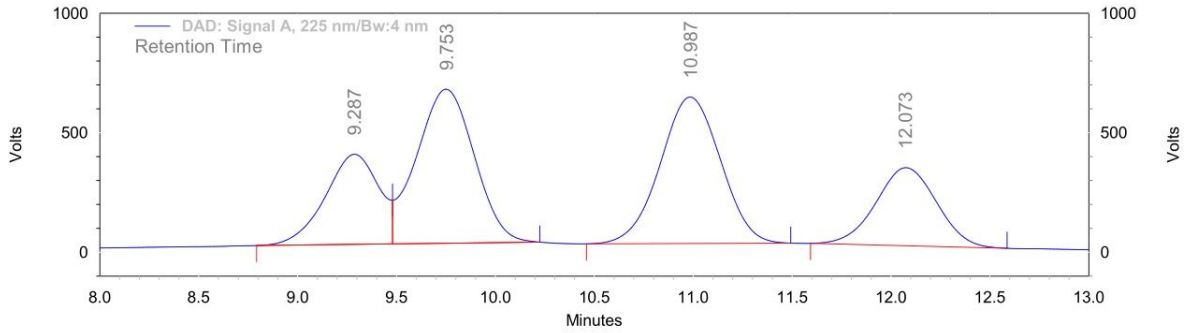
Retention Time	Area	Area %	Height	Height %
17.587	17770176	53.69	411913	57.22
20.593	15328560	46.31	307996	42.78
Totals	33098736	100.00	719909	100.00

Retention time	17.587	20.593
product	(*1S,2R*)	(*1S,2S*)

Figure 4.26: HPLC chromatograms of 1-(3-methoxyphenyl)-2-nitropropan-1-ol. A. racemic standard, B. *Bm*HNL catalyzed synthesis of diastereomers.

5) HPLC chromatograms of 1-(3-methylphenyl)-2-nitropropanol

A)

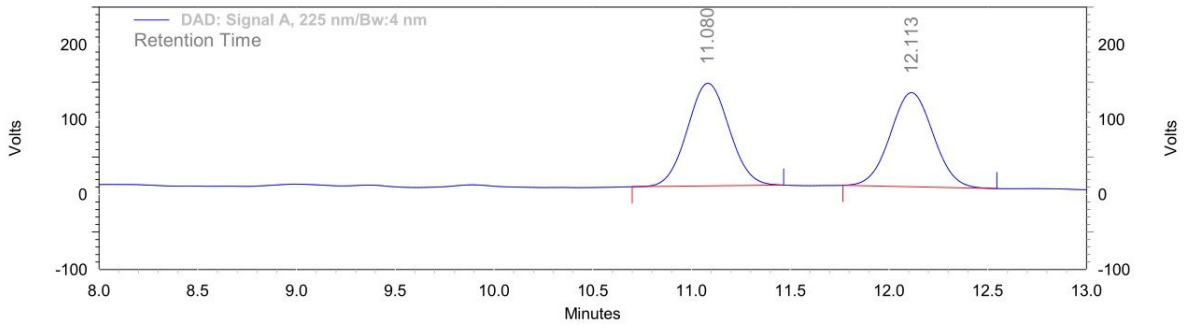


DAD: Signal A,
225 nm/Bw:4 nm
Results

Retention Time	Area	Area %	Height	Height %
9.287	14898772	17.67	790764	19.23
9.753	27510595	32.64	1351797	32.87
10.987	27263243	32.34	1284633	31.24
12.073	14625067	17.35	685198	16.66
Totals	84297677	100.00	4112392	100.00

Retention time	12.073	9.287	10.987	9.753
product	(*1S,2R*)	(*1R,2S*)	(*1S,2S*)	(*1R,2R*)

B)



DAD: Signal A,
225 nm/Bw:4 nm
Results

Retention Time	Area	Area %	Height	Height %
11.080	4242694	51.44	287211	52.14
12.113	4004748	48.56	263616	47.86
Totals	8247442	100.00	550827	100.00

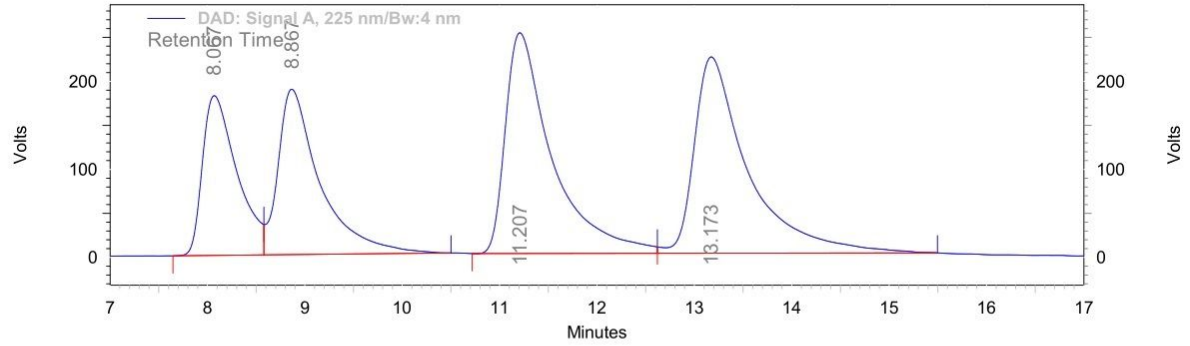
Retention time	12.113	11.08

product	(*1S,2R*)	(*1S,2S*)

Figure 4.27: HPLC chromatograms of 1-(3-methylphenyl)-2-nitropropan-1-ol. A. racemic standard, B. *Bm*HNL catalyzed synthesis of diastereomers.

6) HPLC chromatograms of 1-(4-methylphenyl)-2-nitropropanol

A)

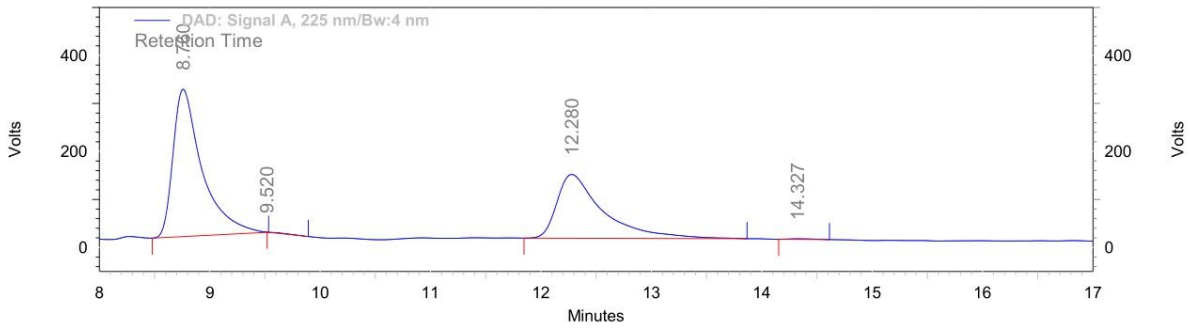


DAD: Signal A,
225 nm/Bw:4 nm
Results

Retention Time	Area	Area %	Height	Height %
8.067	9352700	16.56	380569	21.52
8.867	11744219	20.80	394110	22.28
11.207	17446689	30.90	526034	29.74
13.173	17926331	31.74	467827	26.45
Totals	56469939	100.00	1768540	100.00

Retention time	8.067	8.867	11.207	13.173
product	(*1S,2R*)	(*1R,2S*)	(*1S,2S*)	(*1R,2R*)

B)



DAD: Signal A,
225 nm/Bw:4 nm
Results

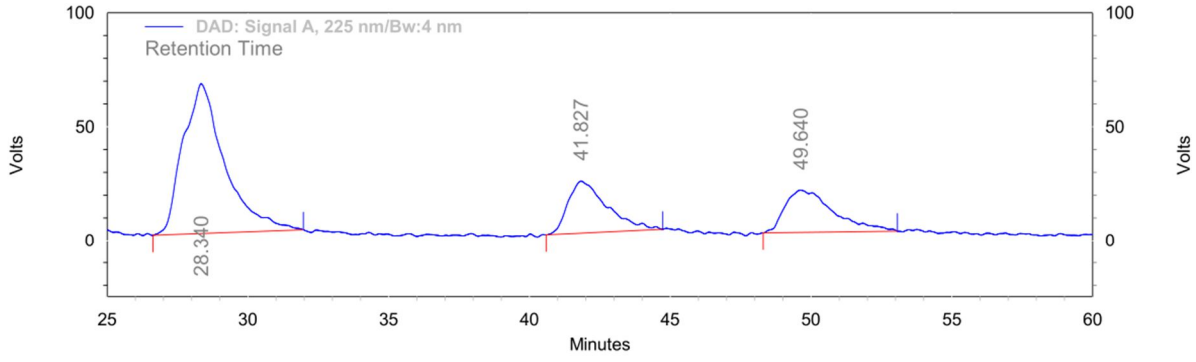
Retention Time	Area	Area %	Height	Height %
8.760	11723030	59.04	643920	69.58
9.520	26610	0.13	0	0.00
12.280	8063037	40.61	278722	30.12
14.327	44032	0.22	2793	0.30
Totals	19856709	100.00	925435	100.00

Retention time	8.76	9.52	12.28	14.327
product	(*1S,2R*)	(*1R,2S*)	(*1S,2S*)	(*1R,2R*)

Figure 4.28: HPLC chromatograms of 1-(4-methylphenyl)-2-nitropropan-1-ol. A. racemic standard, B. *Bm*HNL catalyzed synthesis of diastereomers.

7) HPLC chromatograms of 1-(4-nitrophenyl)-2-nitropropanol

A)

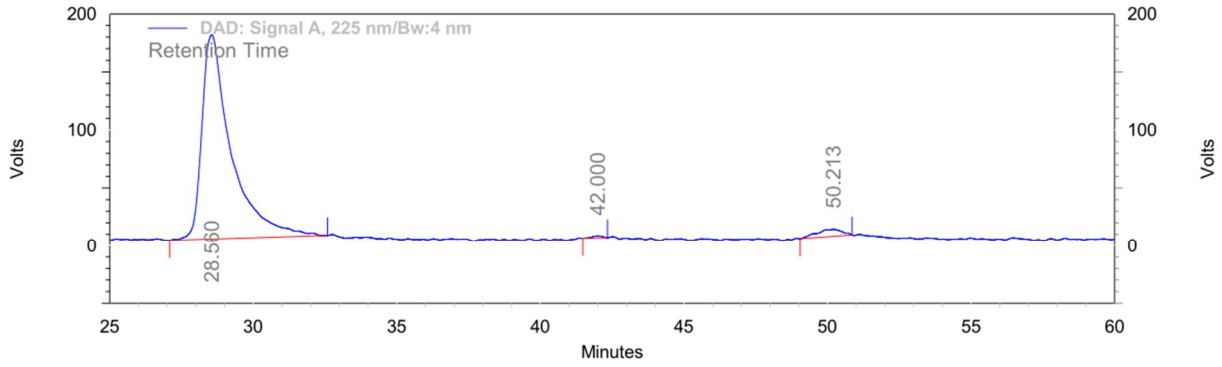


DAD: Signal A,
225 nm/Bw:4 nm
Results

Retention Time	Area	Area %	Height	Height %
28.340	14192792	60.49	137738	61.41
41.827	4600806	19.61	47778	21.30
49.640	4667858	19.90	38765	17.28
Totals	23461456	100.00	224281	100.00

Retention time	28.34	41.827	49.64
product	(*1S,2R*) +(*1R,2S*)	(*1R,2R*)	(*1S,2S*)

B)

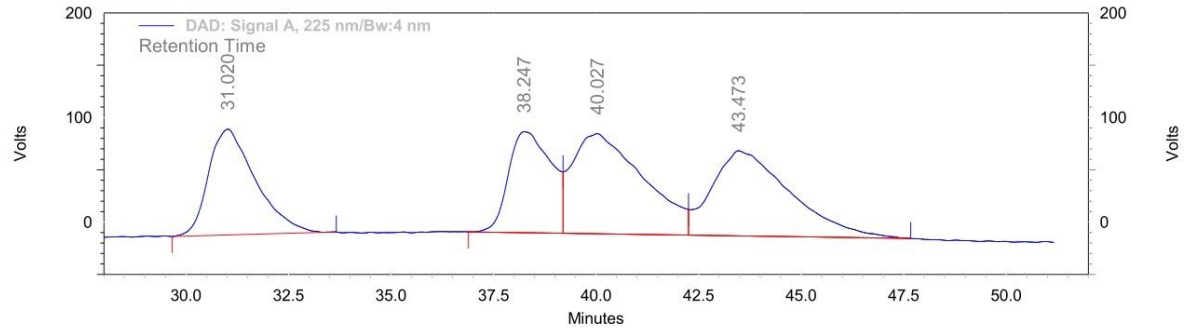


DAD: Signal A,
225 nm/Bw:4 nm
Results

Retention Time	Area	Area %	Height	Height %
28.560	26241378	96.69	369275	95.77
42.000	90338	0.33	3708	0.96
50.213	807480	2.98	12599	3.27
Totals	27139196	100.00	385582	100.00

Retention time	28.56	42	50.21
product	(*1S,2R*) +(*1R,2S*)	(*1R,2R*)	(*1S,2S*)

C)

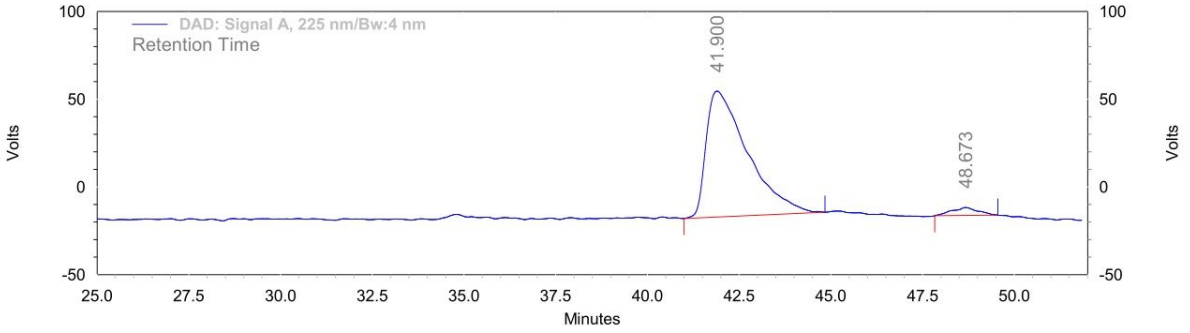


DAD: Signal A,
225 nm/Bw:4 nm
Results

Retention Time	Area	Area %	Height	Height %
31.020	16884143	21.52	212068	26.97
38.247	14692461	18.73	202506	25.76
40.027	24231844	30.89	200951	25.56
43.473	22648743	28.87	170732	21.71
Totals	78457191	100.00	786257	100.00

Retention time	38.24	31.02	40.027	43.473
product	(*1S,2R*)	(*1R,2S*)	(*1S,2S*) / (*1R,2R*)	(*1S,2S*) / (*1R,2R*)

D)



DAD: Signal A,
225 nm/Bw:4 nm
Results

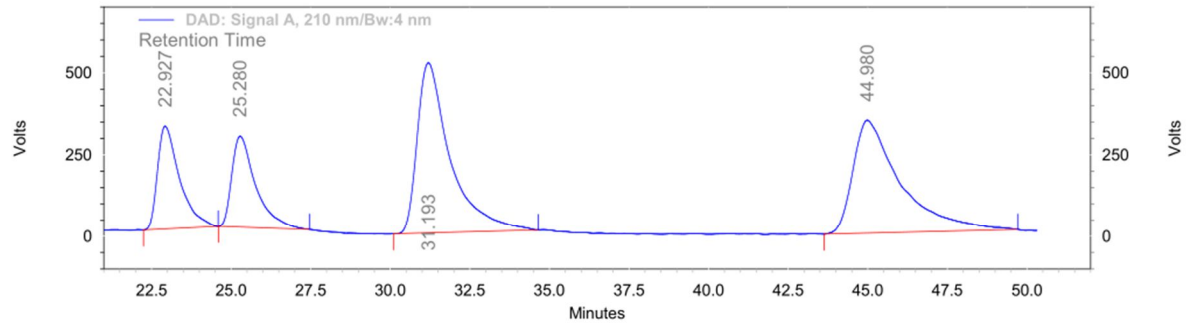
Retention Time	Area	Area %	Height	Height %
41.900	11802475	96.16	150443	94.08
48.673	471185	3.84	9461	5.92
Totals	12273660	100.00	159904	100.00

Retention time	41.9	48.673
product	(*1S,2R*)	(*1S,2S*) / (*1R,2R*)

Figure 4.29: HPLC chromatograms of 1-(4-nitrophenyl)-2-nitropropan-1-ol. A. racemic standard in Lux amylose 1, B. *Bm*HNL catalyzed synthesis of diastereomers analysed in Lux amylose 1, C. racemic standard in CHIRALPAK IB, D *Bm*HNL catalyzed synthesis of diastereomers analysed in CHIRALPAK IB synthesized by *Bm*HNL enzyme.

8) HPLC chromatogram of 1-(2,5-dimethoxyphenyl)-2-nitropropanol

A)

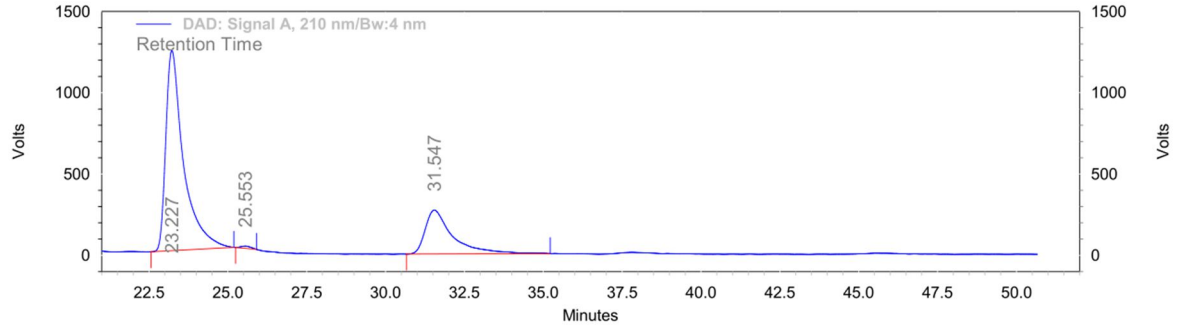


DAD: Signal A, 210 nm/Bw:4 nm
Results

Retention Time	Area	Area %	Height	Height %
22.927	31907066	14.74	659946	21.58
25.280	30551873	14.12	584070	19.10
31.193	78561540	36.30	1089447	35.62
44.980	75382669	34.83	724741	23.70
Totals	216403148	100.00	3058204	100.00

Retention time	22.927	25.28	31.193	44.98
product	(*1S,2R*)	(*1R,2S*)	(*1S,2S*)	(*1R,2R*)

B)



DAD: Signal A,
210 nm/Bw:4 nm
Results

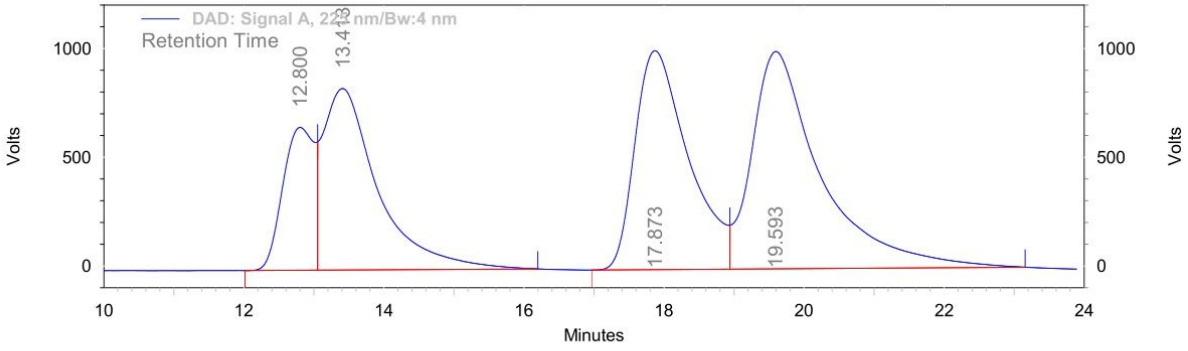
Retention Time	Area	Area %	Height	Height %
23.227	100925735	74.26	2581369	81.29
25.553	639016	0.47	28344	0.89
31.547	34345847	25.27	565750	17.82
Totals	135910598	100.00	3175463	100.00

Retention time	23.227	25.553	31.547
product	(*1S,2R*)	(*1R,2S*)	(*1S,2S*)

Figure 4.30: HPLC chromatograms of 1-(2,5-dimethoxyphenyl)-2-nitropropan-1-ol. A. racemic standard, B. *Bm*HNL catalyzed synthesis of diastereomers.

9) HPLC chromatograms of 1-(4-chlorophenyl)-2-nitropropanol

A)

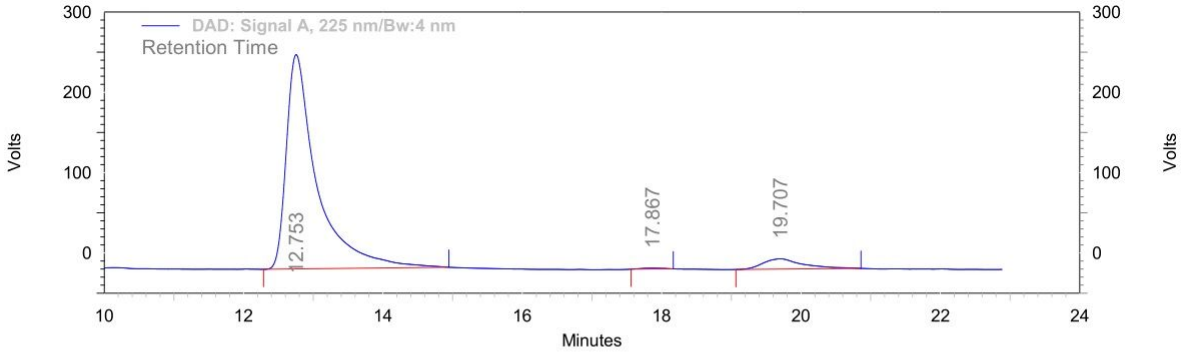


DAD: Signal A,
225 nm/Bw:4 nm
Results

Retention Time	Area	Area %	Height	Height %
12.800	43015506	10.95	1377480	18.78
13.413	94793066	24.12	1749845	23.85
17.873	112018740	28.51	2111907	28.79
19.593	143129224	36.42	2096630	28.58
Totals	392956536	100.00	7335862	100.00

Retention time	12.8	13.413	19.593	17.873
product	(*1S,2R*)	(*1R,2S*)	(*1S,2S*)	(*1R,2R*)

B)



DAD: Signal A, 225 nm/Bw:4 nm
Results

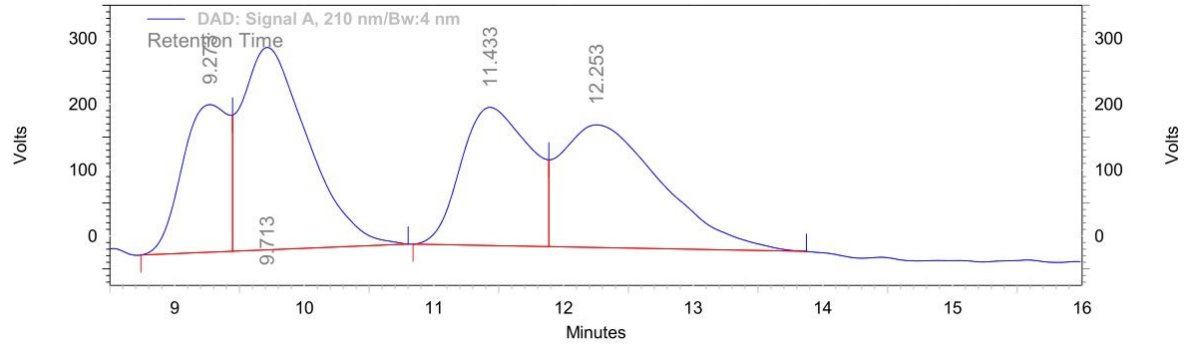
Retention Time	Area	Area %	Height	Height %
12.753	17039270	93.88	559488	95.08
17.867	50734	0.28	2185	0.37
19.707	1060608	5.84	26758	4.55
Totals	18150612	100.00	588431	100.00

Retention time	12.753	19.707	17.867
product	(*1S,2R*)	(*1S,2S*)	(*1R,2R*)

Figure 4.31: HPLC chromatograms of 1-(4-chlorophenyl)-2-nitropropan-1-ol. A. racemic standard, B. *Bm*HNL catalyzed synthesis of diastereomers.

10) HPLC chromatogram of 4 nitro-1-phenylpentan-3-ol

A)

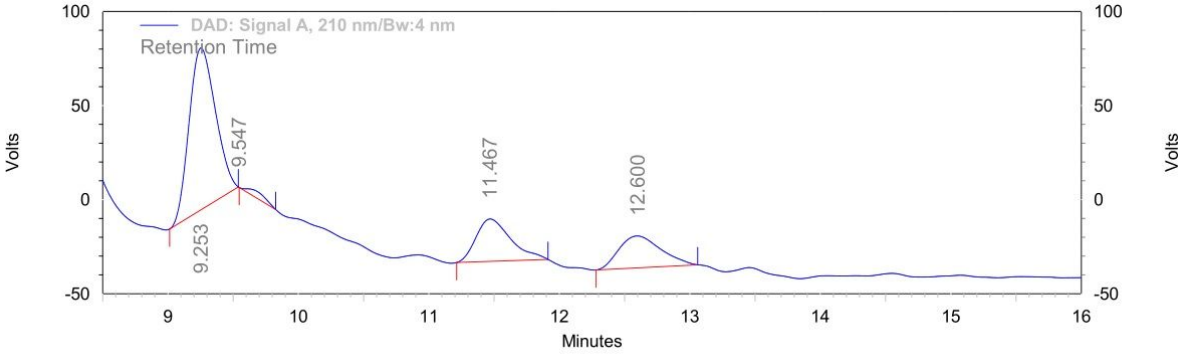


DAD: Signal A,
210 nm/Bw:4 nm
Results

Retention Time	Area	Area %	Height	Height %
9.273	11596841	16.03	469502	24.16
9.713	22979665	31.76	643951	33.14
11.433	16505377	22.81	439698	22.63
12.253	21270926	29.40	390255	20.08
Totals	72352809	100.00	1943406	100.00

Retention time	9.273	9.713	11.433	12.253
product	(*1S,2R*)	(*1R,2S*)	(*1S,2S*)	(*1R,2R*)

B)



DAD: Signal A,
210 nm/Bw:4 nm
Results

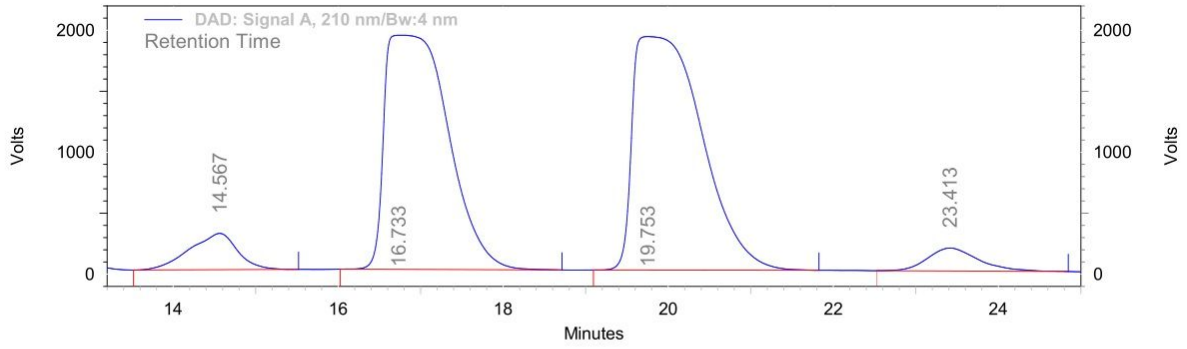
Retention Time	Area	Area %	Height	Height %
9.253	2530326	59.19	180475	68.55
9.547	73622	1.72	0	0.00
11.467	875390	20.48	47248	17.95
12.600	795883	18.62	35538	13.50
Totals	4275221	100.00	263261	100.00

Retention time	9.253	9.547	11.467	12.6
product	(*1S,2R*)	(*1R,2S*)	(*1S,2S*)	(*1R,2R*)

Figure 4.32: HPLC chromatograms of 4 nitro-1-phenylpentan-3-ol. A. racemic standard, B. *Bm*HNL catalyzed synthesis of diastereomers.

11) HPLC Chromatograms for 1-(3-benzyloxyphenyl)-2-nitropropan-1-ol

A)

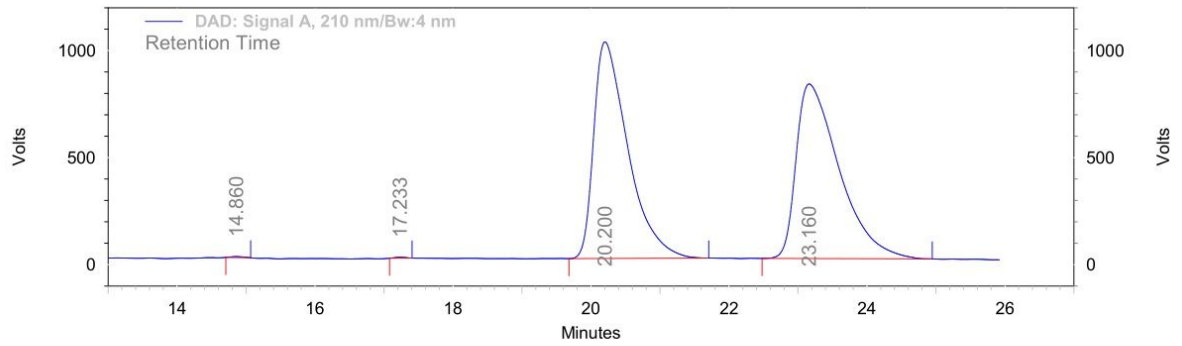


DAD: Signal A, 210 nm/Bw:4 nm
Results

Retention Time	Area	Area %	Height	Height %
14.567	25157973	5.12	624735	6.89
16.733	215931516	43.92	4027649	44.44
19.753	233633687	47.52	4015696	44.31
23.413	16911497	3.44	395145	4.36
Totals	491634673	100.00	9063225	100.00

Retention time	23.413	14.567	19.753	16.733
product	(*1S,2R*)	(*1R,2S*)	(*1S,2S*)	(*1R,2R*)

B)



DAD: Signal A,
210 nm/Bw:4 nm
Results

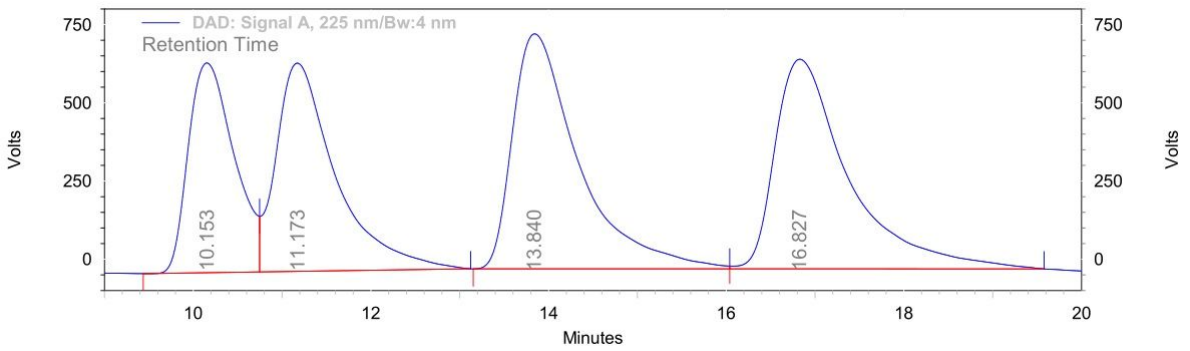
Retention Time	Area	Area %	Height	Height %
14.860	129458	0.09	9808	0.25
17.233	96071	0.07	8281	0.22
20.200	73047099	49.53	2122121	55.12
23.160	74219136	50.32	1710097	44.41
Totals	147491764	100.00	3850307	100.00

Retention time	23.16	14.86	20.2	17.233
product	(*1S,2R*)	(*1R,2S*)	(*1S,2S*)	(*1R,2R*)

Figure 4.33: HPLC chromatograms of 1-(3-benzyloxyphenyl)-2-nitropropan-1-ol. A. *Bm*HNL catalyzed synthesis of diastereomers.

12) HPLC chromatogram of 1-(2-methylphenyl)-2-nitropropan-1-ol

A)

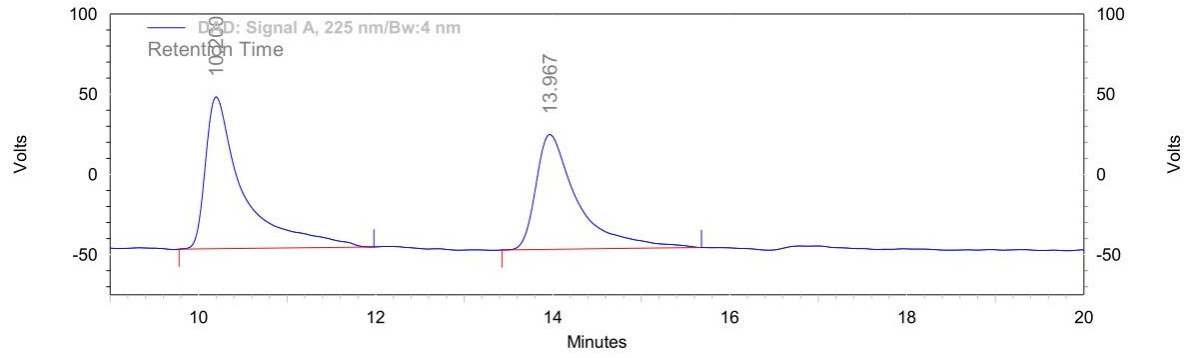


DAD: Signal A,
225 nm/Bw:4 nm
Results

Retention Time	Area	Area %	Height	Height %
10.153	50489453	18.19	1405819	24.31
11.173	64877779	23.38	1395611	24.14
13.840	81256141	29.28	1575055	27.24
16.827	80888509	29.15	1405472	24.31
Totals	277511882	100.00	5781957	100.00

Retention time	10.153	11.173	13.84	16.827
product	(*1S,2R*)	(*1R,2S*)	(*1S,2S*)	(*1R,2R*)

B)



DAD: Signal A,
225 nm/Bw:4 nm
Results

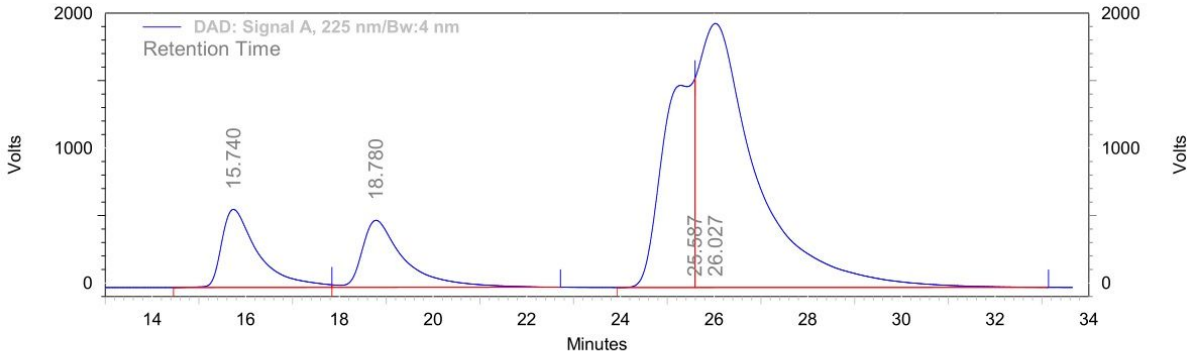
Retention Time	Area	Area %	Height	Height %
10.200	5888795	54.55	198429	56.93
13.967	4907040	45.45	150131	43.07
Totals	10795835	100.00	348560	100.00

Retention time	10.2	13.967
product	(*1S,2R*)	(*1S,2S*)

Figure 4.34: HPLC chromatograms of 1-(2-methylphenyl)-2-nitropropan-1-ol. A. racemic standard, B. *Bm*HNL catalyzed synthesis of diastereomers.

13) HPLC chromatograms of 1-(2-methoxyphenyl)-2-nitropropan-1-ol

A)

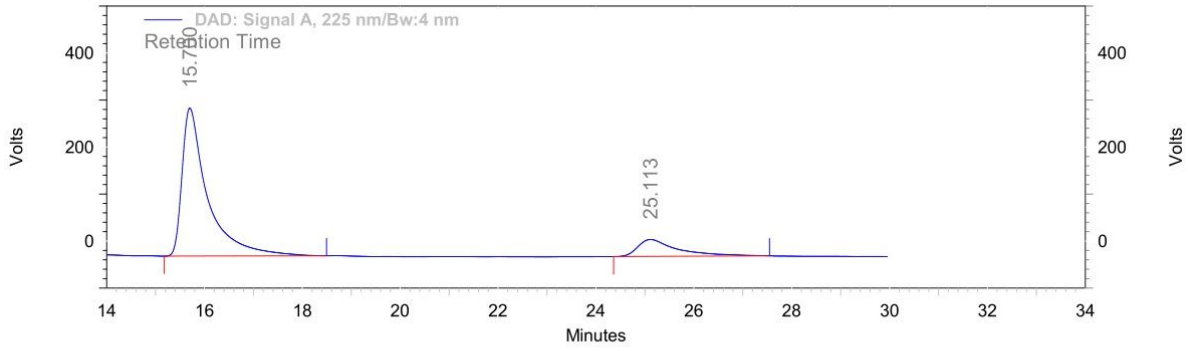


DAD: Signal A,
225 nm/Bw:4 nm
Results

Retention Time	Area	Area %	Height	Height %
15.740	65643564	10.34	1213838	12.64
18.780	65011147	10.24	1042249	10.85
25.587	150800051	23.75	3243057	33.77
26.027	353556277	55.68	4103110	42.73
Totals	635011039	100.00	9602254	100.00

Retention time	15.74	18.78	25.587	26.027
product	(*1S,2R*)	(*1R,2S*)	(*1S,2S*)	(*1R,2R*)

B) *Bm*HNL



DAD: Signal A,
225 nm/Bw:4 nm
Results

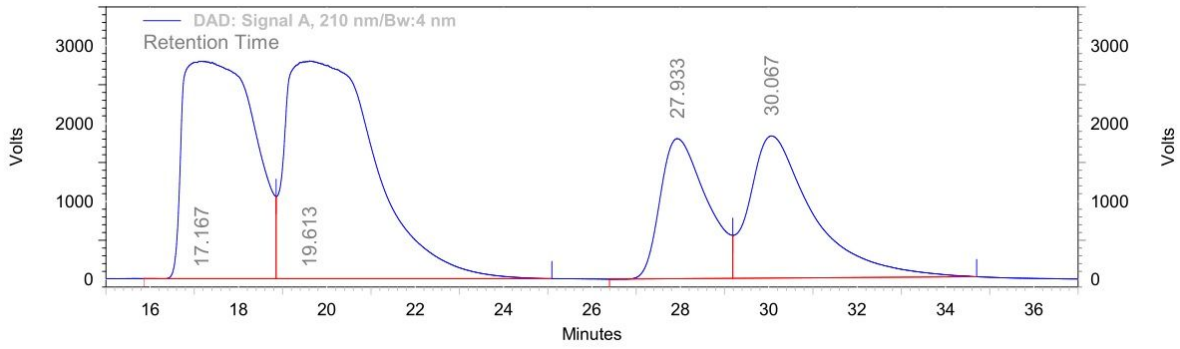
Retention Time	Area	Area %	Height	Height %
15.700	23825496	84.82	660397	89.72
25.113	4263726	15.18	75681	10.28
Totals	28089222	100.00	736078	100.00

Retention time	15.7	25.113
product	(*1S,2R*)	(*1S,2S*)

Figure 4.35: HPLC chromatograms of 1-(2-methoxyphenyl)-2-nitropropan-1-ol. A. racemic standard, B. *Bm*HNL catalyzed synthesis of diastereomers.

14) HPLC chromatograms of 1-napthal-2-nitropropan-1-ol

A)

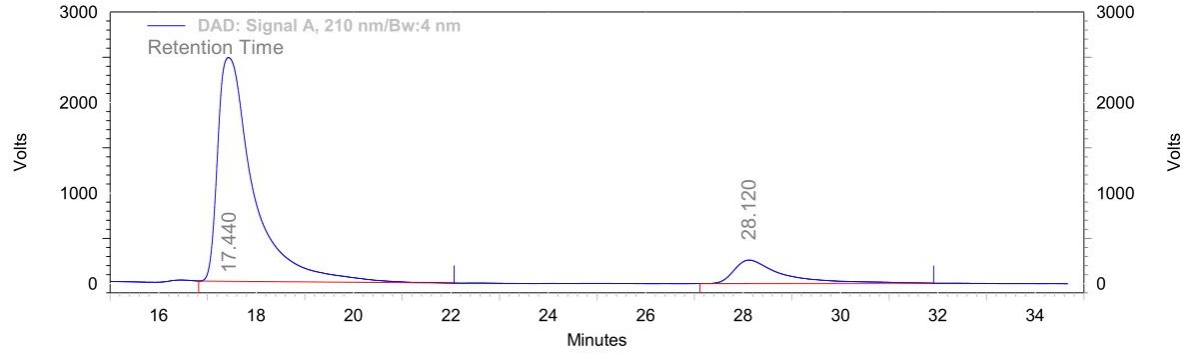


DAD: Signal A,
210 nm/Bw:4 nm
Results

Retention Time	Area	Area %	Height	Height %
17.167	653223027	30.43	5862531	30.31
19.613	830979730	38.71	5867952	30.34
27.933	277629494	12.93	3775579	19.52
30.067	384832144	17.93	3832821	19.82
Totals	2146664395	100.00	19338883	100.00

Retention time	17.167	19.613	27.933	30.067
product	(*1S,2R*)	(*1R,2S*)	(*1S,2S*)	(*1R,2R*)

B)



DAD: Signal A,
210 nm/Bw:4 nm
Results

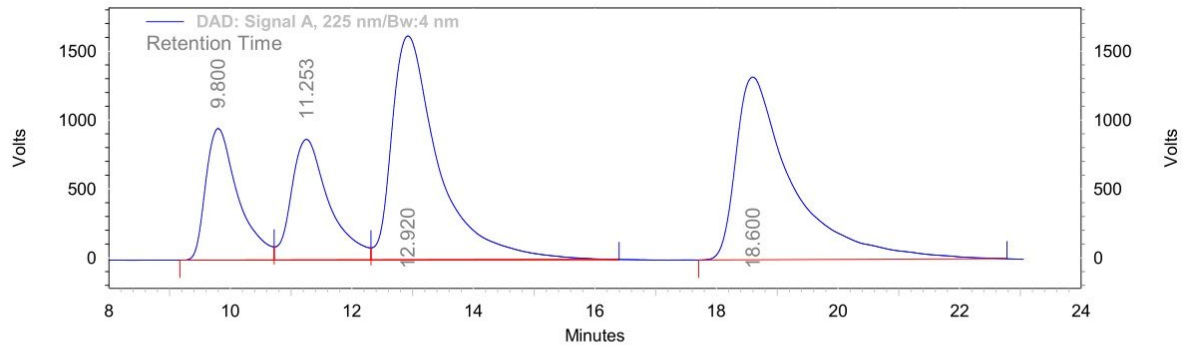
Retention Time	Area	Area %	Height	Height %
17.440	264621126	87.63	5177509	90.54
28.120	37338878	12.37	540803	9.46
Totals	301960004	100.00	5718312	100.00

Retention time	87.63	12.37
product	(*1S,2R*)	(*1S,2S*)

Figure 4.36: HPLC chromatograms of 1-napthal-2-nitropropan-1-ol. A. racemic standard, B. *Bm*HNL catalyzed synthesis of diastereomers.

15) HPLC chromatograms of 1-(3-bromophenyl)-2-nitropropan-1-ol

A)

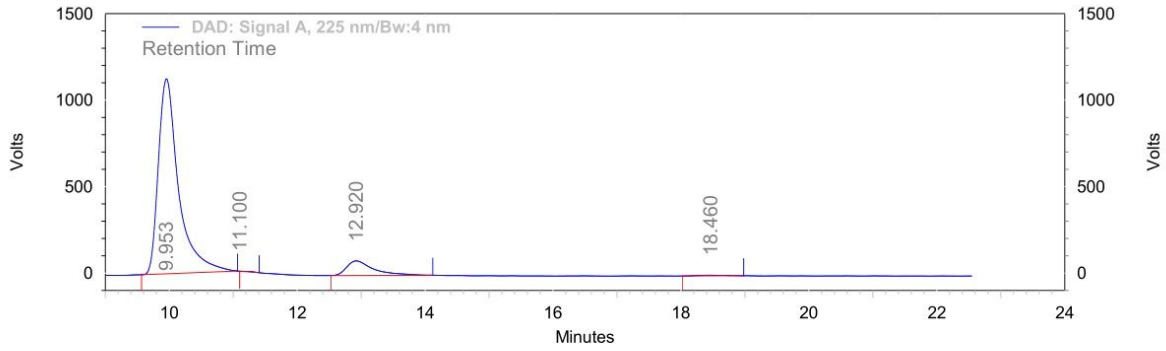


DAD: Signal A,
225 nm/Bw:4 nm
Results

Retention Time	Area	Area %	Height	Height %
9.800	74406413	14.44	2002531	19.97
11.253	79317546	15.39	1835824	18.31
12.920	181947384	35.31	3407644	33.98
18.600	179593926	34.85	2781067	27.74
Totals	515265269	100.00	10027066	100.00

Retention time	9.8	11.253	12.92	18.6
product	(*1S,2R*)	(*1R,2S*)	(*1S,2S*)	(*1R,2R*)

B)



DAD: Signal A,
225 nm/Bw:4 nm
Results

Retention Time	Area	Area %	Height	Height %
9.953	51812573	90.52	2362813	92.76
11.100	55279	0.10	0	0.00
12.920	5145257	8.99	176888	6.94
18.460	223465	0.39	7536	0.30
Totals	57236574	100.00	2547237	100.00

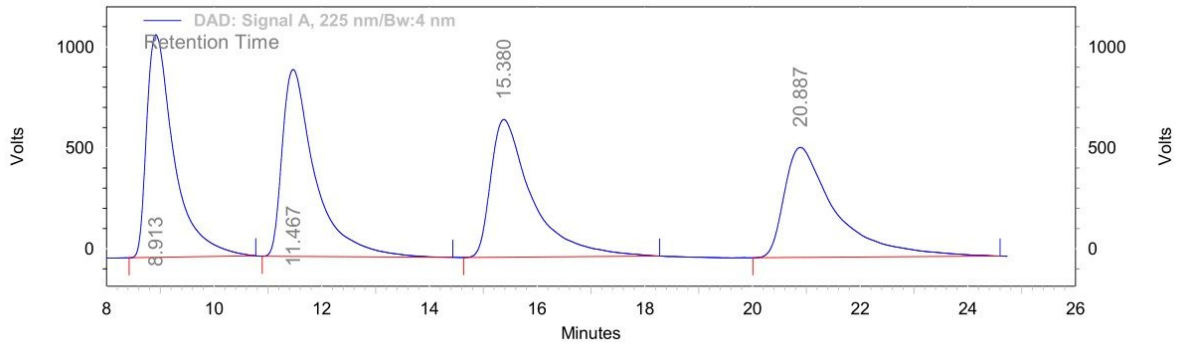
Retention time	9.953	11.1	12.92	18.46

product	(*1S,2R*)	(*1R,2S*)	(*1S,2S*)	(*1R,2R*)

Figure 4.37: HPLC chromatograms of 1-(3-bromophenyl)-2-nitropropan-1-ol. A. racemic standard, B. *Bm*HNL catalyzed synthesis of diastereomers.

16) HPLC chromatograms of 1-(2-bromophenyl)-2-nitropropan-1-ol

A)

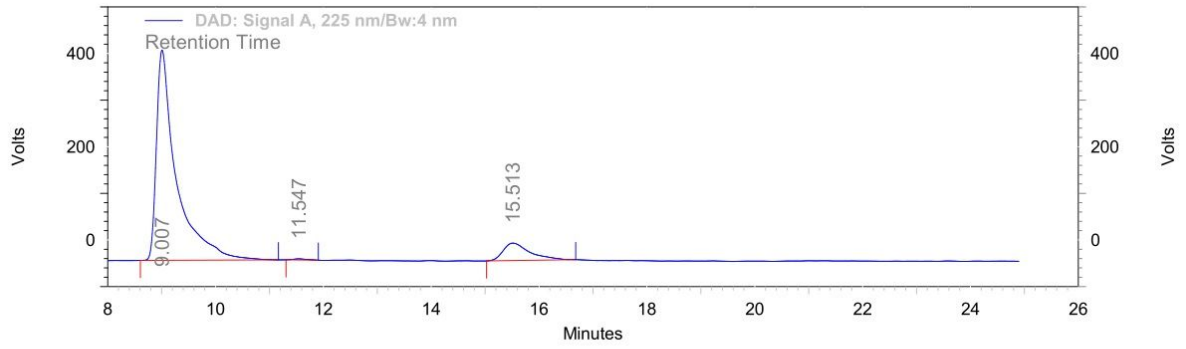


DAD: Signal A,
225 nm/Bw:4 nm
Results

Retention Time	Area	Area %	Height	Height %
8.913	82086933	25.96	2312601	33.87
11.467	82387716	26.05	1941125	28.43
15.380	76156706	24.08	1431259	20.96
20.887	75594275	23.91	1143163	16.74
Totals	316225630	100.00	6828148	100.00

Retention time	8.913	11.467	15.38	20.887
product	(*1S,2R*)	(*1R,2S*)	(*1S,2S*)	(*1R,2R*)

B)



DAD: Signal A, 225 nm/Bw:4 nm
Results

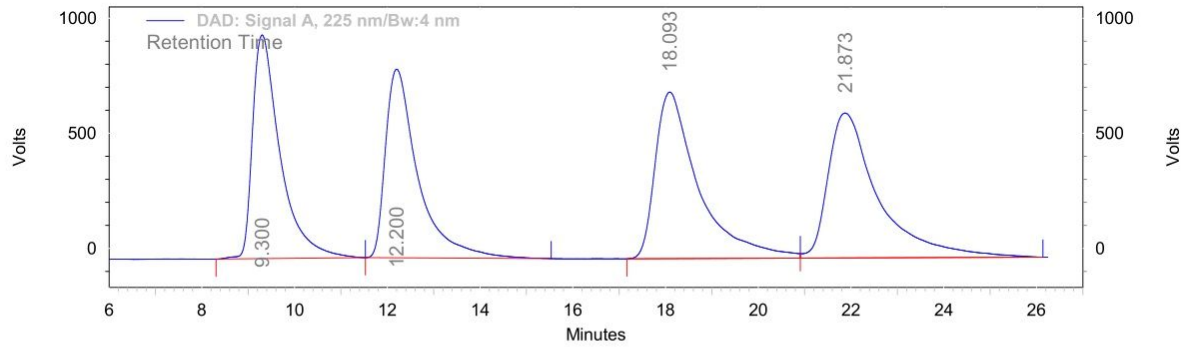
Retention Time	Area	Area %	Height	Height %
9.007	24250029	89.69	946123	91.92
11.547	87655	0.32	4899	0.48
15.513	2701007	9.99	78311	7.61
Totals	27038691	100.00	1029333	100.00

Retention time	9.007	11.547	15.313
product	(*1S,2R*)	(*1R,2S*)	(*1S,2S*)

Figure 4.38: HPLC chromatograms of 1-(2-bromophenyl)-2-nitropropan-1-ol. A. racemic standard, B. *Bm*HNL catalyzed synthesis of diastereomers.

17) HPLC chromatograms of 1-(2,3-dichlorophenyl)-2-nitropropan-1-ol

A)

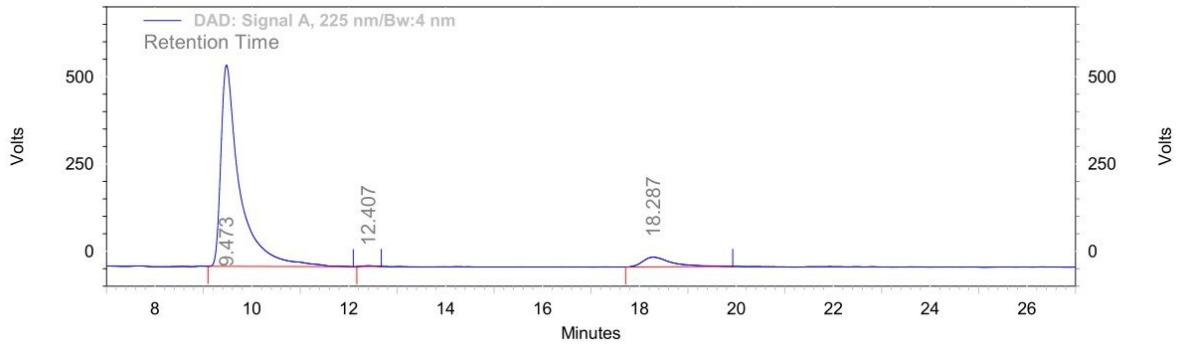


DAD: Signal A,
225 nm/Bw:4 nm
Results

Retention Time	Area	Area %	Height	Height %
9.300	84239109	23.04	2037308	30.90
12.200	83407382	22.81	1718599	26.07
18.093	98415882	26.92	1517694	23.02
21.873	99557404	27.23	1319847	20.02
Totals	365619777	100.00	6593448	100.00

Retention time	9.3	12.2	18.093	21.873
product	(*1S,2R*)	(*1R,2S*)	(*1S,2S*)	(*1R,2R*)

B)



DAD: Signal A,
225 nm/Bw:4 nm
Results

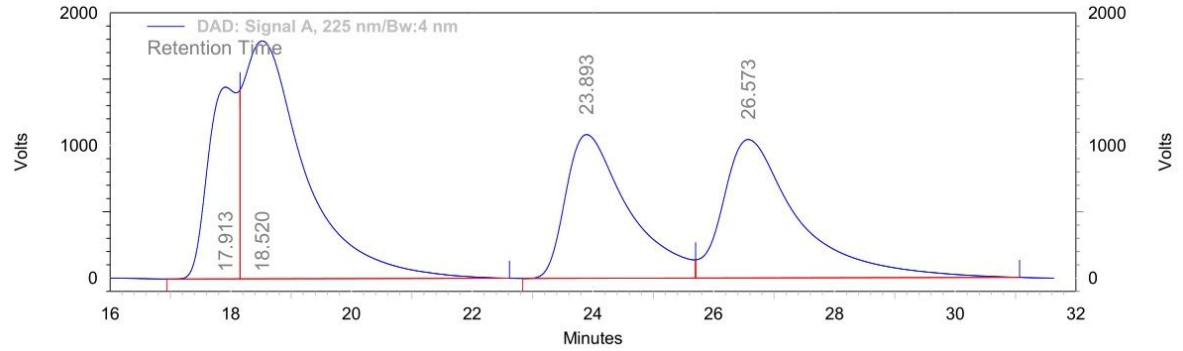
Retention Time	Area	Area %	Height	Height %
9.473	32615277	92.89	1208897	95.05
12.407	86024	0.25	5094	0.40
18.287	2408765	6.86	57914	4.55
Totals	35110066	100.00	1271905	100.00

Retention time	9.473	12.407	18.287
product	(*1S,2R*)	(*1R,2S*)	(*1S,2S*)

Figure 4.39: HPLC chromatograms of 1-(2,3-dichlorophenyl)-2-nitropropan-1-ol. A. racemic standard, B. *Bm*HNL catalyzed synthesis of diastereomers.

18) HPLC chromatograms of 1-(2,3-dimethoxyphenyl)-2-nitropropan-1-ol

A)

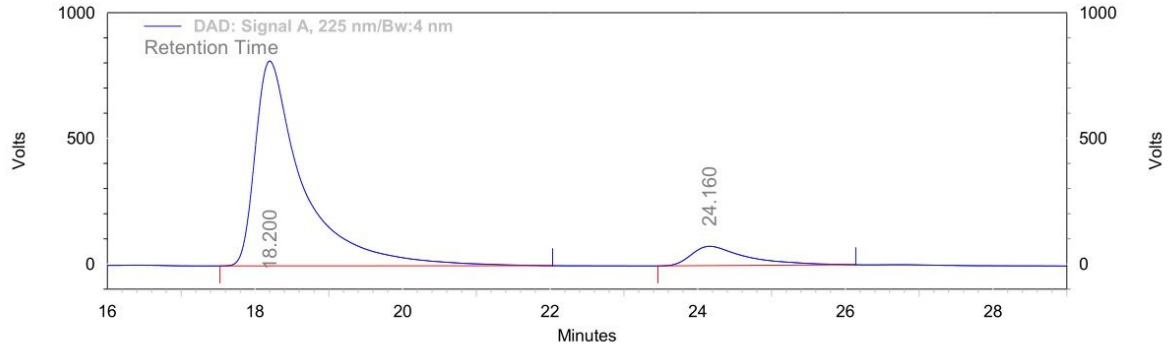


DAD: Signal A,
225 nm/Bw:4 nm
Results

Retention Time	Area	Area %	Height	Height %
17.913	103958295	14.40	3030718	26.93
18.520	264735032	36.68	3759927	33.41
23.893	163861370	22.71	2273034	20.20
26.573	189139413	26.21	2189010	19.45
Totals	721694110	100.00	11252689	100.00

Retention time	17.913	18.52	23.893	26.573
product	(*1S,2R*)	(*1R,2S*)	(*1S,2S*)	(*1R,2R*)

B)



DAD: Signal A,
225 nm/Bw:4 nm
Results

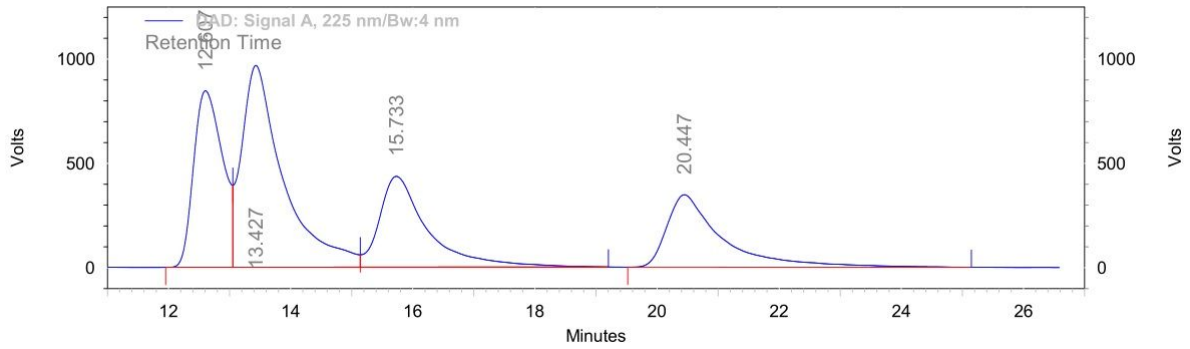
Retention Time	Area	Area %	Height	Height %
18.200	76906453	90.22	1709435	91.39
24.160	8338147	9.78	161117	8.61
Totals	85244600	100.00	1870552	100.00

Retention time	18.2	24.16
product	(*1S,2R*)	(*1S,2S*)

Figure 4.40: HPLC chromatograms of 1-(2,3-dimethoxyphenyl)-2-nitropropan-1-ol. A. racemic standard, B. *Bm*HNL catalyzed synthesis of diastereomers.

19) HPLC chromatograms of 1-(2-nitrophenyl)-2-nitropropan-1-ol

A)

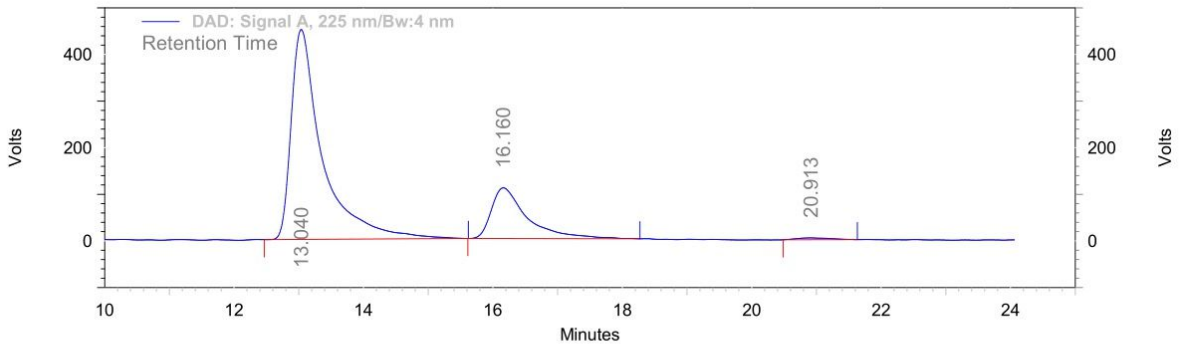


DAD: Signal A,
225 nm/Bw:4 nm
Results

Retention Time	Area	Area %	Height	Height %
12.607	58372180	23.27	1774553	32.59
13.427	96678130	38.53	2028866	37.26
15.733	50040423	19.94	912892	16.77
20.447	45803501	18.26	728671	13.38
Totals	250894234	100.00	5444982	100.00

Retention time	12.607	13.427	15.733	20.447
product	(*1S,2R*)	(*1R,2S*)	(*1S,2S*)	(*1R,2R*)

B)



DAD: Signal A,
225 nm/Bw:4 nm
Results

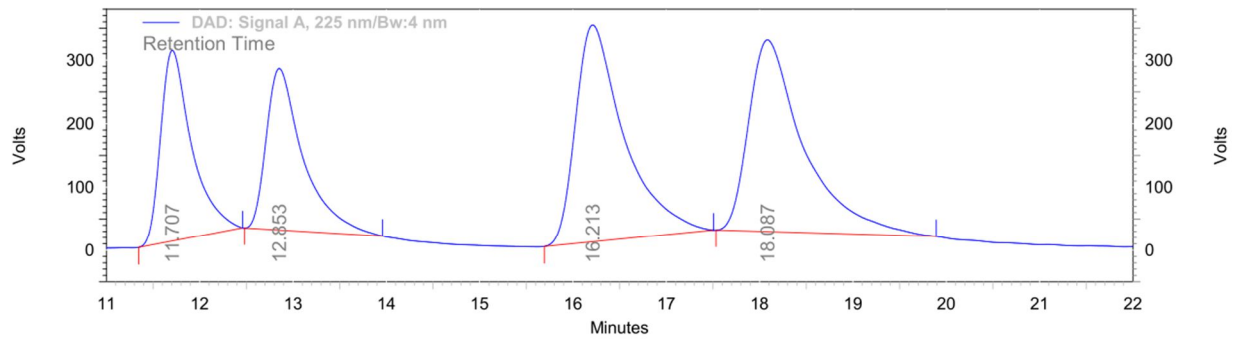
Retention Time	Area	Area %	Height	Height %
13.040	31477124	77.63	944371	79.97
16.160	8763448	21.61	228241	19.33
20.913	309591	0.76	8349	0.71
Totals	40550163	100.00	1180961	100.00

Retention time	13.04	16.16	20.913
product	(*1S,2R*)	(*1S,2S*)	(*1R,2R*)

Figure 4.41: HPLC chromatograms of 1-(2-nitrophenyl)-2-nitropropan-1-ol. A. racemic standard, B. *Bm*HNL catalyzed synthesis of diastereomers.

4.4.19. HPLC chromatograms of (*1S,2R*)-2-NPP synthesized in gram scale by using *Bm*HNL enzyme

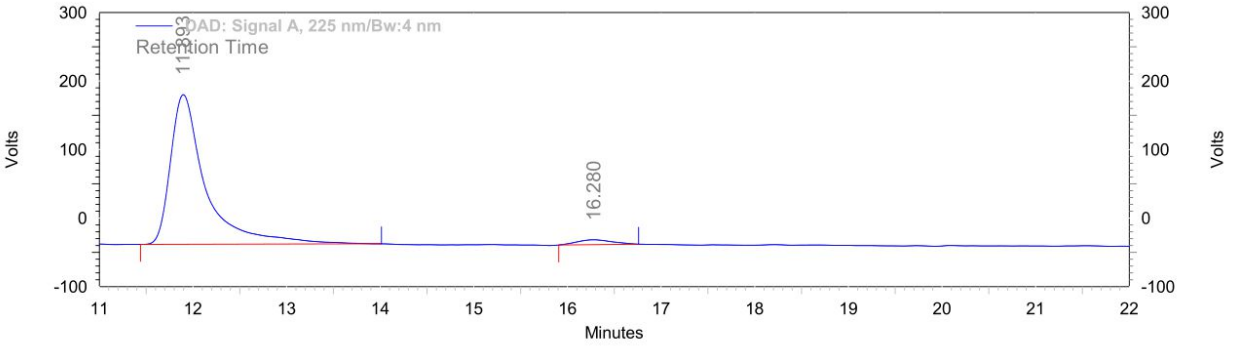
A)



DAD: Signal A,
225 nm/Bw:4 nm
Results

Retention Time	Area	Area %	Height	Height %
11.707	14643237	18.03	630761	25.09
12.853	14678817	18.07	533725	21.23
16.213	25930453	31.92	716364	28.50
18.087	25985937	31.99	633031	25.18
Totals	81238444	100.00	2513881	100.00

B)



DAD: Signal A,
225 nm/Bw:4 nm
Results

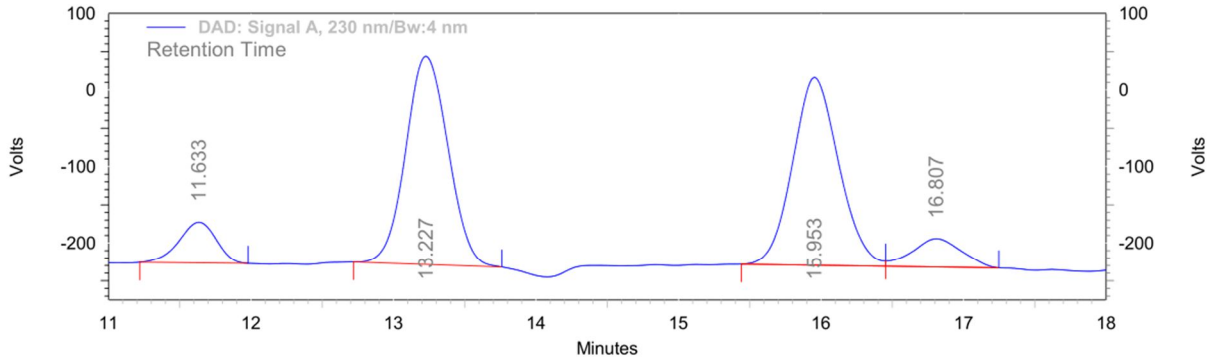
Retention Time	Area	Area %	Height	Height %
11.893	11933913	96.85	457754	96.87
16.280	388417	3.15	14795	3.13
Totals	12322330	100.00	472549	100.00

Figure 4.42: HPLC chromatograms of biocatalyticatally synthesized (*1S,2R*)-2-nitro-1-phenylpropan-1-ol. A. racemic standard, B. *Bm*HNL catalyzed synthesis of diastereomers in gram-scale.

4.4.20. HPLC chromatograms of biocatalytically synthesized 1-nitropropane corresponding β-nitroalcohols starting from different aromatic aldehydes

1) HPLC chromatograms of 2-nitro 1-phenylbutan-1-ol

A)



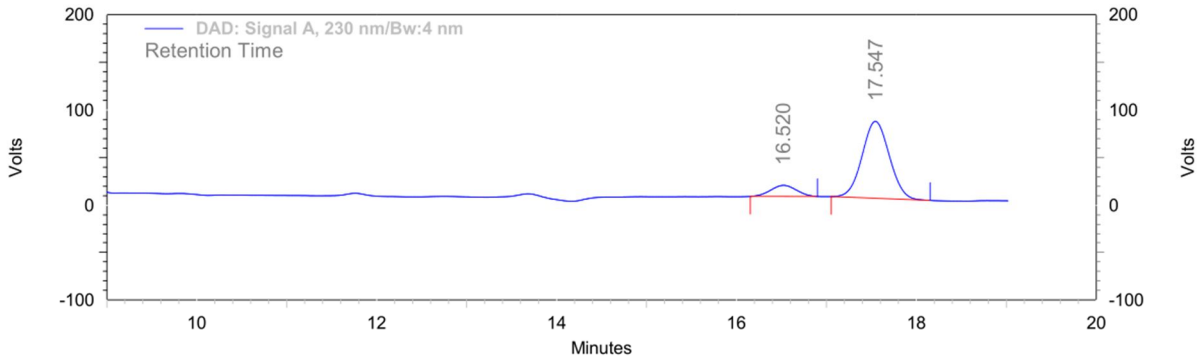
DAD: Signal A,
230 nm/Bw:4 nm
Results

Retention Time	Area	Area %	Height	Height %
11.633	2052710	7.49	112670	8.81
13.227	11821643	43.11	571485	44.69
15.953	11639602	42.45	515829	40.34
16.807	1905197	6.95	78861	6.17

Totals	27419152	100.00	1278845	100.00

Retention time	16.807	11.633	15.953	13.227
product	(*1S,2R*)	(*1R,2S*)	(*1S,2S*)	(*1R,2R*)

B)



DAD: Signal A,
230 nm/Bw:4 nm
Results

Retention Time	Area	Area %	Height	Height %
16.520	486316	12.01	24357	12.59
17.547	3564622	87.99	169061	87.41

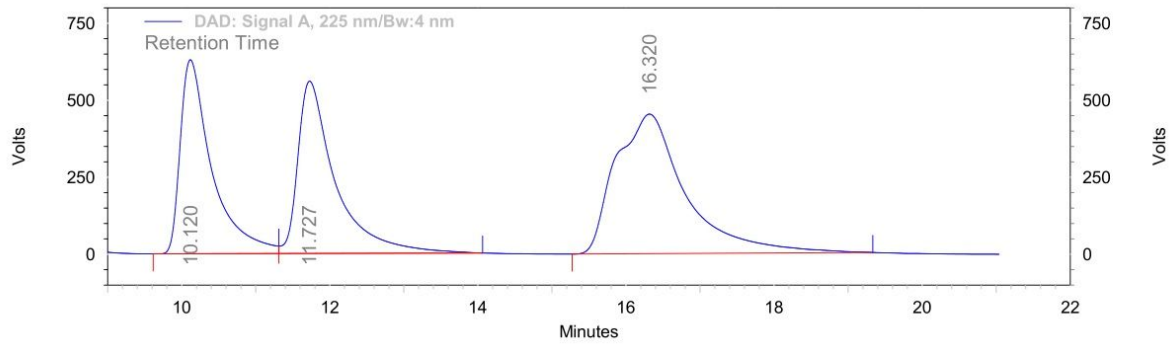
Totals	4050938	100.00	193418	100.00

Retention time	17.547	16.52
product	(*1S,2R*)	(*1S,2S*)

Figure 4.43: HPLC chromatograms of 2-nitro 1-phenylbutan-1-ol. A. racemic standard, B. *Bm*HNL catalyzed synthesis of diastereomers.

2) HPLC chromatograms of 1-(2-methoxyphenyl)-2-nitrobutan-1-ol

A)

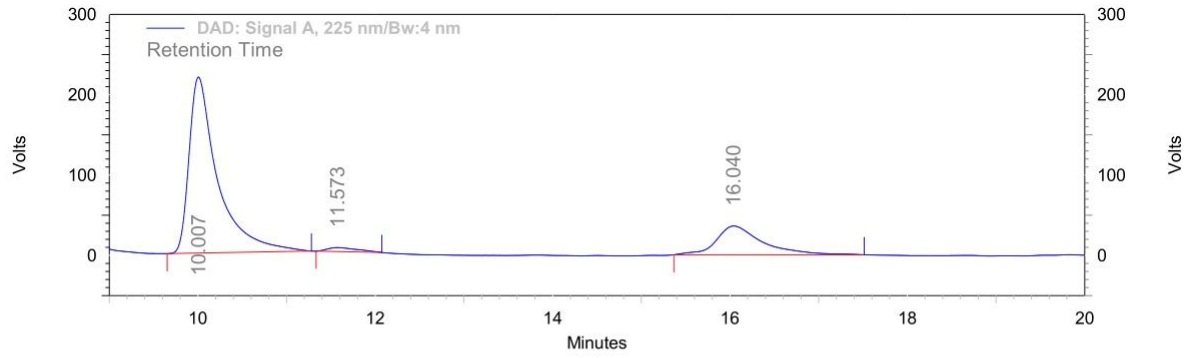


DAD: Signal A,
225 nm/Bw:4 nm
Results

Retention Time	Area	Area %	Height	Height %
10.120	39148091	27.44	1320676	38.34
11.727	41148712	28.84	1173218	34.06
16.320	62379279	43.72	950487	27.60
Totals	142676082	100.00	3444381	100.00

Retention time	10.12	11.727	16.32
product	(*1S,2R*)	(*1R,2S*)	(*1S,2S*) + (*1R,2R*)

B)



DAD: Signal A,
225 nm/Bw:4 nm
Results

Retention Time	Area	Area %	Height	Height %
10.007	10253725	77.58	459429	84.34
11.573	250409	1.89	10300	1.89
16.040	2713624	20.53	74984	13.77

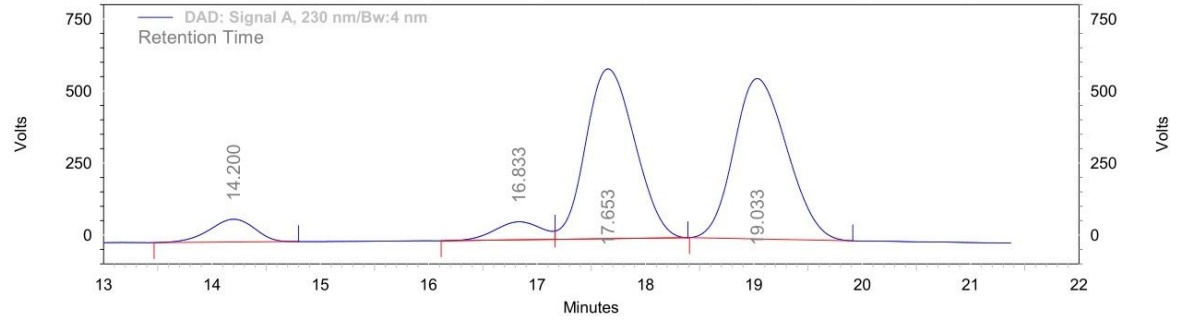
Totals	13217758	100.00	544713	100.00

Retention time	10.007	11.573	16.04
product	(*1S,2R*)	(*1R,2S*)	(*1S,2S*) + (*1R,2R*)

Figure 4.44: HPLC chromatograms of 1-(2-metoxyphenyl)-2-nitrobutan-1-ol. A. racemic standard, B. *Bm*HNL catalyzed synthesis of diastereomers.

3) HPLC chromatograms of 1-(4-chlorophenyl)-2-nitrobutan-1-ol

A)



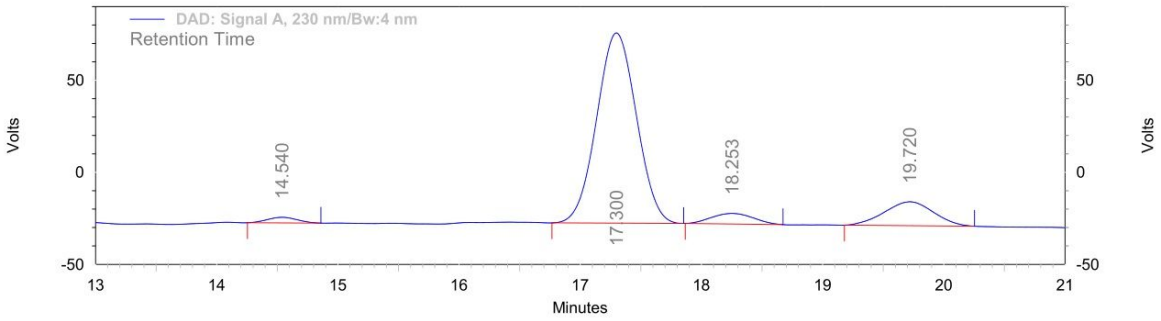
DAD: Signal A,
230 nm/Bw:4 nm
Results

Retention Time	Area	Area %	Height	Height %
14.200	4843759	5.54	165951	6.14
16.833	3923754	4.49	131265	4.86
17.653	38898210	44.47	1236272	45.76
19.033	39803276	45.51	1167902	43.23

Totals	87468999	100.00	2701390	100.00

Retention time	16.833	14.2	17.653	19.033
product	(*1S,2R*)	(*1R,2S*)	(*1S,2S*) / (*1R,2R*)	(*1S,2S*) / (*1R,2R*)

B)



DAD: Signal A,
230 nm/Bw:4 nm
Results

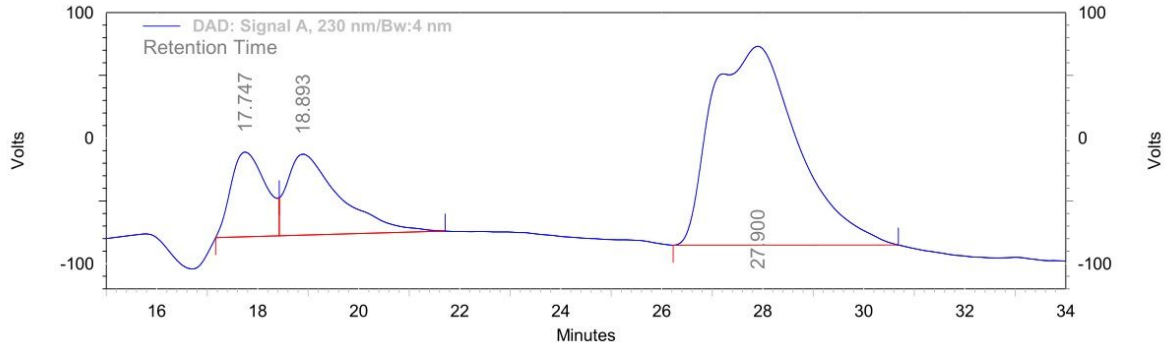
Retention Time	Area	Area %	Height	Height %
14.540	108608	1.78	6311	2.41
17.300	4938682	80.88	216650	82.60
18.253	289738	4.74	12061	4.60
19.720	769194	12.60	27251	10.39
Totals	6106222	100.00	262273	100.00

Retention time	17.3	14.54	18.253	19.720
product	(*1S,2R*)	(*1R,2S*)	(*1S,2S*) / (*1R,2R*)	(*1S,2S*) / (*1R,2R*)

Figure 4.45: HPLC chromatograms of 1-(4-chlorophenyl)-2-nitrobutan-1-ol. A. racemic standard, B. *Bm*HNL catalyzed synthesis of diastereomers.

4) HPLC chromatograms of 1-(4-methylphenyl)-2-nitrobutan-1-ol

A)



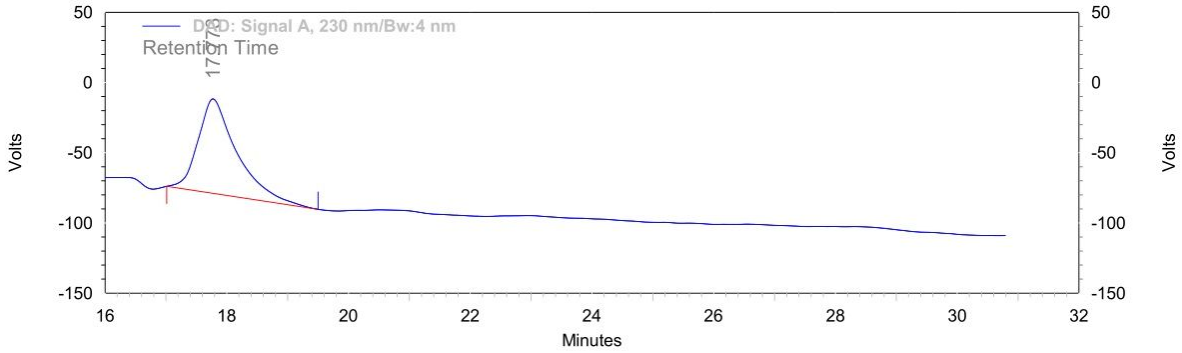
DAD: Signal A,
230 nm/Bw:4 nm
Results

Retention Time	Area	Area %	Height	Height %
17.747	6796281	12.17	141309	23.23
18.893	9865555	17.66	135138	22.21
27.900	39194536	70.17	331972	54.56

Totals	55856372	100.00	608419	100.00

Retention time	17.747	18.893	27.9
product	(*1S,2R*)	(*1R,2S*)	(*1S,2S*) + (*1R,2R*)

B)



DAD: Signal A,
230 nm/Bw:4 nm
Results

Retention Time	Area	Area %	Height	Height %
17.773	6248540	100.00	141021	100.00

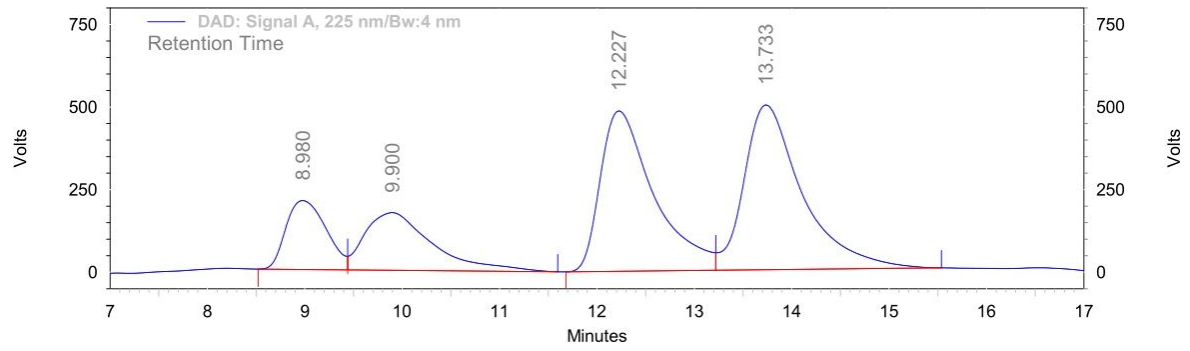
Totals	6248540	100.00	141021	100.00

Retention time	17.773
product	(*1S,2R*)

Figure 4.46: HPLC chromatograms of 1-(4-methylphenyl)-2-nitrobutan-1-ol. A. racemic standard, B. *Bm*HNL catalyzed synthesis of diastereomers.

5) HPLC chromatograms of 1-(3-chlorophenyl)-2-nitrobutan-1-ol

A)

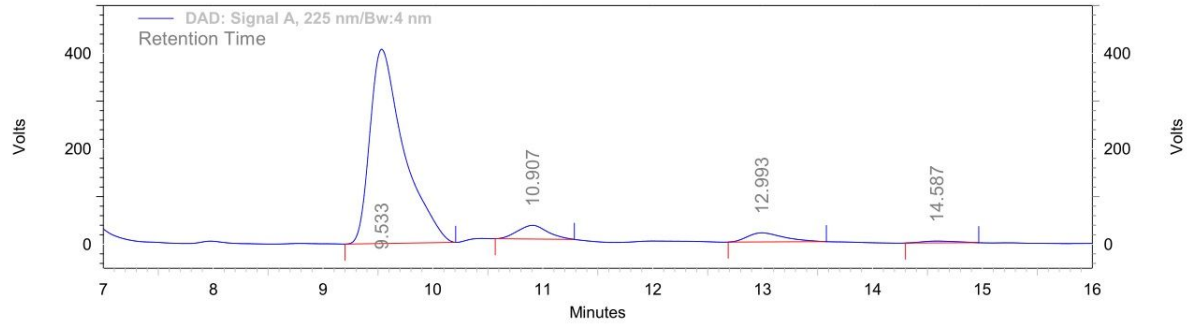


DAD: Signal A,
225 nm/Bw:4 nm
Results

Retention Time	Area	Area %	Height	Height %
8.980	12558851	11.15	437300	15.25
9.900	17613854	15.64	365863	12.76
12.227	38903880	34.55	1018012	35.51
13.733	43538244	38.66	1045952	36.48
Totals	112614829	100.00	2867127	100.00

Retention time	8.980	9.9	12.227	13.733
product	(*1S,2R*)	(*1R,2S*)	(*1S,2S*)	(*1R,2R*)

B)



DAD: Signal A,
225 nm/Bw:4 nm
Results

Retention Time	Area	Area %	Height	Height %
9.533	18237701	89.04	853163	88.80
10.907	1145098	5.59	59959	6.24
12.993	926006	4.52	39867	4.15
14.587	173242	0.85	7810	0.81

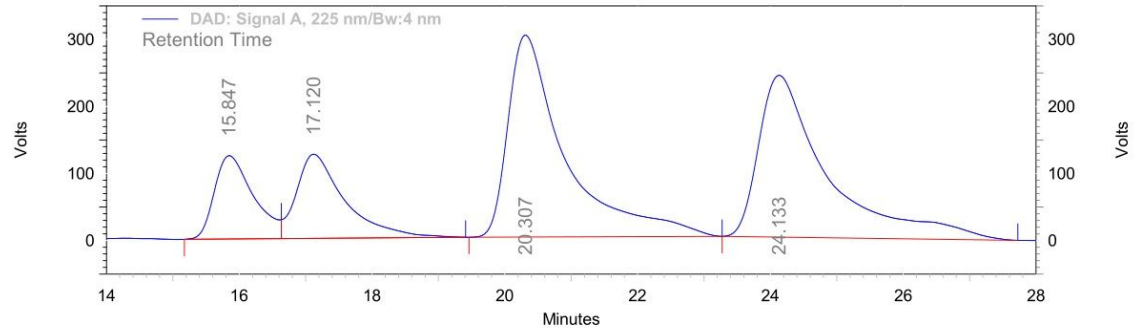
Totals	20482047	100.00	960799	100.00

Retention time	9.533	5.59	4.52	0.85
product	(*1S,2R*)	(*1R,2S*)	(*1S,2S*)	(*1R,2R*)

Figure 4.47: HPLC chromatograms of 1-(3-chlorophenyl)-2-nitrobutan-1-ol. A. racemic standard, B. *Bm*HNL catalyzed synthesis of diastereomers.

6) HPLC chromatograms of 1-(3-methoxyphenyl)-2-nitrobutan-1-ol

A)



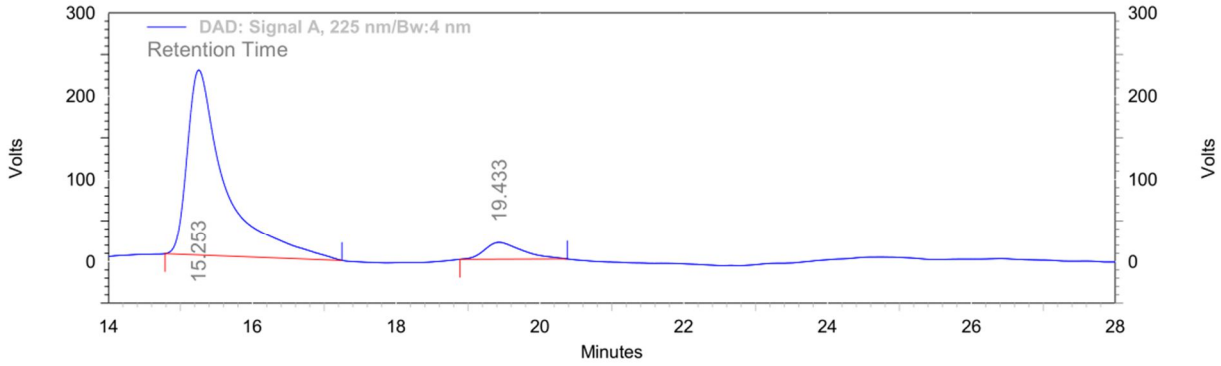
DAD: Signal A,
225 nm/Bw:4 nm
Results

Retention Time	Area	Area %	Height	Height %
15.847	10622166	10.86	260540	15.68
17.120	13284957	13.58	263261	15.85
20.307	37748917	38.58	631541	38.01
24.133	36193749	36.99	505988	30.46

Totals	97849789	100.00	1661330	100.00

Retention time	15.847	17.12	20.307	24.133
product	(*1S,2R*)	(*1R,2S*)	(*1S,2S*)	(*1R,2R*)

B)



DAD: Signal A,
225 nm/Bw:4 nm
Results

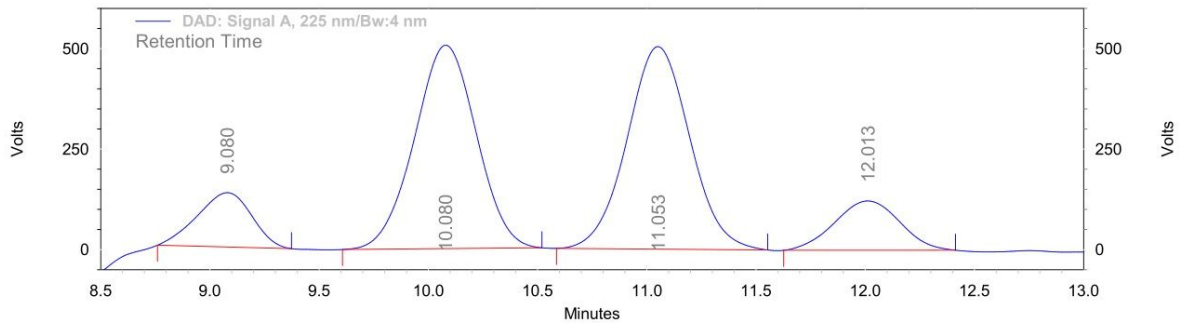
Retention Time	Area	Area %	Height	Height %
15.253	17203201	91.71	467971	91.65
19.433	1555890	8.29	42646	8.35
Totals	18759091	100.00	510617	100.00

Retention time	15.253	19.433
product	(*1S,2R*)	(*1S,2S*)

Figure 4.48: HPLC chromatograms of 1-(3-methoxyphenyl)-2-nitrobutan-1-ol. A. racemic standard, B. *Bm*HNL catalyzed synthesis of diastereomers.

7) HPLC chromatograms of 1-(3-methylphenyl)-2-nitro-1-butanol

A)

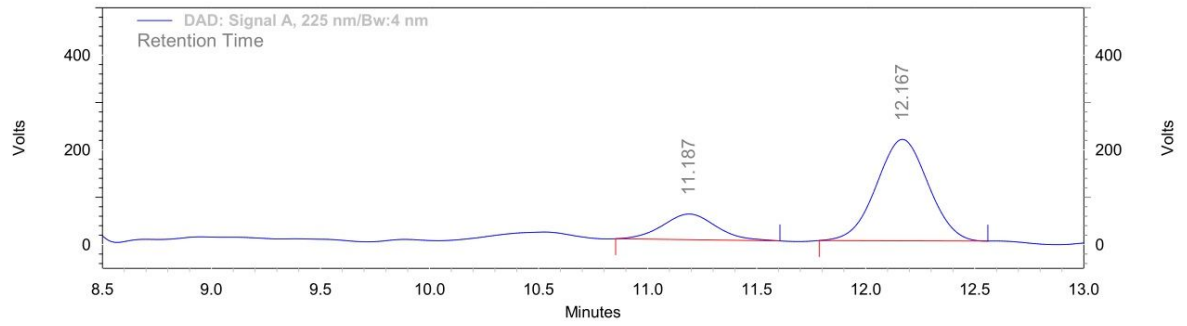


DAD: Signal A,
225 nm/Bw:4 nm
Results

Retention Time	Area	Area %	Height	Height %
9.080	4906691	9.38	283397	10.66
10.080	20936548	40.02	1061379	39.93
11.053	21131028	40.40	1056358	39.74
12.013	5335307	10.20	257222	9.68
Totals	52309574	100.00	2658356	100.00

Retention time	12.013	9.080	11.053	10.08
product	(*1S,2R*)	(*1R,2S*)	(*1S,2S*)	(*1R,2R*)

B)



DAD: Signal A,
225 nm/Bw:4 nm
Results

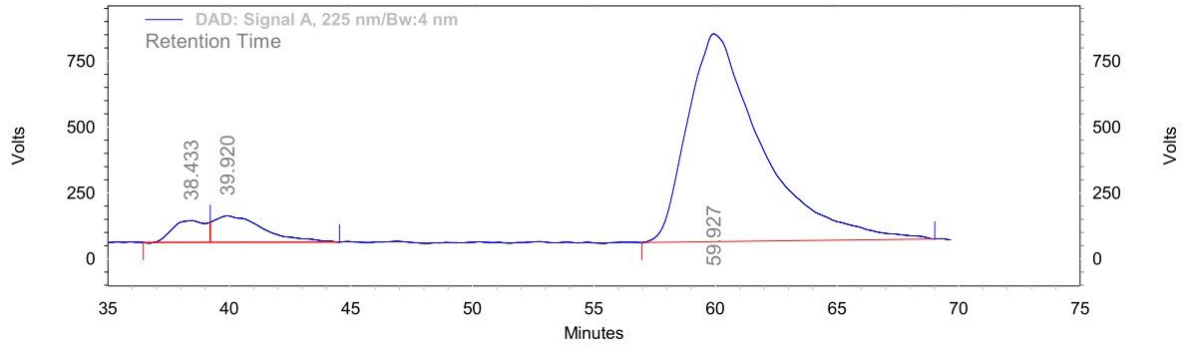
Retention Time	Area	Area %	Height	Height %
11.187	1940453	20.73	113577	20.19
12.167	7420365	79.27	449006	79.81
Totals	9360818	100.00	562583	100.00

Retention time	79.27	20.73
product	(*1S,2R*)	(*1S,2S*)

Figure 4.49: HPLC chromatograms of 1-(3-methylphenyl)-2-nitrobutan-1-ol. A. racemic standard, B. *Bm*HNL catalyzed synthesis of diastereomers.

8) HPLC chromatograms of 2-nitro 1-furalbutan-1-ol

A)



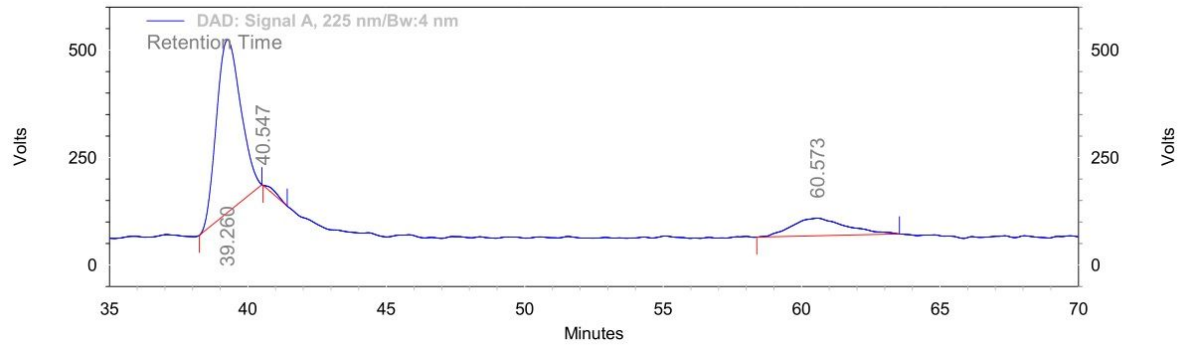
DAD: Signal A,
225 nm/Bw:4 nm
Results

Retention Time	Area	Area %	Height	Height %
38.433	16571226	4.17	173097	8.50
39.920	29813836	7.50	210502	10.34
59.927	351158091	88.33	1652657	81.16

Totals	397543153	100.00	2036256	100.00

Retention time	38.433	39.92	59.927
product	(*1S,2R*)	(*1R,2S*)	(*1S,2S*) + (*1R,2R*)

B)



DAD: Signal A,
225 nm/Bw:4 nm
Results

Retention Time	Area	Area %	Height	Height %
39.260	51304929	80.48	842887	90.79
40.547	587789	0.92	0	0.00
60.573	11857174	18.60	85533	9.21

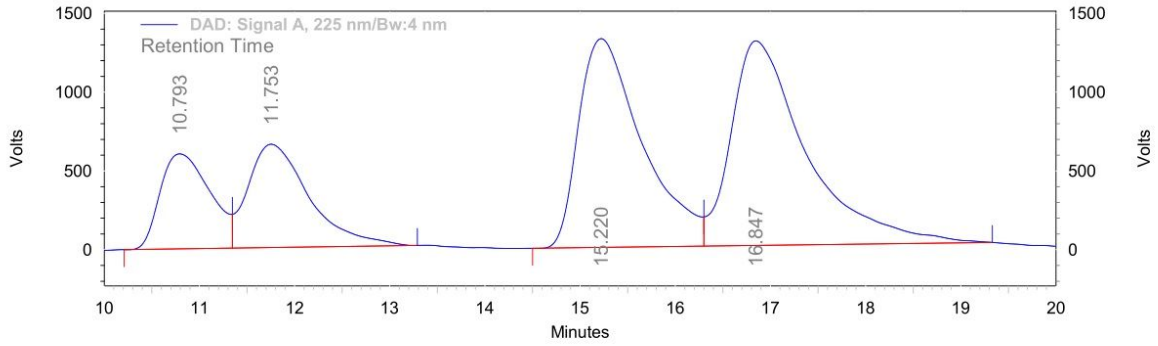
Totals	63749892	100.00	928420	100.00

Retention time	39.26	40.547	60.573
product	(*1S,2R*)	(*1R,2S*)	(*1S,2S*) + (*1R,2R*)

Figure 4.50: HPLC chromatograms of 2-nitro 1-furalbutan-1-ol. A. racemic standard, B. *Bm*HNL catalyzed synthesis of diastereomers.

9) HPLC chromatograms of 1-(3-bromophenyl)-2-nitrobutan-1-ol

A)

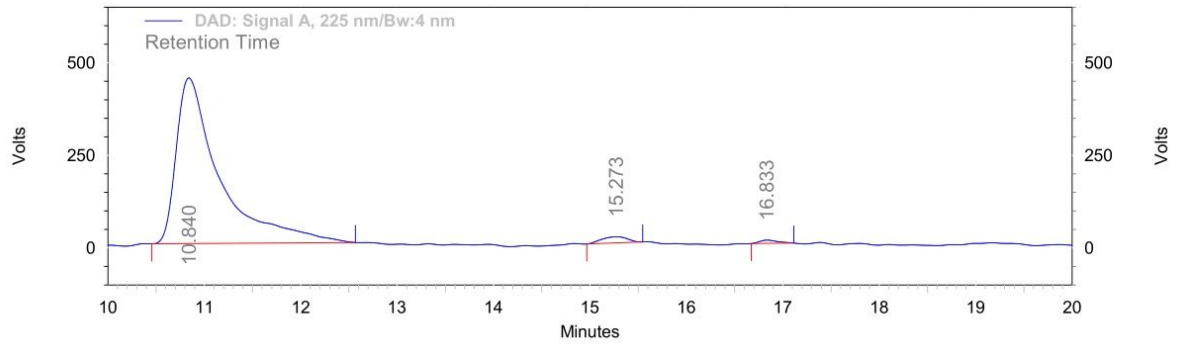


DAD: Signal A,
225 nm/Bw:4 nm
Results

Retention Time	Area	Area %	Height	Height %
10.793	46156558	11.94	1264281	15.53
11.753	61345139	15.87	1374987	16.89
15.220	129109632	33.40	2778687	34.13
16.847	149899568	38.78	2722731	33.45
Totals	386510897	100.00	8140686	100.00

Retention time	10.793	11.753	15.22	16.847
product	(*1S,2R*)	(*1R,2S*)	(*1S,2S*)	(*1R,2R*)

B)



DAD: Signal A,
225 nm/Bw:4 nm
Results

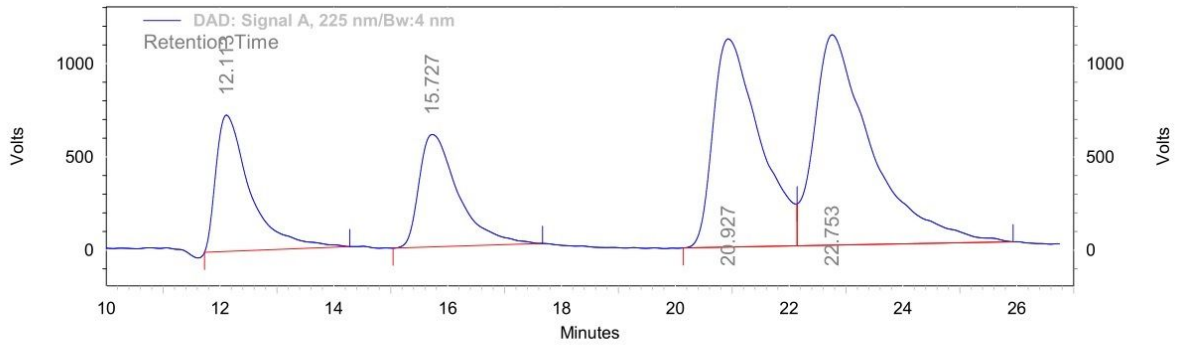
Retention Time	Area	Area %	Height	Height %
10.840	29273744	97.07	938376	94.65
15.273	647386	2.15	34694	3.50
16.833	235636	0.78	18317	1.85
Totals	30156766	100.00	991387	100.00

Retention time	10.84	15.273	16.833
product	(*1S,2R*)	(*1S,2S*)	(*1R,2R*)

Figure 4.51: HPLC chromatograms of 1-(3-bromophenyl)-2-nitrobutan-1-ol. A. racemic standard, B. *Bm*HNL catalyzed synthesis of diastereomers.

10) HPLC chromatograms of 1-(2-bromophenyl)-2-nitrobutan-1-ol

A)

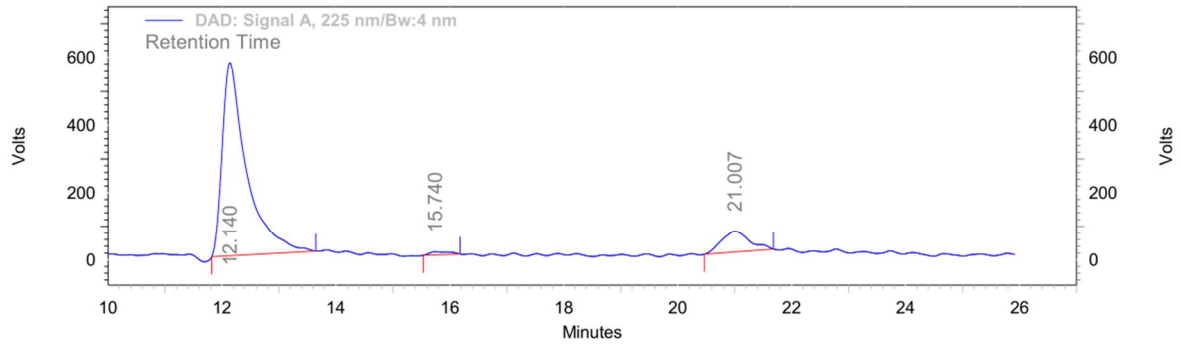


DAD: Signal A,
225 nm/Bw:4 nm
Results

Retention Time	Area	Area %	Height	Height %
12.113	64103981	15.11	1532212	20.43
15.727	60250615	14.20	1263525	16.84
20.927	133897034	31.56	2340538	31.20
22.753	166020897	39.13	2364993	31.53
Totals	424272527	100.00	7501268	100.00

Retention time	12.113	15.727	20.927	22.753
product	(*1S,2R*)	(*1R,2S*)	(*1S,2S*)	(*1R,2R*)

B)



DAD: Signal A,
225 nm/Bw:4 nm
Results

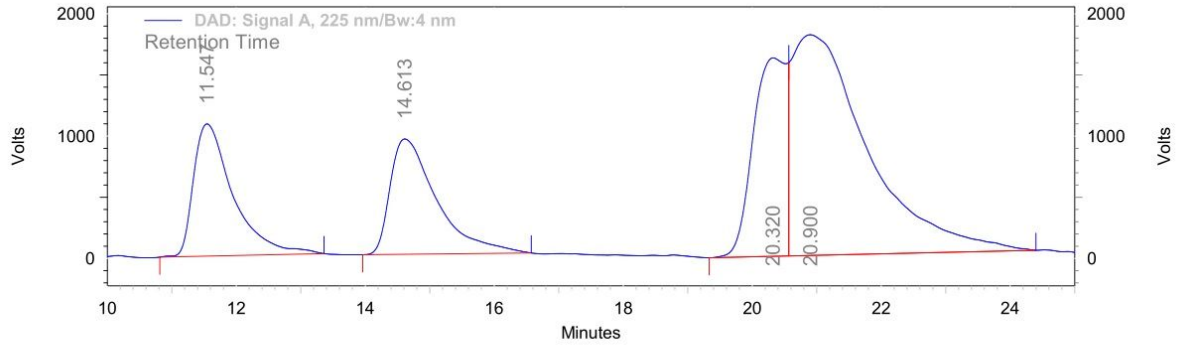
Retention Time	Area	Area %	Height	Height %
12.140	35766769	87.85	1200072	88.89
15.740	479548	1.18	19851	1.47
21.007	4466180	10.97	130198	9.64
Totals	40712497	100.00	1350121	100.00

Retention time	12.14	15.727	20.927	22.753
product	(*1S,2R*)	(*1R,2S*)	(*1S,2S*)	(*1R,2R*)

Figure 4.52: HPLC chromatograms of 1-(2-bromophenyl)-2-nitrobutan-1-ol. A. racemic standard, B. *Bm*HNL catalyzed synthesis of diastereomers.

11) HPLC chromatograms of 1-(2,3-dichlorophenyl)-2-nitrobutan-1-ol

A)

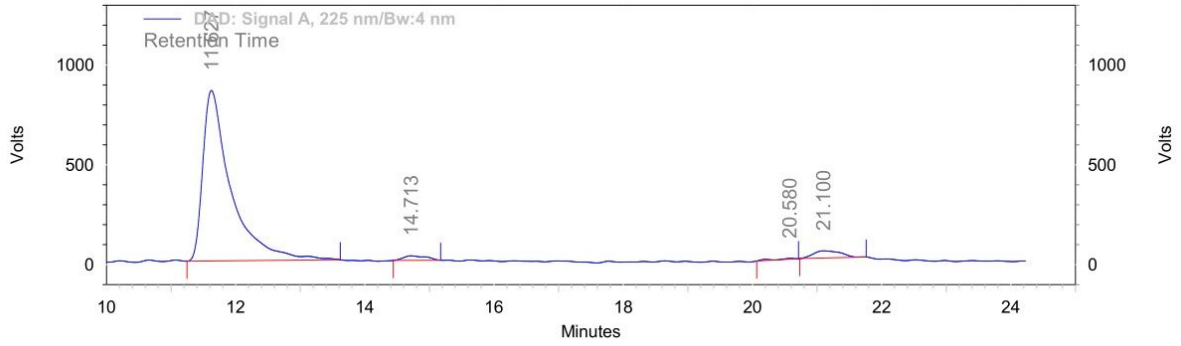


DAD: Signal A,
225 nm/Bw:4 nm
Results

Retention Time	Area	Area %	Height	Height %
11.547	96538767	15.42	2267146	19.83
14.613	98948996	15.80	1978405	17.30
20.320	121986452	19.48	3402722	29.76
20.900	308623717	49.29	3785371	33.11
Totals	626097932	100.00	11433644	100.00

Retention time	11.547	14.613	20.32	20.9
product	(*1S,2R*)	(*1R,2S*)	(*1S,2S*)	(*1R,2R*)

B)



DAD: Signal A,
225 nm/Bw:4 nm
Results

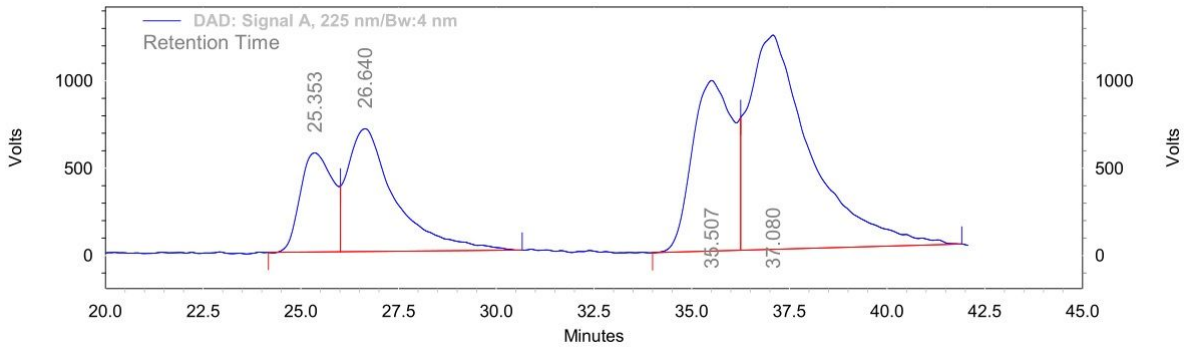
Retention Time	Area	Area %	Height	Height %
11.627	54230477	93.73	1792166	93.16
14.713	1191631	2.06	48178	2.50
20.580	211545	0.37	8129	0.42
21.100	2224951	3.85	75258	3.91
Totals	57858604	100.00	1923731	100.00

Retention time	11.627	14.713	20.58	21.1
product	(*1S,2R*)	(*1R,2S*)	(*1S,2S*)	(*1R,2R*)

Figure 4.53: HPLC chromatograms of 1-(2,3-dichlorophenyl)-2-nitrobutan-1-ol. A. racemic standard, B. *Bm*HNL catalyzed synthesis of diastereomers.

12) HPLC chromatograms of 1-(2-nitrophenyl)-2-nitrobutan-1-ol

A)

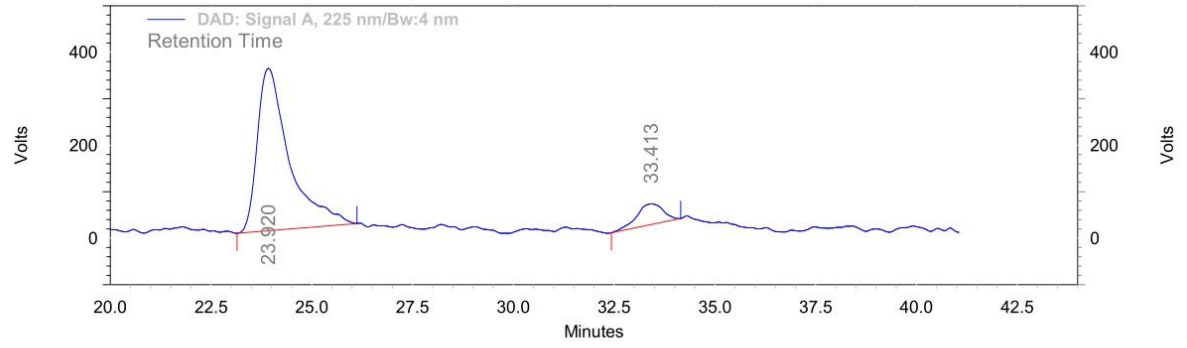


DAD: Signal A,
225 nm/Bw:4 nm
Results

Retention Time	Area	Area %	Height	Height %
25.353	69294142	11.05	1189773	16.34
26.640	125520274	20.01	1474659	20.25
35.507	148650637	23.70	2046996	28.11
37.080	283788196	45.24	2570789	35.30
Totals	627253249	100.00	7282217	100.00

Retention time	25.353	26.64	35.507	37.08
product	(*1S,2R*)	(*1R,2S*)	(*1S,2S*)	(*1R,2R*)

B)



DAD: Signal A,
225 nm/Bw:4 nm
Results

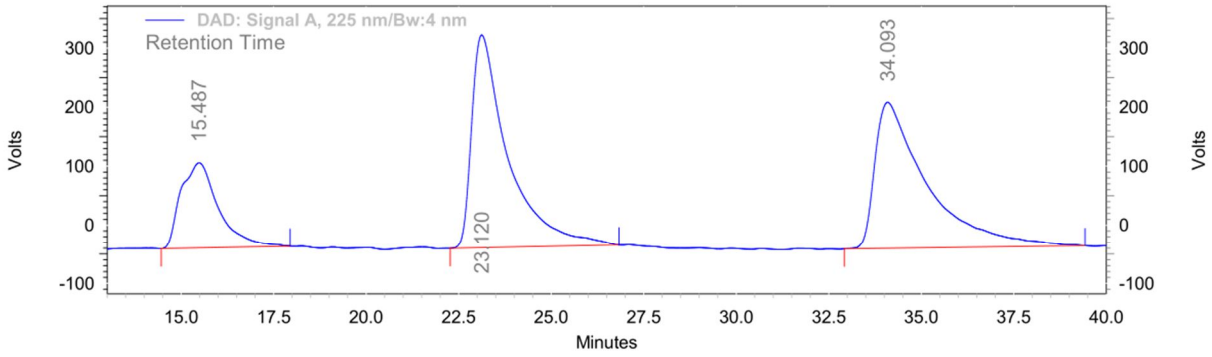
Retention Time	Area	Area %	Height	Height %
23.920	40346191	90.39	732174	88.67
33.413	4290372	9.61	93521	11.33
Totals	44636563	100.00	825695	100.00

Retention time	23.92	33.413
product	(*1S,2R*)	(*1S,2S*)

Figure 4.54: HPLC chromatograms of 1-(2-nitrophenyl)-2-nitrobutan-1-ol. A. racemic standard, B. *Bm*HNL catalyzed synthesis of diastereomers.

13) HPLC chromatograms of 1-(4-nitrophenyl)-2-nitrobutan-1-ol

A)

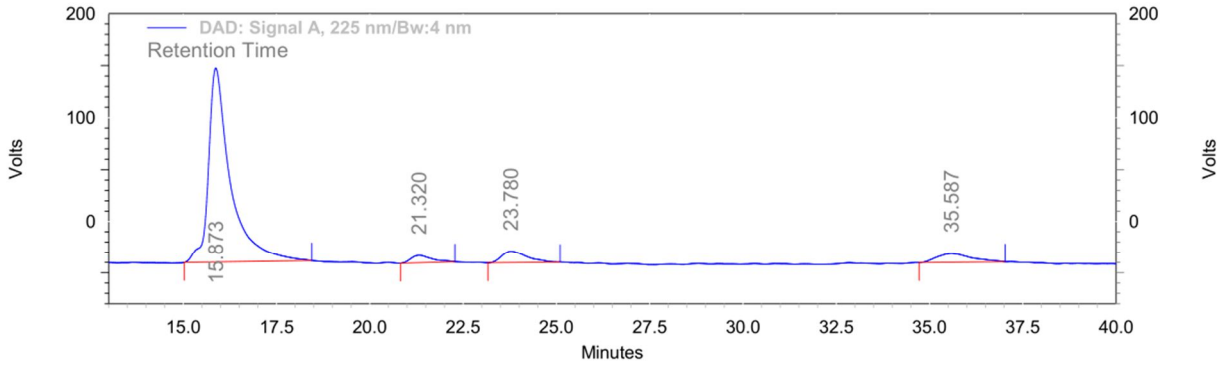


DAD: Signal A,
225 nm/Bw:4 nm
Results

Retention Time	Area	Area %	Height	Height %
15.487	21540139	17.34	304724	19.24
23.120	51748362	41.65	758037	47.87
34.093	50960114	41.01	520928	32.89
Totals	124248615	100.00	1583689	100.00

Retention time	15.487	34.093	23.12
product	(*1S,2R*) + (*1R,2S*)	(*1S,2S*)	(*1R,2R*)

B)

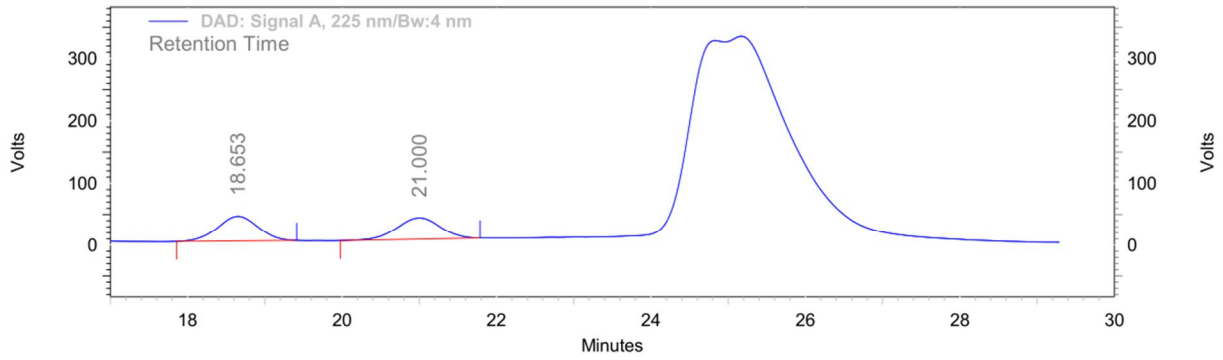


DAD: Signal A,
225 nm/Bw:4 nm
Results

Retention Time	Area	Area %	Height	Height %
15.873	16101075	85.01	392328	87.41
21.320	579424	3.06	14997	3.34
23.780	1098876	5.80	23437	5.22
35.587	1160368	6.13	18087	4.03
Totals	18939743	100.00	448849	100.00

Retention time	15.873	21.32	35.587	23.78
product	(*1S,2R*) + (*1R,2S*)	Aldehyde substrate	(*1S,2S*)	(*1R,2R*)

C)

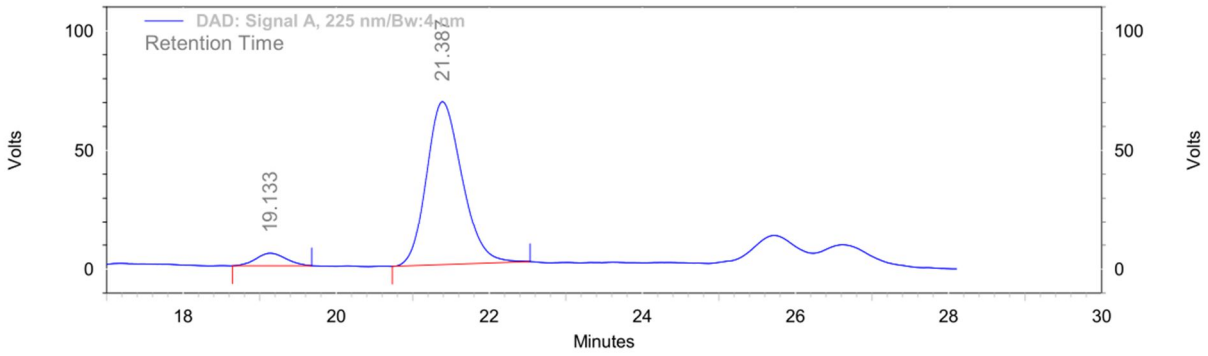


DAD: Signal A,
225 nm/Bw:4 nm
Results

Retention Time	Area	Area %	Height	Height %
18.653	3095774	51.81	84555	53.60
21.000	2879600	48.19	73185	46.40
Totals	5975374	100.00	157740	100.00

Retention time	21	18.563
product	(*1S,2R*)	(*1R,2S*)

D)



DAD: Signal A,
225 nm/Bw:4 nm
Results

Retention Time	Area	Area %	Height	Height %
19.133	301924	6.11	10989	7.11
21.387	4636430	93.89	143628	92.89
Totals	4938354	100.00	154617	100.00

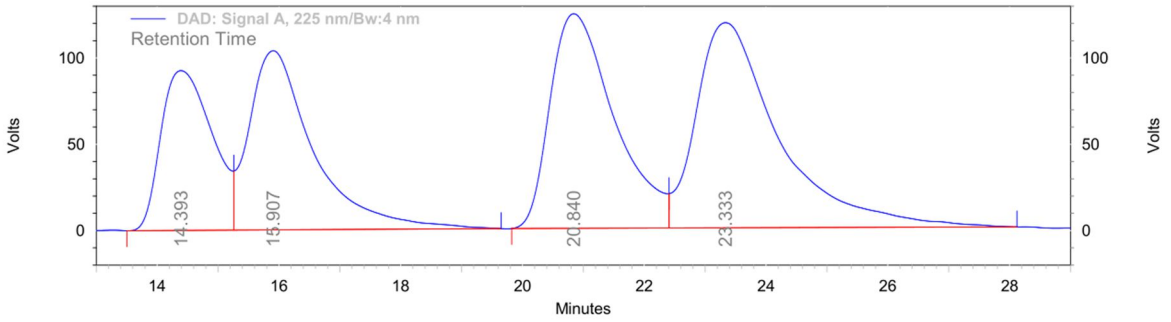
Retention time	21.387	19.133
product	(*1S,2R*)	(*1R,2S*)

Figure 4.55: HPLC chromatograms of 1-(4-nitrophenyl)-2-nitrobutan-1-ol. A. racemic standard in Lux amylose 1, B. *Bm*HNL catalyzed synthesis of diastereomers analysed in Lux amylose 1, C. racemic standard in Lux cellulose 1, D) *Bm*HNL catalyzed synthesis of diastereomers analysed in Lux cellulose 1.

4.4.21. HPLC chromatograms of biocatalytically synthesized *syn* (*1S,2S*)-β-nitroalcohols starting from different aromatic aldehydes and nitroethane via *Bm*HNL catalyzed concomitant Henry and retro-Henry reaction

1) HPLC chromatograms of 2-nitro 1-phenylpropan-1-ol

A)

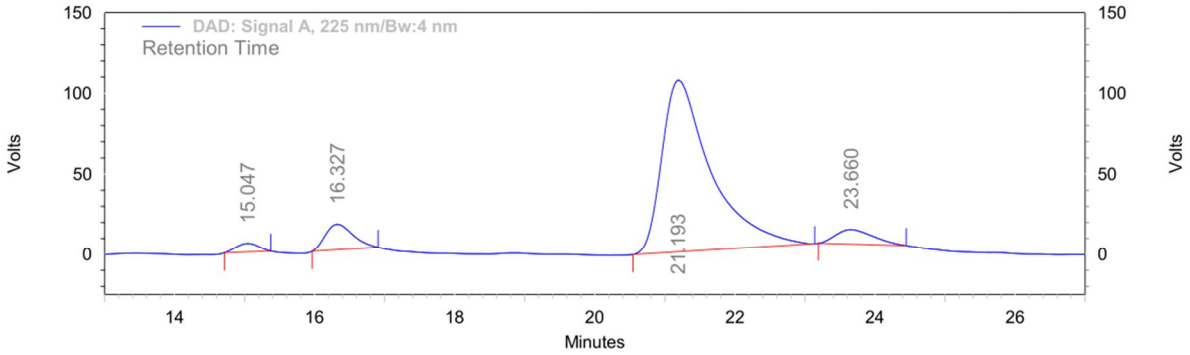


DAD: Signal A,
225 nm/Bw:4 nm
Results

Retention Time	Area	Area %	Height	Height %
14.393	11367115	16.23	194108	21.06
15.907	15931624	22.75	217620	23.61
20.840	19157124	27.36	260728	28.29
23.333	23572464	33.66	249268	27.04
Totals	70028327	100.00	921724	100.00

Retention time	14.393	15.907	20.84	23.333
product	(*1S,2R*)	(*1R,2S*)	(*1S,2S*)	(*1R,2R*)

B)



DAD: Signal A,
225 nm/Bw:4 nm
Results

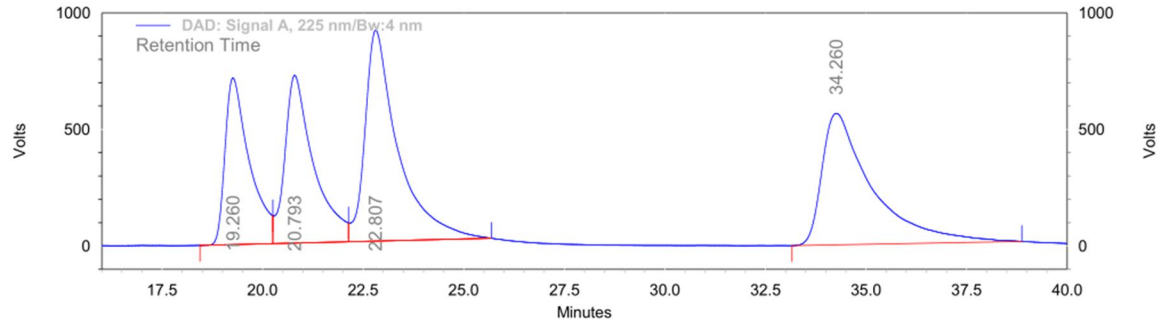
Retention Time	Area	Area %	Height	Height %
15.047	253282	1.98	11518	4.00
16.327	917800	7.17	33463	11.63
21.193	10907647	85.26	223534	77.71
23.660	715105	5.59	19127	6.65
Totals	12793834	100.00	287642	100.00

Retention time	15.047	16.327	21.193	23.66
product	(*1S,2R*)	(*1R,2S*)	(*1S,2S*)	(*1R,2R*)

Figure 4.56: HPLC chromatograms of 2-nitro 1-phenyl propan-1-ol. A. racemic standard, B. *Bm*HNL catalyzed synthesis of diastereomers.

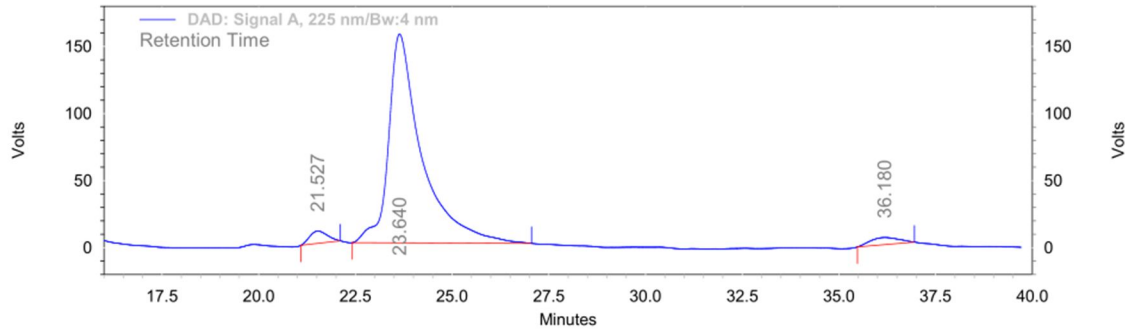
2) HPLC chromatograms of 1-(3-methoxyphenyl)-2-nitropropan-1-ol

A)



Retention time	19.26	20.793	22.807	34.26
product	(*1S,2R*)	(*1R,2S*)	(*1S,2S*)	(*1R,2R*)

B)

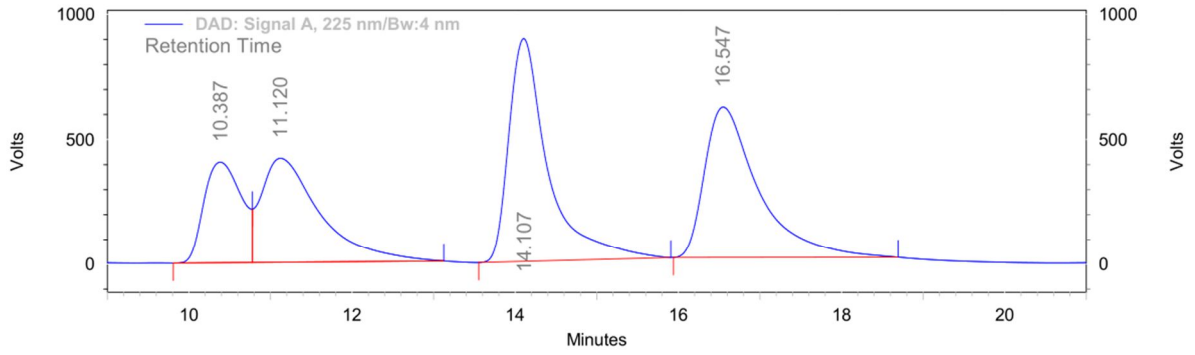


Retention time	21.527	23.64	36.18
product	(*1R,2S*)	(*1S,2S*)	(*1R,2R*)

Figure 4.57: HPLC chromatograms of 1-(3-methoxyphenyl)-2-nitropropan-1-ol. A. racemic standard, B. *Bm*HNL catalyzed synthesis of diastereomers.

3) HPLC chromatograms of 1-(2-methylphenyl)-2-nitropropan-1-ol

A)



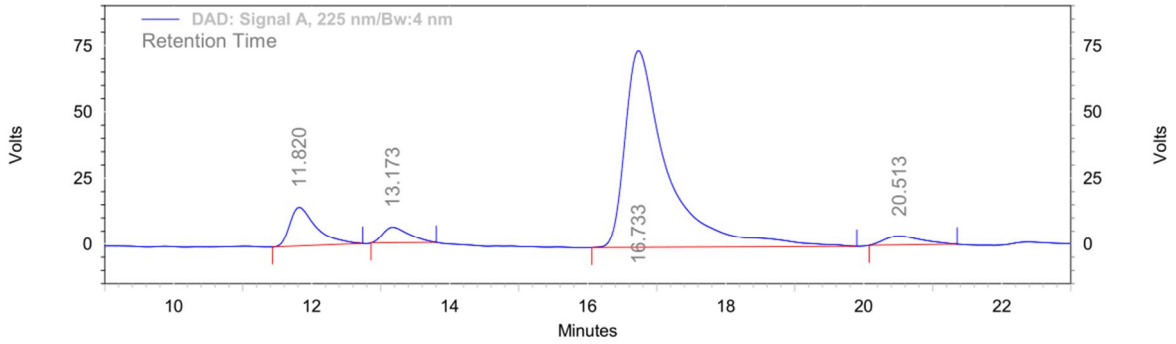
DAD: Signal A,
225 nm/Bw:4 nm
Results

Retention Time	Area	Area %	Height	Height %
10.387	27153262	14.13	848611	17.45
11.120	44096241	22.94	877239	18.04
14.107	62627180	32.58	1871302	38.49
16.547	58347089	30.35	1264972	26.02

Totals	192223772	100.00	4862124	100.00

Retention time	10.387	11.12	14.107	16.547
product	(*1S,2R*)	(*1R,2S*)	(*1S,2S*)	(*1R,2R*)

B)



DAD: Signal A,
225 nm/Bw:4 nm
Results

Retention Time	Area	Area %	Height	Height %
11.820	832631	10.28	31003	14.99
13.173	335864	4.15	12628	6.10
16.733	6660665	82.21	155952	75.38
20.513	273102	3.37	7299	3.53

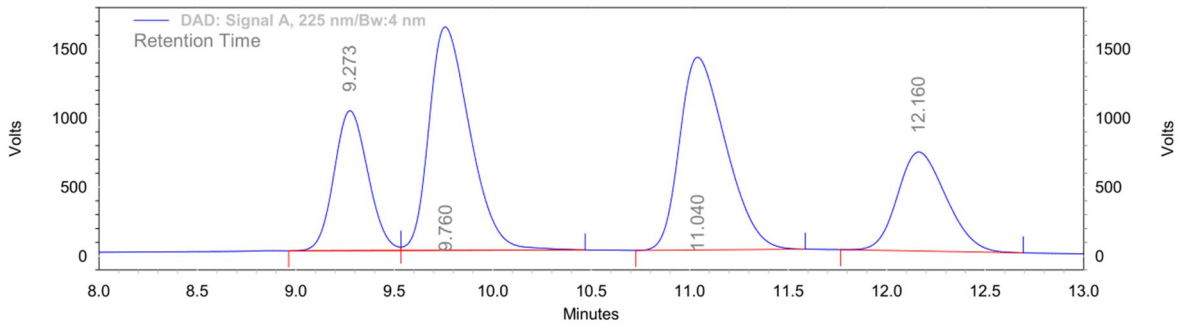
Totals	8102262	100.00	206882	100.00

Retention time	11.82	13.173	16.733	20.513
product	(*1S,2R*)	(*1R,2S*)	(*1S,2S*)	(*1R,2R*)

Figure 4.58: HPLC chromatograms of 1-(2-methylphenyl)-2-nitropropan-1-ol. A. racemic standard, B. *Bm*HNL catalyzed synthesis of diastereomers.

4) HPLC chromatograms of 1-(3-methylphenyl)-2-nitropropan-1-ol

A)

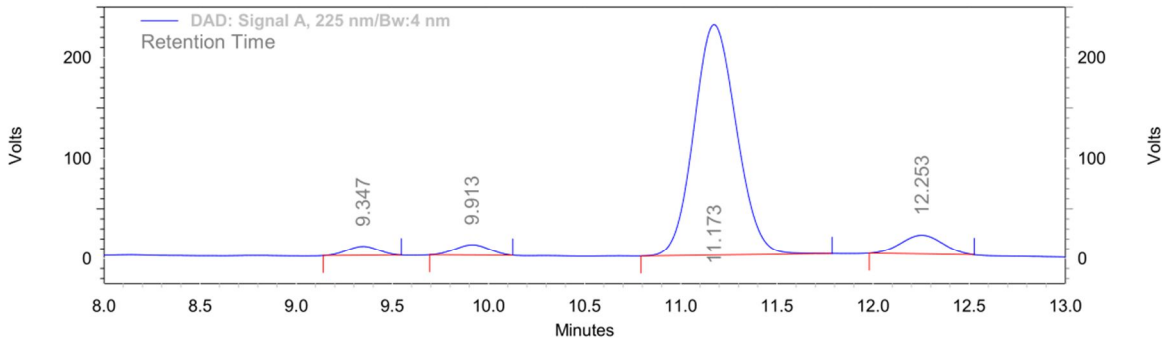


DAD: Signal A, 225 nm/Bw:4 nm
Results

Retention Time	Area	Area %	Height	Height %
9.273	25369224	17.13	2125636	21.36
9.760	48971650	33.08	3393666	34.10
11.040	47917429	32.36	2929016	29.43
12.160	25798623	17.42	1502672	15.10
Totals	148056926	100.00	9950990	100.00

Retention time	12.16	9.273	11.04	9.76
product	(*1S,2R*)	(*1R,2S*)	(*1S,2S*)	(*1R,2R*)

B)



DAD: Signal A,
225 nm/Bw:4 nm
Results

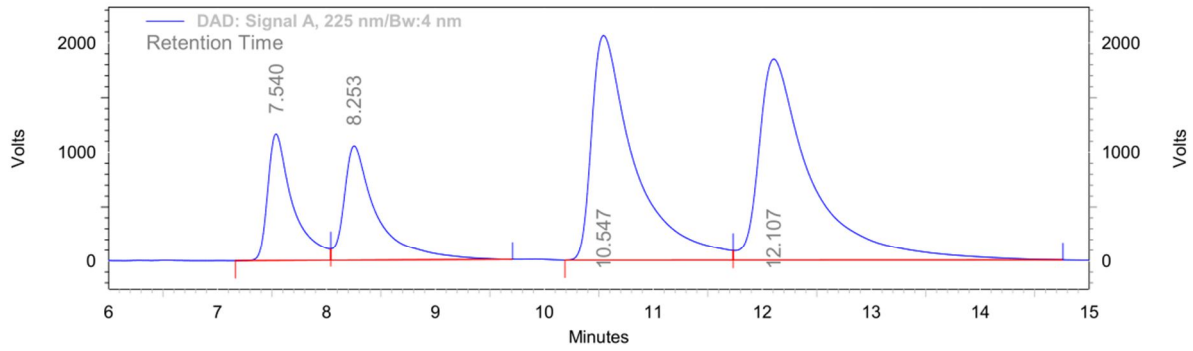
Retention Time	Area	Area %	Height	Height %
9.347	224283	2.63	19674	3.49
9.913	278366	3.27	22390	3.98
11.173	7399114	86.90	480754	85.38
12.253	612597	7.19	40284	7.15
Totals	8514360	100.00	563102	100.00

Retention time	12.253	9.347	11.173	9.913
product	(*1S,2R*)	(*1R,2S*)	(*1S,2S*)	(*1R,2R*)

Figure 4.59: HPLC chromatograms of 1-(3-methylphenyl)-2-nitropropan-1-ol. A. racemic standard, B. *Bm*HNL catalyzed synthesis of diastereomers.

5) HPLC chromatograms of 1-(4-methylphenyl)-2-nitropropan-1-ol

A)

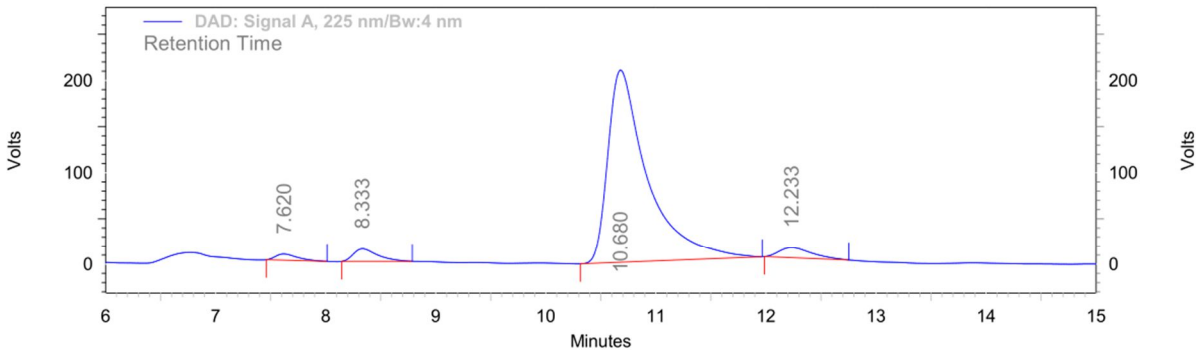


DAD: Signal A,
225 nm/Bw:4 nm
Results

Retention Time	Area	Area %	Height	Height %
7.540	39335762	11.73	2437552	19.01
8.253	46023200	13.72	2202699	17.18
10.547	119680973	35.69	4317493	33.67
12.107	130330612	38.86	3866000	30.15
Totals	335370547	100.00	12823744	100.00

Retention time	7.54	8.253	10.547	12.107
product	(*1S,2R*)	(*1R,2S*)	(*1S,2S*)	(*1R,2R*)

B)



DAD: Signal A,
225 nm/Bw:4 nm
Results

Retention Time	Area	Area %	Height	Height %
7.620	196240	1.62	14338	2.84
8.333	445023	3.67	28934	5.73
10.680	11003180	90.73	438481	86.80
12.233	483198	3.98	23426	4.64
Totals	12127641	100.00	505179	100.00

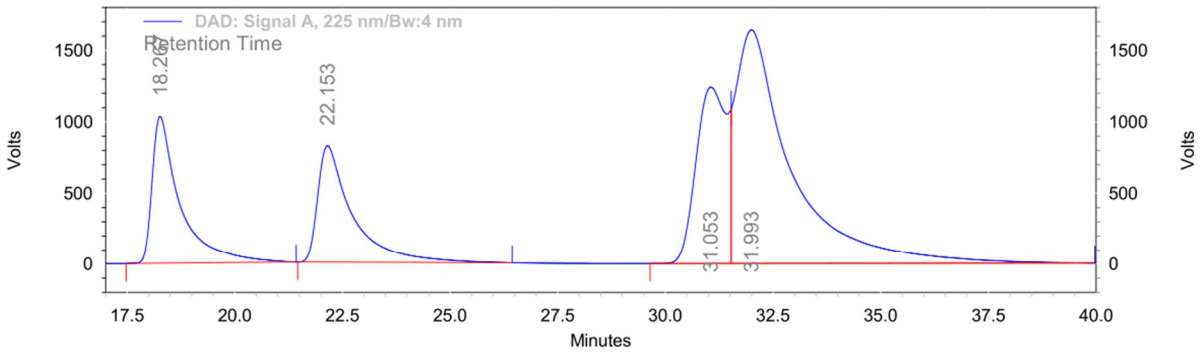
Retention time	7.62	8.333	10.68	12.233

product	(*1S,2R*)	(*1R,2S*)	(*1S,2S*)	(*1R,2R*)

Figure 4.60: HPLC chromatograms of 1-(4-methylphenyl)-2-nitropropan-1-ol. A. racemic standard, B. *Bm*HNL catalyzed synthesis of diastereomers.

6) HPLC chromatograms of 1-(2-methoxyphenyl)-2-nitropropan-1-ol

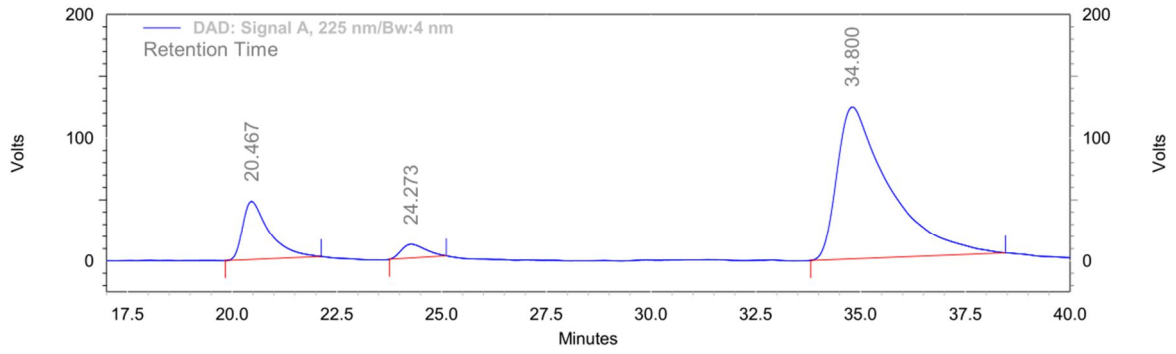
A)



DAD: Signal A,
225 nm/Bw:4 nm
Results

Retention Time	Area	Area %	Height	Height %
18.267	98225505	15.47	2163726	21.81
22.153	96657881	15.23	1718015	17.32
31.053	129307105	20.37	2600096	26.21
31.993	310647031	48.93	3437929	34.66
Totals	634837522	100.00	9919766	100.00

Retention time	18.267	22.153	31.053	31.993
product	(*1S,2R*)	(*1R,2S*)	(*1S,2S*)	(*1R,2R*)



DAD: Signal A, 225 nm/Bw:4 nm Results

Retention Time	Area	Area %	Height	Height %
20.467	4404369	15.78	99587	26.09
24.273	937738	3.36	23365	6.12
34.800	22564314	80.86	258714	67.79
Totals	27906421	100.00	381666	100.00

Retention time	18.267	22.153	31.053	31.993
product	(*1S,2R*)	(*1R,2S*)	(*1S,2S*)	(*1R,2R*)

Figure 4.61: HPLC chromatograms of 1-(2-methoxyphenyl)-2-nitropropan-1-ol. A. racemic standard, B. *Bm*HNL catalyzed synthesis of diastereomers.

4.5. Discussion:

4.5.1. Promiscuous diastereoselective nitroaldol reaction to synthesize (1*S*,2*R*)-2-NPP

To date, only one HNL, i.e., *Hb*HNL is reported to catalyze the diastereoselective synthesis of (*S*)- β -nitroalcohol. *Hb*HNL catalyzed synthesis of (*1S,2R*)-2-NPP from benzaldehyde and nitroethane provided 67% yield with 95% ee and 80% de.[1] Both *Bm*HNL and *Hb*HNL belong to the same α/β hydrolase fold superfamily and share 56% sequence similarity. They also possess similar catalytic machinery, i.e., Asp-His-Ser-Lys-Thr in the active site, which is commonly used for hydrocyanation mechanism. So, after finding the promiscuous nitroaldol activity of *Bm*HNL towards the enantioselective nitromethane addition to a range of aromatic aldehydes,[3] we hypothesized that *Bm*HNL may catalyze the diastereoselective Henry reaction like *Hb*HNL. To our surprise, crude cell lysates of *Bm*HNL catalyzed the stereoselective addition of nitroethane to benzaldehyde and synthesized (*1S,2R*)-2-NPP, the same stereoisomer produced by *Hb*HNL, with 60% conversion, 97% ee and 65% de.

4.5.2. Optimization of reaction conditions of *Bm*HNL catalyzed stereoselective synthesis of (*1S,2R*)-2-NPP

Several important reaction parameters were optimized to improve the production of (*1S,2R*)-2-NPP with respect to % conversion and stereoselectivity. The earlier study of *Hb*HNL used KPB pH 7 towards the synthesis of (*1S,2R*)-2-NPP. [1] *Ac*HNL and *Gt*HNL variants preferred KPB pH 6 to synthesize (*1R,2S*)-2-NPP. [7] We used KPB and CPB varying their pH from 5.5 to 7,

where CPB, pH 5.5 has provided the best results. To find a suitable organic solvent for this biphasic reaction system, five solvents NBA, TBME, DEE, toluene and DIPE were tested. Among them, TBME gave overall best result in terms of % conversion, % ee and % de of (*1S,2R*)-2-NPP. TBME was also used in earlier HNL-catalyzed diastereoselective synthesis of 2-NPP [1,7] and *BmHNL*-catalyzed enantioselective β-nitroalcohols synthesis.[3] Co-substrate nitroethane concentration was optimized in the subsequent experiment. The previous study of *Hb*HNL catalysed diastereoselective Henry reaction used 1:10 stoichiometric ratio between benzaldehyde and nitroethane.[1] We varied nitroethane concentration from 0.75 to 2 M against 20 mM benzaldehyde. *Bm*HNL displayed highest stereoselectivity and good % conversion with 1.75 M nitroethane. Next we evaluated the amount of enzymes as a parameter to optimize. In case of the study of *Hb*HNL, *Ac*HNL and *Gt*HNL variants catalyzed synthesis of 2-NPP, purified proteins were used.[1,7] Since this study involves the usage of the crude enzyme, the amount of enzyme was optimized by varying it from 5-25 mg. An increase in the enzyme activity was observed up to 10 mg, beyond that, the % conversion and % ee remained the same. After optimizing these parameters, *Bm*HNL showed 81% conversion with >99% ee and 80% de of (*1S,2R*)-2-NPP.

4.5.3. *Bm*HNL catalysed stereoselective synthesis of *anti* (*1S,2R*)- stereoisomers of different β-nitroalcohols

Using the optimized biocatalytic reaction conditions, several aldehydes having substituents at different positions of their aromatic ring were converted into corresponding *anti*-diastereomers of β-nitroalcohols. To date, only one (*S*)-selective HNL, i.e., *Hb*HNL, is reported to show such a promiscuous reaction in the production of (*1S,2R*)-2-NPP. *Hb*HNL showed 67% yield and 95% ee with 80% de. [1] Two other (*R*)-selective HNLs, *Gt*HNL and *Ac*HNL have been reported in the synthesis of the opposite isomer from benzaldehyde, but with very poor catalytic activity. [7] Here, we evaluated nineteen diverse aldehydes using nitroethane as a nucleophile and *Bm*HNL demonstrated not only excellent substrate scope but also stereoselectivity in the manufacture of the corresponding (*1S,2R*)-β-nitroalcohols with up to >99% conversion, >99% ee and 93.4% de. *Bm*HNL also exhibited broader nucleophilie promiscuity. It catalysed stereoselective addition of 1-nitropronane to different aldehydes in the synthesis of corresponding (*1S,2R*)-β-nitroalcohols with up to 97% conversion, >99% ee and >99% de. None of these substrates used here (Figure 4.10) except benzaldehyde were studied earlier by HNL catalyzed Henry reaction to produce their *anti* diastereomers starting from their corresponding aldehydes. Even if the biocatalytic methods of synthesis of β-nitroalcohols with two chiral centres to be considered, there exist only one other method, i.e., *Pseudomonas flourescens* lipase catalysed kinetic resolution of racemic 1-(4-chlorophenyl)-2-nitropropanol which provided 77% conversion, but the stereoselectivity of the product was not explicitly mentioned.[9]

4.5.4. Gram scale synthesis of (*1S,2R*)-2-NPP by recycling the *Bm*HNL enzyme

Here preparative scale synthesis of the *anti* diastereoisomer (*1S,2R*)-2-NPP was carried out using purified BmHNL enzyme. The best report to date to synthesize this molecule on an preparative scale was through *Hb*HNL enzyme synthesizing the same compound, did not calculate TTN.[2] However, it achieved a maximum conversion of 67% of 127 mmol of benzaldehyde, yielding 85.1 mmol of product, using 9.27 g of purified enzyme, equivalent to 0.317 mmol of enzyme (*Hb*HNL molecular weight: 29.2 kDa). [10] This resulted in a TTN of

85.1/0.317 = 268, whereas *Bm*HNL enzyme showed a TTN of 13,290 (5460 µmol 2-NPP/ 0.406 µmol *Bm*HNL), almost 50-fold higher than the former (*Bm*HNL molecular weight: 29.5) kDa). [11] Additionally, *Hb*HNL catalyzed reaction showed a substrate to catalyst ratio of only 4495 U/mmol of substrate, 308-fold lower than our *Bm*HNL approach where substrate to catalyst ratio is 14.6 U/ mmol of substrate.

4.6. Conclusions

*Bm*HNL's promiscuous diastereoselective Henry reactions in the stereoselective synthesis of chiral β-nitroalcohols from corresponding aldehydes using nitroethane or 1-nitropropane as a nucleophile is explored. Several reaction parameters for both sets of nitroaldol reactions comprising nitroethane or 1-nitropropane were optimized to obtain enhanced conversion and stereoselectivity of the products. Nineteen aromatic aldehydes were tested to explore the substrate scope of *Bm*HNL towards this reaction using nitroethane. *Bm*HNL displayed broad substrate scope in synthesizing (*1S,2R*) stereoisomers of β-nitroalcohols with up to >99% conversion, up to 99% ee, and up to 93.4% de. Similarly, fourteen substrates were selected along with 1-nitropropane as the nucleophile to synthesize their corresponding β-nitroalcohols which resulted in up to 97% conversion, up to 99% ee, and up to 99% de. Kinetic parameters of *Bm*HNL in the synthesis of (*1S,2R*)-2-NPP were determined that showed catalytic efficiency (k_{cat}/K_M) of 2.6 $mM^{-1}min^{-1}$. *Bm*HNL was found to be extremely stable in the reaction medium containing high substrate concentration, and only 14% activity decreased after incubating it for two months. We have demonstrated the reuse of *Bm*HNL in the reaction medium for 20 consecutive cycles, and yet the enzyme retained 82% of its activity. This recycling approach was employed in performing the gram scale synthesis of (*1R,2S*)-2-NPP. The TTN of this bioconversion was calculated to be 13,290 at the end of ten cycles which is almost 50 times more than the existing *Hb*HNL approach. This enzyme reusability approach significantly improved the enzyme to substrate ratio and it decreased by more than 308 times compared to the *Hb*HNL approach. Lastly, synthesis of (*1S,2S*) *syn* isomer of six β-nitroalcohols was carried out by incubating the same biocatalysis for a longer time. This demonstrates the diastereodivergent synthesis by *Bm*HNL to obtain both *anti* and *syn* Henry products with excellent stereoselectivity.

4.7. References:

1. T. Purkarthofer, K. Gruber, M. Gruber-Khadjawi, K. Waich, W. Skranc, D. Mink, H. Griengl, *Angewandte Chemie International Edition* **2006**, *45*, 3454–3456.

2. M. Gruber-Khadjawi, T. Purkarthofer, W. Skranc, H. Griengl, *Advanced Synthesis & Catalysis* **2007**, *349*, 1445–1450.

3. A. Chatterjee, D. H. S. Rao, S. K. Padhi, *Advanced Synthesis & Catalysis* **2021**, *363*, 5310–5318.

4. B. Kalyanasundar, C. I. Pérez, B. Arroyo, M. Moreno, R. Gutiérrez, *Frontiers in Neuroscience* **2020**, *14*, 572328.

5. S. K. Padhi, *ChemBioChem* **2016**, *18*, 152–160.

6) K. Fuhshuku, Y. Asano, *Journal of Biotechnology* **2011**, *153*, 153–159.

7) M. Bekerle-Bogner, M. Gruber-Khadjawi, H. Wiltsche, R. Wiedner, H. Schwab, K. Steiner, *ChemCatChem* **2016**, *8*, 2214–2216.

8. M. Dadashipour, M. Yamazaki, K. Momonoi, K. Tamura, K. Fuhshuku, Y. Kanase, E. Uchimura, K. Guan, Y. Asano, *Journal of Biotechnology* **2011**, *153*, 100–110.

9) J. C. Borah, J. Boruwa, B. Kalita, A. K. Hazarika, N. C. Barua, *Indian Journal of Chemistry* **2005**, *44*, 1961-1965.

10) M. Hasslacher, M. Schall, M. Hayn, H. Griengl, S. D. Kohlwein, H. Schwab, *Journal of Biological Chemistry* **1996**, *271*, 5884–5891.

11) Y. Asano, N. Kawahara, *Industrial Biotechnology* **2016**, *12*, 91–97

University of Hyderabad
Hyderabad- 500 046, India

PLAGIARISM FREE CERTIFICATE

This is to certify that the similarity index of this thesis as checked by the Library of the University of Hyderabad is 30%. Out of this, 13% similarity has been found from the candidate's (**Ayon Chatterjee**) own publication, which form the adequate part of the thesis. Another 10% is from the M. Sc. theses of my laboratory, where the corresponding students were worked with Ayon Chatterjee for their M. Sc. thesis and used the same protocols that were used by him. This brings to overall plagiarism of the thesis to 30% – 23% = 7%.

The details the of student's publication is as follows:

Paper	% Similarity
1. Ayon Chatterjee, D.H. Sreenivasa Rao, Santosh Kumar Padhi. One-pot enzyme cascade catalyzed asymmetrization of primary alcohols: Synthesis of enantiocomplementary chiral β-nitroalcohols, Adv. Synth. Catal., 2021, 363, 5310-5318.	10% + 2% = 12% (Source No. 2 and 4)
2. 7. D.H. Sreenivasa Rao, Ayon Chatterjee, Santosh Kumar Padhi. Biocatalytic approaches for enantio and diastereoselective synthesis of chiral β-nitroalcohols, Org. Biomol. Chem., 2021, 19, 322-337	1% (Source No. 6)

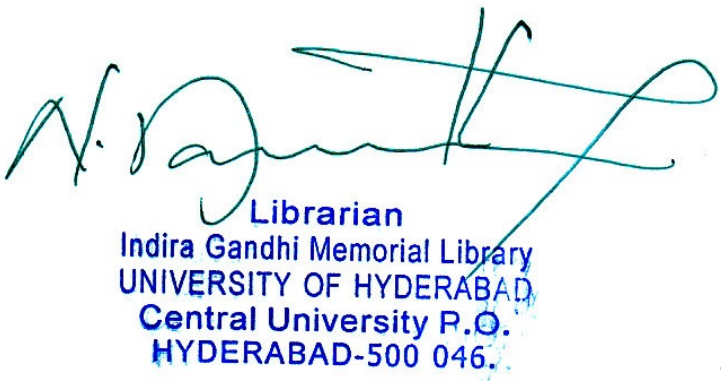
About 7% similarity was identified from external sources in the present thesis, which is in accordance with the regulations of the University. All the publications related to this thesis have been appended at the end of the thesis. Hence the present thesis may be considered to be plagiarism free.

Dr. Santosh Kumar Padhi
Supervisor

Dr. Santosh Kumar Padhi
Associate Professor
Department of Biochemistry
School of Life Science
University of Hyderabad
Hyderabad-500 046. India.

Protein engineering and enzyme cascade in the sustainable stereoselective synthesis of β-nitroalcohols

by Ayon Chatterjee



Submission date: 20-May-2024 03:40PM (UTC+0530)
Submission ID: 2383929981
File name: 2024-05-20-compressed_without_reference_thesis_combined.pdf (11.25M)
Word count: 55575
Character count: 277215

Protein engineering and enzyme cascade in the sustainable stereoselective synthesis of β-nitroalcohols

ORIGINALITY REPORT

30%	12%	27%	17%
SIMILARITY INDEX	INTERNET SOURCES	PUBLICATIONS	STUDENT PAPERS

PRIMARY SOURCES

1	Submitted to University of Hyderabad, Hyderabad Student Paper	10%
2	Ayon Chatterjee, D.H. Sreenivasa Rao, Santosh Padhi. "One-Pot Enzyme Cascade Catalyzed Asymmetrization of Primary Alcohols: Synthesis of Enantiocomplementary Chiral β-Nitroalcohols", Advanced Synthesis & Catalysis, 2021 Publication	10%
3	pubs.rsc.org Internet Source	3%
4	Ayon Chatterjee, D. H. Sreenivasa Rao, Santosh Kumar Padhi. "One-Pot Enzyme Cascade Catalyzed Asymmetrization of Primary Alcohols: Synthesis of Enantiocomplementary Chiral β-Nitroalcohols", Advanced Synthesis & Catalysis, 2021 Publication	2%

Dr. Santosh Kumar Padhi
Associate Professor
Department of Biochemistry
School of Life Science
University of Hyderabad
Hyderabad-500 046. India.

5	www.freepatentsonline.com Internet Source	1 %
6	D. H. Sreenivasa Rao, Ayon Chatterjee, Santosh Kumar Padhi. "Biocatalytic approaches for enantio and diastereoselective synthesis of chiral β-nitroalcohols", Organic & Biomolecular Chemistry, 2020 Publication	1 %
7	Santosh Kumar Padhi, D H Sreenivasa Rao. "Preparation of (S)-β-nitro alcohols by a (R)-selective HNL via enantioselective C-C bond cleavage", ChemBioChem, 2018 Publication	<1 %
8	Dransfield, P.J.. "A unified synthetic strategy toward oroidin-derived alkaloids premised on a biosynthetic proposal", Tetrahedron, 20060529 Publication	<1 %
9	patents.justia.com Internet Source	<1 %
10	Smith, A.B.. "Total synthesis of (-)-salicylihalamide A and related congeners", Tetrahedron, 20020805 Publication	<1 %
11	Submitted to University of South Florida Student Paper	<1 %

Dr. Santosh Kumar Padhi
Associate Professor
Department of Biochemistry
School of Life Science
University of Hyderabad
Hyderabad-500 046. India.

12	Submitted to Savitribai Phule Pune University Student Paper	<1 %
13	hdl.handle.net Internet Source	<1 %
14	Submitted to University of Birmingham Student Paper	<1 %
15	patents.patsnap.com Internet Source	<1 %
16	Submitted to Jawaharlal Nehru Technological University Student Paper	<1 %
17	insight.rpxcorp.com Internet Source	<1 %
18	Submitted to Leiden University Student Paper	<1 %
19	Raphaël Hensienne, Jean-Philippe Cusson, Étienne Chénard, Stephen Hanessian. " Catalytic Lewis and Brønsted acid - diastereoselective benzylic substitutions of -hydroxy- -nitro- and -hydroxy- -azido-alkyl arenes ", Canadian Journal of Chemistry, 2020 Publication	<1 %
20	www.faqs.org Internet Source	<1 %
21	Submitted to Università di Parma Student Paper	

<1%

22 Maurice Michel, Benoît Stijlemans, Dana Michel, Monika Garg, Andreas Geissner, Peter H. Seeberger, Daniel Varón Silva. " Detection of Antibodies Against the African Parasite Using Synthetic glycosylphosphatidylinositol oligosaccharide fragments ", Cold Spring Harbor Laboratory, 2024 <1%
Publication

23 Shin, Y.. "Synthesis and biological evaluation of (-)-dictyostatin and stereoisomers", Tetrahedron, 20070827 <1%
Publication

24 Wei Jin, Xincheng Li, Boshun Wan. "A Highly Diastereo- and Enantioselective Copper(I)-Catalyzed Henry Reaction Using a Bis(sulfonamide)−Diamine Ligand", The Journal of Organic Chemistry, 2011 <1%
Publication

25 escholarship.org <1%
Internet Source

26 Suenaga, K.. "Enantioselective synthesis of aurisides A and B, cytotoxic macrolide glycosides of marine origin", Tetrahedron, 20060814 <1%
Publication

27	Submitted to University of Hong Kong Student Paper	<1%
28	Submitted to Indian Institute of Science Education and Research (IISER) Bhopal Student Paper	<1%
29	Submitted to University of Canberra Student Paper	<1%
30	Submitted to National University of Singapore Student Paper	<1%
31	Va, P.. "Total synthesis of amphidinolide E and amphidinolide E stereoisomers", Tetrahedron, 20070625 Publication	<1%

Exclude quotes	On	Exclude matches	< 14 words
Exclude bibliography	On		

Date of Registration: 04/08/2017
Date of Expiry : 03/8/2025

UNIVERSITY OF HYDERABAD
SCHOOL OF LIFE SCIENCES
DEPARTMENT OF BIOCHEMISTRY

PROFORMA FOR SUBMISSION OF THESIS/DISSERTATION

1. Name of the Candidate : AYON CHATTERJEE.
2. Roll No. : 17LBPH08
3. Year of Registration : 2017
4. Topic : 'Protein engineering and enzyme cascade in the sustainable synthesis of β-nitroalcohols'
5. Supervisor(s) and affiliations : Dr. Santosh Kumar Padhi, Associate professor
6. Whether extension/re-registration granted: (Specify below)
7. Date of submission : 28.05.2024
8. Last class attended on (M.Phil/Pre-Ph.D): 12.04.2023
9. Whether tuition fee for the current period Paid : ✓ Receipt No.& Dt : 1994287434816 ARHDAZ P5 TRANSFER TO 45
10. Whether thesis submission fee paid ✓: Receipt No & Dt : 24052115052962 2 Date - 21/05/2024 (attached) Date - 21/05/202 attached
11. Whether hostel dues cleared ✓ : Receipt No & Dt : 41428 2351169 Date - 21/05/20 (attached)
12. Whether a summary of the dissertation enclosed: Yes

D525/1067 24/5/24

Supervisor(s) Signature:

Dr. Santosh Kumar Padhi
Associate Professor
Department of Biochemistry
School of Life Science
University of Hyderabad
Hyderabad-500 046. India.

Signature of the Head of the Department.

S. V. Nair

अध्यक्ष / Head
जीवरसायनविभाग / Department of Biochemistry
जीवविज्ञान संकाय / School of Life Sciences
हैदराबाद विश्वविद्यालय / University of Hyderabad
हैदराबाद / Hyderabad-500046. INDIA

Signature of the Dean, of the School

सांकेय अध्यक्ष / Dean
जीव विज्ञान संकाय / School of Life Sciences
हैदराबाद विश्वविद्यालय / University of Hyderabad
हैदराबाद / Hyderabad-500 046.

Forwarded on

BC/884 22/5/24

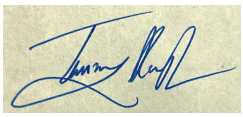
UNIVERSITY OF HYDERABAD

E-Receipt

Received With Thanks from :

Name :	AYON CHATTERJEE
Course :	Ph.D.(Biochemistry)
Rupees :	1200
Purpose :	Thesis Submission
Rs :	1200

Transaction No. :	240521150529622
Date :	May 21, 2024
PG Reference No. :	240521185593454
Application/Reg. No. :	**17LBPH08**
Payment Gateway	ICICI



*** Subject to realization** *** Fees is not refundable** **Authorized Signature**